PROBING THE UBIQUITIN LANDSCAPE

EDITED BY: Huib Ovaa, Monique P. C. Mulder, Zhihao Zhuang, Benedikt M. Kessler and Lei Liu

PUBLISHED IN: Frontiers in Chemistry, Frontiers in Molecular Biosciences and Frontiers in Cell and Developmental Biology

frontiers Research Topics

frontiers

ISSN 1664-8714
ISBN 978-2-88963-825-3
DOI 10.3389/978-2-88963-825-3

About Frontiers

Frontiers is more than just an open-access publisher of scholarly articles: it is a pioneering approach to the world of academia, radically improving the way scholarly research is managed. The grand vision of Frontiers is a world where all people have an equal opportunity to seek, share and generate knowledge. Frontiers provides immediate and permanent online open access to all its publications, but this alone is not enough to realize our grand goals.

Frontiers Journal Series

The Frontiers Journal Series is a multi-tier and interdisciplinary set of open-access, online journals, promising a paradigm shift from the current review, selection and dissemination processes in academic publishing. All Frontiers journals are driven by researchers for researchers; therefore, they constitute a service to the scholarly community. At the same time, the Frontiers Journal Series operates on a revolutionary invention, the tiered publishing system, initially addressing specific communities of scholars, and gradually climbing up to broader public understanding, thus serving the interests of the lay society, too.

Dedication to Quality

Each Frontiers article is a landmark of the highest quality, thanks to genuinely collaborative interactions between authors and review editors, who include some of the world's best academicians. Research must be certified by peers before entering a stream of knowledge that may eventually reach the public - and shape society; therefore, Frontiers only applies the most rigorous and unbiased reviews.
Frontiers revolutionizes research publishing by freely delivering the most outstanding research, evaluated with no bias from both the academic and social point of view. By applying the most advanced information technologies, Frontiers is catapulting scholarly publishing into a new generation.

What are Frontiers Research Topics?

Frontiers Research Topics are very popular trademarks of the Frontiers Journals Series: they are collections of at least ten articles, all centered on a particular subject. With their unique mix of varied contributions from Original Research to Review Articles, Frontiers Research Topics unify the most influential researchers, the latest key findings and historical advances in a hot research area! Find out more on how to host your own Frontiers Research Topic or contribute to one as an author by contacting the Frontiers Editorial Office: researchtopics@frontiersin.org

PROBING THE UBIQUITIN LANDSCAPE

Topic Editors:
Huib Ovaa, Leiden University Medical Center, Netherlands
Monique P. C. Mulder, Leiden University Medical Center, Netherlands
Zhihao Zhuang, University of Delaware, United States
Benedikt M. Kessler, University of Oxford, United Kingdom
Lei Liu, Tsinghua University, China

Citation: Ovaa, H., Mulder, M. P. C., Zhuang, Z., Kessler, B. M., Liu, L., eds. (2020). Probing the Ubiquitin Landscape. Lausanne: Frontiers Media SA.
doi: 10.3389/978-2-88963-825-3

Table of Contents

05 ***In Memoriam: Professor Huib Ovaa (1973-2020): A Uniquely Brilliant and Enthusiastic Scientist, a Pioneer in Chemical Biology and the Ubiquitin Field***
Monique P. C. Mulder and Benedikt M. Kessler

11 ***Editorial: Probing the Ubiquitin Landscape***
Monique P. C. Mulder, Zhihao Zhuang, Lei Liu, Benedikt M. Kessler and Huib Ovaa

13 ***Comprehensive Landscape of Active Deubiquitinating Enzymes Profiled by Advanced Chemoproteomics***
Adán Pinto-Fernández, Simon Davis, Abigail B. Schofield, Hannah C. Scott, Ping Zhang, Eidarus Salah, Sebastian Mathea, Philip D. Charles, Andreas Damianou, Gareth Bond, Roman Fischer and Benedikt M. Kessler

27 ***TULIP2: An Improved Method for the Identification of Ubiquitin E3-Specific Targets***
Daniel Salas-Lloret, Giulia Agabitini and Román González-Prieto

36 ***A High-Throughput Assay for Monitoring Ubiquitination in Real Time***
Tyler G. Franklin and Jonathan N. Pruneda

47 ***Targeted Protein Degradation by Chimeric Small Molecules, PROTACs and SNIPERs***
Mikihiko Naito, Nobumichi Ohoka, Norihito Shibata and Yoshinori Tsukumo

52 ***Recent Developments in Cell Permeable Deubiquitinating Enzyme Activity-Based Probes***
Daniel Conole, Milon Mondal, Jaimeen D. Majmudar and Edward W. Tate

59 ***Linear Ubiquitin Chains: Cellular Functions and Strategies for Detection and Quantification***
Gunnar Dittmar and Konstanze F. Winklhofer

75 ***Strategies to Target Specific Components of the Ubiquitin Conjugation/Deconjugation Machinery***
Neil C. Taylor and Joanna F. McGouran

84 ***SUMO Chains Rule on Chromatin Occupancy***
Jan Keiten-Schmitz, Kathrin Schunck and Stefan Müller

92 ***Strategies to Target ISG15 and USP18 Toward Therapeutic Applications***
Daniel Jiménez Fernández, Sandra Hess and Klaus-Peter Knobeloch

104 ***The Role of Atypical Ubiquitin Chains in the Regulation of the Antiviral Innate Immune Response***
Mariska van Huizen and Marjolein Kikkert

112 ***Hybrid Chains: A Collaboration of Ubiquitin and Ubiquitin-Like Modifiers Introducing Cross-Functionality to the Ubiquitin Code***
David A. Pérez Berrocal, Katharina F. Witting, Huib Ovaa and Monique P. C. Mulder

121 ***Diubiquitin-Based NMR Analysis: Interactions Between Lys6-Linked diUb and UBA Domain of UBXN1***
Dharjath Shahul Hameed, Gabrielle B. A. van Tilburg, Remco Merkx, Dennis Flierman, Hans Wienk, Farid El Oualid, Kay Hofmann, Rolf Boelens and Huib Ovaa

135 ***How to Inactivate Human Ubiquitin E3 Ligases by Mutation***
Cristina Garcia-Barcena, Nerea Osinalde, Juanma Ramirez and Ugo Mayor

149 ***Reporter-Based Screens for the Ubiquitin/Proteasome System***
Maria E. Gierisch, Tatiana A. Giovannucci and Nico P. Dantuma

157 ***Strategy for Development of Site-Specific Ubiquitin Antibodies***
Ila van Kruijsbergen, Monique P. C. Mulder, Michael Uckelmann, Tibor van Welsem, John de Widt, Aldo Spanjaard, Heinz Jacobs, Farid El Oualid, Huib Ovaa and Fred van Leeuwen

170 ***Resolving the Complexity of Ubiquitin Networks***
Katarzyna Kliza and Koraljka Husnjak

189 ***Strategies to Investigate Ubiquitination in Huntington's Disease***
Karen A. Sap and Eric A. Reits

frontiers in Chemistry

EDITORIAL
published: 20 August 2020
doi: 10.3389/fchem.2020.00627

In Memoriam: Professor Huib Ovaa (1973-2020): A Uniquely Brilliant and Enthusiastic Scientist, a Pioneer in Chemical Biology and the Ubiquitin Field

Monique P. C. Mulder[1]* *and Benedikt M. Kessler*[2]*

[1] Department of Cell and Chemical Biology, Oncode Institute, Leiden University Medical Centre, Leiden, Netherlands,
[2] Nuffield Department of Medicine, University of Oxford, Oxford, United Kingdom

Keywords: obituary announcement, pioneer, chemical biology, dedication letter, ubiquitin 26S-proteasome system

A devastating loss of a colleague, mentor, and friend with broad impact on the ubiquitin and chemical biology field. Professor Huib Ovaa had the remarkable ability to integrate chemistry across a seemingly infinite array of biological disciplines, and did so with a contagious enthusiastic, bold, and fearless attitude.

OPEN ACCESS

Edited and reviewed by:
John D. Wade,
University of Melbourne, Australia

***Correspondence:**
Monique P. C. Mulder
M.P.C.Mulder@lumc.nl
Benedikt M. Kessler
benedikt.kessler@ndm.ox.ac.uk

Specialty section:
This article was submitted to Chemical Biology, a section of the journal Frontiers in Chemistry

Received: *12 June 2020*
Accepted: *16 June 2020*
Published: *20 August 2020*

Citation:
Mulder MPC and Kessler BM (2020) In Memoriam: Professor Huib Ovaa (1973-2020): A Uniquely Brilliant and Enthusiastic Scientist, a Pioneer in Chemical Biology and the Ubiquitin Field. Front. Chem. 8:627. doi: 10.3389/fchem.2020.00627

Professor Huib Ovaa (Photo by Duco van Dalen).

CAREER

Huib was born on the 18th of December 1973 and spend most of his childhood in the westernmost and least populous province of the Netherlands, Zeeland. After his high school

education (1987-1993, Middelburg, The Netherlands) he moved to Leiden to study chemistry at Leiden University (1993-1997). He commenced with his Ph.D. research at the same institution in 1997 in the laboratory of the late Prof. Jacques van Boom and spent part of his Ph.D. in the lab of Prof. Blechert at the TU Berlin, Germany. During this time, he was trained in the use of organometallic reactions on carbohydrate derived synthons to construct carbasugars and obtained his doctorate in 2001 with the distinction "Cum Laude." After his Ph.D., Huib moved to the lab of Prof. Hidde Ploegh to perform his postdoctoral research at Harvard Medical School where he, as a fully trained synthetic organic chemist, became familiar with biochemistry and immunology and completed his academic formation.

In 2004 Huib returned to the Netherlands and was appointed Group Leader at the Netherlands Cancer Institute (NKI-AVL) in Amsterdam, where he started his own chemical biology lab. This lab was at the basis of many ubiquitin chemistries, proteasome technologies and MHC-exchange technologies used today and led to the establishment of the biotechnology spinoff company UbiQ. In 2011, Huib received the KNCV (Royal Dutch Chemistry Association) gold medal awarded to the best Dutch chemists under the age of 40 and was appointed Honorary Professor at the Leiden Institute of Chemistry (LIC), Leiden University in 2012. In 2016 Huib became Professor in Chemical Biology and at the same time his "Ovaa lab" moved to the Leiden University Medical Center (LUMC) to become part of the newly created department of Cell and Chemical Biology where he, until his death, supervised his research group and together with Prof. Jacques Neefjes headed the Chemical immunology groups.

MAJOR CONTRIBUTIONS TO THE UBIQUITIN AND CHEMICAL BIOLOGY FIELD

Huib's interest in chemical biology and eventually the ubiquitin proteasome system biology grew while he was conducting his postdoctoral fellowship in the laboratory of Prof. Hidde Ploegh at Harvard Medical School in Boston, USA. As being the only chemistry expert in a research environment of predominantly biologists and immunologists, he was exposed to many biological problems in antigen presentation in immune cells. This provided a perfect fertile ground to spark his interest in applying chemical tools to biological questions. Hidde Ploegh as his postdoctoral mentor encouraged that kind of thinking, in particular its application to immunology and antigen presentation related research. Subsequent discussions with colleagues with immunology expertise led to the realization that there was a need to better understand protein degradation, for antigen processing in the context of MHC class I, but also class II antigens, the latter through cross-presentation. In cells, protein degradation is predominantly mediated by ubiquitin conjugation to protein substrates. At that time, enzymes that recognize and process ubiquitin such as ubiquitin E3 ligases and deubiquitylating enzymes (DUBs) were sparsely characterized, perhaps with the exception of some prominent cases. To better understand ubiquitin-mediated protein degradation, creative thinking was required to face the challenges of generating tools by chemistry-based approaches. DUBs, cleaving ubiquitin chains, offered themselves as an attractive entry point for chemical tool development in forms of "molecular probes" through electrophilic moieties that could trap nucleophilic amino acid side chains of catalytic residues, such as cysteine. Originally, molecular principles borrowed from proteasome and cathepsin probes were transferred to the ubiquitin protein. Initially, the student project of Anna Borodovsky in the Ploegh lab, achieved this enzymatically via a reverse trypsin reaction to create ^{125}I-labeled radioactive ubiquitin active site probes that were used to demonstrate functional interdependence between USP14 and the proteasome proteolytic activity (Borodovsky et al., 2001). With Huib's input, this concept was further developed into a panel of HA-tagged Ub probes with different chemical warheads, which differentially target cellular DUBs, leading to the discovery of ovarian tumor domain containing proteases (OTUs) as a novel subfamily of DUBs (Borodovsky et al., 2002). These studies yet again confirmed that Huib Ovaa had an extraordinary scientific talent and was able to link his remarkable chemical knowledge with relevant biological problems, in particular in the ubiquitin field.

After Huib's return to The Netherlands, he continued to make major contributions in this area. His unusual talent to think "out of the box" provided the framework for unconventional directions, occasionally in dispute with his peers, but provoking some astonishing discoveries.

> *Boris Rodenko, about the early days in the Ovaa lab: "When Huib started as a group leader at the NKI, I was lucky enough to join him as one of his first postdocs. The aptly minted 'chemical biology' group at the NKI started with only a couple of people to conquer the world. Many of the NKI biologists looked at us with suspicious eyes. "We are not Pharma!" was a phrase often uttered by the NKI scientists in those days. Huib and the group would just laugh at this. Little did they know that we had a lot more to offer, but they would soon find out. With lots of energy Huib, and we in his team, started to develop the tools that have been making such an impact in the ubiquitin-proteasome and antigen presentation field ever since. And Huib had a big part not just in the design of the experiments, but also in their execution. In the afterhours and weekends, when the labs were quiet, he would pick a fume hood and started to brew all sorts of fluorescent reagents and probes to be used by the group or by collaborators. You would just pray to the heavens that he didn't pick your fume hood, as typically it would look like a bright pink fluorescent bomb had exploded there after Huib was done."*

For instance, under his directorship and together with his colleagues, the full synthesis of Ub/Ubl probes with remarkable yields was achieved via solid-phase peptide synthesis SPPS (El Oualid et al., 2010; Mulder et al., 2018). This was at odds with the status quo at that time on what solid-phase peptide synthesis technology can achieve, but his trick was to introduce di-amino acid Fmoc building blocks, thereby getting around challenging coupling steps.

Moreover, in collaboration with David Komander, with whom he subsequently has made other landmark contributions to the ubiquitin field, he discovered that terminal alkynes, currently

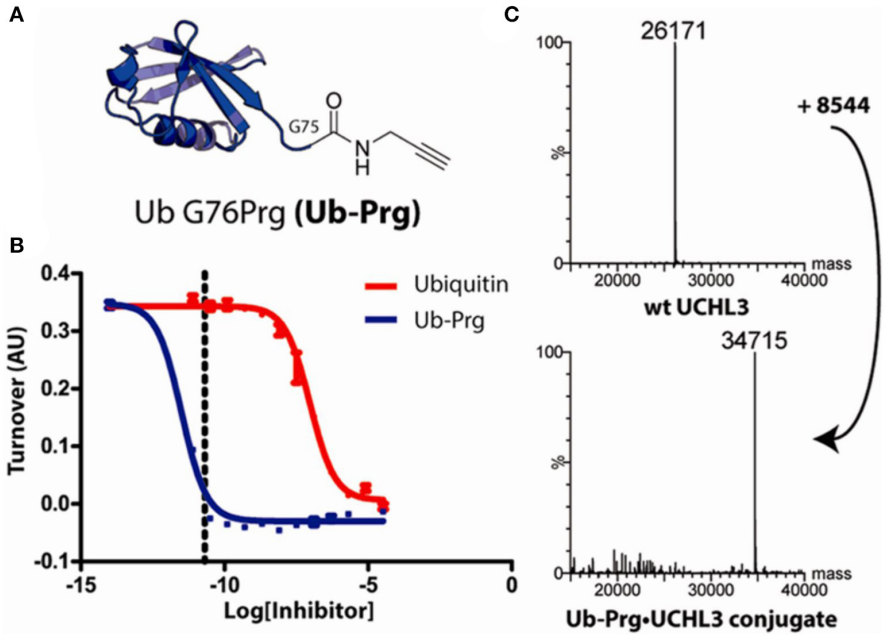

FIGURE 1 | Ub-C-terminal alkyne reacts with UCH-L3 catalytic cysteine (Ekkebus et al., 2013) [With permission –Figure 1.]. **(A)** Structure of ubiquitin propargylamine Ub-PRG. **(B)** Fluorescence polarization-based substrate turnover assay measuring UCHL3 activity, showing Ub-Prg as 105 times more powerful an inhibitor than Ub. Dotted line represents UCHL3 concentration of (60 pM). **(C)** Mass spectra showing UCH-L3 ~ UbPRG adduct formation.

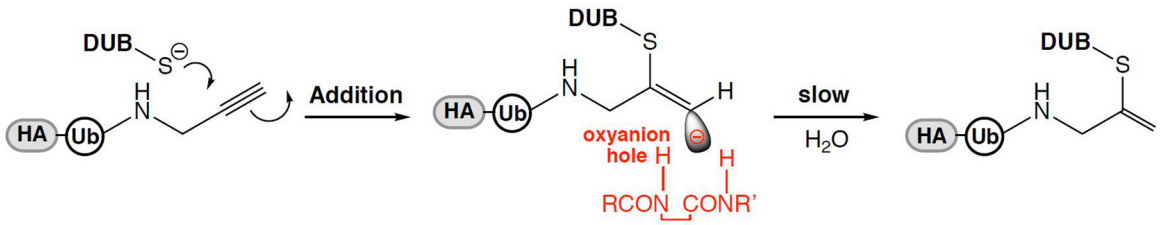

FIGURE 2 | Proposed mechanism for Ub propargyl amine probes via a sterically controlled direct addition reaction with DUBs of the cysteine protease family [Abigail Schofield and Benedikt Kessler].

thought to be poor electrophiles and therefore "orthogonal" to chemical reactions in biological systems, can react with active-site cysteine nucleophiles in proteases (**Figure 1**). Ubiquitin active site probes carrying a propargyl warhead were shown to be compatible with thiol mod in DUBs (Ekkebus et al., 2013). This unexpected reaction involving electron rich alkynes is not yet completely understood, but perhaps is facilitated by the sterically correctly placed oxyanion hole in the catalytic center of proteases such as DUBs, leading to a direct addition reaction yielding a vinyl thioether as covalent adduct (**Figure 2**). Again, this was completely unexpected, at least to occur under physiological conditions, but also applies for other proteases (Arkona and Rademann, 2013; Mons et al., 2019).

Another example is the remarkable elegance of oligo-Ub chain synthesis using a variation of thiolysine chemistry developed in Huib's laboratory (Van Der Heden Van Noort et al., 2017). This represents an optimized large scale and highly reproducible route to orthogonally protected γ-thiolysine and its use was demonstrated in the synthesis of bifunctional ubiquitin monomers (**Figure 3**). The edge of this approach is that these ubiquitin synthons are employed in polymerization reactions, giving access to synthetic poly-ubiquitin chains of defined linkage. In addition, compared to other efforts in synthesizing defined ubiquitin chains in the field, these are practically identical to their native counterparts, even leaving intact iso-peptide bonds after desulphurization.

Gerbrand van der Heden van Noort says: "Huib's way of mentoring was letting you run around the lab and do your own thing. Once in a while he would pop his head around the corner of the lab and ask if you wanted to have a look at your ongoing projects. If declined, he would disappear and put recent literature you might have missed with some unreadable notes on it on your office desk. Huib taught me to not worry about politics or peer pressure, 'just be honest and focus on the science, the rest will fall into place later'. He was extremely proud on his lab, both on the personnel

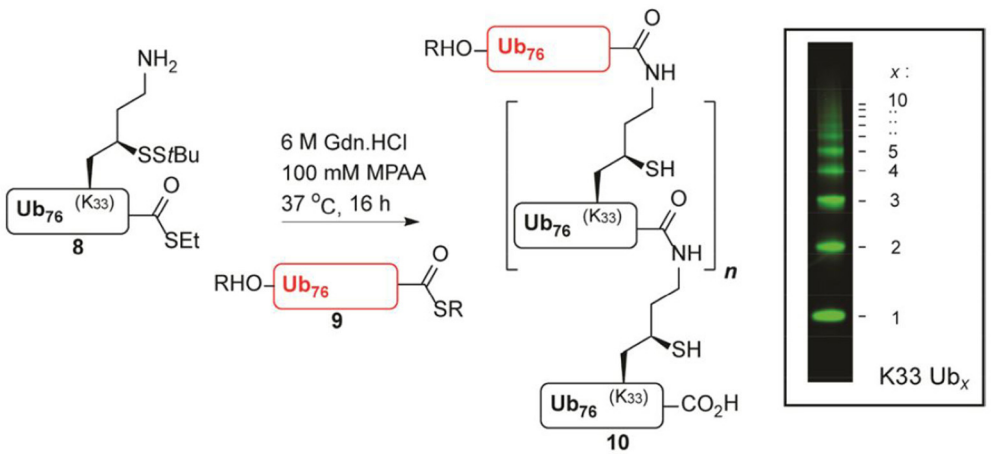

FIGURE 3 | Polymerization reaction of K33 γ-thiolysine ubiquitin thioester (Van Der Heden Van Noort et al., 2017) [With permission—Scheme 3].

and facilities he had at his disposal. Having hard-core organic chemists, peptide chemists, protein chemists, biochemists, structural biologists, cell biologists and everything in between working side by side, he applauded every collaboration between his trainees and often encouraged the 'lone wolfs' amongst us to seek and use each other's expertise."

Ubiquitin based probes and defined Ub-chains have enabled many functional studies in collaboration with other experts in the ubiquitin field with whom Huib has had the chance to work productively, such as Ton Schumacher, David Komander, Titia Sixma, Ivan Dikic, Christopher Lima, Brenda Schulman, Hans-Peter Knobeloch, Jacques Neefjes, and others. The demand for high-quality Ub/Ubl tools in ubiquitin-related research has led to the foundation of the start-up company UbiQ.

More recent developments initiated by Huib and his team included breakthroughs in challenging areas such as the first molecular probes for ubiquitin E3 ligases (Mulder et al., 2016) as well as probes that can target metalloprotease DUBs (Hameed et al., 2019). The latter, which provides access to an interesting subset of the DUB enzyme family, has been attempted previously for many years. It is, however, a reflection of Huib's remarkable efforts that made a change in this area by introducing an efficient zinc-chelator moiety at ubiquitin's C-terminus (**Figure 4**).

Additionally, his input into providing probes for studying DUBs at a cellular level helped to accelerate drug development targeting relevant DUBs in cancer, immunity, and neurodegeneration (Harrigan et al., 2018).

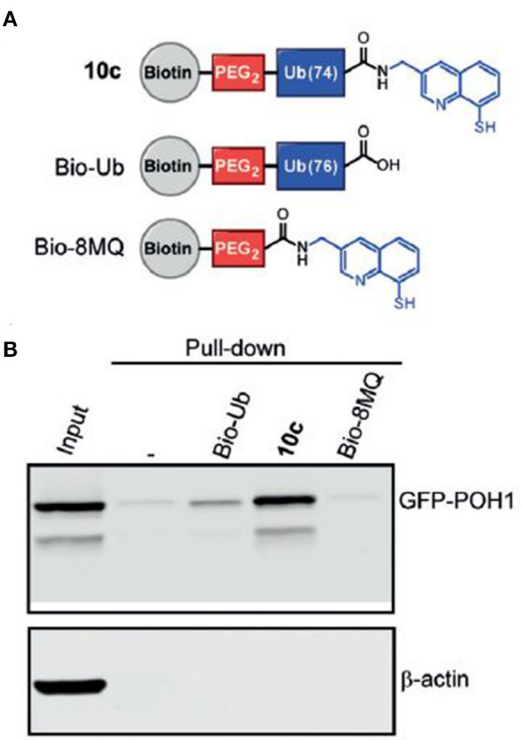

FIGURE 4 | Novel metalloprotease probes (Hameed et al., 2019) [With permission—Figure 5A]. **(A)** Schematic representation of pull-down reagents used in the assay. **(B)** Western Blot analysis of pull-down from cell lysate of HeLa cells overexpressing GFP-POH1.

Dharjath Shahul Hameed says: "Huib's lab has been the launching pad for many students. When I joined his lab as a Master-student intern, I was immediately given the freedom to work on so many ideas that would otherwise be generally shelved for a later day. When I got carried away with some ideas, he immediately reminded me to be practical and pragmatic. He was always up for challenges. There was a time when we faced strong headwinds in our metalloDUB probe project, and he gave us a big push by showing us how to combine chemistry and biology to solve one of the missing pieces of the ubiquitin puzzle. His approach is simple: a great idea executed in a simple way.

When it comes to dealing with paperwork for foreign employees, he made sure we were not distracted by such bureaucracy. He always made sure we focus on research first and let the human resource

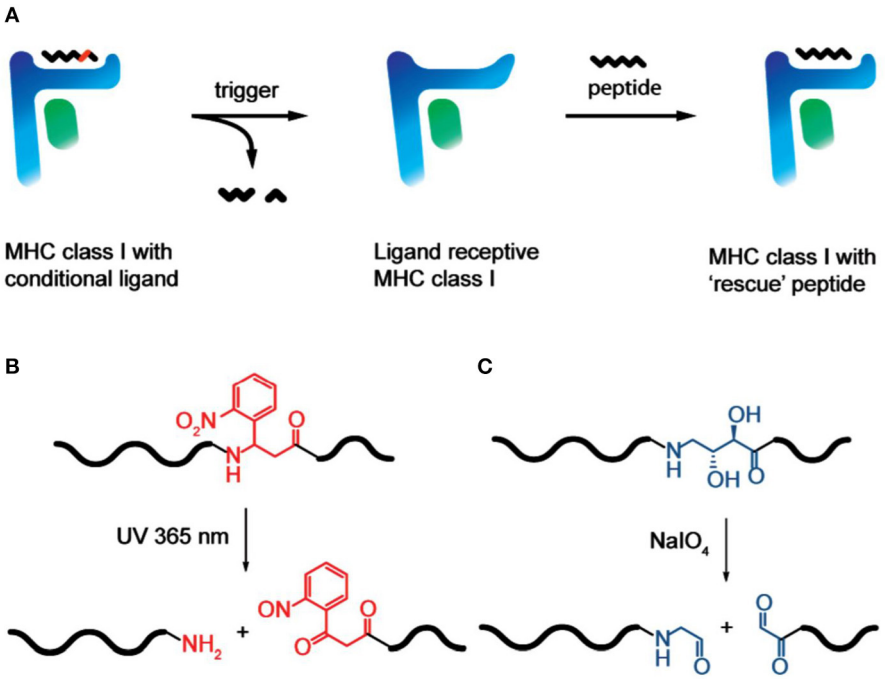

FIGURE 5 | MHC class I peptide loading technology via periodate trigger (Rodenko et al., 2009). [With permission—Figures 1A–C]. **(A)** Conditional MHC class I is treated with a trigger, which cleaves the conditional peptide ligand to afford two fragments that no longer meet minimal affinity requirements and dissociate from the peptide binding groove. The resulting ligandreceptive MHC class I has a short half-life at 37 °C if not stabilized by the binding of a "rescue" ligand. **(B)** Photocleavage of a 2-nitrophenyl-containing conditional peptide ligand, triggered by 365 nm UV light. **(C)** Chemocleavage of a vicinal diol-containing conditional peptide ligand, triggered by the addition of sodium periodate.

management team worry about our visa and work permits. For him, science precedes bureaucracy, even in collaborations. For a foreigner and a student like me, he will remain as one of the best bosses anyone can wish for."

Another unconventional contribution that Huib made, in collaboration with Ton Schumacher, to the field of immunology and antigen presentation was his clever design of MHC class I photoreactive peptides to enable efficient peptide loading (Toebes et al., 2006). The chemical "trick" used here was to introduce a diol-moiety into the antigenic peptide backbone that can be efficiently cleaved by sodium periodate ($NaIO_4$), leading to the cleavage and removal of peptide remnants from the MHC class I peptide groove, making room for other peptides to bind, yielding MHC class I—peptide complexes of defined composition (Rodenko et al., 2009) (**Figure 5**). This elegant technical advance has provided an enormous boost to prepare MHC-I-peptide tools for the detection of circulating T-lymphocytes of a given antigen specificity, extremely relevant to study immune responses to cancer and infection. More recently, he and his colleagues expanded on this early work and developed an efficient method to generate many different MHC-I multimers in parallel using temperature-mediated peptide exchange (Luimstra et al., 2018).

Aysegul Sapmaz says: "I came to Huib's lab as a visiting Ph.D. student with a hardcore molecular biology background but a novice in chemistry. During that time, I was excited to use his magical tools for my Ph.D. study. Even though it was a short stint, I already realized that I would love to continue working with him. When I asked for a postdoc position in his lab, he did not hesitate and immediately said "Yes". From the moment I started in his lab, he always encouraged me to believe in my gut feelings and let me work freely on my own projects even if there was very little overlap with chemistry. He also encouraged me to provide my biological expertise in other chemistry-based projects going on in the lab. This has resulted in several publications in the field of applied chemistry with many more on the way. Huib always supervised the people in his lab by trusting and encouraging them to think out of the box and to do the impossible. When you had interesting results, he got super excited which put his signature big smile on his face. He was a great mentor who always supported his team during difficult times both in their scientific and personal life. He was always proud of his lab that he meticulously built with trust, freedom, and encouragement..."

His lab, jointly run with Prof. Jacques Neefjes, has recently expanded as part of the Chemical Immunology Unit at LUMC, a tribute to their scientific success. Huib was an extraordinary scientist who fearlessly extended his research into a very broad spectrum of the scientific field, as exemplified by one of his more recent publications (Sapmaz et al., 2019). In collaboration with Prof. Jacques Neefjes, they revealed the function of a

previously unidentified DUB, USP32, using molecular biology and biochemistry approaches. His most recent research was geared toward the development of small molecule inhibitor molecules against DUBs as tool compounds and precursors of drug development (Geurink et al., 2019).

Huib has left us way too early as a colleague and exceptional scientist. We could have expected so much more coming from him—he will be remembered as a bright star in the sky of ubiquitin & chemical biology.

AUTHOR CONTRIBUTIONS

MM and BK wrote and edited the manuscript and approved it for publication.

REFERENCES

Arkona, C., and Rademann, J. (2013). Propargyl amides as irreversible inhibitors of cysteine proteases - A lesson on the biological reactivity of alkynes. *Angew. Chem. Int. Ed.* 52, 8210–8212. doi: 10.1002/anie.201303544

Borodovsky, A., Kessler, B. M., Casagrande, R., Overkleeft, H. S., Wilkinson, K. D., and Ploegh, H. L. (2001). A novel active site-directed probe specific for deubiquitylating enzymes reveals proteasome association of USP14. *EMBO J.* 20, 5187–5196. doi: 10.1093/emboj/20.18.5187

Borodovsky, A., Ovaa, H., Kolli, N., Gan-Erdene, T., Wilkinson, K. D., Ploegh, H. L., et al., (2002). Chemistry-based functional proteomics reveals novel members of the deubiquitinating enzyme family. *Chem. Biol.* 9, 1149–1159. doi: 10.1016/S1074-5521(02)00248-X

Ekkebus, R., Van Kasteren, S. I., Kulathu, Y., Scholten, A., Berlin, I., Geurink, P. P., et al. (2013). On terminal alkynes that can react with active-site cysteine nucleophiles in proteases. *J. Am. Chem. Soc.* 135, 2867–2870. doi: 10.1021/ja309802n

El Oualid, F., Merkx, R., Ekkebus, R., Hameed, D. S., Smit, J. J., De Jong, A., et al. (2010). Chemical synthesis of ubiquitin, ubiquitin-based probes, and diubiquitin. *Angew. Chem. Int. Ed.* 49, 10149–10153. doi: 10.1002/anie.201005995

Geurink, P. P., Kooij, R., Sapmaz, A., Liu, S., Xin, B.-T., Janssen, G. M. C., et al. (2019). A small-molecule activity-based probe for monitoring ubiquitin c-terminal hydrolase L1 (UCHL1) activity in live cells and zebrafish embryos. *bioRxiv*. 1–34. doi: 10.1101/827642

Hameed, D. S., Sapmaz, A., Burggraaff, L., Amore, A., Slingerland, C. J., van Westen, G. J. P., et al. (2019). Development of ubiquitin-based probe for metalloprotease deubiquitinases. *Angew. Chem. Int. Ed.* 58, 14477–14482. doi: 10.1002/anie.201906790

Harrigan, J. A., Jacq, X., Martin, N. M., and Jackson, S. P. (2018). Deubiquitylating enzymes and drug discovery: emerging opportunities. *Nat. Rev. Drug Discov.* 17, 57–78. doi: 10.1038/nrd.2017.152

Luimstra, J. J., Garstka, M. A., Roex, M. C. J., Redeker, A., Janssen, G. M. C., van Veelen, P. A., et al. (2018). A flexible MHC class I multimer loading system for large-scale detection of antigen-specific T cells. *J. Exp. Med.* 215, 1493–1504. doi: 10.1084/jem.20180156

Mons, E., Jansen, I. D. C., Loboda, J., van Doodewaerd, B. R., Hermans, J., Verdoes, M., et al. (2019) The alkyne moiety as a latent electrophile in irreversible covalent small molecule inhibitors of cathepsin K. *J. Am. Chem. Soc.* 141, 3507–3514. doi: 10.1021/jacs.8b11027

Mulder, M. P. C., Merkx, R., Witting, K. F., Hameed, D. S., El Atmioui, D., Lelieveld, L., et al. (2018). Total chemical synthesis of SUMO and SUMO-based probes for profiling the activity of SUMO-specific proteases. *Angew. Chem. Int. Ed.* 57, 8958–8962. doi: 10.1002/anie.201803483

Mulder, M. P. C., Witting, K., Berlin, I., Pruneda, J. N., Wu, K. P., Chang, J. G., et al. (2016). A cascading activity-based probe sequentially targets E1-E2-E3 ubiquitin enzymes. *Nat. Chem. Biol.* 12, 523–530. doi: 10.1038/nchembio.2084

Rodenko, B., Toebes, M., Celie, P. H. N., Perrakis, A., Schumacher, T. N. M., and Ovaa, H. (2009). Class I major histocompatibility complexes loaded by a periodate trigger. *J. Am. Chem. Soc.* 131, 12305–2513. doi: 10.1021/ja9037565

Sapmaz, A., Berlin, I., Bos, E., Wijdeven, R. H., Janssen, H., Konietzny, R., et al. (2019). USP32 regulates late endosomal transport and recycling through deubiquitylation of Rab7. *Nat. Commun*. doi: 10.1038/s41467-019-09437-x

Toebes, M., Coccoris, M., Bins, A., Rodenko, B., Gomez, R., Nieuwkoop, N. J., et al. (2006). Design and use of conditional MHC class I ligands. *Nat. Med.* 12, 246–251. doi: 10.1038/nm1360

Van Der Heden Van Noort, G. J., Kooij, R., Elliott, P. R., Komander, D., and Ovaa, H. (2017). Synthesis of poly-ubiquitin chains using a bifunctional ubiquitin monomer. *Org. Lett.* 19, 6490–6493. doi: 10.1021/acs.orglett.7b03085

Conflict of Interest: The authors declare that the research was conducted in the absence of any commercial or financial relationships that could be construed as a potential conflict of interest.

frontiers in Chemistry

EDITORIAL
published: 20 May 2020
doi: 10.3389/fchem.2020.00449

Editorial: Probing the Ubiquitin Landscape

Monique P. C. Mulder[1], Zhihao Zhuang[2], Lei Liu[3], Benedikt M. Kessler[4] and Huib Ovaa[1]*

[1] Department of Cell and Chemical Biology, Oncode Institute, Leiden University Medical Centre, Leiden, Netherlands, [2] Department of Chemistry and Biochemistry, University of Delaware, Newark, DE, United States, [3] Tsinghua-Peking Center for Life Sciences, MOE Key Laboratory of Bioorganic Phosphorus Chemistry & Chemical Biology, Center for Synthetic and Systems Biology, Department of Chemistry, Tsinghua University, Beijing, China, [4] Nuffield Department of Medicine, University of Oxford, Oxford, United Kingdom

Keywords: ubiquitin(-like), activity-based probes, toolbox development, applications, inhibitors, proteomics

Editorial on the Research Topic

Probing the Ubiquitin Landscape

Since the pioneering work of Hershko, Ciechanover and their colleagues 40 years ago, our understanding of one of the most complex and widespread signaling networks in biology has evolved greatly through genetic, proteomic, biochemical, and cell biological studies (Kliza and Husnjak). In this Research Topic, we present a salient collection of original research, methods and review articles that cover novel, promising and recent trends in the ubiquitin(-like) field.

Protein ubiquitination is a powerful post-translational modulator (PTM) as it controls almost every process in cells. To accomplish this, various ubiquitin (Ub) modifications adopt distinct conformations, utilizing what is commonly referred to as the "Ub code", leading to different cellular functions. Modification by ubiquitin of a target protein is tightly controlled by the action of hundreds of regulatory enzymes employed in specific combinations involving three main steps: activation (E1 enzymes), conjugation (E2 enzymes), and ligation (E3 enzymes). To counterbalance ubiquitination, it can be removed from substrate proteins by deubiquitinating enzymes (DUBs). Modification of a substrate protein can occur by a single Ub moiety on a single target lysine (monoubiquitination) or on multiple lysines (multi-monoubiquitination). Additionally, after a single Ub is transferred to the substrate protein, any of the eight amino groups of the initial substrate-conjugated ubiquitin (Lys6, Lys11, Lys27, Lys29, Lys33, Lys48, Lys63, Met1) can be modified with another Ub molecule, yielding polyubiquitin chains of variable linkage type, length, and configuration (homo- vs. heterotypic Ub chains). Though the functional significance of cellular Ub modifications, such as Lys48- and Lys63-linked polyUb chains, are largely known, the biological significance of other homotypic polyUb chains, collectively referred to as atypical Ub chains, is still far from being fully understood. While van Huizen and Kikkert comprehensively review the role of atypical ubiquitin chains in the regulation of antiviral innate immunity pathways, Dittmar and Winklhofer review a distinct type of ubiquitination—linear (Met1-linked) ubiquitination—a transient and spatially regulated modification, complexifying their detection and quantification.

Next to Ub, a vast number of ubiquitin-like (UbL) proteins (e.g., SUMO, Nedd8, ISG15, Ufm1, Fat10) can also be attached to proteins increasing the complexity and fine-tuning cellular responses even further. Keiten-Schmitz et al. review the role of SUMO chains in chromatin dynamics and genome stability networks, whereas Fernández et al. describe ISGylation as well as strategies targeting this PTM for therapeutic applications. Intriguingly, unlike most PTMs such as acetylation and phosphorylation, ubiquitin itself can be highly customized through further post-translational modification by other PTMs, thereby expanding the Ub code for distinct cellular outcomes which either alter the originally encrypted message or encode a completely new one. The

OPEN ACCESS

Edited and reviewed by:
John D. Wade,
University of Melbourne, Australia

****Correspondence:***
Monique P. C. Mulder
M.P.C.Mulder@lumc.nl

Specialty section:
This article was submitted to Chemical Biology, a section of the journal Frontiers in Chemistry

Received: *20 April 2020*
Accepted: *29 April 2020*
Published: *20 May 2020*

Citation:
Mulder MPC, Zhuang Z, Liu L, Kessler BM and Ovaa H (2020) Editorial: Probing the Ubiquitin Landscape. Front. Chem. 8:449. doi: 10.3389/fchem.2020.00449

cross-functionality introduced through additional post-translational modification of Ub molecules by UbL proteins, rendering hybrid Ub/UbL chains, is discussed by Perez Berrocal et al..

Considering the impact of ubiquitination on the regulation of a vast array of fundamental biological processes, dysregulation of this intrinsic process gives rise to numerous diseases ranging from autoimmunity, cancer, and neurodegenerative diseases such as Alzheimer and Huntington's disease (Reits and Sap). During the last few years defects in the ubiquitin-proteasome system (UPS)—a central player in protein quality control facilitating elimination of misfolded or otherwise aberrant proteins—including hampered E3 ligase activity, have been the focus of many studies. Understanding the mechanism of action, as well as identifying which substrates are regulated by a given E3 ligase could provide invaluable knowledge toward the development of therapeutic strategies. Garcia-Barcena et al. review the generation and usage of E3 mutants, thereby highlighting the complexity of this family of enzymes. As the E3 enzymes exhibit different substrate specificity, determining which E3 enzyme maps to which substrate is crucial for our understanding of this complex intrinsic network. Salas-Lloret et al. describe an improved TULIP2 methodology facilitating mass spectrometry toward the identification of E3-substrate networks.

While inhibition of the UPS has proven promising in the treatment of cancer, stimulation of the proteasome has been proposed as a potential therapeutic strategy for neurodegenerative disorders. In the pursuit for novel therapeutics and intervention points, robust assays and tools are key toward understanding and identification of specific components of the UPS. Franklin and Pruneda describe a new assay, UbiReal, that make use of fluorescence polarization to monitor all stages of Ub conjugation and deconjugation in real time, making it a candidate for High-throughput screens (HTS) of activity modulators. In addition, the general functional status of the UPS in cells can be examined using reporter substrates as discussed by Gierisch et al.. More recently technologies have been established that induce targeted protein degradation by chimeric small molecules as reviewed by Naito et al.. These technologies, such as Proteolysis Targeting Chimeras (PROTACs), hijack the cellular machinery for ubiquitination thereby subjecting the ubiquitinated proteins to proteasomal degradation. This promoted several drug development research programs as proteins which had previously been regarded as "undruggable" by traditional small molecule therapies can now be degraded by inducing selective intracellular proteolysis.

With an increased focus on the development of novel therapeutics of ubiquitin(-like) system components, characterization of their dynamics is imminent. Understanding the mechanisms of ubiquitin regulation requires the generation of antibodies or alternative reagents that detect ubiquitin in a site-specific manner. van Kruijsbergen et al. describe a strategy and the encountered challenges toward the development of site-specific ubiquitin antibodies. Together with advances in synthetic strategies for ubiquitin generation, enabling the development of a plethora of ubiquitin activity-based probes (ABPs) and assay reagents, the study of enzymes involved in the complex system of ubiquitination is now within reach. ABPs react covalently at the active site on the enzyme, and thus represent a powerful method to report on specific enzyme activity and to evaluate cellular and physiological enzyme dynamics and function. Taylor and McGouran present the developments made in the "traditional" ubiquitin based ABPs, whereas Conole et al. discuss recent developments in cell-permeable small molecule ABPs. With these advances in the ABP field, activity based protein profiling has emerged as a powerful technique to study these important enzymes as exemplified by the work of Pinto-Fernández et al.. Here, they combined advanced mass spectrometry technology with propargylic-based ubiquitin ABPs to reveal the proportion of active cellular DUBs adding another layer of information in addition to their endogenous expression levels.

Further understanding of the ubiquitin signaling pathway includes the knowhow on how different polyUb chains are recognized by interacting proteins. Often these interacting proteins contain a specific ubiquitin-binding domain (UBD) that bind specifically to polyUb chains, thereby rendering different cellular outcomes. Hameed et al. report on the synthesis of diUb chains, fully 15N-labeled on the distal (N-terminal) Ub and demonstrate their applicability for gaining insights into linkage-selective ubiquitin recognition of a unique UBD.

We believe that our Probing the Ubiquitin Landscape Research Topic demonstrates the multidisciplinary nature of research in the ubiquitin field. Advancement in the field is dependent on increased understanding through interconnected research strategies, thereby allowing development of therapeutics as exemplified in this body of work.

AUTHOR CONTRIBUTIONS

All authors listed have made a substantial, direct and intellectual contribution to the work, and approved it for publication.

Conflict of Interest: The authors declare that the research was conducted in the absence of any commercial or financial relationships that could be construed as a potential conflict of interest.

frontiers in Chemistry

ORIGINAL RESEARCH
published: 29 August 2019
doi: 10.3389/fchem.2019.00592

Comprehensive Landscape of Active Deubiquitinating Enzymes Profiled by Advanced Chemoproteomics

Adán Pinto-Fernández[1,2], Simon Davis[1,2], Abigail B. Schofield[1,3], Hannah C. Scott[1,2], Ping Zhang[1,4], Eidarus Salah[1,5,6], Sebastian Mathea[6,7], Philip D. Charles[1,2], Andreas Damianou[1,2], Gareth Bond[1,4], Roman Fischer[1,2] and Benedikt M. Kessler[1,2]**

[1] University of Oxford, Oxford, United Kingdom, [2] Target Discovery Institute, Nuffield Department of Medicine, University of Oxford, Oxford, United Kingdom, [3] Christ Church, University of Oxford, Oxford, United Kingdom, [4] Ludwig Institute for Cancer Research, University of Oxford, Oxford, United Kingdom, [5] Department of Chemistry, University of Oxford, Oxford, United Kingdom, [6] Structural Genomics Consortium (United Kingdom), Oxford, United Kingdom, [7] Institute of Pharmaceutical Chemistry, Buchmann Institute for Molecular Life Sciences, Goethe University Frankfurt, Frankfurt, Germany

Enzymes that bind and process ubiquitin, a small 76-amino-acid protein, have been recognized as pharmacological targets in oncology, immunological disorders, and neurodegeneration. Mass spectrometry technology has now reached the capacity to cover the proteome with enough depth to interrogate entire biochemical pathways including those that contain DUBs and E3 ligase substrates. We have recently characterized the breast cancer cell (MCF7) deep proteome by detecting and quantifying ~10,000 proteins, and within this data set, we can detect endogenous expression of 65 deubiquitylating enzymes (DUBs), whereas matching transcriptomics detected 78 DUB mRNAs. Since enzyme activity provides another meaningful layer of information in addition to the expression levels, we have combined advanced mass spectrometry technology, pre-fractionation, and more potent/selective ubiquitin active-site probes with propargylic-based electrophiles to profile 74 DUBs including distinguishable isoforms for 5 DUBs in MCF7 crude extract material. Competition experiments with cysteine alkylating agents and pan-DUB inhibitors combined with probe labeling revealed the proportion of active cellular DUBs directly engaged with probes by label-free quantitative (LFQ) mass spectrometry. This demonstrated that USP13, 39, and 40 are non-reactive to probe, indicating restricted enzymatic activity under these cellular conditions. Our extended chemoproteomics workflow increases depth of covering the active DUBome, including isoform-specific resolution, and provides the framework for more comprehensive cell-based small-molecule DUB selectivity profiling.

Keywords: deubiquitylating enzymes, mass spectrometry, proteomics, chemical biology, ubiquitin specific proteases, isoforms

OPEN ACCESS

Edited by:
John D. Wade,
Florey Institute of Neuroscience and Mental Health, Australia

Reviewed by:
Edouard Nice,
Monash University, Australia
Laura Dagley,
Walter and Eliza Hall Institute of Medical Research, Australia

****Correspondence:***
Adán Pinto-Fernández
adan.pintofernandez@ndm.ox.ac.uk
Benedikt M. Kessler
benedikt.kessler@ndm.ox.ac.uk

Specialty section:
This article was submitted to Chemical Biology, a section of the journal Frontiers in Chemistry

Received: *15 June 2019*
Accepted: *09 August 2019*
Published: *29 August 2019*

Citation:
Pinto-Fernández A, Davis S, Schofield AB, Scott HC, Zhang P, Salah E, Mathea S, Charles PD, Damianou A, Bond G, Fischer R and Kessler BM (2019) Comprehensive Landscape of Active Deubiquitinating Enzymes Profiled by Advanced Chemoproteomics. Front. Chem. 7:592. doi: 10.3389/fchem.2019.00592

INTRODUCTION

Ubiquitin (Ub) is a conserved, globular protein consisting of 76 amino acids that can be attached to proteins either in a mono- or polymerized form, impacting on their activity, localization, interactome, and turnover. The covalent attachment of Ub, most frequently to a ε-NH_2 lysine side chain of protein substrates, is catalyzed by the sequential action of three enzymes: E1 activating enzyme, E2 conjugating enzyme, and E3 ligase (Hershko and Ciechanover, 1998). Polymers of Ub can be formed by the addition of one or more monomers to a previously substrate-attached Ub

molecule. These chains provide a code of functional modulations including protein degradation and cellular signaling (Komander and Rape, 2012). Poly-Ub chains can also include Ub-like modifiers (UBLs) (Cappadocia and Lima, 2018) and posttranslational modifications (PTMs) that increase the biological complexity of ubiquitylation (Swatek and Komander, 2016).

Polymerization of Ub is a reversible process carried out by deubiquitylating enzymes (DUBs) that catalyze hydrolysis of Ub–substrate isopeptide bonds (Komander et al., 2009). To date, there are 102 human DUBs that have been grouped into eight different sub-families (Komander et al., 2009; Fraile et al., 2012): Ub-specific proteases (USPs), Ub carboxy-terminal hydrolases (UCHs), ovarian tumor domain containing proteases (OTUs), Machado–Joseph disease protein domain proteases (MJDs or Josephins), JAMM/MPN domain-associated metallopeptidases (JAMMs), motif interacting with Ub-containing novel DUB (MINDYs) (Abdul Rehman et al., 2016), the less studied monocyte chemotactic protein-induced protein (MCPIPs) (Kolattukudy and Niu, 2012), and the recently discovered Zn-finger and UFSP domain protein (ZUFSP) (Haahr et al., 2018; Hermanns et al., 2018; Hewings et al., 2018). Most DUBs (∼80) are classified as cysteine proteases with the exception of JAMM metallopeptidases and inactive (pseudo) DUBs (Nijman et al., 2005; Komander et al., 2009). DUBs have emerged as key enzymes for deciding the fate of most intracellular proteins regarding their function and lifespan. Highly selective and potent DUB inhibitors are now emerging (Kategaya et al., 2017; Lamberto et al., 2017; Turnbull et al., 2017; Gavory et al., 2018; Harrigan et al., 2018; Clague et al., 2019), which, in addition to PROteolysis-TArgeting chimeras (PROTACS) (Mullard, 2019), are paving the way to explore the Ub system in drug discovery development programs by modulating the turnover of key targets in the context of cancer, dementia, and inflammation (Pinto-Fernandez and Kessler, 2016; Harrigan et al., 2018). DUB inhibitor development has been accelerated by the application of Ub activity-based probes (ABPs) (Altun et al., 2011; Turnbull et al., 2017). ABPs contain a specificity motif that targets them to the desired enzyme/class of enzymes and a chemical moiety that reacts covalently with the active site of the enzyme. This has been applicable to study proteases that have a nucleophilic active site, mainly serine hydrolases and cysteine peptidases (Sanman and Bogyo, 2014), but also metalloproteases (Nury et al., 2013; Amara et al., 2018). For DUBs, many different probe architectures have been generated and tested with different selectivity toward DUBs, with those using a molecule of Ub as specificity motif being the more popular ones (Borodovsky et al., 2001, 2002, 2005; Hemelaar et al., 2004). However, di-Ub ABPs mimicking the different poly-Ub linkages have been generated and studied (McGouran et al., 2013), with the linear di-Ub being highly selective toward OTULIN (Weber et al., 2017). Finally, thanks to the utilization of a DUB inhibitor as specificity motif, Ward et al. (2016) managed to synthesize a permeable ABP reactive with a number of DUBs. Different C-terminal chemical moieties enabling Michael additions and nucleophilic displacements have been explored, and more recently, alkynes that react *via* a radical-based mechanism (Ekkebus et al., 2013; Hewings et al., 2017). To determine the subset of DUBs that directly react with probe in addition to binding, DUB-probe reaction centric probes were generated that enrich for Cys-reactive peptides after enzymatic digestion to map covalent sites within reactive DUBs (Hewings et al., 2018). Despite these advances, it is unclear to what extent the entire range of endogenous DUBs expressed that are active in cells are captured.

To address this, we have developed an advanced "activitomics" workflow and compared it against the DUB transcriptome and proteome expressed in MCF7 breast cancer cells. We discriminate between DUBs reactive to probe and non-reactive enzyme species through competition at the enzyme's active-site cysteine combined with quantitative chemoproteomics. The range covered by the cellular DUB activitome, transcriptome (mRNA), and deep proteome (protein) is comparable, revealing an extended landscape of the cellular DUBome.

We acknowledge that it is challenging to compare proteomics data because instrumentation, methods, and software are in constant evolution and all three are quite heterogeneous from lab to lab. In this particular study, we identified 74 DUBs whereas most previous studies reported on between 20 and 40 DUBs. A recent study by Ingrid Wertz' group reported the identification of 61 DUBs (Hewings et al., 2018). Therefore, our study represents the most comprehensive coverage reported so far.

MATERIALS AND METHODS

Contact for Reagent and Resource Sharing

Further information and requests for resources and reagents should be directed to and will be fulfilled by the corresponding authors, BK (benedikt.kessler@ndm.ox.ac.uk) and AP-F (adan.pintofernandez@ndm.ox.ac.uk).

Cell Lines and Reagents

Commercially purchased MCF7 (ATCC Nr HTB-22) cells were cultured in DMEM medium (GIBCO) supplemented with 10% fetal calf serum (FCS; GIBCO), 100 U/ml penicillin (SIGMA), and 100 μg/ml streptomycin (SIGMA) and maintained at 37°C in a humidified atmosphere at 5% CO_2. Other reagents used in this study are listed in **Table 1**.

Ub-Based ABP Synthesis

The construct pTYB-HAUb, comprising the sequences of the human Ub (lacking Gly 76), an intein and a chitin binding domain, plus an HA tag, was used to synthesize HAUb75-MESNa as described previously (Borodovsky et al., 2002). Briefly, Ub–intein–chitin domain fusion protein was expressed in *Escherichia coli* (18 h induction with 0.4 mM IPTG at 17°C). Cell pellets were resuspended in 50 mM HEPES, pH 7.4, 150 mM NaCl, and 0.5 mM TCEP and lysed in a high-pressure homogenizer. The cleared cell extract was loaded onto a 15 ml chitin bead (New England Biolabs) column at a flow rate of 0.5 ml/min. The column was washed with 60 ml of lysis buffer followed by 25 ml of lysis buffer containing 50 mM β-mercaptoethanesulfonic acid sodium salt (MESNa) and incubated overnight at 37°C for the induction of on-column cleavage. HAUb75-MESNa thioester was eluted with 25 ml of lysis buffer and concentrated: approximately

TABLE 1 | Cell lines and reagents.

Reagent or resource	Source	Identifier
ANTIBODIES		
Mouse monoclonal antibody HA (12CA5)	Roche	#11583816001
USP7 pAb	Enzo	#BML-PW0540-0100
GAPDH loading control antibody (GA1R)	Invitrogen	#MA5-15738
Monoclonal Anti-HA-Agarose antibody produced in mouse	SIGMA	#A2095-1ML
CHEMICALS, KITS, ENZYMES, AND OTHERS		
Trypsin (TPCK-treated)	Worthington	#LS003740
Acid-washed glass beads	SIGMA	# G4649
Pierce™ BCA Protein Assay Kit	Thermofisher	#23225
Criterion TGX Gel, 4–15%, 18-well	Bio-Rad	#5671084
Sep-Pak C18 Plus Short Cartridge, 360 mg Sorbent per Cartridge, 55–105 μm Particle Size	Waters	# WAT020515
Chitin resin	New England Biolabs	#S6651L
PD-10 columns	GE Healthcare	#17-0851-01
2-Bromoethylamine	SIGMA	#B65705-25G
Propargylamine	SIGMA	#P50900-5G
EXPERIMENTAL MODELS: CELL LINES		
MCF7 cells	ATCC	HTB-22
Software and Algorithms MaxQuant Software (version 1.5.2)	Open source	http://www.coxdocs.org/doku.php?id=maxquant:start
Perseus Software (version 1.6.2.3)	Open source	http://www.coxdocs.org/doku.php?id=perseus:start
Prism 8	GraphPad	https://www.graphpad.com/scientific-software/prism/

2.5 mg of protein was recovered from a 1-L culture. The N-terminal Met of the HA-tag was frequently processed off during expression, resulting in a mixture of two proteins that behaved identically in labeling experiments.

To synthesize the HA-UbC2Br or HA-UbPA probes, 0.2 mM of 2-bromoethylamine or 250 mM propargylamine was added to a solution of HAUb75-MESNa (1–2 mg/ml) in 500 μl of column buffer, respectively. pH was carefully adjusted to 8 with NaOH, and after 20 min shaking at 1,400 rpm, at room temperature, 100 μl of 2.0 M aqueous HCl was added and the resultant reaction mixture was promptly transferred to a PD10 gravity column for buffer exchange, according to the manufacturer's instructions.

The probe was then aliquoted and frozen at −80°C for storage (no significant deterioration is observed for several months of storage except for HA-UbC2Br, which is prone to hydrolysis). All HA-Ub-derived probes were analyzed by liquid chromatography mass spectrometry (LC-MS) using a 1290 UPLC (Agilent) coupled to a 6560 quadrupole time-of-flight (QToF) mass spectrometer (Agilent) to monitor the reaction and the product detected by $[M+H]^+ = 10{,}197.6221$, with >90% purity.

Preparation of Cell Extracts and Western Blotting

Protein extracts were prepared as follows: Cells were washed with ice-cold PBS and collected into a centrifuge tube in either glass beads lysis buffer (GBL: 50 mM Tris, pH 7.5, 5 mM $MgCl_2$, 0.5 mM EDTA, and 250 mM Sucrose) or glass beads lysis buffer plus 0.2% NP-40 (GBLN). One volume of acid-washed glass beads (Sigma Aldrich, G4649) per 2–3 volumes of ice-cold glass bead buffer (+1 mM DTT) was added to the tube containing the cells and buffer followed by vortexing (10 times in 30 s bursts, returning the samples to the ice for 1–2 min in between) and centrifugation (14,000 *g*, 4°C, 25 min) in order to pellet the glass beads, nuclei, and membranes. The supernatant was carefully transferred to fresh Eppendorf tubes and the pellets were discarded. The protein concentration was determined *via* the Thermo BCA protein assay kit. For Western blotting, 25 μg of protein was then fractionated on Tris–glycine SDS-PAGE gradient (4–15% acrylamide) gels, transferred onto PVDF membranes, and detected with the indicated antibodies using a LI-COR detection system.

DUB Activity-Based Profiling

At least 500 μg of cell extract (corresponding to approximately 1×10^7 cells) in 300 μl of GBL buffer containing 1 mM DTT were utilized for the ABP pulldowns. When profiling a DUB inhibitor, the inhibitor should be added at this point to the desired final concentration and incubated at 37°C for 1 h. Then, ∼10 μg of the HA-Ub-based ABPs were added per 500 μg of sample (Note: this will vary depending on the reactivity of the probe batch and type and may require optimization for complete labeling of the DUB of interest) and incubated at 37°C for 45 min. The reaction was quenched by the addition of SDS to 0.4% (24 μl of a 5% stock per 300 μl) and NP-40 (or IGEPAL CA-630 substitute) to 0.5% (15 μl of a 10% stock per 300 μl), and samples were diluted to 1 ml, 0.5 mg/ml, by the addition of 661 μl of NP-40 lysis buffer [pH 7.4, 50 mM Tris, 0.5% (v/v) NP-40, 150 mM NaCl, and 20 mM $MgCl_2$]. Fifty microliters (25 μg) of sample was aliquoted and denatured by boiling in SDS Laemmli sample buffer for control blotting to assess IP efficiency. To bind and pull down DUB–ABP complexes, 150 μl of anti-HA-Agarose slurry (previously washed four times with NP-40 lysis buffer) was added to the samples and incubated on a rotator overnight at 4°C. After a first centrifugation step (2,000 *g*, 4°C, 1 min), beads were washed four times with 500 μl of NP-40 lysis buffer. Protein complexes were eluted by boiling beads in 110 μl of 2× SDS Laemmli sample buffer and 10% were analyzed by Western blotting after SDS-PAGE, as well as lysate controls.

Mass Spectrometry Experiments (Sample Preparation and Fractionation)

DUB-probe immunoprecipitated sample eluates were diluted to 175 μl with ultra-pure water and reduced with 5 μl of DTT (200 mM in 0.1 M Tris, pH 7.8) for 30 min at 37°C.

Samples were alkylated with 20 µl of iodoacetamide (100 mM in 0.1 M Tris, pH 7.8) for 15 min at room temperature (protected from light), followed by protein precipitation using a double methanol/chloroform extraction method (Wessel and Flugge, 1984). Protein samples were treated with 600 µl of methanol, 150 µl of chloroform, and 450 µl of water, followed by vigorous vortexing. Samples were centrifuged at 17,000 *g* for 3 min, and the resultant upper aqueous phase was removed. Proteins were pelleted following the addition of 450 µl of methanol and centrifugation at 17,000 *g* for 6 min. The supernatant was removed, and the extraction process was repeated. Following the second extraction process, precipitated proteins were re-suspended in 50 µl of 6 M urea and diluted to <1 M urea with 250 µl of 20 mM HEPES (pH 8.0) buffer. Protein digestion was carried out by adding trypsin (from a 1 mg/ml stock in 1 mM HCl) to a ratio 1:100, rocking at 12 rpm and room temperature overnight. Following digestion, samples were acidified to 1% trifluoroacetic acid and desalted on C18 solid-phase extraction cartridges (SEP-PAK plus, Waters), dried, and re-suspended in 2% acetonitrile and 0.1% formic acid for analysis by LC-MS/MS as described below.

Off-line high-pH reverse-phase prefractionation was performed in a similar fashion as in Davis et al. (2017). Briefly, digested material was fractionated using the loading pump of a Dionex Ultimate 3000 HPLC with an automated fraction collector and a Waters Acquity UPLC Peptide BEH C18, 300 Å, 1.7 µm, 1 mm × 100 mm (part no. 186005593) column over a 65 min gradient using basic pH reverse-phase buffers (A: water, pH 10 with ammonium hydroxide; B: 90% acetonitrile, pH 10 with ammonium hydroxide). The gradient consisted of a 15 min wash with 2% B, then increasing to 35% B over 30 min, with a further increase to 95% B in 0.1 min, followed by a 9.9 min wash at 95% B and then returning to 2% in 0.1 min, followed by re-equilibration at 2% B for 9.9 min, all at a flow rate of 100 µl/min with fractions collected every 1 min from 0 to 60 min. One hundred microliters of the fractions was dried and resuspended in 20 µl of 2% acetonitrile/0.1% formic acid for analysis by LC–MS/MS. Fractions were loaded on the LC–MS/MS following concatenation of 60 fractions into 10, combining fractions in a 10-fraction interval (F1 + F11 + F21 + F31 + F41 + F51… to F10 + F20 + F30 + F40 + F50 + F60).

Liquid Chromatography–Mass Spectrometry/Mass Spectrometry (LC-MS/MS)

LC-MS/MS analysis was performed using a Dionex Ultimate 3000 nano-ultra high-pressure reverse-phase chromatography coupled on-line to a Q Exactive HF mass spectrometer (Thermo Scientific) as described previously (Fye et al., 2018). In brief, samples were separated on an EASY-Spray PepMap RSLC C18 column (500 mm × 75 µm, 2 µm particle size, Thermo Scientific) over a 60 min gradient of 2–35% acetonitrile in 5% dimethyl sulfoxide (DMSO), 0.1% formic acid at 250 nL/min. MS1 scans were acquired at a resolution of 60,000 at 200 m/z and the top 12 most abundant precursor ions were selected for high collision dissociation (HCD) fragmentation.

Transcriptomics Analysis of MCF7 Cells

A total of 5 × 10^8 MCF7 cells were grown to ∼90% confluency as described above, harvested by centrifugation at 1,500 rpm, and resuspended in ice-cold PBS, centrifuged again, and pellets were kept at −20°C until analysis. RNA was extracted from cell pellets using the RNeasy Mini Kit (QIAGEN) according to the manufacturer's instructions. mRNA material was further enriched using poly-T oligo column (Manufacturer). The quality of the mRNA was checked by $OD_{260/280nm}$ ratio and found to be ∼2. The cDNA library was prepared using a standardized protocol followed by paired end sequencing using a HiSeq4000 platform (Illumina) at the Oxford Genomics Center (Wellcome Trust Center for Human Genetics, Oxford, UK).

Transcriptomics and Proteomics Data Analysis

For the analysis of transcriptomics data, FASTQ files were converted to Binary-sequence Alignment Format (BAM) files using HISAT2 (v2.1.0) and Samtools (v1.3). Subsequently, BAM files were imported into Perseus software (v1.6.0.2) and genome annotation was performed using the Human Fasta cDNA database (http://www.ensembl.org). Reads per kilo per million (RPKM) values were calculated by a normalization step dividing by the sum (*Normalization* → *Divide*), followed by dividing normalized values by gene length, multiplying by 10^9, and taking the $\log_2$ values (**Table S1**).

For the analysis of proteomics data, the DUB proteome in MCF7 cells was assessed by interrogating the quantified iBAQ values taken from our previous study (Davis et al., 2017) that were then matched to the MCF7 transcriptome using Perseus software (v1.6.0.2) (**Table S2**). For the DUB activitome, all raw MS data files from the HA-IP and high-pH fractionation experiments were analyzed in a combined fashion using MaxQuant (v1.5.5.1) and searched against the UniProt Human database (92,954 entries). Intensity values were used to compare against the DUB proteome and transcriptome (**Table S3**). Zero values were replaced with the value of 1 to allow for displaying the data using scatter plots as shown in **Figures 1C**, **7**. For searches of PTMs, in particular the HA-UbPA probe adduct (112.06 Da) on cysteine residues, each raw MS data file obtained per high-pH fraction analyzed by LC-MS/MS was analyzed using PEAKS software (v 8.5; we used a 1% FDR at protein and peptide level in PEAKS with the −10LogP values of 40 for protein and 23.2 for peptide positive identification) and searched against the UniProt database (UPR_HomoSapiens_20170215). Search parameters were the following: parent mass error tolerance: 10 ppm; fragment mass error tolerance: 0.05 Da; precursor mass search: monoisotopic; enzyme: trypsin; missed cleavages: 2; variable modifications (PEAKS PTM, only the most common listed): deamidation (NQ), oxidation (M), carbamidomethylation (C), acetylation (K), acetylation (N-term), PA Probe adduct (C), maximal variable PTM per peptide: 3.

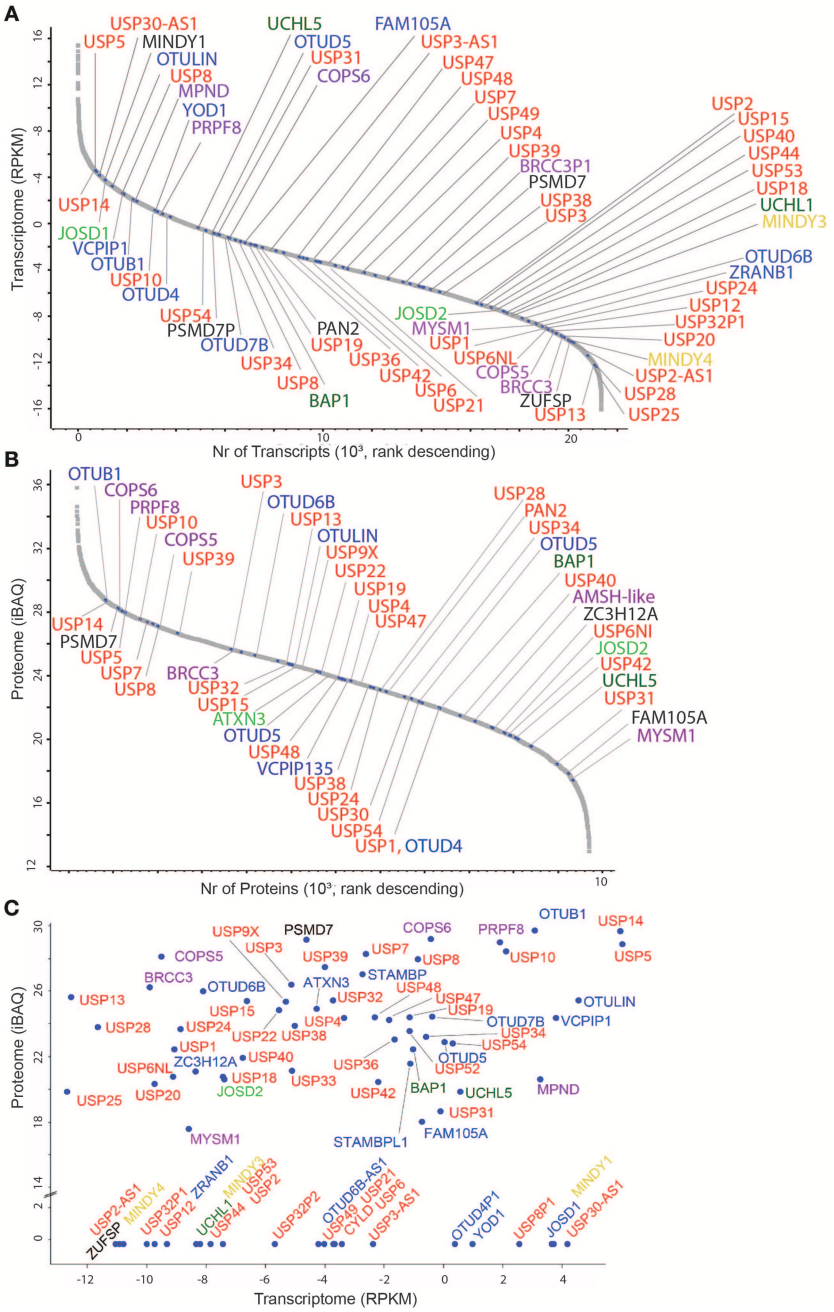

FIGURE 1 | DUB transcriptome and proteome in MCF7 breast cancer cells. **(A)** Transcriptome analysis (single experiment data) listing all quantified mRNAs as reads per Kilobase per million (RPKM) values in descending values. mRNAs encoding DUBs are indicated according to their families: 56 USPs (red), 5 UCHs (dark green), 16 OTUs (blue), 11 JAMMs (purple), 4 MINDYs (yellow), 4 JOS (light green), and 1 ZUP (black). **(B)** Proteome analysis (single experiment data) listing all quantified proteins as intensity-based absolute quantitation (iBAQ) abundances in descending values. DUBs are indicated and colored based on sub-families as stated above. **(C)** Scatter Plot showing mRNA (transcriptome, *X*-axis) and protein (proteome, *Y*-axis) levels of DUBs (indicated in colors according to sub-families).

Generation of the Human DUB Phylogenetic Tree

Genes included in this analysis:

[(CYLD, PAN2, USP17L24, USP1, USP2, USP3_H0YMI, USP3_Q9Y6I, USP4, USP5, USP6, USP7, USP8, USP9X, USP10, USP9Y, USP11, USP12, USP13, USP14, USP15, USP16, USP17L1, USP17L2, USP18, USP19, USP20, USP21, USP22, USP24, USP25, USP26, USP27X, USP28, USP29, USP30, USP31, USP32_K7EK, USP32_Q8NF, USP33, USP34, USP35, USP36, USP37, USP38, USP39, USP40, USP41, USP42, USP43, USP44, USP45, USP46, USP47, USP48, USP49, USP50, USP51, USP53, USP54), (BRCC3, COPS5, COPS6, EIF3F,

EIF3H, MPND, MYSM1, PRPF8, PSMD7, PSMD14, STAMBP, STAMBPL1), (ALG13, OTUB1, OTUB2, OTUD1, OTUD3, OTUD4, OTUD5, OTUD6A, OTUD6B, OTUD7A, OTUD7B, OTULIN, OTULINL, TNFAIP3, VCPIP1, YOD1, ZRANB1), (UCHL1, UCHL3, UCHL5, BAP1), (ATXN3, ATXN3L, JOSD1, JOSD2), (MINDY1, MINDY2, MINDY3, MINDY4)].

The full-length protein sequences for each DUB were extracted from UniProt (https://uniprot.org/). The canonical sequence for each DUB was used as it was determined by UniProt. The protein alignment was performed using MUSCLE (multiple sequence alignment with high accuracy and high throughput). Finally, a constraint ML phylogenetic tree was generated by RAxML (https://raxml-ng.vital-it.ch/#/). The constraint tree was created by including DUBs into the seven known families. The LG Substitution matrix was used. The best fit model tree was further designed initially in the iTOL INTERACTIVE TREE OF LIFE (https://itol.embl.de/) where branched length was ignored, and an unrooted tree style was

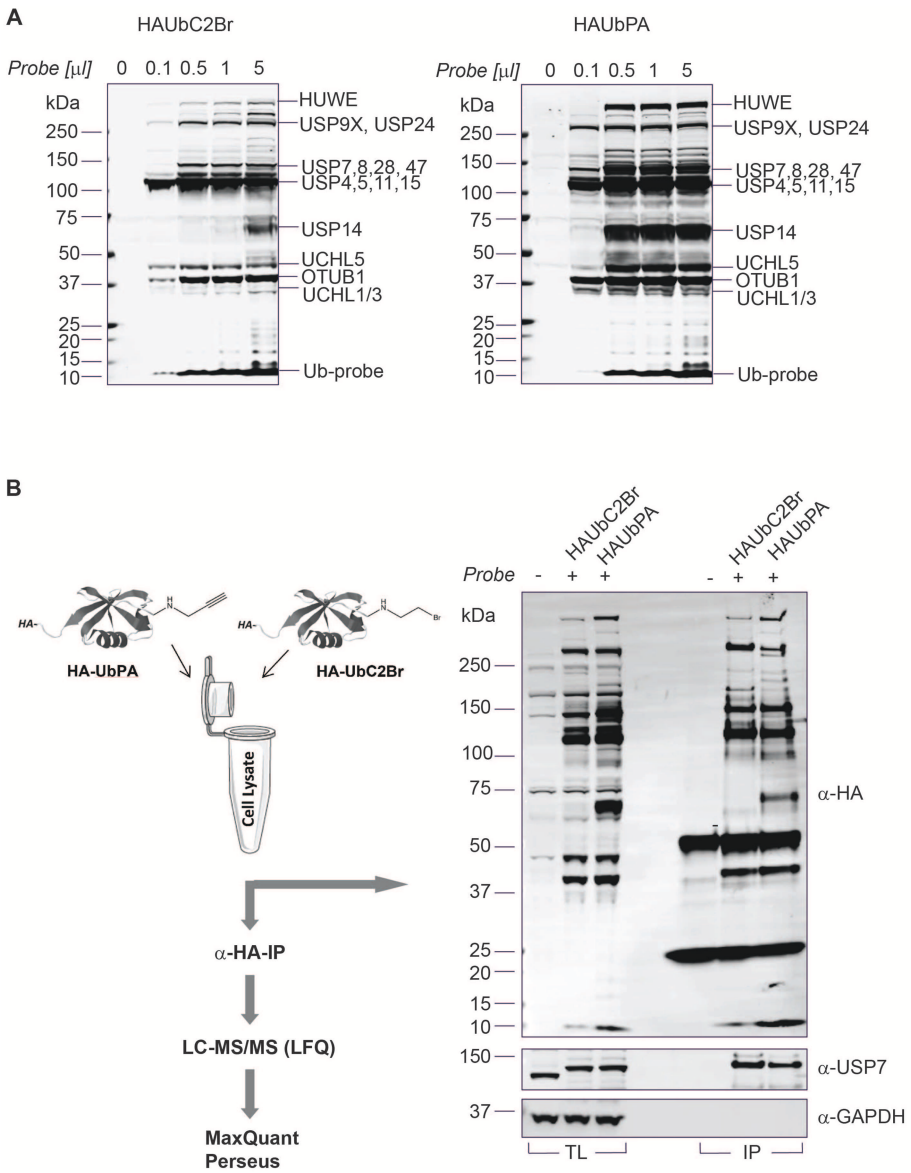

FIGURE 2 | Ub-PA probe chemistry extends DUBome activity-based profiling. **(A)** Titration of HA-UbC2Br (left panel) and HA-UbPA probe (right panel) in MCF7 breast cancer cell extracts, followed by SDS-PAGE separation and analysis by anti-HA immunoblotting. Bands correspond to either DUB-probe or E3 ligase-probe adducts as indicated [based on (Altun et al., 2011) and this study]. **(B)** Left panel: Chemoproteomics workflow for profiling the active DUBome. HA-UbC2Br or HA-UbPA probe is incubated with MCF7 breast cancer cell extracts, followed by anti-HA immunoprecipitation, elution, in-solution trypsin digestion, and label-free quantitative analysis (LFQ) by LC-MS/MS. Right panel: Comparison of HA-UbC2Br and HA-UbPA immunoprecipitated DUBs analyzed by SDS-PAGE and anti-HA, anti-USP7 (positive control), and anti-GAPDH (loading control) immunoblotting.

formed. Finally, the Adobe Illustrator software was then used to finalize the tree.

Data Availability

MCF7 RNA-seq data have been submitted to GEO with the accession number GSE134954.

The mass spectrometry proteomics data have been deposited to the ProteomeXchange Consortium *via* the PRIDE (Perez-Riverol et al., 2019) partner repository with the data set identifier PXD014391.

RESULTS AND DISCUSSION

DUB mRNA and Protein Expression Topology in MCF7 Breast Cancer Cells

To set a baseline, we wished to interrogate the number of DUBs and their abundance at the mRNA and protein level in MCF7 cells, a cell line originally established from the pleural effusion of a 69 year-old woman with metastatic disease (Brooks et al., 1973) and used for breast cancer research for more than 40 years (Comsa et al., 2015). Based on previous studies from our lab and others (Borodovsky et al., 2002; Altun et al., 2011; Turnbull et al., 2017), it appears that MCF-7 has a similar DUB profile to other immortalized cell lines but there are specific DUBs that are expressed in some cell lines and not in MCF-7. For instance, neuronal cells have high levels of active UCHL-1 [also seen to vary considerably in immortalized B-cell lines (Ovaa et al., 2004)], and HEK293 cells (human embryonic kidney) express a recently discovered DUB called ZUP1 (ZUFSP), whereas we were not able to detect either, UCHL-1 or ZUP1, in MCF-7 cells. Therefore, we feel that using the immortalized breast cancer cell line MCF7, we represent most of the endogenous DUBome. To obtain maximal depth, we performed RNA-Seq and pre-fractionation-based deep proteomics, resulting in 21,352 transcripts and 13,728 identified protein groups from which 8,949 were assigned to genes (Davis et al., 2017). In these data sets, we detected 78 DUBs by RNA-seq (76% out of 102 assigned DUBs in the human genome) (**Figure 1A**) and 65 DUBs at the protein level (corresponding to 53 genes) (**Figure 1B**). Interestingly, the DUBs MINDY1/3/4, ZUFSP, UCHL1, and alternative isoforms of OTU and USP subsets were detected only at the mRNA level, whereas others such as USP35, USP30, USP16, UCHL-3, and up to 12 DUBs were present as proteins only (**Figure S1**), suggesting distinct regulatory mechanisms and/or stability of their mRNA vs. protein. Generally, global mRNA expression levels poorly correlated with protein levels (**Figure 1C**), a trait observed in previously reported studies (Maier et al., 2009; Schwanhausser et al., 2011; Wang et al., 2019).

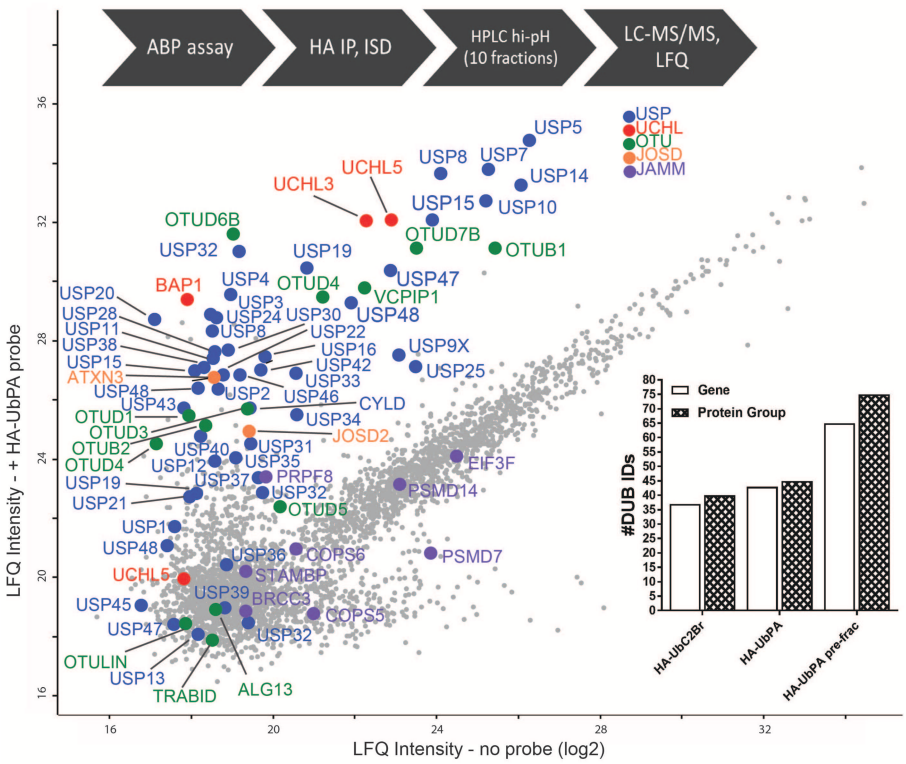

FIGURE 3 | Full DUBome coverage by advanced chemoproteomics. Scatter Plot showing enrichment of DUBs upon labeling and isolation of HA-UbPA activity-based probe pulldown and quantitative analysis by mass spectrometry (concatenation of 60 fractions into 10). *X*-axis—no probe; *Y*-axis—with probe. The experimental workflow is shown on the top. The graph inclusion shows the number of DUBs captured by the HA-UbPA probe with (single experiment data) and without (technical triplicates) high-pH prefractionation post-HA-IP and digestion.

Reactivity of Different Ub Probes Affects Dubome Selectivity

To better gauge DUB cellular function, we aimed to match DUB expression with their activity at a global level using an improved activity-based protein profiling (ABPP)-based workflow (Altun et al., 2011; Turnbull et al., 2017). A limitation for these ABPP studies has been the proteomic technique by itself as well as some DUB targeting selectivity based on the chemical moiety of the probe (Borodovsky et al., 2002). Recently, more sensitive mass spectrometry and the use of reactive-site-centric Ub probes with a vinyl sulfone (VS) or a vinyl methyl ester (VME) revealed less DUB selectivity dependent on the chemical group used, but has also shown that some of them tend to react with non-catalytic cysteine residues, whereas propargylamide (PA)-based probes seem to react more specifically with catalytic cysteines (Hewings et al., 2018). This could be due to the unconventional reactivity of the alkyne in the propargylamide with the thiol group on the catalytic cysteine, which is unusual as electron-rich alkynes are generally poor electrophiles. UbPA reacts with DUB cysteines *via* direct addition to the terminal alkyne to give a vinyl thioether through possible radical-based intermediates (Ekkebus et al., 2013). HA-UbPA is reported to be highly DUB selective, with the exception of the additional labeling of the E3 Ub ligase HUWE1 (Ekkebus et al., 2013). We decided to compare side by side Ub probes with the different reactivities by performing an ABP assay in MCF7 cell lysates, UbPA (direct addition), UbVME (conjugate addition), and UbC2Br (nucleophilic displacement) (**Figure S2A**). As previously described, the UbC2Br probe has a different reactivity profile to cellular DUBs when compared to the VME probe (Borodovsky et al., 2002), in particular with the band corresponding to OTUB1 (theoretical molecular weight: 31,284 Da, ∼37 kDa marker). On the other hand, USP14 (theoretical molecular weight: 56,069 Da, below the 75 kDa marker) is labeled more efficiently by UbVME as compared to UbC2Br. We

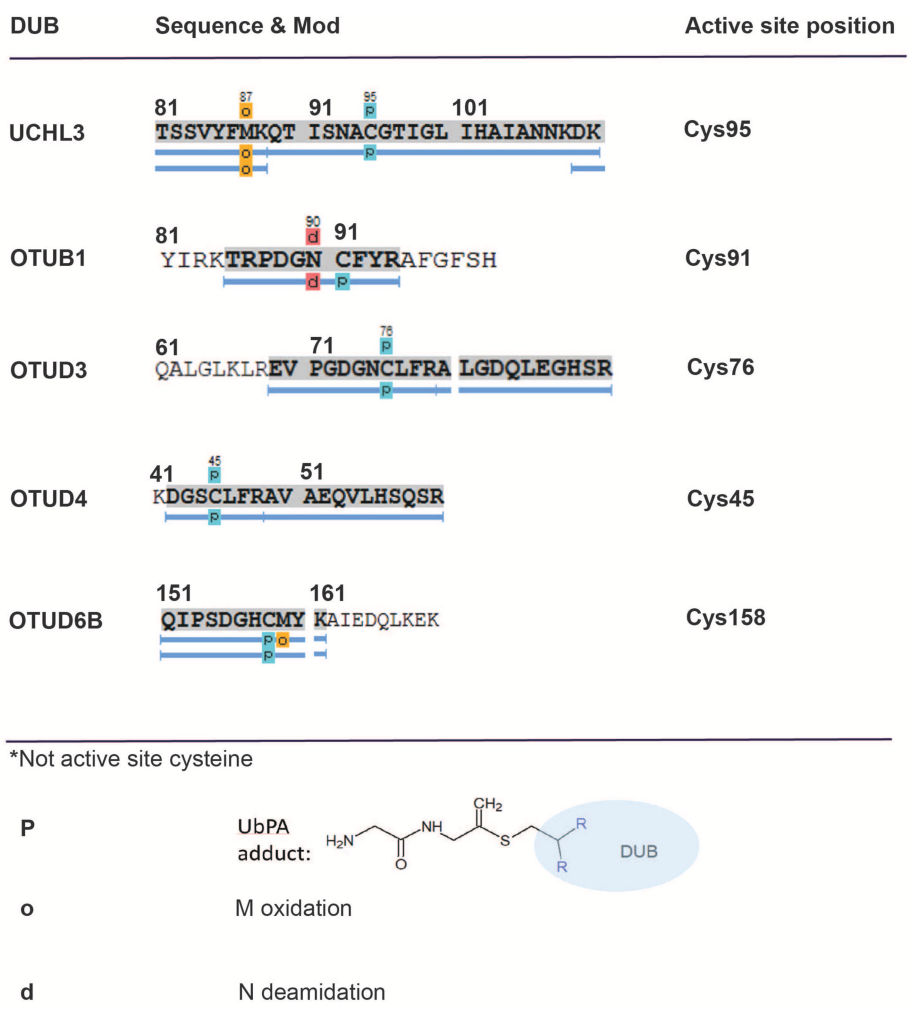

FIGURE 4 | Mapping direct Ub–probe DUB adducts by mass spectrometry. LC-MS/MS analysis of HA-UbPA-labeled DUBs isolated from MCF7 breast cancer cell extracts. Peptide mapping using PEAKS analysis reveals direct cysteine–probe adducts (light blue boxes—P) for the DUBs UCHL3, OTUB1, OTUD3, OTUD4, and OTUD6B. The corresponding MS/MS fragmentation spectra for assigning the Cys–UbPA–probe adducts are listed in **Figures S3A–S3E**.

concluded that the UbPA probe seems to react more efficiently with all cellular DUBs as judged by the visualized bands. To further compare the two probes with the broadest labeling profiles, we performed an ABPP by immunoprecipitating HA-tagged UbPA and UbC2Br probes after labeling MCF7 crude extracts, confirming the greater breadth of cellular DUB labeling with the UbPA probe (**Figure 2A**). We also analyzed probe-captured material by quantitative mass spectrometry (**Figure 2B** and **Table S4**). Both Western blotting and mass spectrometry results confirm the superior reactivity of the UbPA probe over the UbC2Br (**Figure 2A** and **Figure S2A**), being able to identify 44 DUBs with the former and 37 with the latter (**Figure S2B** and **Table S4**).

Improved ABP Using Advanced Proteomics Methodology Expands the Dubome

Since the number of identified DUBs using UbPA in ABPP, although improved, was still not in the range of DUBs expressed in MCF7 cells (**Figure 1**), we decided to explore a more advanced proteomic methodology in order to expand the active DUBome. To this end, we implemented a high-pH pre-fractionation in our classical ABPP workflow after the digestion step (**Figure 2B**) in order to reduce the sample complexity in an orthogonal dimension prior to LC-MS/MS analysis (Wang et al., 2011; Davis et al., 2017). This yielded an increase in the number of DUB identifications from 39 to 74 protein groups, corresponding to 65 DUB genes, greatly expanding the number observed in the conventional ABPP-MS workflow (>92%) [**Figure 3** (inset) and **Figure S2B**]. The number of DUBs detectable *via* the ABP-MS assay is now comparable to the number of expressed DUBs in the same cell line.

Discrimination Between Active Dubs vs. Non-active Dubs

To gain more detailed information about cellular DUB activity captured by our ABPP assay, it was necessary to determine which fraction of enzymes directly reacted with probe and were not enriched only through affinity binding. We addressed this through two experimental approaches. First, we interrogated our data for the presence of Ub-probe adducts, which confirmed the direct reactivity of UCHL3 Cys95, OTUB1 Cys91, OTUD3 Cys76, OTUD4 Cys45, and OTUD6B Cys158 (**Figure 4** and **Figure S3**). MS/MS analysis revealed potentially more UbPA probe adduct sites, also on non-catalytic Cys residues as well as non-DUB proteins, but systematic manual inspection of these revealed insufficient confidence of assignment. It appears that the reactivity of the probe propargyl moiety within DUBs critically depends on the correct positioning identical to the scissile isopeptide bond, which reduces potential "off-target" reactions observed with Ub-probes carrying Michael acceptors or alkyl halides (Hewings et al., 2018). Despite the clear assignment for some DUBs, this approach did not yield a comprehensive overview of DUBs reactive to probe as there were experimental limitations in the detection of tryptic peptides harboring the DUB's catalytic Cys residue, as for most DUBs, the peptide length is unsuitable for LC-MS/MS detection. To overcome this, probe variants with redox release mechanisms have been developed to selectively release probe reactive DUBs, but this was also restricted to a subset of DUBs (de Jong et al., 2017). In our case, we reasoned that probe reactive DUBs could be displaced through a direct competition using cysteine-reactive agents such as N-methylmaleimide (NEM) or the pan-DUB inhibitor PR-619 (Altun et al., 2011; Kramer et al., 2012).

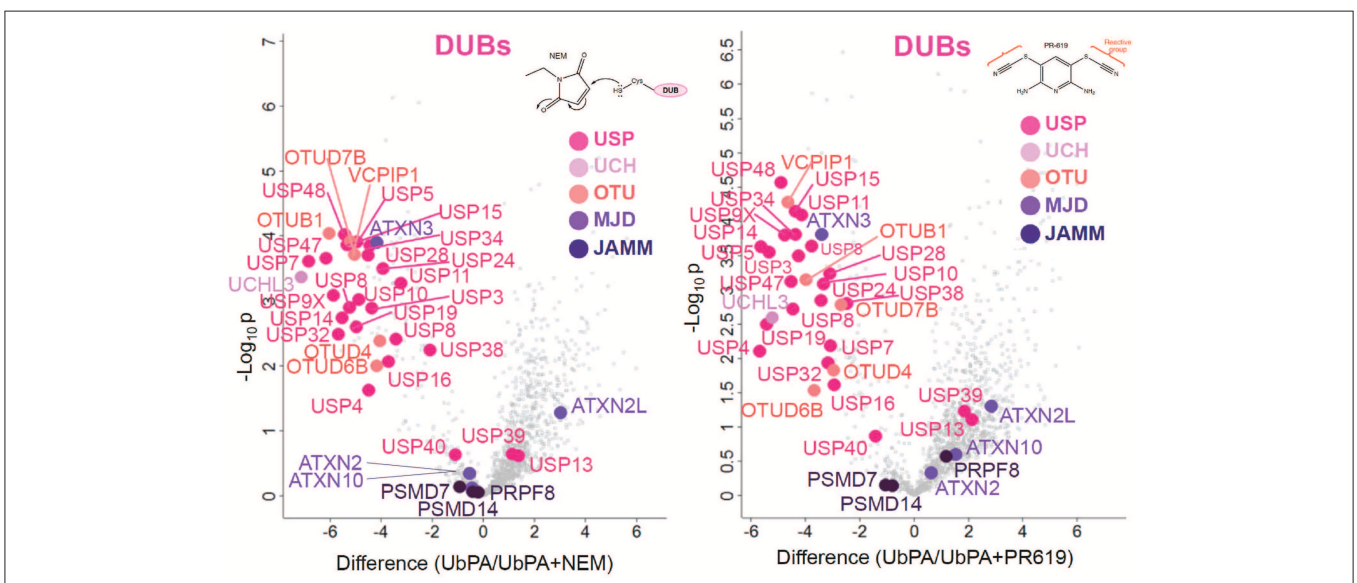

FIGURE 5 | Active vs. non-active DUBs. Volcano plots showing a discrimination between cysteine-reactive and non-reactive DUBs by active-site labeling with HA-UbPA in the presence and absence of *N*-ethylmaleimide (NEM, **Left** panel) and PR-619 (**Right** panel) (data from two biological replicates run in technical duplicates). Displaced reactive DUBs are located in the upper left compartment ([probe alone]−[probe + NEM or PR619]), whereas non-reacting DUBs are left in the lower center area.

DUB-probe competition could be captured by a quantitative ABP-MS experiment. To this end, ABP assays were performed using HA-UbPA probe exposed to MCF7 cell extracts previously treated with excess NEM, PR-619, or DMSO control, followed by enrichment of labeled DUBS and quantitative LC-MS/MS analysis (**Figure 5**). Most cysteine protease DUBs were competed by NEM and PR-619, indicated by their location on the left in the volcano plot with the exception of USP13, USP39, and USP40. As expected, DUB members of the JAMM family were not affected and therefore not displaced. Interestingly, we observe that components of the 26S (e.g., PSMD7) and ATXN network (ATXN2/2L/10) were unchanged, although DUBs that are part of these complexes such as USP14 and ATXN3 are competed away, suggesting flexible complex dynamics. As a specificity control, we did not observe competition of other non-Ub cysteine proteases within the same experimental conditions (**Figure S4**). We concluded that some USPs may have low or no enzymatic activity under these cellular conditions, as can be monitored by our ABPP assay. For instance, USP13 may not directly react to the UbPA probe *via* an active cysteine and that it only binds *via* the Ub scaffold in a non-covalent fashion. Our results suggest that, at least under these circumstances, USP13 appears to be mostly inactive (at least toward the HA-UbPA probe) in an endogenous context where cells are not activated in a particular way, although USP13 was shown to deubiquitylate RAP80 in the context of the DNA damage response (Li et al., 2017). USP39 is a DUB in which the catalytic residue Cys 234 is replaced by an Asp,

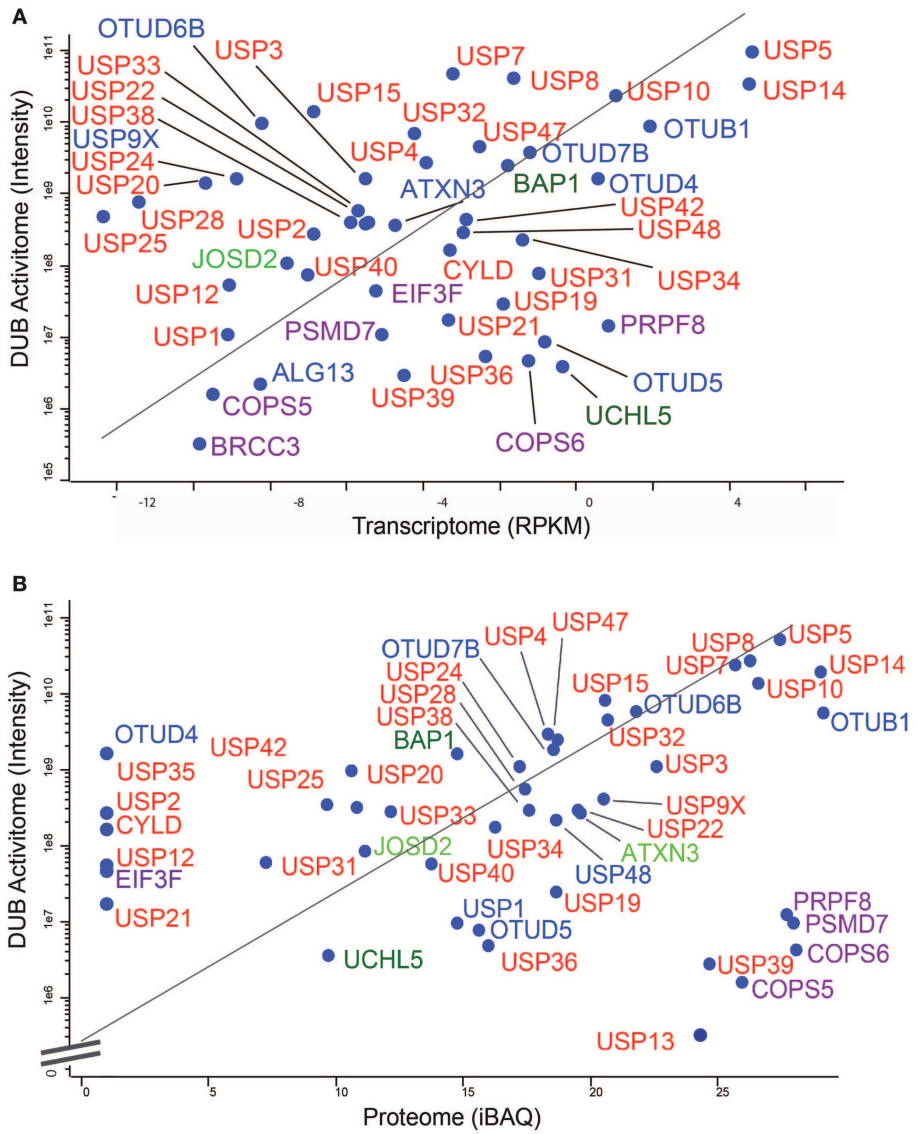

FIGURE 6 | MCF7 DUB activitome vs. transcriptome and proteome. Scatter Plots showing the correlative traits of the transcriptome **(A)** and the proteome **(B)** with the DUB activitome (*X*-axis in both panels). DUBs are indicated in colors respective to their enzyme sub-families.

His 513 by Ser, and Asp 530 by a Glu. Its role in pre-mRNA splicing and regulation of Aurora mRNA seems therefore not dependent on catalytic activity (van Leuken et al., 2008). USP40 appears to be catalytically inactive *in vitro* despite having all the catalytic residues proposed to be important for the catalytic activity (Quesada et al., 2004). To gain further insight, we examined how activity correlates with expression. To do this, we compared the different data sets (**Figure 6**). DUBs identified from 5,761 quantified protein groups that directly matched to genes and mRNA transcripts (**Table S1**) were compared to the expanded DUB "activitome" (**Table S2**), resulting in a three-way comparison of DUB probe-based activity levels with their mRNA (**Figure 6A**) and protein level (**Figure 6B** and **Table S3**). Interestingly, DUB proteome intensities correlated relatively well with the ones from the active DUBome. This is perhaps due to the high affinity of the probe to the target, meaning that more abundant enzymes will have better/faster access to the probe, and they will probably react with it even when their activity is not as high as other less abundant enzymes. Comparing our expanded ABPP approach to the DUB proteogenomic data sets, we could identify six DUBs that were not present in the deep proteome data (CYLD, OTUD1, OTUD7A, USP12, USP2, and USP45; **Figures S1, S2B**), highlighting the importance of studying the active DUBome over regular expression studies. On the other hand, no members of the MINDY and ZUFSP families and most metalloprotease DUBs (JAMMS) are present in our active DUBome data. JAMMs DUBs are not supposed to react with the ABP probes utilized due to the incompatibility of the reaction mechanism of the probe to metalloproteases, and MINDY and ZUFSP proteins do not seem to be expressed in the studied cell line. Since adding a pre-fractionation step helped to get a better representation of the DUBs, we also were able to obtain information about different DUB isoforms. For instance, for USP28, three isoforms produced by alternative splicing have been described (UniProt), from which unique tryptic peptides were assigned to isoform 1 and 2 (**Figure S5**). For OTUD4, four isoforms have been described to be produced by alternative splicing (UniProt). We

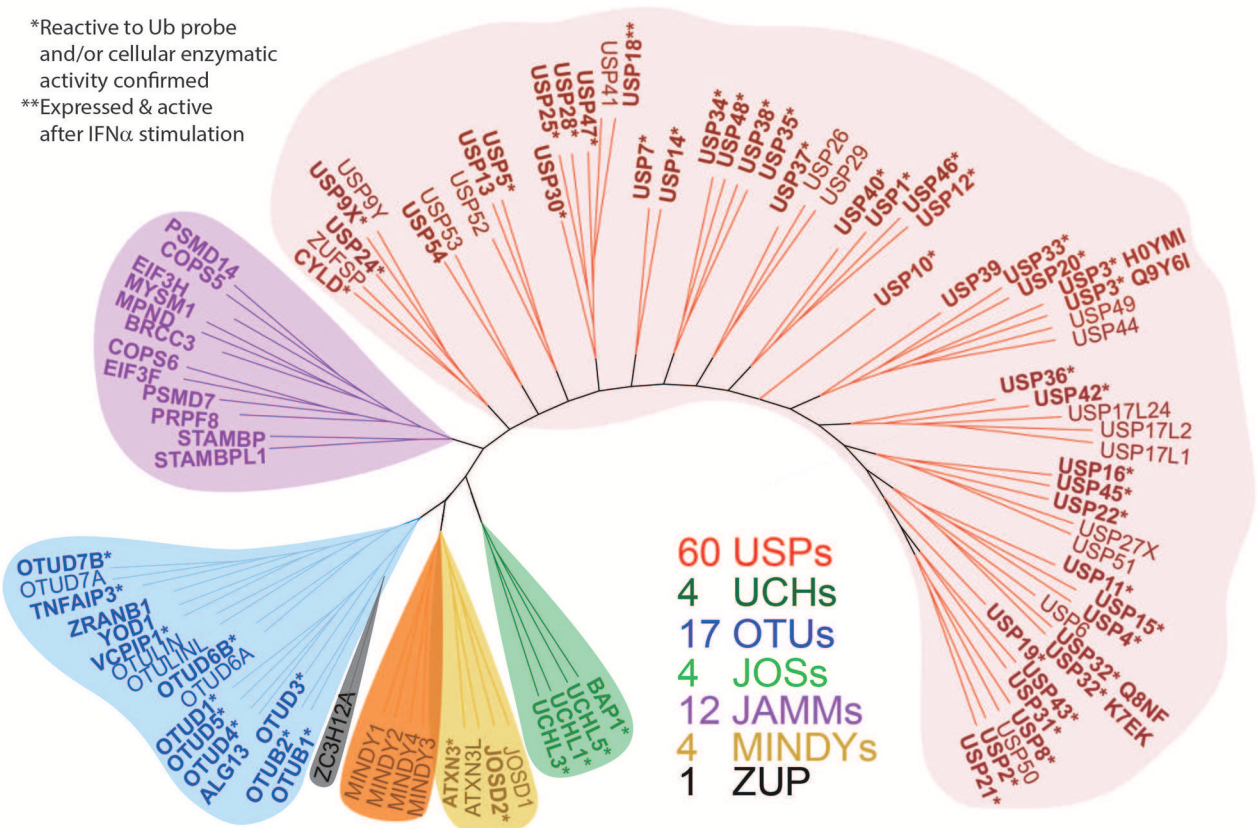

FIGURE 7 | Expanded panel of active DUBs across the different enzyme subfamilies. ML (maximum likelihood) phylogenetic tree of the human DUB family. One hundred and two DUBs of the ubiquitin specific protease (USP), ubiquitin C-terminal hydrolases (UCH), ovarian tumor domain (OTU), JAMM, MINDY, JOS, and ZUP1 families are shown. In bold are the DUBs detected in the cellular proteome by active-site labeling, indicating cellular activity. *indicates inactive DUBs, in part because of mutated catalytic site cysteines and **indicates selective induction by type I interferon (IFN). The gene name nomenclature was used for consistency, but many DUBs have alternative names: ZA20D1 (OTU7B), YOD1 (OTU1/DUBA8), TNFAIP3 (OTUD7C/A20), AMSH (STAMBP1), AMSH-like (STAMBPL1), TL132 (USP32P2), TL132-like (USP32P1), LOC339799 (EIF3FP3), ZRANB1 (TRABID), PSMD14 (RPN11/POH1), USP17L2 (DUB3), OTUD6B (DUBA5, CGI-77), and PAN2 (USP52). In bold are those DUBs detected in the proteome, and the (*) indicates DUBs reactive to UbPA probe.

have detected unique peptides for isoforms 1 and 2, suggesting that they are expressed at the protein level. Interestingly, at the transcriptomics level, an OTUD4P1 pseudogene was detected at high levels, but not the original OTUD4 mRNA (**Figure 1** and **Table S1**). USP15 has been characterized as expressed in four isoforms, from which isoforms 2 and 4 were confirmed at the protein level. USP47 isoform 1 shares peptides with the other forms and so was not distinguishable, but transcriptomics confirms expression of its cognate mRNA (**Table S1**). USP48 is expressed as eight isoforms generated by alternative splicing, from which we confirm the detection of unique peptides corresponding to isoform 1 and a shorter version referred to as A0A0A0MRS6-1 (UniProt) (**Figure S5**). The biological role of these isoforms is not currently understood, but mutations in USP48, potentially affecting the different isoforms differently, have been associated with Cushing's disease (Chen et al., 2018). The function of different DUB isoforms can be quite distinct, such as USP35, whose isoform 1 is an anti-apoptotic factor that inhibits staurosporine- and TNF-related apoptosis-inducing ligand (TRAIL). In contrast, USP35 isoform 2 associates to the endoplasmic reticulum (ER) and is also present at lipid droplets (Leznicki et al., 2018). Another case is USP7, for which two isoforms USP7/USP7S were described that differentially bind to Herpes virus protein and are also phosphorylated not in the same manner, affecting the degradation rate of USP7S independently of USP7 (Khoronenkova et al., 2012). For neither USP35 nor USP7 can we detect unique peptides that would discriminate between these isoforms at the protein level. Together, when we combine the sets of DUB proteomic, transcriptomic, and activitomic profiles, we are extending the global cellular DUB landscape in terms of expression and evidence for enzymatic activity (**Figure 7**). Generally, DUB active-site labeling was better reflected by protein abundance as compared to mRNA levels. Marked exceptions were OTUD4, USP35, USP2, USP21, and CYLD that were all detected by probe labeling, but not at the protein level, indicating very low levels of expression. The extended ABPP profiles provide deeper insights, such as detecting low abundant DUBs, such as USP2, USP21, USP12, USP46, and USP35 that have previously been challenging to be within the detection range (**Table S3** and **Figure S2B**). Our study sets the framework for a better understanding of how physiological and pharmacological interferences affect the DUB enzyme family and their biological pathways at a global scale. Furthermore, it will help to accelerate the development of high-throughput ABP assays with a greater breadth of selectivity panel and to monitor critical DUBs relevant for human disease, as biomarkers or targets for disease modulation in a clinical context.

DATA AVAILABILITY

The datasets generated for this study can be found in the MCF7 RNA-seq data has been submitted to GEO accession number: GSE134954. The mass spectrometry proteomics data have been deposited in ProteomeXchange Consortium via the PRIDE: PXD014391.

AUTHOR CONTRIBUTIONS

This study was conceptualised by BK and AP-F, RF, PC, and SD generated the MCF-7 deep proteome data. RF, SD, PZ, and GB generated the MCF-7 transcriptome data. AS and AP-F performed the ABPP assays and immunoblots. HS performed the high pH fractionation during MS sample preparation for proteomics. AD generated the DUB phylogenetic tree. BK, AP-F, AS, SD, and PC performed the data analysis. ES, SM, and AP-F carried the synthesis of HA-UbC2Br and HA-UbPA ubiquitin-based ABPs (activity-based probes). AP-F and BK wrote the manuscript, and all authors commented on the text.

FUNDING

AP-F and HS were funded by a grant from CRUK/Forma Therapeutics to BK. RF and BK were supported by an award from the Kennedy Trust Fund. AD was supported by an Innovative Technology Enabling Network (ITEN) Award from Pfizer to BK. PC was supported by a grants from the Engineering and Physical Sciences Research Council EPSRC (EP/N034295/1) and the Chinese Academy of Medical Sciences (CAMS) to BK. The authors AP-F, HS, and BK declare competing interests as they have been members of the DUB Alliance funded by FORMA Therapeutics.

ACKNOWLEDGMENTS

We thank members of the Kessler group for helpful discussions.

SUPPLEMENTARY MATERIAL

The Supplementary Material for this article can be found online at: https://www.frontiersin.org/articles/10.3389/fchem.2019.00592/full#supplementary-material

REFERENCES

Abdul Rehman, S. A., Kristariyanto, Y. A., Choi, S. Y., Nkosi, P. J., Weidlich, S., Labib, K., et al. (2016). MINDY-1 is a member of an evolutionarily conserved and structurally distinct new family of deubiquitinating enzymes. *Mol. Cell* 63, 146–155. doi: 10.1016/j.molcel.2016.05.009

Altun, M., Kramer, H. B., Willems, L. I., McDermott, J. L., Leach, C. A., Goldenberg, S. J., et al. (2011). Activity-based chemical proteomics accelerates inhibitor development for deubiquitylating enzymes. *Chem. Biol.* 18, 1401–1412. doi: 10.1016/j.chembiol.2011.08.018

Amara, N., Tholen, M., and Bogyo, M. (2018). Chemical tools for selective activity profiling of endogenously expressed MMP-14 in multicellular models. *ACS Chem. Biol.* 13, 2645–2654. doi: 10.1021/acschembio.8b00562

Borodovsky, A., Kessler, B. M., Casagrande, R., Overkleeft, H. S., Wilkinson, K. D., and Ploegh, H. L. (2001). A novel active site-directed probe specific for deubiquitylating enzymes reveals proteasome association of USP14. *EMBO J.* 20, 5187–5196. doi: 10.1093/emboj/20.18.5187

Borodovsky, A., Ovaa, H., Kolli, N., Gan-Erdene, T., Wilkinson, K. D., Ploegh, H. L., et al. (2002). Chemistry-based functional proteomics reveals novel

members of the deubiquitinating enzyme family. *Chem. Biol.* 9, 1149–1159. doi: 10.1016/S1074-5521(02)00248-X

Borodovsky, A., Ovaa, H., Meester, W. J., Venanzi, E. S., Bogyo, M. S., Hekking, B. G., et al. (2005). Small-molecule inhibitors and probes for ubiquitin- and ubiquitin-like-specific proteases. *Chembiochem* 6, 287–291. doi: 10.1002/cbic.200400236

Brooks, S. C., Locke, E. R., and Soule, H. D. (1973). Estrogen receptor in a human cell line (MCF-7) from breast carcinoma. *J. Biol. Chem.* 248, 6251–6253.

Cappadocia, L., and Lima, C. D. (2018). Ubiquitin-like protein conjugation: structures, chemistry, and mechanism. *Chem. Rev.* 118, 889–918. doi: 10.1021/acs.chemrev.6b00737

Chen, J., Jian, X., Deng, S., Ma, Z., Shou, X., Shen, Y., et al. (2018). Identification of recurrent USP48 and BRAF mutations in Cushing's disease. *Nat. Commun.* 9:3171. doi: 10.1038/s41467-018-05275-5

Clague, M. J., Urbe, S., and Komander, D. (2019). Breaking the chains: deubiquitylating enzyme specificity begets function. *Nat. Rev. Mol. Cell Biol.* 20, 338–352. doi: 10.1038/s41580-019-0099-1

Comsa, S., Cimpean, A. M., and Raica, M. (2015). The story of MCF-7 breast cancer cell line: 40 years of experience in research. *Anticancer Res.* 35, 3147–3154. Available online at: http://ar.iiarjournals.org/content/35/6/3147.full.pdf+html

Davis, S., Charles, P. D., He, L., Mowlds, P., Kessler, B. M., and Fischer, R. (2017). Expanding proteome coverage with CHarge Ordered Parallel Ion aNalysis (CHOPIN) combined with broad specificity proteolysis. *J. Proteome Res.* 16, 1288–1299. doi: 10.1021/acs.jproteome.6b00915

de Jong, A., Witting, K., Kooij, R., Flierman, D., and Ovaa, H. (2017). Release of enzymatically active deubiquitinating enzymes upon reversible capture by disulfide ubiquitin reagents. *Angew. Chem.* 56, 12967–12970. doi: 10.1002/anie.201706738

Ekkebus, R., van Kasteren, S. I., Kulathu, Y., Scholten, A., Berlin, I., Geurink, P. P., et al. (2013). On terminal alkynes that can react with active-site cysteine nucleophiles in proteases. *J. Am. Chem. Soc.* 135, 2867–2870. doi: 10.1021/ja309802n

Fraile, J. M., Quesada, V., Rodriguez, D., Freije, J. M., and Lopez-Otin, C. (2012). Deubiquitinases in cancer: new functions and therapeutic options. *Oncogene* 31 2373–2388. doi: 10.1038/onc.2011.443

Fye, H. K. S., Mrosso, P., Bruce, L., Thezenas, M. L., Davis, S., Fischer, R., et al. (2018). A robust mass spectrometry method for rapid profiling of erythrocyte ghost membrane proteomes. *Clin. Proteomics* 15:14. doi: 10.1186/s12014-018-9190-4

Gavory, G., O'Dowd, C. R., Helm, M. D., Flasz, J., Arkoudis, E., Dossang, A., et al. (2018). Discovery and characterization of highly potent and selective allosteric USP7 inhibitors. *Nat. Chem. Biol.* 14, 118–125. doi: 10.1038/nchembio.2528

Haahr, P., Borgermann, N., Guo, X., Typas, D., Achuthankutty, D., Hoffmann, S., et al. (2018). ZUFSP deubiquitylates K63-linked polyubiquitin chains to promote genome stability. *Mol. Cell* 70, 165–174 e6. doi: 10.1016/j.molcel.2018.02.024

Harrigan, J. A., Jacq, X., Martin, N. M., and Jackson, S. P. (2018). Deubiquitylating enzymes and drug discovery: emerging opportunities. *Nat. Rev. Drug Discov.* 17, 57–78. doi: 10.1038/nrd.2017.152

Hemelaar, J., Galardy, P. J., Borodovsky, A., Kessler, B. M., Ploegh, H. L., and Ovaa, H. (2004). Chemistry-based functional proteomics: mechanism-based activity-profiling tools for ubiquitin and ubiquitin-like specific proteases. *J. Proteome Res.* 3, 268–276. doi: 10.1021/pr0341080

Hermanns, T., Pichlo, C., Woiwode, I., Klopffleisch, K., Witting, K. F., Ovaa, H., et al. (2018). A family of unconventional deubiquitinases with modular chain specificity determinants. *Nat. Commun.* 9:799. doi: 10.1038/s41467-018-03148-5

Hershko, A., and Ciechanover, A. (1998). The ubiquitin system. *Annu. Rev. Biochem.* 67, 425–479. doi: 10.1146/annurev.biochem.67.1.425

Hewings, D. S., Flygare, J. A., Bogyo, M., and Wertz, I. E. (2017). Activity-based probes for the ubiquitin conjugation–deconjugation machinery: new chemistries, new tools, and new insights. *FEBS J.* 284, 1555–1576. doi: 10.1111/febs.14039

Hewings, D. S., Heideker, J., Ma, T. P., AhYoung, A. P., El Oualid, F., Amore, A., et al. (2018). Reactive-site-centric chemoproteomics identifies a distinct class of deubiquitinase enzymes. *Nat. Commun.* 9:1162. doi: 10.1038/s41467-018-03511-6

Kategaya, L., Di Lello, P., Rouge, L., Pastor, R., Clark, K. R., Drummond, J., et al. (2017). USP7 small-molecule inhibitors interfere with ubiquitin binding. *Nature* 550, 534–538. doi: 10.1038/nature24006

Khoronenkova, S. V., Dianova, N. I. I., Ternette, B. M., Kessler, J. L., Parsons, and Dianov, G. L. (2012). ATM-dependent downregulation of USP7/HAUSP by PPM1G activates p53 response to DNA damage. *Mol. Cell* 45, 801–813. doi: 10.1016/j.molcel.2012.01.021

Kolattukudy, P. E., and Niu, J. (2012). Inflammation, endoplasmic reticulum stress, autophagy, and the monocyte chemoattractant protein-1/CCR2 pathway. *Circ. Res.* 110, 174–189. doi: 10.1161/CIRCRESAHA.111.243212

Komander, D., Clague, M. J., and Urbe, S. (2009). Breaking the chains: structure and function of the deubiquitinases. *Nat. Rev. Mol. Cell Biol.* 10, 550–563. doi: 10.1038/nrm2731

Komander, D., and Rape, M. (2012). The ubiquitin code. *Annu. Rev. Biochem.* 81, 203–229. doi: 10.1146/annurev-biochem-060310-170328

Kramer, H. B., Nicholson, B., Kessler, B. M., and Altun, M. (2012). Detection of ubiquitin-proteasome enzymatic activities in cells: application of activity-based probes to inhibitor development. *Biochim. Biophys. Acta* 1823, 2029–2037. doi: 10.1016/j.bbamcr.2012.05.014

Lamberto, I., Liu, X., Seo, H. S., Schauer, N. J., Iacob, R. E., Hu, W., et al. (2017). Structure-guided development of a potent and selective non-covalent active-site inhibitor of USP7. *Cell Chem. Biol.* 24, 1490–1500 e11. doi: 10.1016/j.chembiol.2017.09.003

Leznicki, P., Natarajan, J., Bader, G., Spevak, W., Schlattl, A., Abdul Rehman, S. A., et al. (2018). Expansion of DUB functionality generated by alternative isoforms—USP35, a case study. *J. Cell Sci.* 131:jcs212753. doi: 10.1242/jcs.212753

Li, Y., Luo, K., Yin, Y., Wu, C., Deng, M., Li, L., et al. (2017). USP13 regulates the RAP80–BRCA1 complex dependent DNA damage response. *Nat. Commun.* 8:15752. doi: 10.1038/ncomms15752

Maier, T., Guell, M., and Serrano, L. (2009). Correlation of mRNA and protein in complex biological samples. *FEBS Lett.* 583, 3966–3973. doi: 10.1016/j.febslet.2009.10.036

McGouran, J. F., Gaertner, S. R., Altun, M., Kramer, H. B., and Kessler, B. M. (2013). Deubiquitinating enzyme specificity for ubiquitin chain topology profiled by di-ubiquitin activity probes. *Chem. Biol.* 20, 1447–1455. doi: 10.1016/j.chembiol.2013.10.012

Mullard, A. (2019). First targeted protein degrader hits the clinic. *Nat. Rev. Drug Discov.* 18, 237–239. doi: 10.1038/d41573-019-00043-6

Nijman, S. M., Luna-Vargas, M. P., Velds, A., Brummelkamp, T. R., Dirac, A. M., Sixma, T. K., et al. (2005). A genomic and functional inventory of deubiquitinating enzymes. *Cell* 123, 773–786. doi: 10.1016/j.cell.2005.11.007

Nury, C., Czarny, B., Cassar-Lajeunesse, E., Georgiadis, D., Bregant, S., and Dive, V. (2013). A pan photoaffinity probe for detecting active forms of matrix metalloproteinases. *Chembiochem* 14, 107–114. doi: 10.1002/cbic.201200583

Ovaa, H., Kessler, B. M., Rolen, U., Galardy, P. J., Ploegh, H. L., and Masucci, M. G. (2004). Activity-based ubiquitin-specific protease (USP) profiling of virus-infected and malignant human cells. *Proc. Natl Acad. Sci. U. S. A.* 101, 2253–2258. doi: 10.1073/pnas.0308411100

Perez-Riverol, Y., Csordas, A., Bai, J., Bernal-Llinares, M., Hewapathirana, S., Kundu, D. J., et al. (2019). The PRIDE database and related tools and resources in 2019: improving support for quantification data. *Nucleic Acids Res.* 47, D442–D450. doi: 10.1093/nar/gky1106

Pinto-Fernandez, A., and Kessler, B. M. (2016). DUBbing cancer: deubiquitylating enzymes involved in epigenetics, DNA damage and the cell cycle as therapeutic targets. *Front. Genet.* 7:133. doi: 10.3389/fgene.2016.00133

Quesada, V., Diaz-Perales, A., Gutierrez-Fernandez, A., Garabaya, C., Cal, S., and Lopez-Otin, C. (2004). Cloning and enzymatic analysis of 22 novel human ubiquitin-specific proteases. *Biochem. Biophys. Res. Commun.* 314, 54–62. doi: 10.1016/j.bbrc.2003.12.050

Sanman, L. E., and Bogyo, M. (2014). Activity-based profiling of proteases. *Annu. Rev. Biochem.* 83, 249–273. doi: 10.1146/annurev-biochem-060713-035352

Schwanhausser, B., Busse, D., Li, N., Dittmar, G., Schuchhardt, J., Wolf, J., et al. (2011). Global quantification of mammalian gene expression control. *Nature* 473, 337–342. doi: 10.1038/nature10098

Swatek, K. N., and Komander, D. (2016). Ubiquitin modifications. *Cell Res.* 26, 399–422. doi: 10.1038/cr.2016.39

Turnbull, A. P., Ioannidis, S., Krajewski, W. W., Pinto-Fernandez, A., Heride, C., Martin, A. C. L., et al. (2017). Molecular basis of USP7 inhibition by selective small-molecule inhibitors. *Nature* 550, 481–486. doi: 10.1038/nature24451

van Leuken, R. J., Luna-Vargas, M. P., Sixma, T. K., Wolthuis, R. M., and Medema, R. H. (2008). USP39 is essential for mitotic spindle checkpoint integrity and controls mRNA-levels of aurora B. *Cell Cycle* 7, 2710–2719. doi: 10.4161/cc.7.17.6553

Wang, D., Eraslan, B., Wieland, T., Hallstrom, B., Hopf, T., Zolg, D. P., et al. (2019). A deep proteome and transcriptome abundance atlas of 29 healthy human tissues. *Mol. Syst. Biol.* 15:e8503. doi: 10.15252/msb.20188503

Wang, Y., Yang, F., Gritsenko, M. A., Wang, Y., Clauss, T., Liu, T., et al. (2011). Reversed-phase chromatography with multiple fraction concatenation strategy for proteome profiling of human MCF10A cells. *Proteomics* 11, 2019–2026. doi: 10.1002/pmic.201000722

Ward, J. A., McLellan, L., Stockley, M., Gibson, K. R., Whitlock, G. A., Knights, C., et al. (2016). Quantitative chemical proteomic profiling of ubiquitin specific proteases in intact cancer cells. *ACS Chem. Biol.* 11, 3268–3272. doi: 10.1021/acschembio.6b00766

Weber, A., Elliott, P. R., Pinto-Fernandez, A., Bonham, S., Kessler, B. M., Komander, D., et al. (2017).A linear diubiquitin-based probe for efficient and selective detection of the deubiquitinating enzyme OTULIN. *Cell Chem. Biol.* 24, 1299–1313 e7. doi: 10.1016/j.chembiol.2017.08.006

Wessel, D., and Flugge, U. I. (1984). A method for the quantitative recovery of protein in dilute solution in the presence of detergents and lipids. *Anal. Biochem.* 138, 141–143. doi: 10.1016/0003-2697(84)90782-6

Conflict of Interest Statement: The authors declare that the research was conducted in the absence of any commercial or financial relationships that could be construed as a potential conflict of interest.

frontiers in Chemistry

METHODS
published: 26 November 2019
doi: 10.3389/fchem.2019.00802

TULIP2: An Improved Method for the Identification of Ubiquitin E3-Specific Targets

*Daniel Salas-Lloret, Giulia Agabitini and Román González-Prieto**

González-Prieto Laboratory, Department of Cell and Chemical Biology, Leiden University Medical Center (LUMC), Leiden, Netherlands

Protein modification by Ubiquitin or Ubiquitin-like modifiers is mediated by an enzyme cascade composed of E1, E2, and E3 enzymes. E1s, or ubiquitin-activating enzymes, perform ubiquitin activation. Next, ubiquitin is transferred to ubiquitin-conjugating enzymes or E2s. Finally, ubiquitin ligases or E3s catalyze the transfer of ubiquitin to the acceptor proteins. E3 enzymes are responsible for determining the substrate specificity. Determining which E3 enzyme maps to which substrate is a major challenge that is greatly facilitated by the TULIP2 methodology. TULIP2 methodology is fast, precise, and cost-effective. Compared to the previous TULIP methodology protocol, TULIP2 methodology achieves a more than 50-fold improvement in the purification yield and two orders of magnitude improvement in the signal-to-background ratio after label free quantification by mass spectrometry analysis. The method includes the generation of TULIP2 cell lines, subsequent purification of TULIP2 conjugates, preparation, and analysis of samples by mass spectrometry.

Keywords: ubiquitin, E3 enzymes, proteomics, post-translational modifications, mass spectrometry

OPEN ACCESS

Edited by:
Zhihao Zhuang,
University of Delaware, United States

Reviewed by:
Matthew Robert Pratt,
University of Southern California, United States
Francisco Solano,
University of Murcia, Spain

****Correspondence:***
Román González-Prieto
r.gonzalez_prieto@lumc.nl

Specialty section:
This article was submitted to Chemical Biology, a section of the journal Frontiers in Chemistry

Received: *16 September 2019*
Accepted: *07 November 2019*
Published: *26 November 2019*

Citation:
Salas-Lloret D, Agabitini G and González-Prieto R (2019) TULIP2: An Improved Method for the Identification of Ubiquitin E3-Specific Targets. Front. Chem. 7:802. doi: 10.3389/fchem.2019.00802

INTRODUCTION

The development of liquid chromatography tandem mass spectrometry (LC-MS/MS)-based proteomics technology has boomed in the past years, and, recently, a new strategy termed UbiSite, enabled the identification of around 63,000 unique sites for ubiquitination at endogenous levels of more than 10,000 proteins, including N-terminal ubiquitination (Akimov et al., 2018). The identification of additional ubiquitination sites seems to be a matter of repeating the UbiSite strategy with samples from different sources.

Determining which E3 enzyme is responsible for modifying which substrate is challenging. Different strategies have been proposed for identification of specific E3 substrates. Many of these strategies are based on indirect evidence. For example, investigating differences in the ubiquitin proteome upon overexpression or depletion of a specific E3 (Song et al., 2011; Sarraf et al., 2013; Thompson et al., 2014). Proteins that are enriched or depleted, respectively, in their ubiquitination levels are considered putative ubiquitination substrates for the specific E3 under investigation. However, the complexity of full ubiquitin proteomes is high (Akimov et al., 2018), and low abundant ubiquitination targets might be missed. Furthermore, results obtained from overexpression-based screens might be due to overexpression artifacts. In the case of the knock down-based screens, E3 ligases can be redundant on their targets, and some targets might be missed because their ubiquitination is still performed by another E3 enzyme. E3 enzyme cascades exist, and the absence of a specific ubiquitinated protein might be a result of an epistatic effect. Thus, every target

has to be very carefully verified. As a consequence, indirect approaches are unable to find E3-specific substrates in a reliable manner.

A proposed direct approach is the employment of ubiquitin-activated interaction traps, UBAITs (O'Connor et al., 2015), which work both for Really Interesting New Gene (RING) and Homologous to E6AP C-Terminus (HECT)-type E3 enzymes. The UBAIT approach is based on the utilization of E3 enzyme-ubiquitin fusions. The rationale behind this technique is that, if a linear fusion between a specific E3 and ubiquitin is made, the E3 will be prone to use this ubiquitin to conjugate it to its ubiquitination target. Therefore, the E3 will remain covalently bound to its target after ubiquitination, which allows the later purification of the E3 together with its ubiquitination target. Enabling subsequent identification by LC-MS/MS analysis (**Figure 1**). The main pitfall of the UBait approach is that the purification of the conjugates is based on epitope-antibody interaction, which excludes the possibility of using denaturing buffers. This disadvantage makes it difficult to distinguish between ubiquitination targets and other potential strong interactors of the E3s. Additionally, it is based on overexpression of the constructs, so the occurrence of overexpression-derived artifacts is a possibility.

Nevertheless, using the UBAIT as a base, we optimized and designed a systematic methodology which we termed Targets of Ubiquitin Ligases Identified by Proteomics (TULIP) (Kumar et al., 2017). TULIP methodology employs 10xHIS nickel-based purification, which allows the use of harsh denaturing buffers, solving the drawback of being unable to distinguish between ubiquitination targets and interactors of the E3. Moreover, TULIP methodology is lentiviral based, employing an all-in-one doxycycline-ON system followed by Gateway® cloning cassette and puromycin as selection marker for infected cells. TULIP methodology enables the generation of stable-inducible cell lines where the expression levels can be titrated to near-to-endogenous levels, minimizing the probability of obtaining results due to overexpression. The C-terminal GlyGly motif of ubiquitin is required for conjugation to a target. TULIP plasmids where ubiquitin lacks the C-terminal GlyGly motif (TULIP-ΔGG) are also available as negative controls. Furthermore, catalytically-dead mutants of the E3 enzymes are used as an additional negative control.

In this article, we describe an improved version of the TULIP methodology (Kumar et al., 2017), which we have termed TULIP2. TULIP2 introduces an extra 10xHIS N-terminal tag preceding the Gateway® cloning cassette. The addition of the extra 10xHIS tag results in an average improvement of more than 50 times in terms of purification efficiency of the TULIP conjugates and an improvement of two orders of magnitude in the signal-to-background ratio after mass spectrometry and Label Free Quantification (LFQ) analysis for the SUMO-Targeted Ubiquitin Ligase (STUbL) RNF4.

METHODS

Materials, Reagents, and Antibodies

Dulbecco's modified Eagle's medium, penicillin/streptomycin solution, trypsin-EDTA solution were acquired from Life Technologies (Carlsbad, CA, USA). Fetal bovine serum was from Biowest (Nuaillé, France). Di-sodium hydrogen phosphate dihydrate ($Na_2HPO_4 \bullet 2H_2O$) was from VWR chemicals (Radnor, PA, USA). Sodium dihydrogen phosphate monohydrate ($NaH_2PO_4 \bullet H_2O$), sodium chloride, trifluoroacetic acid, tween-20, puromycin dihydrochloride and imidazole were acquired from Merck (Darmstadt, Germany). Sodium dodecyl sulfate (SDS), MOPS running buffer and Guanidine hydrochloride 99.5+% were acquired from Thermo Fisher Scientific (Waltham, MA, USA). Nonidet P-40, formic acid (LC-MS grade), methanol (chromasol HPLC), acetonitrile (HPLC grade), MG132 (Z-leu-leu-leu-al) ≥90% HPLC, doxycycline, ponceau-S, polyethylenimine (PEI), urea, ammonium bicarbonate, polybrene, β-mercaptoethanol, and Triton X-100 were from Sigma Aldrich (St. Louis, MO, USA). C18 (Octadecyl) matrix for STAGE-tips was from Bioanalytical Technologies 3M Company (St. Paul, MN, USA). Phosphate-Buffered Saline (PBS) was from Fresenius Kabi (Bad Homburg, Germany). TRIS-Base was from Roche (Basel, Switzerland). Velocity DNA polymerase was from Bioline (London, UK). Elk milk powder was from Campina (Zaltbommel, The Netherlands). Rabbit-anti-RNF4 (Eurogentec, custom made, Vyas et al., 2013), HRP-conjugated Donkey-anti-Rabbit secondary antibody was from Thermo Fisher Scientific. Western Bright Quantum Western blotting detection kit was from Advansta (Menlo Park, CA, USA).

Generation of the TULIP2 Toolbox

For the construction of the TULIP2 plasmids, using the previous TULIP plasmid (Kumar et al., 2017), a 1.7 Kbp fragment was amplified by PCR with Velocity DNA polymerase using either FW-NheI-H-TULIP2: AGCTAGCATGCATCAC CATCATCACCACCACCACCATCACCAATCAACAAGT TTGTACAAAAAAGCTGAACG or FW-NheI-HF-TULIP2: AGCTAGCATGCATCACCATCATCACCACCACCACCATC ACGATTACAAGGATGACGACGATAAGCAATCAACAA GTTTGTACAAAAAAGCTGAACG as forward primer for H-TULIP2 and HF-TULIP2, respectively, and RV-TULIP2: AGAATTCCGGATGAGCATTCATCAGG as reverse. PCR fragment was digested with NheI and AgeI restriction enzymes and cloned between the NheI and AgeI sites within the TULIP plasmids.

Generation of TULIP2 Lentiviral Plasmids

TULIP2 plasmids are generated by Gateway® cloning (Thermo Fisher Scientific) according to vendor instructions. LR reactions are performed using a donor plasmid containing an E3 enzyme cDNA without stop codon and a TULIP2 plasmid (**Figure 2**) as destination vector. cDNAs from several E3 enzymes without stop codon can be obtained from repositories such as DNASU (Seiler et al., 2014) or the CCSB Human ORFeome Project (Lamesch et al., 2007). Additionally, cDNAs can also be subcloned into donor vectors by Gateway® cloning BP reactions (Thermo Fisher Scientific). In this article, we use pDONR207-RNF4, which was previously described (Kumar et al., 2017).

Cell Culture

293T and U2OS were cultured in Dulbecco's modified Eagle's medium (DMEM) supplemented with 10% Fetal Bovine Serum

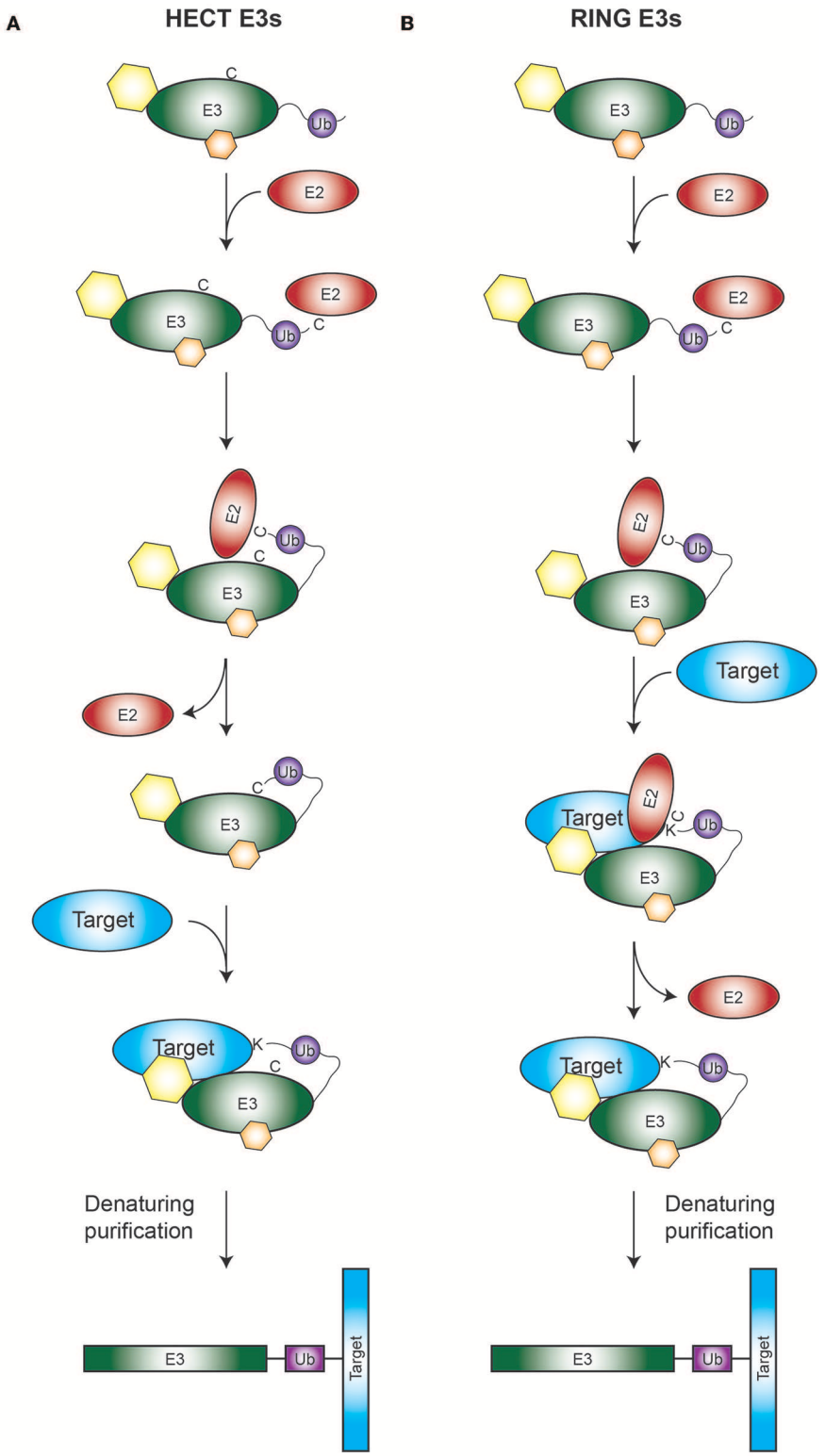

FIGURE 1 | Rationale of the TULIP2 methodology. Rationale is depicted for both HECT **(A)** and RING **(B)** E3 enzymes. **(A)** Activated ubiquitin linearly fused to a HECT E3 of interest will be conjugated to its respective E2 and transferred from the catalytic cysteine of the E2 to the catalytic cysteine of the HECT E3. Next ubiquitin will be transferred from the catalytic cysteine of the E3 to the acceptor lysine of the E3-target protein. Ubiquitination target will remain covalently bound to the E3, enabling the purification of the E3 together with the target protein. **(B)** Similar to A, but in this case the RING E3 catalyzes the transfer of its attached ubiquitin directly from the catalytic cysteine of its respective E2 to the ubiquitination target. Hexagons represent non-covalent interactors of the E3s.

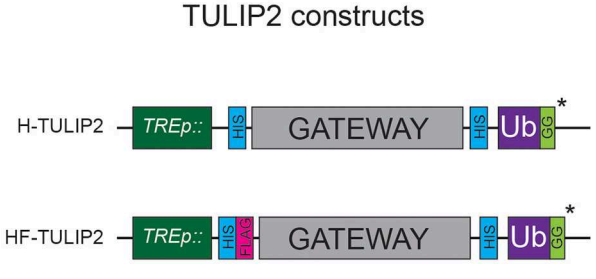

FIGURE 2 | TULIP2 Constructs. Schematic representation of the TULIP2 cloning cassette including the *TRE* promoter, 10xHIS and tandem 10xHIS-FLAG tag, Gateway cloning cassette, linker containing 10xHIS and active ubiquitin. *ΔGG constructs lack the C-terminal GG motif.

(FBS) and 100 U/mL penicillin/100 μg/mL streptomycin at 37°C and 5% CO2 unless specifically specified. The cells were regularly tested for mycoplasma contamination.

TULIP2 Lentivirus Production

293T cells were seeded at 30% confluency in a T175 flask containing 16 mL of DMEM + 10% FBS and allowed to attach overnight. Next, a 2 mL transfection mixture was prepared in 150 mM NaCl containing 7.5 μg pMD2.G (#12259, Addgene), 11.4 μg pMDLg-RRE (#12251, Addgene), 5.4 μg pRSV-REV (#12253, Addgene), 13.7 μg TULIP2 plasmid and 114 μL of 1 mg/mL Polyethylenimine (PEI) solution. All the components were mixed by vortexing and incubated 10 min at room temperature. Subsequently, the transfection mix was added to the cells. The day after transfection, culture medium was replaced by fresh DMEM/FBS/Pen/Strep. Three days after transfection, lentiviral suspension was filtered by passing through a 0.45 μm syringe filter (PN4184, Pall Corporation). Lentiviral particle concentration was determined using the HIV Type 1 p24 antigen ELISA Kit (ZeptoMetrix Corporation).

TULIP2 Cell Lines

U2OS cells were seeded in 15 cm diameter plates at 10% confluency (2×10^6 cells) and allowed to attach overnight. Next day, cell culture medium was replaced with cell culture medium containing 3.2 μg of lentiviral particles and polybrene 8 μg/mL final concentration. Twenty-four hours later, medium was replaced with fresh medium. Three days after lentiviral transduction, TULIP2 construct-positive clones were selected by adding puromycin 3 μg/mL to the culture medium.

Purification of TULIP2 Conjugates

A method overview of TULIP2 methodology is provided in **Figure 3**. Five 15 cm diameter plates of U2OS cells were grown up to 60–80% confluence and the expression of TULIP2 construct was induced with 1 μg/mL doxycycline for 24 h. Next, cells were treated for 5 h with proteasome inhibitor MG132 (Sigma Aldrich) at 10 μM. Subsequently, cells were washed twice with ice-cold PBS, scraped and transferred to a 50 mL tube. Cells were spun down 5 min at 500 × g, supernatant was discarded and cells were transferred to a 15 mL tube with 5 mL PBS. At this point, a 100 μL aliquot was taken to serve as input sample. After spinning down 1 min at 500 x g and discarding supernatant, input sample cells were lysed in 100 μL SNTBS buffer (2% SDS, 1% NP-40, 50 mM TRIS pH 7.5, 150 mM NaCl). Rest of the sample was centrifuged 3 min at 500 × g and the supernatant discarded.

Cell pellet was lysed in 10 mL Guanidinium buffer (6M guanidine-HCl, 0.1M Sodium Phosphate, 10 mM TRIS, pH 7.8). Samples were homogenized at room temperature by sonication using a tip sonicator (Q125 Sonicator, QSonica, Newtown, USA). Sonication was performed at 80% amplitude during 5 s. Subsequently, protein concentration was determined by BiCinchoninic Acid (BCA) Protein Assay Reagent (Thermo Scientific) and sample total protein content was equalized accordingly.

Lysates were supplemented with 5 mM β-mercaptoethanol and 50 mM Imidazole pH 8.0. 100 μL of nickel-nitrilotriacetic acid-agarose (Ni-NTA) beads (QIAGEN), were equilibrated with Guanidinium buffer supplemented with 5 mM β-mercaptoethanol and 50 mM Imidazole pH 8.0, added to the cell lysates and incubated overnight at 4°C under rotation.

After lysate-beads incubation, samples were centrifuged 5 min at 500 × g and the supernatant was discarded. Ni-NTA beads were transferred with 1 mL Wash buffer 1 (6 M Guanidine-HCl, 0.1 M Sodium Phosphate, 10 mM TRIS, 10 mM Imidazole, 5 mM β-mercaptoethanol, 0.2% Triton X-100, pH 7.8) to an Eppendorf LoBind tube (Eppendorf). Centrifuged again, supernatant discarded, and moved to a new LoBind tube with Wash buffer 2 (8 M Urea, 0.1 M Sodium Phosphate, 10 mM TRIS, 10 mM imidazole, 5 mM β-mercaptoethanol, pH 8). Same procedure was repeated with Wash buffer 3 (8 M urea, 0.1 M Sodium Phosphate, 10 mM TRIS, 10 mM imidazole, 5 mM β-mercaptoethanol, pH 6.3). Next, beads were washed twice with Wash buffer 4 (8 M urea, 0.1 M Sodium Phosphate, 10 mM TRIS, 5 mM β-mercaptoethanol, pH 6.3). In every wash step, beads were allowed to equilibrate with the buffer for 15 min under rotation.

The steps for the purification of the TULIP2 conjugates are indicated in a simplified manner in (**Supplementary Protocol 1**).

Trypsin Digestion

After second wash with Wash buffer 4, Ni-NTA beads were separated from the buffer by passing through a 0.45 μm filter Ultrafree-MC-HV spin column (Merck-Millipore) which had been previously equilibrated with 250 μL of ABC buffer (50 mM ammonium bicarbonate). Using 400 μL of ABC buffer, Ni-NTA beads were transferred to a new Eppendorf LoBind tube and 500 ng of sequencing grade modified trypsin (Promega) were added to the ABC buffer-beads suspension. Digestion was performed overnight at 37°C while shaking at 1,400 rpm.

Electrophoresis and Immunoblotting

0.1% of the whole-cell extract (Inputs) and 5% of the HIS-purified proteins (TULIP and TULIP2 conjugates) were separated on Novex 4–12% gradient gels (Thermo Fisher Scientific) using NuPAGE® MOPS SDS running buffer (50 mM MOPS, 50 mM TRIS-base, 0.1% SDS, 1 mM EDTA pH 7.7) and transferred onto Amersham Protran Premium 0.45 NC Nitrocellulose

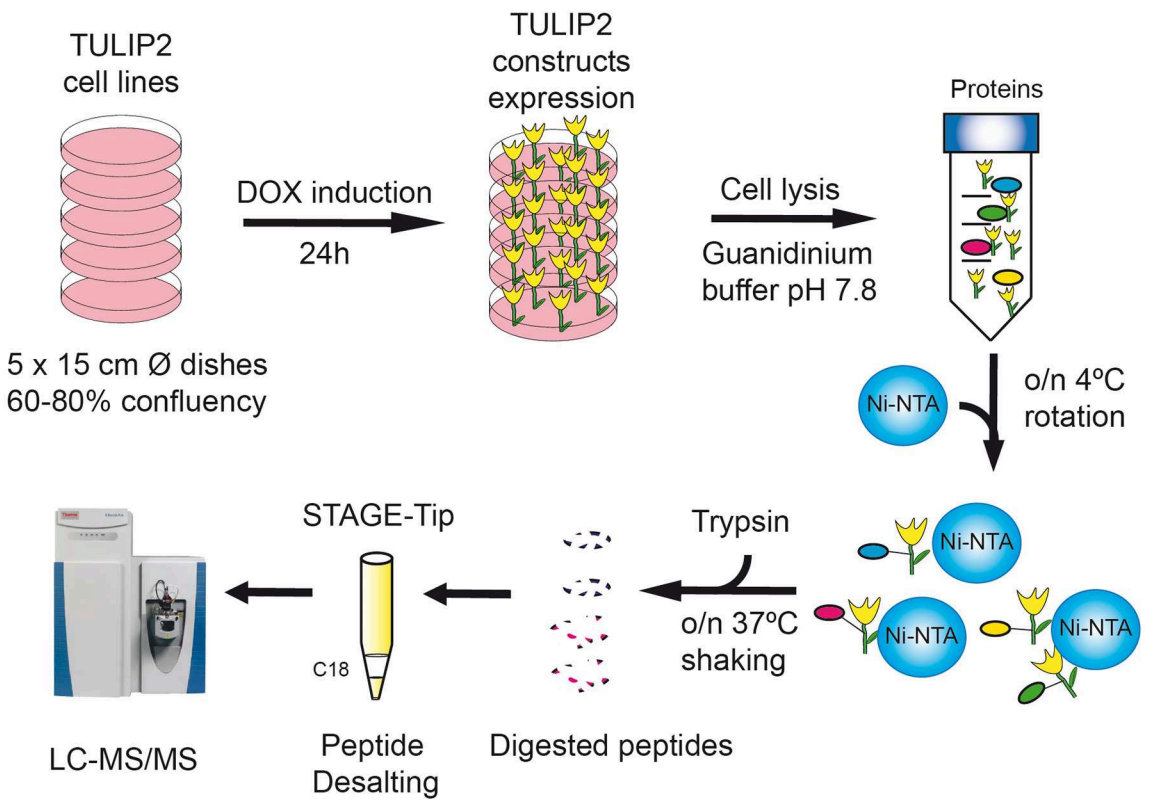

FIGURE 3 | TULIP2 methodology overview. Cells stably containing the E3-TULIP2 expression cassettes are cultured up to 60–80% confluency. The expression of the E3-TULIP2 constructs is induced for 24 h and then they are lysed in Guanidinium buffer and incubated overnight with Ni-NTA beads. Subsequently, beads are washed with different washing buffers and on-the-beads digestion of TULIP2 conjugates with trypsin is performed overnight at 37°C while shaking. Next, digested peptides are desalted by C18 STAGE-Tipping and analyzed by LC-MS/MS.

blotting membrane (GE Healthcare) using a Bolt Mini-Gel system (Thermo Fisher Scientific), which was used for both the gel electrophoresis and the protein transfer to the membrane according to vendor instructions.

Membrane was stained with Ponceau-S (Sigma Aldrich) to determine total amount of protein loaded. Next membrane was de-stained with PBS + 0.1% Tween-20 and, subsequently, was blocked with Blocking solution (8% Elk milk, 0.1% Tween-20 in PBS) for 1 h. Next, membrane was incubated overnight with 2 ml of a 1:2500 dilution of anti-RNF4 antibody in blocking solution. Next day, membranes were washed 3 times 10 min with PBS + 0.1% Tween-20. Subsequently, membranes were incubated for 1 h with a 1:5000 dilution of HRP-conjugated Donkey-anti-rabbit secondary antibody in blocking solution and washed another 3 times 10 min with PBS+0.1% Tween 20.

Chemiluminescence reaction was initiated with Western Bright Quantum Western blotting detection kit and measured in a ChemiDoc^{TM} imaging system (BIO-RAD, Hercules, CA, USA). The quantification of the signal corresponding to the TULIP and TULIP2 constructs was done using FIJI software (Schindelin et al., 2012).

Mass Spectrometry Sample Preparation

Trypsin-digested peptides were separated from the beads by filtering through a 0.45 μm filter Ultrafree-MC-HV spin column (Merck-Millipore) which had been previously equilibrated with 250 μL of ABC buffer. Flow through was collected in an Eppendorf LoBind tube and acidified by adding 2% TriFlourAcetic (TFA) acid. Subsequently, peptides were desalted and concentrated on STAGE-Tips as previously described (Rappsilber et al., 2007). STAGE-Tips were in-house assembled using 200 μL micro pipet tips and a C18 matrix. STAGE-Tips were activated by passing through 100 μL of methanol. Subsequently 100 μL of Buffer B (80% acetonitrile, 0.1% formic acid), 100 μL of Buffer A (0.1% formic acid), the peptide sample, and two times 100 μL Buffer A were passed through the STAGE-tip. Elution was performed in 50 μL of 50% acetonitrile, 0.1% formic acid.

Samples were vacuum dried using a SpeedVac RC10.10 (Jouan, France) and stored at −20°C. Prior to mass spectrometry analysis, samples were reconstituted in 10 μL 0.1% Formic acid and transferred to autoload vials.

LC-MS/MS

All the experiments were performed on an EASY-nLC 1000 system (Proxeon, Odense, Denmark) connected to a Q-Exactive Orbitrap (Thermo Fisher Scientific, Germany) through a nano-electrospray ion source. The Q-Exactive was coupled to a 25 cm silica emitter (FS360-75-15-N-5-C25, NewObjective, Woburn, MA, USA) packed in house with 1.9 μm C18-AQ beads (Reprospher-DE, Pur, Dr. Manish, Ammerbuch-Entringen, Germany).

Twenty percent of the sample was injected in a 100 min chromatography gradient from 0 to 30% acetonitrile and then increasing to 95% acetonitrile prior to column re-equilibration with flow rate of 200 nL/min. The mass spectrometer was operated in a Data-Dependent Acquisition (DDA) mode with a top-10 method and a scan range of 300–1,600 m/z. Full-scan MS spectra were acquired at a target value of 3×10^6 and a resolution of 70,000, and the Higher-Collisional Dissociation (HCD) tandem mass spectra (MS/MS) were recorded at a target value of 1×10^5 and with a resolution of 17,500, an isolation window of 2.2 m/z, and a normalized collision energy (NCE) of 25%. The minimum AGC target was 1×10^4. The maximum MS1 and MS2 injection times were 250 and 60 ms, respectively.

The precursor ion masses of scanned ions were dynamically excluded (DE) from MS/MS analysis for 20 s. Ions with charge 1, and >6, were excluded from triggering MS2 analysis.

Mass Spectrometry Data Analysis

All raw data were analyzed using MaxQuant (version 1.6.7.0) as described previously (Tyanova et al., 2016a). We performed the search against an *in silico* digested UniProt reference proteome for Homo sapiens including canonical and isoform sequences (27th May 2019). Database searches were performed according to standard settings with the following modifications. Digestion with Trypsin/P was used, allowing 4 missed cleavages. Oxidation (M), Acetyl (Protein N-term), and GlyGly (for ubiquitination sites) were allowed as variable modifications with a maximum number of 3. Carbamidomethyl (C) was disabled as a fixed modification. Label-Free Quantification was enabled, not allowing Fast LFQ. All peptides were used for protein quantification.

Output from MaxQuant Data were exported and processed in MS Excel for further filtering, processing of the data, and visualization.

For the statistical analysis of RNF4-TULIP2 samples, output from the analysis in MaxQuant was further processed in the Perseus computational platform (v 1.6.7.0) (Tyanova et al., 2016b). LFQ intensity values were log2 transformed. Potential contaminants and proteins identified by site only or reverse peptide were removed. Samples were grouped in experimental categories and proteins not identified in 3 out of 3 replicates in at least one group were also removed. Missing values were imputed using normally distributed values with a 1.8 downshift (log2) and a randomized 0.3 width (log2) considering whole matrix values. Statistical analysis was performed to determine which proteins were significantly enriched in the wild type RNF4 samples compared to the ΔGG samples (*t*-test with permutation-based False Discovery Rate (FDR) = 0.05 and S0 = 0.1).

RESULTS

TULIP vs. TULIP2

Previously, TULIP methodology was employed to identify the SUMO Targeted Ubiquitin Ligase (STUbL) RNF4 specific ubiquitination targets (Kumar et al., 2017). In order to compare the new TULIP2 methodology with the previous TULIP methodology version, we cloned the RNF4 into the H-TULIP2 plasmids. Next, we generated lentiviral particles containing the RNF4-TULIP2 constructs and used them to stably introduce the RNF4-TULIP2 constructs in U2OS cells by lentiviral transduction. Positive clones were selected with puromycin.

Cells expressing RNF4-TULIP and RNF4-TULIP2 constructs were grown in equal amount, induced for the same time and treated for 5 h with the proteasome inhibitor MG132. Next, cells were lysed and the RNF4-TULIP and RNF4-TULIP2 conjugates were purified in parallel following the TULIP methodology protocol (Gonzalez-Prieto and Vertegaal, 2019) or the TULIP2 method introduced in this article, respectively (**Figure 4A**). Next, whole cell extracts and 5% of the HIS-pulldown samples were analyzed by immunoblotting using an anti-RNF4 antibody (**Figure 4B**). While the RNF4-TULIP2 constructs were expressed relatively higher than their RNF4-TULIP counterparts by a factor of 1.7, the amount of RN4-TULIP2 conjugates purified were 52.2 times higher compared to the amount of RNF4-TULIP conjugates while using the same amount of starting material (**Figure 4C**).

Next, we decided to perform a comparison using three biological replicates of RNF4-TULIP2 samples and the RNF4-TULIP samples from Kumar et al. (2017) both generated after treating with the proteasome inhibitor MG132. In both cases, 20% of the RNF4-TULIP or RNF4-TULIP2 samples were injected in the mass spectrometer and analyzed using the same chromatography gradients. All three biological replicates of each sample set were grouped together for performing comparisons. Signal corresponding to RNF4 was more than 8 times higher in the TULIP2 samples compared to TULIP samples when looking at Intensity or iBAQ MaxQuant output values and more than 5 times in the case of the values of the Label Free Quantification intensity (**Figure 4D**).

Previously, using TULIP methodology, we identified components of the sumoylation machinery and other proteins such as TOP2A, SLFN5, RAD18, and RNF216 as the most important SIM- and MG132-dependent RNF4 targets. Using TULIP2 methodology we were able to increase the number of peptides, the percentage of sequence coverage, intensity, iBAQ, and LFQ intensity values and the number of spectral counts for all these RNF4 direct ubiquitination targets (**Figure 4E**, **Supplementary Dataset 1**).

While TULIP methodology allowed us to identify SUMO E3s and E2 as ubiquitination targets for RNF4, TULIP2 methodology also identified the SUMO E1 enzyme (SAE1/UBA2) as an RNF4 ubiquitination target, indicating that, upon SUMOylation, all the members of the SUMOylation machinery, including E1, E2, and E3 enzymes, are targeted for degradation in an RNF4-dependent manner.

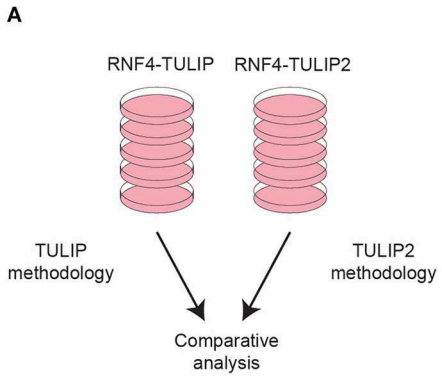

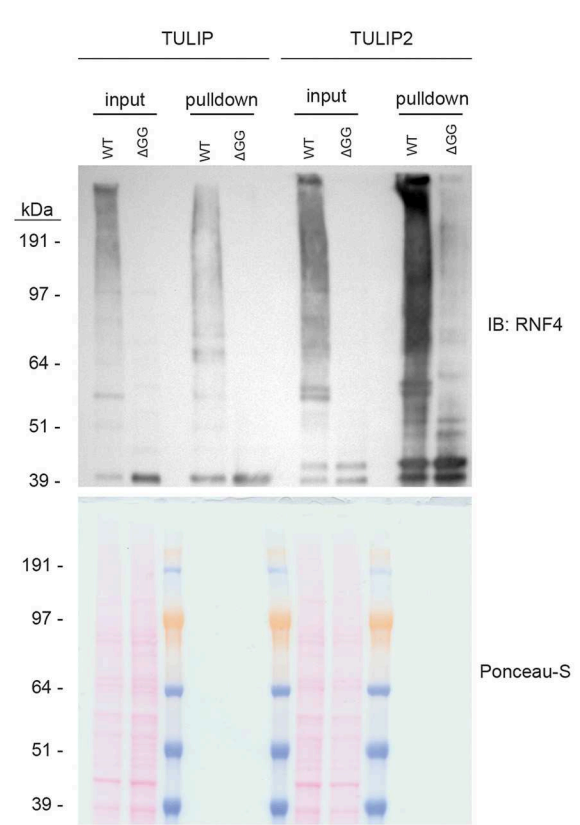

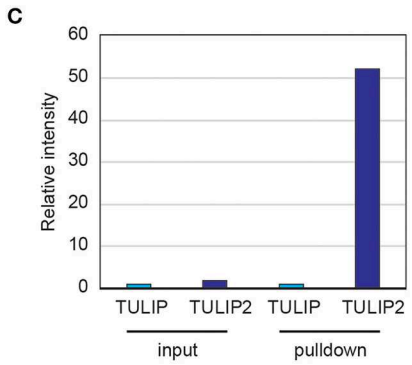

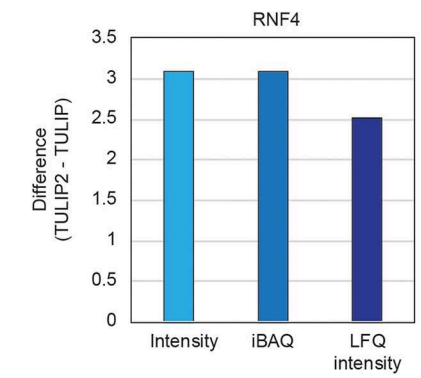

E

Gene name	Peptides		Sequence coverage(%)		Difference (log2)			Spectral counts (MS/MS)	
	TULIP	TULIP2	TULIP	TULIP2	Intensity	iBAQ	LFQ intensity	TULIP	TULIP2
ZNF451	20	20	20,1	20,3	-0,22	-0,22	-0,78	50	51
RNF216	27	50	26,7	35,1	2,48	2,48	1,70	40	153
TOP2A	13	47	10,5	33,1	2,81	2,81	2,40	27	111
PIAS2	6	16	12,2	27,2	2,90	2,90	2,24	7	41
PIAS3	9	13	17,2	29,9	2,96	2,96	1,92	16	49
SLFN5	11	23	13,4	22,7	2,97	2,97	0,84	20	87
RNF4	3	8	23,9	28,7	3,10	3,10	2,51	6	87
PIAS1	11	18	25,5	31,2	3,51	3,51	2,36	21	73
PIAS4	5	11	15,1	23,9	3,59	3,59	1,40	5	32
ZNF451-3	2	11	6,4	25,2	3,66	3,66	3,12	4	26
UBE2I	2	6	16,8	32,1	4,18	4,18	2,86	5	34
RAD18	12	31	26,9	46,1	4,37	4,37	3,18	18	110
NSMCE2	3	9	11,3	38,1	4,83	4,83	∞	4	16
UBA2	0	23	0	44,5	∞	∞	∞	0	55
SAE1	0	15	0	51,2	∞	∞	∞	0	38

FIGURE 4 | TULIP vs. TULIP2. **(A)** Experimental design to compare TULIP vs. TULIP2. **(B).** U2OS cells containing either RNF4-TULIP or RNF4-TULIP2 expression cassettes were induced overnight with doxycycline, lysed and TULIP/TULIP2 conjugates purified according to TULIP or TULIP2 methodology, respectively. The efficiency of the expression and the purification was analyzed by immunoblotting. Ponceau-S is provided as loading control. **(C)** Quantification of the intensity from the immunoblotting analysis performed in **(B)**. Intensity of the signal in TULIP samples is normalized as 1. **(D)** Graph depicting the log2 difference between RNF4-TULIP2 and RNF4-TULIP samples for RNF4 after mass spectrometry analysis in terms of Intensity, iBAQ or LFQ intensity. **(E)** Table indicating the values for number of peptides, sequence coverage, log2 difference of intensities after LC-MS/MS analysis and spectral counts of top RNF4-specific ubiquitination targets comparing RNF4-TULIP and RNF4-TULIP2 samples.

Next, in order to generate a new list of RNF4 ubiquitination targets by using TULIP2 methodology, we performed a second analysis including RNF4-TULIP2 samples and RNF4-TULIP2-ΔGG samples as negative control. We performed 3 biological replicates of each construct in order to perform statistical comparisons. Comparison between the RNF4-TULIP2 and RNF4-TULIP2-ΔGG identified 409 RNF4-TULIP2 conjugated proteins (**Figure 5**, **Supplementary Dataset 2**). Moreover, mass spectrometry analysis also allowed to identify 372 specific ubiquitination sites in 209 proteins (**Supplementary Dataset 3**), including many members of the sumoylation machinery and the previously identified as main ubiquitination targets targeted for degradation by RNF4 in a SUMO-dependent manner.

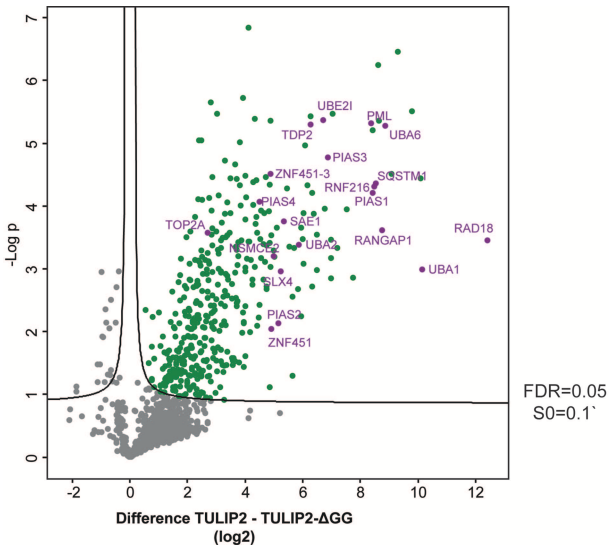

FIGURE 5 | RNF4-TULIP2 ubiquitination targets. Volcano plot depicting RNF4-TULIP2 conjugates comparing to RNF4-TULIP2-ΔGG samples. Each dot represents a protein. Green dots represent proteins that are statistically enriched in the RNF4-TULIP2 samples compared to RNF4-TULIP2-ΔGG samples for an FDR = 0.05 and S0 = 0.1. Purple labeled dots represent proteins relates to the SUMOylation machinery or top main ubiquitination targets previously identified by TULIP methodology.

DISCUSSION, ADVANTAGES, AND PITFALLS

In this article we have performed a comparison between our previously published TULIP methodology (Kumar et al., 2017) and an improved version, which we have termed TULIP2 methodology. Compared to previous version, for the STUbL RNF4, it achieves a more than 50 times improvement in terms of purification efficiency (**Figures 4B,C**). This methodology can be implemented in any laboratory interested in the identification of the ubiquitination targets of a given E3 of interest. Furthermore, the simplification of the protocol by suppressing the elution and size exclusion filter-based sample concentration results in a reduction of the execution costs of the experiments. Moreover, the introduction of the HIS-FLAG TULIP2 plasmids allow the employment of an anti-FLAG tag antibody when a good specific antibody for immunoblotting is not available for the E3 enzyme of interest or for unambiguous identification respect of the endogenous E3 enzyme. Together, all these improvements enable the implementation of the TULIP2 methodology in any research group with access to a mass-spectrometry facility. To facilitate the implementation of the TULIP2 methodology in any laboratory we have included an annotated step-by-step protocol from the induction of the expression of the TULIP2 constructs until the isolation of the trypsin-digested peptides corresponding to the TULIP2 constructs and conjugates.

The improvement achieved by TULIP2 allowed us not only to have a better coverage of the RNF4 ubiquitination targets after mass spectrometry analysis, but also to identify new RNF4 ubiquitination substrates (**Figures 4E, 5**, **Supplementary Datasets 1**, **2**). Moreover, we could determine the specific ubiquitination sites of many of the identified RNF4 targets (**Supplementary Dataset 3**). While previous TULIP methodology allowed us to identify 31 ubiquitination sites on 16 proteins (Kumar et al., 2017), these numbers increased to 372 and 209, respectively, using TULIP2 methodology.

The improvement achieved by TULIP2 methodology facilitates the identification of specific substrates for other E3 enzymes which are less stable, their ubiquitination targets less abundant and/or have a lower ubiquitination activity than RNF4. The identification of the E3-specific ubiquitination substrates using TULIP methodology was still challenging and very large amounts of cells needed to be lysed to obtain the minimum amounts of TULIP conjugates to allow identification by mass spectrometry. TULIP2 methodology solves this major drawback. TULIP2 is straightforward and enables the systematic identification of the specific ubiquitination targets of virtually every HECT- and RING-type E3 enzyme. Using Gateway cloning, any E3-ligase cDNA can be cloned into the TULIP2 plasmids.

Nevertheless, the TULIP2 methodology still shares some limitations with the previous version of the method (Kumar et al., 2017). Some E3-TULIP2 constructs might not be functional due to steric hindrance and the size of the E3 to be cloned into the TULIP2 plasmids is limited by the capacity of the lentiviral particles. As an indication, we have been able to clone E3 enzymes with cDNA sizes up to 6 kilobase pairs. Some E3-TULIP2 constructs might be very rapidly targeted for degradation by the proteasome via autoubiquitination given that the already present ubiquitin moiety is a signal for ubiquitin chain lengthening. Thus, inhibition of the proteasome might be required to be able to purify sufficient amount of TULIP2 conjugates to secure identification by mass spectrometry.

It is also worth noting that, although TULIP2-attached E3s represent a bulky tag that hamper the utilization of the attached ubiquitin by other E3s to ubiquitinate their targets, potentially ubiquitin moieties from the TULIP2 constructs can still be used by other E3s. Thus, including catalytically dead mutants of the E3s of interest as an additional negative control to the ΔGG TULIP2 constructs might be advantageous. Finally, the probability of success in identifying the specific ubiquitination substrates for a given E3 enzyme highly depends on the sensitivity

of the mass spectrometry equipment employed and the amount of sample injected. The signal corresponding to the TULIP2 conjugates is commonly below the signal corresponding to the common unspecific binders to Ni-NTA beads, making good enrichment is critical for successful identification.

DATA AVAILABILITY STATEMENT

TULIP2 construct plasmids are freely available from the González-Prieto lab upon reasonable request.

The mass spectrometry proteomics data have been deposited to the ProteomeXchange Consortium via the PRIDE (Perez-Riverol et al., 2019) partner repository with the dataset identifier PXD015437.

AUTHOR CONTRIBUTIONS

RG-P designed and constructed the TULIP2 plasmids. RG-P, DS-L, and GA performed experiments. GA was supervised by DS-L. RG-P and DS-L made the figures. RG-P wrote the manuscript with input from DS-L. All authors contributed to manuscript revision, read and approved the submitted version.

FUNDING

Work in the González-Prieto lab was supported by the Dutch Cancer Society (KWF-Young Investigator Grant: 11367).

ACKNOWLEDGMENTS

Authors would like to thank Prof. Alfred Vertegaal for infrastructural support.

SUPPLEMENTARY MATERIAL

The Supplementary Material for this article can be found online at: https://www.frontiersin.org/articles/10.3389/fchem.2019.00802/full#supplementary-material

Supplementary Dataset 1 | Values from the mass spectrometry analysis comparing RNF4-TULIP and RNF4-TULIP2.

Supplementary Dataset 2 | Statistical analysis of RNF4-TULIP2 samples compared to RNF4-TULIP2-ΔGG samples.

Supplementary Dataset 3 | Specific ubiquitination sites identified by mass spectrometry in RNF4-TULIP2 samples.

Supplementary Protocol 1 | TULIP2 benchtop step-by-step protocol.

REFERENCES

Akimov, V., Barrio-Hernandez, I., Hansen, S. V. F., Hallenborg, P., Pedersen, A. K., Bekker-Jensen, D. B., et al. (2018). UbiSite approach for comprehensive mapping of lysine and N-terminal ubiquitination sites. *Nat. Struct. Mol. Biol.* 25, 631–640. doi: 10.1038/s41594-018-0084-y

Gonzalez-Prieto, R., and Vertegaal, A. C. O. (2019). "TULIP: targets of ubiquitin ligases identified by proteomics," in *SUMOylation and Ubiquitination: Current and Emerging Concepts*, ed V. G. Wilson (Caister Academic Press), 147–160. doi: 10.21775/9781912530120.10

Kumar, R., Gonzalez-Prieto, R., Xiao, Z., Verlaan-De Vries, M., and Vertegaal, A. C. O. (2017). The STUbL RNF4 regulates protein group SUMOylation by targeting the SUMO conjugation machinery. *Nat. Commun.* 8:1809. doi: 10.1038/s41467-017-01900-x

Lamesch, P., Li, N., Milstein, S., Fan, C., Hao, T., Szabo, G., et al. (2007). hORFeome v3.1: a resource of human open reading frames representing over 10,000 human genes. *Genomics* 89, 307–315. doi: 10.1016/j.ygeno.2006.11.012

O'Connor, H. F., Lyon, N., Leung, J. W., Agarwal, P., Swaim, C. D., Miller, K. M., et al. (2015). Ubiquitin-Activated Interaction Traps (UBAITs) identify E3 ligase binding partners. *EMBO Rep.* 16, 1699–1712. doi: 10.15252/embr.201540620

Perez-Riverol, Y., Csordas, A., Bai, J., Bernal-Llinares, M., Hewapathirana, S., Kundu, D. J., et al. (2019). The PRIDE database and related tools and resources in 2019: improving support for quantification data. *Nucleic Acids Res.* 47, D442–D450. doi: 10.1093/nar/gky1106

Rappsilber, J., Mann, M., and Ishihama, Y. (2007). Protocol for micro-purification, enrichment, pre-fractionation and storage of peptides for proteomics using StageTips. *Nat. Protoc.* 2, 1896–1906. doi: 10.1038/nprot.2007.261

Sarraf, S. A., Raman, M., Guarani-Pereira, V., Sowa, M. E., Huttlin, E. L., Gygi, S. P., et al. (2013). Landscape of the PARKIN-dependent ubiquitylome in response to mitochondrial depolarization. *Nature* 496, 372–376. doi: 10.1038/nature12043

Schindelin, J., Arganda-Carreras, I., Frise, E., Kaynig, V., Longair, M., Pietzsch, T., et al. (2012). Fiji: an open-source platform for biological-image analysis. *Nat. Methods* 9, 676–682. doi: 10.1038/nmeth.2019

Seiler, C. Y., Park, J. G., Sharma, A., Hunter, P., Surapaneni, P., Sedillo, C., et al. (2014). DNASU plasmid and PSI:biology-materials repositories: resources to accelerate biological research. *Nucleic Acids Res.* 42, D1253–D1260. doi: 10.1093/nar/gkt1060

Song, M., Hakala, K., Weintraub, S. T., and Shiio, Y. (2011). Quantitative proteomic identification of the BRCA1 ubiquitination substrates. *J. Proteome Res.* 10, 5191–5198. doi: 10.1021/pr200662b

Thompson, J. W., Nagel, J., Hoving, S., Gerrits, B., Bauer, A., Thomas, J. R., et al. (2014). Quantitative Lys–Gly-Gly (diGly) proteomics coupled with inducible RNAi reveals ubiquitin-mediated proteolysis of DNA damage-inducible transcript 4 (DDIT4) by the E3 ligase HUWE1. *J. Biol. Chem.* 289, 28942–28955. doi: 10.1074/jbc.M114.573352

Tyanova, S., Temu, T., and Cox, J. (2016a). The MaxQuant computational platform for mass spectrometry-based shotgun proteomics. *Nat. Protoc.* 11, 2301–2319. doi: 10.1038/nprot.2016.136

Tyanova, S., Temu, T., Sinitcyn, P., Carlson, A., Hein, M. Y., Geiger, T., et al. (2016b). The *Perseus* computational platform for comprehensive analysis of (prote)omics data. *Nat. Methods* 13, 731–740. doi: 10.1038/nmeth.3901

Vyas, R., Kumar, R., Clermont, F., Helfricht, A., Kalev, P., Sotiropoulou, P., et al. (2013). RNF4 is required for DNA double-strand break repair *in vivo*. *Cell Death Differ.* 20, 490–502. doi: 10.1038/cdd.2012.145

Conflict of Interest: The authors declare that the research was conducted in the absence of any commercial or financial relationships that could be construed as a potential conflict of interest.

frontiers in Chemistry

METHODS
published: 04 December 2019
doi: 10.3389/fchem.2019.00816

A High-Throughput Assay for Monitoring Ubiquitination in Real Time

*Tyler G. Franklin and Jonathan N. Pruneda**

Department of Molecular Microbiology and Immunology, Oregon Health & Science University, Portland, OR, United States

Protein ubiquitination is a highly orchestrated process that controls diverse aspects of human biology. Dysregulation of this process can lead to various disease states including cancer, neurodegeneration, and autoimmunity. It is the correction of these dysregulated pathways, as well as the enticing ability to manipulate protein stability, that have instigated intense research into the therapeutic control of protein ubiquitination. A major bottleneck in the development and validation of small molecule modulators is the availability of a suitable high-throughput assay for enzyme activity. Herein, we present a new assay, which we term UbiReal, that uses fluorescence polarization to monitor all stages of Ub conjugation and deconjugation in real time. We use the assay to validate a chemical inhibitor of the E1 ubiquitin-activating enzyme, as well as to assess the activities and specificities of E2s, E3s, and deubiquitinases. The sensitivity and accessibility of this approach make it an excellent candidate for high-throughput screens of activity modulators, as well as a valuable tool for basic research into the mechanisms of ubiquitin regulation.

Keywords: ubiquitin, high-throughput screen, fluorescence polarization, ubiquitin ligase, deubiquitinase

OPEN ACCESS

Edited by:
Huib Ovaa,
Leiden University Medical Center, Netherlands

Reviewed by:
Alexander Statsyuk,
University of Houston, United States
Danny Huang,
Beatson Institute, University of Glasgow, United Kingdom

****Correspondence:***
Jonathan N. Pruneda
pruneda@ohsu.edu

Specialty section:
This article was submitted to Chemical Biology, a section of the journal Frontiers in Chemistry

Received: *30 September 2019*
Accepted: *12 November 2019*
Published: *04 December 2019*

Citation:
Franklin TG and Pruneda JN (2019) A High-Throughput Assay for Monitoring Ubiquitination in Real Time. Front. Chem. 7:816. doi: 10.3389/fchem.2019.00816

INTRODUCTION

Post-translational regulation through attachment of the small protein modifier ubiquitin (Ub) is a conserved and essential process among all eukaryotic life. Protein ubiquitination can regulate diverse cellular processes including proteasomal degradation as well as protein trafficking, cell cycle regulation, and immune signaling (Komander and Rape, 2012). Ub is typically attached via its carboxy-terminus to a lysine residue on a target protein, resulting in a monoUb modification. The vast diversity of Ub signaling roles arises from additional customization of the monoUb signal. Unlike binary post-translational modifications such as phosphorylation or acetylation, Ub itself is a protein and can thus be further post-translationally modified by e.g., ubiquitination. Ubiquitination of Ub can occur at any of eight classical sites (seven lysine positions and the amino-terminus), creating an array of polymeric Ub (polyUb) chains. MonoUb as well as each polyUb chain type are believed to serve distinct signaling roles, for example chains linked through K48 are the classic proteasomal degradation signal, whereas Met1-linked polyUb serves a specialized role in innate immune signaling (Komander and Rape, 2012; Swatek and Komander, 2016). Additionally, target proteins can be ubiquitinated at multiple sites, further diversifying the versatility of Ub signaling.

In humans, the Ub system is controlled by hundreds of regulatory proteins (Clague et al., 2015). Ubiquitination occurs via a cascade of Ub "writing" enzymes that include an E1 Ub-activating enzyme, an E2 Ub-conjugating enzyme, and an E3 Ub ligase (**Figure 1A**). The E1 Ub-activating enzyme (of which there are two in humans) consumes ATP to activate the Ub carboxy-terminus

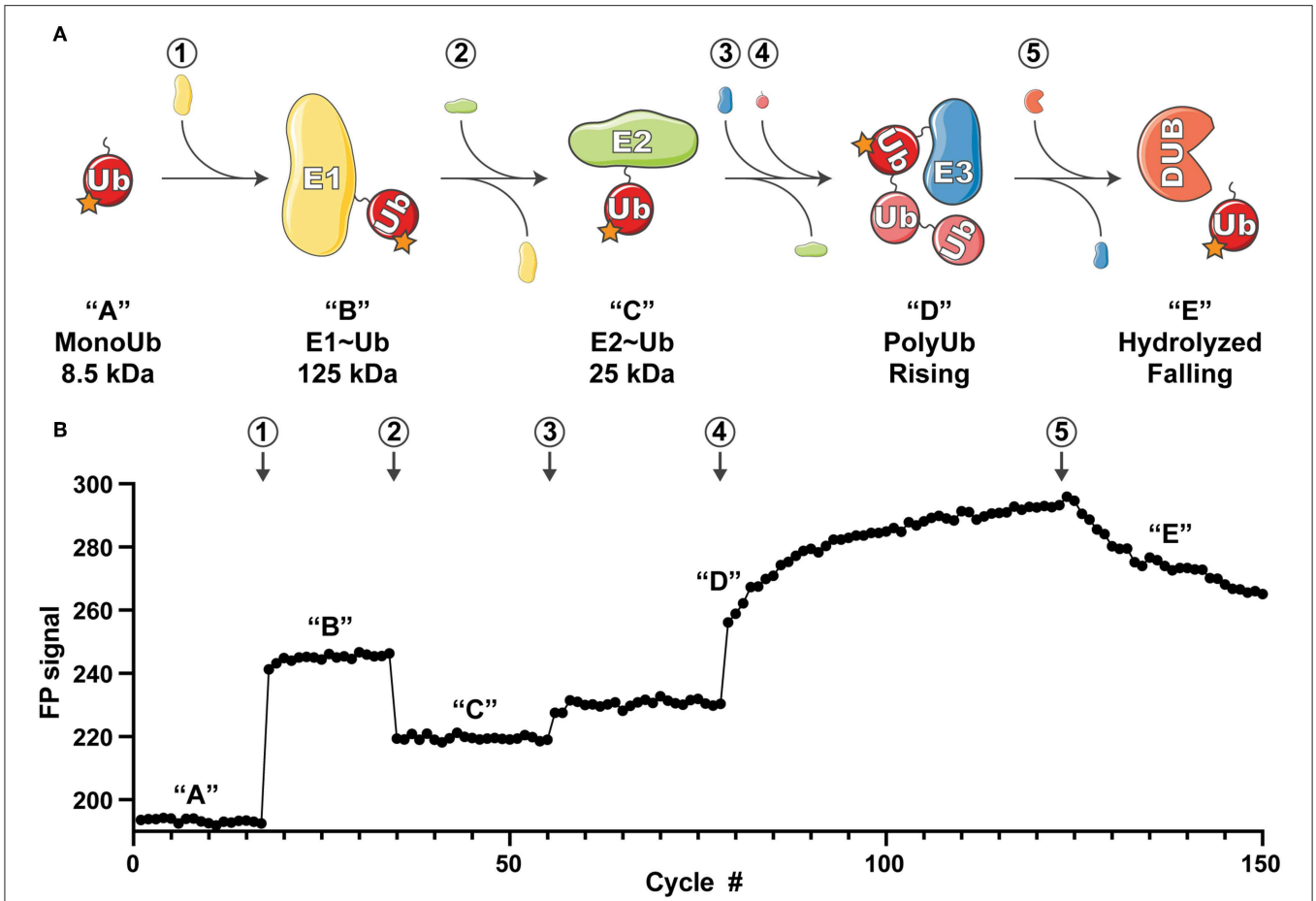

FIGURE 1 | Overview of the UbiReal approach. **(A)** Schematic depicting the sequential states of ubiquitin conjugation that are monitored using UbiReal. Circled numbers indicate the addition of protein and correspond to the data in part **(B)**. Letters in quotations indicate the state of the ubiquitin complex and also correspond to the changes in FP signal observed in (B). Approximate molecular weights of the complexes are provided and reflect the amplitude of the expected FP signal. "Rising" in "D" corresponds to the rising FP signal from the ligation of chains by the E3 enzyme, and "falling" in "E" corresponds to falling FP signal from the activity of a DUB enzyme. (B) Data representing the ability of UbiReal to comprehensively monitor the sequential steps of the ubiquitination pathway. Numbers and letters correspond to protein additions and the states of ubiquitin complexes, respectively, as described in (A). For clarity, data are presented as cycles separated by 30 s. In this representative assay, "1" is the E1 UBE1, "2" is the E2 UBE2D3, "3" is the E3 NleL, "4" is WT Ub, and "5" is the DUB USP21. Graph is the average of two identical, parallel experiments and representative of multiple other UbiReal experimental curves.

onto an E1 active site cysteine, creating a high-energy thioester linkage (E1∼Ub). Next, through a transthiolation reaction the Ub is transferred from the E1 to the active site cysteine of an E2 Ub-conjugating enzyme (of which there are ∼35 in humans), forming the E2∼Ub conjugate. At this stage, the Ub can either be transferred directly onto a substrate lysine in a reaction catalyzed by E3 ligases of the RING/U-box family (of which there are hundreds in humans), or via one additional thioester intermediate in the cases of the HECT and RBR families of E3 ligases (28 and 14 examples in humans, respectively) which utilize their own active site cysteine to receive and transfer Ub onto a substrate. The resulting Ub signals are discriminately interpreted by Ub binding domains (of which there are >150 in humans) that specifically "read" the modification and direct cellular outcomes. Finally, Ub signals can be "erased" by specialized proteases termed deubiquitinases (DUBs, of which there are ∼100 in humans) that can edit or recycle the Ub signal back to its monomeric state (**Figure 1A**).

In total, approximately 5% of human genes encode regulators of Ub signaling. This significant evolutionary investment is illustrative of the strict regulation maintained over Ub signaling across its broad involvement in cellular processes. Perhaps unsurprisingly, breakdown of this regulation can often lead to disease (Popovic et al., 2014). Defects in Ub signaling are linked to many cancers, as the dysregulation of E3 ligase or DUB activities can directly impact the stabilities of tumor suppressors or oncogene products (Kirkin and Dikic, 2011). Ub proteasome system defects are also linked to neurodegenerative disorders, which arise from an inability to degrade toxic protein aggregates (Zheng et al., 2016). In addition to affecting protein stability, aberrant ubiquitination can result in constitutive activation of

Abbreviations: Ub, ubiquitin; FP, fluorescence polarization; DUB, deubiquitinase; HTS, high-throughput screen; T-Ub, TAMRA-Ub; F-Ub, Fluorescein-Ub.

signaling pathways such as NF-κB, leading to autoimmune diseases or tumor formation (Hu and Sun, 2016).

The Ub system is a major focus of recent pharmaceutical research as it offers the opportunity to "drug the undruggable," for example by stabilizing tumor suppressors or inducing the degradation of oncogene products (Huang and Dixit, 2016). The posterchild of successful therapeutics targeting the Ub system is bortezomib (Velcade), which blocks proteasomal degradation of ubiquitinated substrates and is an effective treatment for multiple myeloma (Hideshima et al., 2001). Other efforts have instead targeted the stability of individual proteins. For example, inhibitors of the E3 ligase MDM2 show great promise in preventing p53 ubiquitination, thus rescuing it from degradation (Vassilev et al., 2004). Inhibitors have also been designed to specifically block USP7, a deubiquitinase that would otherwise protect MDM2 from Ub-mediated degradation (Kategaya et al., 2017; Lamberto et al., 2017; Pozhidaeva et al., 2017; Turnbull et al., 2017; Gavory et al., 2018). In an alternative approach, protein-targeting chimeric molecules (PROTACs) can be used to induce the degradation of target proteins by recruiting an E3 Ub ligase (Coleman and Crews, 2018). Thus, we are entering a new era of biomedical research centered around controlling the Ub system as a means to correct disease states.

The development of small molecule modulators of ubiquitination activities hinges upon the availability of robust high-throughput screens (HTS) (Macarrón and Hertzberg, 2009). Currently, screens for DUB activity are much more advanced than those for Ub conjugation. The most widely used substrates for high-throughput DUB assays are Ub-AMC or Ub-Rhodamine, which fluoresce only after cleavage (Dang et al., 1998; Hassiepen et al., 2007). Newer classes of mono- or di-ubiquitin substrates contain a *bona fide* isopeptide linkage and allow for reaction monitoring through either fluorescence polarization (FP) or FRET (Ye et al., 2011; Geurink et al., 2012, 2016; Keusekotten et al., 2013). Still, the available DUB substrates for HTS are very simplified, and do not always accurately reflect the genuine ubiquitinated substrate. In the case of Ub conjugation, screens are much less standardized. It seems that no single method can be applied universally to measure the activities of E1, E2, or E3 enzymes (Sun, 2005; Krist et al., 2016; Foote et al., 2017; Park et al., 2017). Further, most assays require a development step which precludes any kinetic measurement in real time (Sun, 2005; De Cesare et al., 2018). A robust and universal HTS to monitor inhibition or activation along each point in the E1-E2-E3 enzyme cascade would be extremely enabling for both mechanistic studies of Ub transfer as well as small molecule modulator screens.

We present a simple HTS, which we term "UbiReal," that can track all stages of Ub conjugation and deconjugation in real time. Using fluorescently-labeled Ub, we show that every step of the Ub cascade can be measured by FP in a low volume, high-throughput format. Specifically, we demonstrate the utility of UbiReal for measuring E1 activation, E2∼Ub discharge and specificity, E3-dependent Ub chain formation, and DUB-dependent hydrolysis. We highlight the utility of UbiReal for studying small molecule modulators by recapitulating the IC_{50} value of the E1 inhibitor PYR-41 (Yang et al., 2007), as well as for answering basic biochemical questions such as E2-E3 pairing and Ub chain specificity. With minimal adjustment, we are confident that this assay could be applied to any E1/E2/E3/DUB system across both Ub and Ub-like (e.g., NEDD8 or SUMO1/2/3) signaling systems, enabling real time measurement of enzyme activities.

METHODS

Protein Expression and Purification

Fluorescein-Ub (F-Ub), labeled at all primary amines, was purchased from Boston Biochem (U-590). TAMRA-Ub (T-Ub), labeled only at the amino-terminus, was a kind gift from P. Geurink (Leiden University Medical Centre). Wild-type and mutant Ub proteins were prepared according to Pickart and Raasi (2005) with slight modifications. Briefly, Ub was expressed from the pET-17b vector by autoinduction at 37°C for 48 h. Cells were resuspended in 25 mM Tris (pH 8.0), 200 mM sodium chloride and lysed by sonication. The clarified lysate was acidified with perchloric acid to a final concentration of 0.5% v/v. Some Ub mutants were more sensitive to acid precipitation, and in these cases the acid content was limited to 0.2%. The soluble fraction from the acid precipitation was dialyzed into 50 mM sodium acetate (pH 5.0), loaded onto a HiPrep SP FF 16/10 ion exchange column (GE Life Sciences), and eluted with a linear gradient to 500 mM sodium chloride. Ub-containing fractions were pooled, concentrated using an Amicon centrifugal filter (3K MWCO, EMD Millipore), and further purified with a HiLoad Superdex 75 pg size exclusion column equilibrated in 25 mM sodium phosphate (pH 7.4), 150 mM sodium chloride. Purified Ub fractions were pooled, concentrated, and flash frozen for storage at −80°C.

Human E1 (UBE1) was purified by activation to a GST-Ub column, according to Gladkova et al. (2018). UBE2D3, UBE2L3, UBE2N, and NEDD4L were purified from the pGEX6P-1 vector following overnight induction at 18°C with 0.2 mM IPTG. Cells were resuspended in 25 mM Tris (pH 8.0), 200 mM sodium chloride, 2 mM ß-mercaptoethanol and lysed by sonication. The clarified lysate was applied to glutathione agarose resin (Pierce) and washed according to the manufacturer's recommendations. E2s were eluted from the resin by overnight cleavage with GST-3C protease at 4°C, and the resulting protein was dialyzed into 25 mM sodium phosphate (pH 7.4), 150 mM sodium chloride, 1 mM DTT, flash frozen, and stored at −80°C. NleL was purified according to Hospenthal et al. (2013). E4BU was purified according to Nordquist et al. (2010). USP21 was purified according to Ye et al. (2011) with the SUMO tag left intact. OTUB1* and AMSH* were purified according to Michel et al. (2015). ChlaDUB1 was purified according to Pruneda et al. (2016). All proteins were quantified by absorbance at 280 nm.

General Assay Parameters

T-Ub assays were monitored using fluorescence polarization (FP) on a BMG LabTech ClarioStar instrument using settings suitable for the TAMRA fluorophore with an excitation wavelength of 540 nm, an LP 566 nm dichroic mirror, and an emission wavelength of 590 nm. F-Ub assays were similarly monitored, with an excitation wavelength of 482 nm, an LP 504 nm dichroic

mirror, and an emission wavelength of 530 nm. FP experiments were typically 1–2 h in length and FP values were read every 30–60 s with 20 flashes per sample well, unless otherwise noted. FP experiments were performed using Greiner 384-well small-volume HiBase microplates, with samples in 25 mM sodium phosphate (pH 7.4), 150 mM sodium chloride, 10 mM $MgCl_2$ at a final volume of 20 μL unless otherwise noted.

Generally, depending on the assay, a master starting solution was prepared with each component shared by all samples in the assay (e.g., E1, $MgCl_2$, T-Ub), and distributed to each sample well. The master solution components were calculated so that desired concentrations would be achieved in a final 20 μL volume and a volume of <20 μL master solution could be added to each well. Then, the experimental components (e.g., inhibitors, E2s, ATP, etc.) or buffer were added to sample wells such that the final desired volume of 20 μL was achieved.

Complete UbiReal Curve Generation

T-Ub at a final concentration of 100 nM in 25 mM sodium phosphate (pH 7.4), 150 mM sodium chloride, 10 mM $MgCl_2$ and 5 mM ATP was monitored for 17 cycles. After cycle 17, E1 was added to a final concentration of 125 nM and monitored. After cycle 34, UBE2D3 was added to a final concentration of 300 nM and monitored. After cycle 57, NleL was next added to a final concentration of 700 nM and monitored. After cycle 78, unlabeled WT Ub was added to a final concentration of 25 μM and monitored. Finally, after cycle 124, USP21 was added to a final concentration of 250 nM and monitored to cycle 150. FP readings were paused prior to the addition of protein, and resumed after protein had been added to the sample wells. The UbiReal curve shown is the average of two identical sample wells and is representative of several experiments.

E1 Inhibition

0.5 μL of E1 inhibitor PYR-41 (Sigma-Aldrich, N2915) dissolved in DMSO at various dilutions was added to sample wells containing 125 nM E1 and 100 nM T-Ub to final PYR-41 concentrations of 75, 50, 33, 25, 20, 16, 10, 8, 6, 2.5, or 0.5 μM. FP was briefly monitored for 10 cycles before initiating the E1∼Ub charging reaction with a 1 μL addition of ATP to a final concentration of 5 mM. FP was continuously monitored for approximately 1 h, at which point it had stabilized. An uninhibited control sample that received 0.5 μL of DMSO instead of PYR-41 was used to determine the maximal E1∼Ub charging FP signal.

To determine the inhibition of the E1, the FP values for each PYR-41-treated sample were normalized to its starting FP signal before ATP addition (0% activity), and to the final signal of the uninhibited DMSO control, which served as the maximum FP signal in the assay (100% activity). The initial signal in each sample was determined by averaging the 10 values before ATP addition, and the final signal for each sample was determined by averaging the final 10 values. Each sample was prepared in triplicate, and the experiment was performed separately 3 times.

To construct the IC_{50} curve, the unnormalized FP values were used. The final 10 FP values for each sample were averaged and this was used as the final value to plot against the PYR-41 concentration. This was done for each of the 3 separate experiments as before, giving 3 values at each concentration except the 33 μM PYR-41 sample, which had 2 final values. The non-linear regression calculation in GraphPad Prism was used to fit the curve and calculate the final IC_{50} value.

E2 Amino Acid Reactivity

Master solutions resulting in final concentrations of 25 mM sodium phosphate (pH 7.4), 150 mM sodium chloride, 100 nM F-Ub, 10 mM $MgCl_2$, 125 nM E1 and either 5 mM ATP or no ATP were incubated at RT for 10 min before addition to sample wells. FP was monitored for 5 cycles before addition of either UBE2D3 or UBE2L3 to a final concentration of 300 nM, while a subset of UBE2D3 samples also received an addition of E4BU to a final concentration of 2.5 μM. Samples next received an addition of either no amino acid (buffer alone), lysine, or cysteine to a final concentration of 0, 37.5 mM, or 37.5 mM, respectively. Samples were monitored by FP for approximately 2 h.

E3 Ligase Assay

A master solution resulting in final concentrations of 25 mM sodium phosphate (pH 7.4), 150 mM sodium chloride, 10 mM $MgCl_2$, 100 nM T-Ub, 125 nM E1, 2 μM E2 (UBE2D3 or UBE2N) and 2 μM E3 NEDD4L, or a master solution lacking E3 NEDD4L as a control, was added to sample wells. Samples then received a 3 μL addition of either 250 μM WT Ub, lysine-less Ub, methylated Ub, one of the seven Ub K-only mutants, or one of the seven K-R Ub mutants, resulting in a final concentration of 37.5 μM unlabeled Ub in each sample well. The control lacking NEDD4L received WT Ub. FP was monitored for 5 cycles, before initiating the Ub cascade with a 1 μL addition of ATP to a final concentration of 5 mM. FP was monitored for an additional 75 cycles over the course of approximately 2 h. Each sample was prepared in triplicate, with the FP values averaged at each timepoint. The FP value at each time point was normalized to the average of the sample's initial 5 FP values before ATP addition (0% activity), and to the final 5 FP values of the WT Ub sample (100% activity).

DUB Treatment

Ub chains were created in a master solution resulting in final concentrations of 25 mM sodium phosphate (pH 7.4), 150 mM sodium chloride, 10 mM $MgCl_2$, 100 nM T-Ub, 125 nM E1, 2 μM E2 UBE2D3, 2 μM E3 NEDD4L, 50 μM WT Ub, and 5 mM ATP, or a master solution lacking ATP as a control. The master solutions were incubated at 37°C for 1 h while shaking at 500 rpm, and then distributed into sample wells containing a final concentration of 10 mM DTT. FP signal was monitored for 10 cycles before DUB addition.

DUBs were incubated at room temperature for 15 min in 25 mM sodium phosphate (pH 7.4), 150 mM sodium chloride, 10 mM DTT, and 30 mM EDTA. After incubation, DUBs were added to the sample wells containing NEDD4L-generated Ub/T-Ub ubiquitination products. In this assay AMSH had a final concentration of 250 nM, while ChlaDUB1, OTUB1, OTULIN, and USP21 had final concentrations of 600 nM. Following DUB

addition, deubiquitination was monitored for approximately 2 h. The FP values at each timepoint were normalized to the sample's averaged FP value prior to DUB addition (0% activity), and to a corresponding control sample that contained all components except for ATP, representing an unconjugated Ub signal (100% activity).

Data Analysis

Data was first analyzed using the MARS data analysis software from BMG LABTECH. The fluorescence polarization values were calculated by the MARS software using the equation:

$$\boldsymbol{FP} = 1000 \times \frac{\parallel - \perp}{\parallel + \perp} \quad (1)$$

where ∥ and ⊥ are the measured values from the parallel and perpendicular channels, respectively, both in units of mP. Averages and standard deviations of FP data were calculated and plotted using GraphPad Prism.

Z′ values were calculated for each assay according to the equation:

$$\boldsymbol{Z'} = 1 - \frac{(3\sigma_{c+} + 3\sigma_{c-})}{|u_{c+} - u_{c-}|} \quad (2)$$

where μ_{c+} and μ_{c-} are the means of the positive and negative controls, respectively, and σ_{c+} and σ_{c-} are the standard deviations of the positive and negative controls, respectively.

RESULTS

FP is a sensitive measure of a molecule's tumbling behavior in solution. Though primarily used to study protein-protein interactions, previous studies using FP to discriminate monomeric Ub from polyUb chains (Ye et al., 2011; Keusekotten et al., 2013; von Delbrück et al., 2016; Mot et al., 2018) led us to reason that FP could be used to monitor the passage of fluorescent Ub through the entire ubiquitination cascade (**Figure 1A**). Using Ub labeled with tetramethylrhodamine (TAMRA) at its amino-terminus (T-Ub), we could show that conjugation onto the E1 active site resulted in a large shift in FP (**Figure 1B**, step 1). Addition of the E2 Ub-conjugating enzyme UBE2D3 led to rapid formation of the E2∼Ub conjugate, with an intermediate molecular weight and corresponding FP value (**Figure 1B**, step 2). Subsequent addition of the bacterial HECT-type E3 ligase NleL resulted in a modest increase in FP (**Figure 1B**, step 3), which dramatically increased over time following the addition of excess unlabeled Ub into the system (**Figure 1B**, step 4). These Ub modifications (most likely polyUb) could then be removed with the nonspecific DUB USP21, which was evident by a decrease in FP value with time (**Figure 1B**, step 5). Thus, the entire Ub conjugation and deconjugation cycle could be observed in real time simply by tracking the FP of labeled Ub. Our subsequent work with this method focused on analyzing the discrete steps of Ub conjugation and deconjugation to evaluate the utility of UbiReal for measuring activity and specificity.

Focusing first on Ub activation, we measured E1 activity in response to increasing concentrations of the previously described chemical inhibitor PYR-41 (Yang et al., 2007). By incubating E1 with PYR-41 and subsequently initiating the reaction with ATP (**Figure 2A**, step 1), E1∼T-Ub complex formation could be monitored over time (**Figure 2A**). Data were normalized to FP values before ATP addition (0%) and to the endpoint of the DMSO-only control (100%). Effects of PYR-41 addition could be observed as a loss in activity ranging from no to complete inhibition (**Figure 2A**). We noted a moderate degree of variability in our FP measurements, possibly arising from the addition of DMSO, but still calculated an overall Z' value of 0.59 [a measure of signal-to-noise in HTS where values in the range of 0.5–1.0 are considered "excellent" (Zhang et al., 1999)]. E1 activities reported by our assay showed a logarithmic trend with increasing concentration of PYR-41 (**Figure 2B**). Using a non-linear regression, an IC_{50} value for inhibition of E1∼Ub conjugation by PYR-41 under our assay conditions was determined to be 9.15 μM (**Figure 2C**), in agreement with previously reported values (Yang et al., 2007).

Gel-based Ub discharge assays have been used previously to measure the ability of E2 enzymes to transfer Ub onto free amino acids as a simplified model for substrates (Wenzel et al., 2011; Pruneda et al., 2012; Buetow et al., 2018). Using Ub labeled with fluorescein at all primary amines (F-Ub), amino acid reactivity and specificity were measured for the E2 enzymes UBE2D3 and UBE2L3 (**Figure 3A**). Using activated E2∼F-Ub as a starting material, the free amino acids Cys and Lys were added and discharge was measured as the return to unconjugated F-Ub FP values over time (**Figures 3B,C**). As expected from previous work (Wenzel et al., 2011), UBE2D3 demonstrated the ability to transfer F-Ub to both Cys and Lys amino acids (**Figure 3B**), whereas UBE2L3 was largely Cys-specific (**Figure 3C**), indicating that it cannot directly ubiquitinate substrate Lys residues but must act through a HECT/RBR E3 intermediary. As an E2 that can directly ubiquitinate Lys residues, UBE2D3 functions with RING/U-box E3 ligases to efficiently transfer Ub. Addition of the U-box E3 ligase E4BU to the UBE2D3∼F-Ub conjugate already promoted discharge of the thioester linkage (**Figure 3B**, step 1), and in the presence of free Lys resulted in an enhanced rate of Ub transfer (**Figure 3B**, step 2) as observed in previous gel-based assays (Pruneda et al., 2012). Overall, the UbiReal method provided a straightforward approach for observing the specificity and activation of E2 Ub-conjugating enzymes.

E3 ligases traditionally facilitate the final transfer of Ub onto a substrate, but even in the absence of substrate, E3s will often autoubiquitinate themselves or form free Ub chains *in vitro*. Gel-based assays typically report this activity as a "smear" of Ub modifications in the high molecular weight range that is difficult to reliably quantify. As shown in **Figure 1B**, the UbiReal approach can be used to monitor E3 ligase activity, particularly after the addition of excess unlabeled Ub that continually builds high molecular weight products that contain T-Ub. Using a different HECT-type E3 ligase, NEDD4L, we could again show robust ubiquitination activity that builds with time (**Figure 4A**). Importantly, this activity was dependent upon known E2-E3 specificity (Kamadurai et al., 2009), as UBE2D3 could generate

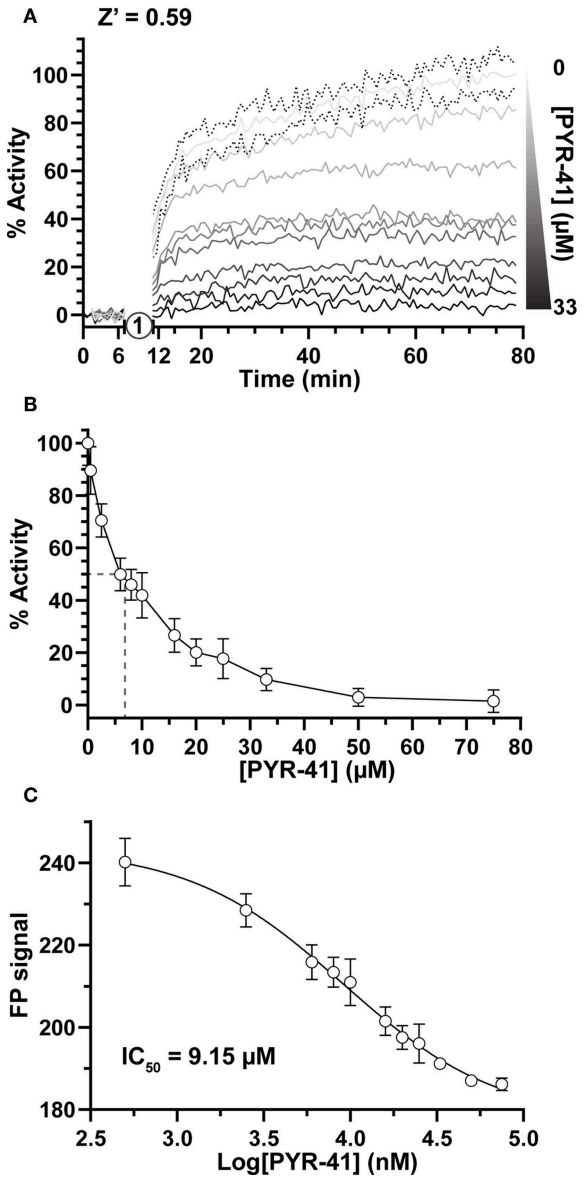

FIGURE 2 | Small molecule inhibition of E1 Ub-activating activity. **(A)** E1∼T-Ub complex inhibition by PYR-41 monitored over time with the UbiReal assay. "1" indicates the addition of ATP to initiate formation of the E1∼T-Ub complex. Increasing concentrations of PYR-41 correspond to reduced E1∼T-Ub complex formation, represented by % Activity. Data points are normalized to FP values after PYR-41 addition, but before ATP addition, and to the FP signal from samples treated with DMSO instead of PYR-41, representing 100% activity. Connected lines represent Mean values, while representative error of ± SD is shown for the 0 μM PYR-41 (DMSO addition) sample. Data are the average of 3 technical replicates for each concentration and representative of all PYR-41 inhibition experiments. **(B)** Inhibition of E1∼T-Ub complex by PYR-41 represented using the end-point FP values at each PYR-41 concentration. The dashed lines represent the approximate PYR-41 concentration at which 50% E1∼T-Ub complex inhibition occurs. Data are normalized as in **(A)**. Data are from 3 separate experiments that each include 3 technical replicates for all PYR-41 concentrations (see section Methods). Data are reported as Mean ± SD. **(C)** IC_{50} graph generated using the end-point FP values as in **(B)**. Data was fitted and an IC_{50} value was calculated using a non-linear regression in GraphPad Prism. Data are from the same experiments as **(B)**, with data reported as Mean ± SD.

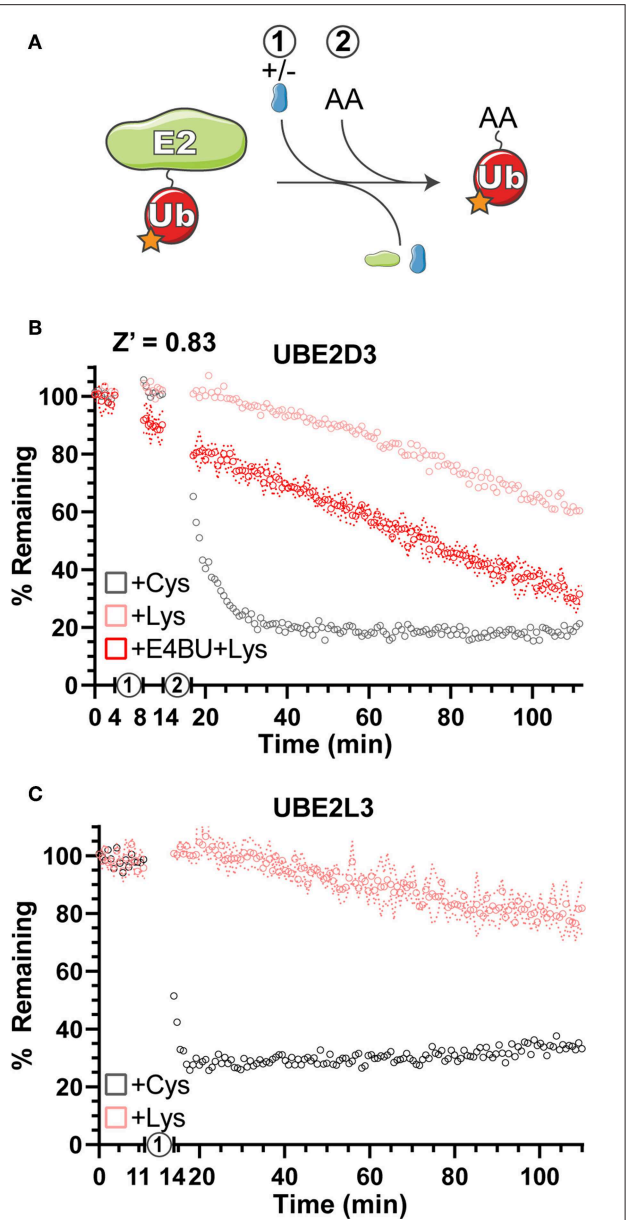

FIGURE 3 | Amino acid reactivity and activation of E2 Ub-conjugating enzymes. **(A)** Reaction schematic depicting E2∼F-Ub discharge onto a substrate amino acid (AA). **(B)** Monitoring discharge of the E2 Ub-conjugating enzyme UBE2D3 from E2∼F-Ub to Lys∼F-Ub or Cys∼F-Ub using UbiReal. "1" indicates the addition of ± E4BU, and "2" indicates the addition of amino acid. Samples are monitored over time, and data are normalized to samples not treated with amino acid (100% remaining) and samples with amino acid but lacking ATP (0% remaining). Data are reported as the Mean values from an experiment with 3 technical replicates, and representative error of Mean ± SD is reported for the UBE2D3+E4BU+Lys sample. **(C)** Discharge of UBE2L3∼F-Ub to Lys∼F-Ub or Cys∼F-Ub over time. "1" represents the addition of amino acid. Data are reported and normalized as in **(B)**, with representative error reported for the UBE2L3+Lys sample.

large ubiquitinated products with NEDD4L but not UBE2N, an E2 that typically functions with UBE2V2 and RING/U-box ligases (**Figure 4A**).

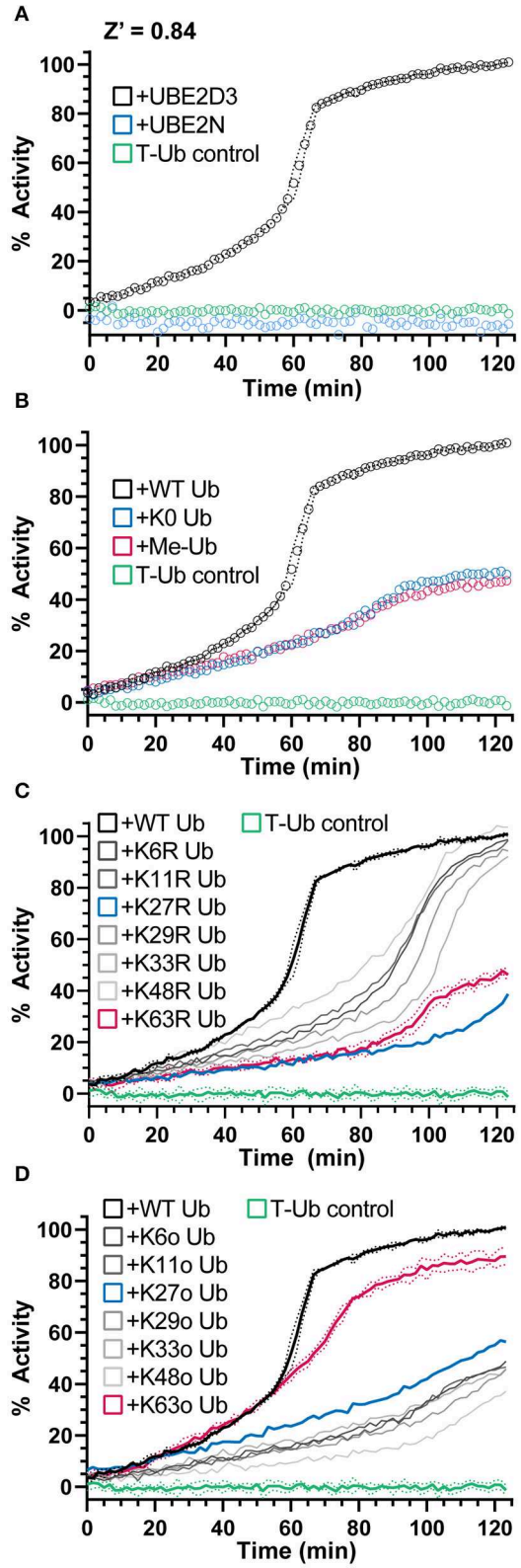

FIGURE 4 | NEDD4L E3 polyUb ligation and chain specificity. **(A)** Ub chain ligation by K63-chain specific NEDD4L and the E2 enzyme UBE2D3 or UBE2N monitored over time using UbiReal. Reactions are initiated with ATP at *(Continued)*

FIGURE 4 | time 0. Data for each sample is normalized to its starting FP value before ATP addition (0% activity) and to the final values of the NEDD4L+UBE2D3+WT Ub sample (100% activity). Data are reported as the Mean from an experiment with 3 technical replicates, with representative error reported as Mean ± SD for the NEDD4L+UBE2D3+WT Ub sample. Data for this and subsequent panels were collected together, and the UBE2D3 and T-Ub data are included as positive and negative controls, respectively, in the panels to follow. **(B)** Monitoring polyUb vs. monoUb formation by NEDD4L and UBE2D3 over time. Reactions are initiated with ATP at time 0. K0 Ub is a mutant lacking all Lys; Me-Ub is methylated at each primary amine. Data are reported and normalized as in **(A)**. **(C)** Ub chain ligation by NEDD4L and UBE2D3 over time using a mutant KR Ub panel that has individual Lys residues mutated to Arg (K63R has every Lys except K63, etc.). Reactions are initiated with ATP at time 0. Data are reported and normalized as in **(A)**, with representative error reported as Mean ± SD for some samples. **(D)** The same experiment as **(C)**. but using a mutant Ko Ub panel that contain only a single Lys residue, with all other Lys mutated to Arg (K63o contains only K63, etc.). Data are reported and normalized as in **(A)**, with representative error reported as Mean ± SD for some samples.

NEDD4L, as a HECT-type E3 ligase, controls the context of the final ubiquitinated product, i.e., mono- vs. polyubiquitination as well as the Ub chain specificity (Kim and Huibregtse, 2009). As the bulk of the ligase-dependent ubiquitination signal develops after an influx of unlabeled Ub, we sought this opportunity to instead supplement mutated Ub that could inform on the type of Ub modification. By supplementing the reaction with K0 Ub (in which all seven Lys residues are mutated to Arg) or Me-Ub (in which all primary amines have been methylated), the FP signal rose to only 50% of that observed with WT Ub (**Figure 4B**). Interestingly, this result suggested that approximately half of the FP signal originated from mono- or multi-mono-autoubiquitination, with the remaining activity originating from chain-building activity of NEDD4L.

To probe the type of polyUb chain formation observed in the NEDD4L reaction, two additional sets of mutated Ub were used. The first set consists of all possible Lys-to-Arg mutants, each eliminating one potential site of chain linkage (e.g., K63R). As expected for the K63-specific ligase NEDD4L, addition of the K63R mutant Ub decreased the ubiquitination signal to levels consistent with the K0 Ub control, whereas most other Lys-to-Arg mutants had little effect on product formation (**Figures 4B,C**). Interestingly, the K27R mutant Ub also produced less ubiquitination signal and could indicate a local disruption in the Ub structure (K27 is the most buried of all Lys) or in some interaction with the conjugation machinery. The second set consists of Ub K-only mutants, in which six of the seven Lys residues have been mutated to Arg leaving only one behind (e.g., K63o). With this panel, only the K63o mutant could generate a ubiquitination signal similar to WT, whereas all other mutants behaved like the K0 Ub control (**Figures 4B,D**). Together, these experiments confirm the K63 specificity of NEDD4L (Maspero et al., 2013) and illustrate the utility of the UbiReal approach for studying E3 ligase activity.

In our initial experiments addressing the measurement of DUB activity, we observed an incomplete reduction in FP signal using the DUB USP21 (**Figure 1B**, step 5), though we expected

the non-specific activity of USP21 toward both mono- and polyubiquitination (Hospenthal et al., 2015) to return the FP signal to unconjugated T-Ub values (**Figure 1A**) To understand the discrepancy, several control experiments were prepared to observe the behavior of USP21 under our assay conditions. The Ub conjugation assay components (T-Ub, E1, UBE2D3, NEDD4L, and WT Ub) were incubated with or without ATP, and this was used as the starting substrate to which each DUB was added. Interestingly, when combined with the –ATP sample that could not support Ub conjugation, the USP21-treated sample increased in FP over time, most likely a result of noncovalent interactions between T-Ub and USP21 (**Figure 5A**). The +ATP sample treated with USP21 decreased to the same FP value as the –ATP sample by the end of the time course, indicating that complete deubiquitination had occurred (**Figure 5A**). For other DUBs like ChlaDUB1, an effector protein from *Chlamydia trachomatis* that preferentially cleaves K63 chains (Pruneda et al., 2016), the background present in the –ATP samples was not as significant as for USP21 (**Figure 5A**), but a –ATP sample was prepared nonetheless for each DUB in subsequent experiments to control for potential background binding. These experiments established a key foundation for the following DUB assays, but also suggest that USP21 most likely suffers from product inhibition resulting from a high affinity for free Ub, as has previously been shown for USP2 (Renatus et al., 2006).

UbiCRest is a powerful method that has been used to determine the type of ubiquitination present in a sample through treatment with Ub chain-specific DUBs (Hospenthal et al., 2015). Though normally interpreted using a gel-based readout, we applied the UbiCRest strategy to NEDD4L-generated ubiquitination in order to detect DUB activity through the release of T-Ub. Using AMSH, an endosome-associated DUB that preferentially cleaves K63 chains, cleavage of the NEDD4L assembly was observed to approximately 40% remaining FP signal, and when combined with USP21, complete cleavage was observed (**Figure 5B**). This result suggested that while AMSH can cleave the K63-linked polyUb, it cannot remove monoUb modifications which likely account for the ∼40% remaining signal (consistent with **Figure 4B**). ChlaDUB1 alone cleaved the Ub assembly to around 20% remaining, and together with USP21 could completely remove all modifications (**Figure 5B**). This suggested that ChlaDUB1, unlike AMSH, appears to be more promiscuous toward monoubiquitination. K48-specific OTUB1 and Met1-specific OTULIN were used as negative controls that should not have deubiquitinating activity toward NEDD4L-generated chains, and the slight drift observed in these samples could be an experimental artifact or low-level cleavage (**Figure 5B**). Taken altogether, the UbiCRest approach for characterizing ubiquitination in our assay was effective at identifying both the amount and type of polyUb present.

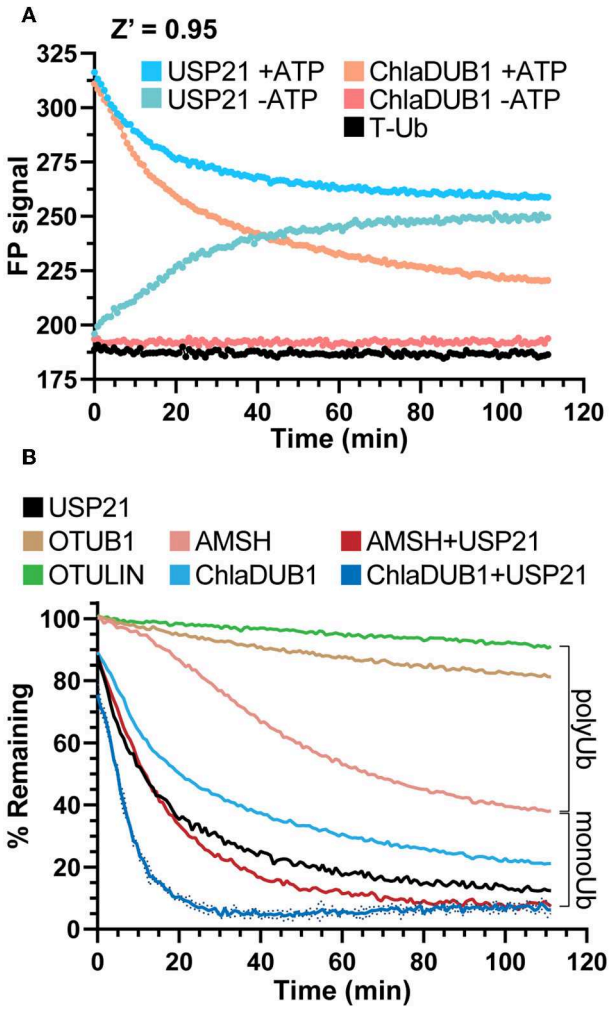

FIGURE 5 | DUB activity and UbiCRest analysis of polyUb chain types. **(A)** Monitoring deubiquitination over time with DUBs USP21 and ChlaDUB1 using UbiReal. Curves show the raw FP signal of USP21 or ChlaDUB1 activity against samples containing a NEDD4L ligation mixture ± ATP. +ATP samples represent DUB activity against NEDD4L-generated chains while –ATP samples represent background FP signal where no ligation activity could occur. Reactions were initiated by addition of the DUB at time 0. +ATP samples are reported as the Mean of 3 technical replicates while –ATP samples are a representative single sample. **(B)** Monitoring deubiquitination over time with DUBs USP21, OTUB1, OTULIN, ChlaDUB1 ± USP21, and AMSH ± USP21. The polyUb and monoUb brackets indicate the observed contributions of monoUb and polyUb in the NEDD4L ligation mixture. Data are from the same assay as **(A)**. and are reported in the same manner, with representative error reported as Mean ± SD for the ChlaDUB1+USP21 sample.

DISCUSSION

In an effort to address a longstanding need for a robust HTS for Ub conjugation, we have designed and tested UbiReal as a real-time assay for monitoring all ubiquitination activities. UbiReal uses commercially-available fluorescently-labeled Ub to track the progression through E1, E2, and E3 enzymes by the molecular weight and resulting fluorescence polarization changes associated with each step. Using this approach, ubiquitination activities can be observed in a highly parallel manner that consumes remarkably little material (on the order of 10 ng of labeled Ub per reaction). Unlike other more specialized approaches, UbiReal offers a universal method

that allows the user to directly observe each consecutive step of Ub conjugation, from the E1 through to the E2, E3, and substrate ubiquitination. Furthermore, the ubiquitination products assembled using this method provide a more complex, realistic substrate that can be used to monitor DUB activity. In our trials, we found that UbiReal was able to provide both quantitative measurements of activity as well as qualitative insights into mechanisms and specificities of Ub transfer.

As a test of its power to assay small molecule modulators, we used UbiReal to monitor the inhibition of E1 Ub-activating function in response to the PYR-41 inhibitor. In a dose-response experiment, we determined the IC_{50} of PYR-41 to be 9.15 μM, consistent with the reported estimation of <10 μM from a radioactive gel-based assay (Yang et al., 2007) and a fluorescent activity-based probe assay (An and Statsyuk, 2013). We chose to analyze this experiment as an endpoint assay as PYR-41 is an irreversible inhibitor, but the same experiment provides kinetic information as well and could easily be used to measure effects of competitive inhibitors on initial velocity. From our experimental control data, we determined Z' values in the range of 0.59–0.95 for all of our directed UbiReal experiments measuring E1, E2, E3, and DUB activities, indicating that under these conditions UbiReal provides excellent signal-to-noise ratios that are compatible with HTS. With minor adjustments, we expect that the UbiReal approach could be an effective HTS for any regulator of ubiquitination.

The UbiReal method was also useful for determining several qualitative aspects of Ub conjugation and deconjugation. Simplified amino acid reactivity assays provide a straightforward measure of E2 enzyme activity, and we showed that UbiReal is able to recapitulate both the reactivity profiles of several E2 enzymes as well as the reactivity enhancement mediated by RING/U-box E3 ligases. By supplementing the reaction with unlabeled Ub, we observed robust E3 ligase activity in the form of autoubiquitination. By changing the nature of the supplemented Ub, we were able to distinguish mono- vs. polyubiquitination as well as determine the preferred Ub chain type. To corroborate this chain type determination, we applied a simplified UbiCRest approach to our assay in order to observe which chain-specific DUBs could reduce the FP of our samples back to a monoUb value. Just as in the gel-based UbiCRest approach, by treating with DUBs singly or in combination, we observed complete, partial, or negligible collapse of FP values that indicate both the chain type and mono- vs. polyUb architecture present in our complex ubiquitinated sample. These proof-of-principle studies indicate the applicability of UbiReal across the entire Ub cascade. Though we focused on aspects of Ub transfer specificity, the same approach could be used to study the mechanisms of Ub transfer, for example by incorporating structure-guided mutations. As an alternative to conventional gel-based assays, UbiReal can provide quantitative information in less time with less material. Furthermore, by separating each stage of Ub transfer, in one assay the user can isolate the precise step (e.g., E2∼Ub formation vs. discharge) that is affected by perturbations such as mutations or small molecule modulators.

Existing HTS for Ub conjugation have primarily focused on observation of the final ubiquitinated substrate. The bulk of these methods rely on either direct detection of Ub following enrichment of substrate (e.g., ELISA), or detection of Ub in close proximity to substrate (e.g., FRET or AlphaScreen). Because these assays are specialized for detecting ubiquitinated substrate, they are not well-suited for monitoring each stage of Ub conjugation separately. Fluorescence polarization provides the unique opportunity to track Ub based on its tumbling rate in solution vis-à-vis its molecular weight. This approach has been used to track different aspects of the Ub system before. By either placing the label on the substrate or the Ub itself, E2- or E3-mediated polyUb chain formation has been observed by increasing FP (von Delbrück et al., 2016; Mot et al., 2018). Specialized Ub substrates can also be used to directly monitor the activities of HECT- or RBR-family E3 ligases by FP, in the absence of E1 or E2 enzymes (Krist et al., 2016; Park et al., 2017). DUB activities have been measured using defined, fluorescently-labeled Ub chains (Ye et al., 2011; Keusekotten et al., 2013). Interestingly, FP has even been used to track the proteasomal degradation of ubiquitinated substrates (Bhattacharyya et al., 2016). It is based on these observations that we developed UbiReal as a generalized approach to observe all consecutive steps of both Ub conjugation and deconjugation in real time.

As with any method, UbiReal does have certain caveats. The most glaring is the dependence on large differences in molecular weight that are required for significant changes in FP. In particular, size similarities between E2, E3, or substrate proteins could pose challenges. One solution to this problem could be to incorporate protein tags, such as GST, to shift molecular weights. A second caveat to our approach is the location of the fluorophore. Though labeling the amino-terminus is routine practice and practically inert for most purposes, it obviously precludes the formation of Met1-linked polyUb. In this case, we expect that the label could instead be conjugated through maleimide chemistry to a Cys residue introduced at, for example, position 20 (von Delbrück et al., 2016). Our tests with two varieties of fluorescent Ub (F-Ub and T-Ub) suggest that other dyes and sites of attachment will also be amenable to UbiReal. Lastly, we recognize that our ability to track fluorescent Ub through each stage of the conjugation process requires a molar excess of conjugating enzymes, which may preclude certain applications of the method. However, if the desired readout does not depend on observing each transfer event (e.g., E2∼Ub formation vs. polyUb formation), the concentrations of each enzyme component can be tuned to suit the reaction requirements.

In sum, we present a simple method that addresses a need for a universal HTS for Ub conjugating activity. UbiReal requires no specialized reagents, only a fluorescently-labeled Ub which is readily available in multiple forms. With only minor optimization, we were able to apply the UbiReal method to measure E1, E2, E3, and DUB activities in separate, controlled experiments. We believe that the robust and scalable nature of this assay will make it useful in HTS for small molecule modulators, and its convenience and quantitative nature makes

it a compelling alternative to the conventional gel-based assays for mechanistic work.

DATA AVAILABILITY STATEMENT

The datasets generated for this study are available on request to the corresponding author.

AUTHOR CONTRIBUTIONS

TF and JP conceptualized the approach, analyzed the data, and wrote the manuscript. TF performed all experiments.

FUNDING

TF was supported by 5T32GM071338-14, Program in Molecular and Cellular Biosciences. JP was supported by Oregon Health & Science University.

ACKNOWLEDGMENTS

The authors would like to thank members of the Pruneda Lab for reagents and discussion, and P. Geurink (Leiden University Medical Centre) for providing the TAMRA-Ub reagent.

REFERENCES

An, H., and Statsyuk, A. V. (2013). Development of activity-based probes for ubiquitin and ubiquitin-like protein signaling pathways. *J. Am. Chem. Soc.* 135, 16948–16962. doi: 10.1021/ja4099643

Bhattacharyya, S., Renn, J. P., Yu, H., Marko, J. F., and Matouschek, A. (2016). An assay for 26S proteasome activity based on fluorescence anisotropy measurements of dye-labeled protein substrates. *Anal. Biochem.* 509, 50–59. doi: 10.1016/j.ab.2016.05.026

Buetow, L., Gabrielsen, M., and Huang, D. T. (2018). Single-turnover RING/U-Box E3-mediated lysine discharge assays. *Methods Mol. Biol.* 1844, 19–31. doi: 10.1007/978-1-4939-8706-1_2

Clague, M. J., Heride, C., and Urbé, S. (2015). The demographics of the ubiquitin system. *Trends Cell Biol.* 25, 417–426. doi: 10.1016/j.tcb.2015.03.002

Coleman, K. G., and Crews, C. M. (2018). Proteolysis-targeting chimeras: harnessing the ubiquitin-proteasome system to induce degradation of specific target proteins. *Annu. Rev. Cancer Biol.* 2, 41–58. doi: 10.1146/annurev-cancerbio-030617-050430

Dang, L. C., Melandri, F. D., and Stein, R. L. (1998). Kinetic and mechanistic studies on the hydrolysis of ubiquitin C-terminal 7-amido-4-methylcoumarin by deubiquitinating enzymes. *Biochemistry* 37, 1868–1879. doi: 10.1021/bi9723360

De Cesare, V., Johnson, C., Barlow, V., Hastie, J., Knebel, A., and Trost, M. (2018). The MALDI-TOF E2/E3 Ligase assay as universal tool for drug discovery in the ubiquitin pathway. *Cell Chem. Biol.* 25, 1117–1127.e4. doi: 10.1016/j.chembiol.2018.06.004

Foote, P. K., Krist, D. T., and Statsyuk, A. V. (2017). High-throughput screening of HECT E3 ubiquitin ligases using UbFluor. *Curr. Protoc. Chem. Biol.* 9, 174–195. doi: 10.1002/cpch.24

Gavory, G., O'Dowd, C. R., Helm, M. D., Flasz, J., Arkoudis, E., Dossang, A., et al. (2018). Discovery and characterization of highly potent and selective allosteric USP7 inhibitors. *Nat. Chem. Biol.* 14, 118–125. doi: 10.1038/nchembio.2528

Geurink, P. P., El Oualid, F., Jonker, A., Hameed, D. S., and Ovaa, H. (2012). A general chemical ligation approach towards isopeptide-linked ubiquitin and ubiquitin-like assay reagents. *Chem. Bio. Chem.* 13, 293–297. doi: 10.1002/cbic.201100706

Geurink, P. P., van Tol, B. D. M., van Dalen, D., Brundel, P. J. G., Mevissen, T. E. T., Pruneda, J. N., et al. (2016). Development of diubiquitin-based FRET probes to quantify ubiquitin linkage specificity of deubiquitinating enzymes. *Chem. Bio. Chem.* 17, 816–820. doi: 10.1002/cbic.201600017

Gladkova, C., Maslen, S. L., Skehel, J. M., and Komander, D. (2018). Mechanism of parkin activation by PINK1. *Nature* 559, 410–414. doi: 10.1038/s41586-018-0224-x

Hassiepen, U., Eidhoff, U., Meder, G., Bulber, J.-F., Hein, A., Bodendorf, U., et al. (2007). A sensitive fluorescence intensity assay for deubiquitinating proteases using ubiquitin-rhodamine110-glycine as substrate. *Anal. Biochem.* 371, 201–207. doi: 10.1016/j.ab.2007.07.034

Hideshima, T., Richardson, P., Chauhan, D., Palombella, V. J., Elliott, P. J., Adams, J., et al. (2001). The proteasome inhibitor PS-341 inhibits growth, induces apoptosis, and overcomes drug resistance in human multiple myeloma cells. *Cancer Res.* 61, 3071–3076.

Hospenthal, M. K., Freund, S. M. V., and Komander, D. (2013). Assembly, analysis and architecture of atypical ubiquitin chains. *Nat. Struct. Mol. Biol.* 20, 555–565. doi: 10.1038/nsmb.2547

Hospenthal, M. K., Mevissen, T. E. T., and Komander, D. (2015). Deubiquitinase-based analysis of ubiquitin chain architecture using Ubiquitin Chain Restriction (UbiCRest). *Nat. Protoc.* 10, 349–361. doi: 10.1038/nprot.2015.018

Hu, H., and Sun, S. C. (2016). Ubiquitin signaling in immune responses. *Cell Res.* 26, 457–483. doi: 10.1038/cr.2016.40

Huang, X., and Dixit, V. M. (2016). Drugging the undruggables: exploring the ubiquitin system for drug development. *Cell Res.* 26, 484–498. doi: 10.1038/cr.2016.31

Kamadurai, H. B., Souphron, J., Scott, D. C., Duda, D. M., Miller, D. J., Stringer, D., et al. (2009). Insights into ubiquitin transfer cascades from a structure of a UbcH5B approximately ubiquitin-HECT(NEDD4L) complex. *Mol. Cell* 36, 1095–1102. doi: 10.1016/j.molcel.2009.11.010

Kategaya, L., Di Lello, P., Rougé, L., Pastor, R., Clark, K. R., Drummond, J., et al. (2017). USP7 small-molecule inhibitors interfere with ubiquitin binding. *Nature* 550, 534–538. doi: 10.1038/nature24006

Keusekotten, K., Elliott, P. R., Glockner, L., Fiil, B. K., Damgaard, R. B., Kulathu, Y., et al. (2013). OTULIN antagonizes LUBAC signaling by specifically hydrolyzing Met1-linked polyubiquitin. *Cell* 153, 1312–1326. doi: 10.1016/j.cell.2013.05.014

Kim, H. C., and Huibregtse, J. M. (2009). Polyubiquitination by HECT E3s and the determinants of chain type specificity. *Mol. Cell Biol.* 29, 3307–3318. doi: 10.1128/MCB.00240-09

Kirkin, V., and Dikic, I. (2011). Ubiquitin networks in cancer. *Curr. Opin. Genet. Dev.* 21, 21–28. doi: 10.1016/j.gde.2010.10.004

Komander, D., and Rape, M. (2012). The ubiquitin code. *Annu. Rev. Biochem.* 81, 203–229. doi: 10.1146/annurev-biochem-060310-170328

Krist, D. T., Park, S., Boneh, G. H., Rice, S. E., and Statsyuk, A. V. (2016). UbFluor: A mechanism-based probe for HECT E3 ligases. *Chem. Sci.* 7, 5587–5595. doi: 10.1039/C6SC01167E

Lamberto, I., Liu, X., Seo, H.-S., Schauer, N. J., Iacob, R. E., Hu, W., et al. (2017). Structure-guided development of a potent and selective non-covalent active-site inhibitor of USP7. *Cell Chem. Biol.* 24, 1490–1500.e11. doi: 10.1016/j.chembiol.2017.09.003

Macarrón, R., and Hertzberg, R. P. (2009). Design and implementation of high-throughput screening assays. *Methods Mol. Biol.* 565, 1–32. doi: 10.1007/978-1-60327-258-2_1

Maspero, E., Valentini, E., Mari, S., Cecatiello, V., Soffientini, P., Pasqualato, S., et al. (2013). Structure of a ubiquitin-loaded HECT ligase reveals the molecular basis for catalytic priming. *Nat. Struct. Mol. Biol.* 20, 696–701. doi: 10.1038/nsmb.2566

Michel, M. A., Elliott, P. R., Swatek, K. N., Simicek, M., Pruneda, J. N., Wagstaff, J. L., et al. (2015). Assembly and specific recognition of k29- and k33-linked polyubiquitin. *Mol. Cell* 58, 95–109. doi: 10.1016/j.molcel.2015.01.042

Mot, A. C., Prell, E., Klecker, M., Naumann, C., Faden, F., Westermann, B., et al. (2018). Real-time detection of N-end rule-mediated ubiquitination via fluorescently labeled substrate probes. *New Phytol.* 217, 613–624. doi: 10.1111/nph.14497

Nordquist, K. A., Dimitrova, Y. N., Brzovic, P. S., Ridenour, W. B., Munro, K. A., Soss, S. E., et al. (2010). Structural and functional characterization

of the monomeric U-box domain from E4B. *Biochemistry* 49, 347–355. doi: 10.1021/bi901620v

Park, S., Foote, P. K., Krist, D. T., Rice, S. E., and Statsyuk, A. V. (2017). UbMES and UbFluor: novel probes for ring-between-ring (RBR) E3 ubiquitin ligase PARKIN. *J. Biol. Chem.* 292, 16539–16553. doi: 10.1074/jbc.M116.773200

Pickart, C. M., and Raasi, S. (2005). Controlled synthesis of polyubiquitin chains. *Meth. Enzymol.* 399, 21–36. doi: 10.1016/S0076-6879(05)99002-2

Popovic, D., Vucic, D., and Dikic, I. (2014). Ubiquitination in disease pathogenesis and treatment. *Nat. Med.* 20, 1242–1253. doi: 10.1038/nm.3739

Pozhidaeva, A., Valles, G., Wang, F., Wu, J., Sterner, D. E., Nguyen, P., et al. (2017). USP7-Specific inhibitors target and modify the enzyme's active site via distinct chemical mechanisms. *Cell Chem. Biol.* 24, 1501–1512.e5. doi: 10.1016/j.chembiol.2017.09.004

Pruneda, J. N., Durkin, C. H., Geurink, P. P., Ovaa, H., Santhanam, B., Holden, D. W., et al. (2016). The Molecular basis for ubiquitin and ubiquitin-like specificities in bacterial effector proteases. *Mol. Cell* 63, 261–276. doi: 10.1016/j.molcel.2016.06.015

Pruneda, J. N., Littlefield, P. J., Soss, S. E., Nordquist, K. A., Chazin, W. J., Brzovic, P. S., et al. (2012). Structure of an E3:E2∼Ub complex reveals an allosteric mechanism shared among RING/U-box ligases. *Mol. Cell* 47, 933–942. doi: 10.1016/j.molcel.2012.07.001

Renatus, M., Parrado, S. G., D'Arcy, A., Eidhoff, U., Gerhartz, B., Hassiepen, U., et al. (2006). Structural basis of ubiquitin recognition by the deubiquitinating protease USP2. *Structure* 14, 1293–1302. doi: 10.1016/j.str.2006.06.012

Sun, Y. (2005). Overview of approaches for screening for ubiquitin ligase inhibitors. *Meth. Enzymol.* 399, 654–663. doi: 10.1016/S0076-6879(05)99043-5

Swatek, K. N., and Komander, D. (2016). Ubiquitin modifications. *Cell Res.* 26, 399–422. doi: 10.1038/cr.2016.39

Turnbull, A. P., Ioannidis, S., Krajewski, W. W., Pinto-Fernandez, A., Heride, C., Martin, A. C. L., et al. (2017). Molecular basis of USP7 inhibition by selective small-molecule inhibitors. *Nature* 550, 481–486. doi: 10.1038/nature24451

Vassilev, L. T., Vu, B. T., Graves, B., Carvajal, D., Podlaski, F., Filipovic, Z., et al. (2004). *In vivo* activation of the p53 pathway by small-molecule antagonists of MDM2. *Science* 303, 844–848. doi: 10.1126/science.1092472

von Delbrück, M., Kniss, A., Rogov, V. V., Pluska, L., Bagola, K., Löhr, F., et al. (2016). The CUE domain of Cue1 aligns growing ubiquitin chains with Ubc7 for rapid elongation. *Mol. Cell* 62, 918–928. doi: 10.1016/j.molcel.2016.04.031

Wenzel, D. M., Lissounov, A., Brzovic, P. S., and Klevit, R. E. (2011). UBCH7 reactivity profile reveals parkin and HHARI to be RING/HECT hybrids. *Nature* 474, 105–108. doi: 10.1038/nature09966

Yang, Y., Kitagaki, J., Lorick, K. L., Ludwig, R. L., Pierre, S. A., Jensen, J. P., et al. (2007). Inhibitors of ubiquitin-activating enzyme (E1), a new class of potential cancer therapeutics. *Cancer Res.* 67, 9472–9481. doi: 10.1158/0008-5472.CAN-07-0568

Ye, Y., Akutsu, M., Reyes-Turcu, F., Enchev, R. I., Wilkinson, K. D., and Komander, D. (2011). Polyubiquitin binding and cross-reactivity in the USP domain deubiquitinase USP21. *EMBO Rep.* 12, 350–357. doi: 10.1038/embor.2011.17

Zhang, J., Chung, T., and Oldenburg, K. (1999). A simple statistical parameter for use in evaluation and validation of high throughput screening assays. *J. Biomol. Screen.* 4, 67–73. doi: 10.1177/108705719900400206

Zheng, Q., Huang, T., Zhang, L., Zhou, Y., Luo, H., Xu, H., et al. (2016). Dysregulation of ubiquitin-proteasome system in neurodegenerative diseases. *Front. Aging Neurosci.* 8:303. doi: 10.3389/fnagi.2016.00303

Conflict of Interest: The authors declare that the research was conducted in the absence of any commercial or financial relationships that could be construed as a potential conflict of interest.

frontiers in Chemistry

MINI REVIEW
published: 10 December 2019
doi: 10.3389/fchem.2019.00849

Targeted Protein Degradation by Chimeric Small Molecules, PROTACs and SNIPERs

Mikihiko Naito, Nobumichi Ohoka, Norihito Shibata and Yoshinori Tsukumo*

Laboratory Molecular Target and Gene Therapy Products, National Institute of Health Sciences, Kawasaki, Japan

Technologies that induce targeted protein degradation by small molecules have been developed recently. Chimeric small molecules such as Proteolysis Targeting Chimeras (PROTACs) and Specific and Non-genetic IAP-dependent Protein Erasers (SNIPERs), and E3 modulators such as thalidomides, hijack the cellular machinery for ubiquitylation, and the ubiquitylated proteins are subjected to proteasomal degradation. This has motivated drug development in industry and academia because "undruggable targets" can now be degraded by targeted protein degradation.

Keywords: PROTAC, SNIPER, E3 modulator, ubiquitin, proteasome, protein degradation

OPEN ACCESS

Edited by:
Monique P. C. Mulder, Leiden University Medical Center, Netherlands

Reviewed by:
Kyung Bo Kim, University of Kentucky, United States
Andrea Testa, University of Dundee, United Kingdom

****Correspondence:***
Mikihiko Naito
miki-naito@nihs.go.jp

Specialty section:
This article was submitted to Chemical Biology, a section of the journal Frontiers in Chemistry

Received: *20 September 2019*
Accepted: *21 November 2019*
Published: *10 December 2019*

Citation:
Naito M, Ohoka N, Shibata N and Tsukumo Y (2019) Targeted Protein Degradation by Chimeric Small Molecules, PROTACs and SNIPERs. Front. Chem. 7:849. doi: 10.3389/fchem.2019.00849

MODALITIES OF RECENT DRUG DEVELOPMENT

Development of a therapeutic antibody and a small molecule inhibitor is the most successful strategy to develop novel molecular target drugs these days (Nelson et al., 2010; Ferguson and Gray, 2018). The targets for antibodies include tumor specific antigens such as human epidermal growth factor receptor 2 (HER2) expressed on breast cancer cells that is recognized by Trastuzumab, and immune suppressive molecules such as programmed death-1 (PD-1) and programmed death-ligand 1 (PD-L1) recognized by Nivolmab and Pembrolizumab, respectively. However, antibodies cannot penetrate into cells, and therefore, target molecules for antibodies are limited to cell surface and extracellular proteins. In contrast, small molecule inhibitors can penetrate into cells and effectively inhibit the function of target proteins, such as kinases and proteases. However, developing small molecule inhibitors against proteins that do not possess enzymatic activity is challenging. Therefore, many intracellular proteins without enzymatic activity are unable to be targeted by antibodies and small molecule inhibitors, and they are sometimes called "undruggable targets." These include scaffold proteins, transcription factors and splicing factors, and account for more than 70% of the proteins expressed in cells.

Accumulating evidence suggests that inducing protein degradation by small molecules represents a promising approach to make "undruggable targets" druggable. There are reports that small molecules, thalidomides and sulfonamides, induce the degradation of "undruggable targets" such as transcription factors (Ikaros and Aiolos) (Krönke et al., 2014; Lu et al., 2014) and a splicing factor (RBM39/CAPERα) (Han et al., 2017; Uehara et al., 2017). Technologies to induce protein degradation by chimeric molecules, Proteolysis Targeting Chimeras (PROTACs) and Specific and Non-genetic IAP-dependent Protein Erasers (SNIPERs), have been developed, which enables rational design of degrader molecules against target proteins of interest. This mini-review provides an overview of the protein degradation technologies.

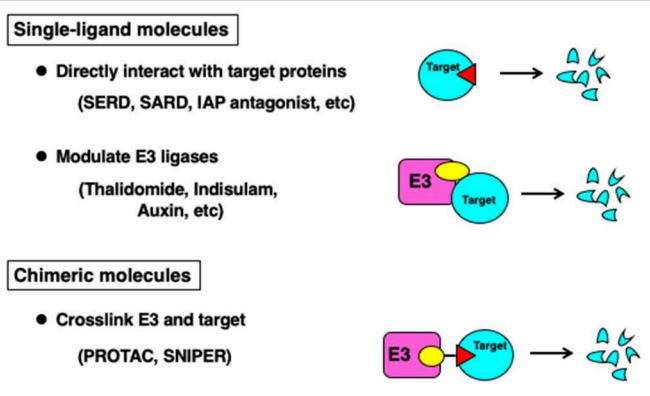

FIGURE 1 | Classification of degrader molecules.

CLASSIFICATION OF DEGRADER MOLECULES

Small molecules that induce degradation of target proteins can be classified into three groups depending on the structure of the compounds and their mode of action (**Figure 1**). The first class is a single-ligand molecule that directly interacts with the target protein to induce degradation. This class of molecules include fulvestrant, a selective estrogen receptor downregulator (SERD) against estrogen receptor-α (ERα) (Osborne et al., 2004) which is approved in the clinic against breast cancers expressing ERα, and a selective androgen receptor downregulator (SARD) against androgen receptor (AR) (Omlin et al., 2015) currently under clinical evaluation. These downregulators are likely to recapitulate the degradation mechanism reported as hydrophobic tagging (Neklesa et al., 2011). Another example in this class is inhibitor of apoptosis protein (IAP) antagonists (Fulda and Vucic, 2012) that induce degradation of cIAP1/2, and some compounds are under clinical development. In addition, Boc3Arg-linked ligands that localize target proteins directly to the 20S proteasome are also grouped in this class (Shi et al., 2016). Thus, molecules in this class can effectively induce degradation of target proteins; however, the number of the proteins targeted for degradation is limited.

The second class of molecules is the single-ligand molecules that interact with E3 ubiquitin ligases to modulate substrate selectivity. This class of molecules is known as E3 modulators and molecular glues. Thalidomide was the first E3 modulator identified and interacts with CRBN (Ito et al., 2010), a substrate recognition subunit of the Cullin-RING-ubiquitin ligase (CRL) complex. Thalidomide and an analog lenalidomide induce the degradation of transcription factors Ikaros and Aiolos (Krönke et al., 2014; Lu et al., 2014). Modification of the side chain of thalidomide alters substrate selectivity, and lenalidomide and CC-885 induce ubiquitylation and degradation of casein kinase 1α (CK1α) (Krönke et al., 2015) and a translation termination factor GSPT1 (Matyskiela et al., 2016), respectively. Sulfonamides such as Indisulam and E7820 are reported to interact with DCAF15, another substrate recognition subunit of the CRL complex, and induce the ubiquitylation and degradation of a splicing factor RBM39/CAPERα (Han et al., 2017; Uehara et al., 2017). Plant hormones including auxin and gibberellin are also categorized in this class. Auxin interacts with F-box proteins TIR1 and AFB2 in the SCF ubiquitin ligase complex, and recruits a transcriptional repressor to be ubiquitylated and degraded by the proteasome, which in turn activates the expression of auxin-responsive genes (Dharmasiri et al., 2005; Kepinski and Leyser, 2005).

The third class is a chimeric molecule, where an E3 ligand and a target ligand are conjugated to form one molecule. This class of molecules was developed under different names such as PROTACs and SNIPERs, but they are designed to crosslink the target protein and an E3 ubiquitin ligase to induce the degradation of the target protein, and therefore, their mode of action is almost identical.

DEVELOPMENT OF CHIMERIC DEGRADER MOLECULES

The first PROTAC reported came from the laboratories of Crews and Deshaies by using a peptide sequence recognized by an F-box protein β-TRCP to recruit the E3 ubiquitin ligase complex involving β-TRCP (Sakamoto et al., 2001). This PROTAC induces ubiquitylation and degradation of a target protein MetAP-2 in an *in vitro* cell-free system, but cannot penetrate into cells efficiently. In collaboration with Ciulli, Crews et al. developed small molecule ligands for VHL (Buckley et al., 2012a,b), and developed small molecule PROTACs (Bondeson et al., 2015; Buckley et al., 2015). These PROTACs induce degradation of various target proteins at nanomolar or sub-nanomolar concentrations in cell culture systems and induce the degradation of target proteins in *in vivo* xenograft models.

We have studied IAP family proteins that are frequently overexpressed in cancer cells and found that a small molecule methyl bestatin (MeBS) induces auto-ubiquitylation and proteasomal degradation of cIAP1 (Sekine et al., 2008). By using MeBS as a ligand for cIAP1, we developed the first SNIPER that induced the degradation of cellular retinoic acid binding protein II (CRABP2) (Itoh et al., 2010). The activity of SNIPERs was then markedly improved by adopting high affinity ligands for IAPs, and the improved SNIPERs at nanomolar concentrations effectively induced degradation of target proteins by recruiting XIAP and cIAP1 (Ohoka et al., 2017, 2018). Some of the SNIPERs were demonstrated to induce degradation of target proteins in an *in vivo* xenograft model, which results in antitumor activity.

Handa et al. reported that CRBN is the direct target of thalidomide that has teratogenic activity (Ito et al., 2010). Bradner et al. then developed another family of chimeric molecules containing thalidomide as a ligand for CRBN that induce degradation of bromo domain proteins (Winter et al., 2015). The thalidomide-based chimeric molecules also induce degradation of target proteins at nanomolar concentrations and show activity

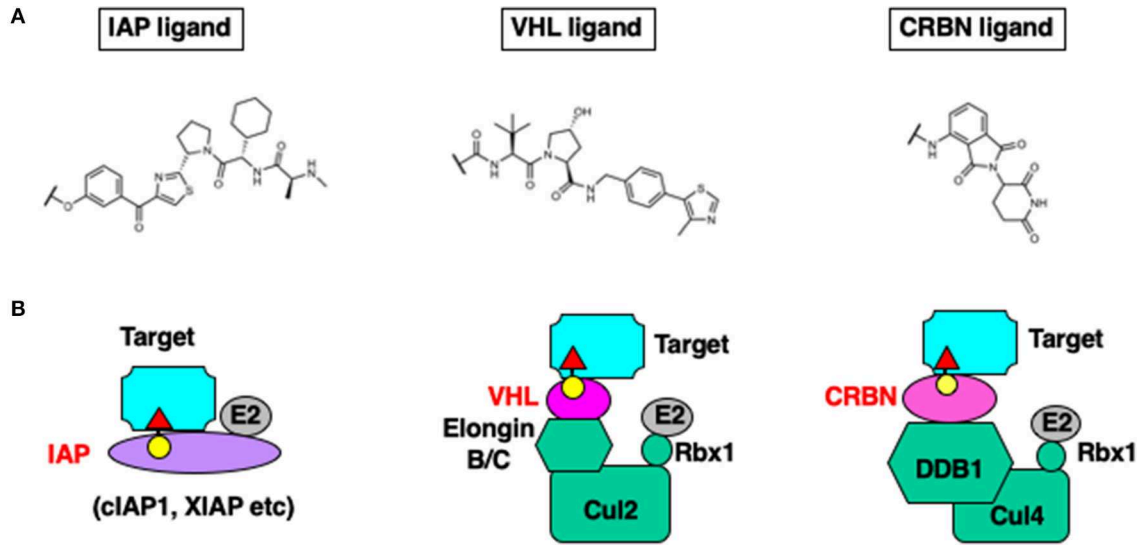

FIGURE 2 | Chemical structure of the E3 ligands **(A)**, and the E3 ligase complexes hijacked by chimeric degraders **(B)**.

in an *in vivo* xenograft model. **Figure 2** illustrates the E3 ligands and ubiquitin ligase complexes recruited to target proteins.

FEATURES OF THE CHIMERIC DEGRADER MOLECULES

Because of the modular structure of chimeric degrader molecules, it is possible to rationally design and develop a novel degrader molecule against a protein of interest by substituting the target ligand. The target ligand does not need to inhibit the activity of the target protein, and therefore, a poor inhibitor that has insufficient activity to inhibit the target protein can be converted to a potent degrader when incorporated into chimeric degrader molecules. Theoretically, a ligand that interacts with any domain of the target protein can effectively capture the target to induce degradation. A higher binding affinity of the target ligand is preferable (Ohoka et al., 2018); however, some target proteins cooperatively interact with E3 ligases in the presence of chimeric molecules (Gadd et al., 2017), implying that low affinity ligands can also be used to develop potent chimeric degraders.

There are only a few E3 ligases among the more than 600 E3 ligases in cells that can currently be successfully recruited to target proteins for degradation. It should be noted that recruiting different E3 ubiquitin ligases to the same target protein results in different degradation potencies (Lai et al., 2016; Shibata et al., 2018), suggesting that finding the best combination of target protein and E3 ligase is important in the development of potent degraders. In this context, it is important to expand the repertoire of E3 ligands to recruit a wide variety of E3 ligases to target proteins. Some of the E3 ubiquitin ligases are expressed in a tissue specific and tumor specific manner. If such an E3 ligase can be recruited to target proteins, we anticipate that degradation of target proteins will be restricted to a tissue type or only tumor cells, which could be more advantageous in terms of selective toxicity. The number of E3 ligands is gradually increasing (Lu et al., 2018; Spradlin et al., 2019; Ward et al., 2019; Zhang X. et al., 2019) but they require improvement to induce degradation at lower concentrations. Recently, cells resistant against PROTACs have been reported (Zhang L. et al., 2019), and the resistance mechanism resides in the alteration of the ubiquitylation machinery rather than the target proteins. To overcome such resistance, it is possible to recruit different E3 ubiquitin ligases to restore the degradation of the target proteins, which further accentuates the importance of developing novel E3 ligands.

CHIMERIC DEGRADER MOLECULES AS PROBES TO UNDERSTAND THE UBIQUITIN CODE

Although ubiquitin was originally identified as an essential factor to induce proteasomal degradation of many proteins, it is widely accepted that ubiquitin plays a role in a variety of cellular phenomena, such as internalization of membrane proteins, autophagy, DNA repair, and signal transduction. The diversity in the linkage and modification of the ubiquitin chain, which is called the ubiquitin code, is assumed to be recognized by different decoder molecules that may mediate different cellular responses (Komander and Rape, 2012). To understand the ubiquitin code in more detail, it would be useful to write a ubiquitin code by chimeric molecules recruiting different E3 ubiquitin ligases to determine whether different cellular responses could be induced by different ubiquitin codes encrypted by various E3 ubiquitin ligases. For this purpose, ubiquitylation of tagged-proteins with chimeric degraders could provide a comprehensive system to

ubiquitylate a variety of target proteins (Neklesa et al., 2011; Natsume et al., 2016; Hattori et al., 2017; Nabet et al., 2018; Okitsu et al., 2018).

CONCLUSION

Technologies to induce targeted protein degradation have been established recently. These technologies are useful for developing novel drugs, and have promoted a number of drug development research programs by pharmaceutical companies, bio-ventures, and academia. The results of the first clinical phase I studies of PROTACs (ARV-110 against AR and ARV-471 against ER) were released recently demonstrating acceptable safety profiles. However, these technologies are still in their infancy and have significant room for improvement. These technologies should be further refined, and ultimately applied to clinical drug development as well as basic research to understand the ubiquitin biology.

AUTHOR CONTRIBUTIONS

MN, NO, NS, and YT wrote and checked the manuscript.

FUNDING

This work was supported in part by grants from the Japan Society for the Promotion of Science (KAKENHI Grants JP18K06567 to NO, and JP16H05090, JP16K15121, and JP18H05502 to MN) and the Japan Agency for Medical Research and Development (AMED Grants JP18ak0101073 and JP18im0210616 to MN, and JP17cm0106124 and JP18ak0101073 to NO).

ACKNOWLEDGMENTS

We thank the Edanz Group (www.edanzediting.com/ac) for editing a draft of this manuscript.

REFERENCES

Bondeson, D. P., Mares, A., Smith, I. E., Ko, E., Campos, S., Miah, A. H., et al. (2015). Catalytic *in vivo* protein knockdown by small-molecule PROTACs. *Nat. Chem. Biol.* 11, 611–617. doi: 10.1038/nchembio.1858

Buckley, D. L., Gustafson, J. L., Van Molle, I., Roth, A. G., Tae, H. S., Gareiss, P. C., et al. (2012a). Small-molecule inhibitors of the interaction between the E3 ligase VHL and HIF1α. *Angew. Chem. Int. Ed. Engl.* 51, 11463–11467. doi: 10.1002/anie.201206231.

Buckley, D. L., Raina, K., Darricarrere, N., Hines, J., Gustafson, J. L., Smith, I. E., et al. (2015). HaloPROTACS: use of small molecule PROTACs to induce degradation of halotag fusion proteins. *ACS Chem. Biol.* 10, 1831–1837. doi: 10.1021/acschembio.5b00442

Buckley, D. L., Van Molle, I., Gareiss, P. C., Tae, H. S., Michel, J., Noblin, D. J., et al. (2012b). Targeting the von Hippel-Lindau E3 ubiquitin ligase using small molecules to disrupt the VHL/HIF-1α interaction. *J. Am. Chem. Soc.* 134, 4465–4468. doi: 10.1021/ja209924v

Dharmasiri, N., Dharmasiri, S., and Estelle, M. (2005). The F-box protein TIR1 is an auxin receptor. *Nature* 435, 441–445. doi: 10.1038/nature03543

Ferguson, F. M., and Gray, N. S. (2018). Kinase inhibitors: the road ahead. *Nat. Rev. Drug Discov.* 17, 353–377. doi: 10.1038/nrd.2018.21

Fulda, S., and Vucic, D. (2012). Targeting IAP proteins for therapeutic intervention in cancer. *Nat. Rev. Drug Discov.* 11, 109–124. doi: 10.1038/nrd3627

Gadd, M. S., Testa, A., Lucas, X., Chan, K. H., Chen, W., Lamont, D. J., et al. (2017). Structural basis of PROTAC cooperative recognition for selective protein degradation. *Nat. Chem. Biol.* 13, 514–521. doi: 10.1038/nchembio.2329

Han, T., Goralski, M., Gaskill, N., Capota, E., Kim, J., Ting, T. C., et al. (2017). Anticancer sulfonamides target splicing by inducing RBM39 degradation via recruitment to DCAF15. *Science*. 356:eaal3755. doi: 10.1126/science.aal3755

Hattori, T., Okitsu, K., Yamazaki, N., Ohoka, N., Shibata, N., Misawa, T., et al. (2017). Simple and efficient knockdown of His-tagged proteins by ternary molecules consisting of a His-tag ligand, a ubiquitin ligase ligand, and a cell-penetrating peptide. *Bioorg. Med. Chem. Lett.* 27, 4478–4481. doi: 10.1016/j.bmcl.2017.08.001

Ito, T., Ando, H., Suzuki, T., Ogura, T., Hotta, K., Imamura, Y., et al. (2010). Identification of a primary target of thalidomide teratogenicity. *Science* 327, 1345–1350. doi: 10.1126/science.1177319

Itoh, Y., Ishikawa, M., Naito, M., and Hashimoto, Y. (2010). Protein knockdown using methyl bestatin-ligand hybrid molecules: design and synthesis of inducers of ubiquitination-mediated degradation of cellular retinoic acid-binding proteins. *J. Am. Chem. Soc.* 132, 5820–5826. doi: 10.1021/ja100691p

Kepinski, S., and Leyser, O. (2005). The Arabidopsis F-box protein TIR1 is an auxin receptor. *Nature* 435, 446–451. doi: 10.1038/nature03542

Komander, D., and Rape, M. (2012). The ubiquitin code. *Annu. Rev. Biochem.* 81, 203–229. doi: 10.1146/annurev-biochem-060310-170328

Krönke, J., Fink, E. C., Hollenbach, P. W., MacBeth, K. J., Hurst, S. N., Udeshi, N. D., et al. (2015). Lenalidomide induces ubiquitination and degradation of CK1alpha in del(5q) MDS. *Nature* 523, 183–188. doi: 10.1038/nature14610

Krönke, J., Udeshi, N. D., Narla, A., Grauman, P., Hurst, S. N., McConkey, M., et al. (2014). Lenalidomide causes selective degradation of IKZF1 and IKZF3 in multiple myeloma cells. *Science* 343, 301–305. doi: 10.1126/science.1244851

Lai, A. C., Toure, M., Hellerschmied, D., Salami, J., Jaime-Figueroa, S., Ko, E., et al. (2016). Modular PROTAC design for the degradation of oncogenic BCR-ABL. *Angew. Chem. Int. Ed. Engl.* 55, 807–810. doi: 10.1002/anie.201507634

Lu, G., Middleton, R. E., Sun, H., Naniong, M., Ott, C. J., Mitsiades, C. S., et al. (2014). The myeloma drug lenalidomide promotes the cereblon-dependent destruction of Ikaros proteins. *Science* 343, 305–309. doi: 10.1126/science.1244917

Lu, M., Liu, T., Jiao, Q., Ji, J., Tao, M., Liu, Y., et al. (2018). Discovery of a Keap1-dependent peptide PROTAC to knockdown Tau by ubiquitination-proteasome degradation pathway. *Eur. J. Med. Chem.* 146, 251–259. doi: 10.1016/j.ejmech.2018.01.063

Matyskiela, M. E., Lu, G., Ito, T., Pagarigan, B., Lu, C. C., Miller, K., et al. (2016). A novel cereblon modulator recruits GSPT1 to the CRL4(CRBN) ubiquitin ligase. *Nature* 535, 252–257. doi: 10.1038/nature18611

Nabet, B., Roberts, J. M., Buckley, D. L., Paulk, J., Dastjerdi, S., Yang, A., et al. (2018). The dTAG system for immediate and target-specific protein degradation. *Nat. Chem. Biol.* 14, 431–441. doi: 10.1038/s41589-018-0021-8

Natsume, T., Kiyomitsu, T., Saga, Y., and Kanemaki, M. T. (2016). Rapid protein depletion in human cells by auxin-inducible degron tagging with short homology donors. *Cell Rep.* 15, 210–218. doi: 10.1016/j.celrep.2016.03.001

Neklesa, T. K., Tae, H. S., Schneekloth, A. R., Stulberg, M. J., Corson, T. W., Sundberg, T. B., et al. (2011). Small-molecule hydrophobic tagging-induced degradation of HaloTag fusion proteins. *Nat. Chem. Biol.* 7, 538–543. doi: 10.1038/nchembio.597

Nelson, A. L., Dhimolea, E., and Reichert, J. M. (2010). Development trends for human monoclonal antibody therapeutics. *Nat. Rev. Drug Discov.* 9, 767–774. doi: 10.1038/nrd3229

Ohoka, N., Morita, Y., Nagai, K., Shimokawa, K., Ujikawa, O., Fujimori, I., et al. (2018). Derivatization of inhibitor of apoptosis protein (IAP) ligands yields improved inducers of estrogen receptor alpha degradation. *J. Biol. Chem.* 293, 6776–6790. doi: 10.1074/jbc.RA117.001091

Ohoka, N., Okuhira, K., Ito, M., Nagai, K., Shibata, N., Hattori, T., et al. (2017). *In vivo* knockdown of pathogenic proteins via specific and nongenetic inhibitor of apoptosis protein (IAP)-dependent protein erasers (SNIPERs). *J. Biol. Chem.* 292, 4556–4570. doi: 10.1074/jbc.M116.768853

Okitsu, K., Hattori, T., Misawa, T., Shoda, T., Kurihara, M., Naito, M., et al. (2018). Development of a small hybrid molecule that mediates degradation of his-tag fused proteins. *J. Med. Chem.* 61, 576–582. doi: 10.1021/acs.jmedchem.7b00413

Omlin, A., Jones, R. J., van der Noll, R., Satoh, T., Niwakawa, M., Smith, S. A., et al. (2015). AZD3514, an oral selective androgen receptor down-regulator in patients with castration-resistant prostate cancer - results of two parallel first-in-human phase I studies. *Invest. New Drugs.* 33, 679–690. doi: 10.1007/s10637-015-0235-5

Osborne, C. K., Wakeling, A., and Nicholson, R. I. (2004). Fulvestrant: an oestrogen receptor antagonist with a novel mechanism of action. *Br. J. Cancer* 90(Suppl. 1), S2–S6. doi: 10.1038/sj.bjc.6601629

Sakamoto, K. M., Kim, K. B., Kumagai, A., Mercurio, F., Crews, C. M., and Deshaies, R. J. (2001). Protacs: chimeric molecules that target proteins to the Skp1-Cullin-F box complex for ubiquitination and degradation. *Proc. Natl. Acad. Sci. U.S.A.* 98, 8554–8559. doi: 10.1073/pnas.141230798

Sekine, K., Takubo, K., Kikuchi, R., Nishimoto, M., Kitagawa, M., Abe, F., et al. (2008). Small molecules destabilize cIAP1 by activating auto-ubiquitylation. *J. Biol. Chem.* 283, 8961–8968. doi: 10.1074/jbc.M709525200

Shi, Y., Long, M. J., Rosenberg, M. M., Li, S., Kobjack, A., Lessans, P., et al. (2016). Boc3Arg-linked ligands induce degradation by localizing target proteins to the 20S proteasome. *ACS Chem. Biol.* 11, 3328–3337. doi: 10.1021/acschembio.6b00656

Shibata, N., Shimokawa, K., Nagai, K., Ohoka, N., Hattori, T., Miyamoto, N., et al. (2018). Pharmacological difference between degrader and inhibitor against oncogenic BCR-ABL kinase. *Sci. Rep.* 8:13549. doi: 10.1038/s41598-018-31913-5

Spradlin, J. N., Hu, X., Ward, C. C., Brittain, S. M., Jones, M. D., Ou, L., et al. (2019). Harnessing the anti-cancer natural product nimbolide for targeted protein degradation. *Nat. Chem. Biol.* 15, 747–755. doi: 10.1038/s41589-019-0304-8

Uehara, T., Minoshima, Y., Sagane, K., Sugi, N. H., Mitsuhashi, K. O., Yamamoto, N., et al. (2017). Selective degradation of splicing factor CAPERalpha by anticancer sulfonamides. *Nat. Chem. Biol.* 13, 675–680. doi: 10.1038/nchembio.2363

Ward, C. C., Kleinman, J. I., Brittain, S. M., Lee, P. S., C., Chung, Y. S., Kim, K., et al. (2019). Covalent ligand screening uncovers a RNF4 E3 ligase recruiter for targeted protein degradation applications. *ACS Chem. Biol.* 14, 2430–2440. doi: 10.1021/acschembio.8b01083

Winter, G. E., Buckley, D. L., Paulk, J., Roberts, J. M., Souza, A., Dhe-Paganon, S., et al. (2015). Drug development. Phthalimide conjugation as a strategy for *in vivo* target protein degradation. *Science* 348, 1376–1381. doi: 10.1126/science.aab1433

Zhang, L., Riley-Gillis, B., Vijay, P., and Shen, Y. (2019). Acquired resistance to BET-PROTACs (proteolysis-targeting chimeras) caused by genomic alterations in core components of E3 ligase complexes. *Mol. Cancer Ther.* 18, 1302–1311. doi: 10.1158/1535-7163.MCT-18-1129

Zhang, X., Crowley, V. M., Wucherpfennig, T. G., Dix, M. M., and Cravatt, B. F. (2019). Electrophilic PROTACs that degrade nuclear proteins by engaging DCAF16. *Nat. Chem. Biol.* 15, 737–746. doi: 10.1038/s41589-019-0279-5

Conflict of Interest: MN received a research fund from Daiichi Sankyo Pharmaceutical Co., Ltd.

The remaining authors declare that the research was conducted in the absence of any commercial or financial relationships that could be construed as a potential conflict of interest.

frontiers in Chemistry

MINI REVIEW
published: 18 December 2019
doi: 10.3389/fchem.2019.00876

Recent Developments in Cell Permeable Deubiquitinating Enzyme Activity-Based Probes

Daniel Conole[1]*, *Milon Mondal*[1], *Jaimeen D. Majmudar*[2] and *Edward W. Tate*[1]

[1] Department of Chemistry, Imperial College London, London, United Kingdom, [2] Medicine Design, Pfizer Inc., Cambridge, MA, United States

Deubiquitinating enzymes (DUBs) function to remove or cleave ubiquitin from post-translationally modified protein substrates. There are about 100 known DUBs in the proteome, and their dysregulation has been implicated a number of disease states, but the specific function of many subclass members remains poorly understood. Activity-based probes (ABPs) react covalently with an active site residue to report on specific enzyme activity, and thus represent a powerful method to evaluate cellular and physiological enzyme function and dynamics. Ubiquitin-based ABPs, such as HA-Ub-VME, an epitope-tagged ubiquitin carrying a C-terminal reactive warhead, are the leading tool for "DUBome" activity profiling. However, these probes are generally cell membrane impermeable, limiting their use to isolated enzymes or lysates. Development of cell-permeable ABPs would allow engagement of DUB enzymes directly within the context of an intact live cell or organism, refining our understanding of physiological and pathological function, and greatly enhancing opportunities for translational research, including target engagement, imaging and biomarker discovery. This mini-review discusses recent developments in small molecule activity-based probes that target DUBs in live cells, and the unique applications of cell-permeable DUB activity-based probes vs. their traditional ubiquitin-based counterparts.

Keywords: deubiquitinase, cell permeability, activity based probe, small molecule, DUB activity, ubiquitin (Ub), deubiquinating enzymes

OPEN ACCESS

Edited by:
Huib Ovaa,
Leiden University Medical Center, Netherlands

Reviewed by:
Eric Robert Strieter,
University of Massachusetts Amherst, United States
Steven Verhelst,
KU Leuven, Belgium

***Correspondence:**
Daniel Conole
d.conole@imperial.ac.uk

Specialty section:
This article was submitted to Chemical Biology, a section of the journal Frontiers in Chemistry

Received: *31 October 2019*
Accepted: *04 December 2019*
Published: *18 December 2019*

Citation:
Conole D, Mondal M, Majmudar JD and Tate EW (2019) Recent Developments in Cell Permeable Deubiquitinating Enzyme Activity-Based Probes. Front. Chem. 7:876. doi: 10.3389/fchem.2019.00876

INTRODUCTION

The Ubiquitin-Proteasome System

The ubiquitin-proteasome system (UPS) has attracted more excitement, scope and promise as a therapeutic target than any system since the rise of the kinome as a druggable protein family. This biological process regulates proteolysis, transcriptional regulation, DNA damage, complex formation, cellular trafficking and localization, inflammation and autophagy, therefore modulation of ubiquitin-proteasome pathways are a potentially rich source of new therapeutic modalities (Fleury and Walker, 2015; Hewings et al., 2017). The key post-translational modification (PTM) in this pathway is ubiquitination, which is catalyzed by the E1–E2–E3-enzyme cascade resulting in isopeptide coupling of a ubiquitin (Ub) C-terminus primarily to a lysine residue of an acceptor protein (Glickman and Ciechanover, 2002). The ubiquitin is then itself elongated to form various branched or linear polyubiquitin chains which, depending on their topology, may lead to varied functional outcomes (Elias et al., 2003; Swatek and Komander, 2016; Haakonsen and Rape, 2019).

Deubiquitinase Enzymes: Function and Importance

In line with the importance of ubiquitination for regulation of many cellular processes, the human genome encodes about 100 deubiquitinating enzymes (DUBs) that can reverse this PTM by hydrolysing the amide bond between mono- and poly-Ub chains, and substrate proteins (Hewings et al., 2017; Clague et al., 2019). Similarly to Ub ligases, DUBs thus regulate protein activity, stability, localization, and interactions (Fleury and Walker, 2015). Although less extensively studied than the much larger class of Ub ligases (numbering over 600), DUBs have attracted intense attention in recent years as promising targets for drug development in various indications, particularly in cancer (D'Arcy and Linder, 2014; D'Arcy et al., 2015). However, significant challenges remain in the identification of selective ligands for DUBs, which would in turn aid in the determination of dynamic DUB substrate profiles among the tens of thousands of Ub sites and diverse Ub polymer topologies, distributed across the majority of proteins in the cell.

DUB Activity-Based Probes

A Brief History

To better understand the function and mechanism of these DUBs, activity-based probes (ABPs) have been developed over the last two decades. There are five DUB sub-types consisting of USPs (ubiquitin-specific proteases), UCHs (ubiquitin carboxy-terminal hydrolases), MJDs (Machado–Josephin domain-containing proteases), OTUs (ovarian tumor proteases) and MINDYs (motif- interacting with ubiquitin-containing novel DUB family) that are papain-type cysteine peptidases (**Figure 1A**). These DUBs possess a catalytic nucleophilic cysteine residue that can be captured covalently by reaction with an electrophilic warhead based ABP (Harrigan et al., 2017; Hewings et al., 2017). Appending a reporter tag to the electrophilic warhead creates an ABP which can inform on DUB selectivity and proteolytic activity, and facilitate novel inhibitor profiling. Distinct from these families are JAMMs (JAB1, MPN, MOV34 family), which are zinc metallopeptidases which are not as well-understood but are likely to require different chemistries for ABP development.

The first generation and most widely employed DUB ABPs contain a mono-Ub recognition element with either a propargylamide or vinyl methyl ester electrophilic group conjugated to the C-terminus of Ub (Borodovsky et al., 2002; de Jong et al., 2012; Ekkebus et al., 2013), and a fluorescent reporter group for detection of the labeled enzyme (Fleury and Walker, 2015; Leestemaker and Ovaa, 2017). Later, this type of ABP was extended to include internal and terminal di-ubiquitin as the targeting element to provide insight into the linkage specificity of DUBs and the nature of their binding interaction with protein substrates (McGouran et al., 2013; Li et al., 2014; Mulder et al., 2014; Flierman et al., 2016).

More recently, a more sophisticated Ub-based ABP incorporated methyl disulphide as the reactive warhead, which allows the release of active DUBs from the ABP under mild conditions, such that they can be isolated from complex cell extracts for further study (de Jong et al., 2017; Leestemaker and Ovaa, 2017).

In-cell Profiling: A New Frontier for DUB Biology

While these various generations of DUB ABPs are widely used and have greatly advanced our knowledge regarding the biological role of DUBs, they can only be employed on cell lysates as the large size of the Ub recognition element(s) precludes cellular permeability (Hewings et al., 2017). Cell lysis causes cytoplasmic and nuclear protein dilution, and disruption of cellular organization and localization, leading to dissociation of important protein-protein interactions (PPIs) necessary for DUB activity and dysregulation of ubiquitination patterns (Claessen et al., 2013; Gui et al., 2018). The consequence is that traditional Ub-based ABPs have limited use for the exploration of dynamic DUB activity profile (Fleury and Walker, 2015), in common with the well-known differences in protease activity profiles measured between lysates and live cells (Hewings et al., 2017).

In order to gain a full understanding of the function of DUBs in the most relevant cellular and physiological setting, the issue of cellular permeability needs to be addressed. Comprehensive reviews of Ub-based ABPs have recently been published and thus the present review focuses on recent work toward cell permeable DUB ABPs (Fleury and Walker, 2015; Hewings et al., 2017; Leestemaker and Ovaa, 2017).

EFFORTS TO ADDRESS DUB ABP CELL PERMEABILITY

Attempts to date to address cell-penetration for DUB ABPs can be divided into four categories: pore-forming toxins (Claessen et al., 2013), electroporation (Mulder et al., 2016), cell-penetrating peptide (CPP) ABPs (Gui et al., 2018) and small-molecule based cell permeable ABPs (Ward et al., 2016, 2019; Geurink et al., 2019; Krabill et al., 2019; Panyain et al., 2019). These are discussed in further detail below and in **Figure 1**.

Pore-Forming Toxins

In 2013, Claessen et al. published a catch-and-release Ub ABP to map the endogenous expression of DUBs and their interacting proteins in semi-intact cells (Claessen et al., 2013). The catch component consisted of a biotin affinity handle, whereas the release motif entailed a cleavable linker (either hydrazine, azobenzene, or levulinoyl ester), accessed through a combination of intein chemistry and sortase-mediated ligation. While this probe improved DUB peptide detection by mass spectrometry (MS), it remained, like those before, cell impermeable. To combat this, the authors of the paper employed perfringolysin O (PFO), a soluble toxin secreted by the pathogen *Clostridium perfringens* that binds cholesterol and forms large homo-oligomeric pore complexes to allow the ABP to cross the cell membrane into the cytosol (**Figure 1B**). Interestingly, they identified 34 DUBs and their interacting partners in non-infected cells, and three additional host DUBs (USP36, USP33, and TRABID) in *chlamydia*-infected HeLa cells that were not detected

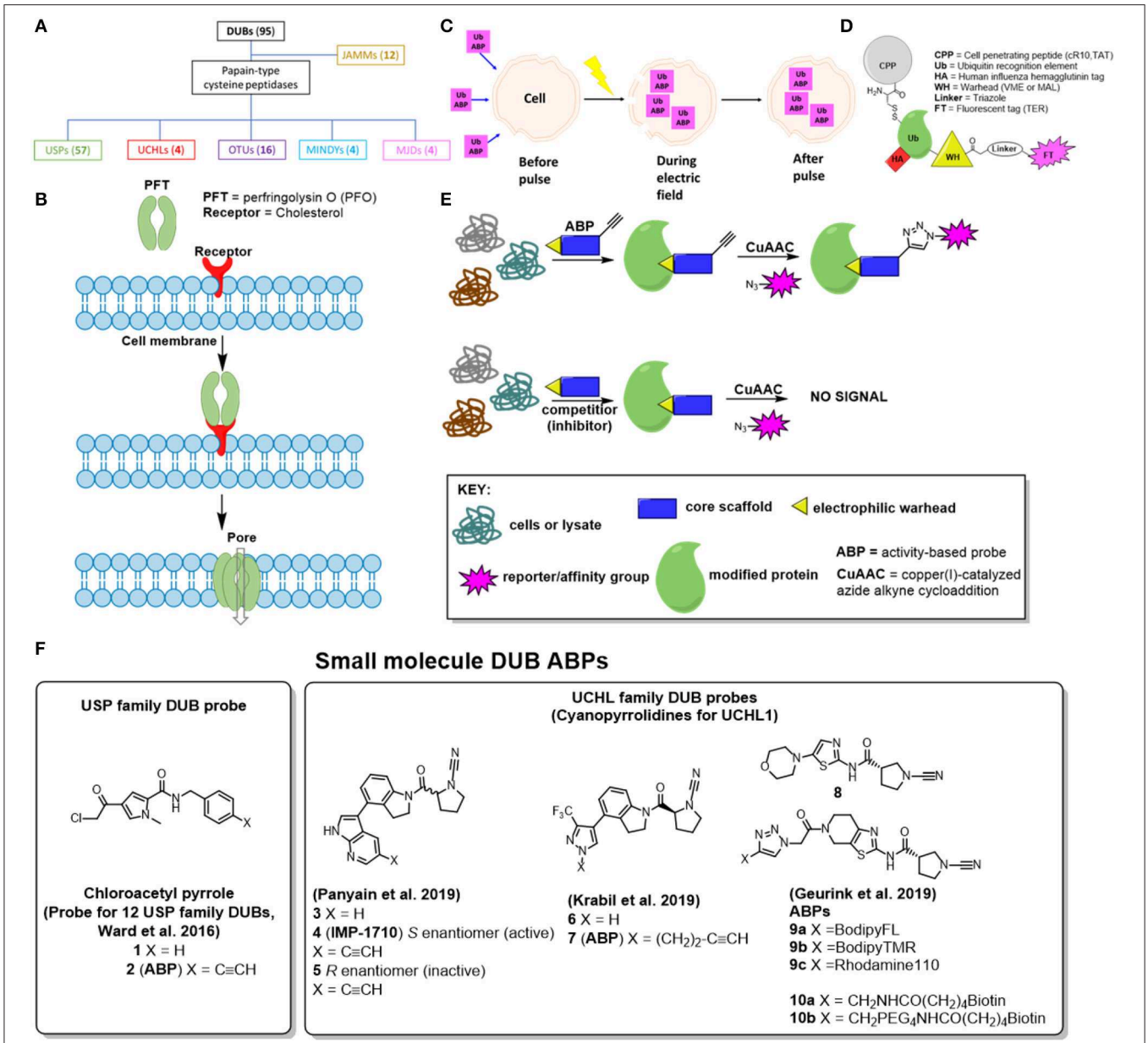

FIGURE 1 | Visual representations of different approaches to address the cell permeability challenge associated with developed DUB ABPs. **(A)** Family tree for DUBs, parenthesis displays how many enzymes are in this sub-family, **(B)** Pore-forming toxins, **(C)** Electroporation, **(D)** Cell penetrating peptide-based DUB ABPs **(E)** Activity-based protein profiling with small molecule-based DUB ABPs—**(F)** Small molecule DUB inhibitors from the literature that have been converted to ABPs.

previously using Ub-VME based ABPs. However, a head-to-head quantitative proteomics analysis (live cells vs. cell lysate) to further support this claim was not undertaken in this study, and this approach has not been widely adopted by other labs.

Electroporation

In another report, a cascading activity-based probe, Ub-Dha (Ub-dehydroalanine) was used to monitor catalysis along the E1, E2, and E3 enzyme trans-thioesterification reaction pathway (Mulder et al., 2016). This probe aimed to capture a dynamic post translational pathway, and although the probe was not designed to interact with DUBs, the approach to deliver it across the cell membrane is relevant for DUB ABP design. To this end, the authors used electroporation, an electrical pulse applied to cells to temporarily induce cell membrane micropore formation (**Figure 1C**). While generally used to transfect exogenous DNA into cells, this technology may be useful for the intracellular delivery of large molecules, such as Ub-Dha (Shi et al., 2018). An advantage of this method, particularly in comparison to pore-forming toxins, is that the pores formed are very small and transient, so cell viability and functionality is usually preserved

(Mukherjee et al., 2018). Consistent with this, the authors report normal cell morphology post-electroporation.

In-gel fluorescence studies showed that labeling of key Ub E1 enzymes (UBA6 and UBE1) in live cells using electroporation occurred on a similar timescale to that in lysates. Also, UBE1 activity could be attenuated with pre-treatment of lysates or live cells with PYR-41 (a small molecule UBE1 inhibitor), further suggesting that electroporation was successfully delivering Ub-Dha into cells. While this method was focused primarily on capturing Ub ligases, four DUBs were also labeled and identified using MS-based quantitative proteomics in HeLa cells. This work was a landmark in Ub ligase profiling, but no data were provided to show whether electroporation in live cells produces significantly different results in DUB labeling compared with that in cell lysates, and the method has not been widely taken up.

Cell-Penetrating Peptide (CPP) Based ABPs

The Zhuang group recently described cell-permeable DUB ABPs consisting of various combinations of polycationic cell-penetrating peptides (CPPs) conjugated to ubiquitin and thiol-reactive warheads (**Figure 1D**; Gui et al., 2018). Chemoselective ligation was employed to attach either a cyclic polyarginine (cR10) or KRKKRRQRRR (TAT) peptide to the Ub N-terminus, whereas propargylamine (PA) or vinyl methyl ester (VME) were used as the electrophilic warhead (Ekkebus et al., 2013). In addition, a disulphide bond was built-in to allow reductive release of the CPP from the ABP once it had entered the cell, and a human influenza hemagglutinin (HA) tag was incorporated for affinity purification. Tetraethyl-rhodamine (TER) fluorescent versions of these ABPs were also synthesized to demonstrate live-cell uptake of CPP-containing probes by live-cell fluorescence confocal microscopy. Importantly, the authors synthesize and evaluate appropriate control probes (without the CPP motifs or thiol-reactive warheads) to demonstrate that the difference in observed live cell DUB labeling can be attributed to these DUB ABP elements.

The authors then profiled the DUBome using HA-tagged ABPs in live cells using immunoblotting and quantitative mass spectrometry proteomic analysis. With respect to immunoblotting, the band profile for live cell DUB labeling with the HA-Cys(cR10)-Ub-PA probe was notably different to that of cell lysates. Using a label-free quantitative proteomics method, 34 DUB proteins were identified after treatment of live HeLa cells with the HA-Cys(cR10)-Ub-PA probe, and 27 of these were found to be significantly enriched [$\log_2$ (fold difference) >2, p-value < 0.05]. Importantly, the authors provide a proteomic level comparison of this probe in live cells vs. cell lysates and demonstrate that treatment of the cell lysate with HA-Cys(cR10)-Ub-PA probe followed by equivalent sample processing results in identification of only 10 DUBs, of which all were also detected in the live cell experiment. Interestingly, the live cell labeling experiment identified DUBs that are present in different organelles, suggesting that the probe is permeating various sub-cellular compartments. Finally, pan-DUB inhibitor PR-619 was employed to test whether these probes could be used for live cell DUB profiling studies and novel DUB inhibitor discovery. PR-619 inhibited intracellular DUB activity in a concentration-dependent manner, and labeling was more pronounced in lysates vs. live cells. This result suggests the nuances that may be missed if DUB activity is not measured in a physiological relevant system.

Small Molecule ABPs

In 2016, Ward et al. published the first small-molecule based DUB ABP, based on a chloroacetylpyrrole scaffold (**1**), which was originally identified from a high-throughput screening (HTS) campaign at Mission Therapeutics (**Figure 1F**; Ward et al., 2016). This compound exhibited potent USP4 and USP11 biochemical activity, and so the authors employed a competitive activity-based protein profiling (ABPP) method to assess whether an alkyne-tagged analog **2** could be used as a live cell DUB ABP for quantitative target engagement. Intriguingly, **2** labeled a total of 12 DUBs in U2OS cells. Furthermore, it was discovered that parent chloroacetylpyrrole (**1**) could compete against alkyne-tagged probe (**2**) in a concentration dependent manner for at least 9 different DUBs, in some cases at sub micromolar concentrations, which is noteworthy considering its structural simplicity. While a direct quantitative mass spectrometry comparison with cell lysate labeling is not reported, the authors demonstrate using a Ub-Rhodamine fluorescent intensity assay that parent chloroacetylpyrrole (**1**) biochemically inhibits 11 of these DUBs at EC_{50} values <10 μM.

As one might expect with a small molecule based ABP, probe **2** also targets many non-DUB proteins, presumably through numerous non-specific reactions with reactive cysteine residues (Ward et al., 2016; Hewings et al., 2017). While this could complicate studies that aim to link a specific function or phenotype to DUB target engagement, the small molecule ABPs still serves as a useful—and to date unique—tool for assessing cellular target engagement and selectivity of novel DUB inhibitors.

More recently, an ABPP approach was also employed to ascertain the molecular explanation for the cellular toxicity of VLX1570 (analog of b-AP15), a small molecule USP14 inhibitor for refractory multiple myeloma that has been put on full clinical hold due to dose limiting toxicity (Ward et al., 2019). The authors prepare an alkyne-tagged version of VLX1570 (structure not shown), and through various immunoblotting and proteomics experiments show high protein target promiscuity, the formation of higher molecular weight complexes, and resultant aggregation and inhibition of CIAPIN1, an important anti-apoptotic protein. This work highlights the importance of determining the protein target activity profile for drug candidates as part of the drug discovery process.

Several potent and selective small molecule covalent inhibitors have emerged for DUBs in the USP and UCHL subfamilies, including in the patent literature (Kemp and Woodrow, 2018; Kemp et al., 2018; Gibson et al., 2019a,b) and these scaffolds present a potential opportunity to design novel cell permeable ABPs. Taking this approach, Panyain et al. in collaboration with Mission Therapeutics designed IMP-1710 (**4**), a highly potent and selective cyanopyrrolidine ABP against UCHL1,

with 40 nM IC_{50} and sensitive detection down to 2 nM ABP in a range of cell types (**Figure 1F**; Panyain et al., 2019). Extensive biochemical, quantitative proteomic and Ub-based probe profiling demonstrated exquisite activity-dependent selectivity for UCHL1 over all other DUBs, and a highly favorable selectivity profile at the whole proteome level. Interestingly, IMP-1710 (**4**) is highly stereoselective, with opposite enantiomer **5** providing an effective inactive control, and could be used to show that the small molecule LDN-57444, previously reported as a UCHL1 tool inhibitor and widely used in the literature, fails to engage UCHL1 biochemically or in cells (Liu et al., 2003). Finally, the authors used compound **3** and IMP-1710 (**4**) to demonstrate the therapeutic potential of UCHL1 inhibition in a model of idiopathic pulmonary fibrosis, without cytotoxicity. Related alkyne-tagged small molecule ABP **7** of cyanopyrrolidine **6** was recently reported by Krabill et al., although this molecule is >150-fold less potent than IMP-1710 (**4**), and is relatively non-specific (**Figure 1F**; Krabill et al., 2019).

In addition, Geurink et al. recently reported some fluorescently labeled (**9a**-**9c**) and biotinylated (**10a**, **10b**) ABPs of related cyanopyrrolidine-based scaffold **8** (**Figure 1F**; Geurink et al., 2019). Through ABPP mass spectrometry the authors demonstrated strong UCHL1 selectivity within the DUB family, with PARK7 - also known as DJ-1, a neuroprotective redox-sensitive chaperone—observed as a majority off-target protein. Additional off-targets were observed by gel electrophoresis at ∼55 kDa; these were not identified by the authors, but based on the work of Panyain et al. these off-targets are likely to be aldehyde dehydrogenases (ALDH). Although the authors demonstrate imaging of probe-labeled proteins in zebrafish embryos, strong off-target labeling of DJ-1 and ALDH may limit the utility of these probes in living systems.

DISCUSSION

Learning From Other Target Classes

Ubiquitin based ABPs have significantly advanced our knowledge of DUB structure, dynamics and function. However, their general inability to cross the cell membrane prevents further understanding concerning DUBs in their native, physiological environment (Fleury and Walker, 2015; Ward et al., 2016; Hewings et al., 2017). The potential applications of cell-permeable DUB ABPs reaches beyond improved understanding of DUBs within a given cell or model organism. Development of cell permeable DUB ABPs may lead to agents that allow direct visualization and quantification of DUB activity in living organisms, and may even extend to the development of DUB-based assays for DUB activity as a clinical biomarker, as well as a tools for preclinical *in vivo* and clinical *ex vivo* evaluation of DUB inhibitors and target engagement (Fleury and Walker, 2015). Basic and translational studies on other hydrolase classes including serine proteases, lipases, caspases, and cathepsins have benefitted greatly from the development of cell permeable ABPs, where significant and sustained research has led to ground-breaking non-invasive *in vivo* imaging probes (Blum et al., 2007; Edgington et al., 2009). In the proteasome field, development of cell permeable ABPs for proteasome and immunoproteasome catalytic subunits such as Dansyl-Ahx3-L3-VS (Berkers et al., 2005) and BodipyFL-Ahx3-L3-VS (Berkers et al., 2007) have become popular tools for in-gel fluorescence imaging, flow cytometry, and fluorescence microscopy in animal tissues (Gan et al., 2019).

The development of small molecule DUB probes is thus a high priority for the field in order for DUB ABPs to match the utility of their counterparts in these other target classes, particularly for *in vivo* applications.

Comparing the Approaches

For a probe to be used as a true ABP, it must be able to capture the protein in its native environment in a strictly activity-dependent manner, features for which cell permeability is critical, ideally through passive diffusion or native uptake mechanisms. Furthermore, an ideal ABP for determining both cellular target engagement and selectivity of novel DUB inhibitors should label a large spectrum of DUBs at a low concentration, preferably 1 μM or lower. Most of the methods reviewed here except a few of the small molecule approaches employ large amounts of probe (>10 μM), precluding their use for cellular discovery of novel reversible or irreversible DUB inhibitors with a weak K_I component (Claessen et al., 2013; Mulder et al., 2016; Gui et al., 2018). Small molecule ABPs, particularly those which cover a majority of the DUBome, would check most of these boxes since they could be used in low concentrations on live cells for short periods of time, enhancing identification of novel DUB inhibitors and our understanding DUB biological functions under various (patho)physiological contexts (**Table 1**).

TABLE 1 | Comparison of various approaches to DUB ABP cellular permeability with respect to the requirements for an ideal DUB ABP.

ABP	Methods of cell entry	Requirements for an ideal DUB ABP		
		Proteins captured in their native environment? (Yes/No/Partial)	ABP labels a large spectrum (>10) of DUBs (Yes/No/Partial)	Can use low (< 1 μM) con-centrations of ABP? (Yes/No/Partial)
Traditional Ubiquitin-based e.g., HA-Ub-VME	None	No	Yes	No
	Pore-forming toxins	Partial	Yes	No
	Electroporation	Partial	Partial	No
	Cell-penetrating peptides	Partial	Yes	No
Small molecules	Passive diffusion	Yes	Partial	Yes

Ub-based ABPs possess a distinct advantage over peptide and small molecule based ABPs because of the specificity of their recognition element, and shortening the recognition element to allow greater cell permeability fails to preserve specificity or activity (Albrow et al., 2011; Safa et al., 2019). Each of the various approaches discussed above to force entry of Ub-based ABPs, including toxin pore formation, electroporation and so-called "cell-penetrating" peptides (CPPs), raise numerous concerns regarding host membrane repair responses that may be triggered as an unintended consequence (Ostolaza et al., 2019). For example, CPPs have been demonstrated to substantially disrupt membrane integrity, causing formation of non-physiological subcellular compartments (Gao et al., 2019). Consequently, there is a chance that upon pore formation that cell homeostasis is disrupted, and either apoptosis, necroptosis or pyroptosis results, which would most likely only be compounded in an *in vivo* environment due to cell signaling (Abdelrazzak et al., 2011; Etxaniz et al., 2018). Each of these approaches also present significant challenges for extended periods of live cell profiling, and are largely inapplicable to whole organism analysis (Shi et al., 2018). CellSqueeze technology, which uses a commercial microfluidics device and pressure system to open membrane pores, may provide an alternative approach to garner higher value from cell-impermeable probes (Szeto et al., 2015; Li et al., 2017). Whether this would improve DUB coverage or better preserve cell integrity remains to be seen, and the method may be difficult to scale.

Small molecule based ABPs, particularly those designed with an alkyne or other biorthogonal enrichment handle for ABPP, can passively diffuse through the cell membrane to afford selective labeling, visualization, and enrichment of active enzymes in a complex proteome without disruption to cellular organization (Martell and Weerapana, 2014; Fleury and Walker, 2015). To date there have been remarkably few successful reports of small molecule DUB ABPs, but two recent examples of a pan-USP ABP and a highly UCHL1-specific ABP have shown the promise of this approach, generating significant interest in the DUB field (Ward et al., 2016; Akinjiyan et al., 2017; Hewings et al., 2017; Wong et al., 2017; Panyain et al., 2019). Issues including probe specificity, DUB spectrum, toxicity and metabolic stability will need to be addressed in order to realize the full potential of cell permeable DUB ABPs and their applications to sophisticated *in vivo* studies such as imaging and biomarker analysis. Focused research from the medicinal chemistry and chemical biology communities, as well as close collaboration with industry partners with deep expertise in DUB inhibitor discovery, will continue to play a key role in this endeavor.

AUTHOR CONTRIBUTIONS

DC prepared the manuscript. JM, ET, and MM reviewed the manuscript and provided comments, suggestions and edits.

FUNDING

This work was supported by Pfizer Inc, and a grant from The European Commission (H2020 Marie Sklodowska Curie Individual Fellowship grant 840690 to MM).

REFERENCES

Abdelrazzak, A. B., O'Neill, P., and Hill, M. A. (2011). Intercellular induction of apoptosis signalling pathways. *Radiat. Prot. Dosimetry* 143, 289–293. doi: 10.1093/rpd/ncq387

Akinjiyan, F. A., Carbonneau, S., and Ross, N. T. (2017). Lead discovery and chemical biology approaches targeting the ubiquitin proteasome system. *Bioorganic Med. Chem. Lett.* 27, 4589–4596. doi: 10.1016/j.bmcl.2017.08.058

Albrow, V. E., Ponder, E. L., Fasci, D., Békés, M., Deu, E., Salvesen, G. S., et al. (2011). Development of small molecule inhibitors and probes of human SUMO deconjugating proteases. *Chem. Biol.* 18, 722–732. doi: 10.1016/j.chembiol.2011.05.008

Berkers, C. R., Van Leeuwen, F. W. B., Groothuis, T. A., Peperzak, V., Van Tilburg, E. W., Borst, J., et al. (2007). Profiling proteasome activity in tissue with fluorescent probes. *Mol. Pharm.* 4, 739–748. doi: 10.1021/mp0700256

Berkers, C. R., Verdoes, M., Lichtman, E., Fiebiger, E., Kessler, B. M., Anderson, K. C., et al. (2005). Activity probe for *in vivo* profiling of the specificity of proteasome inhibitor bortezomib. *Nat. Methods* 2, 357–362. doi: 10.1038/nmeth759

Blum, G., Von Degenfeld, G., Merchant, M. J., Blau, H. M., and Bogyo, M. (2007). Noninvasive optical imaging of cysteine protease activity using fluorescently quenched activity-based probes. *Nat. Chem. Biol.* 3, 668–677. doi: 10.1038/nchembio.2007.26

Borodovsky, A., Ovaa, H., Kolli, N., Gan-Erdene, T., Wilkinson, K. D., Ploegh, H. L., et al. (2002). Chemistry-based functional proteomics reveals novel members of the deubiquitinating enzyme family. *Chem. Biol.* 9, 1149–1159. doi: 10.1016/S1074-5521(02)00248-X

Claessen, J. H. L., Witte, M. D., Yoder, N. C., Zhu, A. Y., Spooner, E., and Ploegh, H. L. (2013). Catch-and-release probes applied to semi-intact cells reveal ubiquitin-specific protease expression in chlamydia trachomatis infection. *ChemBioChem.* 14, 343–352. doi: 10.1002/cbic.201200701

Clague, M. J., Urbé, S., and Komander, D. (2019). Breaking the chains: deubiquitylating enzyme specificity begets function. *Nat. Rev. Mol. Cell Biol.* 20, 338–352. doi: 10.1038/s41580-019-0099-1

D'Arcy, P., and Linder, S. (2014). Molecular pathways: translational potential of deubiquitinases as drug targets. *Clin. Cancer Res.* 20, 3908–3914. doi: 10.1158/1078-0432.CCR-14-0568

D'Arcy, P., Wang, X., and Linder, S. (2015). Deubiquitinase inhibition as a cancer therapeutic strategy. *Pharmacol. Ther.* 147, 32–54. doi: 10.1016/j.pharmthera.2014.11.002

de Jong, A., Merkx, R., Berlin, I., Rodenko, B., Wijdeven, R. H. M., El Atmioui, D., et al. (2012). Ubiquitin-based probes prepared by total synthesis to profile the activity of deubiquitinating enzymes. *ChemBioChem.* 13, 2251–2258. doi: 10.1002/cbic.201200497

de Jong, A., Witting, K., Kooij, R., Flierman, D., and Ovaa, H. (2017). Release of enzymatically active deubiquitinating enzymes upon reversible capture by disulfide ubiquitin reagents. *Angew. Chem.* 56, 12967–12970. doi: 10.1002/anie.201706738

Edgington, L. E., Berger, A. B., Blum, G., Albrow, V. E., Paulick, M. G., Lineberry, N., et al. (2009). Noninvasive optical imaging of apoptosis by caspase-targeted activity-based probes. *Nat. Med.* 15, 967–973. doi: 10.1038/nm.1938

Ekkebus, R., Van Kasteren, S. I., Kulathu, Y., Scholten, A., Berlin, I., Geurink, P. P., et al. (2013). On terminal alkynes that can react with active-site cysteine nucleophiles in proteases. *J. Am. Chem. Soc.* 135, 2867–2870. doi: 10.1021/ja309802n

Elias, J. E., Peng, J., Cheng, D., Thoreen, C. C., Marsischky, G., Schwartz, D., et al. (2003). A proteomics approach to understanding protein ubiquitination. *Nat. Biotechnol.* 21, 921–926. doi: 10.1038/nbt849

Etxaniz, A., González-Bullón, D., Martín, C., and Ostolaza, H. (2018). Membrane repair mechanisms against permeabilization by pore-forming toxins. *Toxins* 10:234. doi: 10.3390/toxins10060234

Fleury, D., and Walker, J. M. (2015). *Book on Proteostasis.* New York, NY: Humana Press (Springer Science+Business Media).

Flierman, D., Van Der Heden Van Noort, G. J., Ekkebus, R., Geurink, P. P., Mevissen, T. E. T., Hospenthal, M. K., et al. (2016). Non-hydrolyzable diubiquitin probes reveal linkage-specific reactivity of deubiquitylating enzymes mediated by S2 pockets. *Cell Chem. Biol.* 23, 472–482. doi: 10.1016/j.chembiol.2016.03.009

Gan, J., Leestemaker, Y., Sapmaz, A., and Ovaa, H. (2019). Highlighting the Proteasome: using fluorescence to visualize proteasome activity and distribution. *Front. Mol. Biosci.* 6:14. doi: 10.3389/fmolb.2019.00014

Gao, X., De Mazière, A., Iaea, D. B., Arthur, C. P., Klumperman, J., Ciferri, C., et al. (2019). Visualizing the cellular route of entry of a cystine-knot peptide with Xfect transfection reagent by electron microscopy. *Sci. Rep.* 9, 1–14. doi: 10.1038/s41598-019-43285-5

Geurink, P. P., Kooij, R., Sapmaz, A., Liu, S., and Xin, B. (2019). A small-molecule activity-based probe for monitoring ubiquitin C-terminal Hydrolase L1 (UCHL1) activity in live cells and zebrafish embryos. *bioRxiv*. doi: 10.1101/827642

Gibson, K. R., Jones, A., and Kemp, M. I. (2019a). US20190055232A1.

Gibson, K. R., Jones, A., Kemp, M. I., Madin, A., Stockley, M. L., Whitlock, G. A., et al. (2019b). US20190010122A1. 1.

Glickman, M. H., and Ciechanover, A. (2002). The ubiquitin-proteasome proteolytic pathway: destruction for the sake of construction. *Physiol. Rev.* 82, 373–428. doi: 10.1152/physrev.00027.2001

Gui, W., Ott, C. A., Yang, K., Chung, J. S., Shen, S., and Zhuang, Z. (2018). Cell-permeable activity-based ubiquitin probes enable intracellular profiling of human deubiquitinases. *J. Am. Chem. Soc.* 140, 12424–12433. doi: 10.1021/jacs.8b05147

Haakonsen, D. L., and Rape, M. (2019). Branching out: improved signaling by heterotypic ubiquitin chains. *Trends Cell Biol.* 29, 704–716. doi: 10.1016/j.tcb.2019.06.003

Harrigan, J. A., Jacq, X., Martin, N. M., and Jackson, S. P. (2017). Deubiquitylating enzymes and drug discovery: emerging opportunities. *Nat. Rev. Drug Discov.* 17, 57–78. doi: 10.1038/nrd.2017.152

Hewings, D. S., Flygare, J. A., Bogyo, M., and Wertz, I. E. (2017). Activity-based probes for the ubiquitin conjugation–deconjugation machinery: new chemistries, new tools, and new insights. *FEBS J.* 284, 1555–1576. doi: 10.1111/febs.14039

Kemp, M. I., Stockley, M., and Jones, A. (2018). US20180194724A1. 1.

Kemp, M. I., and Woodrow, M. D. (2018). US20180362460A1. 1.

Krabill, A. D., Chen, H., Hussain, S., Feng, C., Abdullah, A., Das, C., et al. (2019). Biochemical and cellular characterization of a cyanopyrrolidine covalent Ubiquitin C-terminal hydrolase L1 inhibitor. *ChemBioChem*. doi: 10.1002/cbic.201900434. [Epub ahead of print].

Leestemaker, Y., and Ovaa, H. (2017). Tools to investigate the ubiquitin proteasome system. *Drug Discov. Today Technol.* 26, 25–31. doi: 10.1016/j.ddtec.2017.11.006

Li, G., Liang, Q., Gong, P., Tencer, A. H., and Zhuang, Z. (2014). Activity-based diubiquitin probes for elucidating the linkage specificity of deubiquitinating enzymes. *Chem. Commun.* 50, 216–218. doi: 10.1039/C3CC47382A

Li, J., Wang, B., Juba, B. M., Vazquez, M., Kortum, S. W., Pierce, B. S., et al. (2017). Microfluidic-enabled intracellular delivery of membrane impermeable inhibitors to study target engagement in human primary cells. *ACS Chem. Biol.* 12, 2970–2974. doi: 10.1021/acschembio.7b00683

Liu, Y., Lashuel, H. A., Choi, S., Xing, X., Case, A., Ni, J., et al. (2003). Discovery of inhibitors that elucidate the role of UCH-L1 activity in the H1299 lung cancer cell line. *Chem. Biol.* 10, 837–846. doi: 10.1016/j.chembiol.2003.08.010

Martell, J., and Weerapana, E. (2014). Applications of copper-catalyzed click chemistry in activity-based protein profiling. *Molecules* 19, 1378–1393. doi: 10.3390/molecules19021378

McGouran, J. F., Gaertner, S. R., Altun, M., Kramer, H. B., and Kessler, B. M. (2013). Deubiquitinating enzyme specificity for ubiquitin chain topology profiled by di-ubiquitin activity probes. *Chem. Biol.* 20, 1447–1455. doi: 10.1016/j.chembiol.2013.10.012

Mukherjee, P., Nathamgari, S. S. P., Kessler, J. A., and Espinosa, H. D. (2018). Combined numerical and experimental investigation of localized electroporation-based cell transfection and sampling. *ACS Nano* 12, 12118–12128. doi: 10.1021/acsnano.8b05473

Mulder, M. P. C., El Oualid, F., Ter Beek, J., and Ovaa, H. (2014). A native chemical ligation handle that enables the synthesis of advanced activity-based probes: diubiquitin as a case study. *Chembiochem* 15, 946–949. doi: 10.1002/cbic.201402012

Mulder, M. P. C., Witting, K., Berlin, I., Pruneda, J. N., Wu, K. P., Chang, J. G., et al. (2016). A cascading activity-based probe sequentially targets E1-E2-E3 ubiquitin enzymes. *Nat. Chem. Biol.* 12, 523–530. doi: 10.1038/nchembio.2084

Ostolaza, H., González-Bullón, D., Uribe, K. B., Martín, C., Amuategi, J., and Fernandez-Martínez, X. (2019). Membrane permeabilization by pore-forming RTX toxins: what kind of lesions do these toxins form? *Toxins* 11:354. doi: 10.3390/toxins11060354

Panyain, N., Godinat, A., Lanyon-Hogg, T., Lachiondo-Ortega, S., Will, E. J., Soudy, C., et al. (2019). Discovery of a potent and selective covalent inhibitor and activity-based probe for the deubiquitylating enzyme UCHL1, with anti-fibrotic activity. *chemRxiv*. doi: 10.26434/chemrxiv.10058429

Safa, N., Pettigrew, J. H., Gauthier, T. J., and Melvin, A. T. (2019). Direct measurement of deubiquitinating enzyme activity in intact cells using a protease-resistant, cell-permeable, peptide-based reporter. *Biochem. Eng. J.* 151:107320. doi: 10.1016/j.bej.2019.107320

Shi, J., Ma, Y., Zhu, J., Chen, Y., Sun, Y., Yao, Y., et al. (2018). A review on electroporation-based intracellular delivery. *Molecules* 23, 3044–3063. doi: 10.3390/molecules23113044

Swatek, K. N., and Komander, D. (2016). Ubiquitin modifications. *Cell Res.* 26, 399–422. doi: 10.1038/cr.2016.39

Szeto, G. L., Van Egeren, D., Worku, H., Sharei, A., Alejandro, B., Park, C., et al. (2015). Microfluidic squeezing for intracellular antigen loading in polyclonal B-cells as cellular vaccines. *Sci. Rep.* 5, 1–13. doi: 10.1038/srep10276

Ward, J., Pinto-fernández, A., Cornelissen, L., Bonham, S., Saez, L. D., Riant, O., et al. (2019). Re-evaluating the mechanism of action of α, β-unsaturated carbonyl DUB inhibitors B-AP15 and VLX1570 : a paradigmatic example of unspecific protein crosslinking with michael acceptor motif-containing drugs. *chemRxiv*. doi: 10.26434/chemrxiv.10028444.v1

Ward, J. A., McLellan, L., Stockley, M., Gibson, K. R., Whitlock, G. A., Knights, C., et al. (2016). Quantitative chemical proteomic profiling of ubiquitin specific proteases in intact cancer cells. *ACS Chem. Biol.* 11, 3268–3272. doi: 10.1021/acschembio.6b00766

Wong, Y. K., Zhang, J., Hua, Z. C., Lin, Q., Shen, H. M., and Wang, J. (2017). Recent advances in quantitative and chemical proteomics for autophagy studies. *Autophagy* 13, 1472–1486. doi: 10.1080/15548627.2017.1313944

Conflict of Interest: ET is a founder, shareholder and Director of Myricx Pharma Ltd. JM is an employee of Pfizer Inc.

The remaining authors declare that the research was conducted in the absence of any commercial or financial relationships that could be construed as a potential conflict of interest.

frontiers in Chemistry

REVIEW
published: 10 January 2020
doi: 10.3389/fchem.2019.00915

Linear Ubiquitin Chains: Cellular Functions and Strategies for Detection and Quantification

Gunnar Dittmar[1*†] *and Konstanze F. Winklhofer*[2*†]

[1] *Proteomics of Cellular Signalling, Quantitative Biology Unit, Luxembourg Institute of Health, Strassen, Luxembourg,*
[2] *Department of Molecular Cell Biology, Institute of Biochemistry and Pathobiochemistry, Ruhr University Bochum, Bochum, Germany*

Ubiquitination of proteins is a sophisticated post-translational modification implicated in the regulation of an ever-growing abundance of cellular processes. Recent insights into different layers of complexity have shaped the concept of the ubiquitin code. Key players in determining this code are the number of ubiquitin moieties attached to a substrate, the architecture of polyubiquitin chains, and post-translational modifications of ubiquitin itself. Ubiquitination can induce conformational changes of substrates and alter their interactive profile, resulting in the formation of signaling complexes. Here we focus on a distinct type of ubiquitination that is characterized by an inter-ubiquitin linkage through the N-terminal methionine, called M1-linked or linear ubiquitination. Formation, recognition, and disassembly of linear ubiquitin chains are highly specific processes that are implicated in immune signaling, cell death regulation and protein quality control. Consistent with their role in influencing signaling events, linear ubiquitin chains are formed in a transient and spatially regulated manner, making their detection and quantification challenging.

Keywords: ubiquitin, HOIP, HOIL, SHARPIN, LUBAC, OTULIN, SRM, PRM

OPEN ACCESS

Edited by:
Huib Ovaa, Leiden University Medical Center, Netherlands

Reviewed by:
Donald S. Kirkpatrick, Genentech, Inc., United States
Kazuhiro Iwai, Kyoto University, Japan

***Correspondence:**
Gunnar Dittmar
gunnar.dittmar@lih.lu
Konstanze F. Winklhofer
konstanze.winklhofer@rub.de

[†] *These authors have contributed equally to this work*

Specialty section:
This article was submitted to Chemical Biology, a section of the journal Frontiers in Chemistry

Received: *24 October 2019*
Accepted: *16 December 2019*
Published: *10 January 2020*

Citation:
Dittmar G and Winklhofer KF (2020) Linear Ubiquitin Chains: Cellular Functions and Strategies for Detection and Quantification. Front. Chem. 7:915. doi: 10.3389/fchem.2019.00915

INTRODUCTION

Ubiquitination is a reversible post-translational modification that can affect the function, the fate, and the subcellular localization of the modified substrates, thereby regulating fundamental cellular processes (Akutsu et al., 2016; Swatek and Komander, 2016; Yau and Rape, 2016). The transfer of ubiquitin is catalyzed by an enzymatic cascade involving three enzymes, an E1 ubiquitin-activating enzyme, an E2 ubiquitin-conjugating enzyme, and an E3 ubiquitin ligase. E3 ubiquitin ligases fall into three categories: RING/U-box ligases, RBR (RING-between-RING) ligases, and HECT ligases. The mechanisms of ubiquitin transfer to the target protein varies depending on the E3 ligase type (**Figure 1**). RING ligases facilitate the direct transfer of ubiquitin from a ubiquitin-charged E2 to the substrate. HECT ligases directly bind ubiquitin by forming a thioester intermediate via a catalytic cysteine residue. From this thioester ubiquitin is passed on to a lysine residue of the substrate, generating an isopeptide bond. RBR ligases use a RING/HECT hybrid mechanism. Similarly to RING ligases, they bind an E2 ubiquitin-conjugating enzyme via their RING1 domain. Ubiquitin is then transferred from the E2 to a catalytic cysteine in the RING2 domain forming a transient thioester, similarly to HECT ligases. This ubiquitin moiety is then attached to the target protein.

The ubiquitination machinery requires not only proteins to create the ubiquitin modifications, but also proteins to recognize and remove ubiquitin moieties (**Figure 2**). The ubiquitin signal is decoded and thereby translated into cellular effects by proteins harboring one or

several ubiquitin-binding domains (UBDs), some of which recognize ubiquitin chain topologies with high selectivity (Dikic et al., 2009; Fennell et al., 2018). Reversibility of ubiquitination is ensured by deubiquitinases that hydrolyze isopeptide or peptide bonds between ubiquitin molecules or between ubiquitin and substrate proteins (Dikic et al., 2009; Mevissen and Komander, 2017; Fennell et al., 2018).

Ubiquitination is the most versatile post-translational modification based on variabilities in the number of ubiquitin moieties attached to a substrate, the mode of inter-ubiquitin linkage, and the formation of heterotypic (mixed or branched) ubiquitin chains. Substrate proteins can be modified with single ubiquitin moieties or with polymeric ubiquitin chains. Within polyubiquitin chains, ubiquitin can form eight different linkage types, using one of seven internal lysine residues (K6, K11, K27, K29, K33, K48, K63) or methionine at position 1 (M1). Additional layers of complexity emerge from the formation of heterotypic chains with mixed linkages, branched chains, and the post-translational modification of ubiquitin itself by phosphorylation, acetylation, sumoylation, and neddylation, reminiscent of a sophisticated and highly versatile code. Each linkage-type has a distinct three-dimensional topology allowing interactions with linkage-specific effector proteins, thus resulting in specific biological outcomes (**Figure 3**).

THE LINEAR UBIQUITINATION MACHINERY

M1-linked or linear ubiquitination is characterized by the head-to-tail linkage of ubiquitin molecules via the C-terminal carboxyl group of the donor ubiquitin and the N-terminal methionine of the acceptor ubiquitin. This results in the formation of a peptide bond in contrast to isopeptide formation via the linkage to the epsilon amino group of a lysine residue. The M1 linkage is generated by the linear ubiquitin chain assembly complex (LUBAC) that has first been described in 2006 as a complex of about 600 kDa containing the two RBR E3 ubiquitin ligases HOIP and HOIL-1 (Kirisako et al., 2006). Some years later, the adaptor protein SHARPIN was identified as the third core component of LUBAC (Gerlach et al., 2011; Ikeda et al., 2011; Tokunaga et al., 2011) (**Figure 4**). HOIP is the catalytically active component of LUBAC and the only E3 ubiquitin ligase that can assemble M1-linked ubiquitin based on its unique C-terminal linear ubiquitin chain determining domain (LDD) that positions the N-terminus of the target ubiquitin (Smit et al., 2012; Stieglitz et al., 2012; Yagi et al., 2012; Lechtenberg et al., 2016; Liu et al., 2017). The catalytic activity of HOIP is autoinhibited by its N-terminal domain so that full-length HOIP has no linear ubiquitination activity *in vitro*, in contrast to the N-terminally truncated RBR-LDD domain (Smit et al., 2012; Stieglitz et al., 2012, 2013; Yagi et al., 2012; Liu et al., 2017; Fujita et al., 2018). Binding of the ubiquitin-like (UBL) domain of HOIL-1 and SHARPIN to the ubiquitin-associated domain (UBA) of HOIP releases HOIP from autoinhibition (Smit et al., 2012; Stieglitz et al., 2012, 2013; Liu et al., 2017; Fujita et al., 2018). *In vitro*, the HOIL-1 UBL domain and the SHARPIN UBL domain can separately or synergistically bind to different regions within the UBA domain of HOIP (Liu et al., 2017). Both UBLs can induce conformational changes in the HOIP UBA domain, which allosterically rearrange the orientation between the UBA and RBR-LDD, facilitating E2 loading and promoting catalytic activity of HOIP (Liu et al., 2017). The crystal structure of the trimeric LUBAC core revealed that HOIL-1 and SHARPIN interact with each other via LUBAC-tethering motifs (LTMs) located N-terminally to the UBL domains of both proteins (Fujita et al., 2018). Upon heterodimerization, both LTMs fold into a single globular domain that plays a critical role in stabilizing trimeric LUBAC (Fujita et al., 2018).

HOIL-1 apparently has also catalytic activity. It has been reported to undergo auto-ubiquitination (Tatematsu et al., 2008) and to ubiquitinate oxidized IRP2 (iron regulatory protein 2), thereby inducing IRP2 degradation (Yamanaka et al., 2003). Recombinant HOIL-1 only lacking a C-terminal tail of 32 amino acids was observed to generate high molecular weight ubiquitin chains albeit with low efficiency (Stieglitz et al., 2012; Liu et al., 2017; Fujita et al., 2018). In addition to activating the catalytic core of HOIP, HOIL-1 obviously helps to direct the first ubiquitin toward a lysine residue of the substrate (Smit et al., 2013). The RBR-LDD domain of HOIP does assemble free linear ubiquitin chains *in vitro* but does not modify NEMO (NF-κB essential modifier), a key LUBAC substrate. However, in the presence of catalytically active HOIL-1, linear ubiquitin chain formation at NEMO lysines is efficient (Smit et al., 2013). The assembly of linear ubiquitin chains on substrates by HOIP requires priming of the first ubiquitin on a substrate lysine residue followed by the linkage of an incoming ubiquitin to the N-terminus of the "primed" target ubiquitin. HOIP assembles linear ubiquitin chains preferentially on K63-ubiquitinated substrates, resulting in heterotypic ubiquitin chains (Emmerich et al., 2013, 2016; Fiil et al., 2013; Hrdinka et al., 2016). In support of this notion, the

Abbreviations: BCL10, B cell leukemia/lymphoma 10; cIAP, cellular inhibitor of apoptosis protein; CARD, caspase recruitment domain; CYLD, cylindromatosis lysine 63 deubiquitinase; DLBCL, diffuse large B cell lymphoma; ERAD, endoplasmic reticulum-associated degradation; HOIL-1, haem-oxidized iron-regulatory protein 2 ubiquitin ligase-1; HOIP, HOIL-1-interacting protein; HUWE1, HECT, UBA, and WWE domain containing E3 ubiquitin protein ligase 1; IKK, IκB kinase complex; IRAK, interleukin 1 receptor associated kinase; IRP2, iron regulatory protein 2; KLN1, kinetochore null protein 1; LDD, linear ubiquitin chain determining domain; LPS, lipopolysaccharide; LUBAC, linear ubiquitin chain assembly complex; LUBEL, linear ubiquitin E3 ligase; MALT1, mucosa-associated lymphoid tissue protein-1; MLKL, mixed lineage kinase domain-like; MyD88, myeloid differentiation primary response gene 88; NEMO, NF-κB essential modifier; NF-κB, nuclear factor of kappa light polypeptide gene enhancer in B-cells; NLRP3, NLR family pyrin domain containing 3; NOD, nucleotide binding oligomerization domain containing; ORAS, OTULIN-related inflammatory syndrome; RIG-I, retinoic acid-inducible gene-I; RING, really interesting new gene; RIPK, receptor-interacting serine/threonine-protein kinase; RBR, RING-in-between-RING; SHARPIN, Shank-associated RH domain-interacting protein; SNP, single nucleotide polymorphism; SPATA2, spermatogenesis-associated protein 2; UBA, ubiquitin-associated; UBD, ubiquitin-binding domain; UBAN, ubiquitin-binding domain in ABIN proteins and NEMO; UBL, ubiquitin-like; PIM, PUB-interacting motif; PUB, PNGase/UBA or UBX-containing proteins; TAB, TAK1-binding protein; TAK1, transforming growth factor-β-activated kinase 1; TBK1, TANK binding kinase; TLR, Toll-like receptor; TNF, tumor necrosis factor; TNFR, TNF receptor; TRAF, TNF receptor-associated factor; TRAIL, TNF-related apoptosis-inducing ligand; VCP/p97, valosin-containing protein; XIAP, X-linked inhibitor of apoptosis.

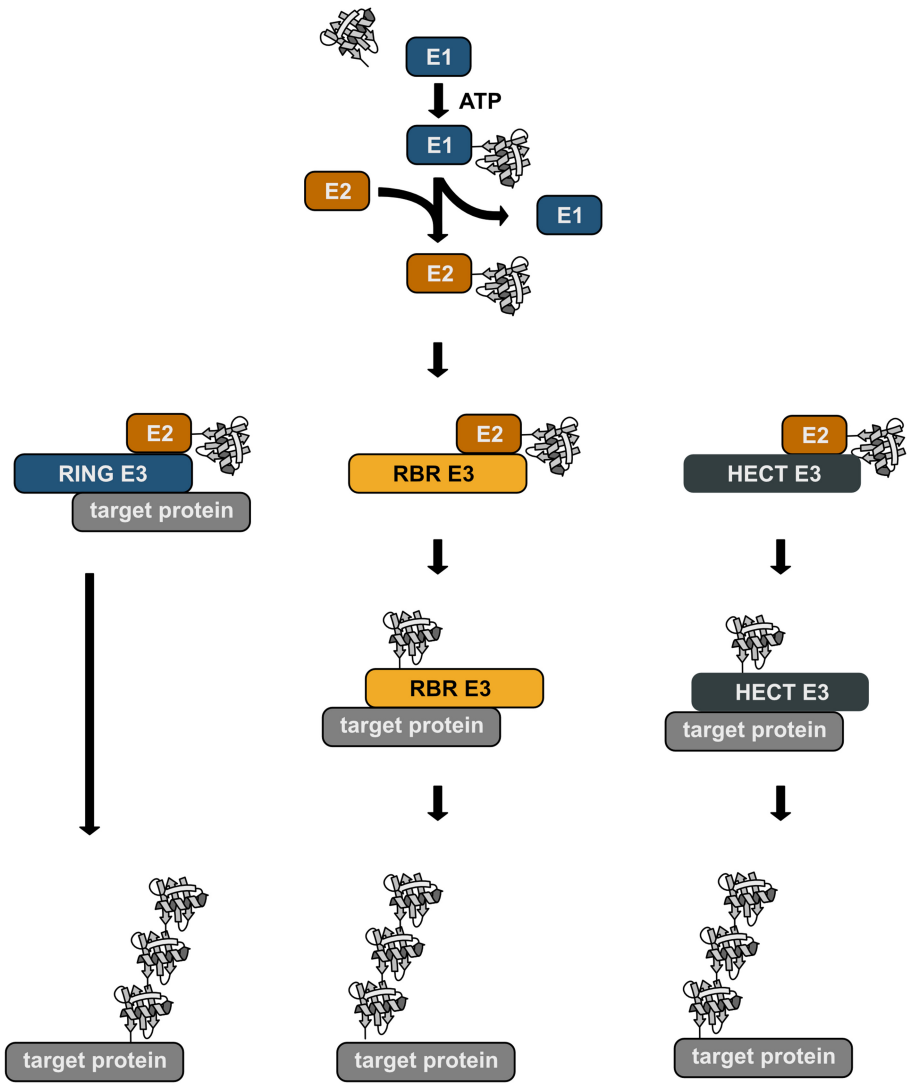

FIGURE 1 | Enzymatic cascade of ubiquitination. Ubiquitin is transferred to the target protein by an enzymatic cascade. Ubiquitin is first bound by an ubiquitin-activating enzyme (E1) using one ATP molecule. The activated ubiquitin is then transferred to a conjugating enzyme (E2). Depending on the type of the E3 ubiquitin ligase that is involved in the ubiquitination process, ubiquitin is directly transferred from the E2 to the target protein with the ligase acting as specific bridging factor (RING ligases). Alternatively, the ubiquitin moiety is transferred to the E3 ligase (RBR and HECT ligases) via a transient thioester bond before it is attached to the target protein by an isopeptide bond.

RBR E3 ubiquitin ligase Parkin can increase LUBAC-mediated linear ubiquitination of NEMO by modifying NEMO with K63-linked ubiquitin (Henn et al., 2007; Sha et al., 2010; Müller-Rischart et al., 2013; Asaoka et al., 2016).

Recently, HOIL-1 was found to act as an atypical E3 ligase by forming an oxyester bond between the C-terminus of ubiquitin and serine or threonine residues (Kelsall et al., 2019). This activity of HOIL-1 is implicated in its auto-ubiquitination and in the modification of substrates within Toll-like receptor signaling, such as IRAK1, IRAK2, and MyD88, by monoubiquitin (Kelsall et al., 2019). Monoubiquitin attached to substrates by HOIL-1 via an oxyester bond can act as a target for further ubiquitination, suggesting a role of HOIL-1 in initiating polyubiquitin chain formation.

Several proteins have been described to interact with linear ubiquitin chains via specific ubiquitin-binding domains (UBDs) (reviewed in Fennell et al., 2018; **Figure 2**). These interactors include proteins with a UBAN (UBD in ABIN proteins and NEMO) domain, such as NEMO, ABIN-1, ABIN-2, ABIN-3, and Optineurin. HOIL-1 and A20 interact via zinc finger domains with M1-linked ubiquitin. In addition, the deubiquitinases OTULIN and CYLD, which both are capable of hydrolyzing M1-linked polyubiquitin, bind to linear ubiquitin chains through their catalytic domains.

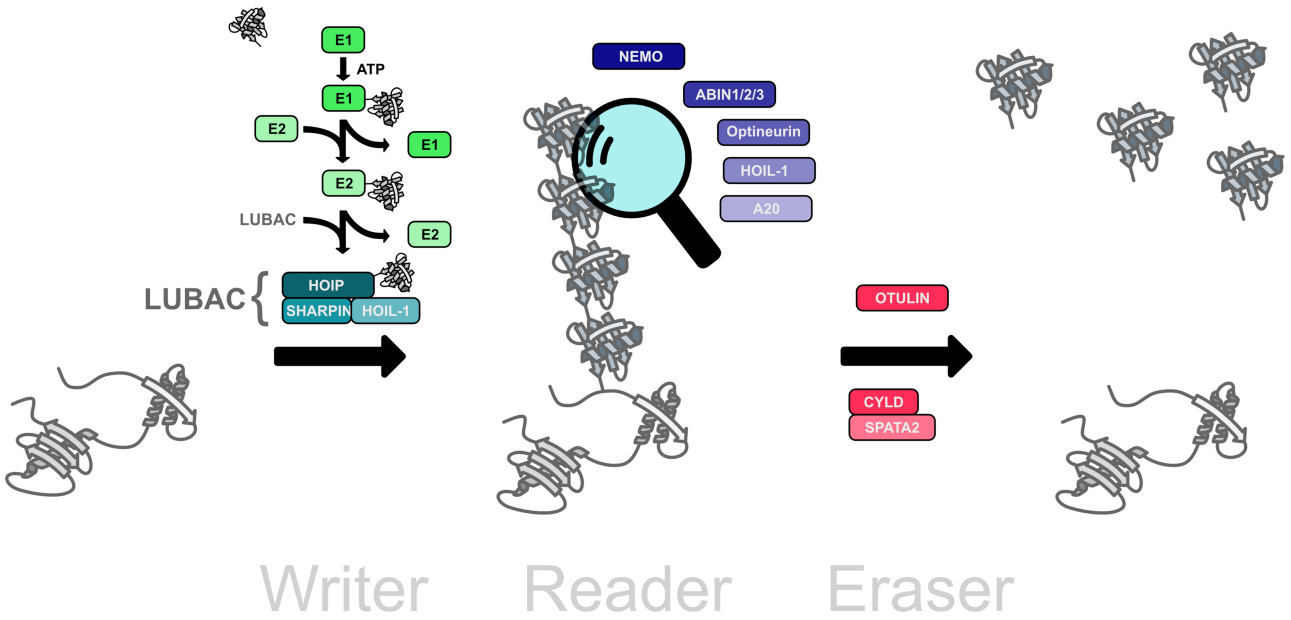

FIGURE 2 | The linear ubiquitination machinery. Linear ubiquitin chains are assembled by LUBAC, the linear ubiquitin chain assembly complex, comprising HOIL, HOIL-1, and SHARPIN (writers). This modification can be translated into a cellular effect by proteins that specifically interact with linear ubiquitin chains (readers). The linear ubiquitination signal can be removed by deubiquitinases that disassemble M1-linked ubiquitin chains (erasers).

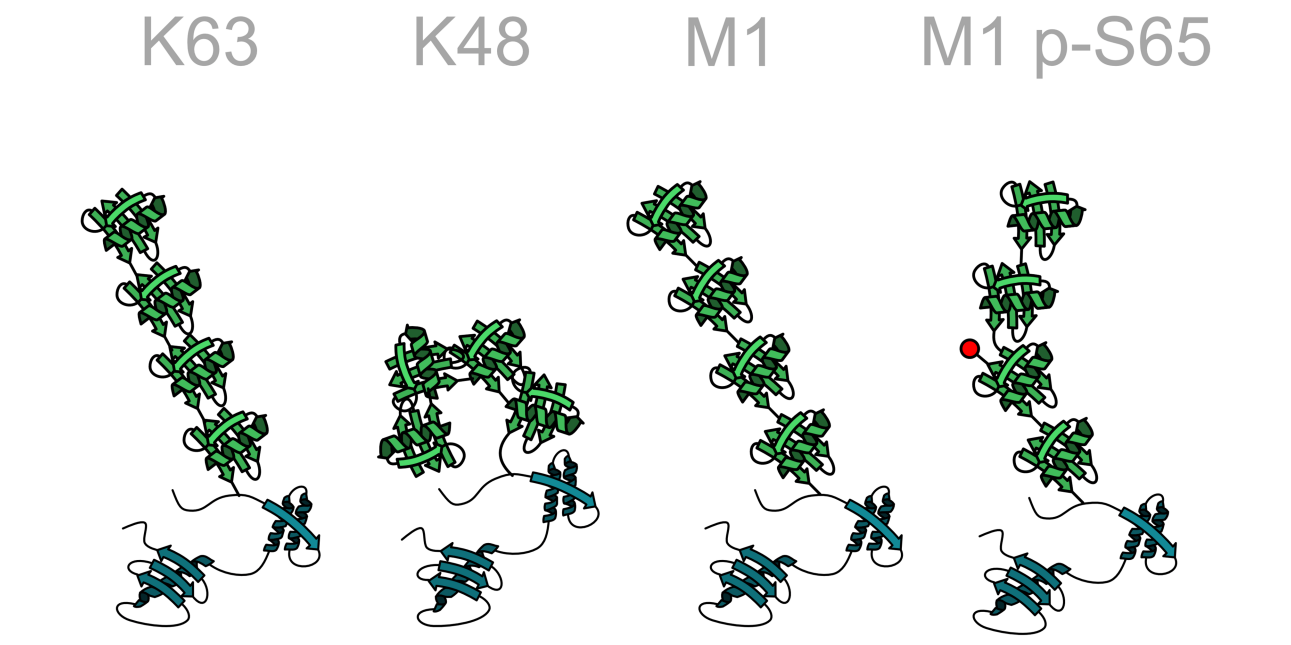

FIGURE 3 | Structural diversity of ubiquitin chains. In homotypic ubiquitin chains ubiquitin monomers are linked to one of seven lysine (K) residues or to the N-terminal methionine (M1). For example, in a K48-linked ubiquitin chain all ubiquitin monomers are linked to lysine 48 of the acceptor ubiquitin moiety. Different linkage types are characterized by specific conformations of the polyubiquitin chain, such as an open or closed conformation. The structure of the chain can be further modified by post-translational modifications of ubiquitin, here indicated by the phosphorylation of serine 65 in a linear ubiquitin chain. Ubiquitin: green; target protein: blue.

OTULIN is the only known deubiquitinase that exclusively disassembles linear ubiquitin chains (Keusekotten et al., 2013; Rivkin et al., 2013). The reason for this specificity is based on two features: First, OTULIN binds with high affinity to M1-linked polyubiquitin and second, it employs a mechanism of ubiquitin-assisted catalysis, implicating activation of the catalytic triad by the proximal ubiquitin moiety (Keusekotten et al., 2013). OTULIN binds to the N-terminal PUB (PNGase/UBA

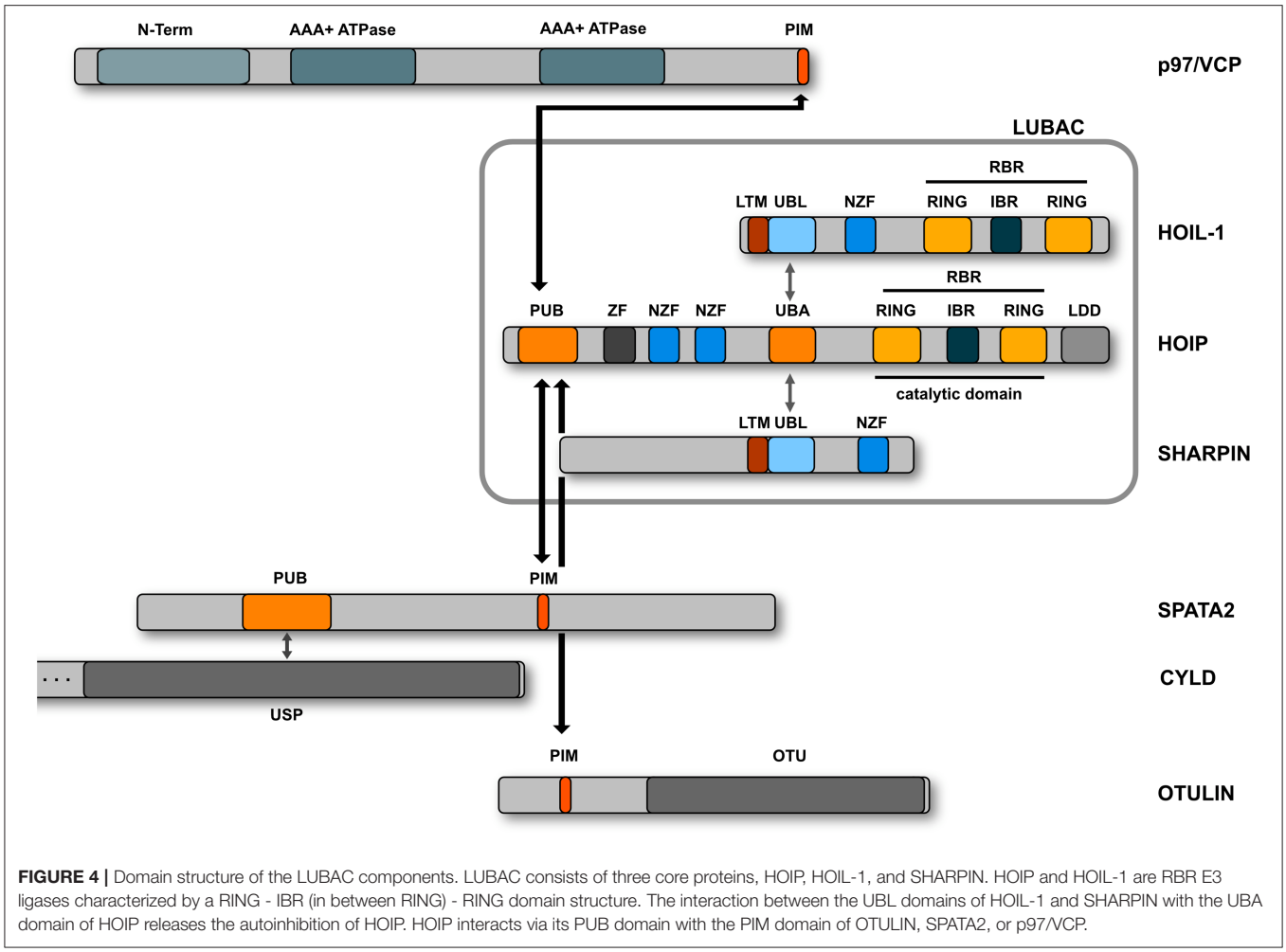

FIGURE 4 | Domain structure of the LUBAC components. LUBAC consists of three core proteins, HOIP, HOIL-1, and SHARPIN. HOIP and HOIL-1 are RBR E3 ligases characterized by a RING - IBR (in between RING) - RING domain structure. The interaction between the UBL domains of HOIL-1 and SHARPIN with the UBA domain of HOIP releases the autoinhibition of HOIP. HOIP interacts via its PUB domain with the PIM domain of OTULIN, SPATA2, or p97/VCP.

or UBX-containing proteins) domain of HOIP via its PUB-interacting motif (PIM) and this interaction seems to be regulated by phosphorylation (Elliott et al., 2014; Schaeffer et al., 2014; Takiuchi et al., 2014). The PUB domain of HOIP can also interact with SPATA2 that binds CYLD and thereby bridges this deubiquitinase to LUBAC (Elliott et al., 2016; Kupka et al., 2016; Schlicher et al., 2016; Wagner et al., 2016). CYLD hydrolyzes both K63- and M1-linked ubiquitin chains (Komander et al., 2009; Sato et al., 2011; Ritorto et al., 2014) and together with OTULIN regulates signaling by linear ubiquitin chains. In contrast to CYLD, OTULIN prevents LUBAC from auto-ubiquitination (Fiil et al., 2013; Keusekotten et al., 2013; Hrdinka et al., 2016; Heger et al., 2018). Importantly, binding of OTULIN and SPATA2 to HOIP is mutually exclusive, since both proteins compete for binding to the PUB domain (Draber et al., 2015; Elliott et al., 2016). Whereas the absence of OTULIN induces a strong increase in the abundance of M1-linked ubiquitin (Rivkin et al., 2013; Damgaard et al., 2016), this is not observed in the absence of CYLD (Draber et al., 2015). It is therefore conceivable that CYLD exerts a ubiquitin chain-editing function by trimming K63-linked chains and influencing K63-M1-hybrid chain formation (Emmerich et al., 2013, 2016; Hrdinka et al., 2016).

CELLULAR FUNCTIONS OF LINEAR UBIQUITIN CHAINS

LUBAC and TNF Signaling

Linear ubiquitin chains generated by LUBAC play a key role in regulating innate and adaptive immunity and inflammatory signaling, for example via the TNF receptor (TNFR1), IL-1 receptor, CD40, TRAIL receptor, Toll-like receptors (TLRs), T and B cell receptors, NOD1 and NOD2 receptors, RIG-I receptors, and the NLRP3 inflammasome (reviewed in Iwai et al., 2014; Hrdinka and Gyrd-Hansen, 2017; Rittinger and Ikeda, 2017; Spit et al., 2019; **Figure 5**). Consistent with the regulation of these pathways by M1-linked ubiquitin, several LUBAC substrates have been identified, such as NEMO, RIPK1, RIPK2, TRADD, TNFR1, IRAK1/2/4, and MyD88 (Haas et al., 2009; Tokunaga et al., 2009; Gerlach et al., 2011; Emmerich et al., 2013; Fiil et al., 2013; Draber et al., 2015; Wertz et al., 2015; Kelsall et al., 2019).

LUBAC function has most widely been studied in the context of TNF signaling (reviewed in Peltzer and Walczak, 2019; Spit et al., 2019). In 2009, LUBAC was shown to activate canonical NF-κB signaling in response to TNF or IL-1 stimulation by conjugating linear ubiquitin chains on

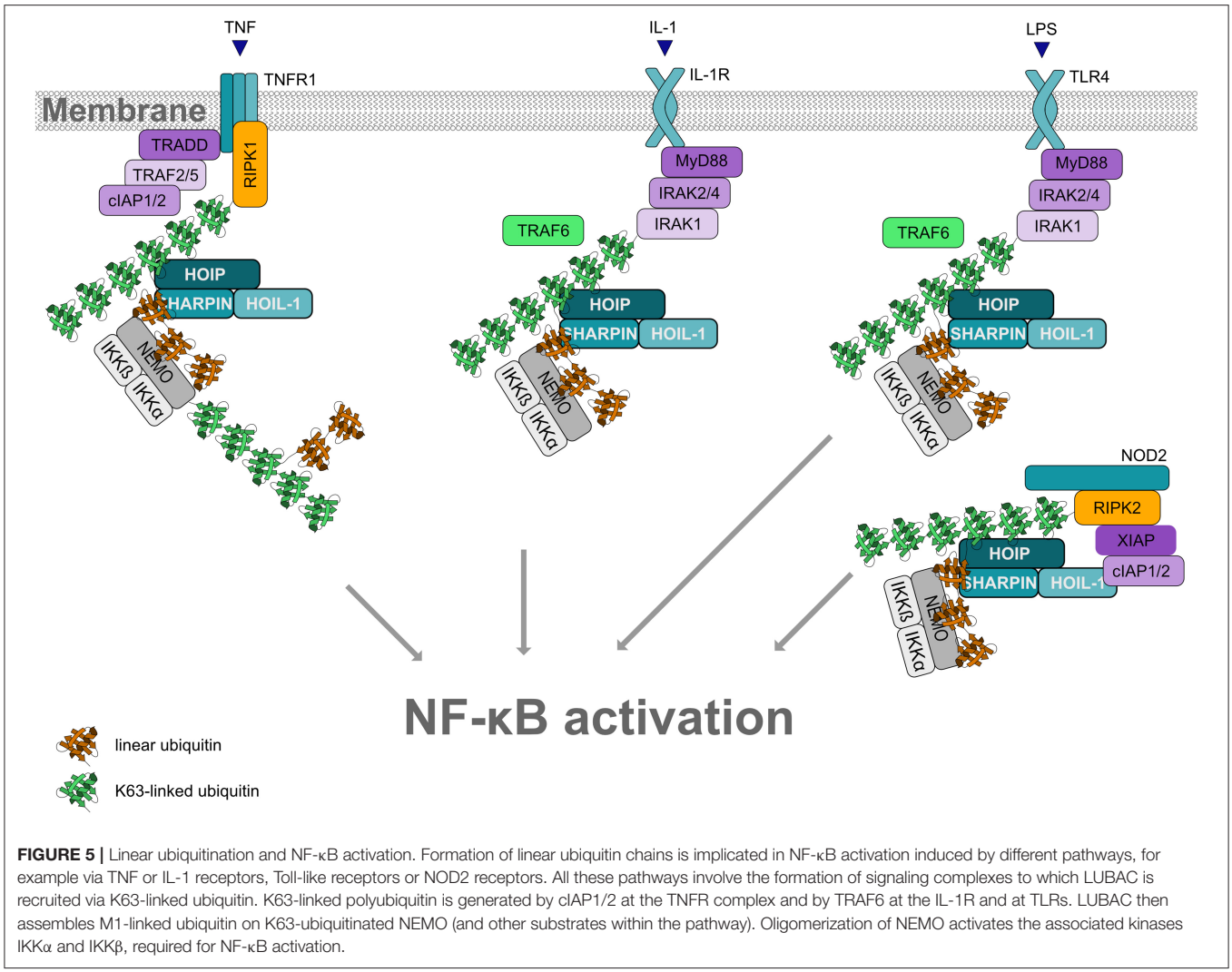

FIGURE 5 | Linear ubiquitination and NF-κB activation. Formation of linear ubiquitin chains is implicated in NF-κB activation induced by different pathways, for example via TNF or IL-1 receptors, Toll-like receptors or NOD2 receptors. All these pathways involve the formation of signaling complexes to which LUBAC is recruited via K63-linked ubiquitin. K63-linked polyubiquitin is generated by cIAP1/2 at the TNFR complex and by TRAF6 at the IL-1R and at TLRs. LUBAC then assembles M1-linked ubiquitin on K63-ubiquitinated NEMO (and other substrates within the pathway). Oligomerization of NEMO activates the associated kinases IKKα and IKKβ, required for NF-κB activation.

NEMO, the core regulatory component of the IκB kinases (IKK) complex (Haas et al., 2009; Tokunaga et al., 2009). Moreover, NEMO harbors a UBAN domain that binds to M1-linked ubiquitin with high affinity (Komander et al., 2009; Rahighi et al., 2009). Upon binding of TNF to its receptor at the plasma membrane, a multiprotein signaling complex, denoted complex I, is assembled, which is regulated by phosphorylation and ubiquitination. K63-linked polyubiquitin generated by cIAP1/2 recruits LUBAC to the activated TNFR1. LUBAC adds linear ubiquitin chains to various substrates, resulting in the formation of mixed K63-/M1-linked heterotypic chains. Since NEMO is not only modified by M1-linked ubiquitin, but also binds to M1-linked ubiquitin via its UBAN domain, linear ubiquitination of NEMO promotes its oligomerization. This induces a conformational change of the associated kinases IKKα and IKKβ within the IKK complex, leading to their activation. Activated IKKs phosphorylate the NF-κB inhibitor IkBα, which is subsequently modified with K48-linked ubiquitin and degraded by the proteasome. Thus, NF-κB heterodimers are released from their inhibitory binding and translocate into the nucleus to regulate the expression of NF-κB target genes. Depending on the cell type and cellular context, NF-κB upregulates pro-survival and/or inflammatory gene expression.

When the formation of the cytoprotective complex I is compromised, for example through defective ubiquitination mediated by either cIAPs or LUBAC, complex II is generated that induces cell death (reviewed in Dondelinger et al., 2016). A crucial player in the transition between complex I and complex II is RIPK1. Phosphorylation of RIPK1 at specific sites for example by TAK1, IKKα, IKKβ, IKKε, or TBK1 has been shown to prevent complex II formation by keeping RIPK1 in an inactive, non-autophosphorylated state (Dondelinger et al., 2015; Annibaldi and Meier, 2018; Lafont et al., 2018; Xu et al., 2018). Notably, TBK1 and IKKε are recruited to complex I mostly by M1-linked ubiquitin (Lafont et al., 2018). Complex II can promote either apoptosis (when caspase-8 is active) or necroptosis, induced by the necrosome formed by RIPK1, RIPK3, and MLKL (reviewed in Peltzer and Walczak, 2019).

LUBAC-Associated Pathologies

In support of a substantial role of LUBAC in regulating immune signaling, mice deficient in the expression of LUBAC components suffer from severe phenotypes. Both HOIP knockout (KO) and HOIL-1 KO mice lacking the UBL domain are not viable and die around E10.5 (Emmerich et al., 2013; Sasaki et al., 2013; Peltzer et al., 2014; Fujita et al., 2018). Interestingly, mice expressing catalytically inactive HOIL-1 (C458S knock-in mice) are viable, since this mutant can still bind and stabilize HOIP in contrast to HOIL-1 lacking the UBL domain (Kelsall et al., 2019). Mice with a spontaneous autosomal recessive loss-of-function mutation in the SHARPIN gene develop chronic proliferative dermatitis, systemic inflammation, and increased apoptosis in the liver, lung, and skin (Seymour et al., 2007; Gerlach et al., 2011; Ikeda et al., 2011; Tokunaga et al., 2011). Notably, defective disassembly of M1-linked ubiquitin has also severe consequences. Mice homozygous for missense mutations interfering with OTULIN function, exhibit embryonic lethality between E12.5 and E14, characterized by vascularization defects and impaired Wnt signaling (Rivkin et al., 2013).

In humans, reduced HOIP expression due to a missense mutation in the HOIP gene causes multiorgan autoinflammation and immunodeficiency (Boisson et al., 2015). These clinical phenotypes widely overlap with those seen in some HOIL-1-deficient patients. Depending on the type of mutation, these patients show autoinflammation and immunodeficiency or polyglucosan storage myopathy (muscular amylopectinosis) and cardiomyopathy (Boisson et al., 2012; Nilsson et al., 2013; Wang et al., 2013). Interestingly, homozygous loss-of-function mutations in the OTULIN gene cause an auto-inflammatory condition, called ORAS (OTULIN-related inflammatory syndrome) or otulipenia that is responsive to anti-TNF treatment (Damgaard et al., 2016; Zhou et al., 2016). These multifaceted pathologies underpin the complex interplay between assembly and disassembly of linear ubiquitin chains, requiring tight regulation and fine-tuned balancing in a cell-type- and context-specific manner.

Given its role in cell death regulation, LUBAC is also associated with oncogenic signaling. Two germline missense single nucleotide polymorphisms (SNPs) in the gene encoding HOIP are enriched in patients suffering from a subtype of diffuse large B cell lymphoma (DLBCL). In activated B cell-like (ABC) DLBCL the constitutive activation of NF-κB mediated by B cell receptor signaling (implicating CARD11, MALT1, and BCL10) and MyD88 signaling is a major pathogenic mechanism, promoting malignant cell survival. The two SNPs identified in ABC DLBCL are located in the UBA domain of HOIP affecting the HOIP/HOIL-1 interface and were shown to enhance LUBAC activity and NF-κB signaling (Yang et al., 2014). In addition, oncogenic CARD11 mutants found in ABC DLBCL spontaneously induce linear ubiquitination of BCL10 by enhancing the interaction between HOIP and BCL10 (Yang et al., 2016b). LUBAC recruitment to BCL10 is promoted by cIAP1/2 which assemble K63-linked ubiquitin chains on BCL10 and on themselves (Yang et al., 2016a). In an siRNA screen, HOIP was identified as a modifier of cisplatin-induced toxicity (MacKay et al., 2014). Depletion of HOIP or expression of catalytically inactive HOIP sensitizes different cancer cell lines to genotoxin-induced apoptotic cell death. Supporting a role of LUBAC in chemotherapy resistance, expression of LUBAC components is significantly higher in cisplatin-resistant cancer cell lines (MacKay et al., 2014) and patient samples and preclinical mouse models of lung squamous cell carcinoma (LSCC) (Ruiz et al., 2019). Moreover, the small molecule HOIP inhibitor gliotoxin sensitizes LSCC cells and mice to cisplatin (Ruiz et al., 2019). A recent study linked LUBAC to chromosome alignment during mitosis. LUBAC was reported to ubiquitinate the kinetochore motor CENP-E that binds in its M1-ubiquitinated form to the linear ubiquitin chain receptor KLN1 (kinetochore null protein 1) at attached kinetochors thereby promoting accurate chromosome segregation (Wu et al., 2019). Whether LUBAC is a feasible drug target to treat malignant diseases needs to be explored in future studies.

LUBAC and Intracellular Bacteria

It has recently been discovered that LUBAC is recruited to the surface of cytosol-invading bacteria, such as *Salmonella enterica* serovar Typhimurium, that have escaped the endocytic pathway and therefore are no longer shielded by host membranes (Zhou et al., 2016; Noad et al., 2017; van Wijk et al., 2017). Bacterial surface components as well as associated host membrane remnants are ubiquitinated by several E3 ubiquitin ligases to generate a ubiquitin coat (Perrin et al., 2004). HOIP binds to this ubiquitin coat via its N-terminal NZF domains (Noad et al., 2017). In addition, the catalytic activity of HOIP is required for its recruitment, suggesting a feed-forward mechanism through synthesizing and binding M1-linked ubiquitin at the bacterial surface (Noad et al., 2017). Linear ubiquitin chains generated by LUBAC recruit the effector proteins NEMO and Optineurin to cytosolic bacteria. As a consequence, two events are induced that independently restrict bacterial proliferation: Local activation of NF-κB mediated by NEMO and stimulation of antibacterial autophagy (xenophagy) mediated by Optineurin (Noad et al., 2017). These effects can be enhanced by decreasing the expression of OTULIN via RNA interference or CRISPR/Cas9 knockout (van Wijk et al., 2012; Noad et al., 2017).

LUBAC and Protein Quality Control

LUBAC is not only recruited to cytosolic bacteria but also to cytosolic protein aggregates, suggesting that assemblies of misfolded proteins are sensed as a special kind of "cellular pathogen" or danger-associated molecular pattern (van Well et al., 2019). We observed that LUBAC modifies misfolded Huntingtin containing a pathogenic polyglutamine expansion (Htt-polyQ) with M1-linked ubiquitin and thereby shapes the ubiquitin coat of these aggregates. Linear ubiquitination of both cytosolic bacteria and aggregates has beneficial cellular effects, yet mediated by different mechanisms (**Figure 6**). HOIP is recruited to protein aggregates by p97/VCP, a triple A-type quality control ATPase that can extract ubiquitinated proteins from macromolecular complexes or lipid membranes. p97/VCP also has a PIM domain which is required for the interaction with the PUB domain of HOIP (Elliott et al., 2014; Schaeffer et al., 2014; Takiuchi et al., 2014). As a consequence of linear ubiquitin

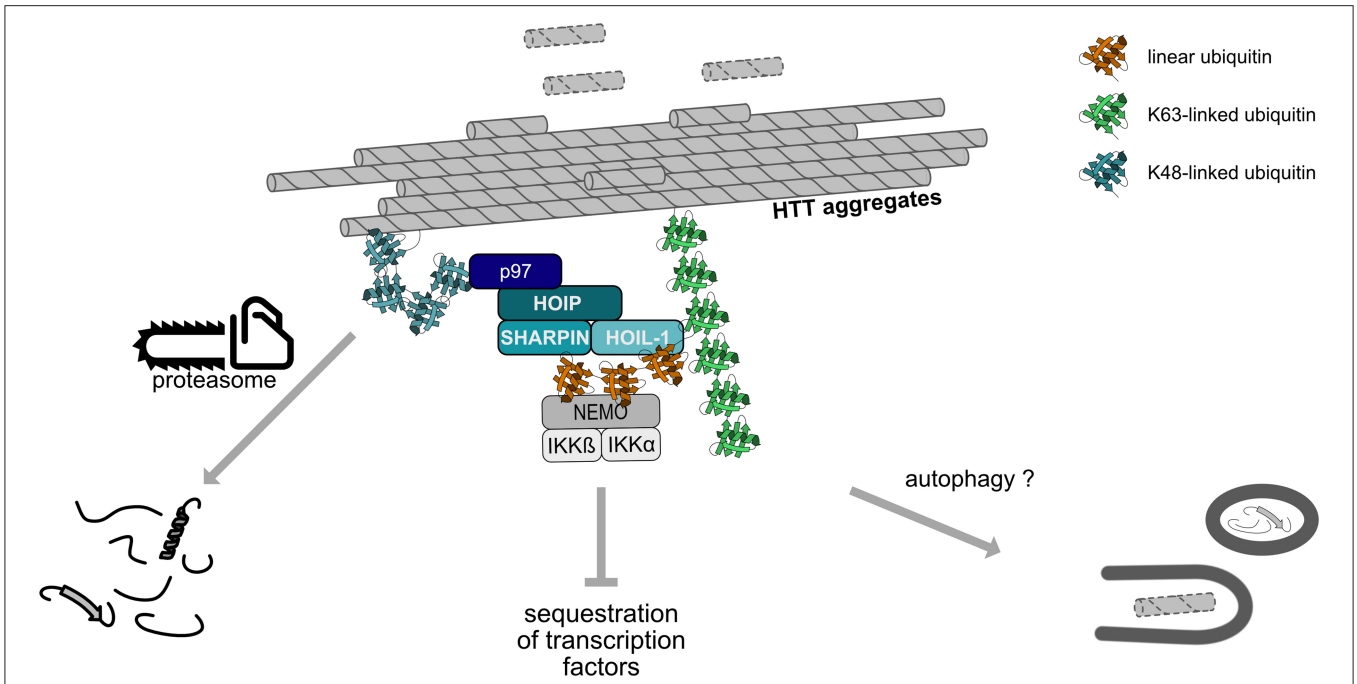

FIGURE 6 | Linear ubiquitination of Huntingtin aggregates. Huntingtin (Htt) aggregates are covered by a ubiquitin coat, including K48- and K63-linked chains. HOIP is recruited to these aggregates in a p97/VCP-dependent manner and together with HOIL-1 and SHARPIN assembles M1-linked ubiquitin chains. Subsequent recruitment of proteins specifically interacting with linear ubiquitin, such as NEMO, remodels the interactive surface of the aggregates. Linear ubiquitination promotes proteasomal degradation of misfolded Htt species and may also increase the removal of aggregates by autophagy.

chain assembly at Htt-polyQ aggregates, the interactive surface of misfolded Huntingtin species is shielded from unwanted interactions, such as the sequestration of low complexity domain-containing transcription factors that causes transcriptional dysregulation in Huntington's disease. Moreover, LUBAC facilitates proteasomal degradation of misfolded Htt-polyQ species in a p97/VCP-dependent manner (van Well et al., 2019).

Interestingly, a *Drosophila* ortholog of HOIP termed LUBEL (linear ubiquitin E3 ligase) is involved in the heat shock response in flies (Asaoka et al., 2016). Flies expressing catalytically inactive LUBEL mutants show climbing defects and reduced survival upon heat stress, which supports a role of linear ubiquitination in protein quality control.

Heterotypic Ubiquitin Chains Implicating M1 Linkage

The formation of heterotypic ubiquitin chains strongly diversifies the structure and hence the functional impact of polyubiquitin chains (Haakonsen and Rape, 2019). Heterotypic chains contain more than one linkage type, resulting in mixed or branched ubiquitin chains. In mixed chains, the ubiquitin molecules are connected by different linkage types but each subunit is connected via a lysine or the N-terminal methionine to only one other ubiquitin molecule. In branched chains, at least one ubiquitin subunit is linked to two or even more ubiquitin molecules, which may result in highly complex chain architectures. The mechanisms underlying heterotypic chain formation have not been uncovered in detail yet, but it is emerging that ubiquitin chain initiation, elongation, and branching often requires an intricate cooperation between different E2 and E3 enzymes.

There is increasing evidence for the formation of various branched ubiquitin chains and their specific role in regulating cellular functions. For example, K11/K48-branched chains are characterized by a higher affinity to the proteasome and to p97/VCP and therefore act as a proteasomal priority signal (Meyer and Rape, 2014). In line with such a function, K11/K48-heterotypic chains have been implicated in cell cycle and protein quality control by promoting rapid and efficient proteasomal degradation of mitosis regulators and misfolded cytoplasmic proteins or ERAD substrates (Meyer and Rape, 2014; Yau et al., 2017; Samant et al., 2018; Leto et al., 2019). A structural analysis of branched K11/K48 tri-ubiquitin revealed a unique hydrophobic interdomain interface between the distal ubiquitins that binds the proteasomal receptor Rpn1 with increased affinity (Boughton et al., 2019). Notably, K29/K48- and K48/K63-branched ubiquitin chains can also mediate efficient proteasomal degradation (Kristariyanto et al., 2015; Ohtake et al., 2018).

In addition to promoting proteasomal degradation, heterotypic ubiquitin chains play a role in regulating signaling pathways, as has been demonstrated for NF-κB signaling. K48/K63-branched ubiquitin chains generated by TRAF6 (K63) and HUWE1 (K48) in response to IL-1 stimulation amplify NF-κB signaling by protecting from CYLD-mediated hydrolysis of K63-linked ubiquitin (Ohtake et al., 2016). M1-linked ubiquitin

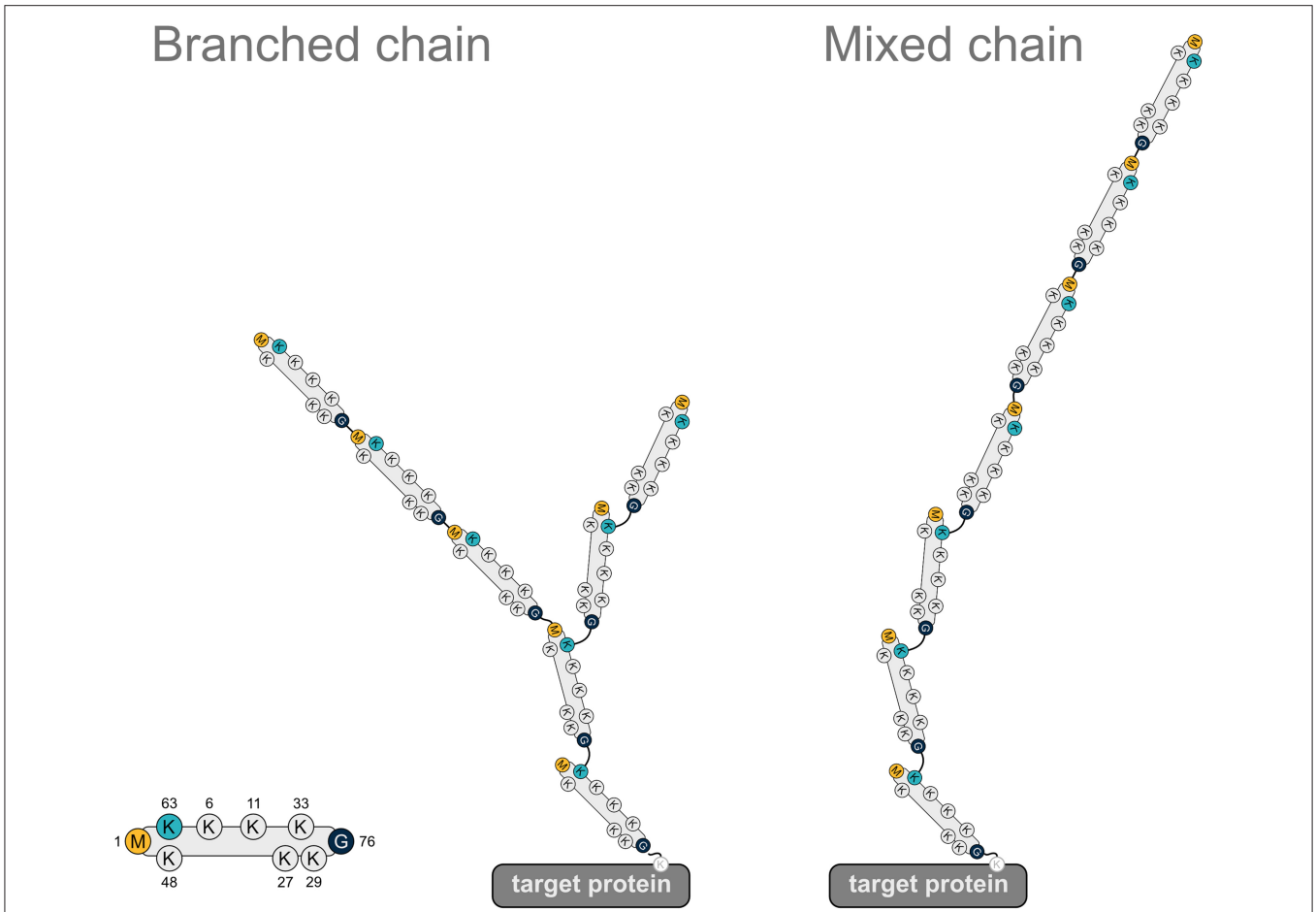

FIGURE 7 | Heterotypic ubiquitin chains implicating M1-linked ubiquitin. Two examples for heterotypic ubiquitin chains containing M1-linked ubiquitin. Linear ubiquitin chains can branch off K63-linked chains via peptide formation between an N-terminal methionine of a ubiquitin molecule within the K63 polyubiquitin and the C-terminal glycine of the incoming ubiquitin (branched chain). Alternatively, the incoming ubiquitin can be added to the N-terminal methionine of the last ubiquitin of the K63-linked chain (mixed chain). G, glycine; K, lysine; M, methionine.

chains are also implicated in the formation of heterotypic chains. In fact, most of the M1-linked chains formed upon IL-1 stimulation are covalently attached to K63-linked chains (Emmerich et al., 2013), although the precise topology (mixed or branched, **Figure 7**) has not been elucidated so far. When K63-linked ubiquitination is inhibited by the deletion of the E2 complex Ubc13-Uev1a, IL-1-induced formation of M1-linked ubiquitin is also strongly reduced, suggesting that K63 ubiquitination is a prerequisite for the formation of M1 ubiquitin chains (Emmerich et al., 2013). In addition to IL-1 signaling, heterotypic M1/K63 ubiquitin chains have been identified upon activation of TNFR1, TLR3, and NOD1 receptors, suggesting that the formation of these hybrid chains is a general feature in innate immune signaling implicating LUBAC (Emmerich et al., 2016). HOIP interacts with K63-linked ubiquitin via its NZF domains, which presumably favors the generation of heterotypic M1/K63 chains (Haas et al., 2009; Emmerich et al., 2013). From a functional perspective, M1/K63 ubiquitin heterotypic chains could act as a platform to co-recruit and concentrate interacting proteins that specifically bind to either K63-linked ubiquitin (such as TAB2 and TAB3 of the TAK1 complex) or M1-linked ubiquitin (such as NEMO of the IKK complex), thereby increasing the efficiency of IKK complex activation (Zhang et al., 2014). It is also conceivable that co-recruitment of regulatory proteins to M1/K63 heterotypic ubiquitin chains helps to fine-tune signaling events in a spatio-temporal manner. In support of this notion, branched M1/K63-linked ubiquitin chains formed upon TNF stimulation inhibit disassembly of K63-linked polyubiquitin by A20 and thus preserve active signaling complexes (Wertz et al., 2015).

DETECTION OF LINEAR CHAINS

Antibodies

The development of chain-specific antibodies by Newton et al. allows the detection of specific chain topologies using western blotting techniques and has been extended by antibodies developed by other groups (Newton et al., 2008; Matsumoto

et al., 2012; Sasaki et al., 2013; Nakayama et al., 2019). The antibodies are raised to specifically recognize the special topology of the ubiquitin chain linkage and can be used for the detection of the chains in western blots, immunocytochemistry and immunohistochemistry (reviewed in van Wijk et al., 2019).

Tandem Ubiquitin Binding Entities (TUBEs)

Ubiquitin signaling is detected by sets of specific reader molecules. These proteins are able to detect besides the position of the ubiquitination also the topology of the chain. The interaction of the ubiquitin signal reader with the ubiquitin chain is mediated by ubiquitin-interacting motifs in these proteins (Watkins et al., 1993; Bertolaet et al., 2001; Wilkinson et al., 2001; Zhang et al., 2008; Rahighi et al., 2009). By fusing several of these interaction motifs into a new detection molecule, a TUBE is created (Hjerpe and Rodríguez, 2008; Hjerpe et al., 2009). The specificity of the single ubiquitin interaction motif is enhanced by the combination and can then be used for enrichment strategies or a far-western blot experiment.

Targeted Proteomics

The rapid development of proteomics in the last decade positioned mass spectrometry-based proteomics (discovery proteomics) as the default technique for the detection of several thousand proteins in a single experiment. Parallel to the development of discovery proteomics a second technique for the analysis of samples has been developed. This technology, targeted proteomics, is focussed on the quantification of a specific set of proteins instead of the identification of as many proteins as possible. Here, a specific set of proteins is selected before the measurement and key peptides for the selected proteins are used. By focussing the measurement on a set of key peptides the measurement gains sensitivity, thus allowing the detection of very small amounts of proteins in the sample. The continuous nature of the measurement ensures that the selected peptides will be detected in all samples, if they are present, and avoid the random selection issues that are associated with a shotgun measurement which are responsible for the generation of missing data points. The disadvantage of the method is the preselection of peptides as it does not allow the detection of any other protein than the preselected ones.

Selected and Parallel Reaction Monitoring (SRM/PRM)

The implementation of the detection method is usually linked to the use of either triple-quadrupole or Q-orbitrap mass spectrometers. For the specific detection of a peptide, the mass spectrometer has to filter for the full mass of the peptide. The selected peptide is then broken down into fragments by collision-induced fragmentation and key fragment masses are selected for detection. For SRM the selection of the precursor mass is done by the first quadrupole, the fragmentation in the second and the third is selecting specific fragments one after the other. The use of PRM allows the parallel measurement of all peptide fragments for a given mass. For increased sensitivity, the quantification is then based on a smaller number of fragments that are selected to avoid interference from co-selected peptides. Usually, the PRM method employs a high-resolution mass spectrometer thus allowing to further reduce the influence of interfering fragments by applying a strong selection based on the high-resolution measurement (**Figure 8**; Lange et al., 2008; Mirzaei et al., 2010; Ordureau et al., 2015; Bourmaud et al., 2016).

The identification of the right fragments across a chromatographic separation depends on the elution time and the precursor/fragment pairs. To ensure the right elution points in the gradient, the use of isotope-labeled standards is recommended. Here the same peptide that is monitored using SRM or PRM is chemically synthesized using an isotope-labeled amino acid. Since the light and heavy peptides are chemically identical the peptides co-elute. The quantification of the peptide can then be done between different runs, given the chromatographic setup is stable enough for a comparison. If the isotope-labeled standard peptide is spiked in at a known concentration it can serve as a standard for absolute quantification of the light counterpart.

Measurement of the Ubiquitin Chain Topology

Post-translational modification by ubiquitin occurs on lysine side chains or the N-terminus of proteins. Here a conjugation cascade connects the C-terminus of ubiquitin to the ε-amino group of lysines or the N-terminal amino group. The target protein can be a protein that is regulated by ubiquitination or ubiquitin itself, forming ubiquitin chains.

Ubiquitin chain topology analysis takes advantage of this unique shape. When a ubiquitin chain is digested with the endoproteinase trypsin key peptides are generated that carry two glycine residues on the side chain. These two remnant residues are coming from the -RGG C-terminus of the next ubiquitin in the chain and are cut off by trypsin during the generation of the peptides (Peng and Gygi, 2001). For the N-terminal ubiquitin fusion, a signature peptide starting with the GG and continuing with the N-terminus of ubiquitin is created by the tryptic digestion. These signature peptides are then used as surrogates for the presence of ubiquitin chains and can be quantified using different targeted proteomics techniques (**Figure 9**). Recently, the Komander group created a viral protease-derived recombinant protease, which recognizes the C-terminus of ubiquitin (Swatek et al., 2018, 2019). The cleavage of the ubiquitin chains occurs after arginine 74 and leaves the GG-remnant on the lysine side chain of ubiquitin or the substrate protein. The analysis of ubiquitin by intact mass spectrometry revealed ubiquitin molecules decorated with several GG-remnants. Quantification of this ubiquitin population shows that 10–20% of the ubiquitin chains are branched (Swatek et al., 2019).

Studies using middle-down proteomics, which is based on a partial tryptic digestion of ubiquitin chains, were able to elucidate the chain length and branching of the polyubiquitin chain (Xu and Peng, 2008; Valkevich et al., 2014; Rana et al., 2017).

A different approach has been developed by Tsuchiya et al. using a TUBE construct with a tryptic digest for the mass spectrometric analysis (trypsin-resistant TUBE, TR-TUBE). The TR-TUBE binds the polyubiquitin chain

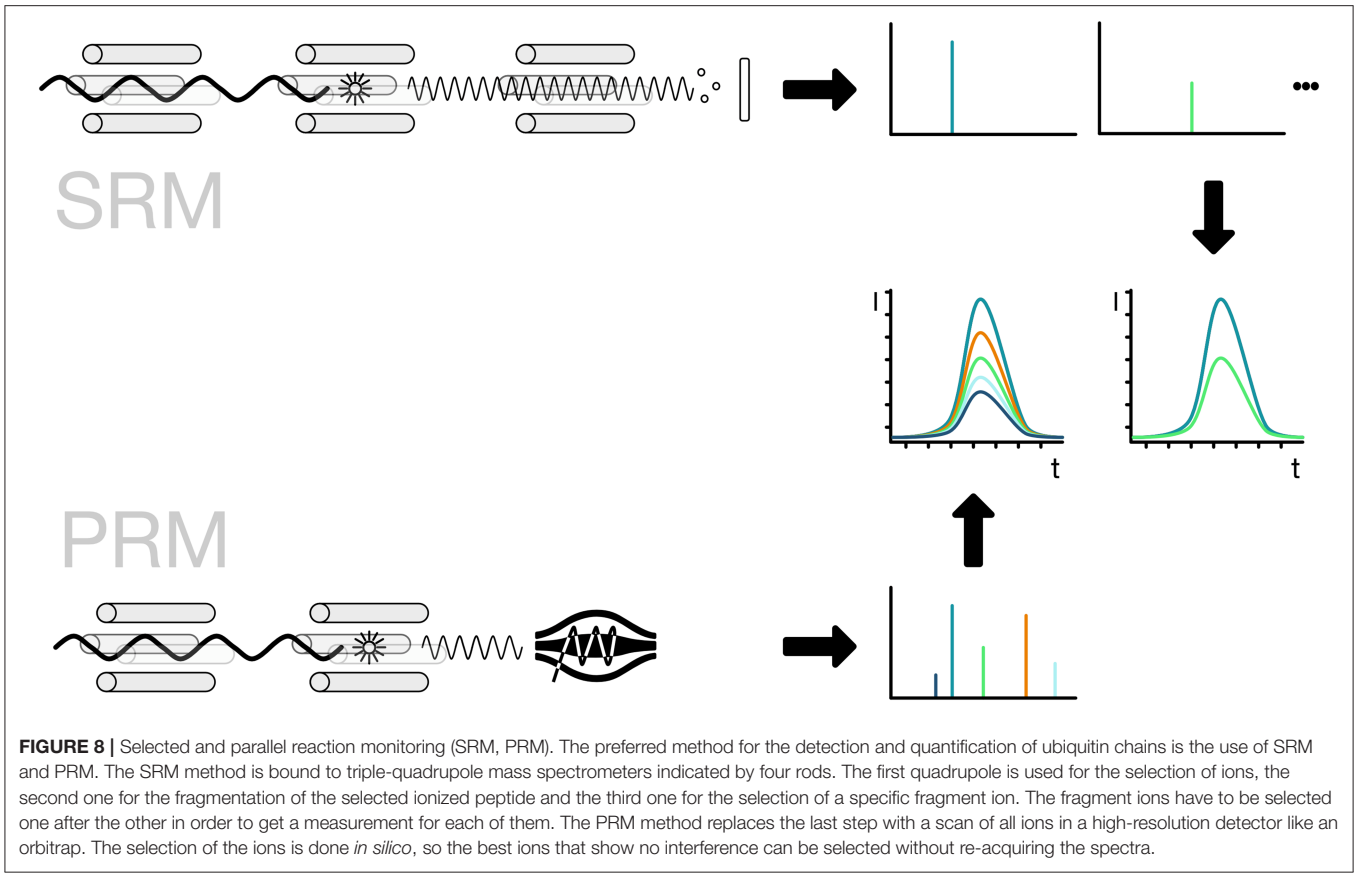

FIGURE 8 | Selected and parallel reaction monitoring (SRM, PRM). The preferred method for the detection and quantification of ubiquitin chains is the use of SRM and PRM. The SRM method is bound to triple-quadrupole mass spectrometers indicated by four rods. The first quadrupole is used for the selection of ions, the second one for the fragmentation of the selected ionized peptide and the third one for the selection of a specific fragment ion. The fragment ions have to be selected one after the other in order to get a measurement for each of them. The PRM method replaces the last step with a scan of all ions in a high-resolution detector like an orbitrap. The selection of the ions is done *in silico*, so the best ions that show no interference can be selected without re-acquiring the spectra.

and is used to pull out the ubiquitinated substrate proteins. In a subsequent tryptic digest the substrate proteins is identified. This allows the distinction of the mono-ubiquitinated proteins from polyubiquitinated ones (Tsuchiya et al., 2018).

Difficulties of Ubiquitin Chain Topology Detection

Ubiquitin-associated signaling can, like other post-translational signals, be erased by two different mechanisms, the dissociation of the ubiquitin chain from the protein target or the degradation of the protein target. While the degradation of the target protein is mostly associated with K48 and K11 chains (Chau et al., 1989; Williamson et al., 2011), the dissociation of ubiquitin chains by deubiquitinating enzymes can occur on all types of chains. For the detection of degradation-mediating chains, the inhibition of the proteasome as the endpoint of the reaction can lead to stabilization of the chains (Kim et al., 2011; Wagner et al., 2011). For the detection of linear chains, proteasome-associated degradation seems to be less important, but the disassembly reaction of chains can severely impair the detection. For the inhibition of the disassembly reaction, several techniques have been employed. The use of highly denaturing agents during the lysis of the cells, using guanidinium hydrochloride (Lectez et al., 2014) or urea (Peng et al., 2003; Bagola et al., 2013), have been proven effective. Other strategies include the precipitation of proteins prior to the extraction using tri-chloric acid (Ziv et al., 2011) or chemical inhibition which is widely used. Most of the deubiquitinating enzymes belong to the class of cysteine proteases which carry a cysteine in the active center of the enzyme. Alkylating agents specific to sulfhydryl groups can be used to modify the active center and thus inactivate the enzyme. N-ethylmalemide and iodoacetamide are widely used, although it has been shown that iodoacetamide can cause unspecific modification of lysine side chains with the same molecular weight as a double-glycine modification (Nielsen et al., 2008), leading to false detection of ubiquitination sites. Other modifications and the inability of certain proteomic search engines to detect ubiquitination appropriately can lead to false-positive identifications as reviewed in Beaudette et al. (2016).

Ubiquitin has a very stable fold and can easily refold after heat or denaturation using chemical agents. This can pose a significant challenge to the accurate quantification of ubiquitin chains using mass spectrometric techniques. The generation of the ubiquitin peptides is dependent on the accessibility of all potential cleavage sites to the proteases used. If ubiquitin is not completely digested this would lead to a significant underestimation of the ubiquitin-derived peptides. Strategies using a two-step digestion protocol under highly denaturing conditions (8M urea) with a protease like endopeptidase lysC in a first step to degrade the protein into smaller pieces, followed by a dilution step and

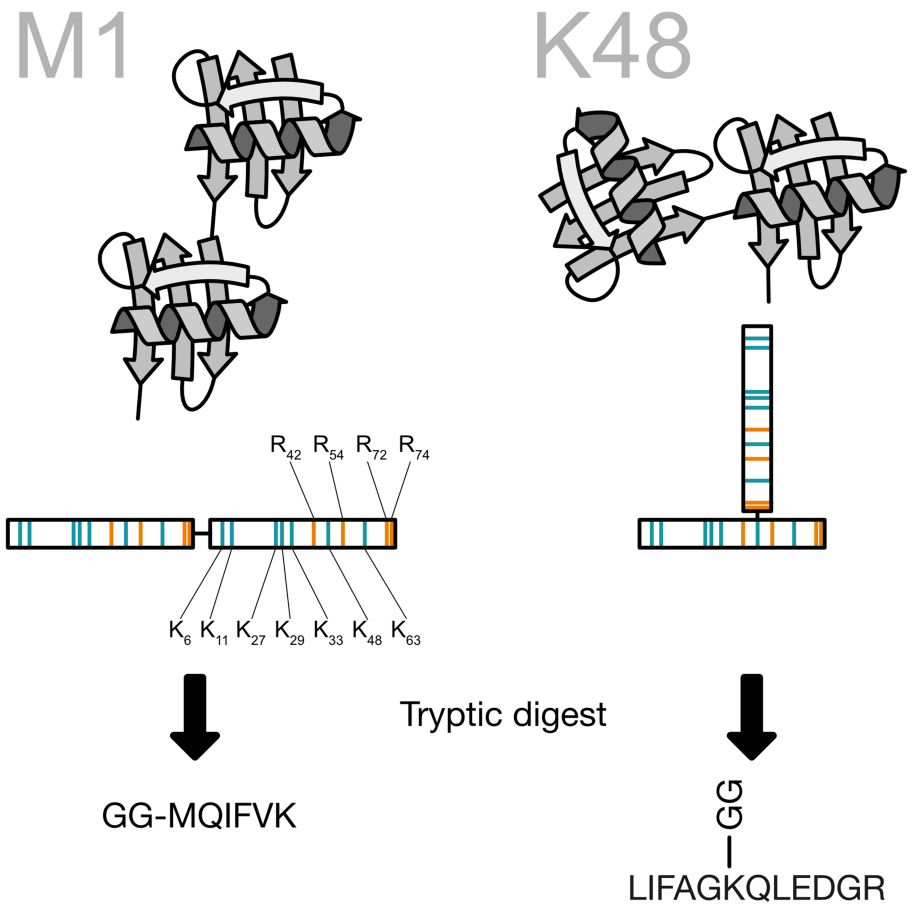

FIGURE 9 | Generation of the ubiquitin chain specific peptides. The C-terminus of ubiquitin is bound to a lysine side chain of the previous ubiquitin. Ubiquitin contains a number of arginine residues that are recognized by the protease trypsin. By cutting after arginine 74 the last two amino acids of ubiquitin are remaining on the lysine side chain and create a peptide, which carries two glycines on the ε-amino group of the lysine. This prevents at the same time a digestion of the modified lysine. All key peptides for ubiquitin chains carry the two glycine residues on a specific lysine side chain except for linear ubiquitin, where the ubiquitin is fused head-to-tail. This particular key peptide carries the two glycine residues on the N-terminus.

the digestion with trypsin, as trypsin is not active under highly denaturing conditions (de Godoy et al., 2008). Alternatively, the addition of mild mass-spectrometry-compatible detergents, like RapiGest, can enhance the sensitivity of the detection (Longworth and Dittmar, 2019).

Advantages and Disadvantages of Using Chain-Specific Antibodies vs. Detection by Mass Spectrometry

The detection of ubiquitin chain topology using antibodies has the obvious advantage of not being dependent on a mass spectrometry laboratory and usually the rapid detection associated with the simple western blot setup. Although the quality of the chain topology-dependent antibodies has improved over time, the quality of the antibody is still dependent on production batches and can vary significantly between batches. The quantification of different chain topologies is difficult and the quantification across different topologies requires high-quality standard to be added to the analysis. The mass spectrometry-based techniques are independent of production batches, but face other challenges. The above-mentioned digestion problem can lead to a significant underestimation of the chains. The determination of ubiquitin topologies is dependent on the detection of a single peptide, which carries the specific modification. Each of the seven characteristic peptides has its own affinity for unspecific absorption to plasticware. In order to prevent the unspecific loss of peptides due to absorption, the use of a carrier (like an *E. coli* digest) has proven effective to prevent losses of the peptides and the spike-in reference peptide (Longworth and Dittmar, 2019). The use of a spike-in reference peptide (Ubi-AQUA) provides the possibility for absolute quantification (Kirkpatrick et al., 2006; Mirzaei et al., 2010; Ordureau et al., 2015). Here special attention to the possibility of losses due to absorption has to be considered, as it can lead to incorrect quantification of the reference standard prior to the spike-in. The quantification of the characteristic peptides can also pose a challenge as

some of the peptides show a tendency for the formation of double peaks that are hard to quantify reliably, although changes to the chromatographic setup can minimize the effect (personal observation).

AUTHOR CONTRIBUTIONS

All authors listed have made a substantial, direct and intellectual contribution to the work, and approved it for publication.

ACKNOWLEDGMENTS

GD is supported by the Luxembourg National Research Fund grants C17/BM/11642138 and SigSing. KW is supported by the Deutsche Forschungsgemeinschaft (WI/2111-6, WI/2111/8), the Michael J. Fox Foundation (Grant Number 16293) and gefördert durch die Deutsche Forschungsgemeinschaft (DFG) im Rahmen der Exzellenzstrategie des Bundes und der Länder—EXC 2033—Projektnummer 390677874—RESOLV.

REFERENCES

Akutsu, M., Dikic, I., and Bremm, A. (2016). Ubiquitin chain diversity at a glance. *J. Cell Sci.* 129, 875–880. doi: 10.1242/jcs.183954

Annibaldi, A., and Meier, P. (2018). Checkpoints in TNF-induced cell death: implications in inflammation and cancer. *Trends Mol. Med.* 24, 49–65. doi: 10.1016/j.molmed.2017.11.002

Asaoka, T., Almagro, J., Ehrhardt, C., Tsai, I., Schleiffer, A., Deszcz, L., et al. (2016). Linear ubiquitination by LUBEL has a role in Drosophila heat stress response. *EMBO Rep.* 17, 1624–1640. doi: 10.15252/embr.201642378

Bagola, K., von Delbrück, M., Dittmar, G., Scheffner, M., Ziv, I., Glickman, M. H., et al. (2013). Ubiquitin binding by a CUE domain regulates ubiquitin chain formation by ERAD E3 ligases. *Mol. Cell* 50, 528–539. doi: 10.1016/j.molcel.2013.04.005

Beaudette, P., Popp, O., and Dittmar, G. (2016). Proteomic techniques to probe the ubiquitin landscape. *Proteomics* 16, 273–287. doi: 10.1002/pmic.201500290

Bertolaet, B. L., Clarke, D. J., Wolff, M., Watson, M. H., Henze, M., Divita, G., et al. (2001). UBA domains of DNA damage-inducible proteins interact with ubiquitin. *Nat. Struct. Biol.* 8, 417–422. doi: 10.1038/87575

Boisson, B., Laplantine, E., Dobbs, K., Cobat, A., Tarantino, N., Hazen, M., et al. (2015). Human HOIP and LUBAC deficiency underlies autoinflammation, immunodeficiency, amylopectinosis, and lymphangiectasia. *J. Exp. Med.* 212, 939–951. doi: 10.1084/jem.20141130

Boisson, B., Laplantine, E., Prando, C., Giliani, S., Israelsson, E., Xu, Z., et al. (2012). Immunodeficiency, autoinflammation and amylopectinosis in humans with inherited HOIL-1 and LUBAC deficiency. *Nat. Immunol.* 13, 1178–1186. doi: 10.1038/ni.2457

Boughton, A. J., Krueger, S., and Fushman, D. (2019). Branching via K11 and K48 Bestows ubiquitin chains with a unique interdomain interface and enhanced affinity for proteasomal subunit Rpn1. *Structure*. doi: 10.1016/j.str.2019.10.008. [Epub ahead of print].

Bourmaud, A., Gallien, S., and Domon, B. (2016). Parallel reaction monitoring using quadrupole-Orbitrap mass spectrometer: principle and applications. *Proteomics* 16, 2146–2159. doi: 10.1002/pmic.201500543

Chau, V., Tobias, J. W., Bachmair, A., Marriott, D., Ecker, D. J., Gonda, D. K., et al. (1989). A multiubiquitin chain is confined to specific lysine in a targeted short-lived protein. *Science* 243, 1576–1583. doi: 10.1126/science.2538923

Damgaard, R. B., Walker, J. A., Marco-Casanova, P., Morgan, N. V., Titheradge, H. L., Elliott, P. R., et al. (2016). The deubiquitinase OTULIN is an essential negative regulator of inflammation and autoimmunity. *Cell* 166, 1215–1230.e20. doi: 10.1016/j.cell.2016.07.019

de Godoy, L. M. F., Olsen, J. V., Cox, J., Nielsen, M. L., Hubner, N. C., Fröhlich, F., et al. (2008). Comprehensive mass-spectrometry-based proteome quantification of haploid versus diploid yeast. *Nature* 455, 1251–1254. doi: 10.1038/nature07341

Dikic, I., Wakatsuki, S., and Walters, K. J. (2009). Ubiquitin-binding domains - from structures to functions. *Nat. Rev. Mol. Cell Biol.* 10, 659–671. doi: 10.1038/nrm2767

Dondelinger, Y., Darding, M., Bertrand, M. J. M., and Walczak, H. (2016). Poly-ubiquitination in TNFR1-mediated necroptosis. *Cell. Mol. Life Sci.* 73, 2165–2176. doi: 10.1007/s00018-016-2191-4

Dondelinger, Y., Jouan-Lanhouet, S., Divert, T., Theatre, E., Bertin, J., Gough, P. J., et al. (2015). NF-κB-independent role of IKKα/IKKβ in preventing RIPK1 kinase-dependent apoptotic and necroptotic cell death during TNF signaling. *Mol. Cell* 60, 63–76. doi: 10.1016/j.molcel.2015.07.032

Draber, P., Kupka, S., Reichert, M., Draberova, H., Lafont, E., de Miguel, D., et al. (2015). LUBAC-recruited CYLD and A20 regulate gene activation and cell death by exerting opposing effects on linear ubiquitin in signaling complexes. *Cell Rep.* 13, 2258–2272. doi: 10.1016/j.celrep.2015.11.009

Elliott, P. R., Leske, D., Hrdinka, M., Bagola, K., Fiil, B. K., McLaughlin, S. H., et al. (2016). SPATA2 links CYLD to LUBAC, activates CYLD, and controls LUBAC signaling. *Mol. Cell* 63, 990–1005. doi: 10.1016/j.molcel.2016.08.001

Elliott, P. R., Nielsen, S. V., Marco-Casanova, P., Fiil, B. K., Keusekotten, K., Mailand, N., et al. (2014). Molecular basis and regulation of OTULIN-LUBAC interaction. *Mol. Cell* 54, 335–348. doi: 10.1016/j.molcel.2014.03.018

Emmerich, C. H., Bakshi, S., Kelsall, I. R., Ortiz-Guerrero, J., Shpiro, N., and Cohen, P. (2016). Lys63/Met1-hybrid ubiquitin chains are commonly formed during the activation of innate immune signalling. *Biochem. Biophys. Res. Commun.* 474, 452–461. doi: 10.1016/j.bbrc.2016.04.141

Emmerich, C. H., Ordureau, A., Strickson, S., Arthur, J. S. C., Pedrioli, P. G. A., Komander, D., et al. (2013). Activation of the canonical IKK complex by K63/M1-linked hybrid ubiquitin chains. *Proc. Natl. Acad. Sci. U.S.A.* 110, 15247–15252. doi: 10.1073/pnas.1314715110

Fennell, L. M., Rahighi, S., and Ikeda, F. (2018). Linear ubiquitin chain-binding domains. *FEBS J.* 285, 2746–2761. doi: 10.1111/febs.14478

Fiil, B. K., Damgaard, R. B., Wagner, S. A., Keusekotten, K., Fritsch, M., Bekker-Jensen, S., et al. (2013). OTULIN restricts Met1-linked ubiquitination to control innate immune signaling. *Mol. Cell* 50, 818–830. doi: 10.1016/j.molcel.2013.06.004

Fujita, H., Tokunaga, A., Shimizu, S., Whiting, A. L., Aguilar-Alonso, F., Takagi, K., et al. (2018). Cooperative domain formation by homologous motifs in HOIL-1L and SHARPIN plays a crucial role in LUBAC stabilization. *Cell Rep.* 23, 1192–1204. doi: 10.1016/j.celrep.2018.03.112

Gerlach, B., Cordier, S. M., Schmukle, A. C., Emmerich, C. H., Rieser, E., Haas, T. L., et al. (2011). Linear ubiquitination prevents inflammation and regulates immune signalling. *Nature* 471, 591–596. doi: 10.1038/nature09816

Haakonsen, D. L., and Rape, M. (2019). Branching out: improved signaling by heterotypic ubiquitin chains. *Trends Cell Biol.* 29, 704–716. doi: 10.1016/j.tcb.2019.06.003

Haas, T. L., Emmerich, C. H., Gerlach, B., Schmukle, A. C., Cordier, S. M., Rieser, E., et al. (2009). Recruitment of the linear ubiquitin chain assembly complex stabilizes the TNF-R1 signaling complex and is required for TNF-mediated gene induction. *Mol. Cell* 36, 831–844. doi: 10.1016/j.molcel.2009.10.013

Heger, K., Wickliffe, K. E., Ndoja, A., Zhang, J., Murthy, A., Dugger, D. L., et al. (2018). OTULIN limits cell death and inflammation by deubiquitinating LUBAC. *Nature* 559, 120–124. doi: 10.1038/s41586-018-0256-2

Henn, I. H., Bouman, L., Schlehe, J. S., Schlierf, A., Schramm, J. E., Wegener, E., et al. (2007). Parkin mediates neuroprotection through activation of IkappaB kinase/nuclear factor-kappaB signaling. *J. Neurosci.* 27, 1868–1878. doi: 10.1523/JNEUROSCI.5537-06.2007

Hjerpe, R., Aillet, F., Lopitz-Otsoa, F., Lang, V., England, P., and Rodriguez, M. S. (2009). Efficient protection and isolation of ubiquitylated proteins using tandem ubiquitin-binding entities. *EMBO Rep.* 10, 1250–1258. doi: 10.1038/embor.2009.192

Hjerpe, R., and Rodríguez, M. S. (2008). Efficient approaches for characterizing ubiquitinated proteins. *Biochem. Soc. Trans.* 36, 823–827. doi: 10.1042/BST0360823

Hrdinka, M., Fiil, B. K., Zucca, M., Leske, D., Bagola, K., Yabal, M., et al. (2016). CYLD Limits Lys63- and Met1-linked ubiquitin at receptor complexes to regulate innate immune signaling. *Cell Rep.* 14, 2846–2858. doi: 10.1016/j.celrep.2016.02.062

Hrdinka, M., and Gyrd-Hansen, M. (2017). The Met1-linked ubiquitin machinery: emerging themes of (De)regulation. *Mol. Cell* 68, 265–280. doi: 10.1016/j.molcel.2017.09.001

Ikeda, F., Deribe, Y. L., Skånland, S. S., Stieglitz, B., Grabbe, C., Franz-Wachtel, M., et al. (2011). SHARPIN forms a linear ubiquitin ligase complex regulating NF-κB activity and apoptosis. *Nature* 471, 637–641. doi: 10.1038/nature09814

Iwai, K., Fujita, H., and Sasaki, Y. (2014). Linear ubiquitin chains: NF-κB signalling, cell death and beyond. *Nat. Rev. Mol. Cell Biol.* 15, 503–508. doi: 10.1038/nrm3836

Kelsall, I. R., Zhang, J., Knebel, A., Arthur, J. S. C., and Cohen, P. (2019). The E3 ligase HOIL-1 catalyses ester bond formation between ubiquitin and components of the Myddosome in mammalian cells. *Proc. Natl. Acad. Sci. U.S.A.* 116, 13293–13298. doi: 10.1073/pnas.1905873116

Keusekotten, K., Elliott, P. R., Glockner, L., Fiil, B. K., Damgaard, R. B., Kulathu, Y., et al. (2013). OTULIN antagonizes LUBAC signaling by specifically hydrolyzing Met1-linked polyubiquitin. *Cell* 153, 1312–1326. doi: 10.1016/j.cell.2013.05.014

Kim, W., Bennett, E. J., Huttlin, E. L., Guo, A., Li, J., Possemato, A., et al. (2011). Systematic and quantitative assessment of the ubiquitin-modified proteome. *Mol. Cell* 44, 325–340. doi: 10.1016/j.molcel.2011.08.025

Kirisako, T., Kamei, K., Murata, S., Kato, M., Fukumoto, H., Kanie, M., et al. (2006). A ubiquitin ligase complex assembles linear polyubiquitin chains. *EMBO J.* 25, 4877–4887. doi: 10.1038/sj.emboj.7601360

Kirkpatrick, D. S., Hathaway, N. A., Hanna, J., Elsasser, S., Rush, J., Finley, D., et al. (2006). Quantitative analysis of *in vitro* ubiquitinated cyclin B1 reveals complex chain topology. *Nat. Cell Biol.* 8, 700–710. doi: 10.1038/ncb1436

Komander, D., Reyes-Turcu, F., Licchesi, J. D. F., Odenwaelder, P., Wilkinson, K. D., and Barford, D. (2009). Molecular discrimination of structurally equivalent Lys 63-linked and linear polyubiquitin chains. *EMBO Rep.* 10, 466–473. doi: 10.1038/embor.2009.55

Kristariyanto, Y. A., Abdul Rehman, S. A., Campbell, D. G., Morrice, N. A., Johnson, C., Toth, R., et al. (2015). K29-selective ubiquitin binding domain reveals structural basis of specificity and heterotypic nature of k29 polyubiquitin. *Mol. Cell* 58, 83–94. doi: 10.1016/j.molcel.2015.01.041

Kupka, S., De Miguel, D., Draber, P., Martino, L., Surinova, S., Rittinger, K., et al. (2016). SPATA2-mediated binding of CYLD to HOIP enables CYLD recruitment to signaling complexes. *Cell Rep.* 16, 2271–2280. doi: 10.1016/j.celrep.2016.07.086

Lafont, E., Draber, P., Rieser, E., Reichert, M., Kupka, S., de Miguel, D., et al. (2018). TBK1 and IKKε prevent TNF-induced cell death by RIPK1 phosphorylation. *Nat. Cell Biol.* 20, 1389–1399. doi: 10.1038/s41556-018-0229-6

Lange, V., Picotti, P., Domon, B., and Aebersold, R. (2008). Selected reaction monitoring for quantitative proteomics: a tutorial. *Mol. Syst. Biol.* 4:222. doi: 10.1038/msb.2008.61

Lechtenberg, B. C., Rajput, A., Sanishvili, R., Dobaczewska, M. K., Ware, C. F., Mace, P. D., et al. (2016). Structure of a HOIP/E2∼ubiquitin complex reveals RBR E3 ligase mechanism and regulation. *Nature* 529, 546–550. doi: 10.1038/nature16511

Lectez, B., Migotti, R., Lee, S. Y., Ramirez, J., Beraza, N., Mansfield, B., et al. (2014). Ubiquitin profiling in liver using a transgenic mouse with biotinylated ubiquitin. *J. Proteome Res.* 13, 3016–3026. doi: 10.1021/pr5001913

Leto, D. E., Morgens, D. W., Zhang, L., Walczak, C. P., Elias, J. E., Bassik, M. C., et al. (2019). Genome-wide CRISPR analysis identifies substrate-specific conjugation modules in ER-associated degradation. *Mol. Cell* 73, 377–389.e11. doi: 10.1016/j.molcel.2018.11.015

Liu, J., Wang, Y., Gong, Y., Fu, T., Hu, S., Zhou, Z., et al. (2017). Structural insights into SHARPIN-mediated activation of HOIP for the linear ubiquitin chain assembly. *Cell Rep.* 21, 27–36. doi: 10.1016/j.celrep.2017.09.031

Longworth, J., and Dittmar, G. (2019). Assessment of ubiquitin chain topology by targeted mass spectrometry. *Methods Mol. Biol.* 1977, 25–34. doi: 10.1007/978-1-4939-9232-4_3

MacKay, C., Carroll, E., Ibrahim, A. F. M., Garg, A., Inman, G. J., Hay, R. T., et al. (2014). E3 ubiquitin ligase HOIP attenuates apoptotic cell death induced by cisplatin. *Cancer Res.* 74, 2246–2257. doi: 10.1158/0008-5472.CAN-13-2131

Matsumoto, M. L., Dong, K. C., Yu, C., Phu, L., Gao, X., Hannoush, R. N., et al. (2012). Engineering and structural characterization of a linear polyubiquitin-specific antibody. *J. Mol. Biol.* 418, 134–144. doi: 10.1016/j.jmb.2011.12.053

Mevissen, T. E. T., and Komander, D. (2017). Mechanisms of deubiquitinase specificity and regulation. *Annu. Rev. Biochem.* 86, 159–192. doi: 10.1146/annurev-biochem-061516-044916

Meyer, H.-J., and Rape, M. (2014). Enhanced protein degradation by branched ubiquitin chains. *Cell* 157, 910–921. doi: 10.1016/j.cell.2014.03.037

Mirzaei, H., Rogers, R. S., Grimes, B., Eng, J., Aderem, A., and Aebersold, R. (2010). Characterizing the connectivity of poly-ubiquitin chains by selected reaction monitoring mass spectrometry. *Mol. Biosyst.* 6, 2004–2014. doi: 10.1039/c005242f

Müller-Rischart, A. K., Pilsl, A., Beaudette, P., Patra, M., Hadian, K., Funke, M., et al. (2013). The E3 ligase parkin maintains mitochondrial integrity by increasing linear ubiquitination of NEMO. *Mol. Cell* 49, 908–921. doi: 10.1016/j.molcel.2013.01.036

Nakayama, Y., Sakamoto, S., Tsuji, K., Ayaki, T., Tokunaga, F., and Ito, H. (2019). Identification of linear polyubiquitin chain immunoreactivity in tau pathology of Alzheimer's disease. *Neurosci. Lett.* 703, 53–57. doi: 10.1016/j.neulet.2019.03.017

Newton, K., Matsumoto, M. L., Wertz, I. E., Kirkpatrick, D. S., Lill, J. R., Tan, J., et al. (2008). Ubiquitin chain editing revealed by polyubiquitin linkage-specific antibodies. *Cell* 134, 668–678. doi: 10.1016/j.cell.2008.07.039

Nielsen, M. L., Vermeulen, M., Bonaldi, T., Cox, J., Moroder, L., and Mann, M. (2008). Iodoacetamide-induced artifact mimics ubiquitination in mass spectrometry. *Nat. Methods* 5, 459–460. doi: 10.1038/nmeth0608-459

Nilsson, J., Schoser, B., Laforet, P., Kalev, O., Lindberg, C., Romero, N. B., et al. (2013). Polyglucosan body myopathy caused by defective ubiquitin ligase RBCK1. *Ann. Neurol.* 74, 914–919. doi: 10.1002/ana.23963

Noad, J., von der Malsburg, A., Pathe, C., Michel, M. A., Komander, D., and Randow, F. (2017). LUBAC-synthesized linear ubiquitin chains restrict cytosol-invading bacteria by activating autophagy and NF-κB. *Nat. Microbiol.* 2:17063. doi: 10.1038/nmicrobiol.2017.63

Ohtake, F., Saeki, Y., Ishido, S., Kanno, J., and Tanaka, K. (2016). The K48-K63 branched ubiquitin chain regulates NF-κB signaling. *Mol. Cell* 64, 251–266. doi: 10.1016/j.molcel.2016.09.014

Ohtake, F., Tsuchiya, H., Saeki, Y., and Tanaka, K. (2018). K63 ubiquitylation triggers proteasomal degradation by seeding branched ubiquitin chains. *Proc. Natl. Acad. Sci. U.S.A.* 115, E1401–E1408. doi: 10.1073/pnas.1716673115

Ordureau, A., Münch, C., and Harper, J. W. (2015). Quantifying ubiquitin signaling. *Mol. Cell* 58, 660–676. doi: 10.1016/j.molcel.2015.02.020

Peltzer, N., Rieser, E., Taraborrelli, L., Draber, P., Darding, M., Pernaute, B., et al. (2014). HOIP deficiency causes embryonic lethality by aberrant TNFR1-mediated endothelial cell death. *Cell Rep.* 9, 153–165. doi: 10.1016/j.celrep.2014.08.066

Peltzer, N., and Walczak, H. (2019). Cell death and inflammation - a vital but dangerous liaison. *Trends Immunol.* 40, 387–402. doi: 10.1016/j.it.2019.03.006

Peng, J., and Gygi, S. P. (2001). Proteomics: the move to mixtures. *J. Mass Spectrom.* 36, 1083–1091. doi: 10.1002/jms.229

Peng, J., Schwartz, D., Elias, J. E., Thoreen, C. C., Cheng, D., Marsischky, G., et al. (2003). A proteomics approach to understanding protein ubiquitination. *Nat. Biotechnol.* 21, 921–926. doi: 10.1038/nbt849

Perrin, A. J., Jiang, X., Birmingham, C. L., So, N. S. Y., and Brumell, J. H. (2004). Recognition of bacteria in the cytosol of Mammalian cells by the ubiquitin system. *Curr. Biol.* 14, 806–811. doi: 10.1016/j.cub.2004.04.033

Rahighi, S., Ikeda, F., Kawasaki, M., Akutsu, M., Suzuki, N., Kato, R., et al. (2009). Specific recognition of linear ubiquitin chains by NEMO is important for NF-kappaB activation. *Cell* 136, 1098–1109. doi: 10.1016/j.cell.2009.03.007

Rana, A. S. J. B., Ambar, S. J., Ge, Y., and Strieter, E. R. (2017). Ubiquitin chain enrichment middle-down mass spectrometry (UbiChEM-MS) reveals cell-cycle dependent formation of Lys11/Lys48 branched ubiquitin chains. *J. Proteome Res.* 16, 3363–3369. doi: 10.1021/acs.jproteome.7b00381

Ritorto, M. S., Ewan, R., Perez-Oliva, A. B., Knebel, A., Buhrlage, S. J., Wightman, M., et al. (2014). Screening of DUB activity and specificity by MALDI-TOF mass spectrometry. *Nat. Commun.* 5:4763. doi: 10.1038/ncomms5763

Rittinger, K., and Ikeda, F. (2017). Linear ubiquitin chains: enzymes, mechanisms and biology. *Open Biol.* 7:170026. doi: 10.1098/rsob.170026

Rivkin, E., Almeida, S. M., Ceccarelli, D. F., Juang, Y.-C., MacLean, T. A., Srikumar, T., et al. (2013). The linear ubiquitin-specific deubiquitinase gumby regulates angiogenesis. *Nature* 498, 318–324. doi: 10.1038/nature12296

Ruiz, E. J., Diefenbacher, M. E., Nelson, J. K., Sancho, R., Pucci, F., Chakraborty, A., et al. (2019). LUBAC determines chemotherapy resistance in squamous cell lung cancer. *J. Exp. Med.* 216, 450–465. doi: 10.1084/jem.20180742

Samant, R. S., Livingston, C. M., Sontag, E. M., and Frydman, J. (2018). Distinct proteostasis circuits cooperate in nuclear and cytoplasmic protein quality control. *Nature* 563, 407–411. doi: 10.1038/s41586-018-0678-x

Sasaki, Y., Sano, S., Nakahara, M., Murata, S., Kometani, K., Aiba, Y., et al. (2013). Defective immune responses in mice lacking LUBAC-mediated linear ubiquitination in B cells. *EMBO J.* 32, 2463–2476. doi: 10.1038/emboj.2013.184

Sato, Y., Fujita, H., Yoshikawa, A., Yamashita, M., Yamagata, A., Kaiser, S. E., et al. (2011). Specific recognition of linear ubiquitin chains by the Npl4 zinc finger (NZF) domain of the HOIL-1L subunit of the linear ubiquitin chain assembly complex. *Proc. Natl. Acad. Sci. U.S.A.* 108, 20520–20525. doi: 10.1073/pnas.1109088108

Schaeffer, V., Akutsu, M., Olma, M. H., Gomes, L. C., Kawasaki, M., and Dikic, I. (2014). Binding of OTULIN to the PUB domain of HOIP controls NF-κB signaling. *Mol. Cell* 54, 349–361. doi: 10.1016/j.molcel.2014.03.016

Schlicher, L., Wissler, M., Preiss, F., Brauns-Schubert, P., Jakob, C., Dumit, V., et al. (2016). SPATA2 promotes CYLD activity and regulates TNF-induced NF-κB signaling and cell death. *EMBO Rep.* 17, 1485–1497. doi: 10.15252/embr.201642592

Seymour, R. E., Hasham, M. G., Cox, G. A., Shultz, L. D., Hogenesch, H., Roopenian, D. C., et al. (2007). Spontaneous mutations in the mouse Sharpin gene result in multiorgan inflammation, immune system dysregulation and dermatitis. *Genes Immun.* 8, 416–421. doi: 10.1038/sj.gene.6364403

Sha, D., Chin, L.-S., and Li, L. (2010). Phosphorylation of parkin by Parkinson disease-linked kinase PINK1 activates parkin E3 ligase function and NF-kappaB signaling. *Hum. Mol. Genet.* 19, 352–363. doi: 10.1093/hmg/ddp501

Smit, J. J., Monteferrario, D., Noordermeer, S. M., van Dijk, W. J., van der Reijden, B. A., and Sixma, T. K. (2012). The E3 ligase HOIP specifies linear ubiquitin chain assembly through its RING-IBR-RING domain and the unique LDD extension. *EMBO J.* 31, 3833–3844. doi: 10.1038/emboj.2012.217

Smit, J. J., van Dijk, W. J., El Atmioui, D., Merkx, R., Ovaa, H., and Sixma, T. K. (2013). Target specificity of the E3 ligase LUBAC for ubiquitin and NEMO relies on different minimal requirements. *J. Biol. Chem.* 288, 31728–31737. doi: 10.1074/jbc.M113.495846

Spit, M., Rieser, E., and Walczak, H. (2019). Linear ubiquitination at a glance. *J. Cell Sci.* 132:jcs208512. doi: 10.1242/jcs.208512

Stieglitz, B., Morris-Davies, A. C., Koliopoulos, M. G., Christodoulou, E., and Rittinger, K. (2012). LUBAC synthesizes linear ubiquitin chains via a thioester intermediate. *EMBO Rep.* 13, 840–846. doi: 10.1038/embor.2012.105

Stieglitz, B., Rana, R. R., Koliopoulos, M. G., Morris-Davies, A. C., Schaeffer, V., Christodoulou, E., et al. (2013). Structural basis for ligase-specific conjugation of linear ubiquitin chains by HOIP. *Nature* 503, 422–426. doi: 10.1038/nature12638

Swatek, K. N., Aumayr, M., Pruneda, J. N., Visser, L. J., Berryman, S., Kueck, A. F., et al. (2018). Irreversible inactivation of ISG15 by a viral leader protease enables alternative infection detection strategies. *Proc. Natl. Acad. Sci. U.S.A.* 115, 2371–2376. doi: 10.1073/pnas.1710617115

Swatek, K. N., and Komander, D. (2016). Ubiquitin modifications. *Cell Res.* 26, 399–422. doi: 10.1038/cr.2016.39

Swatek, K. N., Usher, J. L., Kueck, A. F., Gladkova, C., Mevissen, T. E. T., Pruneda, J. N., et al. (2019). Insights into ubiquitin chain architecture using Ub-clipping. *Nature* 572, 533–537. doi: 10.1038/s41586-019-1482-y

Takiuchi, T., Nakagawa, T., Tamiya, H., Fujita, H., Sasaki, Y., Saeki, Y., et al. (2014). Suppression of LUBAC-mediated linear ubiquitination by a specific interaction between LUBAC and the deubiquitinases CYLD and OTULIN. *Genes Cells* 19, 254–272. doi: 10.1111/gtc.12128

Tatematsu, K., Yoshimoto, N., Okajima, T., Tanizawa, K., and Kuroda, S. (2008). Identification of ubiquitin ligase activity of RBCK1 and its inhibition by splice variant RBCK2 and protein kinase Cbeta. *J. Biol. Chem.* 283, 11575–11585. doi: 10.1074/jbc.M706961200

Tokunaga, F., Nakagawa, T., Nakahara, M., Saeki, Y., Taniguchi, M., Sakata, S.-I., et al. (2011). SHARPIN is a component of the NF-κB-activating linear ubiquitin chain assembly complex. *Nature* 471, 633–636. doi: 10.1038/nature09815

Tokunaga, F., Sakata, S.-I., Saeki, Y., Satomi, Y., Kirisako, T., Kamei, K., et al. (2009). Involvement of linear polyubiquitylation of NEMO in NF-kappaB activation. *Nat. Cell Biol.* 11, 123–132. doi: 10.1038/ncb1821

Tsuchiya, H., Burana, D., Ohtake, F., Arai, N., Kaiho, A., Komada, M., et al. (2018). Ub-ProT reveals global length and composition of protein ubiquitylation in cells. *Nat. Commun.* 9:524. doi: 10.1038/s41467-018-02869-x

Valkevich, E. M., Sanchez, N. A., Ge, Y., and Strieter, E. R. (2014). Middle-down mass spectrometry enables characterization of branched ubiquitin chains. *Biochemistry* 53, 4979–4989. doi: 10.1021/bi5006305

van Well, E. M., Bader, V., Patra, M., Sánchez-Vicente, A., Meschede, J., Furthmann, N., et al. (2019). A protein quality control pathway regulated by linear ubiquitination. *EMBO J.* 38:e100730. doi: 10.15252/embj.2018100730

van Wijk, S. J. L., Fiskin, E., Putyrski, M., Pampaloni, F., Hou, J., Wild, P., et al. (2012). Fluorescence-based sensors to monitor localization and functions of linear and K63-linked ubiquitin chains in cells. *Mol. Cell* 47, 797–809. doi: 10.1016/j.molcel.2012.06.017

van Wijk, S. J. L., Fricke, F., Herhaus, L., Gupta, J., Hötte, K., Pampaloni, F., et al. (2017). Linear ubiquitination of cytosolic *Salmonella typhimurium* activates NF-κB and restricts bacterial proliferation. *Nat Microbiol.* 2:17066. doi: 10.1038/nmicrobiol.2017.66

van Wijk, S. J. L., Fulda, S., Dikic, I., and Heilemann, M. (2019). Visualizing ubiquitination in mammalian cells. *EMBO Rep.* 20:e46520. doi: 10.15252/embr.201846520

Wagner, S. A., Beli, P., Weinert, B. T., Nielsen, M. L., Cox, J., Mann, M., et al. (2011). A proteome-wide, quantitative survey of *in vivo* ubiquitylation sites reveals widespread regulatory roles. *Mol. Cell. Proteomics* 10:M111.013284. doi: 10.1074/mcp.M111.013284

Wagner, S. A., Satpathy, S., Beli, P., and Choudhary, C. (2016). SPATA2 links CYLD to the TNF-α receptor signaling complex and modulates the receptor signaling outcomes. *EMBO J.* 35, 1868–1884. doi: 10.15252/embj.201694300

Wang, K., Kim, C., Bradfield, J., Guo, Y., Toskala, E., Otieno, F. G., et al. (2013). Whole-genome DNA/RNA sequencing identifies truncating mutations in RBCK1 in a novel Mendelian disease with neuromuscular and cardiac involvement. *Genome Med.* 5:67. doi: 10.1186/gm471

Watkins, J. F., Sung, P., Prakash, L., and Prakash, S. (1993). The *Saccharomyces cerevisiae* DNA repair gene RAD23 encodes a nuclear protein containing a ubiquitin-like domain required for biological function. *Mol. Cell. Biol.* 13, 7757–7765. doi: 10.1128/MCB.13.12.7757

Wertz, I. E., Newton, K., Seshasayee, D., Kusam, S., Lam, C., Zhang, J., et al. (2015). Phosphorylation and linear ubiquitin direct A20 inhibition of inflammation. *Nature* 528, 370–375. doi: 10.1038/nature16165

Wilkinson, C. R. M., Seeger, M., Hartmann-Petersen, R., Stone, M., Wallace, M., Semple, C., et al. (2001). Proteins containing the UBA domain are able to bind to multi-ubiquitin chains. *Nat. Cell Biol.* 3, 939–943. doi: 10.1038/ncb1001-939

Williamson, A., Banerjee, S., Zhu, X., Philipp, I., Iavarone, A. T., and Rape, M. (2011). Regulation of ubiquitin chain initiation to control the timing of substrate degradation. *Mol. Cell* 42, 744–757. doi: 10.1016/j.molcel.2011.04.022

Wu, M., Chang, Y., Hu, H., Mu, R., Zhang, Y., Qin, X., et al. (2019). LUBAC controls chromosome alignment by targeting CENP-E to attached kinetochores. *Nat. Commun.* 10:273. doi: 10.1038/s41467-018-08043-7

Xu, D., Jin, T., Zhu, H., Chen, H., Ofengeim, D., Zou, C., et al. (2018). TBK1 suppresses RIPK1-driven apoptosis and inflammation during development and in aging. *Cell* 174, 1477–1491.e19. doi: 10.1016/j.cell.2018.07.041

Xu, P., and Peng, J. (2008). Characterization of polyubiquitin chain structure by middle-down mass spectrometry. *Anal. Chem.* 80, 3438–3444. doi: 10.1021/ac800016w

Yagi, H., Ishimoto, K., Hiromoto, T., Fujita, H., Mizushima, T., Uekusa, Y., et al. (2012). A non-canonical UBA-UBL interaction forms the linear-ubiquitin-chain assembly complex. *EMBO Rep.* 13, 462–468. doi: 10.1038/embor.2012.24

Yamanaka, K., Ishikawa, H., Megumi, Y., Tokunaga, F., Kanie, M., Rouault, T. A., et al. (2003). Identification of the ubiquitin–protein ligase that recognizes oxidized IRP2. *Nat. Cell Biol.* 5, 336–340. doi: 10.1038/ncb952

Yang, Y., Kelly, P., Shaffer, A. L. III, Schmitz, R., Yoo, H. M., Liu, X., et al. (2016a). Targeting non-proteolytic protein ubiquitination for the treatment of diffuse large B Cell lymphoma. *Cancer Cell* 29, 494–507. doi: 10.1016/j.ccell.2016.03.006

Yang, Y., Schmitz, R., Mitala, J., Whiting, A., Xiao, W., Ceribelli, M., et al. (2014). Essential role of the linear ubiquitin chain assembly complex in lymphoma revealed by rare germline polymorphisms. *Cancer Discov.* 4, 480–493. doi: 10.1158/2159-8290.CD-13-0915

Yang, Y.-K., Yang, C., Chan, W., Wang, Z., Deibel, K. E., and Pomerantz, J. L. (2016b). Molecular determinants of scaffold-induced linear ubiquitinylation of B cell lymphoma/leukemia 10 (Bcl10) during T cell receptor and oncogenic caspase recruitment domain-containing protein 11 (CARD11) Signaling. *J. Biol. Chem.* 291, 25921–25936. doi: 10.1074/jbc.M116.754028

Yau, R., and Rape, M. (2016). The increasing complexity of the ubiquitin code. *Nat. Cell Biol.* 18, 579–586. doi: 10.1038/ncb3358

Yau, R. G., Doerner, K., Castellanos, E. R., Haakonsen, D. L., Werner, A., Wang, N., et al. (2017). Assembly and function of heterotypic ubiquitin chains in cell-cycle and protein quality control. *Cell* 171, 918–933.e20. doi: 10.1016/j.cell.2017.09.040

Zhang, D., Raasi, S., and Fushman, D. (2008). Affinity makes the difference: nonselective interaction of the UBA domain of ubiquilin-1 with monomeric ubiquitin and polyubiquitin chains. *J. Mol. Biol.* 377, 162–180. doi: 10.1016/j.jmb.2007.12.029

Zhang, J., Clark, K., Lawrence, T., Peggie, M. W., and Cohen, P. (2014). An unexpected twist to the activation of IKKβ: TAK1 primes IKKβ for activation by autophosphorylation. *Biochem. J* 461, 531–537. doi: 10.1042/BJ20140444

Zhou, Q., Yu, X., Demirkaya, E., Deuitch, N., Stone, D., Tsai, W. L., et al. (2016). Biallelic hypomorphic mutations in a linear deubiquitinase define otulipenia, an early-onset autoinflammatory disease. *Proc. Natl. Acad. Sci. U.S.A.* 113, 10127–10132. doi: 10.1073/pnas.1612594113

Ziv, I., Matiuhin, Y., Kirkpatrick, D. S., Erpapazoglou, Z., Leon, S., Pantazopoulou, M., et al. (2011). A perturbed ubiquitin landscape distinguishes between ubiquitin in trafficking and in proteolysis. *Mol. Cell. Proteomics* 10:M111.009753. doi: 10.1074/mcp.M111.009753

Conflict of Interest: The authors declare that the research was conducted in the absence of any commercial or financial relationships that could be construed as a potential conflict of interest.

frontiers in Chemistry

MINI REVIEW
published: 10 January 2020
doi: 10.3389/fchem.2019.00914

Strategies to Target Specific Components of the Ubiquitin Conjugation/Deconjugation Machinery

*Neil C. Taylor and Joanna F. McGouran**

School of Chemistry and Trinity Biomedical Sciences Institute, Trinity College Dublin, Dublin, Ireland

The regulation of ubiquitination status in the cell is controlled by ubiquitin ligases acting in tandem with deubiquitinating enzymes. Ubiquitination controls many key processes in the cell from division to death making its tight regulation key to optimal cell function. Activity based protein profiling has emerged as a powerful technique to study these important enzymes. With around 100 deubiquitinating enzymes and 600 ubiquitin ligases in the human genome targeting a subclass of these enzymes or even a single enzyme is a compelling strategy to unpick this complex system. In this review we will discuss different approaches adopted, including activity-based probes centered around ubiquitin-protein, ubiquitin-peptide and mutated ubiquitin scaffolds. We examine challenges faced and opportunities presented to increase specificity in activity-based protein profiling of the ubiquitin conjugation/deconjugation machinery.

Keywords: activity-based protein profiling, ubiquitin, protein modification, deubiquitinating enzymes, probe

OPEN ACCESS

Edited by:
Huib Ovaa, Leiden University Medical Center, Netherlands

Reviewed by:
Tony T. Huang, New York University, United States
James Frederick Burrows, Queen's University Belfast, United Kingdom

****Correspondence:***
Joanna F. McGouran
jmcgoura@tcd.ie

Specialty section:
This article was submitted to Chemical Biology, a section of the journal Frontiers in Chemistry

Received: *14 October 2019*
Accepted: *16 December 2019*
Published: *10 January 2020*

Citation:
Taylor NC and McGouran JF (2020) Strategies to Target Specific Components of the Ubiquitin Conjugation/Deconjugation Machinery. Front. Chem. 7:914. doi: 10.3389/fchem.2019.00914

INTRODUCTION

Ubiquitin is a small protein that is added post-translationally to substrate proteins, modulating their activity and interactions (Goldstein et al., 1975). It has a major role in DNA repair (Jentsch et al., 1987), transcriptional regulation (Hochstrasser and Varshavsky, 1990), cell cycle (Ciechanover et al., 1984; Finley et al., 1984), and stress responses (Ciechanover et al., 1984; Finley et al., 1984) amongst others. Ubiquitin is added to substrate proteins *via* E1, E2, and E3 enzymes (Ciechanover et al., 1982; Hershko et al., 1983) activating, conjugating and ligating ubiquitin, culminating in isopeptide bond formation between a lysine residue of the substrate protein and the C-terminus of ubiquitin (Hunt and Dayhoff, 1977).

Substrates can be modified with monoubiquitin (Haglund et al., 2003; Carter et al., 2007) or polyubiquitin chains linked by isopeptide bonds between an ubiquitin C-terminus and one of the seven lysine residues or N-terminus of another ubiquitin (Hershko and Heller, 1985). The linkage types afford distinct topologies, essential in determining the substrate protein's fate (Chau et al., 1989; Peng et al., 2003; Xu et al., 2009).

Deubiquitinating enzymes (DUBs) possess ubiquitin C-terminal hydrolytic activity, removing ubiquitin (Pickart and Rose, 1985; Hough and Rechsteiner, 1986). The human genome encodes ∼100 DUBs, split into six families; ubiquitin-specific proteases (USPs), ubiquitin C-terminal hydrolases (UCHs), ovarian tumor proteases (OTUs), Machado-Josephin domain proteases (MJDs), the JAB1/MPN/MOV34 family (JAMMs) and the motif interacting with Ub-containing novel DUB (MINDY) family. All families, excluding the JAMM zinc metalloproteases, are cysteine proteases and will be the focus of this review (Hanpude et al., 2015; Abdul Rehman et al., 2016). Given the diversity in ubiquitin chain length, linkage type and protein substrate, DUB specificity is key to biological function.

Dysregulation of the enzymes involved in ubiquitin signaling can result in disease states. Genes encoding the DUBs CYLD and BAP1 are established tumor suppressor genes, often mutated in cancer phenotypes (Zhao et al., 2011). Additionally, members of the OTU family are upregulated in several cancer types (Carneiro et al., 2014). There is also a growing number of studies linking DUBs to neurological diseases (Bhattacharyya et al., 2012; Imai et al., 2012; Xilouri et al., 2012). Mutations in members of the ubiquitin cascade have been implicated in similar disorders (Bernassola et al., 2008; Popovic et al., 2014). The importance of these enzymes in cellular processes and disease states has created demand for molecular tools to assist their study.

Activity-based probes target only the active form of an enzyme allowing for the identification and characterization of active enzymes within complex cellular milieus. They provide a more accurate picture of an enzyme's influence in a cell in comparison to traditional transcriptomic or proteomic screens which do not account for differences in activity, caused by post translational modifications or other inhibitory effects. Probes targeting DUBs based on monoubiquitin have been successful in characterizing new DUB family members (Borodovsky et al., 2002) aiding the crystallization of DUBs (Misaghi et al., 2005) and assessing novel DUB inhibitors (Kramer et al., 2012). The first example of an activity-based probe targeting DUBs consisted of a vinyl sulfone "warhead" in place of the C-terminal glycine residue of ubiquitin (Borodovsky et al., 2001). A variety of thiol-reactive electrophiles have since been reported (Borodovsky et al., 2002; Love et al., 2009; Ekkebus et al., 2013; de Jong et al., 2017). These probes provide information about global DUB activity with some also shown to react with members of the conjugation machinery (Mulder et al., 2016). Recently, large biological screens using these probes have aided in the development of a new chemoproteomic method that could potentially be used to identify the labeling site of any covalent modifier (Hewings et al., 2018). A similar screen demonstrated how chemoproteomics can be used to study DUBs in a more comprehensive manner (Pinto-Fernández et al., 2019). These examples elegantly demonstrate the depth of knowledge that can be obtained using these probes.

Recently, focus has shifted toward the development of probes to target specific subsets of ubiquitin conjugation/deconjugation machinery to allow for more precise investigations of their activity. Using the knowledge that the binding domain recognizing ubiquitin, the C-terminal adduct, chain length and linkage type all affect the specificity of these enzymes, new generations of probe have been developed. The generation of selective probes harbors significant challenges and this review will focus on the design and synthesis of probes to tackle this problem.

PROBES FOR DEUBIQUITINATING ENZYMES

Mutated Ubiquitin Probes

The binding interactions of DUBs are mediated by ubiquitin-binding domains. An innovative strategy based on mutation of WT ubiquitin to enhance/diminish specific interactions between ubiquitin and DUB binding domains was developed by Ernst et al. (2013). It involved random mutation of Ubiquitin and selection through phage display assays. Although the ubiquitin variants were able to pull out endogenous deubiquitinating enzymes in a selective manner their primary design and use was for inhibition or enhancement of endogenous DUB/Ligase activity though cellular expression. Several DUBS and ligases have been targeted in this manner (Zhang et al., 2013, 2016; Gabrielsen et al., 2017; Gorelik and Sidhu, 2017). Ovaa and co-workers extended this methodology to generate USP7 selective activity-based probes using ubiquitin variants developed by Zhang et al. (Ernst et al., 2013; Zhang et al., 2013, 2016) and computational models as starting points for mutations (Gjonaj et al., 2019). Probes incorporated a C-terminal alkyne warhead for covalent capture and an N-terminal Rhodamine dye. Rounds of screening were monitored by probe labeling of HAP1 cell lysate. Interestingly low reactivity was seen for mutants reported to be strong binders in previous phage display assays (Zhang et al., 2013, 2016; Gabrielsen et al., 2017), potentially due to incorrect alignment of the warhead in these variants (Gjonaj et al., 2019). However, an iterative approach screening >120 total variants afforded a probe with high USP7 selectivity.

Ubiquitin-Peptide Probes

DUBs show specificity toward different chain linkage types and the substrate protein. Therefore, extending the probe scaffold by appending an ubiquitin or target protein peptide onto the C-terminus of a Ubiquitin probe beyond the electrophilic trap can increase specificity.

The first example by Iphöfer et al. generated ubiquitin linkage mimics (Iphofer et al., 2012). Peptide sequences were coupled to a warhead containing linker followed by reaction with HA-Ub_{75}-thioester. Probes with peptide sequences reflecting the K48 and K63 regions were tested in Jurkat cell lysate. Differences in labeling were seen between the probes which were both restricted in comparison to the Ub-VME probe. These probes were the first step toward determining DUB selectivity using an activity-based probe approach. The strategy is broadly applicable and laid excellent groundwork but results in a linker two atoms longer than the natural substrate and, as with all peptide probes, selectivity determined by the tertiary structure of the substrate protein is lost.

A further example of this probe type was developed by the Chatrerjee laboratory in 2016 using a selenocystine ligation (Whedon et al., 2016). The approach is similar to that developed by Brik and co-workers (Haj-Yahya et al., 2014), however the use of selenocysteine allowed for Cysteine residues within the peptide. A peptide centered on K117 of TRIM25 was used, containing two Cys residues and a Met alongside the SeCys introduced at position 117. Ligation of the selenium with Ub_{75}-thioester and subsequent Se to N acyl shift resulted in the ubiquitinated peptide bearing a SeCys at Ub_{76}. Selective alkylation of Selenium at low pH afforded the DHA probe in the presence of Cys residues. TRIM25 is known to be deubiquitiniated by USP15 suggesting potential USP15 probe selectivity, however this was not investigated. Reactivity was demonstrated with recombinant USP15, showing predominantly

active site labeling. This work extended the DHA methodology to allow the presence of cysteine in peptides/proteins. The low pH (3.4) of the selective alkylation could however limit the utility for protein conjugation. Also, the presence of a native isopeptide bond in the scissile position may affect probe stability in complex systems.

Diubiquitin Probes

Shortly following Iphöfer et al. several diubiquitin probes were created, further extending the probe scaffold. McGouran et al. generated the first full length diubiquitin probes (McGouran et al., 2013). A "warhead" bearing an alkyne handle was coupled to HA-Ub_{75}-thioester. An azidohomoalanine incorporated into the proximal ubiquitin allowed triazole formation to generate the probes. All linkage types were mimicked and probe selectivity was quantified in HEK293T cell lysate. Distinct labeling profiles were observed between the probes without selectivity for a single DUB. The method is broadly applicable, although incompatible with multiple methionine residues. The linker is four atoms longer than in the natural substrate but is uncleavable, providing a robust probe.

In 2014 the Zhuang laboratory developed an alternative method using a warhead bearing a sulfur reactive group (Li et al., 2014). This was coupled to Ub_{75}-thioester. The proximal HA-ubiquitin containing a single cysteine at the 48/63 position was reacted to generate two diubiquitin activity-based probes (**Figure 1A**). The probes were tested in HEK293T cell lysate again giving distinct labeling profiles. This elegant method affords a non-hydrolyzable linker of the correct length, although it is incompatible with multiple cysteine residues. Recently, this probe was one of a panel that were used to report the mechanism by which USP9X recognizes substrates in a linkage specific manner by using a combination of activity-based labeling and crystallization studies. This study described previously unreported mechanistic and structural recognition features of these enzymes showing how these probes provide a useful insight into enzyme activity (Paudel et al., 2019).

Brik and co-workers took a strategy using dehydroalanine formation (Haj-Yahya et al., 2014), based on their previous non-cleavable diubiquitin synthesis (Kumar et al., 2010). Native chemical ligation and desulfurization to furnish the electrophilic trap in the form of a DHA gave the linear, 48 and 63 linked probes. To accomplish this, the relevant nitrogen of the proximal ubiquitin was selectively deprotected and coupled to a protected cysteine. After deprotection the sulfur reacts with Ub_{75}-thioester followed by an S to N acyl shift and dehydroalanine formation (**Figure 1B**). In this probe design, and all subsequent probes based on this strategy, the native isopeptide bond is still present and the electrophilic trap is two (branched probes) or three (linear probe) atoms from the native position. These probes could therefore either trap or be cleaved by active DUBs. Interestingly the K63 probes labeled recombinant DUBs and the linear probe showed only cleavage with the DUBs tested. The K48 probe showed both labeling and cleavage.

Ovaa and co-workers also utilized the elimination of sulfur to give a Michael acceptor in their final step (Mulder et al., 2014). Orthogonally protected diaminnocutyric acid replaced the lysine residue of interest. A short sulfur containing linker was coupled prior to ligation and desulfurization to afford the diubiquitin probes. This was carried out for all 7 lysine linkages and affords a linkage that matches the native length and is not degraded by DUBs. All probes were tested with recombinant DUBs, the K11 and K48 probes were also tested in EL4 lysate. Both were seen to display a restricted labeling pattern in comparison to the VME probe and were later used to characterize Cezanne (Mevissen et al., 2016). In addition to this, the probe was used to elucidate the linkage specificity of Mug105, which along with ZUSFP, was identified as a founding member of a novel family of DUBs (Hermanns et al., 2018).

Although all the Diubiquitin probes demonstrated more selective labeling patterns than mono ubiquitin probes the linear probe generated by Krappmann and co-workers (Weber et al., 2017) was the first to show single DUB selectivity. Using an approach similar to Brik and co-workers, an N-terminal cysteine was introduced to the proximal ubiquitin allowing native chemical ligation to a Ub_{75}-thioester and desulfurization to afford a dehydroalanine war head. This resulted in a linear probe with the native linker length and an electrophilic trap one bond away from the scissile peptide bond. This probe structure, once optimized by removal of the C-terminal glycine, proved to be selective for OTULIN in cell lysate (Weber et al., 2017).

Li and co-workers used photoaffinity labeling for their K27 linked diubiquitin probe (Tan et al., 2017). They took a native chemical ligation approach using a biotinylated proximal ubiquitin functionalized at K27 with a cysteine coupled to the ε-N. This was ligated to Ub_{75}-NH_2NH_2 to afford the native isopeptide bond adjacent to a single cysteine. Sulfur alkylation installed the photo crosslinking group to the probes. A slightly broader reactivity profile was seen in comparison to the corresponding DHA probe in HEK293F lysate. The synthetic method could be easily applied to other systems and resulted in a native linker length. Due to the nature of photo-crosslinking, proteins which bind K27 linked ubiquitin can also be detected and the presence of the native isopeptide bond gives the possibility of cleavage of the probe. As the photo-crosslinking doesn't require an active site cysteine this method can also profile metalloprotease DUBs.

In 2011 Ye et al. generated a noncleavable linear diubiquitin with a C-terminal aldehyde via expression of a diubiquitn-intein construct (Ye et al., 2011). This aided study of USP21 by crystallization although its potential as an activity based probe was not explored.

In 2016 Ovaa and co-workers fully expanded the diubiquitin probe concept to probe the S1-S2 pocket of DUBs (Flierman et al., 2016). To this end they generated triazole linked non-cleavable diubiquitins bearing a C-terminal thioester on the proximal ubiquitin. A propargyl warhead was introduced to generate the probe (**Figure 1D**). This design allowed examination of DUB activity for diubiquitin binding in the S1-S2 pocket without degradation of the probe should it enter the S1'-S1 pocket. All 7 lysine linked diubiquitins were generated and the K6, 11 & 48 probes were tested in EL4 cells, showing different labeling patterns. DUBs with low reported specificity when probing the S1'-S1 pocket can display specificity in probing the S1-S2 pocket as demonstrated by the SARS PLpro DUB (Bekes et al., 2016).

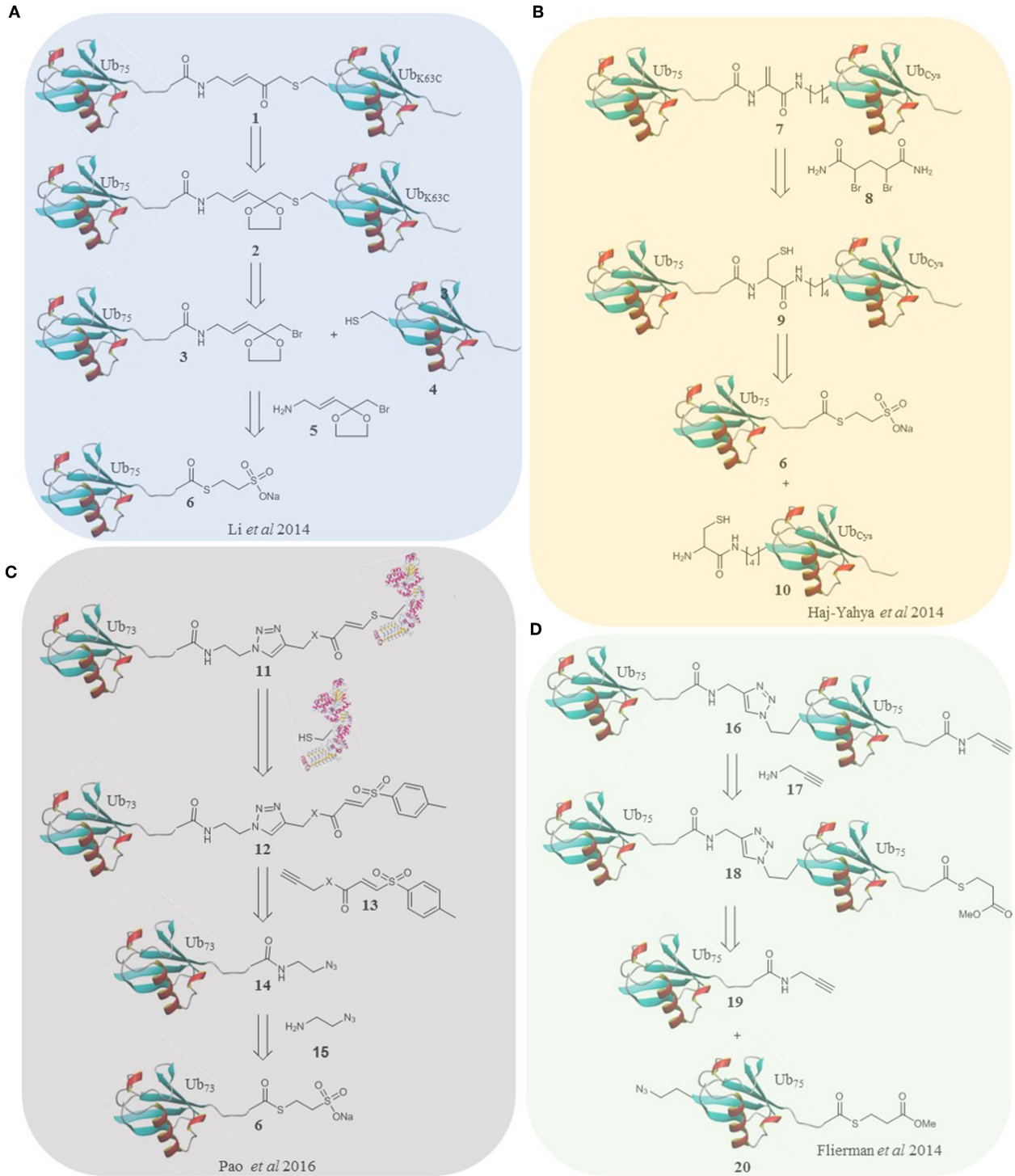

FIGURE 1 | Retrosynthesis of selected probes. **(A)** A methodology reported by Li et al. utilizes an α-bromo-vinylketal to link Ub_{75} thioester **6** and the mutated Ub monomer **4**. Deprotection of the ketal of 2 unmasks a Michael acceptor within the linker of the probe **1**. **(B)** Haj-Yahya et al. synthesized a diubiquitin probe based on DHA as the electrophilic warhead. NCL is used to link Ub monomers **6** and **10**, positioning a cysteine residue at position 76 of the distal Ub which is then converted to DHA using the dibromide reagent **7**. **(C)** Pao et al. expanded on the TDAE methodology to incorporate a Ub monomer and E2 enzyme in a single probe. Alkyne functionalized TDAE **13** is coupled to azido functionalized Ub monomer **14** using copper catalyzed cycloaddition. A subsequent reaction with an E2 enzyme eliminates the tosyl component of the TDAE **12**, affording the final probe **11** containing a Michael acceptor. **(D)** Flieman et al. use copper catalyzed cycloaddition to conjugate two modified Ub monomers **19** and **20**. Propargyl amine **17** was reacted with the C-terminus of the proximal monomer to yield probe **16**.

This was the first time a DUB was proven to be specific for K48 linked chains over monoubiquitin, exhibiting how these probes are superior, at least in some cases, at elucidating poly ubiquitin linkage specificity in DUBs.

In 2019, Tong and co-workers extended the concept a step further by generating triubiquitin activity-based probes. The probes bear a native isopeptide bond between the proximal and middle ubiquitin and a warhead between the middle and distal ubiquitin (Paudel et al., 2019). The proximal K63 linked diubiquitin was generated enzymatically with the middle ubiquitin harboring a K63C mutation to allow ligation through the same methodology as employed by the Zhuang lab (Li et al., 2014). These probes gave insights into the binding modes of USP9X. Although using the probes in more complex milieus would be complicated by the cleavable isopeptide bond it demonstrates the limitless scope of such approaches (Paudel et al., 2019).

Ubiquitin-Protein Conjugate Probes for Deubiquitinating Enzymes

To further unpick DUB specificity the challenging aim of generating Ubiquitin-protein conjugate probes has been addressed. In 2018 Brick (Meledin et al., 2018) and Zhuang (Gong et al., 2018) both extended their conjugation methodologies to create Ub-protein probes. Brik and co-workers targeted ubiquitinated α-globin, forming DHA at the single cysteine (104) present in α-globin and coupling to a thiol bearing thiazolidine. Deprotection allowed ligation to Biotin-Ub_{75}-thioester. A further DHA formation step installed the electrophilic trap into the Ubiquitin-α-globin conjugate. This strategy utilizes the single cysteine present in α-globin and its proximity to a ubiquitination site at K100. Quantitation of probe activity in erythrocyte lysate detected enrichment of several DUBs including USP15, which was confirmed with the natural substrate and was also shown to deubiquitinate the K119 position in an independent study (Sun et al., 2018).

This methodology was extended by the development of selective deprotection of three cysteine protecting groups using palladium species in order to make a Ubiquitinated Histone probe (Jbara et al., 2018). The multiple cysteines present allowed NCL to build the target protein which was desulfurised prior to release of the final thiol for Ub_{75}-thioester conjugation and DHA formation. The probe mimicked K119 ubiquitinated H2A. Nucleosome particles were reconstituted avoiding reducing conditions for DHA stability, and labeling by Calypso/ASK was confirmed. Although the methodology is powerful in the breadth of application as it could allow multiple cysteines in the peptide/protein the utility in complex systems may be limited by the native isopeptide bond.

The Zhuang laboratory used their warhead containing linker strategy to generate ubiquitin-PCNA probes representing K107 and K164 ubiquitinated PCNA. This strategy is elegant in its simplicity although it required mutation of the four cysteines in PCNA to ensure site selectivity. These probes displayed differences in the affinity enrichment of deubiquitinating enzymes in Yeast. The K164 probe enriched several DUBs whilst the K107 probe showed only modest enrichment.

PROBES FOR UBIQUITIN CONJUGATION MACHINERY

Ubiquitin is added to substrate proteins by E1, E2, and E3 enzymes (Ciechanover et al., 1982; Hershko et al., 1983). Dysregulation of these enzymes is associated with certain cancers and neurodegenerative disorders (Bernassola et al., 2008; Popovic et al., 2014). There has therefore been a demand to develop probes for these enzymes analogous to those targeting DUBs.

Ubiquitin-Adenine Probes

Monoubiquitin probes have been demonstrated to label ubiquitin conjugation machinery (Kamadurai et al., 2009; Love et al., 2009; Kim et al., 2011; Ekkebus et al., 2013; Maspero et al., 2013; Byrne et al., 2017) however they lack specificity. Tan and co-workers (Lu et al., 2010) developed E1 targeting probes by mimicking the adenylate intermediate formed in the E1 active site. Native chemical ligation of Ub_{71}-thioester introduced the modified C-terminus of the protein. The modified C-terminus contained an electrophilic trap at the 74 position and a 5′-sulfonyladenosine-based modification. The probe labeled recombinant E1s and aided crystallization but was not tested in more complex systems. Additionally, the C-terminal ubiquitin sequence is altered and truncated which may affect selectivity. This probe design was used in subsequent studies to provide insight into structural changes within E1 enzymes during adenylation (Hann et al., 2019).

An and Statsyuk (2016) also took a native chemical ligation approach to target E1 enzymes. Flag-Ub_{75}-thioester was coupled to cysteine-conjugated adenine moieties. The cysteine was then converted to DHA to furnish an electrophilic trap. The site of attack is three atoms away from the native position relative to ubiquitin and the lack of phosphate group mimic potentially reduces binding. Nonetheless, covalent labeling was observed with UBA1. The probes react specifically with their cognate E1 enzymes over Ubl conjugation machinery. However, some reactivity was observed with the DUB IsoT which also appeared to cleave the probe. This represents a limitation for cell lysate, but the probes provided an effective strategy to study E1 enzymes.

Modified E2 Probes

More recently, Virdee and co-workers employed tosyl-substituted doubly activated enes (TDAEs) to sequentially functionalize thiols at a single carbon center for profiling E1 enzyme activity (Stanley et al., 2015). The single cysteine in E2 UBE2N was reacted with TDAEs to form E2-based probes for E1 activity. Labeling of E1 UBA1 was observed and enhanced by co-incubation with Ub and ATP. Endogenous UBA1 was selectively labeled in HEK293 lysate.

Ubiquitin-Protein Probes for E3 Ligases

Elaborated TDAE probes aimed to specifically target the E3 ligase Parkin by incorporating ubiquitin into the probe (Pao et al., 2016). Ub_{73}-thioester was reacted with azidoaminoethane to afford Ub-azide. Alkyne functionalized acrylate and acrylamide were used to prepare two TDAE functionalized ubiquitin monomers. A single cysteine mutant of His-UBE2L3 was reacted with the monomers to form the E2-Ub conjugate probes

(**Figure 1C**). The triazole linker and electrophile replace residues 74-76 of ubiquitin. The electrophilic trap is one atom from the native position. The active site of Parkin was labeled by both probes. Furthermore, the probes were stable and inert to recombinant DUBs. Virdee et al. demonstrated an application in profiling primary fibroblasts from Parkinson's disease patients. Licchesi and co-workers (Byrne et al., 2017) later showed these probes react with NEDD4, UBE3C and HECTD1.

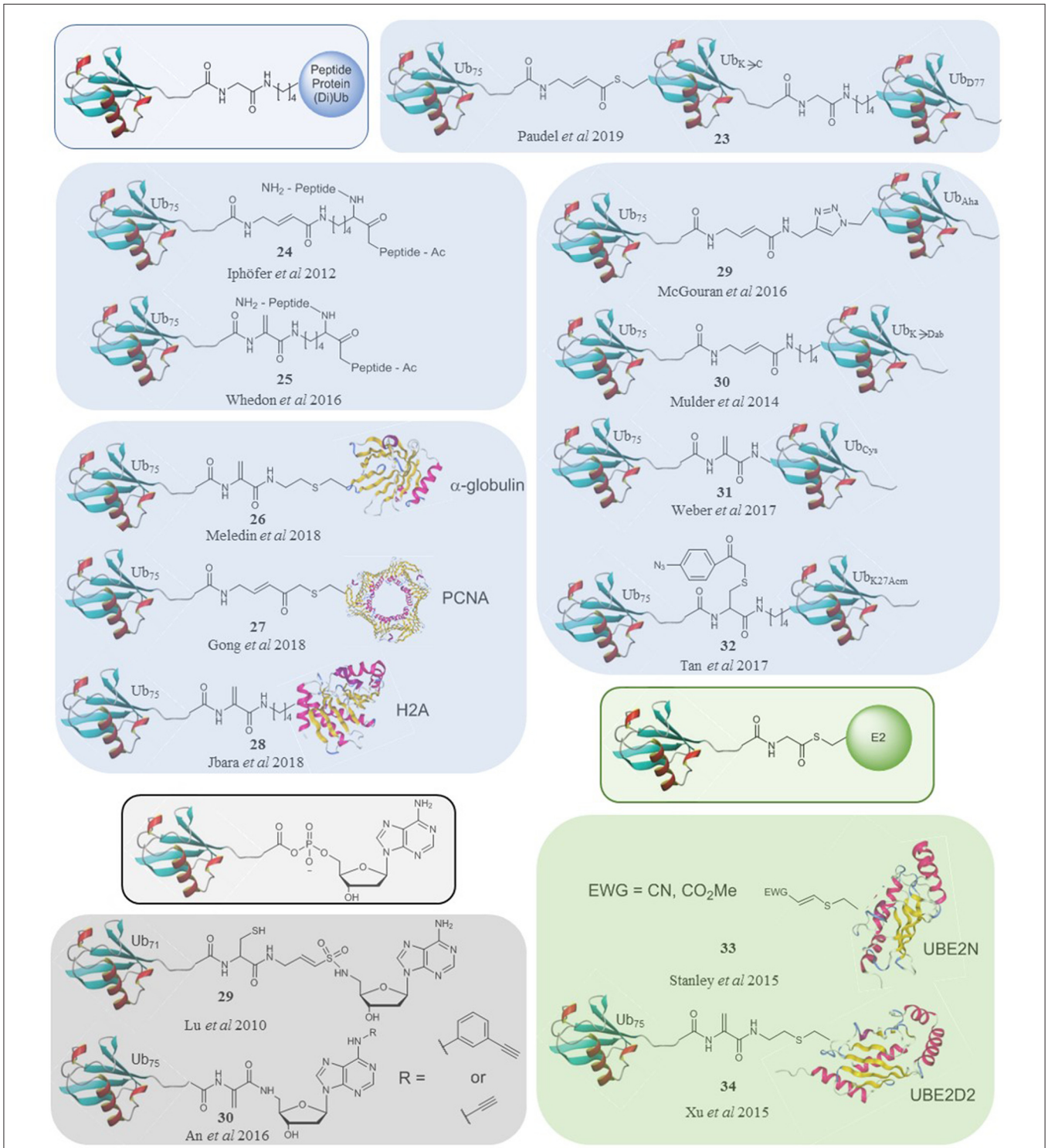

FIGURE 2 | A selection of ubiquitin-based probes that specifically target subsets of DUBs (blue), E1s (black) and E3s (green) compared to the natural substrates of their targets (framed).

Although not specific for a single E3, the synthetic approach is broadly applicable.

Shi and co-workers (Xu et al., 2019) designed a probe consisting of mutated UBE2D2, bearing a single cysteine, conjugated to Biotin-Ub_{75}-NH_2NH_2 using native chemical ligation followed by Dha formation. The probes were tested against catalytic domains of NEDD4 and UBE3C, labeling both active sites. Probing HeLa cells saw enrichment of several E3 enzymes, with strong enrichment of NEDD4. This work demonstrates an alternative route to E2-Ub probes however the linker is three atoms longer than the native and the electrophilic trap is presented two and five atoms away from Ub and UBE2D2, respectively.

CONCLUSION

Several approaches have been taken to confer selectivity to activity-based probes for ubiquitin conjugation/deconjugation machinery (**Figure 2**). Mutation of ubiquitin has proved successful following several rounds of screening. Expansion of this method to include unnatural amino acids could prove to be powerful. Ubiquitin-peptide and diubiquitin structures, except for the OTULIN probe, did not yield probes selective for a single enzyme but they did lay much of the groundwork for generating the more complex ubiquitin-protein probes. Furthermore, di and triubiquitin probes can allow probing of ubiquitin binding pockets of DUBs beyond the S1'-S1 pocket. Several ubiquitin-protein conjugate probes now exist giving us new levels of detail. Existing and new methodology has also been applied to explore ubiquitin conjugation machinery. Selectivity was tested in recombinant and cellular systems, with probes varying in linker length, positioning of electrophilic trap and stability to DUBs as well as compatibility requirements. Many probes have proven to be excellent tools to study these complex pathways and have already provided valuable insights into the mechanistic and structural features of target enzymes (Bekes et al., 2016; Hann et al., 2019; Paudel et al., 2019) as well in the characterization of new family members (Hermanns et al., 2018) and identification of potential disease markers in patient samples (Pao et al., 2016).

Certain conjugate probes are limited due to their hydrolysable linkers and despite several well-designed solutions, many of the probes also do not perfectly mimic the linker length or trap position of the wild-type substrate. There is therefore scope for optimisation of the probe design and implementation of new chemistry for the synthesis of novel probes. Furthermore, these probes are currently limited by their lack of cell permeability. Recent work demonstrated that incorporation of cleavable cell-penetrating peptides can help deliver monoubiquitin probes into a cell (Gui et al., 2018). Application of this methodology to conjugate probes could enable the development of cell-permeable versions. Additionally, large scale biological screens combined with the latest chemoproteomic methods, similar to those carried out using monoubiquitin probes, could provide a more resolved picture of DUB activity using these more specific probes (Hewings et al., 2018; Pinto-Fernández et al., 2019). Overall, the expansion and combination of methods reviewed herein could open further possibilities, ultimately affording a panel of probes capable of targeting specific subsets or even individual enzymes. This could provide a more comprehensive view of DUB and ubiquitin conjugating enzyme activity in cells.

AUTHOR CONTRIBUTIONS

JM and NT drafted and edited the manuscript.

FUNDING

This work was funded by Trinity College Dublin.

ACKNOWLEDGMENTS

JM and NT would like to acknowledge Trinity College Dublin and the School of Chemistry for funding.

REFERENCES

Abdul Rehman, S. A., Kristariyanto, Y. A., Choi, S. Y., Nkosi, P. J., Weidlich, S., Labib, K., et al. (2016). MINDY-1 is a member of an evolutionarily conserved and structurally distinct new family of deubiquitinating enzymes. *Mol. Cell* 63, 146–155. doi: 10.1016/j.molcel.2016.05.009

An, H., and Statsyuk, A. V. (2016). Facile synthesis of covalent probes to capture enzymatic intermediates during E1 enzyme catalysis. *Chem. Commun.* 52, 2477–2480. doi: 10.1039/c5cc08592f

Bekes, M., van der Heden van Noort, G. J., Ekkebus, R., Ovaa, H., Huang, T. T., and Lima, C. D. (2016). Recognition of Lys48-linked di-ubiquitin and deubiquitinating activities of the SARS coronavirus papain-like protease. *Mol. Cell* 62, 572–585. doi: 10.1016/j.molcel.2016.04.016

Bernassola, F., Karin, M., Ciechanover, A., and Melino, G. (2008). The HECT family of E3 ubiquitin ligases: multiple players in cancer development. *Cancer Cell* 14, 10–21. doi: 10.1016/j.ccr.2008.06.001

Bhattacharyya, B. J., Wilson, S. M., Jung, H., and Miller, R. J. (2012). Altered neurotransmitter release machinery in mice deficient for the deubiquitinating enzyme Usp14. *Am. J. Physiol. Cell Physiol.* 302, C698–C708. doi: 10.1152/ajpcell.00326.2010

Borodovsky, A., Kessler, B. M., Casagrande, R., Overkleeft, H. S., Wilkinson, K. D., and Ploegh, H. L. (2001). A novel active site-directed probe specific for deubiquitylating enzymes reveals proteasome association of USP14. *EMBO J.* 20, 5187–5196. doi: 10.1093/emboj/20.18.5187

Borodovsky, A., Ovaa, H., Kolli, N., Gan-Erdene, T., Wilkinson, K. D., Ploegh, H. L., et al. (2002). Chemistry-based functional proteomics reveals novel members of the deubiquitinating enzyme family. *Chem. Biol.* 9, 1149–1159. doi: 10.1016/s1074-5521(02)00248-x

Byrne, R., Mund, T., and Licchesi, J. D. F. (2017). Activity-based probes for HECT E3 ubiquitin ligases. *Chembiochem* 18, 1415–1427. doi: 10.1002/cbic.201700006

Carneiro, A. P., Reis, C. F., Morari, E. C., Maia, Y. C., Nascimento, R., Bonatto, J. M., et al. (2014). A putative OTU domain-containing protein 1 deubiquitinating enzyme is differentially expressed in thyroid cancer and identifies less-aggressive tumours. *Br. J. Cancer* 111, 551–558. doi: 10.1038/bjc.2014.331

Carter, S., Bischof, O., Dejean, A., and Vousden, K. H. (2007). C-terminal modifications regulate MDM2 dissociation and nuclear export of p53. *Nat. Cell Biol.* 9, 428–435. doi: 10.1038/ncb1562

Chau, V., Tobias, J. W., Bachmair, A., Marriott, D., Ecker, D. J., Gonda, D. K., et al. (1989). A multiubiquitin chain is confined to specific lysine in a targeted short-lived protein. *Science* 243, 1576–1583. doi: 10.1126/science.2538923

Ciechanover, A., Elias, S., Heller, H., and Hershko, A. (1982). "Covalent affinity" purification of ubiquitin-activating enzyme. *J. Biol. Chem.* 257, 2537–2542.

Ciechanover, A., Finley, D., and Varshavsky, A. (1984). Ubiquitin dependence of selective protein degradation demonstrated in the mammalian cell cycle mutant ts85. *Cell* 37, 57–66. doi: 10.1016/0092-8674(84)90300-3

de Jong, A., Witting, K., Kooij, R., Flierman, D., and Ovaa, H. (2017). Release of enzymatically active deubiquitinating enzymes upon reversible capture by disulfide ubiquitin reagents. *Angew. Chem. Int. Ed. Engl.* 56, 12967–12970. doi: 10.1002/anie.201706738

Ekkebus, R., van Kasteren, S. I., Kulathu, Y., Scholten, A., Berlin, I., Geurink, P. P., et al. (2013). On terminal alkynes that can react with active-site cysteine nucleophiles in proteases. *J. Am. Chem. Soc.* 135, 2867–2870. doi: 10.1021/ja309802n

Ernst, A., Avvakumov, G., Tong, J., Fan, Y., Zhao, Y., Alberts, P., et al. (2013). A strategy for modulation of enzymes in the ubiquitin system. *Science* 339, 590–595. doi: 10.1126/science.1230161

Finley, D., Ciechanover, A., and Varshavsky, A. (1984). Thermolability of ubiquitin-activating enzyme from the mammalian cell cycle mutant ts85. *Cell* 37, 43–55. doi: 10.1016/0092-8674(84)90299-x

Flierman, D., van der Heden van Noort, G. J., Ekkebus, R., Geurink, P. P., Mevissen, T. E., Hospenthal, M. K., et al. (2016). Non-hydrolyzable diubiquitin probes reveal linkage-specific reactivity of deubiquitylating enzymes mediated by S2 pockets. *Cell Chem. Biol.* 23, 472–482. doi: 10.1016/j.chembiol.2016.03.009

Gabrielsen, M., Buetow, L., Nakasone, M. A., Ahmed, S. F., Sibbet, G. J., Smith, B. O., et al. (2017). A general strategy for discovery of inhibitors and activators of RING and U-box E3 ligases with ubiquitin variants. *Mol. Cell.* 68:456–470.e10. doi: 10.1016/j.molcel.2017.09.027

Gjonaj, L., Sapmaz, A., Gonzalez-Prieto, R., Vertegaal, A. C. O., Flierman, D., and Ovaa, H. (2019). USP7: combining tools towards selectivity. *Chem. Commun.* 55, 5075–5078. doi: 10.1039/c9cc00969h

Goldstein, G., Scheid, M., Hammerling, U., Schlesinger, D. H., Niall, H. D., and Boyse, E. A. (1975). Isolation of a polypeptide that has lymphocyte-differentiating properties and is probably represented universally in living cells. *Proc. Natl. Acad. Sci. U.S.A.* 72, 11–15. doi: 10.1073/pnas.72.1.11

Gong, P., Davidson, G. A., Gui, W., Yang, K., Bozza, W. P., and Zhuang, Z. (2018). Activity-based ubiquitin-protein probes reveal target protein specificity of deubiquitinating enzymes. *Chem. Sci.* 9, 7859–7865. doi: 10.1039/c8sc01573b

Gorelik, M., and Sidhu, S. S. (2017). Specific targeting of the deubiquitinase and E3 ligase families with engineered ubiquitin variants. *Bioeng. Transl. Med.* 2, 31–42. doi: 10.1002/btm2.10044

Gui, W., Ott, C. A., Yang, K., Chung, J. S., Shen, S., and Zhuang, Z. (2018). Cell-permeable activity-based ubiquitin probes enable intracellular profiling of human deubiquitinases. *J. Am. Chem. Soc.* 140, 12424–12433. doi: 10.1021/jacs.8b05147

Haglund, K., Sigismund, S., Polo, S., Szymkiewicz, I., Di Fiore, P. P., and Dikic, I. (2003). Multiple monoubiquitination of RTKs is sufficient for their endocytosis and degradation. *Nat. Cell Biol.* 5, 461–466. doi: 10.1038/ncb983

Haj-Yahya, N., Hemantha, H. P., Meledin, R., Bondalapati, S., Seenaiah, M., and Brik, A. (2014). Dehydroalanine-based diubiquitin activity probes. *Org. Lett.* 16, 540–543. doi: 10.1021/ol403416w

Hann, Z. S., Ji, C., Olsen, S. K., Lu, X., Lux, M. C., Tan, D. S., et al. (2019). Structural basis for adenylation and thioester bond formation in the ubiquitin E1. *Proc. Natl. Acad. Sci. U.S.A.* 116, 15475–15484. doi: 10.1073/pnas.1905488116

Hanpude, P., Bhattacharya, S., Dey, A. K., and Maiti, T. K. (2015). Deubiquitinating enzymes in cellular signaling and disease regulation. *IUBMB Life* 67, 544–555. doi: 10.1002/iub.1402

Hermanns, T., Pichlo, C., Woiwode, I., Klopffleisch, K., Witting, K. F., Ovaa, H., et al. (2018). A family of unconventional deubiquitinases with modular chain specificity determinants. *Nat. Commun.* 9:799. doi: 10.1038/s41467-018-03148-5

Hershko, A., and Heller, H. (1985). Occurrence of a polyubiquitin structure in ubiquitin-protein conjugates. *Biochem. Biophys. Res. Commun.* 128, 1079–1086. doi: 10.1016/0006-291x(85)91050-2

Hershko, A., Heller, H., Elias, S., and Ciechanover, A. (1983). Components of ubiquitin-protein ligase system. Resolution, affinity purification, and role in protein breakdown. *J. Biol. Chem.* 258, 8206–8214.

Hewings, D. S., Heideker, J., Ma, T. P., AhYoung, A. P., El Oualid, F., Amore, A., et al. (2018). Reactive-site-centric chemoproteomics identifies a distinct class of deubiquitinase enzymes. *Nat. Commun.* 9:1162. doi: 10.1038/s41467-018-03511-6

Hochstrasser, M., and Varshavsky, A. (1990). *In vivo* degradation of a transcriptional regulator: the yeast alpha 2 repressor. *Cell* 61, 697–708. doi: 10.1016/0092-8674(90)90481-s

Hough, R., and Rechsteiner, M. (1986). Ubiquitin-lysozyme conjugates. Purification and susceptibility to proteolysis. *J. Biol. Chem.* 261, 2391–2399.

Hunt, L. T., and Dayhoff, M. O. (1977). Amino-terminal sequence identity of ubiquitin and the nonhistone component of nuclear protein A24. *Biochem. Biophys. Res. Commun.* 74, 650–655. doi: 10.1016/0006-291x(77)90352-7

Imai, S., Mamiya, T., Tsukada, A., Sakai, Y., Mouri, A., Nabeshima, T., et al. (2012). Ubiquitin-specific peptidase 46 (Usp46) regulates mouse immobile behavior in the tail suspension test through the GABAergic system. *PLoS ONE* 7:e39084. doi: 10.1371/journal.pone.0039084

Iphofer, A., Kummer, A., Nimtz, M., Ritter, A., Arnold, T., Frank, R., et al. (2012). Profiling ubiquitin linkage specificities of deubiquitinating enzymes with branched ubiquitin isopeptide probes. *Chembiochem* 13, 1416–1420. doi: 10.1002/cbic.201200261

Jbara, M., Laps, S., Morgan, M., Kamnesky, G., Mann, G., Wolberger, C., et al. (2018). Palladium prompted on-demand cysteine chemistry for the synthesis of challenging and uniquely modified proteins. *Nat. Commun.* 9:3154. doi: 10.1038/s41467-018-05628-0

Jentsch, S., McGrath, J. P., and Varshavsky, A. (1987). The yeast DNA repair gene RAD6 encodes a ubiquitin-conjugating enzyme. *Nature* 329, 131–134. doi: 10.1038/329131a0

Kamadurai, H. B., Souphron, J., Scott, D. C., Duda, D. M., Miller, D. J., Stringer, D., et al. (2009). Insights into ubiquitin transfer cascades from a structure of a UbcH5B approximately ubiquitin-HECT(NEDD4L) complex. *Mol. Cell* 36, 1095–1102. doi: 10.1016/j.molcel.2009.11.010

Kim, H. C., Steffen, A. M., Oldham, M. L., Chen, J., and Huibregtse, J. M. (2011). Structure and function of a HECT domain ubiquitin-binding site. *EMBO Rep.* 12, 334–341. doi: 10.1038/embor.2011.23

Kramer, H. B., Nicholson, B., Kessler, B. M., and Altun, M. (2012). Detection of ubiquitin-proteasome enzymatic activities in cells: application of activity-based probes to inhibitor development. *Biochim. Biophys. Acta* 1823, 2029–2037. doi: 10.1016/j.bbamcr.2012.05.014

Kumar, K. S., Spasser, L., Erlich, L. A., Bavikar, S. N., and Brik, A. (2010). Total chemical synthesis of di-ubiquitin chains. *Angew. Chem. Int. Ed. Engl.* 49, 9126–9131. doi: 10.1002/anie.201003763

Li, G., Liang, Q., Gong, P., Tencer, A. H., and Zhuang, Z. (2014). Activity-based diubiquitin probes for elucidating the linkage specificity of deubiquitinating enzymes. *Chem. Commun.* 50, 216–218. doi: 10.1039/c3cc47382a

Love, K. R., Pandya, R. K., Spooner, E., and Ploegh, H. L. (2009). Ubiquitin C-terminal electrophiles are activity-based probes for identification and mechanistic study of ubiquitin conjugating machinery. *ACS Chem. Biol.* 4, 275–287. doi: 10.1021/cb9000348

Lu, X., Olsen, S. K., Capili, A. D., Cisar, J. S., Lima, C. D., and Tan, D. S. (2010). Designed semisynthetic protein inhibitors of Ub/Ubl E1 activating enzymes. *J. Am. Chem. Soc.* 132, 1748–1749. doi: 10.1021/ja9088549

Maspero, E., Valentini, E., Mari, S., Cecatiello, V., Soffientini, P., Pasqualato, S., et al. (2013). Structure of a ubiquitin-loaded HECT ligase reveals the molecular basis for catalytic priming. *Nat. Struct. Mol. Biol.* 20, 696–701. doi: 10.1038/nsmb.2566

McGouran, J. F., Gaertner, S. R., Altun, M., Kramer, H. B., and Kessler, B. M. (2013). Deubiquitinating enzyme specificity for ubiquitin chain topology profiled by di-ubiquitin activity probes. *Chem. Biol.* 20, 1447–1455. doi: 10.1016/j.chembiol.2013.10.012

Meledin, R., Mali, S. M., Kleifeld, O., and Brik, A. (2018). Activity-based probes developed by applying a sequential dehydroalanine formation strategy to expressed proteins reveal a potential alpha-globin-modulating deubiquitinase. *Angew. Chem. Int. Ed. Engl.* 57, 5645–5649. doi: 10.1002/anie.201800032

Mevissen, T. E. T., Kulathu, Y., Mulder, M. P. C., Geurink, P. P., Maslen, S. L., Gersch, M., et al. (2016). Molecular basis of Lys11-polyubiquitin specificity in the deubiquitinase Cezanne. *Nature* 538, 402–405. doi: 10.1038/nature19836

Misaghi, S., Galardy, P. J., Meester, W. J., Ovaa, H., Ploegh, H. L., and Gaudet, R. (2005). Structure of the ubiquitin hydrolase UCH-L3 complexed with a suicide substrate. *J. Biol. Chem.* 280, 1512–1520. doi: 10.1074/jbc.M410770200

Mulder, M. P., El Oualid, F., ter Beek, J., and Ovaa, H. (2014). A native chemical ligation handle that enables the synthesis of advanced activity-based probes: diubiquitin as a case study. *Chembiochem* 15, 946–949. doi: 10.1002/cbic.201402012

Mulder, M. P., Witting, K., Berlin, I., Pruneda, J. N., Wu, K. P., Chang, J. G., et al. (2016). A cascading activity-based probe sequentially targets E1-E2-E3 ubiquitin enzymes. *Nat. Chem. Biol.* 12, 523–530. doi: 10.1038/nchembio.2084

Pao, K. C., Stanley, M., Han, C., Lai, Y. C., Murphy, P., Balk, K., et al. (2016). Probes of ubiquitin E3 ligases enable systematic dissection of parkin activation. *Nat. Chem. Biol.* 12, 324–331. doi: 10.1038/nchembio.2045

Paudel, P., Zhang, Q., Leung, C., Greenberg, H. C., Guo, Y., Chern, Y. H., et al. (2019). Crystal structure and activity-based labeling reveal the mechanisms for linkage-specific substrate recognition by deubiquitinase USP9X. *Proc. Natl. Acad. Sci. U.S.A.* 116, 7288–7297. doi: 10.1073/pnas.1815027116

Peng, J., Schwartz, D., Elias, J. E., Thoreen, C. C., Cheng, D., Marsischky, G., et al. (2003). A proteomics approach to understanding protein ubiquitination. *Nat. Biotechnol.* 21, 921–926. doi: 10.1038/nbt849

Pickart, C. M., and Rose, I. A. (1985). Ubiquitin carboxyl-terminal hydrolase acts on ubiquitin carboxyl-terminal amides. *J. Biol. Chem.* 260, 7903–7910.

Pinto-Fernández, A., Davis, S., Schofield, A. B., Scott, H. C., Zhang, P., Salah, E., et al. (2019). Comprehensive landscape of active deubiquitinating enzymes profiled by advanced chemoproteomics. *Front. Chem.* 7:592. doi: 10.3389/fchem.2019.00592

Popovic, D., Vucic, D., and Dikic, I. (2014). Ubiquitination in disease pathogenesis and treatment. *Nat. Med.* 20, 1242–1253. doi: 10.1038/nm.3739

Stanley, M., Han, C., Knebel, A., Murphy, P., Shpiro, N., and Virdee, S. (2015). Orthogonal thiol functionalization at a single atomic center for profiling transthiolation activity of E1 activating enzymes. *ACS Chem. Biol.* 10, 1542–1554. doi: 10.1021/acschembio.5b00118

Sun, H., Meledin, R., Mali, S. M., and Brik, A. (2018). Total chemical synthesis of ester-linked ubiquitinated proteins unravels their behavior with deubiquitinases. *Chem. Sci.* 9, 1661–1665. doi: 10.1039/c7sc04518b

Tan, X. D., Pan, M., Gao, S., Zheng, Y., Shi, J., and Li, Y. M. (2017). A diubiquitin-based photoaffinity probe for profiling K27-linkage targeting deubiquitinases. *Chem. Commun.* 53, 10208–10211. doi: 10.1039/c7cc05504h

Weber, A., Elliott, P. R., Pinto-Fernandez, A., Bonham, S., Kessler, B. M., Komander, D., et al. (2017). A linear diubiquitin-based probe for efficient and selective detection of the deubiquitinating enzyme OTULIN. *Cell Chem. Biol.* 24:1299–1313.e7. doi: 10.1016/j.chembiol.2017.08.006

Whedon, S. D., Markandeya, N., Rana, A. S., Weller, C. E., Senger, N. A., Turecek, F., et al. (2016). Selenocysteine as a latent bioorthogonal electrophilic probe for deubiquitylating enzymes. *J. Am. Chem. Soc.* 138, 13774–13777. doi: 10.1021/jacs.6b05688

Xilouri, M., Kyratzi, E., Pitychoutis, P. M., Papadopoulou-Daifoti, Z., Perier, C., Vila, M., et al. (2012). Selective neuroprotective effects of the S18Y polymorphic variant of UCH-L1 in the dopaminergic system. *Hum. Mol. Genet.* 21, 874–889. doi: 10.1093/hmg/ddr521

Xu, L., Fan, J., Wang, Y., Zhang, Z., Fu, Y., Li, Y. M., et al. (2019). An activity-based probe developed by a sequential dehydroalanine formation strategy targets HECT E3 ubiquitin ligases. *Chem. Commun.* 55, 7109–7112. doi: 10.1039/c9cc03739j

Xu, P., Duong, D. M., Seyfried, N. T., Cheng, D., Xie, Y., Robert, J., et al. (2009). Quantitative proteomics reveals the function of unconventional ubiquitin chains in proteasomal degradation. *Cell* 137, 133–145. doi: 10.1016/j.cell.2009.01.041

Ye, Y., Akutsu, M., Reyes-Turcu, F., Enchev, R. I., Wilkinson, K. D., and Komander, D. (2011). Polyubiquitin binding and cross-reactivity in the USP domain deubiquitinase USP21. *EMBO Rep.* 12, 350–357. doi: 10.1038/embor.2011.17

Zhang, W., Wu, K. P., Sartori, M. A., Kamadurai, H. B., Ordureau, A., Jiang, C., et al. (2016). System-wide modulation of HECT E3 ligases with selective ubiquitin variant probes. *Mol. Cell* 62, 121–136. doi: 10.1016/j.molcel.2016.02.005

Zhang, Y., Zhou, L., Rouge, L., Phillips, A. H., Lam, C., Liu, P., et al. (2013). Conformational stabilization of ubiquitin yields potent and selective inhibitors of USP7. *Nat. Chem. Biol.* 9, 51–58. doi: 10.1038/nchembio.1134

Zhao, Y., Thornton, A. M., Kinney, M. C., Ma, C. A., Spinner, J. J., Fuss, I. J., et al. (2011). The deubiquitinase CYLD targets Smad7 protein to regulate transforming growth factor β (TGF-β) signaling and the development of regulatory T cells. *J. Biol. Chem.* 286, 40520–40530. doi: 10.1074/jbc.M111.292961

Conflict of Interest: The authors declare that the research was conducted in the absence of any commercial or financial relationships that could be construed as a potential conflict of interest.

frontiers in Cell and Developmental Biology

MINI REVIEW
published: 10 January 2020
doi: 10.3389/fcell.2019.00343

SUMO Chains Rule on Chromatin Occupancy

*Jan Keiten-Schmitz†, Kathrin Schunck† and Stefan Müller**

Institute of Biochemistry II, Medical Faculty, Goethe University, Frankfurt, Germany

The dynamic and reversible post-translational modification of proteins and protein complexes with the ubiquitin-related SUMO modifier regulates a wide variety of nuclear functions, such as transcription, replication and DNA repair. SUMO can be attached as a monomer to its targets, but can also form polymeric SUMO chains. While monoSUMOylation is generally involved in the assembly of protein complexes, multi- or polySUMOylation may have very different consequences. The evolutionary conserved paradigmatic signaling process initiated by multi- or polySUMOylation is the SUMO-targeted Ubiquitin ligase (StUbL) pathway, where the presence of multiple SUMO moieties primes ubiquitylation by the mammalian E3 ubiquitin ligases RNF4 or RNF111, or the yeast Slx5/8 heterodimer. The mammalian SUMO chain-specific isopeptidases SENP6 or SENP7, or yeast Ulp2, counterbalance chain formation thereby limiting StUbL activity. Many facets of SUMO chain signaling are still incompletely understood, mainly because only a limited number of polySUMOylated substrates have been identified. Here we summarize recent work that revealed a highly interconnected network of candidate polySUMO modified proteins functioning in DNA damage response and chromatin organization. Based on these datasets and published work on distinct polySUMO-regulated processes we discuss overarching concepts in SUMO chain function. We propose an evolutionary conserved role of polySUMOylation in orchestrating chromatin dynamics and genome stability networks by balancing chromatin-residency of protein complexes. This concept will be exemplified in processes, such as centromere/kinetochore organization, sister chromatid cohesion, DNA repair and replication.

Keywords: RNF4, StUbL, SENP6, PolySUMOylation, SUMO chains

OPEN ACCESS

Edited by:
Huib Ovaa,
Leiden University Medical Center, Netherlands

Reviewed by:
Jürgen Dohmen,
University of Cologne, Germany
Ivo A. Hendriks,
University of Copenhagen, Denmark

***Correspondence:**
Stefan Müller
ste.mueller@em.uni-frankfurt.de

†These authors have contributed equally to this work

Specialty section:
This article was submitted to Cellular Biochemistry, a section of the journal Frontiers in Cell and Developmental Biology

Received: *03 November 2019*
Accepted: *03 December 2019*
Published: *10 January 2020*

Citation:
Keiten-Schmitz J, Schunck K and Müller S (2020) SUMO Chains Rule on Chromatin Occupancy. Front. Cell Dev. Biol. 7:343. doi: 10.3389/fcell.2019.00343

THE SUMO PATHWAY AND ITS INTERSECTION WITH UBIQUITIN

Post-translational modification with the ubiquitin-related modifier SUMO provides a rapid and reversible way to control protein functions. Lower eukaryotes, such as *Saccharomyces cerevisiae* express a single SUMO form, also known as Smt3, while in humans three conjugatable SUMO paralogs (SUMO1, SUMO2, and SUMO3) are found (Flotho and Melchior, 2013; Cappadocia and Lima, 2018). At the amino acid level SUMO1 is 50% identical to SUMO2/3, which differ in only two amino acid residues. Conjugation of SUMO to lysine residues of targets proceeds via a multi-step enzymatic pathway involving a dimeric E1 activating enzyme (SAE1/SAE2), an E2 conjugating enzyme (Ubc9) and a relatively small set of SUMO E3 ligases. Attachment of SUMO generally modulates protein-protein interactions through binding of SUMO conjugates

to interaction partners harboring specific SUMO interaction motifs, termed SIMs (Raman et al., 2013; Husnjak et al., 2016). Multiple SUMO-SIM mediated protein-protein interactions are commonly involved in the assembly of larger protein complexes. Much like ubiquitin, SUMO can be attached as a monomer on single or multiple lysine sites of a target protein generating mono- or multiSUMOylated proteins. Additionally, SUMO can also form polymeric chains through the attachment of one SUMO molecule to internal lysine residues of another SUMO moiety. SUMO chains are typically induced in response to cellular stress and preferentially assemble via lysine residue 11 in SUMO2/3 (Ulrich, 2008; Vertegaal, 2010). However, alternatively linked non-canonical SUMO2/3 chains, mixed SUMO1-SUMO2/3 chains as well as SUMO2/3 chains capped with SUMO1, have been found (Matic et al., 2008; Gartner et al., 2018; Sriramachandran et al., 2019). One signaling process initiated by SUMO chains is the SUMO-targeted Ubiquitin ligase (StUbL) pathway. In this evolutionary conserved pathway, poly- (or multi-) SUMOylated proteins are recognized by E3 ubiquitin ligases that contain specific binding modules for these structures. The best-characterized StUbLs are the budding yeast Slx5/Slx8 heterodimer and the mammalian RING-type ubiquitin ligases RNF4 and RNF111 (Sriramachandran and Dohmen, 2014; Kumar and Sabapathy, 2019). They all contain poly- or multi-SUMO binding modules and catalyze either non-proteolytic or proteolytic ubiquitylation of proteins modified by multiple SUMO moieties. Depending on the cooperating ubiquitin E2 enzyme, RNF4 and RNF111 can mediate either K63- or K48 ubiquitylation. RNF4 also synthesizes hybrid SUMO-ubiquitin chains by ubiquitylating lysine residues on SUMO (Guzzo et al., 2012). Similarly to other PTMs SUMOylation is a reversible and dynamic modification. Deconjugation of SUMO from targets is catalyzed by SUMO-specific isopeptidases. The best-characterized isopeptidases belong to the ULP/SENP family of cysteine proteases, which share a conserved catalytic domain (Hickey et al., 2012; Kunz et al., 2018). In *S. cerevisiae,* Ulp1 and Ulp2 act as SUMO deconjugases, while human cells express six SENP family members. SENP1, SENP2, SENP3 and SENP5 are evolutionary derived from the Ulp1 branch, while SENP6 and SENP7 are related to the Ulp2 subtype. Ulp2, as well as SENP6 and SENP7 preferentially act on SUMO chains thereby countering the StUbL pathway. While SENP6 and SENP7 antagonize the StUbL pathway by limiting SUMO chain formation, two deubiquitylating enzymes, namely USP7 and USP11, possibly counter RNF4 signaling by catalyzing the removal of ubiquitin from SUMO2 polymers (Hendriks et al., 2015; Lecona and Fernandez-Capetillo, 2016; Lecona et al., 2016).

Despite these mechanistic insights, cellular signaling by SUMO chains is still incompletely understood. This is mainly due to the fact that so far the cellular substrates undergoing dynamic polySUMOylation were not well defined. To fill this gap, recent unbiased proteomic screens have focused on the identification of targets for the chain-specific isopeptidase SENP6 (Liebelt et al., 2019; Wagner et al., 2019). To this end alterations in SUMO conjugation were determined following inactivation of SENP6 by siRNA- or shRNA-mediated knock-down. Even though some changes might be indirect, these studies revealed a comprehensive list of candidate substrates of SUMO chain modification. Based on these datasets and other published work we give an overview of cellular networks that are controlled by polySUMOylation. The integrated proteomics dataset of candidate SENP6 targets revealed a highly interconnected network of proteins functioning in DNA damage response and DNA repair networks as well as chromatin organization. Importantly, SENP6 seems to limit SUMO chain formation of protein groups that are part of larger protein assemblies (**Figure 1**). This is exemplified for the constitutive centromere-associated network (CCAN) (**Figure 1**, red subcluster) and SMC (structural maintenance of chromosomes) complexes, such as the SMC1/3 cohesin complex (**Figure 1**, green subcluster) and the SMC5/6 complex (**Figure 1,** magenta subcluster).

SUMO CHAINS AS ORGANIZERS OF KINETOCHORES/CENTROMERES

A first hint for a role of SUMO, and in particular SUMO chains, in centromere organization was provided by genetic data from yeast. In fact, both Smt3 and Ulp2/Smt4 were initially identified in a high copy suppressor screen of a temperature sensitive mutation in the centromeric Mif2 protein, the yeast ortholog of the mammalian inner kinetochore protein CENP-C (Meluh and Koshland, 1995). Subsequent work in vertebrates indeed revealed that the restriction of SUMO chain formation by SENP6, the human ortholog Ulp2, is essential for the proper assembly of kinetochore/centromere structures. Dasso and co-workers demonstrated that SENP6 depletion enhanced SUMOylation and proteasomal degradation of CENP-I, thereby preventing deposition of the CENP-H/I/K subcomplex on kinetochores (Mukhopadhyay et al., 2010; Mukhopadhyay and Dasso, 2010). Co-depletion of the StUbL RNF4 together with SENP6 at least partially restored these defects, suggesting that RNF4 and SENP6 function antagonistically in this context. Indeed, it was further demonstrated that in the absence of SENP6 the polySUMOylated CENP-H/I/K complex is targeted by RNF4 for ubiquitylation and proteasomal degradation. The authors concluded that this leads to the loss of the CENP-H/I/K complex from kinetochores thereby causing defects in spindle assembly and mitotic progression. The CENP-H/I/K subcomplex is part of the constitutive centromere associated network (CCAN), which localizes to the centromere throughout the cell cycle and bridges the histone H3 variant CENP-A at centromeric chromatin to the microtubule-binding machinery (**Figure 2B**). Two recent unbiased proteomic screens now confirmed that SENP6 not only counters SUMO chain formation on CENP-I, but also on CENP-H and CENP-K. Moreover, it appears that multiple subunits within all other CCAN subcomplexes undergo unrestricted polySUMOylation in the absence of SENP6 (Liebelt et al., 2019; Wagner et al., 2019). Importantly, in cells lacking SENP6 polySUMOylation of these CCAN components coincides with their loss from centromeres (Liebelt et al., 2019). Surprisingly, polySUMOylation

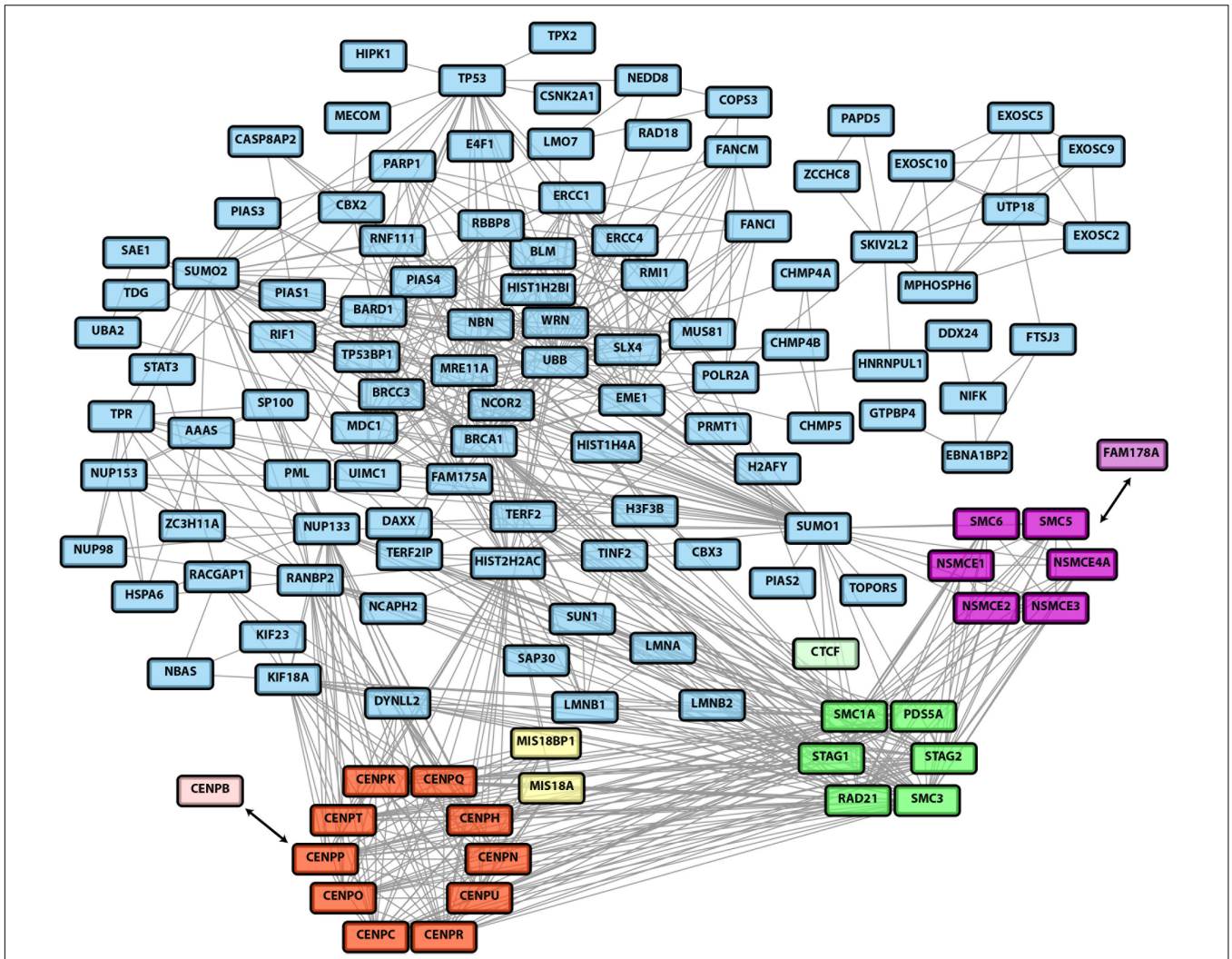

FIGURE 1 | A network of SENP6 targets identified by two recent unbiased proteomic studies (Liebelt et al., 2019; Wagner et al., 2019). Candidate SENP6 targets identified in both studies were combined into a single dataset. This dataset was then used for the generation of a network using the STRING database (version 11.0, https://string-db.org). Only highest confidence interactions (interaction score > 0.9) were considered. Experiments and databases were used as interaction sources. Disconnected nodes were removed from the network. The network data was imported into Cytoscape. The core components of the constitutive centromere associated network (CCAN) are highlighted as red subcluster. The associated CENP-B and the CENP-A targeting factors Mis18A/Mis18BP1 are depicted in light red and yellow, respectively. The cohesion complex is represented by the green subcluster (with the CTCF targeting factor in light green) and the SMC5/6 complex is highlighted in magenta. The SMC5/6 recruitment factor FAM178A/Slf2 is shown in pink.

did not trigger their ubiquitylation and proteasome dependent degradation leading to the conclusion that polySUMO chain formation on CCAN proteins *per se* rather than subsequent RNF4 mediated ubiquitylation affects their proper deposition at centromeres (**Figure 2B**). Notably, however, the canonical RNF4-SENP6 StUbL pathway is critically involved in centromere architecture by controlling the centromeric deposition and/or maintenance of the master organizer CENP-A (Fu et al., 2019; Liebelt et al., 2019). This is not mediated by SUMOylation of CENP-A itself, but by RNF4 regulating the stability of the CENP-A recruitment factor Mis18BP1 (Fu et al., 2019; Liebelt et al., 2019). Noteworthy, in the yeast *S. cerevisiae* the CENP-A ortholog Cse4 is targeted for degradation by the Slx5/8 StUbL thereby preventing its mislocalization to euchromatin (Ohkuni et al., 2016). In mammalian cells, CENP-B dynamics at centromeres is also likely directly regulated by SUMO-primed RNF4-dependent proteasomal degradation (Maalouf et al., 2018), which is consistent with the identification of CENP-B as a major SENP6 target in proteomic studies (Liebelt et al., 2019; Wagner et al., 2019). Importantly, kinetochore-association of the motor protein CENP-E was also shown to depend on SUMO homeostasis at centromers (Zhang et al., 2008).

Altogether these data clearly indicate that the global architecture of centromere/kinetochores largely depends on the coordinated formation and editing of SUMO chains. Conclusive evidence defines SENP6 as the essential chain-limiting activity in

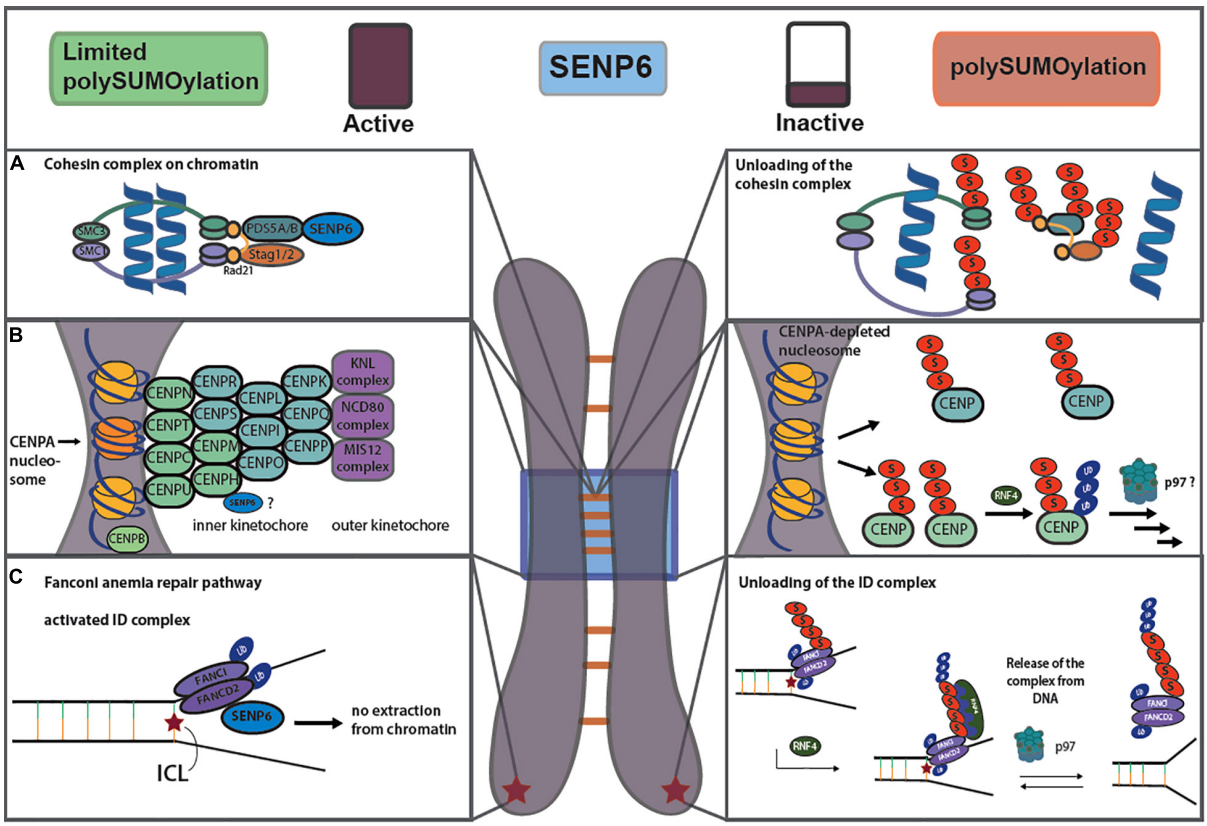

FIGURE 2 | Balancing SUMO chain formation controls chromatin residency of the cohesion complex **(A)**, the centromere network **(B)** and the FA repair pathway **(C)**. For details see text.

this process and underscores a main role of SENP6 in protecting at least a subset of centromeric proteins from entering the StUbL pathway. Why only a subset of polySUMOylated centromeric proteins are channeled into this pathway and how the proposed polySUMO-mediated, but ubiquitin-independent impairment of centromeric CCAN deposition occurs are future key questions.

SUMO CHAINS AS REGULATORS OF SMC COMPLEXES

Structural maintenance of chromosomes complexes consist of multi-subunit annular structures that encircle DNA molecules and function in the organization and compaction of chromosomes. In eukaryotes there are three distinct SMC complexes, cohesin (SMC1/3), condensin (SMC2/4) and the SMC5/6 complex (Haering and Gruber, 2016). These evolutionary conserved complexes have central functions during chromosome segregation and genome maintenance. All SMC complexes share a common ring-like architecture comprising two SMC proteins that are connected to each other via a kleisin subunit. Additional factors typically associated with the kleisin subunit exhibit regulatory functions, in particular in chromatin loading or release of the complexes. Genetic and biochemical data from both lower and higher eukaryotes suggest that SUMO chain formation on SMC complexes is a critical determinant for their chromatin association.

The cohesion core complex is composed of the SMC1-SMC3 scaffold and the kleisin Rad21, which is associated with the HEAT repeat proteins STAG1 or STAG2 and PDS5A or PDS5B (Haering and Gruber, 2016). A main function of the cohesion ring in cycling cells is to hold sister chromatids together after DNA replication in S phase. In double-strand break (DSB) repair, the cohesin complex promotes homologous recombination in conjunction with the SMC5/6 complex (see below) by maintaining sister chromatids in close proximity. Cohesins also control gene expression by generating DNA loops that juxtapose enhancer and promoter elements. This particular function likely involves the CTCF protein as a cohesin targeting factor that tethers cohesins to specific CTCF binding sites. Loading and maintenance of cohesin in interphase involves the Rad21-associated PDS5A/B protein, although the underlying mechanism is not entirely clear. Data in both higher and lower eukaryotes now suggest that PDS5 at least partly functions by recruitment of a SUMO chain-editing activity to the cohesin core complex (**Figure 2A**) (Baldwin et al., 2009; Wagner et al., 2019). We detected an association of chromatin-associated PDS5 with SENP6 and found that SENP6 limits the polySUMOylation of PDS5 and all cohesin core components (Wagner et al., 2019). Lack

of SENP6 affects sister chromatid cohesion and goes along with reduced chromatin association of RAD21 and STAG2 again linking unbalanced SUMOylation with perturbations in proper chromatin-residency and/or degradation (Wagner et al., 2019). Notably, in budding yeast, Ulp2 also controls SUMOylation of Pds5, and Ulp2 mutants are as well defective in cohesin maintenance (D'ambrosio and Lavoie, 2014). Moreover, in Pds5 mutants the yeast Rad21 ortholog is degraded by the StUbL pathway. Finally, in fission yeast SUMOylation of the SMC1/SMC3 orthologues Pms1 and Pms3 was specifically increased in a Slx8 mutant (Kohler et al., 2015). Notably, upon exposure of cells to DNA damaging agents cohesin subunits are SUMOylated by the SMC5/6-associated E3 ligase NSMCE2/MMS21 in yeast and mammals, and SUMOylation was reported to promote DSB repair through homologous recombination (McAleenan et al., 2012; Wu et al., 2012). Based on these findings we hypothesize that an initial monoSUMOylation event on cohesins promotes the establishment of cohesion, while their subsequent multi- or polySUMO-induced ubiquitylation promotes the dissolution of cohesion. SENP6/Ulp2 association with cohesins is therefore needed to keep cohesion hypersumoylation in check until dissolution should happen (**Figure 2A**). A key question in this yet speculative model remains how SENP6/Ulp2 targeting and/or activity is controlled. Given that the Plk1 ortholog Cdc5 interacts with yeast Ulp2 and opposes Ulp2 functions in centromeric cohesion, it is tempting to speculate that the phosphorylation status of Ulp2 determines its activity or localization (Baldwin et al., 2009). Investigating a potential phospho-dependent regulation of SENP6 is as well an attractive aspect for future studies.

Importantly, polySUMOylation of the two cohesin-related SMC complexes, condensin and SMC5/6 is also controlled by SENP6. Condensins promote chromatin compaction to prepare for chromosome segregation during mitosis. In humans two condensin complexes are found (Haering and Gruber, 2016). Condensin II resides in the cell nucleus during interphase and controls the early stage of chromosome condensation, whereas condensin I associates with chromosomes after nuclear envelope breakdown at the end of prophase. In both complexes the DNA encircling ring is formed by SMC2-SMC4 and the kleisin CAPH (Condensin I) or CAPH2 (Condensin II). In the condensin I complex CAPH is associated with the HEAT repeat proteins CAPD2 and CAPG, while CAPH2 in condensin II complexes is bound to CAPD3 and CAPG2. We detected a physical association of SENP6 with the CAPH2, CAPG2 subunits of condensin II and observed a strong increase in SUMOylation of the kleisin subunit CAPH2 in the absence of SENP6 (Wagner et al., 2019). The functional consequence of CAPH2 hyperSUMOylation in mammalian cells is not yet clear. However, deletion of Ulp2 in budding yeast affects is proper targeting to the rDNA locus (Strunnikov et al., 2001). Moreover, in fission yeast, condensin subunits were identified as Slx5/8 substrates (Kohler et al., 2015). Altogether these data are consistent with the idea that SENP6 is a crucial regulator of cohesion and condensin function by controlling their chromatin residency in conjunction with the RNF4 pathway. This concept can possibly be expanded to the SMC5-SMC6 complex, which is crucial for repair of DNA DSB and for replication stress tolerance. In the SMC5/6 complex the kleisin NSMCE4 forms a ring structure together with SMC5-SMC6 (Haering and Gruber, 2016). Among the regulatory factors associated with the complex are the ubiquitin-ligase NSMCE1 and the SUMO ligase NSMCE2, alias MMS21, and NSMCE3. MS data in SENP6 depleted cells show an enhanced SUMOylation of the core complex (SMC5, SMC6, NSMCE4) as well as NSCME1-3 (Liebelt et al., 2019). Moreover, NSMCE2 levels are strongly downregulated under these conditions indicating that polySUMOylation channels it into the RNF4 pathway (Wagner et al., 2019). This is consistent with proteomic data identifying NSMCE2 as a *bona fide* RNF4 substrate (Kumar et al., 2017). To better understand these processes future experiments should focus on the regulation of SENP6 during cell cycle progression and in response to DNA damage.

SUMO CHAINS IN DNA REPAIR AND THE DNA DAMAGE RESPONSE (DDR)

In both lower and higher eukaryotes StUBLs contribute to the maintainance of genome stability (Heideker et al., 2009; Kumar and Sabapathy, 2019). A recurrent theme in DDR pathways is the SUMO-regulated turnover of repair factors at sites of DNA damage. SUMO-primed ubiquitylation appears to have a key role in extraction or clearance of DNA repair factors from chromatin. One well established example for this process has been delineated in the Fanconi anemia (FA) repair pathway (Gibbs-Seymour et al., 2015; Xie et al., 2015; **Figure 2C**). The canonical function of the FA pathway is the repair of DNA inter-strand cross-links (ICLs) that, if unrepaired, are prone to convert to double strand breaks. In the FA pathway, a network of repair factors cooperates to preserve genomic integrity by stabilizing replication forks, and by alleviating replication stress resulting from ICLs. FANC proteins can been subdivided into three groups, where group I comprises the FANC core complex that functions as a ubiquitin ligase monoubiquitylating the group II proteins FANCI and FANCD2, known as the ID complex. This monoubiquitylation is required for ID localization to the lesion and the subsequent coordination of the repair by group III proteins. Repair involves the recruitment of structure-specific endonucleases and the HR repair machinery. Importantly, data by Mailand and co-workers provide evidence that SUMO-primed K48 and K63-linked ubiquitylation by RNF4 facilitates the removal of the activated ID complex from the sites of DNA lesions (Gibbs-Seymour et al., 2015). For unloading RNF4 cooperates with the p97 segregase and its adaptor protein DVC1/Spartan. SENP6 antagonizes this pathway by limiting SUMO-chain formation on FANCI, most likely at the sites of DNA damage. In accordance with this data, the unbiased proteomics screens for SENP6 targets and binding proteins confirmed the physical association of SENP6 with the ID complex as well as increased SUMOylation of FANCI in the absence of SENP6 (Wagner et al., 2019). Moreover, in SENP6 depleted cells FANCD2 protein levels were strongly reduced indicating that in cells lacking SENP6, FANCD2 is not only extracted from chromatin but subsequently degraded

by the StUbL pathway (Wagner et al., 2019). Altogether these data support the model that polySUMOylation in conjunction with RNF4, limits the dosage of activated ID complex at DNA lesions. It has been proposed that this regulatory circuit helps to avoid the prolonged, potentially dangerous localization of the structure-specific endonucleases to the chromatin (Gibbs-Seymour et al., 2015). Notably, SENP6 substrate profiling revealed that components of the endonuclease complexes itself, such as SLX4, ERCC1 or ERCC4 are as well targets of SENP6 and SLX4 is a *bona fide* RNF4 target (Kumar et al., 2017; Liebelt et al., 2019; Wagner et al., 2019). This possibly indicates that the StUbL pathway clears ID and endonuclease complexes from the DNA damage sites in a concerted action. In support of a coordinated clearance of the FA machinery FANCA, a component of the core complex, was also shown to be targeted for degradation by the SUMO-RNF4 pathway (Xie et al., 2015). The general concept of a polySUMO-primed StUbL-dependent eviction of protein complexes from chromatin appears to be a more widespread mechanism in DNA repair pathways. For example, in homologous recombination (HR) RNF4 controls the turnover of the replication protein A (RPA) at DNA damage sites (Galanty et al., 2012; Yin et al., 2012). In RNF4-depleted cells RPA is not properly replaced by the HR factor RAD51. SUMO-StUbL mediated extraction of repair factors is not limited to HR. In nucleotide excision repair (NER) the StUbL RNF111 promotes K63-linked ubiquitylation of the SUMOylated XPC repair factor, thereby promoting the release of XPC from damaged DNA after NER initiation (van Cuijk et al., 2015).

SUMO CHAINS AT REPLISOMES

Several lines of evidence point to a regulatory role of SUMO chains and the StUbL pathway in unperturbed DNA replication and under replication stress. A recurrent theme is again that the extent of SUMO- or Ub-SUMO chains governs the association of the replication machinery with chromatin. This has been very recently nicely exemplified for the budding yeast Dbf4-Cdc7 kinase complex, which mediates DNA replication initiation by phosphorylating the replicative MCM helicase complex (Psakhye et al., 2019). SUMO chains prime the replication engaged Dbf4-Cdc7 for Slx5/8-mediated degradation. Ulp2, which is directly associated with Dbf4, protects the complex from ubiquitylation thereby safeguarding replication initiation. This concept was expanded by the identification of additional factors, including the MCM helicase itself, as SUMO-chain-modified degradation-prone substrates of Ulp2 and Slx5/Slx8. The authors therefore propose SUMO-chain/Ulp2-protease-regulated proteasomal degradation as a mechanism that times the availability of functionally engaged SUMO-modified protein pools during replication.

Limiting the formation of Ub-SUMO conjugates at replisomes is also an important mechanism that safeguards replication progression in mammalian cells. USP7 was identified as a DUB that removes ubiquitin from SUMO. Intriguingly, upon USP7 inhibition, SUMOylated proteins are collectively displaced from the replisome, which fully abrogates DNA replication, both by limiting fork progression and the firing of new origins (Lecona and Fernandez-Capetillo, 2016; Lecona et al., 2016).

CONCLUDING REMARKS

Altogether, the above-mentioned data strongly support a general role of polySUMOylation and the StUbL pathway in controlling the chromatin association of proteins and protein complexes. This also implies that mono- and polySUMOylation of the same protein or protein complex may have fundamentally different consequences. MonoSUMOylation can facilitate the assembly of DNA-associated protein complexes by fostering SUMO-SIM dependent complex formations. PolySUMOylation in turn primes the complexes for StUbL-mediated proteolytic or non-proteolytic ubiquitylation and displacement from chromatin in conjunction with the p97 machinery. DNA can directly trigger SUMOylation, as exemplified by DNA-dependent activation of the NSMCE2/Mms21 ligase in the SMC5/6 complex (Varejao et al., 2018). A key function of chain-trimming SUMO isopeptidases would therefore be to protect the complexes from polySUMOylation until release should occur. In line with this idea it has been proposed that SENPs are required to restrict an "over before it has begun" repair response (Garvin et al., 2019). Consistent with this scenario SENP6 localizes to sites of DNA damage in response to DNA damaging stimuli. StUBL-mediated clearance of protein complexes is likely not limited to replication or DNA repair processes, but seems as well play a role in promoter clearance during transcription (Martin et al., 2009; Rosonina et al., 2012; Ng et al., 2015; Akhter and Rosonina, 2016). However, the polySUMO-StUbL system does not always act in unloading chromatin-associated complexes, but can also prevent deposition to chromatin by acting on the soluble nucleoplasmic fraction of distinct complexes. This was initially shown for the CENH/I/K complex, which is degraded by RNF4 in S phase, and is now also exemplified on the CENP-A loading factor M18BP1 (Fu et al., 2019; Liebelt et al., 2019). Since SENP6 was not detected at centromeres in mitotic or in interphase cells it is likely that in these cases SENP6 limits hypersumoylation of centromere/kinetochore organizers in the nucleoplasmic fraction. How hyperSUMOylation alone without subsequent ubiquitylation controls chromatin residency of proteins in mammalian cells is unclear. Importantly, however, in both *S. pombe* and *S. cerevisiae* it has been shown that Cdc48/p97, in conjunction with its cofactor Ufd1, is targeted to SUMOylated proteins (Nie et al., 2012; Bergink et al., 2013). Moreover, Cdc48/p97 displaces the Rad52-Rad51 repair complex from chromatin in a SUMO-mediated, but ubiquitin-independent process (Bergink et al., 2013). Future work needs to uncover whether distinct p97 cofactors in mammalian cells are also solely dependent on polySUMO chains rather than ubiquitylation.

AUTHOR CONTRIBUTIONS

JK-S and KS designed and prepared the figures and corrected the manuscript. SM wrote the manuscript.

FUNDING

The work was funded by DFG Collaborative Research Centers SFB815, SFB1177 and DFG grant MU-1764/4.

ACKNOWLEDGMENTS

We thank all members of our group and members of IBC2 for constructive feedback and discussions.

REFERENCES

Akhter, A., and Rosonina, E. (2016). Chromatin association of Gcn4 is limited by post-translational modifications triggered by its DNA-binding in *Saccharomyces cerevisiae*. *Genetics* 204, 1433–1445. doi: 10.1534/genetics.116.194134

Baldwin, M. L., Julius, J. A., Tang, X., Wang, Y., and Bachant, J. (2009). The yeast SUMO isopeptidase Smt4/Ulp2 and the polo kinase Cdc5 act in an opposing fashion to regulate sumoylation in mitosis and cohesion at centromeres. *Cell Cycle* 8, 3406–3419. doi: 10.4161/cc.8.20.9911

Bergink, S., Ammon, T., Kern, M., Schermelleh, L., Leonhardt, H., and Jentsch, S. (2013). Role of Cdc48/p97 as a SUMO-targeted segregase curbing Rad51-Rad52 interaction. *Nat. Cell Biol.* 15, 526–532. doi: 10.1038/ncb2729

Cappadocia, L., and Lima, C. D. (2018). Ubiquitin-like protein conjugation: structures, chemistry, and mechanism. *Chem. Rev.* 118, 889–918. doi: 10.1021/acs.chemrev.6b00737

D'ambrosio, L. M., and Lavoie, B. D. (2014). Pds5 prevents the PolySUMO-dependent separation of sister chromatids. *Curr. Biol.* 24, 361–371. doi: 10.1016/j.cub.2013.12.038

Flotho, A., and Melchior, F. (2013). Sumoylation: a regulatory protein modification in health and disease. *Annu. Rev. Biochem.* 82, 357–385. doi: 10.1146/annurev-biochem-061909-093311

Fu, H., Liu, N., Dong, Q., Ma, C., Yang, J., Xiong, J., et al. (2019). SENP6-mediated M18BP1 deSUMOylation regulates CENP-A centromeric localization. *Cell Res.* 29, 254–257. doi: 10.1038/s41422-018-0139-y

Galanty, Y., Belotserkovskaya, R., Coates, J., and Jackson, S. P. (2012). RNF4, a SUMO-targeted ubiquitin E3 ligase, promotes DNA double-strand break repair. *Genes Dev.* 26, 1179–1195. doi: 10.1101/gad.188284.112

Gartner, A., Wagner, K., Holper, S., Kunz, K., Rodriguez, M. S., and Muller, S. (2018). Acetylation of SUMO2 at lysine 11 favors the formation of non-canonical SUMO chains. *EMBO Rep.* 19:e46117. doi: 10.15252/embr.201846117

Garvin, A. J., Walker, A. K., Densham, R. M., Chauhan, A. S., Stone, H. R., Mackay, H. L., et al. (2019). The deSUMOylase SENP2 coordinates homologous recombination and nonhomologous end joining by independent mechanisms. *Genes Dev.* 33, 333–347. doi: 10.1101/gad.321125.118

Gibbs-Seymour, I., Oka, Y., Rajendra, E., Weinert, B. T., Passmore, L. A., Patel, K. J., et al. (2015). Ubiquitin-SUMO circuitry controls activated fanconi anemia ID complex dosage in response to DNA damage. *Mol. Cell.* 57, 150–164. doi: 10.1016/j.molcel.2014.12.001

Guzzo, C. M., Berndsen, C. E., Zhu, J., Gupta, V., Datta, A., Greenberg, R. A., et al. (2012). RNF4-dependent hybrid SUMO-ubiquitin chains are signals for RAP80 and thereby mediate the recruitment of BRCA1 to sites of DNA damage. *Sci. Signal.* 5:ra88. doi: 10.1126/scisignal.2003485

Haering, C. H., and Gruber, S. (2016). SnapShot: smc protein complexes part I. *Cell* 164, 326.e1–326.e1. doi: 10.1016/j.cell.2015.12.026

Heideker, J., Perry, J. J. P., and Boddy, M. N. (2009). Genome stability roles of SUMO-targeted ubiquitin ligases. *DNA Repair (Amst)* 8, 517–524. doi: 10.1016/j.dnarep.2009.01.010

Hendriks, I. A., Schimmel, J., Eifler, K., Olsen, J. V., and Vertegaal, A. C. (2015). Ubiquitin-specific protease 11 (USP11) deubiquitinates hybrid small ubiquitin-like modifier (SUMO)-ubiquitin chains to counteract RING finger protein 4 (RNF4). *J. Biol. Chem.* 290, 15526–15537. doi: 10.1074/jbc.M114.618132

Hickey, C. M., Wilson, N. R., and Hochstrasser, M. (2012). Function and regulation of SUMO proteases. *Nat. Rev. Mol. Cell Biol.* 13, 755–766. doi: 10.1038/nrm3478

Husnjak, K., Keiten-Schmitz, J., and Muller, S. (2016). Identification and characterization of SUMO-SIM interactions. *Methods Mol. Biol.* 1475, 79–98. doi: 10.1007/978-1-4939-6358-4_6

Kohler, J. B., Tammsalu, T., Jorgensen, M. M., Steen, N., Hay, R. T., and Thon, G. (2015). Targeting of SUMO substrates to a Cdc48-Ufd1-Npl4 segregase and STUbL pathway in fission yeast. *Nat. Commun.* 6:8827. doi: 10.1038/ncomms9827

Kumar, R., Gonzalez-Prieto, R., Xiao, Z., Verlaan-De Vries, M., and Vertegaal, A. C. O. (2017). The STUbL RNF4 regulates protein group SUMOylation by targeting the SUMO conjugation machinery. *Nat. Commun.* 8:1809. doi: 10.1038/s41467-017-01900-x

Kumar, R., and Sabapathy, K. (2019). RNF4-A paradigm for SUMOylation-mediated ubiquitination. *Proteomics* 19:e1900185. doi: 10.1002/pmic.201900185

Kunz, K., Piller, T., and Muller, S. (2018). SUMO-specific proteases and isopeptidases of the SENP family at a glance. *J. Cell Sci.* 131:jcs211904. doi: 10.1242/jcs.211904

Lecona, E., and Fernandez-Capetillo, O. (2016). A SUMO and ubiquitin code coordinates protein traffic at replication factories. *Bioessays* 38, 1209–1217. doi: 10.1002/bies.201600129

Lecona, E., Rodriguez-Acebes, S., Specks, J., Lopez-Contreras, A. J., Ruppen, I., Murga, M., et al. (2016). USP7 is a SUMO deubiquitinase essential for DNA replication. *Nat. Struct. Mol. Biol.* 23, 270–277. doi: 10.1038/nsmb.3185

Liebelt, F., Jansen, N. S., Kumar, S., Gracheva, E., Claessens, L. A., Verlaan-De Vries, M., et al. (2019). The poly-SUMO2/3 protease SENP6 enables assembly of the constitutive centromere-associated network by group deSUMOylation. *Nat. Commun.* 10:3987. doi: 10.1038/s41467-019-11773-x

Maalouf, J. E., Texier, P., Erliandri, I., Cohen, C., Corpet, A., Catez, F., et al. (2018). CENP-B dynamics at centromeres is regulated by a SUMOylation/ubiquitination and proteasomal-dependent degradation mechanism involving the SUMO-targeted ubiquitin E3 ligase RNF4. *bioRxiv[Preprint]*

Martin, N., Schwamborn, K., Schreiber, V., Werner, A., Guillier, C., Zhang, X. D., et al. (2009). PARP-1 transcriptional activity is regulated by sumoylation upon heat shock. *EMBO J.* 28, 3534–3548. doi: 10.1038/emboj.2009.279

Matic, I., Van Hagen, M., Schimmel, J., Macek, B., Ogg, S. C., Tatham, M. H., et al. (2008). In vivo identification of human small ubiquitin-like modifier polymerization sites by high accuracy mass spectrometry and an in vitro to in vivo strategy. *Mol. Cell. Proteomics* 7, 132–144. doi: 10.1074/mcp.M700173-MCP200

McAleenan, A., Cordon-Preciado, V., Clemente-Blanco, A., Liu, I. C., Sen, N., Leonard, J., et al. (2012). SUMOylation of the alpha-kleisin subunit of cohesin is required for DNA damage-induced cohesion. *Curr. Biol.* 22, 1564–1575. doi: 10.1016/j.cub.2012.06.045

Meluh, P. B., and Koshland, D. (1995). Evidence that the MIF2 gene of Saccharomyces cerevisiae encodes a centromere protein with homology to the mammalian centromere protein CENP-C. *Mol. Biol. Cell* 6, 793–807. doi: 10.1091/mbc.6.7.793

Mukhopadhyay, D., Arnaoutov, A., and Dasso, M. (2010). The SUMO protease SENP6 is essential for inner kinetochore assembly. *J. Cell Biol.* 188, 681–692. doi: 10.1083/jcb.200909008

Mukhopadhyay, D., and Dasso, M. (2010). The fate of metaphase kinetochores is weighed in the balance of SUMOylation during S phase. *Cell Cycle* 9, 3194–3201. doi: 10.4161/cc.9.16.12619

Ng, C. H., Akhter, A., Yurko, N., Burgener, J. M., Rosonina, E., and Manley, J. L. (2015). Sumoylation controls the timing of Tup1-mediated transcriptional deactivation. *Nat. Commun.* 6:6610. doi: 10.1038/ncomms7610

Nie, M., Aslanian, A., Prudden, J., Heideker, J., Vashisht, A. A., Wohlschlegel, J. A., et al. (2012). Dual recruitment of Cdc48 (p97)-Ufd1-Npl4 ubiquitin-selective segregase by small ubiquitin-like modifier protein (SUMO) and ubiquitin in SUMO-targeted ubiquitin ligase-mediated genome stability functions. *J. Biol. Chem.* 287, 29610–29619. doi: 10.1074/jbc.M112.379768

Ohkuni, K., Takahashi, Y., Fulp, A., Lawrimore, J., Au, W. C., Pasupala, N., et al. (2016). SUMO-Targeted Ubiquitin Ligase (STUbL) Slx5 regulates proteolysis of centromeric histone H3 variant Cse4 and prevents its mislocalization to euchromatin. *Mol. Biol. Cell.* 27, 1500–1510. doi: 10.1091/mbc.E15-12-0827

Psakhye, I., Castellucci, F., and Branzei, D. (2019). SUMO-chain-regulated proteasomal degradation timing exemplified in DNA replication initiation. *Mol. Cell* 76, 632.e6–645.e6. doi: 10.1016/j.molcel.2019.08.003

Raman, N., Nayak, A., and Muller, S. (2013). The SUMO system: a master organizer of nuclear protein assemblies. *Chromosoma* 122, 475–485. doi: 10.1007/s00412-013-0429-6

Rosonina, E., Duncan, S. M., and Manley, J. L. (2012). Sumoylation of transcription factor Gcn4 facilitates its Srb10-mediated clearance from promoters in yeast. *Genes Dev.* 26, 350–355. doi: 10.1101/gad.184689.111

Sriramachandran, A. M., and Dohmen, R. J. (2014). SUMO-targeted ubiquitin ligases. *Biochim. Biophys. Acta* 1843, 75–85. doi: 10.1016/j.bbamcr.2013.08.022

Sriramachandran, A. M., Meyer-Teschendorf, K., Pabst, S., Ulrich, H. D., Gehring, N. H., Hofmann, K., et al. (2019). Arkadia/RNF111 is a SUMO-targeted ubiquitin ligase with preference for substrates marked with SUMO1-capped SUMO2/3 chain. *Nat. Commun.* 10:3678. doi: 10.1038/s41467-019-11549-3

Strunnikov, A. V., Aravind, L., and Koonin, E. V. (2001). *Saccharomyces cerevisiae* SMT4 encodes an evolutionarily conserved protease with a role in chromosome condensation regulation. *Genetics* 158, 95–107.

Ulrich, H. D. (2008). The fast-growing business of SUMO chains. *Mol. Cell* 32, 301–305. doi: 10.1016/j.molcel.2008.10.010

van Cuijk, L., Van Belle, G. J., Turkyilmaz, Y., Poulsen, S. L., Janssens, R. C., Theil, A. F., et al. (2015). SUMO and ubiquitin-dependent XPC exchange drives nucleotide excision repair. *Nat. Commun.* 6:7499. doi: 10.1038/ncomms8499

Varejao, N., Ibars, E., Lascorz, J., Colomina, N., Torres-Rosell, J., and Reverter, D. (2018). DNA activates the Nse2/Mms21 SUMO E3 ligase in the Smc5/6 complex. *EMBO J.* 37:e98306. doi: 10.15252/embj.201798306

Vertegaal, A. C. (2010). SUMO chains: polymeric signals. *Biochem. Soc. Trans.* 38, 46–49. doi: 10.1042/BST0380046

Wagner, K., Kunz, K., Piller, T., Tascher, G., Holper, S., Stehmeier, P., et al. (2019). The SUMO isopeptidase SENP6 functions as a rheostat of chromatin residency in genome maintenance and chromosome dynamics. *Cell Rep.* 29, 480.5–494.e5. doi: 10.1016/j.celrep.2019.08.106

Wu, N., Kong, X., Ji, Z., Zeng, W., Potts, P. R., Yokomori, K., et al. (2012). Scc1 sumoylation by Mms21 promotes sister chromatid recombination through counteracting Wapl. *Genes Dev.* 26, 1473–1485. doi: 10.1101/gad.193615.112

Xie, J., Kim, H., Moreau, L. A., Puhalla, S., Garber, J., Al Abo, M., et al. (2015). RNF4-mediated polyubiquitination regulates the Fanconi anemia/BRCA pathway. *J. Clin. Invest.* 125, 1523–1532. doi: 10.1172/JCI79325

Yin, Y., Seifert, A., Chua, J. S., Maure, J. F., Golebiowski, F., and Hay, R. T. (2012). SUMO-targeted ubiquitin E3 ligase RNF4 is required for the response of human cells to DNA damage. *Genes Dev.* 26, 1196–1208. doi: 10.1101/gad.189274.112

Zhang, X. D., Goeres, J., Zhang, H., Yen, T. J., Porter, A. C., and Matunis, M. J. (2008). SUMO-2/3 modification and binding regulate the association of CENP-E with kinetochores and progression through mitosis. *Mol. Cell.* 29, 729–741. doi: 10.1016/j.molcel.2008.01.013

Conflict of Interest: The authors declare that the research was conducted in the absence of any commercial or financial relationships that could be construed as a potential conflict of interest.

frontiers in Chemistry

REVIEW
published: 21 January 2020
doi: 10.3389/fchem.2019.00923

Strategies to Target ISG15 and USP18 Toward Therapeutic Applications

Daniel Jiménez Fernández[1], *Sandra Hess*[1,2] *and Klaus-Peter Knobeloch*[1]*

[1] Faculty of Medicine, Institute of Neuropathology, University of Freiburg, Freiburg, Germany, [2] Faculty of Biology, University of Freiburg, Freiburg, Germany

The interferon (IFN)-stimulated gene product 15 (ISG15) represents an ubiquitin-like protein (Ubl), which in a process termed ISGylation can be covalently linked to target substrates via a cascade of E1, E2, and E3 enzymes. Furthermore, ISG15 exerts functions in its free form both, as an intracellular and as a secreted protein. In agreement with its role as a type I IFN effector, most functions of ISG15 and ISGylation are linked to the anti-pathogenic response. However, also key roles in other cellular processes such as protein translation, cytoskeleton dynamics, exosome secretion, autophagy or genome stability and cancer were described. Ubiquitin-specific protease 18 (USP18) constitutes the major ISG15 specific protease which counteracts ISG15 conjugation. Remarkably, USP18 also functions as a critical negative regulator of the IFN response irrespective of its enzymatic activity. Concordantly, lack of USP18 function causes fatal interferonopathies in humans and mice. The negative regulatory function of USP18 in IFN signaling is regulated by various protein–protein interactions and its stability is controlled via proteasomal degradation. The broad repertoire of physiological functions and regulation of ISG15 and USP18 offers a variety of potential intervention strategies which might be of therapeutic use. Due to the high mutation rates of pathogens which are often species specific and constantly give rise to a variety of immune evasion mechanisms, immune effector systems are under constant evolutionarily pressure. Therefore, it is not surprising that considerable differences in ISG15 with respect to function and sequence exist even among closely related species. Hence, it is essential to thoroughly evaluate the translational potential of results obtained in model organisms especially for therapeutic strategies. This review covers existing and conceptual assay systems to target and identify modulators of ISG15, ISGylation, USP18 function, and protein–protein interactions within this context. Strategies comprise mouse models for translational perspectives, cell-based and biochemical assays as well as chemical probes.

Keywords: ISG15, USP18, STAT2, ubiquitin, protein–protein interaction, IFN, Immunity, transgenic mice

OPEN ACCESS

Edited by:
Lei Liu,
Tsinghua University, China

Reviewed by:
Francisco Solano,
University of Murcia, Spain
Chen Zhao,
Shanghai Public Health Clinical Center, Fudan University, China

***Correspondence:**
Klaus-Peter Knobeloch
klaus-peter.knobeloch@uniklinik-freiburg.de

Specialty section:
This article was submitted to Chemical Biology, a section of the journal Frontiers in Chemistry

Received: *16 October 2019*
Accepted: *18 December 2019*
Published: *21 January 2020*

Citation:
Jiménez Fernández D, Hess S and Knobeloch K-P (2020) Strategies to Target ISG15 and USP18 Toward Therapeutic Applications. Front. Chem. 7:923. doi: 10.3389/fchem.2019.00923

INTRODUCTION

ISGylation

ISG15 is one of the genes most strongly induced by type I interferon and was the first Ubiquitin-like modifier (Ubl) identified (Blomstrom et al., 1986; Haas et al., 1987). Analogous to ubiquitin, Ubls like ISG15, small ubiquitin-related modifier (SUMO), human leukocyte antigen (HLA)-F adjacent transcript 10 (FAT10) or neural precursor cell expressed, developmentally down-regulated

8 (NEDD8) can be covalently linked to target proteins to alter a variety of biological processes.

ISG15 is composed of two Ubl domains connected by a flexible polypeptide hinge region. Each domain is formed by four β-sheets and a single α-helix (Narasimhan et al., 2005) reminiscent of the ubiquitin structure. The C-terminal tail of ISG15 contains the LRLRGG motif which is essential for the conjugation to target proteins. Like ubiquitin, ISG15 can be covalently attached to lysine residues of target proteins (through the ε-amino group) via the LRLRGG motif (Loeb and Haas, 1992).

Analogous to the ubiquitin conjugation system, ISGylation is mediated by the consecutive action of a three-step catalytic cascade, where all the enzymes are induced by type I IFNs (**Figure 1**). E1-activating enzymes bind to Ub (or ISG15) and, mediated by ATP-Mg^{+2}, form a complex that catalyzes Ub (or ISG15) C-terminal acyl adenylation (Tokgoz et al., 2006). Subsequently, a catalytic cysteine on the E1 enzyme interacts with the ubiquitin-AMP or ISG15-AMP complex undergoing acyl substitution that leads to thioester bond formation and the release of an AMP group. After that, through a transthiolation reaction, an E2 cysteine residue replaces the E1 enzyme. E2-conjugating enzymes catalyze the isopeptide bond formation but also contribute to substrate specificity. E3-ligase enzymes bind the E2-ubiquitin thioester, recognize the protein substrate and catalyze the transfer of ubiquitin or ISG15 from the E2 enzyme to the target protein (Zhang and Zhang, 2011).

In sharp contrast to ubiquitin, which is highly conserved among different species, the amino acid (AA) composition of ISG15 and its effector functions can differ substantially among species. ISG15 has only been identified in vertebrates, and murine ISG15 and its human counterpart share only 64% homology and 76% similarity on the AA level. This is most likely caused by high evolutionary pressure on anti-pathogenic immune effector functions which need to adapt to immune evasion mechanisms from rapidly mutating pathogens.

One of the features that substantially differ in the ISGylation mechanisms between murine and human ISG15 is the use of certain enzymes. The E1 ubiquitin-activating enzyme E1 homolog (UBE1L/UBA7) is a common enzyme for human and mouse in the ISG15 system (Kim et al., 2006), whereas the E1 counterparts for ubiquitin are ubiquitin-like modifier activating enzyme 1 (UBA1) and ubiquitin-like modifier activating enzyme 6 (UBA6) (Pelzer et al., 2007). Ubiquitin/ISG15-conjugating enzyme E2 L6 (UBCH8) and UBCM8 represent the human and murine E2 conjugating enzymes in ISGylation, respectively. Both share only 76% AA identity, whereas E2 conjugating enzymes for other ubl systems show 95–100% identity (Kim et al., 2004). UBCH8 also interacts with the E1-activating enzyme from the Ub conjugation system which indicates an overlap of both conjugation systems at the level of the E2 enzyme (Zhao et al., 2004). However, the enzyme ubiquitin-conjugating enzyme E2 L3 (UBE2L3/UBCH7) represents the dominant conjugating enzyme in ubiquitination as the K_M values uncover a 36-fold higher affinity of UBE1L to UBCH7 as compared to UBCH8 (Durfee et al., 2008). Four cellular ISG15 E3 ligases have been identified so far. Human E3 ISG15–protein ligase HERC5 (HERC5) and the murine counterpart E3 ISG15–protein ligase HERC6 (HERC6) are the dominant E3 ligases in ISGylation that coordinate the conjugation of ISG15 to substrates. Interestingly, both mISG15 and hISG15 can be conjugated either by hHERC5 or mHERC6 (Wong et al., 2006; Ketscher et al., 2012). Furthermore, the E3 ubiquitin-protein ligases estrogen-responsive finger protein (EFP) (Zou and Zhang, 2006), human homolog of Drosophila ariadne-1 (HHARI) (Okumura et al., 2007), and tripartite motif-containing protein 25 (TRIM25) (Park et al., 2016) were also reported to mediate ISGylation.

It was shown that ISGylation can occur in a cotranslational process favoring modification of newly synthesized proteins. As in infected cells mainly viral proteins are translated, ISGylation can interfere with pathogen protein function as shown for capsid assembly of the papilloma virus (Durfee et al., 2010). Furthermore, cellular proteins involved in antiviral defense or export of viral particles were shown to be ISGylated (Perng and Lenschow, 2018).

USP18 Functions: DeISGylation and Negative Regulation of the IFN Response

Ubiquitination and Ubl-conjugation pathways can be reversed by the action of deubiquitinating enzymes (DUBs). These proteases remove or trim Ub/Ubl residues from target proteins. Most of

Abbreviations: IFN, Interferon; ISG15, IFN-stimulated gene product 15; Ubl, Ubiquitin-like protein; USP18, Ubiquitin-specific protease 18; STAT2, Signal transducer and activator of transcription 2; ABPs, Activity-based probes; SUMO, Small ubiquitin-related modifier; FAT10, Human leukocyte antigen (HLA)-F adjacent transcript 10; NEDD8, Neural precursor cell expressed, developmentally down-regulated 8; AA, Amino acid; UBE1L, Ubiquitin-activating enzyme E1 homologue; UBA1, Ubiquitin-like modifier activating enzyme 1; UBA6, Ubiquitin-like modifier activating enzyme 6; UBCH8, Ubiquitin/ISG15-conjugating enzyme E2 L6 in human; UBCM8, Ubiquitin/ISG15-conjugating enzyme E2 L6 in mouse; UBE2L3/UBCH7, Ubiquitin-conjugating enzyme E2 L3; HERC5, E3 ISG15-protein ligase HERC5; HERC6, E3 ISG15-protein ligase HERC6; h, Human; m, Murine; EFP, Estrogen-responsive finger protein; HHARI, Human homolog of Drosophila ariadne-1; TRIM25, Tripartite motif-containing protein 25; DUB, Deubiquitinating enzyme; MERS-CoV, Middle East respiratory syndrome coronavirus; CCHFV, Crimean-Congo hemorrhagic fever virus; SARS-CoV, Severe acute respiratory syndrome coronavirus; PLP, Papain-like protease; IBB1, ISG15-binding box1; IBB2, ISG15-binding box2; IFNAR2, IFN-α/β receptor 2; JAK1, Janus kinase 1; SKP2, S-phase kinase-associated protein 2; BCG, Bacillus Calmette–Guérin; PBMCs, Peripheral blood mononuclear cells; IL, Interleukin; NK, Natural killer; LFA-1, leukocyte function associated antigen-1; UBAIT, Ubiquitin-activated interaction trap; UPS, Ubiquitin-proteasome system; UAE, Ubiquitin activation enzyme (E1); CDC34, Human ubiquitin-conjugating enzyme E2 R1; UBC13-UEV1A, Ubiquitin-conjugating enzyme variant; UBE2N, Ubiquitin-conjugating enzyme E2 N; ICAM1, Intercellular Adhesion Molecule 1; VS, Vinyl methyl sulfone; VME, Vinyl methyl ester; PRG, Propargylamide; ct-ISG15, C-terminal Ubl domain of ISG15; SPPS, Solid-phase peptide chemistry; FMOC, 9-fluorenylmethoxycarbonyl; HTS, High-throughput drug screening; amc, 7-Amino-4-methylcoumarin; FP, Fluorescence polarization; TAMRA, 5-carboxytetra-methylrhodamine; CHO, Aldehyde; AGS, Aicardi-Goutières syndrome; PTS, Pseudo-TORCH syndrome; MS, Mass spectroscopy; BMDMs, Bone marrow derived macrophages; VACV, Vaccinia virus; OXPHOS, Oxidative phosphorylation; FMD, Foot-and-mouth disease; IP, Immunoprecipitation; LC, Liquid chromatography; PROTACs, Proteolysis Targeting Chimeras; BRET, Bioluminescence Resonance Energy Transfer; FRET, Fluorescence resonance energy transfer.

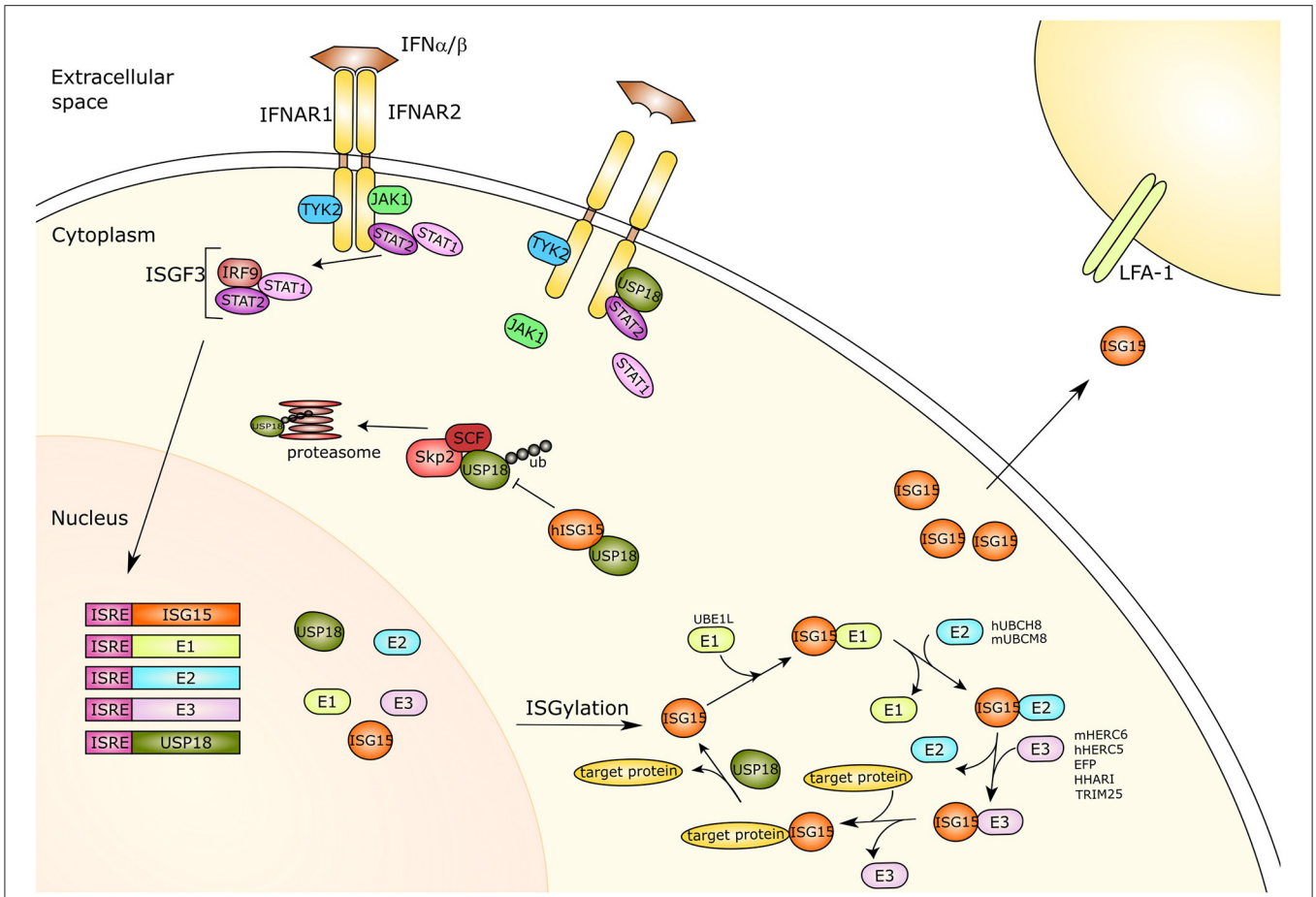

FIGURE 1 | Type-I interferon signaling and ISG15. Type I interferon (IFN) binds its receptor causing the dimerization of the two subunits IFNAR1 and IFNAR2 and thus the activation of the JAK-STAT pathway. The receptor associated kinases TYK2 and JAK1 induce recruitment and phosphorylation of STAT1 and STAT2. The phosphorylated proteins translocate to the nucleus and together with IRF9 form a trimer called ISGF3. This trimer acts as a transcriptional activator and is capable of binding to the ISRE of IFN response genes activating their expression. ISG15 and its three conjugating enzymes E1-activating enzyme (UBE1L), E2-conjugating enzyme (hUBCH8, mUBCM8) and E3 ligases (hHERC5/mHERC6, EFP, HHARI, TRIM25), as well as the ISG15 protease USP18 are all IFN-response genes. ISG15 is linked to target proteins via its conjugation system, which is counteracted by USP18 protease activity. Moreover, free ISG15 can act as a cytokine binding to LFA-1, subsequently inducing IFN-γ secretion by natural killer cells and T lymphocytes. Furthermore, USP18 also plays an important role as a negative regulator of IFN type I signaling. USP18 can interact with IFNAR2 and STAT2, competing with JAK1 for receptor binding and thus inhibiting signal transduction. The SCF^{Skp2} complex binds USP18 by mediating its poly-ubiquitination and proteasomal degradation, which is inhibited by ISG15 in human cells only. IFNAR, Interferon alpha/beta receptor; Tyk2, Tyrosine kinase 2; JAK1, Janus Kinase 1; STAT1/2, Signal transducer and activator of transcription 1/2; IRF9, Interferon regulatory factor 9; ISGF3, Interferon-stimulated gene factor 3; ISRE, Interferon-sensitive response element; ISG15, IFN-response gene 15; UBE1L, Ubiquitin-activating enzyme E1 homolog; h, human; hUBCH8, Ubiquitin/ISG15-conjugating enzyme E2 L6 in human; m, mouse; mUBCM8, Ubiquitin/ISG15-conjugating enzyme E2 L6 in mouse; mHERC6, E3 ISG15-protein ligase HERC6 in mouse; hHERC5, E3 ISG15-protein ligase HERC5 in mouse; EFP, Estrogen-responsive finger protein; HHARI, Human homolog of Drosophila ariadne-1; TRIM25, Tripartite motif-containing protein 25; USP18, Ubiquitin-specific protease 18; LFA-1, Lymphocyte function-associated antigen 1; ub, ubiquitin; SCF, Skp, cullin, F-box protein; Skp2, S-phase kinase-associated protein 2.

the endogenous proteases from the USP family recognize and deconjugate ubiquitin. However, a small group of proteins from the USP family have been reported to show cross-reactivity and deconjugate ISG15 and ubiquitin, as is the case for USP2, USP5, USP13, USP14, and USP21 (Catic et al., 2007; Ye et al., 2011; Basters et al., 2017).

In addition, many viruses and bacteria have evolved ways to revoke ISGylation as an immune evasion mechanism. Examples of these viral ISG15 proteases were found in the Middle East respiratory syndrome coronavirus (MERS-CoV) (Mielech et al., 2014); Crimean-Congo hemorrhagic fever virus (CCHFV) (Frias-Staheli et al., 2007) or severe acute respiratory syndrome coronavirus (SARS-CoV) (Bekes et al., 2016). They all encode papain-like proteases (PLPs) that impair the host innate immune response.

In contrast to cross-reactive isopeptidases, USP18 is an endogenous ISG15-specific protease that shows no reactivity toward ubiquitin (Malakhov et al., 2002; Basters et al., 2014; Ronau et al., 2016) and it represents the major ISG15 isopeptidase *in vivo* (Ketscher et al., 2012). In order to define the structural function relationship for this specificity, Basters et al., identified the molecular determinants by solving the crystal structures

of mouse USP18 alone and in complex with mouse ISG15. USP18 specificity toward ISG15 is mediated by a small interaction interface of two defined areas within the USP18 sequence, termed ISG15-binding box1 and box2 (IBB-1 and IBB-2, respectively). IBB-1 interacts through hydrophobic contact with ISG15. In ISG15, the side chain of His149 stablizes π-π stacking contact to the aromatic AA Trp121. The IBB1 region, which comprises the USP18 residues Ala138, Leu142, and His251, forms a hydrophobic pocket that specifically accommodates the bulky aromatic side chains of ISG15. Furthermore, the side chains of Pro128 (ISG15) and Leu142 (USP18) contribute to further stability. Of note, replacement of the USP18 residues corresponding to the IBB-1 region, by the homologous residues of the ubiquitin specific protease USP7, resulted in lower affinity toward ISG15. Within the IBB-2 region, the USP18 residues Thr262 and Gln259 interact with the ISG15 residues Gln114, His116, and Gln119 through hydrogen bonds. Likewise, replacement of the USP18 residues corresponding to the IBB-2 region, by the homologous residues of the ubiquitin specific protease USP7, resulted in lower affinity toward ISG15. Moreover, only the ISG15 C-terminal domain (AA residues 77-155) is necessary and sufficient for USP18 binding and activation. Structural data demonstrated that only the ISG15 C-terminal but not the N-terminal UBL domain binds USP18. *In vitro* assays revealed that USP18 cleaved the ISG15 C-terminal domain as effectively as it cleaved full-length ISG15 (Basters et al., 2017).

Independent of its deconjugating activity, USP18 binds to the IFN-α/β receptor 2 (IFNAR2) complex, where it competes with Janus kinase 1 (JAK1), and thereby negatively regulates type I IFN signaling (Malakhova et al., 2006). Remarkably, USP18 requires Signal transducer and activator of transcription 2 (STAT2) for exerting its inhibitory effect on IFN signaling and IFN-stimulated gene expression (Arimoto et al., 2017) (**Figure 1**). In humans, binding of free ISG15 prevents proteasomal degradation of USP18 by the S-phase kinase-associated protein 2 (SKP2) and thus is critical to ensure negative regulation of IFN-α/β immunity by stabilizing USP18 (Tokarz et al., 2004; Zhang et al., 2015). However, murine ISG15 appears not to influence the stability of mouse USP18 or IFNAR signaling underlining species specific peculiarities (Knobeloch et al., 2005; Osiak et al., 2005; Zhang et al., 2015).

ISG15 as a Secreted Protein

ISG15 in its unconjugated form has been reported to be released from cells exerting cytokine like activity. Although ISG15 does not have a leader signal sequence to direct its secretion, it has been shown that certain cell types are capable of releasing ISG15 to the extracellular space. Such cell types are epithelial-derived cell lines, fibroblasts, monocytes, neutrophils and lymphocytes (Knight and Cordova, 1991; Bogunovic et al., 2012; Sun et al., 2016). Extracellular ISG15 has been detected in the media of cells as well as in the serum of patients treated with IFN-α/β (D'Cunha et al., 1996). Early work suggested that secreted ISG15 elicits IFN-γ secretion from lymphocytes (Recht et al., 1991). Bacillus Calmette–Guérin (BCG) can also induce IFN-γ secretion from control peripheral blood mononuclear cells (PBMCs) when stimulated with recombinant human ISG15 (Bogunovic et al., 2012). In normal control patients, extracellular interleukin (IL)-12 played a synergistic role with ISG15 stimulating the release of IFN-γ and IL-10. Both, natural killer (NK) cells and T lymphocytes secreted IFN-γ in response to IL-12 and ISG15 (Bogunovic et al., 2012). However, IFN-γ secretion was not detected in PBMCs from ISG15-deficient patients and that defect leads to susceptibility to mycobacterial disease and autoinflammation (Bogunovic et al., 2012).

Recently, the adhesion molecule leukocyte function associated antigen-1 (LFA-1) has been identified as the receptor for extracellular ISG15 (Swaim et al., 2017) (**Figure 1**). To identify this receptor, ISG15 ubiquitin-activated interaction trap (UBAIT) was employed (O'Connor et al., 2015).

PRINCIPAL STRATEGIES TO REGULATE THE ISG15 CONJUGATION SYSTEM

Many researchers have focused their efforts on the study and characterization of the ubiquitin system (Hershko and Ciechanover, 1998). The ubiquitin-proteasome system (UPS) represents the main mechanism of protein degradation and the regulation of every step within this mechanism is crucial to prevent several disorders and diseases such as tumor development and progression. A recent example of an existing drug that targets the ubiquitin system is the adenosine sulfamate inhibitor, TAK-243, which inhibits the ubiquitin activation enzyme (E1) (UAE/UBA1) (Hyer et al., 2018). TAK-243 has entered phase I trial studies for the treatment of patients with relapsed or refractory acute myeloid leukemia, refractory myelodysplastic syndrome or chronic myelomonocytic leukemia (NCT03816319).

Two other compounds have been described to target UAE/UBA1: PYR-41, a cell permeable inhibitor that blocks the catalytic cysteine (Yang et al., 2007) and panepophenanthrin, a fungal product which inhibits ubiquitin thioester formation (Sekizawa et al., 2002). The pyrazolidine compound 4-[4-(5-nitro-furan-2-ylmethylene)-3,5-dioxo-pyrazolidin-1-yl]-benzoic acid ethyl ester was shown to inhibit UBA1. Likewise, the analog drug PYZD-4409, that carries a pyrazolidine pharmacophore, also inhibited UBA1 activation and therefore subsequent transfer of ubiquitin from the E1 to the E2 enzyme. This effect resulted in tumor growth delay in a mouse model of leukemia (Xu et al., 2010b). Besides ubiquitin, a NEDD8 activating enzyme (NAE) inhibitor has been characterized. MLN492 is a nucleotide analog that binds to UBA3/NAE1 (NEDD8 E1 enzyme) and inhibits NAE function in cells and suppresses the growth of human tumor xenografts. This chemical has entered phase II studies with promising results as an anti-cancer drug in acute myelogenous leukemia (AML) or high-grade myelodysplastic syndrome (MDS) (Soucy et al., 2009).

The drug CC0651 works as an allosteric inhibitor of the human ubiquitin-conjugating enzyme E2 R1 (CDC34) (Ceccarelli et al., 2011). Binding of CC0651 to CDC34 causes secondary structural rearrangements preventing the ubiquitin transfer to substrates. In this case, ubiquitin thioester formation

is not compromised and neither is the interaction with E1 and E3 enzymes. Hence, it shows the importance of the E2 enzymatic step as a regulation point in the process of ubiquitination. In addition, NSC697923 has been developed to target ubiquitin-conjugating enzyme variant (UBC13-UEV1A), an E2-conjugating enzyme, blocking ubiquitin transfer to the substrate (Pulvino et al., 2012). Furthermore, BAY 11-7082 interacts with the ubiquitin-conjugating enzyme E2 N (UBE2N) and modifies the reactive cysteine residue of the E2 enzyme (Strickson et al., 2013).

Analogous to ubiquitin or other UBL modification systems, the cascade of conjugation enzymes comprise targets to affect ISGylation. Likewise, USP18 inhibition (see below) represents a strategy to stabilize ISGylation. Furthermore, the ISG15 cell surface receptor represents a target to modulate ISG15 function. As indicated before, ISG15 also exists as an unconjugated protein and it has been proposed to function as a cytokine (Swaim et al., 2017). The ISG15 cell surface receptor LFA-1 is a heterodimeric complex that comprises two subunits, CD11a/αL and CD18/β2. The CD11a/αL domain forms part of the binding site for both Intercellular Adhesion Molecule 1 (ICAM1) (Shimaoka et al., 2003) and ISG15. However, determinants of the αL domain recognized by ISG15 and ICAM1 are different and biochemically and biologically separable (Swaim et al., 2017). Extracellular ISG15 plays an important role in the secretion of cytokines such as IL-10 or IFNγ. Therefore, ISG15 can be potentially exploited to boost cytokine secretion (Swaim et al., 2017). In contrast, targeting LFA-1 receptor or specifically one of the two heterodimers that form the receptor would conceptually lessen the impact of extracellular ISG15 activity by blocking its receptor.

USP18 ACTIVITY ASSAYS

Activity-based probes (ABPs) are a helpful tool to study the activity of DUBs and Ubl-specific proteases. One of the main advantages of using ABPs over other substrate-based probes is that ABPs covalently attach to the active site of the target protein (Ovaa, 2007; Verdoes and Verhelst, 2016). Many proteases are secreted in their inactive forms and require post-translational modifications to become active. These modifications can be either irreversible, via proteolysis, or reversible by pH change or protein complex formation (Hewings et al., 2017). The characterization of DUBs in biological processes benefits from ABPs as protein activity is rather important and classical methods such as western blotting or proteomics techniques are not suitable to deduce enzyme activity. Furthermore, fluorogenic substrates are a valuable tool for kinetic studies as they are turned over by the target enzyme and as a consequence the resulting fluorescent signal will be proportional to enzyme activity.

As mentioned before, USP18 specifically deconjugates ISG15 from substrates (Malakhov et al., 2002). Specific ABPs for USP18 proteases have been developed (Ekkebus et al., 2013; Basters et al., 2017). In analogy to ABPs for ubiquitin, these probes have been synthesized by replacing the C-terminal residue of ISG15 with an electrophilic moiety, such as—VS (Vinyl methyl sulfone), VME (Vinyl methyl ester), or PRG (Propargylamide) (Ekkebus et al., 2013; Basters et al., 2017). These probes work as a C-terminal electrophilic trap and they were synthesized with intein chemistry (Hemelaar et al., 2004) (**Figure 2**). The use of these ISG15 probes represents a valuable tool to evaluate the enzymatic activity of DUBs.

ISG15-VME covalently binds the active-site cysteine via thioether bond forming a covalent complex. The sulfur atom of the active-site cysteine of the DUB interacts with the carbon (β) atom of the VME moiety forming a thiol bond (Boudreaux et al., 2010). ISG15-VME and ISG15-VS form covalent adducts via a Michael-type (1,4) addition. Vinyl sulfone reactions can be performed under physiological conditions (e.g., aqueous media, slightly alkaline pH) which preserves the biological function of the proteins (Morales-Sanfrutos et al., 2010).

ISG15-VS results in the formation of a covalent complex between USP18 and ISG15. The reaction results in a covalent adduct that can be detected by SDS/PAGE as an upwards shift in molecular mass. A similar experiment was conducted making use of the equivalent propargylamide probe, ISG15-PRG, with USP18-ISG15 complex formation. ISG15-PRG forms a vinyl thioether with the DUB active site cysteine residue. The reaction depends on a direct nucleophilic attack on the internal alkyne carbon as a result of the developing carbanion stabilization by the "oxyanion hole" of the active site (Ekkebus et al., 2013; Hewings et al., 2017). Conversely, Ub-VS or Ub-PRG did not react with USP18 demonstrating that USP18 does not exert enzymatic activity toward ubiquitin (Basters et al., 2014, 2017).

The crystal structure of mouse USP18 in complex with mouse ISG15 displayed extensive interaction between the ISG15 C-terminal Ubl domain and the palm and thumb domain of USP18 (Basters et al., 2017). A good example for the use of an ISG15-PRG probe was the validation of the ISG15 C-terminal domain as necessary and sufficient for USP18 binding. Here, either only the C-terminal Ubl domain of ISG15 (ct-ISG15) or full-length ISG15 were fused to -PRG to form the respective ct-ISG15-PRG and ISG15-PRG probes. Both probes reacted with the active site cysteine of USP18 and formed a covalent complex. Furthermore, USP18 cleaved ct-ISG15 as effectively as it cleaved full-length ISG15 from cellular substrates (Basters et al., 2017).

Synthesis of the ISG15 C-terminal Ubl domain was carried out through solid-phase peptide chemistry (SPPS). Briefly, SPPS is an automated synthesis method used for the production of synthetic peptides. This technology allows assembly of a peptide chain through successive reactions of amino acids or derivatives. The activated carboxyl moiety of each incoming amino acid is linked to the α-amino group of the subsequent amino acid. The new α-amino group gets protected by 9-fluorenylmethoxycarbonyl (Fmoc) to avoid unintended peptide bond formation at this site until the incoming amino acid is added to the sequence. In addition, reactive side chains on the amino acids are protected by ester, ether and urethane derivative complex formation during the synthesis of the synthetic peptide (El Oualid et al., 2010). Recently, the synthesis of the N-terminal domain together with the C-terminal domain, comprising the 155 amino acid protein mISG15, has been reported (Xin et al., 2019). Most of the ISG15 functions, especially those related to deISGylation, is attributed to its C-terminal domain. The full length synthesis of mISG15

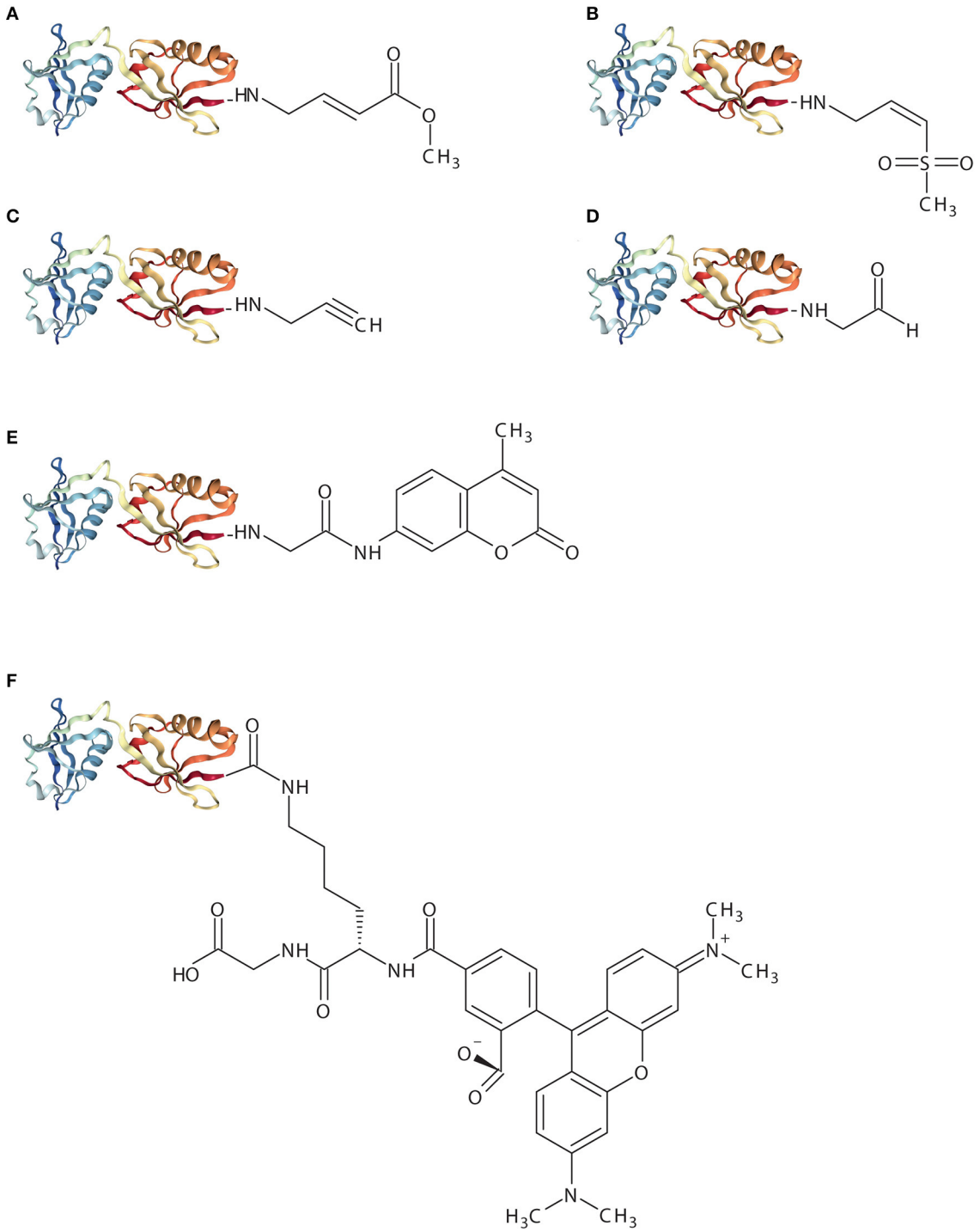

FIGURE 2 | Schematic representation of ISG15-based assay reagents. The X-ray crystal structure represents mouse ISG15 (PDB: 5TLA) and implies $ISG15_{1-155}$. **(A)**, ISG15-VME **(B)**, ISG15-VS **(C)**, ISG15-PRG **(D)**, ISG15-CHO **(E)**, ISG15-AMC **(F)**, ISG15-TAMRA-(5-thioLys)-Gly.

will elucidate specific roles associated to the N-terminal domain within ISG15.

High-throughput drug screening (HTS) studies in combination with enzymatic assays using ubiquitin-7-Amino-4-methylcoumarin (Ub-amc) have been extensively used for the identification of small molecules inhibiting USP protease activity (Hirayama et al., 2007). Hydrolysis of the fluorophore amc group upon cleavage of the isopeptidase bond by a specific protein results in a quantifiable fluorescence signal. ISG15-amc was used to demonstrate USP18 activity and specificity toward

ISG15 (Basters et al., 2012) (**Figure 2**). Therefore, the ISG15-amc probe can also be used to monitor activity of other deISGylases (e.g., viral ISG15 DUBs).

ISG15-Rhodamine represents a fluorescence polarization (FP) assay reagent where ISG15 is quenched to the green fluorescence rhodamine 110 cationic dye by its C-terminus. The substrate was synthesized from $ISG15^{C76S}$ and 5-carboxytetramethylrhodamine (TAMRA)-labeled 5-thioLys-Gly dipeptide. The linkage between the C-terminal Gly of ISG15 and a Lys side chain resembles natural ISG15-linked substrates more precisely (Tirat et al., 2005; Geurink et al., 2012; Swatek et al., 2018). Likewise, hydrolysis of the TAMRA-Lys-Gly complex by a specific protein results in a quantifiable fluorescence signal. Hence, incubation of ISG15-TAMRA with USP18 led to a dose-dependent decrease of polarization values (in millipolarization), indicative of proteolytic cleavage of the substrate (Basters et al., 2014) (**Figure 2**).

The reversible ISG15 aldehyde inhibitor, ISG15-CHO, does not yield a stable adducted enzyme but it still represents a highly specific inhibitor of ISG15-specific isopeptidases (Siklos et al., 2015) (**Figure 2**). This probe blocks the hydrolysis of poly-ISG15 chains on substrate proteins *in vitro*. However, aldehyde inhibitors suffer metabolic oxidation/reduction modifications and pH-dependent hydrate formation that results in deficient stability and bioavailability. Such drawbacks limit the progress of aldehyde inhibitors to the clinic.

ISG15- AND USP18-RELATED DISEASES

Due to the critical role of the ISG15 system in antimicrobial host defense it is appealing to exploit this endogenous effector system therapeutically. Within this context, human patients lacking functional ISG15 represent valuable subjects of investigation to define physiological and molecular functions. Six patient cases with ISG15 deficiency from three non-related families have been reported (Bogunovic et al., 2012; Zhang et al., 2015).

In mice, ISG15 plays an important role in host response to viral infection. It has been shown to protect from viral-induced lethality using different pathogens (Perng and Lenschow, 2018). However, ISG15-null patients appear not to be more susceptible to viral infections (Bogunovic et al., 2012). Conversely, ISG15 deficient patients even showed enhanced antiviral protection (Speer et al., 2016). Three of the ISG15 deficient patients suffered from seizures and displayed intracranial calcification, which is a common phenotype for patients with Aicardi-Goutières syndrome (AGS) (Zhang et al., 2015). In humans, binding of free ISG15 prevents proteasomal degradation of USP18 by SKP2 (Tokarz et al., 2004) and is critical to ensure negative regulation of IFN-α/β immunity by stabilizing USP18 (Zhang et al., 2015). The three ISG15 deficient individuals showed hyper-responsiveness to type-I IFN stimulation due to the fact that human USP18 stability relies heavily on human ISG15. Thus, in the absence of ISG15 USP18 would no longer be able to function as a negative regulator of type-I IFN signaling (Zhang et al., 2015). The regulatory function of ISG15 to stabilize USP18 is not seen in mice (Speer et al., 2016). Recently, USP18 deficient patients were identified (Meuwissen et al., 2016). These patients' life expectancy is quite short and they die shortly after birth due to massive dysregulation of type-I IFN signaling. Five Pseudo-TORCH syndrome (PTS) patients showed recessive loss-of-function mutations of USP18 leading to severe immune inflammation with calcification and polymicrogyria. USP18 deficient patients represent the first case of a genetic disorder of PTS caused by dysregulation of the response to type I IFNs. This situation makes USP18 an interesting therapeutic target, as USP18 agonists might be a strategy to dampen type-I IFNs overabundance. Alternatively, USP18 antagonists or strategies promoting USP18 degradation could promote the beneficial effect of therapeutic IFNs used in multiple sclerosis, hairy cell leukemia, and melanoma (Meuwissen et al., 2016).

Studies in mice lacking USP18 uncovered a key role of USP18 to maintain microglial quiescence under homeostatic conditions (Goldmann et al., 2015; Schwabenland et al., 2019). USP18 negatively regulates the activation of STAT1 upon interaction with IFNAR2 (Malakhova et al., 2006). Interestingly, this regulatory function is independent from USP18 catalytic activity as it was also observed in knock-in mice ($USP18^{C61A/C61A}$), expressing enzymatically inactive USP18. $USP18^{C61A/C61A}$ mice showed increased resistance against virus infections, but in contrast to $USP18^{-/-}$ mice, $USP18^{C61A/C61A}$ knock-in mice did not display fatal IFN hypersensitivity, brain injury or increased lethality (Ketscher et al., 2015). Based on the analysis of $USP18^{C61A/C61A}$ mice, selective inhibition of USP18 proteolytic activity might be used as an antiviral strategy.

IDENTIFICATION OF ISG15 SUBSTRATES

To gain further insight into ISG15 targets, it would be interesting to define ISG15 modified proteins on a proteome wide base (ISGylome) to identify specific ISG15 modifications sites, and to uncover common principles of ISG15 modification. Several proteomics studies have identified hundreds of cellular but also viral substrates (Giannakopoulos et al., 2005; Zhao et al., 2005). In these studies, ISG15-modified proteins were purified from IFN-β-treated cells by using both affinity selection and mass spectroscopy (MS-MS) to identify ISG15 target proteins. Later, a new study compared the proteomes of $ISG15^{+/+}$ and $ISG15^{-/-}$ bone marrow derived macrophages (BMDMs) upon vaccinia virus (VACV) infection (Baldanta et al., 2017). Here, they evaluated the presence of ISGylated proteins in total extracts from $ISG15^{+/+}$ and $ISG15^{-/-}$ BMDMs that were left untreated or treated with IFN or VACV. The results indicated mitochondrial dysfunction and oxidative phosphorylation (OXPHOS) in $ISG15^{-/-}$ mice (Baldanta et al., 2017). Further analysis of the ISG15 target proteins will shed light on the different functions of ISG15 in the innate immune system.

Recently, Swatek et al. (2018) have elucidated a mechanism to identify virus-induced modified proteins upon foot-and-mouth disease (FMD). The viral leader protease, Lb^{pro}, mainly targeted ISG15 showing high activity and specificity for ISG15 over other Ubl proteins. Lb^{pro} cleaves the peptide bond preceding

the ISG15 C-terminal GlyGly motif; consequently cleaved ISG15 can no longer be reconjugated, leading to shut down of the ISG15 modification system. Unlike Lb^{pro}, USP18-mediated ISG15 cleavage leads to ISG15 recycling since USP18 cleaves the isopeptide linkage after the C-terminal GlyGly motif and ISG15 remains competent for reconjugation. Lb^{pro} activity has been quantified using fluorescence polarization assay reagents (Swatek et al., 2018). Importantly, Lb^{pro} represents a new tool to uncover virus-induced GlyGly remnants on substrate proteins using an anti-GlyGly antibody already used for ubiquitin MS-MS research.

Peptide enrichment by immunoprecipitation (IP) technology is developed to quantitatively profile modification sites in cellular proteins. Ubiquitin as well as other Ubls can be covalently linked to lysine residues of target proteins. The bead-conjugated Lys-ε-GG antibody specifically recognizes the GlyGly remnant left after trypsin digestion of modified proteins (Udeshi et al., 2013). Enrichment upon Lys-ε-GG antibody IP coupled with liquid chromatography (LC) tandem MS-MS analysis leads to the identification of a substantial number of proteins modified with ubiquitin or Ubls. Ubiquitin and some Ubls share a common diglycine adduct upon digestion with trypsin. The identification of ISG15-modified sequences would represent a valuable tool to characterize new molecular pathways in situations of homeostasis or disease-related conditions. Recently, the endogenous *in vivo* ISGylome in mouse liver, following *Listeria* infection has been mapped. In this study, authors employed Lys-ε-GG antibody IP in wildtype and $ISG15^{-/-}$ mice followed by LC tandem MS-MS analysis. Comparison of the datasets allowed to identify and distinguish ISGylated sites from ubiquitin sites *in vivo* (Zhang et al., 2019). Similar approaches have already been used in several cell systems to identify different post-translational modifications such as, phosphorylation (Rush et al., 2005), ubiquitination (Xu et al., 2010a; Kim et al., 2011), acetylation (Weinert et al., 2011; Kori et al., 2017), methylation and SUMOylation (Impens et al., 2014; Lamoliatte et al., 2017).

NOVEL TECHNOLOGIES TO TARGET USP18

Proteolysis Targeting Chimeras (PROTACs) or degronimids are reagents that recruit a protein of interest to a specific ubiquitin E3 ligase. The E3 ligase induces its ubiquitination followed by subsequent degradation by the proteasome. These probes are bifunctional small molecules that combine a target-binding warhead and E3 ubiquitin ligase-recruiting moiety by a chemical linker (Sakamoto et al., 2001; Stanton et al., 2018). This drug discovery strategy differs from classical methods that focus on targeting the protein of interest by specific inhibitors or its receptor ligands. Interestingly, ARV-110 represents the first oral PROTACs drug that has been approved by the FDA for the treatment of patients with metastatic castration-resistant prostate cancer (NCT03888612). PROTACS targeting USP18 might represent an interesting approach to specifically degrade USP18 and thus enhance type I IFN signaling.

Beside direct destabilization, targeting the interaction of USP18 with important proteins such as STAT2 or ISG15 might constitute an option to interfere with its function.

A sophisticated technique to directly study protein–protein interaction within a cellular context is the BRET (Bioluminescence Resonance Energy Transfer) assay where dipole-dipole energy is transferred from a luciferase to a fluorophore. For the successful energy transfer, the excitation spectrum of the acceptor fluorophore has to overlap with the bioluminescence spectrum generated by the luciferase (Ciruela, 2008). Similar to fluorescence resonance energy transfer (FRET), this transfer is dependent on close proximity (<10 nm) between the donor/acceptor pair (Wu and Brand, 1994; Pfleger and Eidne, 2006). Thus, genetic fusion of this system to proteins of interest can be used to measure their protein interaction. This is achieved by creating fusion constructs of the donor luciferase with one protein of interest and the acceptor with a second protein of interest.

In the case of NanoBRET™, NanoLuc® represents a genetically modified luciferase, originating from the deep sea shrimp *Oplophorus gracilirostris* that acts as donor. Genetic engineering and the use of a novel coelenterazine derivate (Furimazine) resulted in a brighter luminescence, with a narrower spectrum and higher protein stability compared to the traditional RLuc (Hall et al., 2012). For the acceptor fusion, a red-emitting fluorophore is linked to the HaloTag® protein (Machleidt et al., 2015). HaloTag® is a modified bacterial haloalkane dehydrogenase which can covalently bind fluorescent dyes or other molecules of interest through a chloroalkane linker allowing for tailoring the Tag for each individual experimental setup (Los et al., 2008; Machleidt et al., 2015).

DISCUSSION AND FUTURE PERSPECTIVES

Multiple strategies have been proposed to modulate ISG15 function in the immune system. The endogenous ISG15-specific protease, USP18, shows no reactivity toward ubiquitin (Malakhov et al., 2002; Basters et al., 2014; Ronau et al., 2016) and represents the major ISG15 isopeptidase *in vivo*.

How the negative regulation of type I IFN by USP18 is precisely mediated is only starting to become clearer in recent years, and additional proteins and factors involved await discovery. Moreover, it is unknown whether the enzymatic and the non-enzymatic functions of USP18 are really exerted in an independent manner or can influence each other. Protein–protein interaction assays such as NanoBRET™ represent a technique to monitor protein–protein interactions involving USP18, STAT2, IFNAR, and ISG15 more closely. As a cell-based assay, it appears to be well-suited to analyze the interaction of two proteins of interest under physiological conditions nicely complementing biochemical assays.

Traditional strategies to inhibit enzyme activity have focused on the development and synthesis of small molecules that bind to the active side of a protein of interest in order to decrease its activity. However, besides the classical biochemical protease

assay where recombinant USP18 is used in combination with ISG15-TAMRA (Basters et al., 2014), a screening system suitable to monitor direct USP18-ISG15 binding could be helpful.

In the classical approach targeting a protease, a small molecule needs to show activity toward the enzymatic activity either by blocking the binding pocket or allosteric mechanisms. This highly specific requirement often makes it difficult to identify suitable compounds even in HTS approaches. However, libraries of covalent inhibitors could be beneficial for chemical screens to identify new compounds.

PROTACs represent a very elegant strategy to target difficult druggable proteins by selectively targeting their degradation through the proteasome (Sakamoto et al., 2001; Stanton et al., 2018). Target proteins with low affinities for PROTACs can still be targeted and further degraded as long as the formation of the PROTACs complex generates sufficient protein–protein interactions between the target protein and the E3 ligase (Bondeson et al., 2018). It is therefore important to consider other parameters such as an adequate linker or a specific E3 ligase on top of traditional inhibitor specificity. As described above, the ISG15-TAMRA/recombinant USP18 assay represents a HTS compatible system to identify inhibitors of USP18 enzymatic activity. Compounds identified in such a screen are expected to bind USP18 with high affinity or even covalently and thus should also constitute interesting building blocks for PROTACs aiming to degrade the entire USP18 protein. Rather than only stabilizing ISGylation PROTACS directed against USP18 would be expected to also boost the type I IFN response as USP18 can no longer exert its negative regulatory function at the IFNAR. Thus, targeted degradation of USP18 might at least conceptually be a strategy to enhance the therapeutic use of type I IFNs in antiviral, antineoblastic and autoimmune applications. Currently, there are several mouse models to study the function of ISG15: ISG15$^{-/-}$ (Osiak et al., 2005), UbE1L$^{-/-}$ (Kim et al., 2006), USP18$^{-/-}$ (Ritchie et al., 2002) and USP18$^{C61A/C61A}$ mice (Ketscher et al., 2015). ISG15$^{-/-}$ mice lack both free ISG15 and ISG15 conjugates. UbE1L$^{-/-}$ mice show higher basal and inducible levels of free ISG15; however, these mice lack ISG15 conjugates. USP18$^{-/-}$ mice present higher basal and inducible levels of ISG15 modified proteins. The USP18$^{C61A/C61A}$ mouse expresses a catalytic inactive form of USP18 and thus mimics the scenario of USP18 protease activity repression via a small molecule inhibitor. This mouse model shows enhanced ISGylation levels because of the USP18 protease inactivation whereas they do not show apparent phenotypic alterations (Ketscher et al., 2015). Furthermore, no abnormalities were identified in USP18$^{C61A/C61A}$ mice backcrossed to C57BL/6, a genetic background, in which USP18$^{-/-}$ mice display malformations that leads to embryonic lethality around embryonic day 15.5 (E15.5) (Ketscher et al., 2015). The use of a humanized ISG15 mouse model where murine ISG15 is replaced by its human counterpart would represent an interesting *in vivo* model to study species-specific differences in ISG15 with respect to substrate recognition and antipathogenic activity. It is known that E1, E2, and E3 enzymes can be exchanged between mouse and human and that mUSP18 can efficiently deconjugate ISGylated substrates derived from IFN treated human cells (Ketscher et al., 2012). Therefore, this mouse model would shed light on how murine and human ISG15 can target proteins upon infection with different pathogens.

In conclusion, the use of all these different mouse models in combination with enrichment of modified peptides by IP and further MS-MS technology, developed to quantitatively profile modification sites in cellular proteins, represent valuable tools to unravel the ISGylome in situations of homeostasis or disease-related conditions.

AUTHOR CONTRIBUTIONS

DJ and K-PK discussed and developed the concept of the review. DJ, SH, and K-PK edited the manuscript. DJ and K-PK wrote the manuscript.

FUNDING

This work was supported by a grant from the Deutsche Forschungsgemeinschaft KN 590/7-1 and BMBF (BacVirISG15).

REFERENCES

Arimoto, K. I., Lochte, S., Stoner, S. A., Burkart, C., Zhang, Y., Miyauchi, S., et al. (2017). STAT2 is an essential adaptor in USP18-mediated suppression of type I interferon signaling. *Nat. Struct. Mol. Biol.* 24, 279–289. doi: 10.1038/nsmb.3378

Baldanta, S., Fernandez-Escobar, M., Acin-Perez, R., Albert, M., Camafeita, E., Jorge, I., et al. (2017). ISG15 governs mitochondrial function in macrophages following vaccinia virus infection. *PLoS Pathog.* 13:e1006651. doi: 10.1371/journal.ppat.1006651

Basters, A., Geurink, P. P., El Oualid, F., Ketscher, L., Casutt, M. S., Krause, E., et al. (2014). Molecular characterization of ubiquitin-specific protease 18 reveals substrate specificity for interferon-stimulated gene 15. *FEBS J.* 281, 1918–1928. doi: 10.1111/febs.12754

Basters, A., Geurink, P. P., Rocker, A., Witting, K. F., Tadayon, R., Hess, S., et al. (2017). Structural basis of the specificity of USP18 toward ISG15. *Nat. Struct. Mol. Biol.* 24, 270–278. doi: 10.1038/nsmb.3371

Basters, A., Ketscher, L., Deuerling, E., Arkona, C., Rademann, J., Knobeloch, K. P., et al. (2012). High yield expression of catalytically active USP18 (UBP43) using a trigger factor fusion system. *BMC Biotechnol.* 12:56. doi: 10.1186/1472-6750-12-56

Bekes, M., van der Heden van Noort, G. J., Ekkebus, R., Ovaa, H., Huang, T. T., and Lima, C. D. (2016). Recognition of Lys48-linked di-ubiquitin and deubiquitinating activities of the SARS coronavirus papain-like protease. *Mol. Cell* 62, 572–585. doi: 10.1016/j.molcel.2016.04.016

Blomstrom, D. C., Fahey, D., Kutny, R., Korant, B. D., and Knight, E. Jr. (1986). Molecular characterization of the interferon-induced 15-kDa protein. molecular cloning and nucleotide and amino acid sequence. *J. Biol. Chem.* 261, 8811–8816.

Bogunovic, D., Byun, M., Durfee, L. A., Abhyankar, A., Sanal, O., Mansouri, D., et al. (2012). Mycobacterial disease and impaired IFN-γ immunity in humans with inherited ISG15 deficiency. *Science* 337, 1684–1688. doi: 10.1126/science.1224026

Bondeson, D. P., Smith, B. E., Burslem, G. M., Buhimschi, A. D., Hines, J., Jaime-Figueroa, S., et al. (2018). Lessons in PROTAC design from selective

degradation with a promiscuous warhead. *Cell Chem. Biol.* 25, 78–87.e75. doi: 10.1016/j.chembiol.2017.09.010

Boudreaux, D. A., Maiti, T. K., Davies, C. W., and Das, C. (2010). Ubiquitin vinyl methyl ester binding orients the misaligned active site of the ubiquitin hydrolase UCHL1 into productive conformation. *Proc. Natl. Acad. Sci. U.S.A.* 107, 9117–9122. doi: 10.1073/pnas.0910870107

Catic, A., Fiebiger, E., Korbel, G. A., Blom, D., Galardy, P. J., and Ploegh, H. L. (2007). Screen for ISG15-crossreactive deubiquitinases. *PLoS ONE* 2:e679. doi: 10.1371/journal.pone.0000679

Ceccarelli, D. F., Tang, X., Pelletier, B., Orlicky, S., Xie, W., Plantevin, V., et al. (2011). An allosteric inhibitor of the human Cdc34 ubiquitin-conjugating enzyme. *Cell* 145, 1075–1087. doi: 10.1016/j.cell.2011.05.039

Ciruela, F. (2008). Fluorescence-based methods in the study of protein-protein interactions in living cells. *Curr. Opin. Biotechnol.* 19, 338–343. doi: 10.1016/j.copbio.2008.06.003

D'Cunha, J., Ramanujam, S., Wagner, R. J., Witt, P. L., Knight, E. Jr., and Borden, E. C. (1996). *In vitro* and *in vivo* secretion of human ISG15, an IFN-induced immunomodulatory cytokine. *J. Immunol.* 157, 4100–4108.

Durfee, L. A., Kelley, M. L., and Huibregtse, J. M. (2008). The basis for selective E1-E2 interactions in the ISG15 conjugation system. *J. Biol. Chem.* 283, 23895–23902. doi: 10.1074/jbc.M804069200

Durfee, L. A., Lyon, N., Seo, K., and Huibregtse, J. M. (2010). The ISG15 conjugation system broadly targets newly synthesized proteins: implications for the antiviral function of ISG15. *Mol. Cell* 38, 722–732. doi: 10.1016/j.molcel.2010.05.002

Ekkebus, R., van Kasteren, S. I., Kulathu, Y., Scholten, A., Berlin, I., Geurink, P. P., et al. (2013). On terminal alkynes that can react with active-site cysteine nucleophiles in proteases. *J. Am. Chem. Soc.* 135, 2867–2870. doi: 10.1021/ja309802n

El Oualid, F., Merkx, R., Ekkebus, R., Hameed, D. S., Smit, J. J., de Jong, A., et al. (2010). Chemical synthesis of ubiquitin, ubiquitin-based probes, and diubiquitin. *Angew. Chem. Int. Ed Engl.* 49, 10149–10153. doi: 10.1002/anie.201005995

Frias-Staheli, N., Giannakopoulos, N. V., Kikkert, M., Taylor, S. L., Bridgen, A., Paragas, J., et al. (2007). Ovarian tumor domain-containing viral proteases evade ubiquitin- and ISG15-dependent innate immune responses. *Cell Host Microbe.* 2, 404–416. doi: 10.1016/j.chom.2007.09.014

Geurink, P. P., El Oualid, F., Jonker, A., Hameed, D. S., and Ovaa, H. (2012). A general chemical ligation approach towards isopeptide-linked ubiquitin and ubiquitin-like assay reagents. *Chembiochem* 13, 293–297. doi: 10.1002/cbic.201100706

Giannakopoulos, N. V., Luo, J. K., Papov, V., Zou, W., Lenschow, D. J., Jacobs, B. S., et al. (2005). Proteomic identification of proteins conjugated to ISG15 in mouse and human cells. *Biochem. Biophys. Res. Commun.* 336, 496–506. doi: 10.1016/j.bbrc.2005.08.132

Goldmann, T., Zeller, N., Raasch, J., Kierdorf, K., Frenzel, K., Ketscher, L., et al. (2015). USP18 lack in microglia causes destructive interferonopathy of the mouse brain. *EMBO J.* 34, 1612–1629. doi: 10.15252/embj.201490791

Haas, A. L., Ahrens, P., Bright, P. M., and Ankel, H. (1987). Interferon induces a 15-kilodalton protein exhibiting marked homology to ubiquitin. *J. Biol. Chem.* 262, 11315–11323.

Hall, M. P., Unch, J., Binkowski, B. F., Valley, M. P., Butler, B. L., Wood, M. G., et al. (2012). Engineered luciferase reporter from a deep sea shrimp utilizing a novel imidazopyrazinone substrate. *ACS Chem. Biol.* 7, 1848–1857. doi: 10.1021/cb3002478

Hemelaar, J., Borodovsky, A., Kessler, B. M., Reverter, D., Cook, J., Kolli, N., et al. (2004). Specific and covalent targeting of conjugating and deconjugating enzymes of ubiquitin-like proteins. *Mol. Cell. Biol.* 24, 84–95. doi: 10.1128/MCB.24.1.84-95.2004

Hershko, A., and Ciechanover, A. (1998). The ubiquitin system. *Annu. Rev. Biochem.* 67, 425–479. doi: 10.1146/annurev.biochem.67.1.425

Hewings, D. S., Flygare, J. A., Bogyo, M., and Wertz, I. E. (2017). Activity-based probes for the ubiquitin conjugation-deconjugation machinery: new chemistries, new tools, and new insights. *FEBS J.* 284, 1555–1576. doi: 10.1111/febs.14039

Hirayama, K., Aoki, S., Nishikawa, K., Matsumoto, T., and Wada, K. (2007). Identification of novel chemical inhibitors for ubiquitin C-terminal hydrolase-L3 by virtual screening. *Bioorg. Med. Chem.* 15, 6810–6818. doi: 10.1016/j.bmc.2007.07.016

Hyer, M. L., Milhollen, M. A., Ciavarri, J., Fleming, P., Traore, T., Sappal, D., et al. (2018). A small-molecule inhibitor of the ubiquitin activating enzyme for cancer treatment. *Nat. Med.* 24, 186–193. doi: 10.1038/nm.4474

Impens, F., Radoshevich, L., Cossart, P., and Ribet, D. (2014). Mapping of SUMO sites and analysis of SUMOylation changes induced by external stimuli. *Proc. Natl. Acad. Sci. U.S.A.* 111, 12432–12437. doi: 10.1073/pnas.1413825111

Ketscher, L., Basters, A., Prinz, M., and Knobeloch, K. P. (2012). mHERC6 is the essential ISG15 E3 ligase in the murine system. *Biochem. Biophys. Res. Commun.* 417, 135–140. doi: 10.1016/j.bbrc.2011.11.071

Ketscher, L., Hannss, R., Morales, D. J., Basters, A., Guerra, S., Goldmann, T., et al. (2015). Selective inactivation of USP18 isopeptidase activity *in vivo* enhances ISG15 conjugation and viral resistance. *Proc. Natl. Acad. Sci. U.S.A.* 112, 1577–1582. doi: 10.1073/pnas.1412881112

Kim, K. I., Giannakopoulos, N. V., Virgin, H. W., and Zhang, D. E. (2004). Interferon-inducible ubiquitin E2, Ubc8, is a conjugating enzyme for protein ISGylation. *Mol. Cell. Biol.* 24, 9592–9600. doi: 10.1128/MCB.24.21.9592-9600.2004

Kim, K. I., Yan, M., Malakhova, O., Luo, J. K., Shen, M. F., Zou, W., et al. (2006). Ube1L and protein ISGylation are not essential for alpha/beta interferon signaling. *Mol. Cell. Biol.* 26, 472–479. doi: 10.1128/MCB.26.2.472-479.2006

Kim, W., Bennett, E. J., Huttlin, E. L., Guo, A., Li, J., Possemato, A., et al. (2011). Systematic and quantitative assessment of the ubiquitin-modified proteome. *Mol. Cell* 44, 325–340. doi: 10.1016/j.molcel.2011.08.025

Knight, E. Jr., and Cordova, B. (1991). IFN-induced 15-kDa protein is released from human lymphocytes and monocytes. *J. Immunol.* 146, 2280–2284.

Knobeloch, K. P., Utermohlen, O., Kisser, A., Prinz, M., and Horak, I. (2005). Reexamination of the role of ubiquitin-like modifier ISG15 in the phenotype of UBP43-deficient mice. *Mol. Cell. Biol.* 25, 11030–11034. doi: 10.1128/MCB.25.24.11030-11034.2005

Kori, Y., Sidoli, S., Yuan, Z. F., Lund, P. J., Zhao, X., and Garcia, B. A. (2017). Proteome-wide acetylation dynamics in human cells. *Sci. Rep.* 7:10296. doi: 10.1038/s41598-017-09918-3

Lamoliatte, F., McManus, F. P., Maarifi, G., Chelbi-Alix, M. K., and Thibault, P. (2017). Uncovering the SUMOylation and ubiquitylation crosstalk in human cells using sequential peptide immunopurification. *Nat. Commun.* 8:14109. doi: 10.1038/ncomms14109

Loeb, K. R., and Haas, A. L. (1992). The interferon-inducible 15-kDa ubiquitin homolog conjugates to intracellular proteins. *J. Biol. Chem.* 267, 7806–7813.

Los, G. V., Encell, L. P., McDougall, M. G., Hartzell, D. D., Karassina, N., Zimprich, C., et al. (2008). HaloTag: a novel protein labeling technology for cell imaging and protein analysis. *ACS Chem. Biol.* 3, 373–382. doi: 10.1021/cb800025k

Machleidt, T., Woodroofe, C. C., Schwinn, M. K., Mendez, J., Robers, M. B., Zimmerman, K., et al. (2015). NanoBRET–a novel BRET platform for the analysis of protein-protein interactions. *ACS Chem. Biol.* 10, 1797–1804. doi: 10.1021/acschembio.5b00143

Malakhov, M. P., Malakhova, O. A., Kim, K. I., Ritchie, K. J., and Zhang, D. E. (2002). UBP43 (USP18) specifically removes ISG15 from conjugated proteins. *J. Biol. Chem.* 277, 9976–9981. doi: 10.1074/jbc.M109078200

Malakhova, O. A., Kim, K. I., Luo, J. K., Zou, W., Kumar, K. G., Fuchs, S. Y., et al. (2006). UBP43 is a novel regulator of interferon signaling independent of its ISG15 isopeptidase activity. *EMBO J.* 25, 2358–2367. doi: 10.1038/sj.emboj.7601149

Meuwissen, M. E., Schot, R., Buta, S., Oudesluijs, G., Tinschert, S., Speer, S. D., et al. (2016). Human USP18 deficiency underlies type 1 interferonopathy leading to severe pseudo-TORCH syndrome. *J. Exp. Med.* 213, 1163–1174. doi: 10.1084/jem.20151529

Mielech, A. M., Kilianski, A., Baez-Santos, Y. M., Mesecar, A. D., and Baker, S. C. (2014). MERS-CoV papain-like protease has deISGylating and deubiquitinating activities. *Virology* 450–451, 64–70. doi: 10.1016/j.virol.2013.11.040

Morales-Sanfrutos, J., Lopez-Jaramillo, J., Ortega-Munoz, M., Megia-Fernandez, A., Perez-Balderas, F., Hernandez-Mateo, F., et al. (2010). Vinyl sulfone: a

versatile function for simple bioconjugation and immobilization. *Org. Biomol. Chem.* 8, 667–675. doi: 10.1039/B920576D

Narasimhan, J., Wang, M., Fu, Z., Klein, J. M., Haas, A. L., and Kim, J. J. (2005). Crystal structure of the interferon-induced ubiquitin-like protein ISG15. *J. Biol. Chem.* 280, 27356–27365. doi: 10.1074/jbc.M502814200

O'Connor, H. F., Lyon, N., Leung, J. W., Agarwal, P., Swaim, C. D., Miller, K. M., et al. (2015). Ubiquitin-activated interaction traps (UBAITs) identify E3 ligase binding partners. *EMBO Rep.* 16, 1699–1712. doi: 10.15252/embr.201540620

Okumura, F., Zou, W., and Zhang, D. E. (2007). ISG15 modification of the eIF4E cognate 4EHP enhances cap structure-binding activity of 4EHP. *Genes Dev.* 21, 255–260. doi: 10.1101/gad.1521607

Osiak, A., Utermohlen, O., Niendorf, S., Horak, I., and Knobeloch, K. P. (2005). ISG15, an interferon-stimulated ubiquitin-like protein, is not essential for STAT1 signaling and responses against vesicular stomatitis and lymphocytic choriomeningitis virus. *Mol. Cell. Biol.* 25, 6338–6345. doi: 10.1128/MCB.25.15.6338-6345.2005

Ovaa, H. (2007). Active-site directed probes to report enzymatic action in the ubiquitin proteasome system. *Nat. Rev. Cancer* 7, 613–620. doi: 10.1038/nrc2128

Park, J. H., Yang, S. W., Park, J. M., Ka, S. H., Kim, J. H., Kong, Y. Y., et al. (2016). Positive feedback regulation of p53 transactivity by DNA damage-induced ISG15 modification. *Nat. Commun.* 7:12513. doi: 10.1038/ncomms12513

Pelzer, C., Kassner, I., Matentzoglu, K., Singh, R. K., Wollscheid, H. P., Scheffner, M., et al. (2007). UBE1L2, a novel E1 enzyme specific for ubiquitin. *J. Biol. Chem.* 282, 23010–23014. doi: 10.1074/jbc.C700111200

Perng, Y. C., and Lenschow, D. J. (2018). ISG15 in antiviral immunity and beyond. *Nat. Rev. Microbiol.* 16, 423–439. doi: 10.1038/s41579-018-0020-5

Pfleger, K. D., and Eidne, K. A. (2006). Illuminating insights into protein-protein interactions using bioluminescence resonance energy transfer (BRET). *Nat. Methods* 3, 165–174. doi: 10.1038/nmeth841

Pulvino, M., Liang, Y., Oleksyn, D., DeRan, M., Van Pelt, E., Shapiro, J., et al. (2012). Inhibition of proliferation and survival of diffuse large B-cell lymphoma cells by a small-molecule inhibitor of the ubiquitin-conjugating enzyme Ubc13-Uev1A. *Blood* 120, 1668–1677. doi: 10.1182/blood-2012-02-406074

Recht, M., Borden, E. C., and Knight, E. Jr. (1991). A human 15-kDa IFN-induced protein induces the secretion of IFN-gamma. *J. Immunol.* 147, 2617–2623.

Ritchie, K. J., Malakhov, M. P., Hetherington, C. J., Zhou, L., Little, M. T., Malakhova, O. A., et al. (2002). Dysregulation of protein modification by ISG15 results in brain cell injury. *Genes Dev.* 16, 2207–2212.

Ronau, J. A., Beckmann, J. F., and Hochstrasser, M. (2016). Substrate specificity of the ubiquitin and Ubl proteases. *Cell Res.* 26, 441–456. doi: 10.1038/cr.2016.38

Rush, J., Moritz, A., Lee, K. A., Guo, A., Goss, V. L., Spek, E. J., et al. (2005). Immunoaffinity profiling of tyrosine phosphorylation in cancer cells. *Nat. Biotechnol.* 23, 94–101. doi: 10.1038/nbt1046

Sakamoto, K. M., Kim, K. B., Kumagai, A., Mercurio, F., Crews, C. M., and Deshaies, R. J. (2001). Protacs: chimeric molecules that target proteins to the Skp1-Cullin-F box complex for ubiquitination and degradation. *Proc. Natl. Acad. Sci. U.S.A.* 98, 8554–8559. doi: 10.1073/pnas.141230798

Schwabenland, M., Mossad, O., Peres, A. G., Kessler, F., Maron, F. J. M., Harsan, L. A., et al. (2019). Loss of USP18 in microglia induces white matter pathology. *Acta Neuropathol. Commun.* 7:106. doi: 10.1186/s40478-019-0757-8

Sekizawa, R., Ikeno, S., Nakamura, H., Naganawa, H., Matsui, S., Iinuma, H., et al. (2002). Panepophenanthrin, from a mushroom strain, a novel inhibitor of the ubiquitin-activating enzyme. *J. Nat. Prod.* 65, 1491–1493. doi: 10.1021/np020098q

Shimaoka, M., Xiao, T., Liu, J. H., Yang, Y., Dong, Y., Jun, C. D., et al. (2003). Structures of the alpha L I domain and its complex with ICAM-1 reveal a shape-shifting pathway for integrin regulation. *Cell* 112, 99–111. doi: 10.1016/S0092-8674(02)01257-6

Siklos, M., BenAissa, M., and Thatcher, G. R. (2015). Cysteine proteases as therapeutic targets: does selectivity matter? A systematic review of calpain and cathepsin inhibitors. *Acta Pharm. Sin B* 5, 506–519. doi: 10.1016/j.apsb.2015.08.001

Soucy, T. A., Smith, P. G., Milhollen, M. A., Berger, A. J., Gavin, J. M., Adhikari, S., et al. (2009). An inhibitor of NEDD8-activating enzyme as a new approach to treat cancer. *Nature* 458, 732–736. doi: 10.1038/nature07884

Speer, S. D., Li, Z., Buta, S., Payelle-Brogard, B., Qian, L., Vigant, F., et al. (2016). ISG15 deficiency and increased viral resistance in humans but not mice. *Nat. Commun.* 7:11496. doi: 10.1038/ncomms11496

Stanton, B. Z., Chory, E. J., and Crabtree, G. R. (2018). Chemically induced proximity in biology and medicine. *Science* 359:eaao5902. doi: 10.1126/science.aao5902

Strickson, S., Campbell, D. G., Emmerich, C. H., Knebel, A., Plater, L., Ritorto, M. S., et al. (2013). The anti-inflammatory drug BAY 11-7082 suppresses the MyD88-dependent signalling network by targeting the ubiquitin system. *Biochem. J.* 451, 427–437. doi: 10.1042/BJ20121651

Sun, L., Wang, X., Zhou, Y., Zhou, R. H., Ho, W. Z., and Li, J. L. (2016). Exosomes contribute to the transmission of anti-HIV activity from TLR3-activated brain microvascular endothelial cells to macrophages. *Antiviral Res.* 134, 167–171. doi: 10.1016/j.antiviral.2016.07.013

Swaim, C. D., Scott, A. F., Canadeo, L. A., and Huibregtse, J. M. (2017). Extracellular ISG15 signals cytokine secretion through the LFA-1 integrin receptor. *Mol. Cell 68*, 581–590.e585. doi: 10.1016/j.molcel.2017.10.003

Swatek, K. N., Aumayr, M., Pruneda, J. N., Visser, L. J., Berryman, S., Kueck, A. F., et al. (2018). Irreversible inactivation of ISG15 by a viral leader protease enables alternative infection detection strategies. *Proc. Natl. Acad. Sci. U.S.A.* 115, 2371–2376. doi: 10.1073/pnas.1710617115

Tirat, A., Schilb, A., Riou, V., Leder, L., Gerhartz, B., Zimmermann, J., et al. (2005). Synthesis and characterization of fluorescent ubiquitin derivatives as highly sensitive substrates for the deubiquitinating enzymes UCH-L3 and USP-2. *Anal. Biochem.* 343, 244–255. doi: 10.1016/j.ab.2005.04.023

Tokarz, S., Berset, C., La Rue, J., Friedman, K., Nakayama, K., Nakayama, K., et al. (2004). The ISG15 isopeptidase UBP43 is regulated by proteolysis via the SCFSkp2 ubiquitin ligase. *J. Biol. Chem.* 279, 46424–46430. doi: 10.1074/jbc.M403189200

Tokgoz, Z., Bohnsack, R. N., and Haas, A. L. (2006). Pleiotropic effects of ATP.Mg2+ binding in the catalytic cycle of ubiquitin-activating enzyme. *J. Biol. Chem.* 281, 14729–14737. doi: 10.1074/jbc.M513562200

Udeshi, N. D., Mertins, P., Svinkina, T., and Carr, S. A. (2013). Large-scale identification of ubiquitination sites by mass spectrometry. *Nat. Protoc.* 8, 1950–1960. doi: 10.1038/nprot.2013.120

Verdoes, M., and Verhelst, S. H. (2016). Detection of protease activity in cells and animals. *Biochim. Biophys. Acta* 1864, 130–142. doi: 10.1016/j.bbapap.2015.04.029

Weinert, B. T., Wagner, S. A., Horn, H., Henriksen, P., Liu, W. R., Olsen, J. V., et al. (2011). Proteome-wide mapping of the Drosophila acetylome demonstrates a high degree of conservation of lysine acetylation. *Sci. Signal.* 4:ra48. doi: 10.1126/scisignal.2001902

Wong, J. J., Pung, Y. F., Sze, N. S., and Chin, K. C. (2006). HERC5 is an IFN-induced HECT-type E3 protein ligase that mediates type I IFN-induced ISGylation of protein targets. *Proc. Natl. Acad. Sci. U.S.A.* 103, 10735–10740. doi: 10.1073/pnas.0600397103

Wu, P., and Brand, L. (1994). Resonance energy transfer: methods and applications. *Anal. Biochem.* 218, 1–13. doi: 10.1006/abio.1994.1134

Xin, B. T., Gan, J., Fernandez, D. J., Knobeloch, K. P., Geurink, P. P., and Ovaa, H. (2019). Total chemical synthesis of murine ISG15 and an activity-based probe with physiological binding properties. *Org. Biomol. Chem.* 17, 10148–10152.

Xu, G., Paige, J. S., and Jaffrey, S. R. (2010a). Global analysis of lysine ubiquitination by ubiquitin remnant immunoaffinity profiling. *Nat. Biotechnol.* 28, 868–873. doi: 10.1038/nbt.1654

Xu, G. W., Ali, M., Wood, T. E., Wong, D., Maclean, N., Wang, X., et al. (2010b). The ubiquitin-activating enzyme E1 as a therapeutic target for the treatment of leukemia and multiple myeloma. *Blood* 115, 2251–2259. doi: 10.1182/blood-2009-07-231191

Yang, Y., Kitagaki, J., Dai, R. M., Tsai, Y. C., Lorick, K. L., Ludwig, R. L., et al. (2007). Inhibitors of ubiquitin-activating enzyme (E1), a new class of potential cancer therapeutics. *Cancer Res.* 67, 9472–9481. doi: 10.1158/0008-5472.CAN-07-0568

Ye, Y., Akutsu, M., Reyes-Turcu, F., Enchev, R. I., Wilkinson, K. D., and Komander, D. (2011). Polyubiquitin binding and cross-reactivity in the USP domain deubiquitinase USP21. *EMBO Rep.* 12, 350–357. doi: 10.1038/embor.2011.17

Zhang, D., and Zhang, D. E. (2011). Interferon-stimulated gene 15 and the protein ISGylation system. *J. Interferon Cytokine Res.* 31, 119–130. doi: 10.1089/jir.2010.0110

Zhang, X., Bogunovic, D., Payelle-Brogard, B., Francois-Newton, V., Speer, S. D., Yuan, C., et al. (2015). Human intracellular ISG15 prevents interferon-α/β over-amplification and auto-inflammation. *Nature* 517, 89–93. doi: 10.1038/nature13801

Zhang, Y., Thery, F., Wu, N. C., Luhmann, E. K., Dussurget, O., Foecke, M., et al. (2019). The *in vivo* ISGylome links ISG15 to metabolic pathways and autophagy upon *Listeria monocytogenes infection*. *Nat. Commun.* 10:5383. doi: 10.1038/s41467-019-13393-x

Zhao, C., Beaudenon, S. L., Kelley, M. L., Waddell, M. B., Yuan, W., Schulman, B. A., et al. (2004). The UbcH8 ubiquitin E2 enzyme is also the E2 enzyme for ISG15, an IFN-alpha/beta-induced ubiquitin-like protein. *Proc. Natl. Acad. Sci. U.S.A.* 101, 7578–7582. doi: 10.1073/pnas.0402528101

Zhao, C., Denison, C., Huibregtse, J. M., Gygi, S., and Krug, R. M. (2005). Human ISG15 conjugation targets both IFN-induced and constitutively expressed proteins functioning in diverse cellular pathways. *Proc. Natl. Acad. Sci. U.S.A.* 102, 10200–10205. doi: 10.1073/pnas.0504754102

Zou, W., and Zhang, D. E. (2006). The interferon-inducible ubiquitin-protein isopeptide ligase (E3) EFP also functions as an ISG15 E3 ligase. *J. Biol. Chem.* 281, 3989–3994. doi: 10.1074/jbc.M510787200

Conflict of Interest: The authors declare that the research was conducted in the absence of any commercial or financial relationships that could be construed as a potential conflict of interest.

frontiers in Cell and Developmental Biology

MINI REVIEW
published: 22 January 2020
doi: 10.3389/fcell.2019.00392

The Role of Atypical Ubiquitin Chains in the Regulation of the Antiviral Innate Immune Response

*Mariska van Huizen and Marjolein Kikkert**

Department of Medical Microbiology, LUMC Center for Infectious Diseases, Leiden University Medical Center, Leiden, Netherlands

It is well established that polyubiquitin chains, in particular those linked through K48 and K63, play a key role in the regulation of the antiviral innate immune response. However, the role of the atypical chains linked via any of the other lysine residues (K6, K11, K27, K29, and K33) and the M1-linked linear chains have not been investigated very well yet in this context. This is partially due to a lack of tools to study these linkages in their biological context. Interestingly though, recent findings underscore the importance of the atypical chains in the regulation of the antiviral immune response. This review will highlight the most important advances in the study of the role of atypical ubiquitin chains, particularly in the regulation of intracellular antiviral innate immune signaling pathways. We will also discuss the development of new tools and how these can increase our knowledge of the role of atypical ubiquitin chains.

Keywords: atypical ubiquitination, K27-linked ubiquitin, innate immune response, antiviral signaling, interferon, NFκB

OPEN ACCESS

Edited by:
Benedikt M. Kessler, University of Oxford, United Kingdom

Reviewed by:
Yuqi Wang, Saint Louis University, United States
Ulrike Resch, Medical University of Vienna, Austria

***Correspondence:**
Marjolein Kikkert
m.kikkert@lumc.nl

Specialty section:
This article was submitted to Cellular Biochemistry, a section of the journal Frontiers in Cell and Developmental Biology

Received: *02 October 2019*
Accepted: *24 December 2019*
Published: *22 January 2020*

Citation:
van Huizen M and Kikkert M (2020) The Role of Atypical Ubiquitin Chains in the Regulation of the Antiviral Innate Immune Response. Front. Cell Dev. Biol. 7:392. doi: 10.3389/fcell.2019.00392

INTRODUCTION

Virus infection triggers an immediate response in the host cell, termed the innate immune response. The basic innate immune response pathways, operational in virtually every cell type, have been comprehensively reviewed elsewhere (Schneider et al., 2014; Sparrer and Gack, 2015; Chen et al., 2016). In summary, they comprise a variety of signaling cascades that are initiated by the recognition of pathogen-associated molecular patterns by intra- and extracellular pattern recognition receptors (PRRs). An important class of intracellular PRRs are those that recognize viral nucleic acids in the cytosol. The retinoic acid-inducible gene-I (RIG-I)-like receptors (RLRs) recognize double-stranded RNA (dsRNA), whereas cyclic GMP-AMP synthase (cGAS) recognizes dsDNA. Activation of RLRs and the cGAS-STING pathway leads to a signaling cascade converging at the transcription factors NFκB and IRF3 and -7, which induce the production of proinflammatory cytokines and type I interferons (IFN), respectively (**Figure 1**).

Ubiquitin plays a crucial role in the activation and downregulation of the innate immune response. Conjugation of ubiquitin onto lysine residues of target proteins by E1, E2, and E3 enzymes and deconjugation by deubiquitinating enzymes (DUBs) can modulate the function, localization,

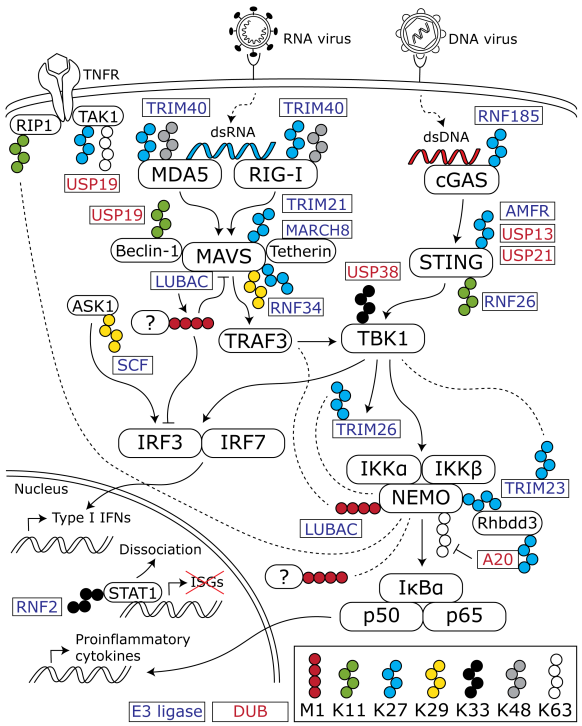

FIGURE 1 | Overview of ubiquitin chains that modulate the antiviral innate immune response. Cytosolic viral nucleic acids are recognized by the dsRNA sensors MDA5 and RIG-I and the dsDNA sensor cGAS. These activate downstream signaling cascades that converge at TBK1 and lead to subsequent activation of the transcription factors IRF3 and -7 and the NFκB subunits p50 and p65. IRF3 and -7 induce the production of type I IFNs, whereas p50 and p65 stimulate proinflammatory cytokine production. In addition to K48- and K63-linked chains, atypical chains are important regulators of the activation and downregulation of the innate immune response. For the sake of clarity, K48- and K63-linked chains are only depicted when an interaction with one of the atypical chains is shown in the discussed literature. Blocks with rounded corners present key innate immune factors, whereas rectangles represent E3 ligases (blue text) and DUBs (red text) that (de)conjugate the indicated chains. Dashed lines indicate an interaction between the connected protein and ubiquitin chains.

and abundance of the ubiquitinated target (Heaton et al., 2016). Moreover, polyubiquitin chains can be formed by conjugation of a subsequent ubiquitin molecule to one of the lysine residues or the N-terminal methionine of the previous ubiquitin molecule. These polyubiquitin chains have different topologies, thereby creating a complex ubiquitin code that can direct many different outcomes (Komander and Rape, 2012; Kulathu and Komander, 2012). Regulation of the innate immune response by polyubiquitination is well characterized for K48- and K63-linked chains (reviewed in Davis and Gack, 2015). However, knowledge of the role of the atypical linkages, linked via any of the other lysine residues or the N-terminal methionine, is still rather limited. Here we focus on the role of linear, K11-, K27-, K29-, and K33-linked chains in the innate immune response and the tools that are available to study these chains. **Table 1** summarizes the functions of atypical ubiquitination in innate immune responses, and associated E3 enzymes and DUBs, as will be discussed below.

LINEAR CHAINS ARE IMPORTANT REGULATORS OF NEMO AND NFκB SIGNALING

Since the discovery of the linear ubiquitin chain assembly complex (LUBAC) that uniquely catalyzes the formation of linear chains, it has become evident that LUBAC and linear chains are crucial for the activation of nuclear factor κB (NFκB) signaling (Kirisako et al., 2006; Gerlach et al., 2011; Tokunaga et al., 2011). Linear chains are especially important for tumor necrosis factor α (TNFα) signaling, but are also involved in other immune signaling pathways (Spit et al., 2019). One important mechanism in the activation of NFκB, is the interaction of linear chains with NFκB essential modulator (NEMO). NEMO is part of the IKK complex that phosphorylates NFκB inhibitor α (IκBα), thereby releasing the NFκB subunits p50 and p65, which then act as transcription factors and induce the transcription of proinflammatory cytokines. The UBAN domain (ubiquitin binding in ABIN proteins and NEMO) of NEMO has a strong binding-preference for linear chains, although some studies indicate that it can also bind longer K63-linked chains. NEMO mutants that cannot bind linear chains or NEMO chimeras in which the UBAN domain is replaced by the NZF domain of TAB2, a ubiquitin-binding domain (UBD) that binds specifically to K63-linked chains, cannot activate NFκB upon TNFα stimulation (Rahighi et al., 2009; Hadian et al., 2011; Kensche et al., 2012). Altogether, these studies show that NEMO UBAN has a strong preference for linear chains, and that this is required and sufficient for NFκB activation.

In addition to its binding to linear chains, NEMO is also a substrate for the conjugation of linear chains by LUBAC (Tokunaga et al., 2009). Furthermore, association of LUBAC with NEMO mediates the interaction between NEMO and TRAF3, which then leads to the disruption of the MAVS-TRAF3 complex. This results in NFκB activation and inhibition of type I IFN signaling (Belgnaoui et al., 2012). LUBAC has also been found to interact with MAVS. Hepatitis B virus-induced recruitment of the E3 ligases Parkin and LUBAC to MAVS leads to the formation of linear chains. Interaction of MAVS with these chains results in a disruption of the MAVS signalosome and downstream IRF3 activation, thereby inhibiting the type I IFN response. It is unclear to which substrate these chains are conjugated (Khan et al., 2016).

In summary, linear chains potentiate NFκB signaling, while inhibiting type I IFN signaling.

K11-LINKED CHAINS REGULATE THE DEGRADATION OF INNATE IMMUNE FACTORS

K11-linked ubiquitination is associated with the regulation of the cell cycle and proteasome-mediated degradation (Meyer and Rape, 2014; Grice and Nathan, 2016; Yau et al., 2017). By regulating the degradation of innate immune factors, K11-linked ubiquitination can affect the innate immune response. For example, RNF26-mediated K11-linked ubiquitination of STING

TABLE 1 | Overview of the functions of atypical ubiquitination and the associated E3 enzymes and DUBs.

Ubiquitin linkage	Modifying enzyme	Substrate	Functional outcome	References
Linear	LUBAC[a]	?	Interaction of NEMO with linear chains potentiates NFκB activation.	Rahighi et al., 2009; Hadian et al., 2011; Kensche et al., 2012
		NEMO	Upregulates NFκB activation and disrupts MAVS-TRAF3 interaction, thereby inhibiting IRF3 activation and the IFN response.	Tokunaga et al., 2009; Belgnaoui et al., 2012
		?	Interaction of MAVS with LUBAC leads to the formation of linear chains that disrupt the MAVS signalosome and prevent downstream signaling.	Khan et al., 2016
K11	RNF26[a]	STING	Inhibits STING degradation, leading to increased type I IFN and cytokine production.	Qin et al., 2014
	USP19[b]	Beclin-1	Stabilizes Beclin-1 and limits type I IFN production by disrupting the interaction between RIG-I and MAVS.	Jin et al., 2016
	?	RIP1	Interacts with NEMO.	Dynek et al., 2010
K27	TRIM23[a]	NEMO	Leads to NFκB and IRF3 activation.	Arimoto et al., 2010
		NEMO and Rhbdd3	Recruits the DUB A20 to remove K63-linked chains from NEMO, thereby preventing excessive NFκB activation.	Liu et al., 2014
	TRIM23[a]	TRIM23	Activates TBK1 and thereby induces antiviral autophagy.	Sparrer et al., 2017
	TRIM26[a]	TRIM26	Interacts with NEMO, leading to increased type I IFN and cytokine production.	Ran et al., 2016
	TRIM40[a]	RIG-I and MDA5	Induces proteasome-mediated degradation of RIG-I and MDA5, thereby inhibiting the type I IFN response.	Zhao et al., 2017
	TRIM21[a]	MAVS	Enhances type I IFN production.	Liu H. et al., 2018; Xue et al., 2018
	MARCH8[a]	MAVS	Induces autophagy-mediated degradation of MAVS, thereby restricting the type I IFN response.	Jin et al., 2017
	RNF185[a]	cGAS	Induces IRF3 activation and the production of type I IFNs and proinflammatory cytokines.	Wang et al., 2017
	AMFR[a]	STING	Recruits TBK1 to STING and induces IRF3 activation and the production of type I IFNs and proinflammatory cytokines.	Wang Q. et al., 2014
	USP13 and USP21[b]	STING	Inhibits IRF3 activation and the production of type I IFNs and proinflammatory cytokines.	Chen et al., 2017; Sun et al., 2017
	USP19[b]	TAK1	Inhibition of proinflammatory cytokine production.	Lei et al., 2019
K27 and K29	RNF34[a]	MAVS	Induces autophagy-mediated degradation of MAVS, thereby restricting the type I IFN response.	He et al., 2019
K29	SKP1-Cullin-Fbx21[a]	ASK1	Induces IFNβ and IL-6 production.	Yu et al., 2016
K33	USP38[b]	TBK1	Prevents TBK1 degradation and induces IRF3 activation.	Lin et al., 2016
	RNF2[a]	STAT1	Suppresses ISG transcription.	Liu S. et al., 2018

This table summarizes the E3 enzymes and DUBs that (de)conjugate atypical ubiquitin chains in the context of the innate immune response and the effects of (de)conjugation of these chains on the innate immune response. [a]Indicates that the modifying enzyme is an E3 ligase, whereas [b]indicates that the enzyme is a DUB.

causes inhibition of STING degradation. Thereby, the production of type I IFNs and proinflammatory cytokines is potentiated (Qin et al., 2014). On the other hand, RNF26 can induce autophagy-mediated degradation of IRF3, which limits the production of type I IFNs. This is dependent on the E3 ligase activity of RNF26, but the authors could not identify which ubiquitin linkage is involved (Qin et al., 2014). Overall, it seems that RNF26, partially via K11-linked ubiquitination, can both prevent and promote the induction of type I IFNs via the degradation of its target, and that this is under strict temporal regulation.

The presence of K11- and K48-linked chains on Beclin-1, a protein interacting with MAVS, has been associated with proteasome-mediated degradation of Beclin-1 (Jin et al., 2016). Removal of K11-linked chains by the DUB USP19 prevents this and leads to Beclin-1 stabilization. Stabilized Beclin-1 induces autophagy and inhibits the interaction between RIG-I and MAVS, thereby limiting the production of type I IFNs upon SeV or vesicular stomatitis virus (VSV) infection. This way, K11-linked ubiquitination of Beclin-1 indirectly inhibits autophagy and promotes the type I IFN response by inducing Beclin-1 degradation (Jin et al., 2016).

Lastly, there is some evidence that NEMO can bind K11-linked chains, which are for example conjugated to receptor-interacting serine/threonine-protein kinase 1 (RIP1), a kinase associated with the TNFα receptor (Dynek et al., 2010). However, it is unclear what the effects of this interaction are.

K27-LINKED CHAINS: BALANCING ACTIVATION AND INHIBITION?

It is becoming more and more evident that K27-linked chains are important regulators of the innate immune response. The first evidence for this came from a study by Arimoto et al. (2010).

They showed that E3 ligase TRIM23 can conjugate K27-linked chains to NEMO and that this is required for the induction of NFκB and IRF3 upon activation of RLR signaling (Arimoto et al., 2010). K27-linked chains on NEMO subsequently serve as an interaction platform for other factors that regulate the innate immune response. This is for example illustrated by binding of Rhbdd3, a serine protease that regulates epidermal growth factor signaling, to K27-linked chains on NEMO. This leads to K27-linked ubiquitination of Rhbdd3 and recruitment of the DUB A20. A20 then removes K63-linked chains from NEMO, thereby preventing excessive NFκB activation. By this mechanism, Rhbdd3 was shown to control the activation of dendritic cells and to limit Th17 cell-mediated colitis in mice (Liu et al., 2014).

TRIM23 is also auto-ubiquitinated with K27-linked chains. As a result, TRIM23 activates TBK1 by its GTPase activity. TBK1 subsequently phosphorylates the selective autophagy receptor p62, which leads to the induction of autophagy upon infection with several different DNA and RNA viruses (Sparrer et al., 2017).

Another E3 ligase that is auto-ubiquitinated with K27-linked chains is TRIM26. Upon activation of RLR signaling, TBK1 phosphorylates TRIM26, leading to TRIM26 auto-ubiquitination. NEMO then interacts with the K27-linked chains conjugated to TRIM26, which induces the expression of proinflammatory cytokines, type I IFNs, and interferon stimulated genes (ISGs) (Ran et al., 2016).

Another E3 ligase of the TRIM family, TRIM40, was shown to conjugate K27- and K48-linked chains to the dsRNA sensors RIG-I and Melanoma Differentiation-Associated protein 5 (MDA5). This leads to attenuation of RNA virus-induced RLR signaling. Mechanistically, TRIM40-mediated ubiquitination of RIG-I and MDA5 induces proteasome-mediated degradation of these proteins (Zhao et al., 2017). Therefore, the authors conclude that both K27- and K48-linked chains are involved in proteasome-mediated degradation. However, they do not discriminate between the functions of these two linkages. Since K48-linked chains have strongly been linked to proteasome-mediated degradation, it may be likely that the proteasome-mediated degradation could be attributed to K48-linked ubiquitination, while the role of K27-linked chains in degradation of RIG-I and MDA5 remains unclear.

Lastly, TRIM21 has been suggested to catalyze K27-linked ubiquitination of MAVS (Liu H. et al., 2018; Xue et al., 2018). TRIM21 expression is induced by infection with different RNA viruses and it potentiates the innate immune response (Liu H. et al., 2018; Xue et al., 2018). These studies clearly demonstrate that TRIM21 has antiviral effects. However, the presented Western blots which show that TRIM21 exerts its effects via K27-linked ubiquitination are not very convincing, and this should be further investigated.

Another E3 ligase that can conjugate K27-linked chains to MAVS, is MARCH8 (Jin et al., 2017). MARCH8 is recruited to MAVS by Tetherin, an ISG that restricts the release of enveloped viruses (Evans et al., 2010). Recruitment of MARCH8 by Tetherin induces K27-linked ubiquitination of MAVS followed by the degradation of MAVS by selective autophagy. This provides a negative feedback loop by which the innate immune response is restricted (Jin et al., 2017). Another E3 ligase that induces autophagic degradation of MAVS, is RNF34. RNF34 catalyzes both K27- and K29-linked ubiquitination of MAVS (He et al., 2019). However, the authors also show that RNF34 is important for the clearance of damaged mitochondria by mitophagy, so the question is whether the degradation of MAVS is specific or is a result of mitophagy (He et al., 2019).

RNF185-mediated K27-linked ubiquitination of cGAS, and AMFR-mediated K27-linked ubiquitination of STING both lead to the induction of a proinflammatory and antiviral response upon stimulation with different DNA ligands or infection with the DNA virus herpes simplex virus 1 (HSV-1). K27-linked ubiquitination of cGAS and STING is required for TBK1 activation (Wang Q. et al., 2014; Wang et al., 2017). Mechanistically, K27-linked chains on STING are responsible for the recruitment of TBK1 to STING (Wang Q. et al., 2014). The DUBs USP13 and USP21 were shown to remove K27-linked ubiquitin from STING (Chen et al., 2017; Sun et al., 2017). These studies confirmed that K27-linked ubiquitin activates the immune response upon infection with several DNA viruses or the intracellular bacterium *Listeria monocytogenes* (Chen et al., 2017; Sun et al., 2017).

TGFβ-activated kinase 1 (TAK1) is a protein that is activated by various inflammatory stimuli and subsequently induces activation of NFκB signaling. TAK1 activation is strongly regulated by posttranslational modifications, including K48- and K63-linked ubiquitination (Hirata et al., 2017). Recently, it was shown that TAK1 can also be K27-linked ubiquitinated and that both K27- and K63-linked chains can mediate the interaction with TAK1-binding protein 2 (TAB2) and TAB3. Removal of K27- and K63-linked chains by USP19 inhibited TNFα- and IL-1β-induced NFκB activation, suggesting that these ubiquitin chains normally activate TAK1 downstream signaling (Lei et al., 2019). However, the authors could not discriminate between the role of K27- and K63-linked chains, due to technical constraints.

In summary, K27-linked chains are important activators of the innate immune response, in this context often conjugated by members of the TRIM family but also by other E3 ligases. These chains are also part of negative feedback loops that prevent excessive inflammation and immunopathology, hence K27-linked ubiquitin chains could be used to give a temporary controlled boost to the innate immune system, when this is deemed necessary by the cell.

K29-LINKED CHAINS ON ASK1 ACTIVATE IRF3

Very little is known about the role of K29-linked ubiquitination in the innate immune response. It has been shown that the SKP1-Cullin-Fbx21 (SCF) E3 ligase complex is activated upon VSV and HSV-1 infection. This complex then catalyzes K29-linked ubiquitination of apoptosis signal-regulating kinase 1 (ASK1), thereby inducing phosphorylation of JNK1/2, p38, and IRF3, and activation of the transcription factor activator

protein-1 (AP-1). Altogether, this leads to the production of IFNβ and interleukin-6 (Yu et al., 2016). However, it remains to be elucidated how virus infection leads to the activation of ASK1 signaling.

K33-LINKED CHAINS MODULATE RLR AND TYPE I IFN SIGNALING

K33-linked ubiquitination is associated with cGAS-STING- and RLR-induced type I IFN signaling. Upon infection with different DNA and RNA viruses, TBK1 is K33-linked ubiquitinated, which leads to IRF3 activation (Lin et al., 2016). This can be reversed by the DUB USP38. USP38-mediated removal of K33-linked ubiquitin is associated with an increase in K48-linked ubiquitination and subsequent proteasome-mediated degradation of TBK1, thereby downregulating the antiviral response (Lin et al., 2016). Another study describes K33-linked ubiquitination of the type I IFN-induced transcription factor STAT1. This is mediated by the E3 ligase RNF2. Upon interferon stimulation, RNF2 binds to STAT1 in the nucleus and mediates K33-linked ubiquitination of the STAT1 DNA binding domain. This leads to the dissociation of STAT1 from the promotor of several ISGs, thereby suppressing the production of ISGs (Liu S. et al., 2018). These two studies demonstrate two different ways in which K33-linked chains can be involved in the regulation of the innate immune response. Further studies are necessary to elucidate how these mechanisms complement each other and regulate RLR and interferon signaling.

TOOLS TO STUDY SPECIFIC UBIQUITIN LINKAGES IN THEIR BIOLOGICAL CONTEXT

Probably the most reliable technique to identify specifically linked ubiquitin chains on a purified substrate or in the total cellular ubiquitin pool, is using mass spectrometry. However, this is relatively elaborate, and may not be available to all researchers. Furthermore, this does not allow the identification of specific ubiquitin linkages conjugated to a specific substrate in cells. Most biochemical studies that try to identify specific ubiquitin linkages therefore rely on expression of ubiquitin mutants that contain only one lysine residue (KX-only mutants) or individual lysine-to-arginine substitutions (KXR mutants). These are then individually co-transfected into cells together with the other proteins of interest. However, using this approach it is hard to study the role of a specific ubiquitin linkage in the innate immune response, as most cultured cells, such as the often-used 293T cells, have important deficiencies in these pathways (Burdette et al., 2011; Lin et al., 2014). Therefore, one should use cells that have an intact innate immune system, however, transfection of these cells is usually rather inefficient and subsequent virus infection is very hard. Another frequently used method are *in vitro* ubiquitination and deubiquitination assays. Although these can be a helpful tool, such assays do not take into account the subcellular localization of the proteins involved and do not allow to study the effects of a specific chain on a specific target in the innate immune response. Therefore, methods are needed to directly detect specific ubiquitin linkages in cells. For linear, K11-, K27-, K48-, and K63-linked chains, linkage-specific antibodies have been generated (Newton et al., 2008; Matsumoto et al., 2010, 2012). These have been used with varying results, and in most cases they hardly produce any specific signal when used in cell lysates. The generation of linkage-specific antibodies is apparently very challenging, which is probably due to the sometimes very subtle structural differences between different ubiquitin chains.

An alternative to antibodies are affimers. These are small scaffold proteins of which the sequence is based on a phytocystatin consensus sequence (Tiede et al., 2014, 2017). The insertion of two variable peptide regions into this sequence was used to construct a phage-display library that can be screened for any protein of interest (Tiede et al., 2014). Michel et al. (2017) have described the development of an affimer against K6-linked ubiquitin. This affimer was used successfully in pull downs, Western blotting, and confocal microscopy (Michel et al., 2017). Using the affimer, the cellular E3 ligase that catalyzes K6-linked ubiquitination, a DUB with strong preference for K6-linked ubiquitin and a substrate could be identified (Gersch et al., 2017; Michel et al., 2017; Heidelberger et al., 2018). In addition, an affimer against K33-linked ubiquitin was developed. However, this affimer also recognized K11-linked ubiquitin (Michel et al., 2017). Most likely this is the result of heterogeneity in the conformation of polyubiquitin chains, which is why chains linked via different residues can have closely resembling conformations (Wang Y. et al., 2014). Although this shows that it can be hard to achieve linkage-specificity, affimers could be a powerful alternative for antibodies.

In addition to methods that directly detect a specific type of ubiquitin chain, linkage-specific DUBs can be used to discriminate between different linkages in a cell lysate or on a target that was precipitated using pull-downs. The following linkage-specific DUBs are available: OTULIN for linear chains, Cezanne for K11-linked chains, Otubain-1 for K48-linked chains, and AMSH or OTUD1 for K63-linked chains (Mevissen et al., 2013). No DUBs are known that have specificity for K6-, K27-, K29-, and K33-linked chains. However, OTUD3 and USP30 have a strong preference for K6- and K11-linked chains, whereas TRABID has a strong preference for K29- and K33-linked chains. When OTUD3 or USP30 are used in combination with Cezanne, the discrimination between K6- and K11-linked chains can be made (Mevissen et al., 2013; Cunningham et al., 2015). Based on this principle, a method was developed termed ubiquitin chain restriction (UbiCRest) in which *in vitro* ubiquitinated proteins, cell lysates, or precipitated immunocomplexes are incubated with a combination of the aforementioned linkage-specific DUBs (Hospenthal et al., 2015).

The UBDs of linkage-specific DUBs and other proteins that interact with specific ubiquitin linkages can also be exploited as biosensors. TRABID has 3 NZF domains that can bind a variety of different ubiquitin chains. The NZF1 domain specifically binds

K29- and K33-linked chains (Kristariyanto et al., 2015). This NZF1 domain was used to pull down polyubiquitin chains from cells. Subsequently, the immunocomplexes were treated with the Crimean-Congo Hemorrhagic Fever virus OTU (vOTU) DUB to discriminate between K29- and K33-linked chains (Akutsu et al., 2011; Kristariyanto et al., 2015). According to the authors, vOTU cleaves all types of ubiquitin chains except for K29-linked chains (Kristariyanto et al., 2015). Contrary to this, there is also evidence that vOTU cleaves all linkages except for linear chains (Mevissen et al., 2013). Using their approach, the authors showed that K29-linked ubiquitin can be part of heterotypic chains containing also K48-linked ubiquitin (Kristariyanto et al., 2015). Two other biosensors have been described, one that is based on the UBAN domain of NEMO and recognizes linear chains and one that is based on the NZF domain of TAB2 and recognizes K63-linked chains. These domains were coupled to GFP and could thereby be used in microscopy and live cell imaging (van Wijk et al., 2012; Greenfeld et al., 2015). Although these biosensors are a valuable tool, their development depends on the availability of a UBD that specifically binds to a certain ubiquitin linkage.

Another method to obtain insight in the cellular function of a specific ubiquitin linkage has been developed by Xu et al. (2009). They developed a tetracycline-inducible RNAi system with which the expression of all four ubiquitin genes can be knocked down and replaced by a KXR mutant. Using cells expressing K63R ubiquitin, they could show that K63-linked chains are required for IKK activation, but only by IL-1β and not by TNFα (Xu et al., 2009). Although this setup is laborious to create and leads to a general depletion of a specific ubiquitin linkage, this strategy can be very useful in elucidating the role of a certain linkage in the innate immune response or any other signaling cascade of interest.

In summary, for M1-, K48- and K63-linked chains rather well-functioning antibodies, linkage-specific DUBs, and UBD-based biosensors exist, whereas for most of the other linkages, including K27- and K33-linked chains, very few or no tools are available. Potentially, new UBDs could be developed based on the structure of UBDs in complex with ubiquitin chains for which no specific UBD is known. By structure-guided mutagenesis, it would in theory be possible to develop new biosensors that recognize for example K27- or K33-linked chains.

CONCLUSION

The innate immune response is a crucial first line of defense against virus infection and is responsible for the recruitment of innate immune cells to the site of infection and the induction of the adaptive response. However, overactivation of the innate response can lead to excessive inflammation and immunopathology. Therefore, activation of the innate immune response is subject to strong regulation. Besides phosphorylation, this is strongly mediated by ubiquitination. The variety in ubiquitin chains, each with their unique properties, enables very precise fine-tuning of the innate immune response. Some linkages, such as linear chains, are currently almost exclusively linked to the innate immune response. However, most linkages are involved in many different processes. K27-linked chains seem to function mainly as activators of the innate immune response, although they can also have inhibitory effects. For K29- and K33-linked ubiquitin, too little data is available to define whether they have a specific role in the innate immune response. In addition to these homotypic chains that are linked via one specific lysine residue, hybrid or mixed chains exist as well (Akutsu et al., 2016). M1/K63-linked hybrid chains can serve as unique scavengers that recruit TAK1, IKKα, and IKKβ via the K63 linkage, and NEMO via the M1 linkage (Emmerich et al., 2013). Overall, the ubiquitin code has a fascinating complexity and elucidating more of this will give us important insight into the intricate interactions that regulate the innate immune response.

AUTHOR CONTRIBUTIONS

MH wrote the original draft of the manuscript. MH and MK contributed to the manuscript revision, and read and approved the submitted version.

FUNDING

This work was supported by a research grant from the Dutch Research Council (NWO) to MH (NWO 022.006.010).

REFERENCES

Akutsu, M., Dikic, I., and Bremm, A. (2016). Ubiquitin chain diversity at a glance. *J. Cell Sci.* 129, 875–880. doi: 10.1242/jcs.183954

Akutsu, M., Ye, Y., Virdee, S., Chin, J. W., and Komander, D. (2011). Molecular basis for ubiquitin and ISG15 cross-reactivity in viral ovarian tumor domains. *Proc. Natl. Acad. Sci. U.S.A.* 108, 2228–2233. doi: 10.1073/pnas.1015287108

Arimoto, K., Funami, K., Saeki, Y., Tanaka, K., Okawa, K., Takeuchi, O., et al. (2010). Polyubiquitin conjugation to NEMO by triparite motif protein 23 (TRIM23) is critical in antiviral defense. *Proc. Natl. Acad. Sci. U.S.A.* 107, 15856–15861. doi: 10.1073/pnas.1004621107

Belgnaoui, S. M., Paz, S., Samuel, S., Goulet, M. L., Sun, Q., Kikkert, M., et al. (2012). Linear ubiquitination of NEMO negatively regulates the interferon antiviral response through disruption of the MAVS-TRAF3 complex. *Cell Host Microbe* 12, 211–222. doi: 10.1016/j.chom.2012.06.009

Burdette, D. L., Monroe, K. M., Sotelo-Troha, K., Iwig, J. S., Eckert, B., Hyodo, M., et al. (2011). STING is a direct innate immune sensor of cyclic di-GMP. *Nature* 478, 515–518. doi: 10.1038/nature10429

Chen, Q., Sun, L., and Chen, Z. J. (2016). Regulation and function of the cGAS-STING pathway of cytosolic DNA sensing. *Nat. Immunol.* 17, 1142–1149. doi: 10.1038/ni.3558

Chen, Y., Wang, L., Jin, J., Luan, Y., Chen, C., Li, Y., et al. (2017). p38 inhibition provides anti-DNA virus immunity by regulation of USP21 phosphorylation and STING activation. *J. Exp. Med.* 214, 991–1010. doi: 10.1084/jem.20161387

Cunningham, C. N., Baughman, J. M., Phu, L., Tea, J. S., Yu, C., Coons, M., et al. (2015). USP30 and parkin homeostatically regulate atypical ubiquitin chains on mitochondria. *Nat. Cell Biol.* 17, 160–169. doi: 10.1038/ncb3097

Davis, M. E., and Gack, M. U. (2015). Ubiquitination in the antiviral immune response. *Virology* 479-480, 52–65. doi: 10.1016/j.virol.2015.02.033

Dynek, J. N., Goncharov, T., Dueber, E. C., Fedorova, A. V., Izrael-Tomasevic, A., Phu, L., et al. (2010). c-IAP1 and UbcH5 promote K11-linked

polyubiquitination of RIP1 in TNF signalling. *EMBO J.* 29, 4198–4209. doi: 10.1038/emboj.2010.300

Emmerich, C. H., Ordureau, A., Strickson, S., Arthur, J. S. C., Pedrioli, P. G. A., Komander, D., et al. (2013). Activation of the canonical IKK complex by K63/M1-linked hybrid ubiquitin chains. *Proc. Natl. Acad. Sci. U.S.A.* 110, 15247–15252. doi: 10.1073/pnas.1314715110

Evans, D. T., Serra-Moreno, R., Singh, R. K., and Guatelli, J. C. (2010). BST-2/tetherin: a new component of the innate immune response to enveloped viruses. *Trends Microbiol.* 18, 388–396. doi: 10.1016/j.tim.2010.06.010

Gerlach, B., Cordier, S. M., Schmukle, A. C., Emmerich, C. H., Rieser, E., Haas, T. L., et al. (2011). Linear ubiquitination prevents inflammation and regulates immune signalling. *Nature* 471, 591–596. doi: 10.1038/nature09816

Gersch, M., Gladkova, C., Schubert, A. F., Michel, M. A., Maslen, S., and Komander, D. (2017). Mechanism and regulation of the Lys6-selective deubiquitinase USP30. *Nat. Struct. Mol. Biol.* 24, 920–930. doi: 10.1038/nsmb.3475

Greenfeld, H., Takasaki, K., Walsh, M. J., Ersing, I., Bernhardt, K., Ma, Y., et al. (2015). TRAF1 coordinates polyubiquitin signaling to enhance Epstein-Barr Virus LMP1-mediated growth and survival pathway activation. *PLoS Pathog.* 11:e1004890. doi: 10.1371/journal.ppat.1004890

Grice, G. L., and Nathan, J. A. (2016). The recognition of ubiquitinated proteins by the proteasome. *Cell. Mol. Life Sci.* 73, 3497–3506. doi: 10.1007/s00018-016-2255-5

Hadian, K., Griesbach, R. A., Dornauer, S., Wanger, T. M., Nagel, D., Metlitzky, M., et al. (2011). NF-kappaB essential modulator (NEMO) interaction with linear and lys-63 ubiquitin chains contributes to NF-kappaB activation. *J. Biol. Chem.* 286, 26107–26117. doi: 10.1074/jbc.M111.233163

He, X., Zhu, Y., Zhang, Y., Geng, Y., Gong, J., Geng, J., et al. (2019). RNF34 functions in immunity and selective mitophagy by targeting MAVS for autophagic degradation. *EMBO J.* 38:e100978. doi: 10.15252/embj.2018100978

Heaton, S. M., Borg, N. A., and Dixit, V. M. (2016). Ubiquitin in the activation and attenuation of innate antiviral immunity. *J. Exp. Med.* 213, 1–13. doi: 10.1084/jem.20151531

Heidelberger, J. B., Voigt, A., Borisova, M. E., Petrosino, G., Ruf, S., Wagner, S. A., et al. (2018). Proteomic profiling of VCP substrates links VCP to K6-linked ubiquitylation and c-Myc function. *EMBO Rep.* 19:e44754. doi: 10.15252/embr.201744754

Hirata, Y., Takahashi, M., Morishita, T., Noguchi, T., and Matsuzawa, A. (2017). Post-translational modifications of the TAK1-TAB complex. *Int. J. Mol. Sci.* 18:E205. doi: 10.3390/ijms18010205

Hospenthal, M. K., Mevissen, T. E. T., and Komander, D. (2015). Deubiquitinase-based analysis of ubiquitin chain architecture using ubiquitin chain restriction (UbiCRest). *Nat. Protoc.* 10, 349–361. doi: 10.1038/nprot.2015.018

Jin, S., Tian, S., Chen, Y., Zhang, C., Xie, W., Xia, X., et al. (2016). USP19 modulates autophagy and antiviral immune responses by deubiquitinating Beclin-1. *EMBO J.* 35, 866–880. doi: 10.15252/embj.201593596

Jin, S., Tian, S., Luo, M., Xie, W., Liu, T., Duan, T., et al. (2017). Tetherin suppresses type I interferon signaling by targeting MAVS for NDP52-mediated selective autophagic degradation in human cells. *Mol. cell* 68, 308.e4–322.e4. doi: 10.1016/j.molcel.2017.09.005

Kensche, T., Tokunaga, F., Ikeda, F., Goto, E., Iwai, K., and Dikic, I. (2012). Analysis of nuclear factor-kappaB (NF-kappaB) essential modulator (NEMO) binding to linear and lysine-linked ubiquitin chains and its role in the activation of NF-kappaB. *J. Biol. Chem.* 287, 23626–23634. doi: 10.1074/jbc.M112.347195

Khan, M., Syed, G. H., Kim, S. J., and Siddiqui, A. (2016). Hepatitis B virus-induced parkin-dependent recruitment of linear ubiquitin assembly complex (LUBAC) to mitochondria and attenuation of innate immunity. *PLoS Pathog.* 12:e1005693. doi: 10.1371/journal.ppat.1005693

Kirisako, T., Kamei, K., Murata, S., Kato, M., Fukumoto, H., Kanie, M., et al. (2006). A ubiquitin ligase complex assembles linear polyubiquitin chains. *EMBO J.* 25, 4877–4887. doi: 10.1038/sj.emboj.7601360

Komander, D., and Rape, M. (2012). The ubiquitin code. *Annu. Rev. Biochem.* 81, 203–229. doi: 10.1146/annurev-biochem-060310-170328

Kristariyanto, Y. A., Abdul Rehman, S. A., Campbell, D. G., Morrice, N. A., Johnson, C., Toth, R., et al. (2015). K29-selective ubiquitin binding domain reveals structural basis of specificity and heterotypic nature of k29 polyubiquitin. *Mol. Cell* 58, 83–94. doi: 10.1016/j.molcel.2015.01.041

Kulathu, Y., and Komander, D. (2012). Atypical ubiquitylation - the unexplored world of polyubiquitin beyond Lys48 and Lys63 linkages. *Nat. Rev. Mol. Cell Biol.* 13, 508–523. doi: 10.1038/nrm3394

Lei, C. Q., Wu, X., Zhong, X., Jiang, L., Zhong, B., and Shu, H. B. (2019). USP19 Inhibits TNF-alpha- and IL-1beta-Triggered NF-kappaB activation by deubiquitinating TAK1. *J. Immunol.* 203, 259–268. doi: 10.4049/jimmunol.1900083

Lin, A. H., Burrascano, C., Pettersson, P. L., Ibañez, C. E., Gruber, H. E., and Jolly, D. J. (2014). Blockade of type I interferon (IFN) production by retroviral replicating vectors and reduced tumor cell responses to IFN likely contribute to tumor selectivity. *J. Virol.* 88, 10066–10077. doi: 10.1128/JVI.02300-13

Lin, M., Zhao, Z., Yang, Z., Meng, Q., Tan, P., Xie, W., et al. (2016). USP38 inhibits Type I interferon signaling by editing TBK1 ubiquitination through NLRP4 signalosome. *Mol. Cell* 64, 267–281. doi: 10.1016/j.molcel.2016.08.029

Liu, H., Li, M., Song, Y., and Xu, W. (2018). TRIM21 restricts coxsackievirus B3 replication, cardiac and pancreatic injury via interacting with MAVS and positively regulating IRF3-Mediated Type-I interferon production. *Front. Immunol.* 9:2479. doi: 10.3389/fimmu.2018.02479

Liu, J., Han, C., Xie, B., Wu, Y., Liu, S., Chen, K., et al. (2014). Rhbdd3 controls autoimmunity by suppressing the production of IL-6 by dendritic cells via K27-linked ubiquitination of the regulator NEMO. *Nat. Immunol.* 15, 612–622. doi: 10.1038/ni.2898

Liu, S., Jiang, M., Wang, W., Liu, W., Song, X., Ma, Z., et al. (2018). Nuclear RNF2 inhibits interferon function by promoting K33-linked STAT1 disassociation from DNA. *Nat. Immunol.* 19, 41–52. doi: 10.1038/s41590-017-0003-0

Matsumoto, M. L., Dong, K. C., Yu, C., Phu, L., Gao, X., Hannoush, R. N., et al. (2012). Engineering and structural characterization of a linear polyubiquitin-specific antibody. *J. Mol. Biol.* 418, 134–144. doi: 10.1016/j.jmb.2011.12.053

Matsumoto, M. L., Wickliffe, K. E., Dong, K. C., Yu, C., Bosanac, I., Bustos, D., et al. (2010). K11-linked polyubiquitination in cell cycle control revealed by a K11 linkage-specific antibody. *Mol. Cell* 39, 477–484. doi: 10.1016/j.molcel.2010.07.001

Mevissen, T. E., Hospenthal, M. K., Geurink, P. P., Elliott, P. R., Akutsu, M., Arnaudo, N., et al. (2013). OTU deubiquitinases reveal mechanisms of linkage specificity and enable ubiquitin chain restriction analysis. *Cell* 154, 169–184. doi: 10.1016/j.cell.2013.05.046

Meyer, H. J., and Rape, M. (2014). Enhanced protein degradation by branched ubiquitin chains. *Cell* 157, 910–921. doi: 10.1016/j.cell.2014.03.037

Michel, M. A., Swatek, K. N., Hospenthal, M. K., and Komander, D. (2017). Ubiquitin linkage-specific affimers reveal insights into K6-linked ubiquitin signaling. *Mol. cell* 68, 233.e5–246.e5. doi: 10.1016/j.molcel.2017.08.020

Newton, K., Matsumoto, M. L., Wertz, I. E., Kirkpatrick, D. S., Lill, J. R., Tan, J., et al. (2008). Ubiquitin chain editing revealed by polyubiquitin linkage-specific antibodies. *Cell* 134, 668–678. doi: 10.1016/j.cell.2008.07.039

Qin, Y., Zhou, M. T., Hu, M. M., Hu, Y. H., Zhang, J., Guo, L., et al. (2014). RNF26 temporally regulates virus-triggered type I interferon induction by two distinct mechanisms. *PLoS Pathog.* 10:e1004358. doi: 10.1371/journal.ppat.1004358

Rahighi, S., Ikeda, F., Kawasaki, M., Akutsu, M., Suzuki, N., Kato, R., et al. (2009). Specific recognition of linear ubiquitin chains by NEMO is important for NF-kappaB activation. *Cell* 136, 1098–1109. doi: 10.1016/j.cell.2009.03.007

Ran, Y., Zhang, J., Liu, L. L., Pan, Z. Y., Nie, Y., Zhang, H. Y., et al. (2016). Autoubiquitination of TRIM26 links TBK1 to NEMO in RLR-mediated innate antiviral immune response. *J. Mol. Cell Biol.* 8, 31–43. doi: 10.1093/jmcb/mjv068

Schneider, W. M., Chevillotte, M. D., and Rice, C. M. (2014). Interferon-stimulated genes: a complex web of host defenses. *Annu. Rev. Immunol.* 32, 513–545. doi: 10.1146/annurev-immunol-032713-120231

Sparrer, K. M., and Gack, M. U. (2015). Intracellular detection of viral nucleic acids. *Curr. Opin. Microbiol.* 26, 1–9. doi: 10.1016/j.mib.2015.03.001

Sparrer, K. M. J., Gableske, S., Zurenski, M. A., Parker, Z. M., Full, F., Baumgart, G. J., et al. (2017). TRIM23 mediates virus-induced autophagy via activation of TBK1. *Nat. Microbiol.* 2, 1543–1557. doi: 10.1038/s41564-017-0017-2

Spit, M., Rieser, E., and Walczak, H. (2019). Linear ubiquitination at a glance. *J. Cell Sci.* 132:jcs208512. doi: 10.1242/jcs.208512

Sun, H., Zhang, Q., Jing, Y. Y., Zhang, M., Wang, H. Y., Cai, Z., et al. (2017). USP13 negatively regulates antiviral responses by deubiquitinating STING. *Nat. Commun.* 8:15534. doi: 10.1038/ncomms15534

Tiede, C., Bedford, R., Heseltine, S. J., Smith, G., Wijetunga, I., Ross, R., et al. (2017). Affimer proteins are versatile and renewable affinity reagents. *eLife* 6:e24903. doi: 10.7554/eLife.24903

Tiede, C., Tang, A. A., Deacon, S. E., Mandal, U., Nettleship, J. E., Owen, R. L., et al. (2014). Adhiron: a stable and versatile peptide display scaffold for molecular recognition applications. *Protein Eng. Des. Sel.* 27, 145–155. doi: 10.1093/protein/gzu007

Tokunaga, F., Nakagawa, T., Nakahara, M., Saeki, Y., Taniguchi, M., Sakata, S., et al. (2011). SHARPIN is a component of the NF-kappaB-activating linear ubiquitin chain assembly complex. *Nature* 471, 633–636. doi: 10.1038/nature09815

Tokunaga, F., Sakata, S., Saeki, Y., Satomi, Y., Kirisako, T., Kamei, K., et al. (2009). Involvement of linear polyubiquitylation of NEMO in NF-kappaB activation. *Nat. Cell Biol.* 11, 123–132. doi: 10.1038/ncb1821

van Wijk, S. J., Fiskin, E., Putyrski, M., Pampaloni, F., Hou, J., Wild, P., et al. (2012). Fluorescence-based sensors to monitor localization and functions of linear and K63-linked ubiquitin chains in cells. *Mol. Cell* 47, 797–809. doi: 10.1016/j.molcel.2012.06.017

Wang, Q., Huang, L., Hong, Z., Lv, Z., Mao, Z., Tang, Y., et al. (2017). The E3 ubiquitin ligase RNF185 facilitates the cGAS-mediated innate immune response. *PLoS Pathog.* 13:e1006264. doi: 10.1371/journal.ppat.1006264

Wang, Q., Liu, X., Cui, Y., Tang, Y., Chen, W., Li, S., et al. (2014). The E3 ubiquitin ligase AMFR and INSIG1 bridge the activation of TBK1 kinase by modifying the adaptor STING. *Immunity* 41, 919–933. doi: 10.1016/j.immuni.2014.11.011

Wang, Y., Tang, C., Wang, E., and Wang, J. (2014). PolyUbiquitin chain linkage topology selects the functions from the underlying binding landscape. *PLoS Comput. Biol.* 10:e1003691. doi: 10.1371/journal.pcbi.1003691

Xu, M., Skaug, B., Zeng, W., and Chen, Z. J. (2009). A ubiquitin replacement strategy in human cells reveals distinct mechanisms of IKK activation by TNFalpha and IL-1beta. *Mol. Cell* 36, 302–314. doi: 10.1016/j.molcel.2009.10.002

Xue, B., Li, H., Guo, M., Wang, J., Xu, Y., Zou, X., et al. (2018). TRIM21 promotes innate immune response to RNA viral infection through Lys27-linked polyubiquitination of MAVS. *J. Virol.* 92:e00321-18. doi: 10.1128/JVI.00321-18

Yau, R. G., Doerner, K., Castellanos, E. R., Haakonsen, D. L., Werner, A., Wang, N., et al. (2017). Assembly and function of heterotypic ubiquitin chains in cell-cycle and protein quality control. *Cell* 171, 918.e20–933.e20. doi: 10.1016/j.cell.2017.09.040

Yu, Z., Chen, T., Li, X., Yang, M., Tang, S., Zhu, X., et al. (2016). Lys29-linkage of ASK1 by Skp1-Cullin 1-Fbxo21 ubiquitin ligase complex is required for antiviral innate response. *eLife* 5:e14087. doi: 10.7554/eLife.14087

Zhao, C., Jia, M., Song, H., Yu, Z., Wang, W., Li, Q., et al. (2017). The E3 ubiquitin ligase TRIM40 attenuates antiviral immune responses by targeting MDA5 and RIG-I. *Cell Rep.* 21, 1613–1623. doi: 10.1016/j.celrep.2017.10.020

Conflict of Interest: The authors declare that the research was conducted in the absence of any commercial or financial relationships that could be construed as a potential conflict of interest.

frontiers in Chemistry

MINI REVIEW
published: 22 January 2020
doi: 10.3389/fchem.2019.00931

Hybrid Chains: A Collaboration of Ubiquitin and Ubiquitin-Like Modifiers Introducing Cross-Functionality to the Ubiquitin Code

*David A. Pérez Berrocal, Katharina F. Witting, Huib Ovaa and Monique P. C. Mulder**

Department of Cell and Chemical Biology, Chemical Immunology, Leiden University Medical Center, Oncode Institute, Leiden, Netherlands

The Ubiquitin CODE constitutes a unique post-translational modification language relying on the covalent attachment of Ubiquitin (Ub) to substrates, with Ub serving as the minimum entity to generate a message that is translated into different cellular pathways. The creation of this message is brought about by the dedicated action of writers, erasers, and readers of the Ubiquitin CODE. This CODE is greatly expanded through the generation of polyUb chains of different architectures on substrates thus regulating their fate. Through additional post-translational modification by Ub-like proteins (UbL), hybrid Ub/UbL chains, which either alter the originally encrypted message or encode a completely new one, are formed. Hybrid Ub/UbL chains are generated under both stress or physiological conditions and seem to confer improved specificity and affinity toward their cognate receptors. In such a manner, their formation must play a specific, yet still undefined role in cellular signaling and thus understanding the UbCODE message is crucial. Here, we discuss the evidence for the existence of hybrid Ub/UbL chains in addition to the current understanding of its biology. The modification of Ub by another UbL complicates the deciphering of the spatial and temporal order of events warranting the development of a hybrid chain toolbox. We discuss this unmet need and expand upon the creation of tailored tools adapted from our previously established toolkit for the Ubiquitin Proteasome System to specifically target these hybrid Ub/UbL chains.

Keywords: ubiquitin-like modifiers, hybrid chains, SUMO and ubiquitin signaling, NEDD8, ISG15, proteotoxic conditions, stress conditions, toolbox

OPEN ACCESS

Edited by:
Laszlo Otvos, Olpe LLC, United States

Reviewed by:
Gary Kleiger, University of Nevada, Las Vegas, United States
Gunnar Dittmar, Luxembourg Institute of Health (LIH), Luxembourg

***Correspondence:**
Monique P. C. Mulder
m.p.c.mulder@lumc.nl

Specialty section:
This article was submitted to Chemical Biology, a section of the journal Frontiers in Chemistry

Received: *22 October 2019*
Accepted: *20 December 2019*
Published: *22 January 2020*

Citation:
Pérez Berrocal DA, Witting KF, Ovaa H and Mulder MPC (2020) Hybrid Chains: A Collaboration of Ubiquitin and Ubiquitin-Like Modifiers Introducing Cross-Functionality to the Ubiquitin Code. Front. Chem. 7:931. doi: 10.3389/fchem.2019.00931

INTRODUCTION

Ubiquitin (Ub) is a 76 amino acid, highly conserved protein among eukaryotes post-translationally modifying proteins thereby dictating almost every fundamental cellular process. Malfunction of its action drives diverse pathologies such as cancer and neurological disorders like Parkinson's, Alzheimer's, and Huntington's disease (McNaught et al., 2001; Du and Mei, 2013; Ciechanover and Kwon, 2015). It exerts its action through the covalent attachment of its C-terminus to the target substrates by an orchestrated enzymatic cascade composed by three different enzyme families

named E1, E2, E3 (writers of the code) (**Figure 1A**). This conjugation process, commonly referred to as ubiquitination, is initiated once the E1 activating enzyme catalyzes adenylation of the C-terminus of Ub at the expense of ATP thereby forming a high-energy E1-Ub thioester. Afterwards, the activated Ub is transferred by trans-thioesterification to the cysteine of the E2 conjugating enzyme which allows E3 ligase mediated Ub conjugation the substrate lysine residue through a stable peptide bond. Ub transfer to the substrate can be carried out by three different mechanisms depending on the nature of participating E3 ligase [RING, HECT, and RING-in-between-RING (RBR)] (Zheng and Shabek, 2017). Activated Ub can be transferred onto the catalytic cysteine of the HECT E3s via a transthioesterification reaction followed by conjugation to the lysine residue of the substrate. Alternatively, transfer of the E2-Ub thioester to the substrate lysine is accomplished by the contribution of a scaffolding RING E3 enzyme accommodating both the E2-Ub complex and the substrate. RBR E3s catalyze Ub conjugation by a concerted RING/HECT hybrid mechanism in which the RING1 domain recruits the E2-Ub complex, followed by thioester transfer of Ub to a cysteine in the RING2 domain (Spratt et al., 2014).

Different ubiquitination patterns can be observed depending on the constitution of the lysine residues of the substrate, giving rise to mono-ubiquitination or multi mono-ubiquitination, respectively. Additionally, this enzymatic process can be repeated by utilizing the ε-amine functionality of any of the seven internal lysine residues or the N-terminal amine of Ub. Thus, self-conjugation of Ub to any of these residues permits the formation of eight different homogenous polymeric Ub chains (M1, K6/11/27/29/33/48/63). Due to the different disposition adopted by each of these Ub linkages, a wide variety of cellular signaling (Akutsu et al., 2016) events can be modulated all exerting different biological outcomes. For instance, Lys-48 and Lys-63 linked poly-Ub, the best characterized polymeric chains are mainly involved in proteasome mediated protein degradation and cell signaling respectively, whereas the cellular responses of the remaining linkages, known as atypical chains, remains

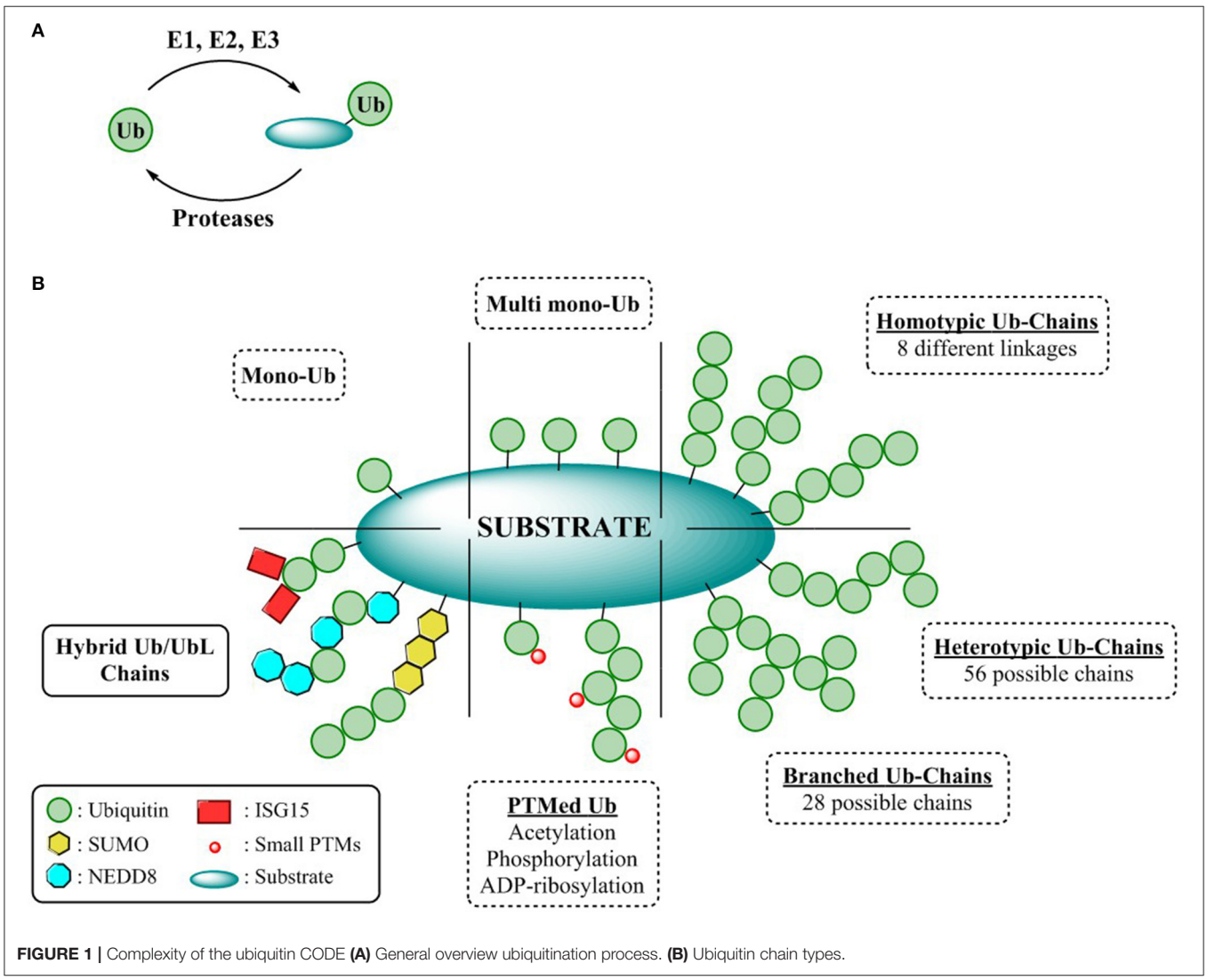

FIGURE 1 | Complexity of the ubiquitin CODE **(A)** General overview ubiquitination process. **(B)** Ubiquitin chain types.

undefined (Kulathu and Komander, 2012). Furthermore, complexity can be augmented through permutation of linkages, either through modification of different internal lysines (branched chains) or by repetition of different linkages within the chain (heterologous/mixed chains) thereby endowing the UbCODE with an extraordinary versatility and specificity (Nakasone et al., 2013; Stolz and Dikic, 2018; Haakonsen and Rape, 2019) (**Figure 1B**).

To counterbalance ubiquitination and further sculpting the physiological effects or rescuing proteins destined for proteasomal degradation, dedicated proteases known as deubiquitinases (DUBs) not only remove mono-Ub from their substrates, but also alter Ub chain topology (editors of the code) (Leznicki and Kulathu, 2017). Alternatively, modulating the formation and processing of Ub chains can be achieved through their interaction with Ubiquitin Binding Domains (UBDs). These UBDs are endowed with a specific affinity toward Ub or Ub chains permitting the modulation of both chain elongation as well as governing the interaction of the Ub chains with the substrates (Dikic et al., 2009).

While Ubiquitin represents the minimum entity to express a code, the Ubiquitin CODE as coined by Komander and Rape, it is a highly complex, yet still elusive signaling system reliant on the interplay of its "writers," "editors," and "readers" (Komander and Rape, 2012). Nonetheless, intricacy arises when Ub, is further "PTMylated" by the classical modifications such as acetylation (Ohtake et al., 2015), phosphorylation (Herhaus and Dikic, 2015), or ribosylation (Vivelo et al., 2019), or even by some Ubiquitin-like proteins (UbL). Structurally and biochemically similar to Ub, UbLs are covalently attached to the lysine residues of their substrates through the sequential action of dedicated activating, conjugating, and ligating enzymes. Conjugation of UbLs to Ub and vice versa, results in hybrid chains, expanding the utility of the Ubiquitin CODE to enable an extensive crosstalk among the different UbL pathways and the UPS (Schmidt and Dikic, 2006; Schimmel et al., 2008; Geoffroy and Hay, 2009; Hjerpe et al., 2012a) (**Figure 1B**). However, the assembly, topology, architecture, as well as the encoded information of these Ub/UbLs hybrid chains remains cryptic warranting the development of suitable reagents to decipher this intricate CODE.

Given the breadth of this review, we will focus on evidence supporting the existence of these Hybrid Chains with ubiquitin-like modifiers mainly composed of Ub and the UbL proteins NEDD8, SUMO, and ISG15 as well as the future potential for this emerging field. Additionally, we will touch upon the crosstalk between the Ubiquitin and the Ubiquitin-like enzyme cascades that cooperate to form hybrid Ub/UbL chains.

UBIQUITIN-LIKE PROTEINS AND HYBRID CHAIN FORMATION

Small Ubiquitin-Related Modifier (SUMO)

SUMOylation, which is involved in a large plethora of fundamental cellular processes, is catalyzed through the interplay of specific enzymes and counteracted by the action of SUMO specific isopeptidases (Pichler et al., 2017). The SUMO family is composed by three different members known as SUMO-1, -2, and -3, which, subsequent to the exposure of their C-terminal di-glycine signature, are conjugated onto specific lysines embedded within a SUMO consensus motif (ψ-Lys-X-Glu, with ψ encoding a hydrophobic residue of their substrates) (Geiss-Friedlander and Melchior, 2007). While the most predominant isoforms SUMO-2 and SUMO-3 are virtually identical and mainly form K11-linked polymeric chains (Matic et al., 2008; Hendriks et al., 2014), SUMO-1 bears only a 50% sequence similarity and does not form polymeric chains give the absence of the necessary conserved lysine residue within the consensus motif (Saitoh and Hinchey, 2000). However, it has been shown that SUMO-1 can be linked to the end of a poly-SUMO-2/-3 chain, effectively terminating chain growth (Matic et al., 2008). Formation of SUMO-2/-3 chains is elicited upon cellular stressors such as heat shock (Saitoh and Hinchey, 2000) and their recognition is mediated by SUMO interactive motifs (SIMs)- specific regions interacting with SUMO and SUMO polymers (Song et al., 2004).

Hybrid SUMO-Ub Chains

In addition to modification with SUMO itself, several proteomic studies have identified that Ubiquitination at various lysines in SUMO-1–3 can occur (Danielsen et al., 2011; Wagner et al., 2012; Hendriks et al., 2014; Hendriks and Vertegaal, 2016). Interestingly, while SUMO-1 cannot be SUMOylated, it is Ubiquitinated at six lysine residues most likely inducing a different response than Ubiquitinated SUMO-2/3 (Hendriks and Vertegaal, 2016). Thus, given the sheer number of Ubiquitination sites in SUMO a plethora of hybrid chains combinations are possible.

Intriguingly, proteomics revealed not only the vast number of modification possibilities on the different SUMO isoforms, but also allowed to identify whether the modification occurs on SUMO or on the Ubiquitin lysines (Hendriks et al., 2014, 2017), further increasing the complexity (**Figure 2A**). The hybrid chains predominantly occur upon specific stressors (Hendriks et al., 2014) (**Figure 2A**) and despite the advances in detection and elucidation of the branched architecture of SUMO-Ub hybrid chains, comprehending their cellular function is still in its infancy. Discerning their physiological roles is of utmost importance since the architecture of hybrid SUMO-Ub chains expands the potential for distinct signaling events by SUMO and Ub.

SUMO-Ub Chain Signaling

Hybrid chains can be recognized by a variety of receptors containing tandem SUMO-interacting motifs (SIMs) and UBDs. Moreover, to counterbalance or alter the effect of SUMOylation, subsequent ubiquitination of poly-SUMOylated proteins, catalyzed by SUMO-targeted Ubiquitin ligases (STUbls) can ensue. Upon recognition of the poly-SUMO signal through virtue of their SIMs, STUbls install a specific Ub-linkage onto the lysine of the SUMO-modification (Sriramachandran and Dohmen, 2014). Although, SUMO-Ub chains were primarily identified on proteins impending proteasomal degradation (Lallemand-Breitenbach et al., 2008; Tatham et al., 2008; Erker

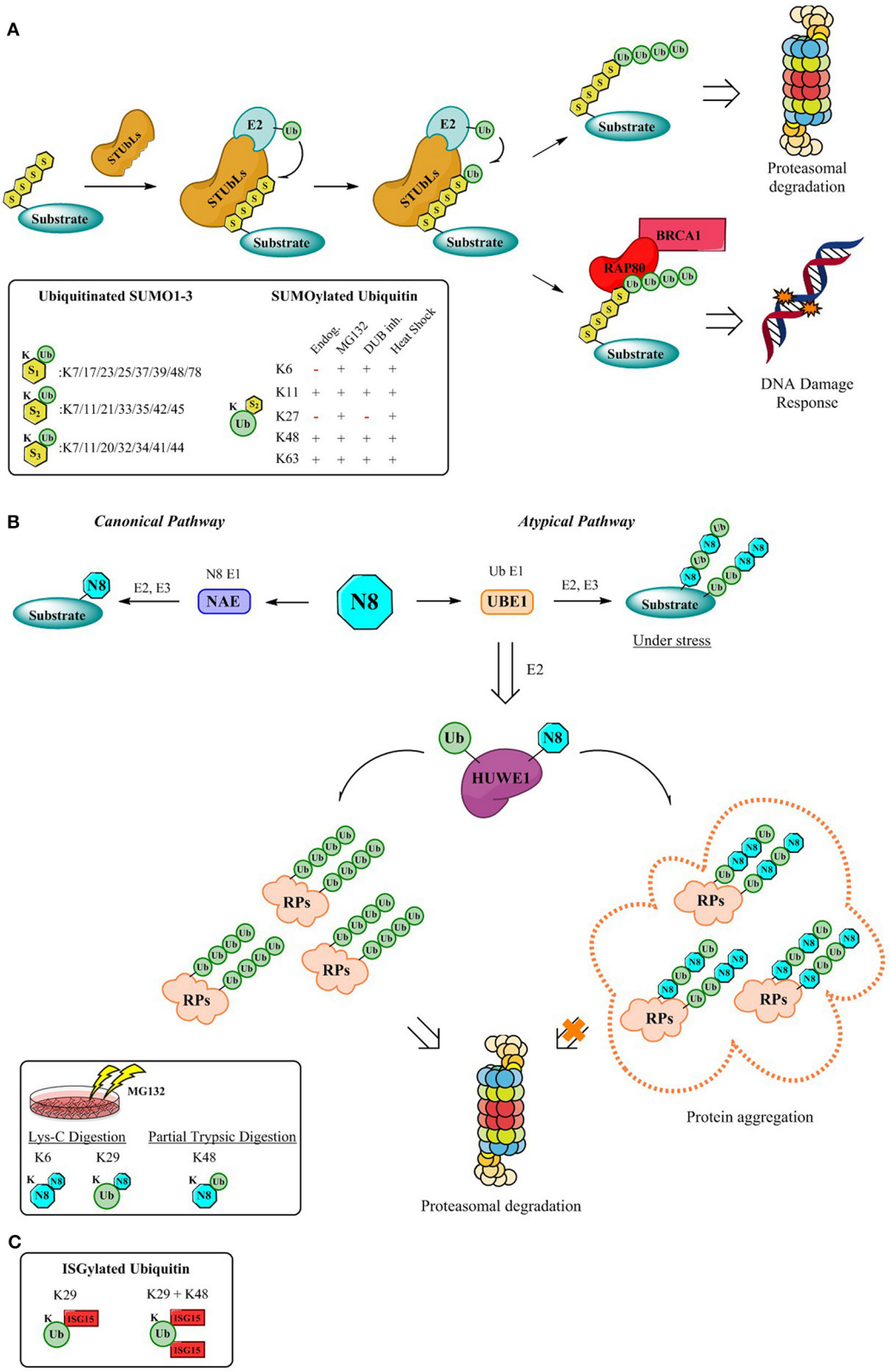

FIGURE 2 | Mechanism for the formation of hybrid chains. **(A)** StubLs containing tandem of SIMS recognize polySUMO2/3 chains and poly-ubiquitinate in a linkage specific manner the PolySUMO chains targeting them for enhanced proteasomal degradation (Aillet et al., 2012) or initiates signaling for DDR events through the RAP80/BRCA1 complex (Guzzo et al., 2012). The insert highlights ubiquitinitated SUMO1-3 (Hendriks and Vertegaal, 2016) and SUMOylated Ubiquitin identified by

(Continued)

FIGURE 2 | proteomics so far (Hendriks et al., 2014). **(B)** Canonical and atypical pathways (Leidecker et al., 2012) and dual activity of HUWE1 under stress conditions which lead to formation of hybrid chains which protect the UPS by via the formation of aggregates that are no longer processed by the proteasome (Maghames et al., 2018). The insert displays identified Ub-Nedd8 linkages (Leidecker et al., 2012). **(C)** Although the mechanism for the formation of ISG15 hybrid chains is still outstanding, data supporting the existence of Ub-ISG15 is available. First, K29 gets ISGylated, followed by K48 as the second ISG15 site (Fan et al., 2015).

et al., 2013; McIntosh et al., 2018), roles in maintaining genome stability (Guzzo et al., 2012; Nie and Boddy, 2016) have been assigned more recently through the K63 poly-ubiquitination of poly-SUMO chains (**Figure 2A**). Here RNF4, a STUbl, mediates poly-ubiquitination of SUMOylated proteins, thereby evoking the recruitment of RAP80 and its subsequent interaction with BRCA1 complex, to promote genomic stability (Guzzo et al., 2012). Another example involves Arkadia which ubiquitinates SUMOylated xeroderma pigmentosum C (XPC), a pivotal player in nucleotide excision repair, driving XPC to UV-damaged DNA sites (Poulsen et al., 2013).

DUBs such as USP11 can trim or reverse ubiquitination on hybrid SUMO-Ub chains to modulate the associated cellular responses (Hendriks et al., 2015). Thus, the amalgamation of ubiquitination and SUMOylation resembles an efficacious strategy to confer both specificity and increased affinity to the target proteins (Aillet et al., 2012; Guzzo et al., 2012).

Neural Precursor Cell Expressed, Developmentally Downregulated 8 (NEDD8)

Akin to SUMOylation, Neddylation is accomplished by its own specific enzymes and is counterbalanced by a few dedicated proteases (Enchev et al., 2015). Given the similarities between Ubiquitin and Nedd8, it is unsurprising that both have the propensity to form hybrid chains. However, the formation of Ubiquitin-Nedd8 hybrid chains occurs predominantly in response to proteotoxic stress, perhaps as a mechanism to dampen cellular signaling in this context or to protect the UPS from proteotoxicity (Maghames et al., 2018; Santonico, 2019). Neddylation and the Nedd8 enzyme cascade have been demonstrated to be crucial to the development of neurological disorders (Dil Kuazi et al., 2003; Mori et al., 2005; Chen et al., 2012; Lu et al., 2013). Thus, given the protective role of Ubiquitin-Nedd8 hybrid chains against proteotoxic stress, these complex posttranslational modifications may play a pivotal role in the pathogenesis and progression of neurodegenerative diseases (Ross and Poirier, 2004; Gestwicki and Garza, 2012; Dantuma and Bott, 2014; Valastyan and Lindquist, 2014; Sweeney et al., 2017).

In an attempt to elucidate the architecture of the hybrid chains several hybrid linkages were determined by SILAC-based proteomics upon proteasomal inhibition (Leidecker et al., 2012) (**Figure 2B**). Neddylation occurs via the interplay of enzymes relying on its own specificity and is referred to as the "Canonical" pathway. However, under stress conditions such as proteasome inhibition, oxidative stress, or heat shock Neddylation is mediated "atypically" by the Ubiquitin activating enzyme UBE1 instead (Hjerpe et al., 2012a,b; Leidecker et al., 2012). This tight synchronization of the Ubiquitin and Nedd8 systems to fine-tune the cellular response during proteotoxic stress has been observed not only for UBE1, but also for also for the E3 ligase HUWE1, a crucial component of the Protein Quality Control (PQC) pathway (Xirodimas et al., 2008; Sung et al., 2016a,b), which targets ribosomal proteins (RPs) and protects the UPS from stress-induced toxicity by ribosomal protein aggregation (Maghames et al., 2018) (**Figure 2B**). Importantly, during the persistence of stress, the unconjugated Ub pool is rapidly depleted triggering Neddylation through the Ubiquitin pathway and targeting several substrates typically ubiquitinated (Leidecker et al., 2012) (**Figure 2B**). Akin to the sophisticated regulatory system provided by DUBs, research underscores that Nedd8-Ub hybrid chains seem to be modulated in a similar fashion by DUBs subsequent to cellular stress (Leidecker et al., 2012; Singh et al., 2012, 2014).

Interferon (IFN)-Stimulated Gene 15 (ISG15)

Firstly identified upon IFN treatment on Ehrlich ascites tumor cells (Farrell et al., 1979), ISG15 had initially not been identified as an Ubiquitin-like protein, until cross-reactivity toward Ub antibodies suggested the existence of UbL proteins (Haas et al., 1987). Unlike all other UbLs, ISG15 is composed of two Ub like domains tethered by a "hinge" polypeptide sequence. Analogous to Ub, ISG15 can be conjugated onto the target substrates through the orchestrated interplay of its E1, E2, and E3 enzymes through its exposed C-terminal glycine (Perng and Lenschow, 2018). Given its increased activation upon interferon stimulation, conjugation of ISG15 to protein substrates plays a crucial role in the antiviral response and thereby constituting a key contributor to innate immunity (Harty et al., 2009; Durfee et al., 2010; Perng and Lenschow, 2018).

In contrast to Ub, SUMO and NEDD8 (Jones et al., 2008), ISG15 has not been reported to generate polymeric chains and does not seem to have specific ISG15-interacting motifs. Although some studies have suggested an antagonistic relationship of Ub and ISG15 in certain contexts such as during tumorigenesis (Liu et al., 2003; Desai et al., 2006; Kim et al., 2006; Malakhova and Zhang, 2008; Wood et al., 2011), evidence of a crosstalk between ISG15 and Ub conjugation pathways still remains perplexing. Unexpectedly, a proteomic study revealed that ISG15 was conjugated to Ub (Giannakopoulos et al., 2005), and further investigation by Zhang et al. corroborated the formation of hybrid ISG15-Ub chains (Fan et al., 2015) (**Figure 2C**).

Little is known about the biological function of these hybrid Ub-ISG15 chains, but it has been established that they do not act as proteasomal degradation signals. Thus, ISG15 could potentially function as a chain termination moiety to rescue ubiquitylated proteins from degradation. However, given the fact that ISG15 is predominantly conjugated to Ub via K29, a

plausible role of these hybrid chains could be modulation of K29-Ub mediated biological signaling (Kulathu and Komander, 2012). Moreover, this type of hybrid chains could trigger new signaling pathways exerting different biological outcomes, but the assignment of their biological role is a daunting task since no ISG15 interactive motifs have been identified and readers containing both UIM and ISG15 interacting motifs cannot be predicted.

PERSPECTIVES

Considering the impact of ubiquitination on regulating a vast array of fundamental biological processes, with dysregulation of the dedicated enzymes giving rise to pathologies such as cancer and neurodegenerative diseases, understanding its function merited the development and innovation of respective tools. Advances in synthetic strategies for generating ubiquitin, constituted a qualitative leap forward in the development of a plethora of ubiquitin assay reagents and numerous activity-based probes (ABPs) enabling study of enzymes involved in the complex system of ubiquitination (El Oualid et al., 2010; Ekkebus et al., 2013; Hameed et al., 2017).

The modification of Ub by another UbL complicates the deciphering of the spatial and temporal order of events, as well as the underlying biological role of this modification, underscoring the urgent need for new next generation ABPs and assay reagents. The lack of a robust methodology to chemically access some UbL proteins has hampered the study on the biological role that hybrid chains display as well as the identification of their readers, writers, erasers, and interpreters. Generating such complex hybrid chains is a challenging feat as the E2/E3 enzymes generating these linkages *in vitro* remain unknown. So far, only (semi)-synthetic strategies for obtaining ubiquitinated Rub1, the yeast NEDD8 homolog (Singh et al., 2014) and SUMO-2-K63diUb hybrid chains (Bondalapati et al., 2017) have been reported. Only in the last decade, efforts to devise synthetic strategies for UbL proteins such as Nedd8 (Mulder et al., 2014), SUMO (Dobrota et al., 2012; Wucherpfennig et al., 2014; Mulder et al., 2018) and Ufm1 (Ogunkoya et al., 2012; Witting et al., 2018) have been undertaken. More recently, ISG15 synthesis has been accomplished as a modular synthesis of both domains and its subsequent ligation (Xin et al., 2019). These developments in the chemical synthesis of UbL proteins in combination with the advancements made in polyUb probes (Mulder et al., 2014; Flierman et al., 2016; Paudel et al., 2019) open a new avenue to UbL and hybrid Ub/UbL reagents allowing research on their respective enzymatic cascades, but also enabling in depth studies on their crosstalk with ubiquitin.

Mass spectrometry (MS) has become an invaluable tool in the quest for understanding cell signaling and in particular to study the UPS (Heap et al., 2017). This type of proteomics relies on the isolation and enrichment of the target proteins through affinity-based approaches (Mattern et al., 2019) such as affimers, antibodies targeting the di-Glycine signature, anti/mini/nanobodies, endogenous tags, biotin, and molecular entities based in the repetition of UBDs and SIMs capturing poly-Ub and SUMO chains, respectively (TUBES and SUBES) (Hjerpe et al., 2009; Da Silva-Ferrada et al., 2013) with a high affinity. However, many of these approaches cannot be undertaken in the study toward hybrid Ub-UbL biology since they are not endowed with specific affinity toward these linkages or due to the shared homology under Ub and UbL proteins as exemplified by the shared GG remnant after enzymatic digestion. To overcome these pitfalls, an UbiSite antibody approach (Akimov et al., 2018) which relies on LysC digestion has recently been described to allow differentiation among Ub and UbL proteins. The translation of the existing affinity technologies toward hybrid chains and UbL proteins would facilitate the understanding of the crosstalk among the different Ub-UbL proteins. For example, an elegant combination of SIMs and UBDs, a mixed TUBE/SUBE approach, could potentially enrich for substrates endowed with hybrid chains generated by STUbLs. Unsurprisingly due to the high similarity of Nedd8 and Ub, all known binding domains with affinity for Nedd8 display cross-reactivity with Ub. Recently, the first specific binding domain for Nedd8 was reported (Castagnoli et al., 2019) and thus a similar approach as the TUBES/SUBES could potentially be designed, "NEBES."

Furthermore, a proteomic approach called Ubi-clipping (Swatek et al., 2019) has shown the great percentage (10–20%) of which branched chains are present in polymeric forms of Ub. This method relies on an engineered version of an ISG15-specificenzyme that partially removes Ub from substrates and leave the characteristic diglycine signature on Ub while simultaneously allowing the identification of different branched architectures. The translation of such technology into the hybrid chains field would shed light on the different architectures that such chains exhibit. In addition to this innovation, the generation of specific antibodies toward the linkage of hybrid chains, in a similar fashion as the first Ub branched K11/K48 antibody (Yau et al., 2017) could be a feasible approach toward the generation a Hybrid Chain Tool Box.

Despite the recent advances made in developing innovative reagents on the Ubiquitin-field, there are still many conundrums to be resolved regarding the writers, editors and readers of this part of the Ub CODE. The origin of the identified Ub-SUMO linkages in which Ub is SUMOylated is still unclear, the possibility of a parallel mechanism such as the STUbL in which SUMO ligases target polyUb-chains and SUMOylate (UbTSLs) them might explain their existence. The enzymes catalyzing the formation of Ub-ISG15 hybrid chains are still unknown and efforts to identify them should be undertaken. Moreover, the formation of these hybrid chains confers an extra layer of complexity to the CODE that could be translated into terms of specificity and increased affinity that the "readers" display for them. Such readers must be endowed with "hybrid" recognition domains which could be screened by bioinformatic analysis as exemplified in the discovery of RAP80 (Nie and Boddy, 2016). It has been shown that hybrid chains are processed by the proteasome more efficiently compared with poly-Ub or poly-SUMO chains. This pronounced affinity could be derived from the improved recognition of either a proteasome subunit or of a shuttle protein containing

the aforementioned "hybrid" recognition domains. For the Ub-Nedd8 and Ub-ISG15 hybrid chains, the field is less explored and hybrid chain recognition domains still need to be identified.

The fact that Ub and UbL proteins can generate this array of chains, conferring new architectures and topology to the chains and thereby triggering different signaling events, increases complexity of the already intricate Ubiquitin CODE. The current knowledge regarding hybrid-chain formation is based upon chain formation between Ub and UbL proteins. However, a recent report revealed that a small fraction of NEDD8 becomes modified by K0-SUMO (Hendriks et al., 2017). Although SUMOylation of NEDD8 is likely to be a very rare event, it does extend the knowledge regarding hybrid chain cross-talk and opens a new perspective to the intrinsic code (Hendriks et al., 2014). The creation of tailored tools specific toward these hybrid chains by adapting the methodology already applied for the study of the Ubiquitin Proteasome System will augment our knowledge about hybrid chains.

AUTHOR CONTRIBUTIONS

DP, KW, and MM wrote sections of the manuscript. All authors contributed to manuscript revision, read, and approved the submitted version.

FUNDING

This work was supported by the European Union's Horizon 2020 research and innovation programme under the Marie Skłodowska-Curie grant agreement No. 765445. MM was supported by an Off Road grant (ZonMw #451001024).

REFERENCES

Aillet, F., Lopitz-Otsoa, F., Egaña, I., Hjerpe, R., Fraser, P., Hay, R. T., et al. (2012). Heterologous SUMO-2/3-ubiquitin chains optimize IκBα degradation and NF-κB activity. *PLoS ONE* 7:e51672. doi: 10.1371/journal.pone.0051672

Akimov, V., Barrio-Hernandez, I., Hansen, S. V. F., Hallenborg, P., Pedersen, A.-K., Bekker-Jensen, D. B., et al. (2018). UbiSite approach for comprehensive mapping of lysine and N-terminal ubiquitination sites. *Nat. Struct. Mol. Biol.* 25, 631–640. doi: 10.1038/s41594-018-0084-y

Akutsu, M., Dikic, I., and Bremm, A. (2016). Ubiquitin chain diversity at a glance. *J. Cell Sci.* 129, 875–880. doi: 10.1242/jcs.183954

Bondalapati, S., Eid, E., Mali, S. M., Wolberger, C., and Brik, A. (2017). Total chemical synthesis of SUMO-2-Lys63-linked diubiquitin hybrid chains assisted by removable solubilizing tags. *Chem. Sci.* 8, 4027–4034. doi: 10.1039/C7SC00488E

Castagnoli, L., Mandaliti, W., Nepravishta, R., Valentini, E., Mattioni, A., Procopio, R., et al. (2019). Selectivity of the CUBAN domain in the recognition of ubiquitin and NEDD8. *FEBS J.* 286, 653–677. doi: 10.1111/febs.14752

Chen, Y., Neve, R. L., and Liu, H. (2012). Neddylation dysfunction in Alzheimer's disease. *J. Cell. Mol. Med.* 16, 2583–2591. doi: 10.1111/j.1582-4934.2012.01604.x

Ciechanover, A., and Kwon, Y. T. (2015). Degradation of misfolded proteins in neurodegenerative diseases: therapeutic targets and strategies. *Exp. Mol. Med.* 47:e147. doi: 10.1038/emm.2014.117

Da Silva-Ferrada, E., Xolalpa, W., Lang, V., Aillet, F., Martin-Ruiz, I., de la Cruz-Herrera, C. F., et al. (2013). Analysis of SUMOylated proteins using SUMO-traps. *Sci. Rep.* 3:1690. doi: 10.1038/srep01690

Danielsen, J. M., Sylvestersen, K. B., Bekker-Jensen, S., Szklarczyk, D., Poulsen, J. W., Horn, H., et al. (2011). Mass spectrometric analysis of lysine ubiquitylation reveals promiscuity at site level. *Mol. Cell. Proteomics* 10:M110.003590. doi: 10.1074/mcp.M110.003590

Dantuma, N. P., and Bott, L. C. (2014). The ubiquitin-proteasome system in neurodegenerative diseases: precipitating factor, yet part of the solution. *Front. Mol. Neurosci.* 7:70. doi: 10.3389/fnmol.2014.00070

Desai, S. D., Haas, A. L., Wood, L. M., Tsai, Y. C., Pestka, S., Rubin, E. H., et al. (2006). Elevated expression of ISG15 in tumor cells interferes with the ubiquitin/26S proteasome pathway. *Cancer Res.* 66, 921–928. doi: 10.1158/0008-5472.CAN-05-1123

Dikic, I., Wakatsuki, S., and Walters, K. J. (2009). Ubiquitin-binding domains — from structures to functions. *Nat. Rev. Mol. Cell Biol.* 10:659. doi: 10.1038/nrm2767

Dil Kuazi, A., Kito, K., Abe, Y., Shin, R.-W., Kamitani, T., and Ueda, N. (2003). NEDD8 protein is involved in ubiquitinated inclusion bodies. *J. Pathol.* 199, 259–266. doi: 10.1002/path.1283

Dobrota, C., Fasci, D., Hadade, N. D., Roiban, G. D., Pop, C., Meier, V. M., et al. (2012). Glycine fluoromethylketones as SENP-specific activity based probes. *Chembiochem* 13, 80–84. doi: 10.1002/cbic.201100645

Du, W., and Mei, Q.-B. (2013). Ubiquitin-proteasome system, a new anti-tumor target. *Acta Pharmacol. Sin.* 34, 187–188. doi: 10.1038/aps.2012.192

Durfee, L. A., Lyon, N., Seo, K., and Huibregtse, J. M. (2010). The ISG15 conjugation system broadly targets newly synthesized proteins: implications for the antiviral function of ISG15. *Mol. Cell* 38, 722–732. doi: 10.1016/j.molcel.2010.05.002

Ekkebus, R., van Kasteren, S. I., Kulathu, Y., Scholten, A., Berlin, I., Geurink, P. P., et al. (2013). On terminal alkynes that can react with active-site cysteine nucleophiles in proteases. *J. Am. Chem. Soc.* 135, 2867–2870. doi: 10.1021/ja309802n

El Oualid, F., Merkx, R., Ekkebus, R., Hameed, D. S., Smit, J. J., de Jong, A., et al. (2010). Chemical synthesis of ubiquitin, ubiquitin-based probes, and diubiquitin. *Angew. Chem.* 49, 10149–10153. doi: 10.1002/anie.201005995

Enchev, R. I., Schulman, B. A., and Peter, M. (2015). Protein neddylation: beyond cullin-RING ligases. *Nat. Rev. Mol. Cell Biol.* 16, 30–44. doi: 10.1038/nrm3919

Erker, Y., Neyret-Kahn, H., Seeler, J. S., Dejean, A., Atfi, A., and Levy, L. (2013). Arkadia, a novel SUMO-targeted ubiquitin ligase involved in PML degradation. *Mol. Cell. Biol.* 33, 2163–2177. doi: 10.1128/MCB.01019-12

Fan, J.-B., Arimoto, K.-L., Motamedchaboki, K., Yan, M., Wolf, D. A., and Zhang, D.-E. (2015). Identification and characterization of a novel ISG15-ubiquitin mixed chain and its role in regulating protein homeostasis. *Sci. Rep.* 5:12704. doi: 10.1038/srep12704

Farrell, P. J., Broeze, R. J., and Lengyel, P. (1979). Accumulation of an mRNA and protein in interferon-treated Ehrlich ascites tumour cells. *Nature* 279, 523–525. doi: 10.1038/279523a0

Fliermann, D., van Noort, G. J. V., Ekkebus, R., Geurink, P. P., Mevissen, T. E. T., Hospenthal, M. K., et al. (2016). Non-hydrolyzable diubiquitin probes reveal linkage-specific reactivity of deubiquitylating enzymes mediated by S2 pockets. *Cell Chem. Biol.* 23, 472–482. doi: 10.1016/j.chembiol.2016.03.009

Geiss-Friedlander, R., and Melchior, F. (2007). Concepts in sumoylation: a decade on. *Nat. Rev. Mol. Cell Biol.* 8, 947–956. doi: 10.1038/nrm2293

Geoffroy, M. C., and Hay, R. T. (2009). An additional role for SUMO in ubiquitin-mediated proteolysis. *Nat. Rev. Mol. Cell Biol.* 10, 564–568. doi: 10.1038/nrm2707

Gestwicki, J. E., and Garza, D. (2012). Protein quality control in neurodegenerative disease. *Prog. Mol. Biol. Transl. Sci.* 107, 327–353. doi: 10.1016/B978-0-12-385883-2.00003-5

Giannakopoulos, N. V., Luo, J. K., Papov, V., Zou, W., Lenschow, D. J., Jacobs, B. S., et al. (2005). Proteomic identification of proteins conjugated to ISG15 in mouse and human cells. *Biochem. Biophys. Res. Commun.* 336, 496–506. doi: 10.1016/j.bbrc.2005.08.132

Guzzo, C. M., Berndsen, C. E., Zhu, J., Gupta, V., Datta, A., Greenberg, R. A., et al. (2012). RNF4-dependent hybrid SUMO-ubiquitin chains are signals for RAP80

and thereby mediate the recruitment of BRCA1 to sites of DNA damage. *Sci. Signal.* 5:ra88. doi: 10.1126/scisignal.2003485

Haakonsen, D. L., and Rape, M. (2019). Branching out: improved signaling by heterotypic ubiquitin chains. *Trends Cell Biol.* 29, 704–716. doi: 10.1016/j.tcb.2019.06.003

Haas, A. L., Ahrens, P., Bright, P. M., and Ankel, H. (1987). Interferon induces a 15-kilodalton protein exhibiting marked homology to ubiquitin. *J. Biol. Chem.* 262, 11315–11323.

Hameed, D. S., Sapmaz, A., and Ovaa, H. (2017). How chemical synthesis of ubiquitin conjugates helps to understand ubiquitin signal transduction. *Bioconjug. Chem.* 28, 805–815. doi: 10.1021/acs.bioconjchem.6b00140

Harty, R. N., Pitha, P. M., and Okumura, A. (2009). Antiviral activity of innate immune protein ISG15. *J. Innate Immun.* 1, 397–404. doi: 10.1159/000226245

Heap, R. E., Gant, M. S., Lamoliatte, F., Peltier, J., and Trost, M. (2017). Mass spectrometry techniques for studying the ubiquitin system. *Biochem. Soc. Trans.* 45, 1137–1148. doi: 10.1042/BST20170091

Hendriks, I. A., D'Souza, R. C., Yang, B., Verlaan-de Vries, M., Mann, M., and Vertegaal, A. C. (2014). Uncovering global SUMOylation signaling networks in a site-specific manner. *Nat. Struct. Mol. Biol.* 21, 927–936. doi: 10.1038/nsmb.2890

Hendriks, I. A., Lyon, D., Young, C., Jensen, L. J., Vertegaal, A. C., and Nielsen, M. L. (2017). Site-specific mapping of the human SUMO proteome reveals co-modification with phosphorylation. *Nat. Struct. Mol. Biol.* 24, 325–336. doi: 10.1038/nsmb.3366

Hendriks, I. A., Schimmel, J., Eifler, K., Olsen, J. V., and Vertegaal, A. C. (2015). Ubiquitin-specific protease 11 (USP11). Deubiquitinates hybrid Small Ubiquitin-like Modifier (SUMO)-ubiquitin chains to counteract RING Finger Protein 4 (RNF4). *J. Biol. Chem.* 290, 15526–15537. doi: 10.1074/jbc.M114.618132

Hendriks, I. A., and Vertegaal, A. C. (2016). A comprehensive compilation of SUMO proteomics. *Nat. Rev. Mol. Cell Biol.* 17, 581–595. doi: 10.1038/nrm.2016.81

Herhaus, L., and Dikic, I. (2015). Expanding the ubiquitin code through post-translational modification. *EMBO Rep.* 16, 1071–1083. doi: 10.15252/embr.201540891

Hjerpe, R., Aillet, F., Lopitz-Otsoa, F., Lang, V., England, P., and Rodriguez, M. S. (2009). Efficient protection and isolation of ubiquitylated proteins using tandem ubiquitin-binding entities. *EMBO Rep.* 10, 1250–1258. doi: 10.1038/embor.2009.192

Hjerpe, R., Thomas, Y., Chen, J., Zemla, A., Curran, S., Shpiro, N., et al. (2012a). Changes in the ratio of free NEDD8 to ubiquitin triggers NEDDylation by ubiquitin enzymes. *Biochem. J.* 441, 927–936. doi: 10.1042/BJ20111671

Hjerpe, R., Thomas, Y., and Kurz, T. (2012b). NEDD8 overexpression results in neddylation of ubiquitin substrates by the ubiquitin pathway. *J. Mol. Biol.* 421, 27–29. doi: 10.1016/j.jmb.2012.05.013

Jones, J., Wu, K., Yang, Y., Guerrero, C., Nillegoda, N., Pan, Z. Q., et al. (2008). A targeted proteomic analysis of the ubiquitin-like modifier nedd8 and associated proteins. *J. Proteome Res.* 7, 1274–1287. doi: 10.1021/pr700749v

Kim, K. I., Yan, M., Malakhova, O., Luo, J. K., Shen, M. F., Zou, W., et al. (2006). Ube1L and protein ISGylation are not essential for alpha/beta interferon signaling. *Mol. Cell. Biol.* 26, 472–479. doi: 10.1128/MCB.26.2.472-479.2006

Komander, D., and Rape, M. (2012). The ubiquitin code. *Annu. Rev. Biochem.* 81, 203–229. doi: 10.1146/annurev-biochem-060310-170328

Kulathu, Y., and Komander, D. (2012). Atypical ubiquitylation - the unexplored world of polyubiquitin beyond Lys48 and Lys63 linkages. *Nat. Rev. Mol. Cell Biol.* 13, 508–523. doi: 10.1038/nrm3394

Lallemand-Breitenbach, V., Jeanne, M., Benhenda, S., Nasr, R., Lei, M., Peres, L., et al. (2008). Arsenic degrades PML or PML-RARalpha through a SUMO-triggered RNF4/ubiquitin-mediated pathway. *Nat. Cell Biol.* 10, 547–555. doi: 10.1038/ncb1717

Leidecker, O., Matic, I., Mahata, B., Pion, E., and Xirodimas, D. P. (2012). The ubiquitin E1 enzyme Ube1 mediates NEDD8 activation under diverse stress conditions. *Cell Cycle* 11, 1142–1150. doi: 10.4161/cc.11.6.19559

Leznicki, P., and Kulathu, Y. (2017). Mechanisms of regulation and diversification of deubiquitylating enzyme function. *J. Cell Sci.* 130, 1997–2006. doi: 10.1242/jcs.201855

Liu, M., Li, X. L., and Hassel, B. A. (2003). Proteasomes modulate conjugation to the ubiquitin-like protein, ISG15. *J. Biol. Chem.* 278, 1594–1602. doi: 10.1074/jbc.M208123200

Lu, B., Al-Ramahi, I., Valencia, A., Wang, Q., Berenshteyn, F., Yang, H., et al. (2013). Identification of NUB1 as a suppressor of mutant Huntingtin toxicity via enhanced protein clearance. *Nat. Neurosci.* 16:562. doi: 10.1038/nn.3367

Maghames, C. M., Lobato-Gil, S., Perrin, A., Trauchessec, H., Rodriguez, M. S., Urbach, S., et al. (2018). NEDDylation promotes nuclear protein aggregation and protects the Ubiquitin Proteasome System upon proteotoxic stress. *Nat. Commun.* 9:4376. doi: 10.1038/s41467-018-06365-0

Malakhova, O. A., and Zhang, D. E. (2008). ISG15 inhibits Nedd4 ubiquitin E3 activity and enhances the innate antiviral response. *J. Biol. Chem.* 283, 8783–8787. doi: 10.1074/jbc.C800030200

Matic, I., van Hagen, M., Schimmel, J., Macek, B., Ogg, S. C., Tatham, M. H., et al. (2008). *In vivo* Identification of human small ubiquitin-like modifier polymerization sites by high accuracy mass spectrometry and an *in vitro* to *in vivo* strategy. *Moll Cell Proteomics* 7, 132–144. doi: 10.1074/mcp.M700173-MCP200

Mattern, M., Sutherland, J., Kadimisetty, K., Barrio, R., and Rodriguez, M. S. (2019). Using ubiquitin binders to decipher the ubiquitin code. *Trends Biochem. Sci.* 44, 599–615. doi: 10.1016/j.tibs.2019.01.011

McIntosh, D. J., Walters, T. S., Arinze, I. J., and Davis, J. (2018). Arkadia (RING finger protein 111). Mediates sumoylation-dependent stabilization of Nrf2 through K48-linked ubiquitination. *Cell. Physiol. Biochem.* 46, 418–430. doi: 10.1159/000488475

McNaught, K. S. P., Olanow, C. W., Halliwell, B., Isacson, O., and Jenner, P. (2001). Failure of the ubiquitin–proteasome system in Parkinson's disease. *Nat. Rev. Neurosci.* 2, 589–594. doi: 10.1038/35086067

Mori, F., Nishie, M., Piao, Y.-S., Kito, K., Kamitani, T., Takahashi, H., et al. (2005). Accumulation of NEDD8 in neuronal and glial inclusions of neurodegenerative disorders. *Neuropathol. Appl. Neurobiol.* 31, 53–61. doi: 10.1111/j.1365-2990.2004.00603.x

Mulder, M. P. C., El Oualid, F., ter Beek, J., and Ovaa, H. (2014). A native chemical ligation handle that enables the synthesis of advanced activity-based probes: diubiquitin as a case study. *Chembiochem* 15, 946–949. doi: 10.1002/cbic.201402012

Mulder, M. P. C., Merkx, R., Witting, K. F., Hameed, D. S., El Atmioui, D., Lelieveld, L., et al. (2018). Total chemical synthesis of SUMO and SUMO-based probes for profiling the activity of SUMO-specific proteases. *Angew. Chem.* 57, 8958–8962. doi: 10.1002/anie.201803483

Nakasone, M. A., Livnat-Levanon, N., Glickman, M. H., Cohen, R. E., and Fushman, D. (2013). Mixed-linkage ubiquitin chains send mixed messages. *Structure* 21, 727–740. doi: 10.1016/j.str.2013.02.019

Nie, M., and Boddy, M. N. (2016). Cooperativity of the SUMO and ubiquitin pathways in genome stability. *Biomolecules* 6:14. doi: 10.3390/biom6010014

Ogunkoya, A. O., Pattabiraman, V. R., and Bode, J. W. (2012). Sequential alpha-ketoacid-hydroxylamine (KAHA). ligations: synthesis of C-terminal variants of the modifier protein UFM1. *Angew. Chem.* 51, 9693–9697. doi: 10.1002/anie.201204144

Ohtake, F., Saeki, Y., Sakamoto, K., Ohtake, K., Nishikawa, H., Tsuchiya, H., et al. (2015). Ubiquitin acetylation inhibits polyubiquitin chain elongation. *EMBO Rep.* 16, 192–201. doi: 10.15252/embr.201439152

Paudel, P., Zhang, Q., Leung, C., Greenberg, H. C., Guo, Y., Chern, Y.-H., et al. (2019). Crystal structure and activity-based labeling reveal the mechanisms for linkage-specific substrate recognition by deubiquitinase USP9X. *Proc. Natl. Acad. Sci. U.S.A.* 116, 7288–7297. doi: 10.1073/pnas.1815027116

Perng, Y. C., and Lenschow, D. J. (2018). ISG15 in antiviral immunity and beyond. *Nat. Rev. Microbiol.* 16, 423–439. doi: 10.1038/s41579-018-0020-5

Pichler, A., Fatouros, C., Lee, H., and Eisenhardt, N. (2017). SUMO conjugation - a mechanistic view. *Biomol. Concepts* 8, 13–36. doi: 10.1515/bmc-2016-0030

Poulsen, S. L., Hansen, R. K., Wagner, S. A., van Cuijk, L., van Belle, G. J., Streicher, W., et al. (2013). RNF111/Arkadia is a SUMO-targeted ubiquitin ligase that facilitates the DNA damage response. *J. Cell Biol.* 201, 797–807. doi: 10.1083/jcb.201212075

Ross, C. A., and Poirier, M. A. (2004). Protein aggregation and neurodegenerative disease. *Nat. Med.* 10, S10–S17. doi: 10.1038/nm1066

Saitoh, H., and Hinchey, J. (2000). Functional heterogeneity of small ubiquitin-related protein modifiers SUMO-1 versus SUMO-2/3. *J. Biol. Chem.* 275, 6252–6258. doi: 10.1074/jbc.275.9.6252

Santonico, E. (2019). "New insights into the mechanisms underlying NEDD8 structural and functional specificities," in *Ubiquitin Proteasome System Current Insights into Mechanism Cellular Regulation and Disease* (IntechOpen). Available online at: https://www.intechopen.com/books/ubiquitin-proteasome-system-current-insights-into-mechanism-cellular-regulation-and-disease

Schimmel, J., Larsen, K. M., Matic, I., van Hagen, M., Cox, J., Mann, M., et al. (2008). The ubiquitin-proteasome system is a key component of the SUMO-2/3 cycle. *Mol. Cell. Proteomics* 7, 2107–2122. doi: 10.1074/mcp.M800025-MCP200

Schmidt, M. H. H., and Dikic, I. (2006). Ubiquitin and NEDD8: brothers in arms. *Sci. STKE* 2006:pe50. doi: 10.1126/stke.3622006pe50

Singh, R. K., Sundar, A., and Fushman, D. (2014). Nonenzymatic rubylation and ubiquitination of proteins for structural and functional studies. *Angew. Chem.* 53, 6120–6125. doi: 10.1002/anie.201402642

Singh, R. K., Zerath, S., Kleifeld, O., Scheffner, M., Glickman, M. H., and Fushman, D. (2012). Recognition and cleavage of related to ubiquitin 1 (Rub1). and Rub1-ubiquitin chains by components of the ubiquitin-proteasome system. *Mol. Cell. Proteomics* 11, 1595–1611. doi: 10.1074/mcp.M112.022467

Song, J., Durrin, L. K., Wilkinson, T. A., Krontiris, T. G., and Chen, Y. (2004). Identification of a SUMO-binding motif that recognizes SUMO-modified proteins. *Proc. Natl. Acad. Sci. U.S.A.* 101, 14373–14378. doi: 10.1073/pnas.0403498101

Spratt, D. E., Walden, H., and Shaw, G. S. (2014). RBR E3 ubiquitin ligases: new structures, new insights, new questions. *Biochem. J.* 458, 421–437. doi: 10.1042/BJ20140006

Sriramachandran, A. M., and Dohmen, R. J. (2014). SUMO-targeted ubiquitin ligases. *Biochim. Biophys. Acta* 1843, 75–85. doi: 10.1016/j.bbamcr.2013.08.022

Stolz, A., and Dikic, I. (2018). Heterotypic ubiquitin chains: seeing is believing. *Trends Cell Biol.* 28, 1–3. doi: 10.1016/j.tcb.2017.11.005

Sung, M. K., Porras-Yakushi, T. R., Reitsma, J. M., Huber, F. M., Sweredoski, M. J., Hoelz, A., et al. (2016a). A conserved quality-control pathway that mediates degradation of unassembled ribosomal proteins. *eLife* 5:e19105. doi: 10.7554/eLife.19105.026

Sung, M. K., Reitsma, J. M., Sweredoski, M. J., Hess, S., and Deshaies, R. J. (2016b). Ribosomal proteins produced in excess are degraded by the ubiquitin-proteasome system. *Mol. Biol. Cell* 27, 2642–2652. doi: 10.1091/mbc.e16-05-0290

Swatek, K. N., Usher, J. L., Kueck, A. F., Gladkova, C., Mevissen, T. E. T., Pruneda, J. N., et al. (2019). Insights into ubiquitin chain architecture using Ub-clipping. *Nature* 572, 533–537. doi: 10.1038/s41586-019-1482-y

Sweeney, P., Park, H., Baumann, M., Dunlop, J., Frydman, J., Kopito, R., et al. (2017). Protein misfolding in neurodegenerative diseases: implications and strategies. *Transl. Neurodegener.* 6:6. doi: 10.1186/s40035-017-0077-5

Tatham, M. H., Geoffroy, M. C., Shen, L., Plechanovova, A., Hattersley, N., Jaffray, E. G., et al. (2008). RNF4 is a poly-SUMO-specific E3 ubiquitin ligase required for arsenic-induced PML degradation. *Nat. Cell Biol.* 10, 538–546. doi: 10.1038/ncb1716

Valastyan, J. S., and Lindquist, S. (2014). Mechanisms of protein-folding diseases at a glance. *Dis. Models Mech.* 7, 9–14. doi: 10.1242/dmm.013474

Vivelo, C. A., Ayyappan, V., and Leung, A. K. L. (2019). Poly(ADP-ribose)-dependent ubiquitination and its clinical implications. *Biochem. Pharmacol.* 167, 3–12. doi: 10.1016/j.bcp.2019.05.006

Wagner, S. A., Beli, P., Weinert, B. T., Schölz, C., Kelstrup, C. D., Young, C., et al. (2012). Proteomic analyses reveal divergent ubiquitylation site patterns in murine tissues. *Mol. Cell. Proteomics* 11, 1578–1585. doi: 10.1074/mcp.M112.017905

Witting, K. F., van der Heden van Noort, G. J., Kofoed, C., Talavera Ormeno, C., El Atmioui, D., Mulder, M. P. C., et al. (2018). Generation of the UFM1 toolkit for profiling UFM1-specific proteases and ligases. *Angew. Chem.* 57, 14164–14168. doi: 10.1002/anie.201809232

Wood, L. M., Sankar, S., Reed, R. E., Haas, A. L., Liu, L. F., McKinnon, P., et al. (2011). A novel role for ATM in regulating proteasome-mediated protein degradation through suppression of the ISG15 conjugation pathway. *PLoS ONE* 6:e16422. doi: 10.1371/journal.pone.0016422

Wucherpfennig, T. G., Pattabiraman, V. R., Limberg, F. R., Ruiz-Rodriguez, J., and Bode, J. W. (2014). Traceless preparation of C-terminal alpha-ketoacids for chemical protein synthesis by alpha-ketoacid-hydroxylamine ligation: synthesis of SUMO2/3. *Angew. Chem.* 53, 12248–12252. doi: 10.1002/anie.201407014

Xin, B.-T., Gan, J., Fernandez, D. J., Knobeloch, K.-P., Geurink, P. P., and Ovaa, H. (2019). Total chemical synthesis of murine ISG15 and an activity-based probe with physiological binding properties. *Org. Biomol. Chem.* 17, 10148–10152. doi: 10.1039/C9OB02127B

Xirodimas, D. P., Sundqvist, A., Nakamura, A., Shen, L., Botting, C., and Hay, R. T. (2008). Ribosomal proteins are targets for the NEDD8 pathway. *EMBO Rep.* 9, 280–286. doi: 10.1038/embor.2008.10

Yau, R. G., Doerner, K., Castellanos, E. R., Haakonsen, D. L., Werner, A., Wang, N., et al. (2017). Assembly and function of heterotypic ubiquitin chains in cell-cycle and protein quality control. *Cell* 171, 918–933.e20. doi: 10.1016/j.cell.2017.09.040

Zheng, N., and Shabek, N. (2017). Ubiquitin ligases: structure, function, and regulation. *Annu. Rev. Biochem.* 86, 129–157. doi: 10.1146/annurev-biochem-060815-014922

Conflict of Interest: HO is shareholder of the reagent company UbiQ Bio BV.

The remaining authors declare that the research was conducted in the absence of any commercial or financial relationships that could be construed as a potential conflict of interest.

frontiers in Chemistry

ORIGINAL RESEARCH
published: 22 January 2020
doi: 10.3389/fchem.2019.00921

Diubiquitin-Based NMR Analysis: Interactions Between Lys6-Linked diUb and UBA Domain of UBXN1

Dharjath Shahul Hameed[1,2], *Gabrielle B. A. van Tilburg*[1,2], *Remco Merkx*[1†], *Dennis Flierman*[1,2], *Hans Wienk*[3†], *Farid El Oualid*[1,4†], *Kay Hofmann*[5], *Rolf Boelens*[3] *and Huib Ovaa*[1,2*]

[1] Department of Cell Biology II, The Netherlands Cancer Institute, Amsterdam, Netherlands, [2] Department of Cell and Chemical Biology, Oncode Institute, Leiden University Medical Centre, Leiden, Netherlands, [3] NMR Spectroscopy, Bijvoet Center for Biomolecular Research, Utrecht University, Utrecht, Netherlands, [4] UbiQ Bio BV, Amsterdam, Netherlands, [5] Institute for Genetics, University of Cologne, Cologne, Germany

OPEN ACCESS

Edited by:
Laszlo Otvos,
Olpe LLC, United States

Reviewed by:
Norelle Daly,
James Cook University, Australia
Carlos A. Castaneda,
Syracuse University, United States
Yogesh Kulathu,
University of Dundee,
United Kingdom

***Correspondence:**
Huib Ovaa
H.Ovaa@lumc.nl

†Present address:
Remco Merkx,
Medicines Evaluation Board, Utrecht, Netherlands
Hans Wienk and Farid El Oualid,
Division of Biochemistry and Oncode Institute, The Netherlands Cancer Institute, Amsterdam, Netherlands

Specialty section:
This article was submitted to Chemical Biology, a section of the journal Frontiers in Chemistry

Received: 11 September 2019
Accepted: 18 December 2019
Published: 22 January 2020

Citation:
Shahul Hameed D, van Tilburg GBA, Merkx R, Flierman D, Wienk H, El Oualid F, Hofmann K, Boelens R and Ovaa H (2020) Diubiquitin-Based NMR Analysis: Interactions Between Lys6-Linked diUb and UBA Domain of UBXN1. Front. Chem. 7:921. doi: 10.3389/fchem.2019.00921

Ubiquitination is a process in which a protein is modified by the covalent attachment of the C-terminal carboxylic acid of ubiquitin (Ub) to the ε-amine of lysine or N-terminal methionine residue of a substrate protein or another Ub molecule. Each of the seven internal lysine residues and the N-terminal methionine residue of Ub can be linked to the C-terminus of another Ub moiety to form 8 distinct Ub linkages and the resulting differences in linkage types elicit different Ub signaling pathways. Cellular responses are triggered when proteins containing ubiquitin-binding domains (UBDs) recognize and bind to specific polyUb linkage types. To get more insight into the differences between polyUb chains, all of the seven lysine-linked di-ubiquitin molecules (diUbs) were prepared and used as a model to study their structural conformations in solution using NMR spectroscopy. We report the synthesis of diUb molecules, fully ^{15}N-labeled on the distal (N-terminal) Ub moiety and revealed their structural orientation with respect to the proximal Ub. As expected, the diUb molecules exist in different conformations in solution, with multiple conformations known to exist for K6-, K48-, and K63-linked diUb molecules. These multiple conformations allow structural flexibility in binding with UBDs thereby inducing unique responses. One of the well-known but poorly understood UBD-Ub interaction is the recognition of K6 polyubiquitin by the ubiquitin-associated (UBA) domain of UBXN1 in the BRCA-mediated DNA repair pathway. Using our synthetic ^{15}N-labeled diUbs, we establish here how a C-terminally extended UBA domain of UBXN1 confers specificity to K6 diUb while the non-extended version of the domain does not show any linkage preference. We show that the two distinct conformations of K6 diUb that exist in solution converge into a single conformation upon binding to this extended form of the UBA domain of the UBXN1 protein. It is likely that more of such extended UBA domains exist in nature and can contribute to linkage-specificity in Ub signaling. The isotopically labeled diUb compounds described here and the use of NMR to study their interactions with relevant partner molecules will help accelerate our understanding of Ub signaling pathways.

Keywords: isotope labeled diubiquitin, NMR, extended UBA domain, UBXN1, solid phase peptide synthesis

INTRODUCTION

Ubiquitin (Ub) is a small protein of 76 amino acids, involved in the post-translational modification of several proteins in cells (Hochstrasser, 1996; Hershko and Ciechanover, 1998). Ub is attached to a target protein in a process called ubiquitination which employs a specific combination of three enzyme classes: Ub activating enzyme E1, Conjugating enzyme E2, and Ub ligase E3 (Scheffner et al., 1995). On the other hand, ubiquitin can be removed from its substrates by enzymes called deubiquitinases (DUBs) (Komander et al., 2009a). Ub is attached to a target protein as a monomer or as a polymeric chain (polyUb) in which individual Ub molecules are attached via their C-terminal residue to one of the seven lysine residues (K6, K11, K27, K29, K33, K48, and K63) or the N-terminal methionine residue of other Ub molecules (Meierhofer et al., 2008; Akutsu et al., 2016). Different types of Ub modifications cause different responses, such as regulation of protein turnover and DNA-repair signaling and are therefore ubiquitination is essential in maintaining cellular homoeostasis. The polyUb chains vary in length, type of linkage (homotypic or branched) and the position of the modified lysine residues in target proteins (Li and Ye, 2008). Recognition of different polyUb chains by Ub binding domains (UBDs) is essential for stimulation of Ub signaling pathways.

The enzymatic assembly of all but K27-linked homotypical ubiquitin chains can be achieved by using the required combination of ubiquitinating E1-E2-E3 enzymes (Zhang et al., 2005; Hospenthal et al., 2013; Michel et al., 2015; Faggiano et al., 2016). However, there is lack of control over the length of polyUb chains generated when using enzymatic methods and this often requires either mutating the Ub monomer to halt the chain extension or using extensive purification methods to separate different Ub polymers. In addition, such techniques are known for being less selective and require post-synthesis clean-up of undesired chains using chain-specific DUBs. This results in low yields and long preparation times. To circumvent this, in the past years, we and others have reported the synthesis of ubiquitin chains using chemical tools (El Oualid et al., 2010; Kumar et al., 2010; Moyal et al., 2012; van der Heden van Noort et al., 2017). The use of a thiolysine handle at the sites of ubiquitination and the omission of enzymes resulted in the generation of diUbs of all seven isopeptide linkages (Merkx et al., 2013). These chains have been used extensively to study the biochemical properties of DUBs (Faesen et al., 2011; Licchesi et al., 2011).

To study the structural behavior of diUb molecules in solution by nuclear magnetic resonance spectroscopy (NMR), segmental isotope-labeled diUb reagents can be a valuable tool. Such a diUb molecule consists of a labeled Ub moiety linked to an unlabeled Ub moiety at defined positions. Synthesis of labeled diUb molecules has been reported previously relying on expressing recombinant Ub using an evolved tRNA/tRNA-synthetase system, followed by selective deprotection, chemical ligation and purification of diUb molecules (Castañeda C. et al., 2011; Castañeda C. A. et al., 2011). These diUb molecules can be used to study the intermolecular interactions with other proteins involved in the ubiquitin pathway.

It has been reported that Ub chain interactions with other proteins frequently involve a hydrophobic patch containing residues such as Leucine 8, Isoleucines 36 and 44, and Valine 70 on the ubiquitin surface (**Figure 1**, labeled in red) (Sloper-Mould et al., 2001). This patch is also involved in interactions between the Ub monomers in a diUb molecule or in polyUb chains. However, the position of interacting residues and the strength of the interaction between monomers differ for each Ub linkage (Wang et al., 2014). Although structural information on commercially available K48 (van Dijk et al., 2005; Ryabov and Fushman, 2007; Zhang et al., 2009) and K63 (Komander et al., 2009b; Weeks et al., 2009; Liu et al., 2015; He et al., 2016) Ub chains and other atypical Ub chains of K6- (Virdee et al., 2010; Hospenthal et al., 2013), K11- (Bremm et al., 2010; Matsumoto et al., 2010; Castañeda et al., 2013), K27- (Gao et al., 2016), K29- (Kristariyanto et al., 2015a), and K33- (Castañeda C. A. et al., 2011; Kristariyanto et al., 2015b; Michel et al., 2015) linkages is available, a comparative study on diUb structural dynamics in solution is necessary to get an idea on the differences in structure of different Ub linkages. Since structure-function relationships are known to be directive in ubiquitin signaling, it is essential to uncover the structural details of diUb molecules. For obtaining structural details, X-ray crystallography and increasingly also single-particle EM can be used to obtain high-resolution snapshots of protein folding and interactions of diUb molecules with some of their interacting proteins. On the other hand, NMR spectroscopy can provide a more dynamic view on structural transitions due to changes in environmental conditions and allows kinetic analyses of binding and dissociation between proteins and their interacting partners. In this study, we synthesized all seven isopeptide-linked diUbs using native chemical ligation of different proximal lysine-Ubs to a distal ^{15}N-labeled Ub. A comparative study on the interactions between the ^{15}N-labeled distal Ub and the unlabeled proximal Ub for each of the diUb linkages showed different interaction details in good agreement with previously reported data (Castañeda et al., 2016a,b). Furthermore, we demonstrate here the usefulness of these tools for gaining structural insights into the selective recognition of a unique Ub-binding domain (UBD) for a diUb linkage.

Each ubiquitin linkage-type leads to a different response in cells, based on their recognition by specific proteins containing a UBD. UBDs provide a structural basis for different responses by recruiting Ub chains and other proteins associated in their respective pathway. For example, the DNA repair pathway is one of the crucial pathways in cells that utilize polyUb signaling and is essential in maintaining genomic integrity during or after cell division. DNA damage can be repaired by several mechanisms (Schwertman et al., 2016). Among them, Non-Homologous End Joining (NHEJ) and Homologous Recombination (HR) are the most prevalent DNA-damage repair pathways. It has been observed that a Ubiquitin ligase called BRCA1 is involved in both of these DNA repair pathways. BRCA1 is an oncogene that is mainly associated with the prevalence of breast cancer (Rosen et al., 2003).

The BRCA-mediated DNA repair pathway involves the recognition of K6 polyubiquitin chains on BRCA1 protein

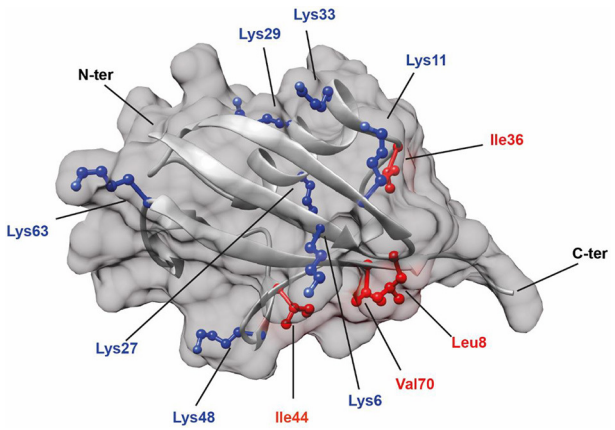

FIGURE 1 | Structure of Ub (PDB: 1UBQ) showing the positions of all seven lysine residues (colored in blue). In addition, hydrophobic residues (colored in red) known to be involved in protein interactions are also highlighted.

by another protein called UBXN1 (Ohta et al., 2011). The UBXN1 protein contains a UBD that belongs to the family of ubiquitin-associated domain (UBA) at its N-terminal tail (Wu-Baer et al., 2010). The UBA domain is one of the earliest types of defined ubiquitin-binding domains described in literature (Hofmann and Bucher, 1996). These domains are short (about 45 amino acids) polypeptide sequences and are frequently observed in the enzymes associated with the ubiquitin machinery. The UBA domains usually consists of three alpha-helix modules which include a highly conserved hydrophobic surface that can bind efficiently with hydrophobic areas of Ub or polyUb chains (Mueller and Feigon, 2002). The UBA sequences are conserved among proteins and enzymes involved in the proteasome degradation pathway (Chen et al., 2001) and in DNA repair (Kozlov et al., 2007).

Although it has been established that the UBA domain of UBXN1 can specifically recognize a K6 polyUb chain attached to the BRCA1 Ub ligase (Wu-Baer et al., 2010), the mode of interaction between the isolated UBA domain and the K6-Ub chain is largely unknown. Using our synthetic diUbs and biophysical techniques, we established how only an extended version of the UBA domain (UBAext1-52) of the UBXN1 protein binds selectively to K6 diUb. To illustrate the interaction of K6 diUb with UBAext1-52 of the UBXN1 protein, we monitored their titration by NMR and revealed which residues in the distal Ub of the K6 diUb molecule are important for this interaction. Understanding this interaction between the extended UBA domain and K6 Ub chains will help in understanding the interaction preference over other Ub chains.

MATERIALS AND METHODS

Expression of UBE1 Enzyme and ^{15}N Isotopic Labeling of Ubiquitin

All chemicals were obtained from Sigma unless stated otherwise. The ubiquitin-activating enzyme (UBA1) was recombinantly expressed with N-terminally fused hexahistidine tag (His6-tag). The enzyme was expressed in BL21 *E.coli* cells by adding 1 mM IPTG when the OD600 reached 0.6, followed by culturing the cells at 18°C overnight. Cells were then sonicated in a lysis buffer containing 20 mM Tris-HCl, 250 mM NaCl and 5 mM 2-Mercaptoethanol at pH 8. The supernatant was incubated with TALON® metal affinity resin and after two washing steps, the UBA1 was eluted at 250 mM Imidazole concentration in the elution buffer. The imidazole was removed from the buffer using 10 kDa cut-off spin columns (Millipore). The final concentration of the enzyme was measured using a Nanodrop™.

^{15}N-enriched ubiquitin was expressed as an untagged protein using a pET2A expression system in BL21 *E.coli* cells in minimal essential medium. The M9 minimal essential medium contained 50 mM Na_2HPO_4, 50 mM KH_2PO_4, 5 mM Na_2SO_4, 50 mM $^{15}NH_4Cl$, 2 mM $MgSO_4$, 0.01% glycerol, 0.001% glucose, and 0.004% lactose (inducer). After expression by autoinduction at 37°C overnight, cells were spun down at 3,700 G for 10 min and resuspended in Milli-Q™ water containing protease inhibitor cocktail tablets. Then the suspension was heated to 85°C for 30 min, cooled down to room temperature and added with 0.3 mg DNase per 50 mL suspension along with 10 mM $MgSO_4$. After heating again at 85°C for 30 min, the cell lysate was spun down at 20,000 rcf. The supernatant was purified by cation-exchange chromatography at 4°C using AKTA Unichromat 1500- "PRO" system (15 × 185 mm column packed with Workbeads™ 40 S) with two mobile phases: 50 mM NaOAc, pH 4.5 (solvent A), and 1 M NaCl in 50 mM NaOAc (solvent B), pH 4.5 (Flow-rate 5 mL/min). All fractions were checked on an SDS-PAGE gel. The pure fractions collected from the cation-exchange column were re-purified over a C18 Atlantis preparative reverse-phase HPLC on a Shimadzu Prominence system using two mobile phases: A = 0.05% TFA in water and B = 0.05% TFA in CH_3CN (Column temperature 40°C, flow rate 7.5 mL/min, UV-signal is measured at 230 and 254 nm). Typical ubiquitin yields were 80 mg/L of cell culture.

Preparation of Lysine-Linked Diubiquitin Molecules

The ^{15}N-Ub-MESNa thioester was obtained according to a previously reported procedure with >95% yield, which was then purified using RP-HPLC and lyophilized (Oualid et al., 2012). ^{15}N-Ub-MESNa thioester ligations were performed using the following conditions: 125 mM HEPES-NaOH pH 8; 100 mM MESNa; 10 mM $MgCl_2$; 10 mM ATP and 250 nM UBA1 enzyme at a concentration of 550 μM ^{15}N Ubiquitin. The ^{15}N-Ub-MESNa thioester was then purified using reversed-phase HPLC (RP-HPLC). Ub (K6, K11, K27, K29, K33, K48, and K63) δ-thiolysine derivatives were prepared using chemical synthesis on a solid phase. Diubiquitins were synthesized using a previously reported procedure (El Oualid et al., 2010). Native chemical ligation was performed by adding equal amounts of ^{15}N Ub MESNa thioester and thiolysine-Ub to a final concentration of 50 mg/mL in 6 M Gnd.HCl 0.2 M sodium phosphate buffer pH 8 containing 100 mM MPAA and 50 mM TCEP. After overnight ligation, the product was analyzed by LCMS and then diluted

in desulphurization mix to a final concentration of 1 mg/ml protein (Diubiquitin). This mix contains 6 M Gnd.HCl 0.2 M sodium phosphate buffer pH 6.8, 200 mM TCEP, 50 mM reduced Glutathione, and 50 mM radical initiator VA-044 (2,2'-Azobis[2-(2-imidazolin-2-yl)propane]dihydrochloride). After overnight desulphurization, the product was analyzed by LCMS and purified with RP-HPLC.

Preparation of UBA Peptides

UBA(1-42) and UBA(ext1-52) peptides were synthesized at 2 μmol scales, coupled with TAMRA on the N-terminus and purified by reversed-phase HPLC. Stock concentrations of TAMRA-UBA peptides were measured using a standard curve of TAMRA-K-G from 0 to 800 nM in 20 mM Tris pH 7.6 and 150 mM NaCl.

The amino acid sequence of the UBA domain of the UBXN1 protein is as follows:

```
         10          20          30
MAELTALESL IEMGFPRGRA EKALALTGNQ
         40          50
GIEAAMDWLM EHEDDPDVDE PL.
```

Analysis of Ubiquitin and Diubiquitin Molecules

The Ub and diUb molecules were analyzed by 12% Nu-PAGE SDS gel electrophoresis using MES buffer and Seablue plus 2® as a protein marker. Isolated products with an expected molecular weight (MW) of 17,212 Da were observed as a single band in the gel at around 17 kDa. The MW of the product were also confirmed by LC/MS using a Phenomenex Kinetex C18 (2.1 × 50 mm, 2.6 μm) column (flow rate: 0.8 mL/min; runtime: 6 min; mobile phases: A = 1% CH_3CN, 0.1% formic acid in water and B = 1% water and 0.1% formic acid in CH_3CN; column T = 40°C. Protocol: 0–0.5 min: 5% B; 0.5–4 min: 5–95% B gradient; 4–5.5 min: 95% B). Final yields were measured after freeze-drying the product.

For Circular Dichroism (CD) measurements, a JASCO CD J1000 machine was used (UMC, Utrecht, the Netherlands). Samples were dissolved in DMSO and then diluted in NMR buffer containing 20 mM NaH_2PO_4 pH 6.8 to a final concentration of 4 μM. Measurements were performed at 25°C using wavelengths ranging from 260 to 185 nm in a span of 100 m deg. The scanning speed was 20 nm/min and measurements from 10 experiments were averaged. After CD measurements, the samples were subjected to BCA assay to determine actual concentrations. Based on the observed values of CD measurements and concentration from BCA assay, CD plots were prepared.

NMR Measurements

Freeze-dried ubiquitin and diubiquitin samples were dissolved in 5% DMSO (Biosolve) in Milli-Q® water and then redissolved in NMR buffer containing 20 mM $NaPO_4$ pH 6.8 and 10% D_2O. Then, samples were taken in 15 ml 3.5 kDa Millipore spin filter tubes and spun-washed with three volumes of NMR buffer until DMSO was almost completely removed (LC/MS analysis). Concentrated samples were diluted to 500 μL with NMR buffer and the final concentration was determined using BCA assay using ubiquitin as standard. The pH was carefully measured using a Mettler TOLEDO pH probe.

All NMR studies were carried out on a Bruker 900 MHz spectrometer with a TCI cryoprobe, at 298 K (25°C). [^{1}H, ^{15}N] HSQC-spectra were acquired, processed and calibrated using standard methods. Chemical Shift Perturbations (CSPs) were calculated by comparing the [^{1}H, ^{15}N] HSQC spectra of mono Ub with that of each of the diUb molecules/ The CSP was calculated according to the following formula

$$CSP = \sqrt{(0.2\Delta\delta N)^2 + (\Delta\delta H)^2}$$

where ΔδH and ΔδN are the chemical shift differences for ^{1}H and ^{15}N, respectively.

The spectra of K6 diUb indicated two different co-existing conformations. An "open conformation" was assigned based on similarity with the mono-Ub spectrum.

Fluorescence Polarization and Microscale Thermophoresis Measurements

Fluorescence polarization (FP) measurements were performed at room temperature preceded by overnight incubation of UBA(ext1-52) domain with diubiquitin at 4°C. Total assay volume was 20 μL in black 384-well plates (low volume, flat bottom, non-binding surface; Corning®; ref 3820). All diubiquitin variants and concentrations were measured in triplicate. The concentration of synthetic TMR-labeled UBA domain was unchanged at 5 nM while diubiquitin was added in six steps of increasing concentrations from 0.78 to 25 μM. A UBA domain-only control (0 μM diubiquitin) was used to normalize measured FP values to 0. For these measurements, native diubiquitins were used and prepared as described previously (El Oualid et al., 2010). DiUbs were additionally purified by gel filtration on a HiLoad 16/600 superdex 75 pg column (GE Healthcare) in 20 mM Tris pH 7.6 and 150 mM NaCl. The measurements were carried out in a FP binding buffer (20 mM Tris pH 7.6, 150 mM NaCl, 0.5 mg/ml BGG, 1% TX-100). Before each measurement, the plates were briefly centrifuged for 1 min at 4°C and 500 G. Read-out was performed on a PHERAstar plate reader (BMG labtech) using a TAMRA filter. Statistical analyses were performed with GraphPad Prism 7 software using non-linear regression analysis [one site binding (hyperbola)].

Microscale thermophoresis (MST) measurements were carried out using the synthetic TAMRA-UBAdomains in FP binding buffer. Concentrations of K6 diUb ranged from 1.53 to 50 μM. Samples were incubated for 30 min to allow binding and measured in hydrophobic capillaries on a Monolith NT.115 reader (NanoTemper Technologies, Munich, Germany) using 30% LED and 40% IR-laser power. The analysis was performed with GraphPad Prism 7 software using non-linear regression analysis [log (inhibitor) vs. response (three parameters)].

RESULTS

diUb Synthesis and Validation by Gel, LCMS

Diubiquitin molecules were synthesized using our previously established native chemical ligation procedure (**Figure 2**) (El Oualid et al., 2010). Briefly, the different proximal Ub moieties, containing a δ-thiolysine building block instead of a lysine residue, were generated using Fmoc SPPS. The distal ^{15}N-Ub part was prepared by recombinant bacterial expression in ^{15}N-ammonia enriched M9 minimal medium and converted to ^{15}N-Ub MESNa thioester using UbE1 enzyme and MESNa. The proximal and ^{15}N-distal Ub precursors were ligated using native chemical ligation conditions. The product was then subjected to chemical desulfurization using TCEP and VA-044 and finally purified by reversed-phase HPLC.

The purified product was dissolved in DMSO and refolded into NMR buffer (20 mM $NaPO_4$ pH 6.8 and 10% D_2O). ^{15}N-Ub was also purified by HPLC and refolded using the same procedure. To check for proper folding, the products were examined by Circular Dichroism (CD) using commercially available Ub as a control. Based on SDS-PAGE analysis (**Supplementary Figure S1A**), the CD spectra (**Supplementary Figure S1B**) and LC/MS analysis, the distal ^{15}N labeled diUbs (**Supplementary Figures S14–S21**) are found to be pure and properly refolded.

Comparison of NMR Data of Monoub and diUb Molecules

By NMR, a 2D [^{1}H.^{15}N] HSQC spectrum was obtained for ^{15}N-Ub (**Supplementary Figure S2**). Although most of the signals were identified and assigned according to a previously reported data (Cornilescu et al., 1998), signals corresponding to Met1, Glu24, and Gly53 backbone amides were missing. The data showed that monoUb is properly folded.

We compared the [^{1}H, ^{15}N] HSQC spectra of each of the different ^{15}N-diUb molecules (**Supplementary Figures S3–S9**) (hereafter referred to as diUbs) to that of monomeric ^{15}N-Ub to reveal interactions between the distal Ub and proximal Ub moieties. Chemical shift perturbations (CSP) were calculated from ^{1}H to ^{15}N resonance frequency-differences between signals of the same residue in both monoUb and diUb spectra. This was plotted in a graph, illustrating the influence of the attached proximal Ub on residues in the ^{15}N-distal Ub moiety (**Figure 3**). Previously using a similar approach, the K48 (van Dijk et al., 2005; Hirano et al., 2011; Lai et al., 2012) and K63 (Jacobson et al., 2009; Liu et al., 2015) diUbs have been extensively studied. In our experiments, we also analyzed the NMR spectrum of all other diUb molecules.

CSPs are useful in determining the changes in the local environment of amino acids, which can be attributed to direct or indirect interactions but cannot be differentiated as such. All diUb spectra showed a common CSP behavior in the C-terminal region of the distal Ub module, where the isopeptide linkage with the proximal Ub module is located. However, the hydrophobic region in Ub including the residues of Leu8, Ile36, Ile44, and Val70 and its surroundings also showed CSPs to a varying degree of magnitude and signal shift directions. In the case of K6 diUb, spectral changes were mostly observed for Leu8, Ile36, and a small region in the second beta-sheet covering residues Thr12, Ile13, and Thr14. K11 diUb showed similar behavior encompassing residues Thr9, Ile13, Thr14, and Arg42. Here, Lys48, which is in the hydrophobic region surrounding Ile44 residue, was also disturbed. The elusive K27 diUb showed changes for Thr9 and Lys48 nearby the hydrophobic patch that surrounds Leu8 and Ile44 residues, respectively. K29 diUb showed disturbances in Leu8, Ile13, Thr14, and Lys48, similar to that of K11 diUb. Intriguingly, the spectra of K27 diUb and K29 diUb show variation likely because the lys29 residue in K29 diUb is more solvent-exposed compared to lys27 in K27 diUb. Similar effects as with K29 diUb were also observed for K33 diUb. K48 diUb, which is the most studied so far, showed CSPs for Val5, Ile13, areas around Ile44 and Val70, encompassing the hydrophobic patch of Ub, suggesting a compact folding as had been observed in X-ray crystal structures of K48 polyUb chains (Varadan et al., 2005). Finally, K63 diUb shows the least interactions between the distal Ub and proximal Ub, in line with the reported open conformations known for K63 linked Ub chains. Comparing the overall CSPs of each of the diUbs measured in our NMR experiment, we observed that K6 diUb, K11 diUb, K29 diUb, and K48 diUb showed more perturbations than K27 diUb, K33 diUb, and K63 diUb.

Of particular interest was the K6 diUb spectrum which showed signal-doubling for Thr12, Ile13, and Thr14 and residues Asp32 and Ile36 (**Figures 4A–E**). After ruling out the presence of impurities in the K6 diUb sample (**Supplementary Figures S1A**, **S15**), we further analyzed this phenomenon. Based on the reported crystal structure for K6 diUb, the region around Asp32 and Ile36 is away from the interface between the two Ub moieties (Virdee et al., 2010). Our data suggest that there is a second conformation in solution. Assuming that relaxation properties and NMR lineshapes between the two conformations are similar we estimate the major and minor populations in an approximate ratio of 70:30 for K6 diUb (**Figure 4**). In the major conformation, Leu8, Asp32, and Ile36 could interact with Thr12, Ile13, and Thr14 residues ("loop-in" conformation) which is in agreement with a compact diUb fold. In the minor conformation, there is less effect from Ile36 and therefore less perturbations are seen in Thr12, Ile13, and Thr14 residues ("loop-out" conformation) indicating that this K6 diUb conformation is less compact than the closed one but comparable to K48 diUb.

A Novel C-Terminally Extended UBA Domain of the UBXN1 Protein Binds Specifically to K6-Linked Diubiquitin *in vitro*

K6-linked polyubiquitin chains are known to be involved in BRCA-mediated DNA repair (Ohta et al., 2011). The BRCA1 protein forms a complex with BARD1 to gain its ubiquitin ligating activity. In addition to ubiquitinating many substrates involved in the DNA repair pathway with K6-linked polyUb chains (Sato et al., 2008), the BRCA1-BARD1 heterodimer complex can also auto-ubiquitinate itself with K6-linked polyUb

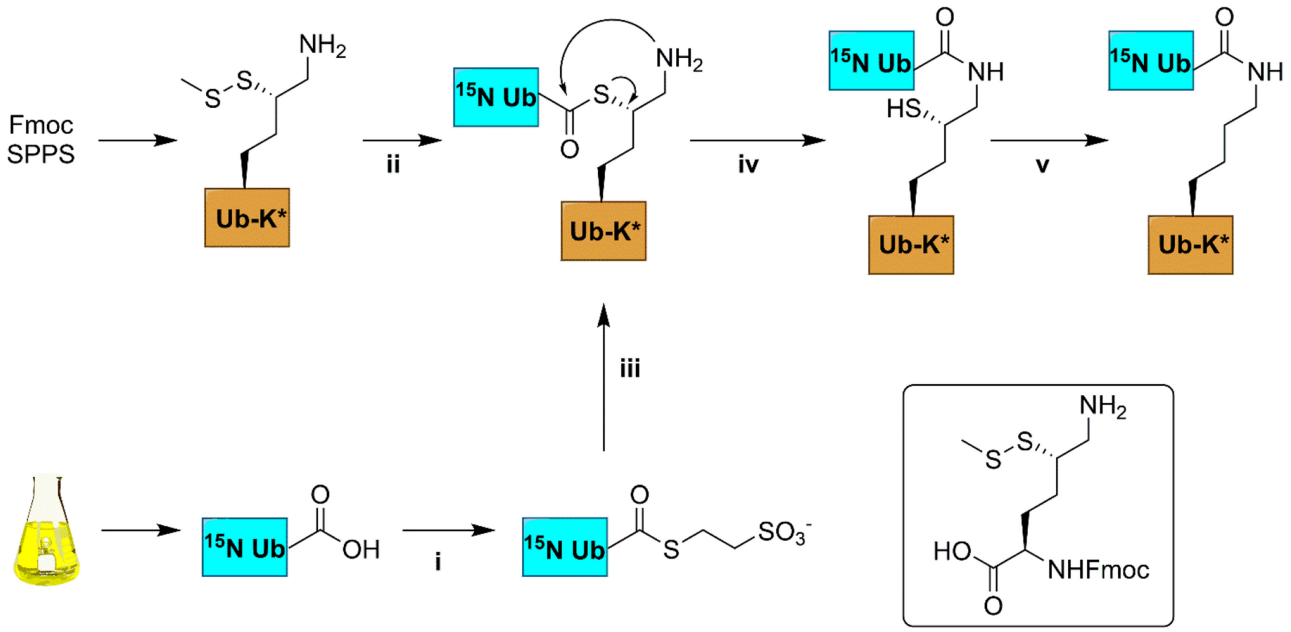

FIGURE 2 | Schematic representation of the synthesis of ^{15}N-labeled diUb. ^{15}N-Ub was expressed in a bacterial expression system; thiolysine (inset) containing Ub was synthesized from Fmoc-based SPPS. (i) 100 nM UbE1, 100 mM MESNa, pH 8; (ii) 50 mM TCEP, 6 M Gnd.HCl; (iii) Ub-thiolysine after step (ii), 100 mM MPAA, 6M Gnd.HCl, pH 8; (iv) room temperature, overnight incubation; (v) buffer exchange to remove MPAA, 100 mM TCEP, 100 mM VA-044, 6 M Gnd.HCl, pH 7.

chains (Chen et al., 2002; Wu-Baer et al., 2010). In this auto-ubiquitinated state, BRCA1-BARD1 ligase activity is significantly reduced by binding to the protein UBXN1 (Wu-Baer et al., 2010). UBXN1 contains an N-terminal UBA domain (residues 1–42) that binds to K6-linked polyubiquitin chains conjugated to BRCA1, while the C-terminal sequences of UBXN1 bind the BRCA1/BARD1 heterodimer in a ubiquitin-independent fashion (Wu-Baer et al., 2010). However, the isolated UBA(1-42) domain of UBXN1 did not bind with K6 polyUb chains, while deletion of this section in full length protein did abolish K6 interaction. This implied to us that there might be more residues beyond the UBA domain that are important for the K6-linked ubiquitin interaction (Wu-Baer et al., 2010).

To study this in more detail, we set out to investigate the specificity of the UBXN1 UBA domain for K6 diUb molecules using a Fluorescence Polarization (FP) binding assay in which TAMRA-labeled UBA peptide was added to different concentrations of unlabeled diUbs of all linkage types. Consistent with the findings of Wu-Baer et al., we also did not observe binding of K6 diubiquitin with the canonical UBA domain (1-42) of UBXN1 (**Supplementary Figure S10**) (Wu-Baer et al., 2010). On comparing the UBA domains of other proteins, we found that the 10 amino acids following the C-terminus of all conventional UBA domains that we compared showed the existence of a conserved sequence (**Table 1**). Interestingly when looking at the alignment, a previously unnoticed WxxxH motif was found to be conserved only in the extended versions of the UBA domain and not the shorter ones. To investigate whether this C-terminally extended version of the UBA domain of UBXN1 had any effect on binding to K6 diUb, we repeated the FP binding assay with the UBA (1-52) domain. We observed a tight and linkage specific binding to K6 diubiquitin (**Figure 5**). We quantified the linkage specific binding of UBA(ext1-52) to K6 diUb with an approximate K_d of 1.43 ± 0.31 μM which was validated with an orthogonal technique called microscale thermophoresis (MST) and found a similar K_d value of 1.05 ± 0.12 μM.

Carefully analyzing the NMR structures of the isolated UBA domains of UBASH3A (pdb: 2CRN), UBASH3B (pdb: 2CPW), UBAC1 (pdb: 2DAI), USP5 UBA2 (pdb: 2DAK), and USP13 (pdb: 2LBC), we found that all three alpha-helices in the conventional UBA domain are structurally conserved whereas the first few residues of the 10 residues extending from the C-terminus starts from the last alpha-helix and then becomes largely unstructured (**Figure 6**). The C-terminal UBA extension in UBXN1 seemingly adds to K6 diubiquitin specificity and further research is needed to investigate whether this holds true for the other proteins containing this conserved C-terminal UBA extension and thereby establishing a functional role of this conserved motif.

NMR of K6 diUb With the UBA (1-52) Domain of UBXN1 Provides an Insight Into the Mode of Interaction

To further study the interaction between the UBA(ext1-52) domain of UBXN1 and K6 diUb, we titrated the UBA(ext1-52) with ^{15}N-K6 diUb and monitored this by NMR. Signals corresponding to Lys 48, Gln49, Leu69, Leu71, and Leu73

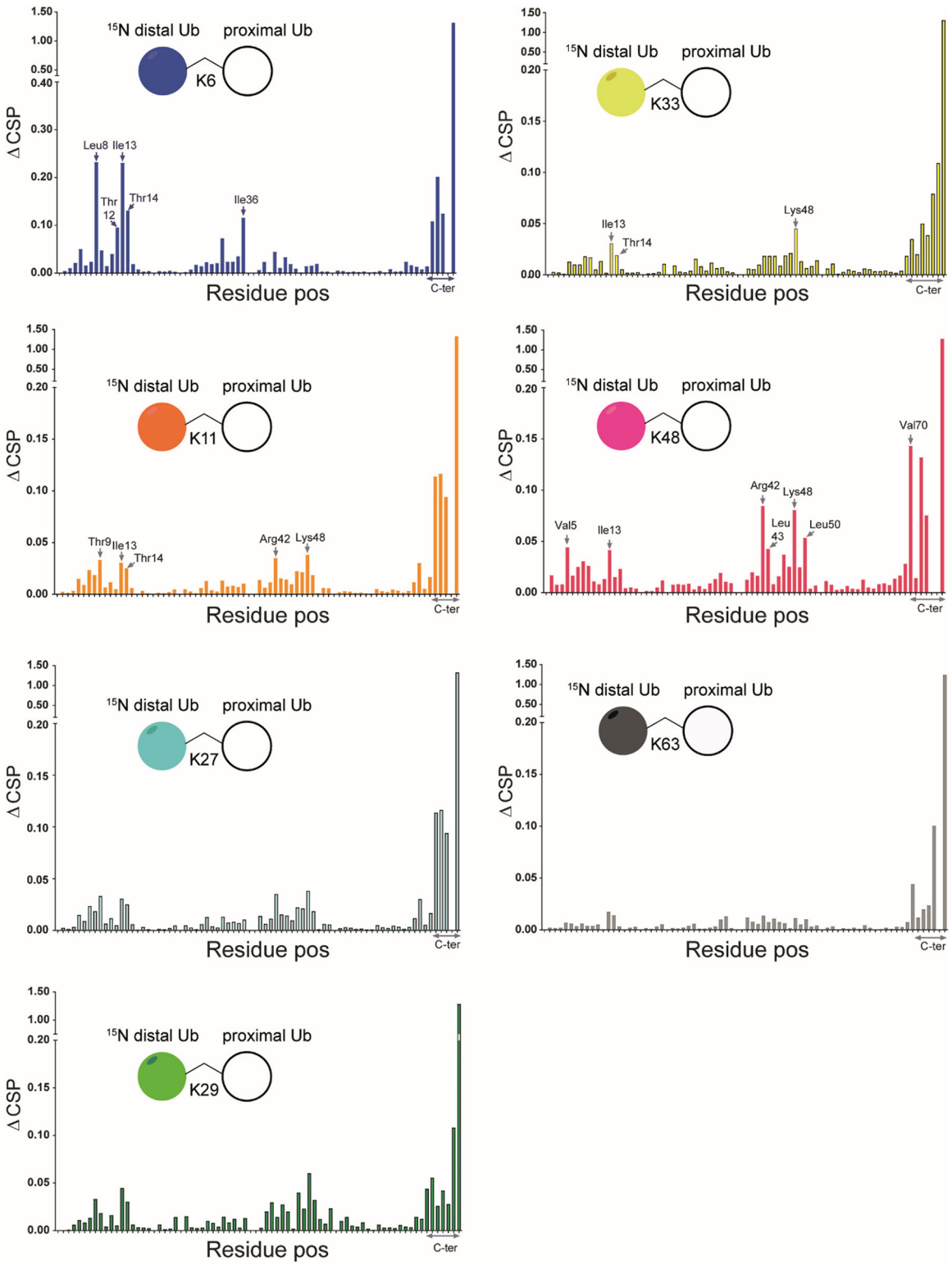

FIGURE 3 | CSPs calculated for all isopeptide linked diUbs by comparison of ^{15}N-^{1}H HSQC spectrum of mono-Ub with that of each of the ^{15}N-labeled diUb. Pictorial representations of each of the diUbs are shown (in each panel). In general, the C-terminal residues in all diUbs show CSP due to their covalent bonding with the second unlabeled Ub. However, other residues also show changes, indicating their possible interaction with the unlabeled proximal Ub. The residues that show major CSP besides the C-terminal region are labeled.

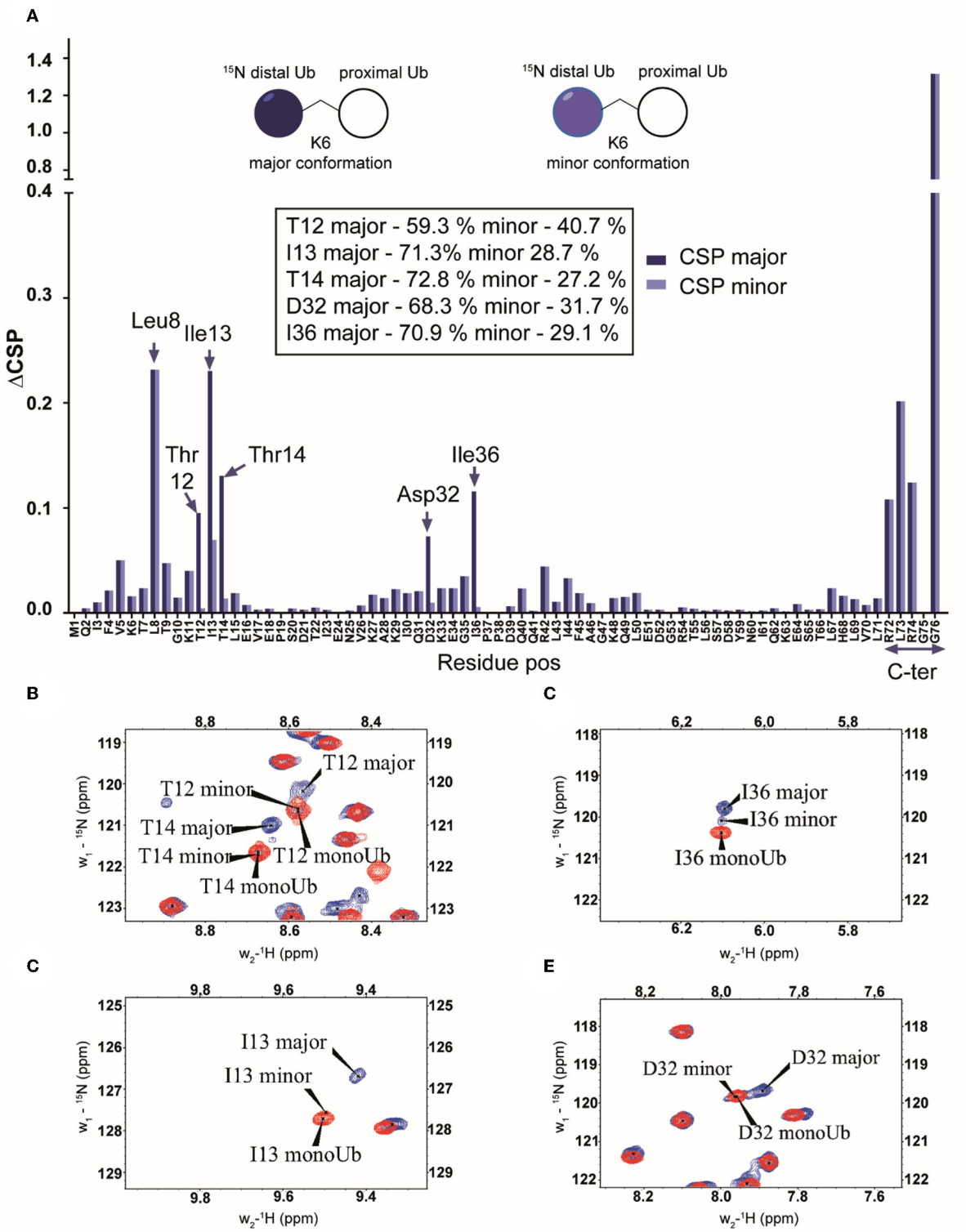

FIGURE 4 | (A) Chemical shift perturbations calculated by comparing the ^{15}N-^{1}H spectrum of mono-Ub and the distally ^{15}N-labeled K6-diUb (structural representation in inset). Although most of the signals are less affected, certain residues like Leu8, Thr12-Thr14, Ile36, and the C-terminal tail from Arg72 to Gly76 are all shifted significantly. This indicates a change in the electronic environment of these residues, which may be attributed to interactions with the unlabeled proximal-Ub. Leu8 and Ile36 show a considerable migration relative to other residues. In addition, signal doubling is observed for Asp32 and Ile36 in K6-diUb. **(B–E)** NMR spectral regions showing ^{15}N-^{1}H peaks of Thr12, Ile13, Thr14, Asp32, and Ile36 of K6 diUb (blue) compared with monoUb (red).

TABLE 1 | Comparison of UBA domain sequences from different Ub binding proteins.

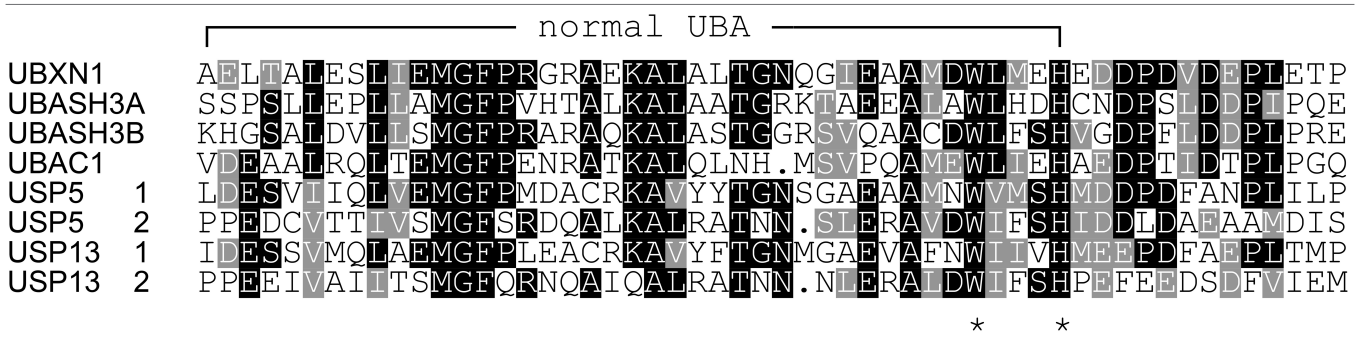

The C-terminal extension adds about 10 amino acids at the C-terminal end of the conventional UBA domain. Moreover, all extended UBA domains have a totally invariant WxxxH motif within the 3rd helix. While this region is part of the conventional UBA fold, the conservation of this motif is only found in extended UBA-domain-containing members. The Trp and His residue in the conserved WxxxH motif is indicated with a star (*).

disappeared after adding more than 1 equivalent of UBA(ext1-52), suggesting that these sites are in direct interaction with the UBA peptide. For other residues, signal shifts were observed. The CSP results indicated a distinct role of the hydrophobic patch on the distal Ub moiety that encompasses the residues Leu8, Ile44, Ala46, and Val70. Moreover, the residues Val5 to Thr9, Lys11, Ile13, and Thr14, surrounding Leu8 of the distal Ub, were also perturbed (**Figure 7A**, **Supplementary Figure S11**). Interestingly, shifts in Thr12, Ile13, and Thr14 were observed and explained previously as the "loop-in" and "loop-out" conformations for K6 diUb (Hospenthal et al., 2013).

Some signals that were split in the reference spectrum converged upon the addition of UBA(ext1-52) peptide. For example, Thr12, Ile13, and Thr14 were split in the unbound K6 diUb spectrum, but upon adding increasing concentrations of the UBA(ext1-52) peptide, their signals converged (**Supplementary Figure S12**). This indicates that the two different conformations of K6 diUb change into a single conformation upon binding with UBA(ext1-52) peptide. The fact that Ile44 and Leu8 show higher CSP values implying that the K6 diUb molecule is changing preferring the "loop-out" conformation upon interacting with the UBA peptide. However, residues Asp32 and Ile36 (**Supplementary Figure S13**) remained doubled, suggesting that the binding to the UBA(ext1-52) domain has local effects, but does not affect the structure of the entire distal Ub module.

Using the known X-ray crystal structure of K6 diUb, the interacting residues were mapped on the Ub surface (**Figures 7B,C**). It appears that the residues interacting with the extended UBA peptide are positioned away from the proximal Ub moiety. The fact that the Leu8 residue of distal Ub is positioned at the interface between the distal Ub and proximal Ub moieties may suggest a dual role for this residue in interacting with both the proximal Ub and UBA peptide.

DISCUSSION

Structures of all seven isopeptide-linked diUb molecules have been characterized using X-ray crystallography (Weeks et al., 2009; Bremm et al., 2010; Virdee et al., 2010; Hirano et al., 2011; Kristariyanto et al., 2015a,b; Pan et al., 2016). These crystal structures broadly fall into two categories: compact (K6, K48, K11, K27, K29, K33) and open (M1, K63) conformations (Wang et al., 2014). Some Ub chains, however, are known to exist in intermediate forms in solution. For example, K48 chains obtain two different conformations in addition to several intermediate structures (Lai et al., 2012). This structural flexibility is essential to facilitate polyUb signaling where K48 polyUb chains contribute to proteasomal degradation (Jacobson et al., 2009). Although they mainly exist in a compact conformation, 10% of K48 Ub chains exist in an open conformation exposing the hydrophobic patches to make these accessible for interactions with proteins such as the UBA domain of hHR23A which leads to the recruitment of K48 poly-ubiquitinated substrates for proteasomal degradation (Varadan et al., 2005). In another study, the K48 diUb molecule has been found to exist predominantly in an open conformation (Hirano et al., 2011). It is clear that the existence of multiple conformations of K48 polyUb chains in cells are essential to bind with different proteins and elicit different responses and further research is needed to study the structural dynamics of K48 polyUb chains in cells. Although X-ray data can reveal different conformations of diUb molecules, solution NMR is convenient to study the dynamics between different conformations and interactions with specific binding domains. Moreover, control of the environment in NMR experiments offers freedom to study solution structures at different physiological conditions, pH or temperature. Given the advances in chemical synthesis of Ub and Ub molecules containing thiolysine, we were able to generate distally labeled diUbs and studied the interactions between the two Ub moieties from the perspective of distal Ub. The synthesis of Ub chains by genetic incorporation of protected lysine residues using modified tRNA synthetases followed by selective chemical ligation and deprotection has also enabled generating diUb molecules of all linkages which were then analyzed by NMR spectroscopy (Castañeda et al., 2016b). Both approaches have demonstrated the advantages of using chemoenzymatic procedures to make diUb molecules to study their structural dynamics related to functionality.

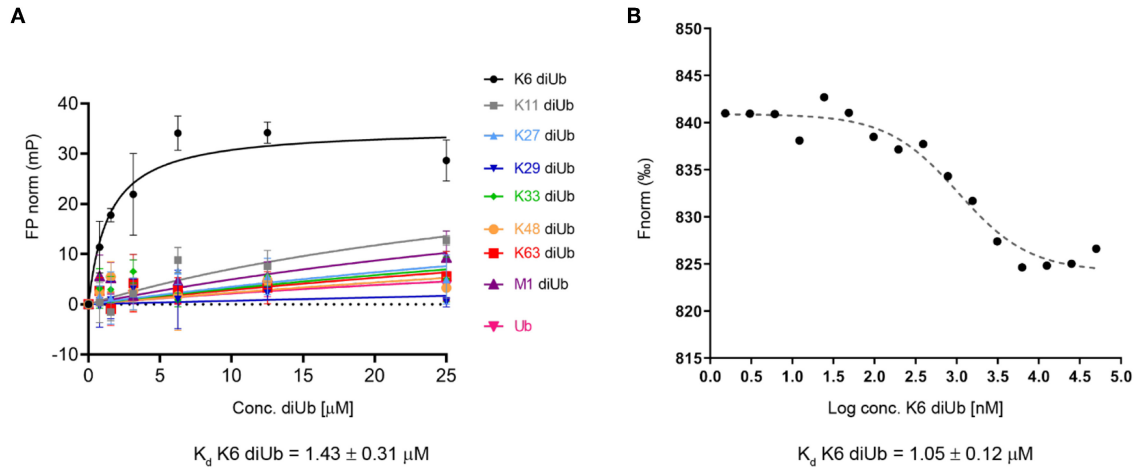

FIGURE 5 | (A) Fluorescence polarization assay using a TAMRA-labeled UBXN1 UBA(ext1-52) domain and different concentrations of all 8 homotypical diUbs and monoUb. **(B)** Microscale thermophoresis binding curve of K6 diUb to TAMRA-labeled UBA(ext1-52) from UBXN1. These experiments show the preference and tight binding of UBA(ext1-52) to K6 diUb.

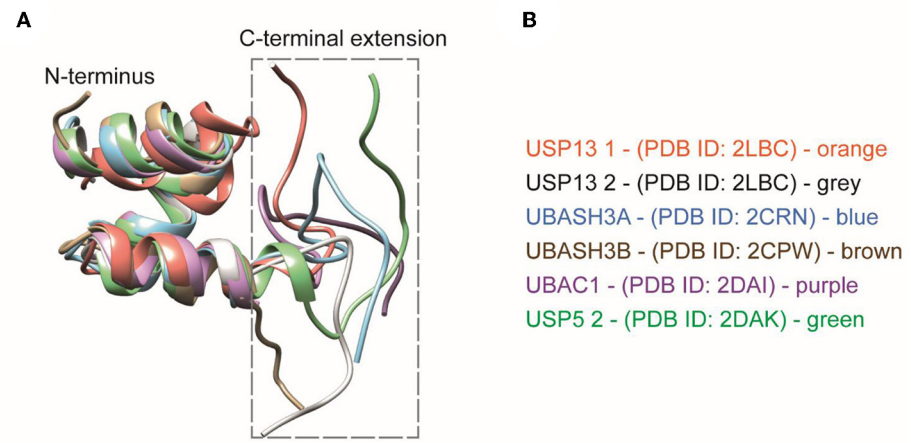

FIGURE 6 | (A) Structural comparisons of extended UBA domains. The C-terminal extension of all the UBA domains mentioned here is found to be disordered. **(B)** The UBA-domain containing proteins are color coded along with their respective PDB IDs.

For a better understanding of ubiquitin signaling pathway, it is essential to know how polyUb-specific interacting proteins recognize different polyUb chains. These interacting proteins often contain a specific UBD that can bind to specific polyUb chains, leading to different cellular responses. The best-studied Ub-interaction system is the K48 polyUb chain type and its corresponding interacting protein hHR23a in the proteasomal degradation system. Recently, it has been shown that hHR23a protein also recognizes K27 Ub chains, thereby implicating it in the DNA repair mechanism (Castañeda et al., 2016b). Although K48 chains are readily available for *in-vitro* studies, K27 chains are impossible to make via biochemical strategies and recombinant enzymes. Hence the chemical synthesis of these chains, such as shown in this study, may develop into a valuable tool in identifying the interacting proteins and establish a mechanism of binding.

DNA repair pathways are essential for the maintenance of the integrity of genomic DNA. The DNA repair pathway requires the efficient action of different protein complexes including the BRCA complex. Ubiquitination also plays an essential role in this pathway by adding different ubiquitin chains onto the proteins involved. For instance, the BRCA/ABRAXIS protein complex can be polyubiquitinated with K6, K48, and K63 polyUb chains by different sets of ubiquitin ligation enzymes and each of these modifications leads to different responses in the cell. Of special interest is the polyubiquitination with K6 chains which leads to recruitment of the DNA polymerase complex to restart DNA synthesis after DNA repair has been accomplished (Morris and Solomon, 2004). For K6 polyUb chains, UBXN1 acts as a specific

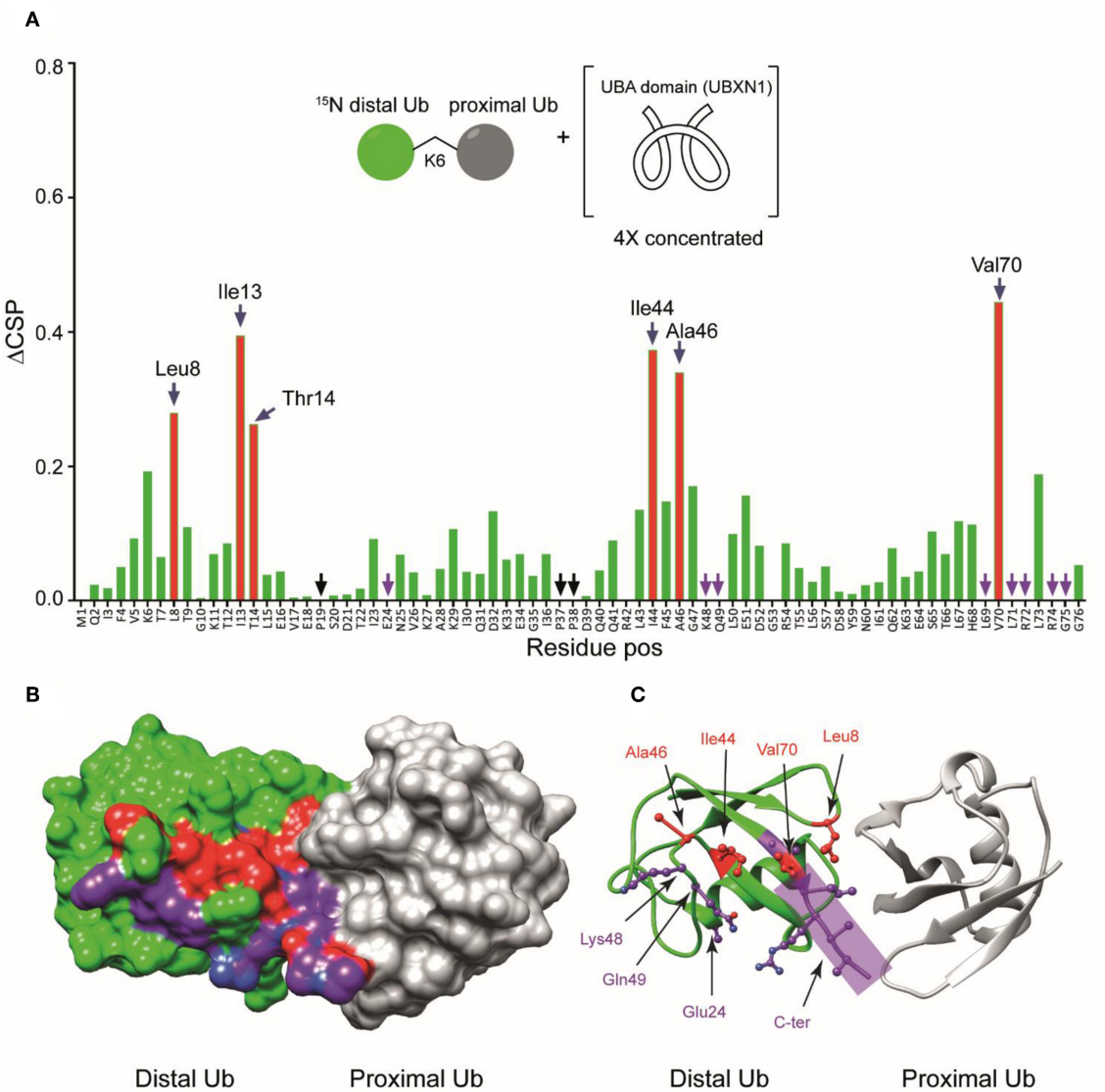

FIGURE 7 | (A) Unlabeled UBA(ext1-52) domain of UBXN1 was added in different concentrations to ^{15}N-K6 diUb and the CSPs were monitored. At a ratio of 4:1 (UBA(ext1–52) domain:K6 diUb), residues Leu8, Ile44, Ala46, and Val70 (red bars, labeled) shifted more than the rest. Other residues like Tyr 59 remain unchanged. **(B)** X-ray crystal structure of a K6 diUb (PDB: 2XEW) showing the residues that were perturbed according to CSP. Residues that shifted more are colored in red. Residues whose signal disappeared upon addition of UBA(ext1-52) peptide are represented in purple. **(C)** The same structure in figure **(B)** but showing the positions of side chains of the residues that were affected upon UBA(ext1-52) binding. Several perturbed residues are found to be positioned on the surface away from proximal Ub.

receptor protein and its UBA domain has been reported to be involved in chain recognition. However, the exact mode of binding has not been shown using any biophysical methods so far. In this study, we showed that to achieve binding to K6-linked ubiquitin, instead of the canonical UBXN1 UBA (1-42) domain, an extended version of the UBXN1 UBA domain, UBA(ext1-52), is needed. For the first time, we gain structural insight into the recognition of this elusive K6-specific ubiquitin-binding domain. Our results suggest that different conformations of K6 chains are locked into one dominant conformation upon binding with the UBXN1 UBA(ext1-52) domain. The additional 10 amino acids long C-terminal extension of the conventional UBA domain is found to be conserved among different proteins and is therefore important to study this in more detail in future experiments.

CONCLUSION

We have synthesized all isopeptide-linked distally ^{15}N labeled diUb chains using native chemical ligation. This allowed us to study their conformations in solution and the interactions of the distal Ub moiety with the proximal Ub moiety by NMR. We also established that the additional C-terminal residues of the

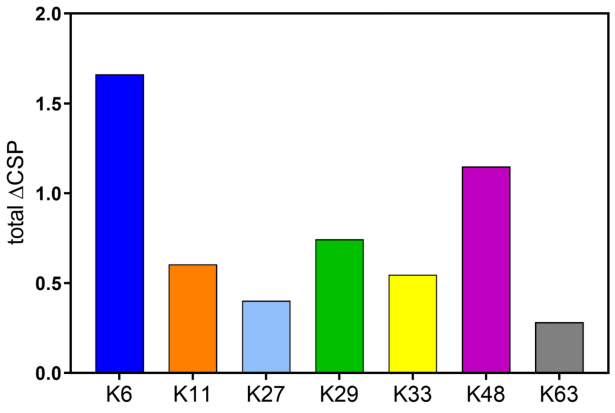

FIGURE 8 | Sum of CSPs of residues in distal Ub of all diUbs excluding the C-terminal tail interactions which happen due to the proximity of isopeptide bond, and not exclusively due to the interaction between the interface of the distal and proximal Ub.

conventional UBA domain of UBXN1 protein are essential in binding specifically with K6 diUb molecule.

Upon comparing different diubiquitins of each linkage, we observed that K48-, K6-, K29-, and K11- diUbs were in a relatively closed conformation while K33-, K27-, and K63- diUbs were in a more open conformation. The CSPs revealed that K6 diUb exhibits the most closed conformation among all diubiquitins, whereas K63 exhibits the most open conformation. In general, calculating the total CSPs of all residues in each of the diUb spectra, excluding the C-terminal tail encompassing residues 70 to 76, provided a tentative overview on the degree of compactness for each of the diUb molecules (**Figure 8**). In addition, we found that certain diUbs like K6 diUb, K48 diUb, and K63 diUb exist in more than one conformation. For instance, in K6 diUb the residues Val5, Thr12, Ile13, Thr14, Asp32, and Ile36 gave rise to two signals.

Using our synthetic ^{15}N diUbs, we established how only an extended version of the UBA domain (UBAext1-52) of the UBXN1 protein binds selectively to K6 diUb, using NMR titration experiments, revealing the crucial residues in the distal Ub of K6 diUb important for this interaction. With this, we demonstrate the applicability of these ^{15}N labeled diUb chains as tools for gaining structural insights into the selective recognition of a unique UBD for a diUb linkage.

DATA AVAILABILITY STATEMENT

The datasets generated for this study are available on request to the corresponding author.

AUTHOR CONTRIBUTIONS

DS and RM prepared the Ub and diUb reagents for NMR measurements. GT did the FP and MST measurements for UBA(ext1-52) and diUb interactions. HW measured the NMR spectra. DS and HW analyzed the NMR data. DF, FE, and KH provided valuable suggestions and ideas. RB and HO supported the work with grants from NWO.

FUNDING

Work in the Ovaa lab was supported by NWO (VICI grant 724.013.002). NMR experiments were performed at the SONNMRLSF facility, financially supported by an NWO-Groot Grant 175.107.301.10.

ACKNOWLEDGMENTS

We would like to thank Henk Hilkmann and Dris el Atmioui for providing synthetic ubiquitin mutants and ubiquitin-binding domains. We would like to thank Dr. Monique Mulder, Dr. Gerbrand J. van der Heden van Noort and Stephan Scherpe for critical reading.

SUPPLEMENTARY MATERIAL

The Supplementary Material for this article can be found online at: https://www.frontiersin.org/articles/10.3389/fchem.2019.00921/full#supplementary-material

REFERENCES

Akutsu, M., Dikic, I., and Bremm, A. (2016). Ubiquitin chain diversity at a glance. *J. Cell Sci.* 129, 875–880. doi: 10.1242/jcs.183954

Bremm, A., Freund, S. M., and Komander, D. (2010). Lys11-linked ubiquitin chains adopt compact conformations and are preferentially hydrolyzed by the deubiquitinase Cezanne. *Nat. Struct. Mol. Biol.* 17, 939–947. doi: 10.1038/nsmb.1873.

Castañeda, C., Liu, J., Chaturvedi, A., Nowicka, U., Cropp, T. A., and Fushman, D. (2011). Nonenzymatic assembly of natural polyubiquitin chains of any linkage composition and isotopic labeling scheme. *J. Am. Chem. Soc.* 133, 17855–17868. doi: 10.1021/ja207220g

Castañeda, C. A., Chaturvedi, A., Camara, C. M., Curtis, J. E., Krueger, S., and Fushman, D. (2016a). Linkage-specific conformational ensembles of non-canonical polyubiquitin chains. *Phys. Chem. Chem. Phys.* 18, 5771–5788. doi: 10.1039/c5cp04601g

Castañeda, C. A., Dixon, E. K., Walker, O., Chaturvedi, A., Nakasone, M. A., Curtis, J. E., et al. (2016b). Linkage via K27 bestows ubiquitin chains with unique properties among polyubiquitins. *Structure* 24, 423–436. doi: 10.1016/j.str.2016.01.007

Castañeda, C. A., Kashyap, T. R., Nakasone, M. A., Krueger, S., and Fushman, D. (2013). Unique structural, dynamical, and functional properties of k11-linked polyubiquitin chains. *Structure* 21, 1168–1181. doi: 10.1016/j.str.2013.04.029

Castañeda, C. A., Spasser, L., Bavikar, S. N., Brik, A., and Fushman, D. (2011). Segmental isotopic labeling of ubiquitin chains to unravel monomer-specific molecular behavior. *Angew. Chem. Int. Ed. Engl.* 50, 11210–11214. doi: 10.1002/anie.201104649

Chen, A., Kleiman, F. E., Manley, J. L., Ouchi, T., and Pan, Z. Q. (2002). Autoubiquitination of the BRCA1*BARD1 RING ubiquitin ligase. *J. Biol. Chem.* 277, 22085–22092. doi: 10.1074/jbc.M201252200

Chen, L., Shinde, U., Ortolan, T. G., and Madura, K. (2001). Ubiquitin-associated (UBA) domains in Rad23 bind ubiquitin and promote

inhibition of multi-ubiquitin chain assembly. *EMBO Rep.* 2, 933–938. doi: 10.1093/embo-reports/kve203

Cornilescu, G., Marquardt, J. L., Ottiger, M., and Bax, A. (1998). Validation of protein structure from anisotropic carbonyl chemical shifts in a dilute liquid crystalline phase. *J. Am. Chem. Soc.* 120, 6836–6837. doi: 10.1021/ja9812610

El Oualid, F., Merkx, R., Ekkebus, R., Hameed, D. S., Smit, J. J., de Jong, A., et al. (2010). Chemical synthesis of ubiquitin, ubiquitin-based probes, and diubiquitin. *Angew. Chem. Int. Ed. Engl.* 49, 10149–10153. doi: 10.1002/anie.201005995

Faesen, A. C., Luna-Vargas, M. P., Geurink, P. P., Clerici, M., Merkx, R., van Dijk, W. J., et al. (2011). The differential modulation of USP activity by internal regulatory domains, interactors and eight ubiquitin chain types. *Chem. Biol.* 18, 1550–1561. doi: 10.1016/j.chembiol.2011.10.017

Faggiano, S., Alfano, C., and Pastore, A. (2016). The missing links to link ubiquitin: methods for the enzymatic production of polyubiquitin chains. *Anal. Biochem.* 492, 82–90. doi: 10.1016/j.ab.2015.09.013

Gao, S., Pan, M., Zheng, Y., Huang, Y., Zheng, Q., Sun, D., et al. (2016). Monomer/oligomer quasi-racemic protein crystallography. *J. Am. Chem. Soc.* 138, 14497–14502. doi: 10.1021/jacs.6b09545

He, F., Wollscheid, H. P., Nowicka, U., Biancospino, M., Valentini, E., Ehlinger, A., et al. (2016). Myosin VI contains a compact structural motif that binds to ubiquitin chains. *Cell Rep.* 14, 2683–2694. doi: 10.1016/j.celrep.2016.01.079

Hershko, A., and Ciechanover, A. (1998). The ubiquitin system. *Annu. Rev. Biochem.* 67, 425–479. doi: 10.1146/annurev.biochem.67.1.425

Hirano, T., Serve, O., Yagi-Utsumi, M., Takemoto, E., Hiromoto, T., Satoh, T., et al. (2011). Conformational dynamics of wild-type Lys-48-linked diubiquitin in solution. *J. Biol. Chem.* 286, 37496–37502. doi: 10.1074/jbc.M111.256354

Hochstrasser, M. (1996). Ubiquitin-dependent protein degradation. *Annu. Rev. Genet.* 30, 405–439. doi: 10.1146/annurev.genet.30.1.405

Hofmann, K., and Bucher, P. (1996). The UBA domain: a sequence motif present in multiple enzyme classes of the ubiquitination pathway. *Trends Biochem. Sci.* 21, 172–173. doi: 10.1016/S0968-0004(96)30015-7

Hospenthal, M. K., Freund, S. M., and Komander, D. (2013). Assembly, analysis and architecture of atypical ubiquitin chains. *Nat. Struct. Mol. Biol.* 20, 555–565. doi: 10.1038/nsmb.2547

Jacobson, A. D., Zhang, N. Y., Xu, P., Han, K. J., Noone, S., Peng, J., et al. (2009). The lysine 48 and lysine 63 ubiquitin conjugates are processed differently by the 26 s proteasome. *J. Biol. Chem.* 284, 35485–35494. doi: 10.1074/jbc.M109.052928

Komander, D., Clague, M. J., and Urbé, S. (2009a). Breaking the chains: structure and function of the deubiquitinases. *Nat. Rev. Mol. Cell Biol.* 10, 550–563.

Komander, D., Reyes-Turcu, F., Licchesi, J. D., Odenwaelder, P., Wilkinson, K. D., and Barford, D. (2009b). Molecular discrimination of structurally equivalent Lys 63-linked and linear polyubiquitin chains. *EMBO Rep.* 10, 466–473. doi: 10.1038/embor.2009.55

Kozlov, G., Nguyen, L., Lin, T., De Crescenzo, G., Park, M., and Gehring, K. (2007). Structural basis of ubiquitin recognition by the ubiquitin-associated (UBA) domain of the ubiquitin ligase EDD. *J. Biol. Chem.* 282, 35787–35795. doi: 10.1074/jbc.M705655200

Kristariyanto, Y. A., Abdul Rehman, S. A., Campbell, D. G., Morrice, N. A., Johnson, C., Toth, R., et al. (2015a). K29-selective ubiquitin binding domain reveals structural basis of specificity and heterotypic nature of k29 polyubiquitin. *Mol. Cell* 58, 83–94. doi: 10.1016/j.molcel.2015.01.041

Kristariyanto, Y. A., Choi, S. Y., Rehman, S. A., Ritorto, M. S., Campbell, D. G., Morrice, N. A., et al. (2015b). Assembly and structure of Lys33-linked polyubiquitin reveals distinct conformations. *Biochem. J.* 467, 345–352. doi: 10.1042/BJ20141502

Kumar, K. S., Spasser, L., Erlich, L. A., Bavikar, S. N., and Brik, A. (2010). Total chemical synthesis of di-ubiquitin chains. *Angew. Chem. Int. Ed. Engl.* 49, 9126–9131. doi: 10.1002/anie.201003763

Lai, M. Y., Zhang, D., Laronde-Leblanc, N., and Fushman, D. (2012). Structural and biochemical studies of the open state of Lys48-linked diubiquitin. *Biochim. Biophys. Acta* 1823, 2046–2056. doi: 10.1016/j.bbamcr.2012.04.003

Li, W., and Ye, Y. (2008). Polyubiquitin chains: functions, structures, and mechanisms. *Cell Mol. Life Sci.* 65, 2397–2406. doi: 10.1007/s00018-008-8090-6

Licchesi, J. D., Mieszczanek, J., Mevissen, T. E., Rutherford, T. J., Akutsu, M., Virdee, S., et al. (2011). An ankyrin-repeat ubiquitin-binding domain determines TRABID's specificity for atypical ubiquitin chains. *Nat. Struct. Mol. Biol.* 19, 62–71. doi: 10.1038/nsmb.2169

Liu, Z., Gong, Z., Jiang, W. X., Yang, J., Zhu, W. K., Guo, D. C., et al. (2015). Lys63-linked ubiquitin chain adopts multiple conformational states for specific target recognition. *Elife* 4:e05767. doi: 10.7554/eLife.05767

Matsumoto, M. L., Wickliffe, K. E., Dong, K. C., Yu, C., Bosanac, I., Bustos, D., et al. (2010). K11-linked polyubiquitination in cell cycle control revealed by a K11 linkage-specific antibody. *Mol. Cell* 39, 477–484. doi: 10.1016/j.molcel.2010.07.001

Meierhofer, D., Wang, X., Huang, L., and Kaiser, P. (2008). Quantitative analysis of global ubiquitination in HeLa cells by mass spectrometry. *J. Proteome Res.* 7, 4566–4576. doi: 10.1021/pr800468j

Merkx, R., de Bruin, G., Kruithof, A., van den Bergh, T., Snip, E., Lutz, M., et al. (2013). Scalable synthesis of γ-thiolysine starting from lysine and a side by side comparison with δ-thiolysine in non-enzymatic ubiquitination. *Chem. Sci.* 4, 4494–4498. doi: 10.1039/C3SC51599K

Michel, M. A., Elliott, P. R., Swatek, K. N., Simicek, M., Pruneda, J. N., Wagstaff, J. L., et al. (2015). Assembly and specific recognition of k29- and k33-linked polyubiquitin. *Mol. Cell* 58, 95–109. doi: 10.1016/j.molcel.2015.01.042

Morris, J. R., and Solomon, E. (2004). BRCA1: BARD1 induces the formation of conjugated ubiquitin structures, dependent on K6 of ubiquitin, in cells during DNA replication and repair. *Hum. Mol. Genet.* 13, 807–817. doi: 10.1093/hmg/ddh095

Moyal, T., Bavikar, S. N., Karthikeyan, S. V., Hemantha, H. P., and Brik, A. (2012). Polymerization behavior of a bifunctional ubiquitin monomer as a function of the nucleophile site and folding conditions. *J. Am. Chem. Soc.* 134, 16085–16092. doi: 10.1021/ja3078736

Mueller, T. D., and Feigon, J. (2002). Solution structures of UBA domains reveal a conserved hydrophobic surface for protein-protein interactions. *J. Mol. Biol.* 319, 1243–1255. doi: 10.1016/S0022-2836(02)00302-9

Ohta, T., Sato, K., and Wu, W. (2011). The BRCA1 ubiquitin ligase and homologous recombination repair. *FEBS Lett.* 585, 2836–2844. doi: 10.1016/j.febslet.2011.05.005

Oualid, F. E., Hameed, D. S., Atmioui, D. E., Hilkmann, H., and Ovaa, H. (2012). Synthesis of atypical diubiquitin chains. *Methods Mol. Biol.* 832, 597–609. doi: 10.1007/978-1-61779-474-2_42

Pan, M., Gao, S., Zheng, Y., Tan, X., Lan, H., Tan, X., et al. (2016). Quasi-racemic X-ray structures of K27-linked ubiquitin chains prepared by total chemical synthesis. *J. Am. Chem. Soc.* 138, 7429–7435. doi: 10.1021/jacs.6b04031

Rosen, E. M., Fan, S., Pestell, R. G., and Goldberg, I. D. (2003). BRCA1 gene in breast cancer. *J. Cell Physiol.* 196, 19–41. doi: 10.1002/jcp.10257

Ryabov, Y., and Fushman, D. (2007). Structural assembly of multidomain proteins and protein complexes guided by the overall rotational diffusion tensor. *J. Am. Chem. Soc.* 129, 7894–7902. doi: 10.1021/ja071185d

Sato, K., Rajendra, E., and Ohta, T. (2008). The UPS: a promising target for breast cancer treatment. *BMC Biochem.* 9 (Suppl. 1):S2. doi: 10.1186/1471-2091-9-S1-S2

Scheffner, M., Nuber, U., and Huibregtse, J. M. (1995). Protein ubiquitination involving an E1-E2-E3 enzyme ubiquitin thioester cascade. *Nature* 373, 81–83. doi: 10.1038/373081a0

Schwertman, P., Bekker-Jensen, S., and Mailand, N. (2016). Regulation of DNA double-strand break repair by ubiquitin and ubiquitin-like modifiers. *Nat. Rev. Mol. Cell Biol.* 17, 379–394. doi: 10.1038/nrm.2016.58

Sloper-Mould, K. E., Jemc, J. C., Pickart, C. M., and Hicke, L. (2001). Distinct functional surface regions on ubiquitin. *J. Biol. Chem.* 276, 30483–30489. doi: 10.1074/jbc.M103248200

van der Heden van Noort, G. J., Kooij, R., Elliott, P. R., Komander, D., and Ovaa, H. (2017). Synthesis of poly-ubiquitin chains using a bifunctional ubiquitin monomer. *Org. Lett.* 19, 6490–6493. doi: 10.1021/acs.orglett.7b03085

van Dijk, A. D., Fushman, D., and Bonvin, A. M. (2005). Various strategies of using residual dipolar couplings in NMR-driven protein docking: application to Lys48-linked di-ubiquitin and validation against 15N-relaxation data. *Proteins* 60, 367–381. doi: 10.1002/prot.20476

Varadan, R., Assfalg, M., Raasi, S., Pickart, C., and Fushman, D. (2005). Structural determinants for selective recognition of a Lys48-linked polyubiquitin chain by a UBA domain. *Mol. Cell* 18, 687–698. doi: 10.1016/j.molcel.2005.05.013

Virdee, S., Ye, Y., Nguyen, D. P., Komander, D., and Chin, J. W. (2010). Engineered diubiquitin synthesis reveals Lys29-isopeptide specificity of an OTU deubiquitinase. *Nat. Chem. Biol.* 6, 750–757. doi: 10.1038/nchembio.426

Wang, Y., Tang, C., Wang, E., and Wang, J. (2014). PolyUbiquitin chain linkage topology selects the functions from the underlying binding landscape. *PLoS Comput. Biol.* 10:e1003691. doi: 10.1371/journal.pcbi.1003691

Weeks, S. D., Grasty, K. C., Hernandez-Cuebas, L., and Loll, P. J. (2009). Crystal structures of Lys-63-linked tri- and di-ubiquitin reveal a highly extended chain architecture. *Proteins* 77, 753–759. doi: 10.1002/prot.22568

Wu-Baer, F., Ludwig, T., and Baer, R. (2010). The UBXN1 protein associates with autoubiquitinated forms of the BRCA1 tumor suppressor and inhibits its enzymatic function. *Mol. Cell Biol.* 30, 2787–2798. doi: 10.1128/MCB.01056-09

Zhang, M., Windheim, M., Roe, S. M., Peggie, M., Cohen, P., Prodromou, C., et al. (2005). Chaperoned ubiquitylation–crystal structures of the CHIP U box E3 ubiquitin ligase and a CHIP-Ubc13-Uev1a complex. *Mol. Cell* 20, 525–538. doi: 10.1016/j.molcel.2005.09.023

Zhang, N., Wang, Q., Ehlinger, A., Randles, L., Lary, J. W., Kang, Y., et al. (2009). Structure of the s5a:k48-linked diubiquitin complex and its interactions with rpn13. *Mol. Cell* 35, 280–290. doi: 10.1016/j.molcel.2009.06.010

Conflict of Interest: FE and HO declare competing financial interests as shareholder of UbiQ Bio BV.

The remaining authors declare that the research was conducted in the absence of any commercial or financial relationships that could be construed as a potential conflict of interest.

frontiers in Cell and Developmental Biology

REVIEW
published: 04 February 2020
doi: 10.3389/fcell.2020.00039

How to Inactivate Human Ubiquitin E3 Ligases by Mutation

*Cristina Garcia-Barcena[1], Nerea Osinalde[2], Juanma Ramirez[1] and Ugo Mayor[1,3]**

[1] Department of Biochemistry and Molecular Biology, Faculty of Science and Technology, University of the Basque Country (UPV/EHU), Leioa, Spain, [2] Department of Biochemistry and Molecular Biology, Faculty of Pharmacy, University of the Basque Country (UPV/EHU), Vitoria-Gasteiz, Spain, [3] Ikerbasque – Basque Foundation for Science, Bilbao, Spain

E3 ubiquitin ligases are the ultimate enzymes involved in the transfer of ubiquitin to substrate proteins, a process that determines the fate of the modified protein. Numerous diseases are caused by defects in the ubiquitin-proteasome machinery, including when the activity of a given E3 ligase is hampered. Thus, inactivation of E3 ligases and the resulting effects at molecular or cellular level have been the focus of many studies during the last few years. For this purpose, site-specific mutation of key residues involved in either protein interaction, substrate recognition or ubiquitin transfer have been reported to successfully inactivate E3 ligases. Nevertheless, it is not always trivial to predict which mutation(s) will block the catalytic activity of a ligase. Here we review over 250 site-specific inactivating mutations that have been carried out in 120 human E3 ubiquitin ligases. We foresee that the information gathered here will be helpful for the design of future experimental strategies.

Keywords: ubiquitin, E3, mutation, ligase, inactivation

OPEN ACCESS

Edited by:
Benedikt M. Kessler, University of Oxford, United Kingdom

Reviewed by:
Richard Chahwan, University of Zurich, Switzerland
Yasuhito Ishigaki, Kanazawa Medical University, Japan

***Correspondence:**
Ugo Mayor
ugo.mayor@ehu.eus

Specialty section:
This article was submitted to Cellular Biochemistry, a section of the journal Frontiers in Cell and Developmental Biology

Received: *17 October 2019*
Accepted: *16 January 2020*
Published: *04 February 2020*

Citation:
Garcia-Barcena C, Osinalde N, Ramirez J and Mayor U (2020) How to Inactivate Human Ubiquitin E3 Ligases by Mutation. Front. Cell Dev. Biol. 8:39. doi: 10.3389/fcell.2020.00039

UBIQUITINATION, THE UBIQUITIN CODE AND E3 LIGASES

Ubiquitin is a 76-amino-acid protein, highly conserved among organisms (Zuin et al., 2014), used–through the ubiquitin-proteasome system- to regulate many cellular processes. Proteins are covalently modified on their Lys residues with ubiquitin via amide isopeptide linkages (Laney and Hochstrasser, 1999). Frequently, ubiquitinated proteins are targeted for degradation through the proteasomal system on an ATP hydrolysis-dependent manner (Hershko and Ciechanover, 1998; Komander and Rape, 2012). But protein ubiquitination participates in a plethora of additional cellular responses including regulation of gene expression, cell signalling, cell cycle, DNA repair and apoptosis (Pickart, 2001; Gilberto and Peter, 2017).

The ubiquitination reaction requires the coordinated action of three types of enzymes termed E1, E2, and E3. First, ubiquitin is activated with ATP in a process carried out by an activating E1 enzyme. Once ubiquitin is activated, it is transferred to the Cys on the active site of a conjugating E2 enzyme. Finally, ubiquitin is generally linked to a Lys of the target protein through an isopeptide bond, formed between the C-terminal carboxyl group of ubiquitin and the ε-amino group of the Lys. Substrate specificity in ubiquitination is attributed to E3 ligases, who are able to interact with both the ubiquitin-charged E2 and the substrates to be modified (Metzger et al., 2014). Like most post-translational modifications (PTMs), ubiquitination is reversible and deubiquitinating enzymes (DUBs) are responsible for hydrolysing the isopeptide bond between ubiquitin and substrate proteins or between ubiquitin molecules.

Proteins can be modified by ubiquitin in a wide range of manners. For instance, in addition to Lys, ubiquitin can be conjugated via a peptide bond to the N-terminal amino group of the substrates (Ciechanover and Ben-Saadon, 2004), as well as to Cys or Ser/Thr residues by thio- or oxy-ester bonds, respectively (Wang et al., 2012). Substrates can be mono-ubiquitinated, meaning modified in a single residue by only one ubiquitin. Multi-mono-ubiquitination occurs when several residues of a given protein are simultaneously modified with one ubiquitin each. Poly-ubiquitination occurs when the C-terminus of another ubiquitin associates to one of the seven Lys (Lys6, Lys11, Lys27, Lys29, Lys33, Lys48, and Lys63) or the N-terminal Met (Met1) on the previously added ubiquitin molecules. Consequently, a ubiquitin chain is formed on the target protein. Depending on how ubiquitin residues are bound together, different ubiquitin chain architectures can be formed: (i) homogenous, if the Lys used throughout the chain is the same (e.g., Lys48-linked chains), (ii) heterogeneous, if they alternate (e.g., Lys48-Lys11-linked chains) and (iii) branched, if multiple Lys of the same ubiquitin are modified at the same time. Altogether, ubiquitin can generate a huge amount of different types of modifications on any given protein (Komander and Rape, 2012). Consequently, ubiquitin-mediated cellular responses will depend not only on the specific residues of the substrate that are modified but also on the topology of the ubiquitin chains that are formed.

Eukaryotic cells express hundreds of ubiquitin E3 ligases, which can operate in different cellular contexts, respond to numerous cellular signals, and process diverse protein substrates (Zheng and Shabek, 2017). Ubiquitin E3 ligases have been classically classified in two different groups, based on conserved structural domains and the mechanism by which ubiquitin is transferred: RING (really interesting new gene)-type E3s and HECT (homologous to the E6AP carboxyl terminus)-type E3s. Whereas RING E3 ligases directly transfer the ubiquitin from the E2-ubiquitin complex to the substrate (**Figure 1A**), HECT-type E3s transfer ubiquitin to their own catalytic Cys before linking it to the substrate (**Figure 1B**; Deshaies and Joazeiro, 2009). Additionally, a third group of E3s, that combines features from both RING- and HECT-type E3 families, has been established: the RING between RING (RBR) family (**Figure 1C**). RBR and RING E3s share RING binding domains, but RBR family members have the ability to generate a thioester intermediate with ubiquitin, as HECT-type E3s do (Morreale and Walden, 2016).

Typically, one E3 ligase is able to modify several substrates, as well as to bind different E2s. The same protein can, therefore, be ubiquitinated by different E2/E3 combinations, which will lead to different ubiquitination patterns (Metzger et al., 2014). Substrate recognition by HECT-type E3 ligases depends on protein-protein interactions that are mediated by specific motifs typically located in the N-terminal of the HECT domain (Scheffner and Kumar, 2014). Substrate recognition by RING-type E3s is achieved either through regions of the E3 other than the RING domain, in the case of monomeric E3s, or through substrate recognition elements in other domains, in the case of multi-subunit RING E3s (Metzger et al., 2014). On the other hand, some studies have reported that substrate proteins have a short linear sequence, known as degron, important in the regulation of protein degradation rates. Not all degron are ubiquitin-dependent, but if they are, it appears that they facilitate the recognition of the substrate protein by the E3 ligase. Degrons can be modified by kinases and other enzymes. These modifications appear to be crucial for timing the interaction between E3 and substrate, even though they are not always necessary and many substrates of HECT-type E3s and CRLs are able to recognise their substrates in their native forms (Kanelis et al., 2001; Kamadurai et al., 2009; Rotin and Kumar, 2009; Fukutomi et al., 2014; Muńoz-Escobar et al., 2015). In order to increase the specificity toward their substrates, many E3 ligases, such as TRIMs, are able to form homo- and heterodimers and recognise multiple degrons located in the same substrate (Li et al., 2014). Moreover, the effect is summatory and a robust degron may have the same effect as two weak degrons (Welcker et al., 2013).

The role mediated by E3 ligases is so crucial, that their activity must be tightly controlled in order to ensure they solely act when necessary. Oligomerisation is one of the mechanisms that modulate the activity of HECT- and RING-type E3s. For instance, structural studies suggest that the trimeric arrangement of E6AP activates the ligase (Ronchi et al., 2014), whereas homodimerisation of the HECT domain of HUWE1 results in enzyme inactivity (Sander et al., 2017). RING-type E3s can act as independent enzymes, but most of them tend to form homo- or heterodimers, and even more complex multi-subunit assemblies in order to mediate ubiquitination (Metzger et al., 2014). For instance, RING E3 ligases cIAP, RNF4, BIRC7, IDOL, CHIP, and Prp19 homodimerize, and RING domains of both units interact with E2 proteins. By contrast, RING-type E3 ligases BRCA1-BARD1, Mdm2-MdmX, and RING1B-Bmi1 form heterodimers. While BRCA1 and Mdm2 have the ability to interact with E2 proteins, their partners do not. But they function as enhancers of ligase activity and interact with substrates (Brzovic et al., 2001; Joukov et al., 2001; Wang et al., 2004; Cao et al., 2005).

In this review we aim to provide a detailed description of mutations in ubiquitin E3 ligases, with the outlook that such detailed and structured catalog of mutants will provide a pattern to be considered by future researchers when designing new mutations on their E3 ligases.

MUTATIONS ON RING-TYPE E3 LIGASES

RING-type E3s are conserved from human to yeast. It is estimated that the human genome encodes above 600 different RING-type E3s. The RING domain was first characterised by Freemont et al. (1991). The canonical sequence for this 40–60 amino acid long domain is Cys-X_2-Cys-$X_{(9-39)}$-Cys-$X_{(1-3)}$-His-$X_{(2-3)}$-Cys-X_2-Cys-$X_{(4-48)}$-Cys-X_2-Cys. The conserved Cys residues (seven in total) and the single His are disposed in a "cross-brace" topology to coordinate two zinc ions and stabilise its structure (**Figure 2**; Deshaies and Joazeiro, 2009).

Initially, the role of RING domains was uncertain, although it was known they were involved in protein-protein interactions as well as in a wide range of cellular processes (Deshaies and Joazeiro, 2009). However, it was not until 1997 that the function

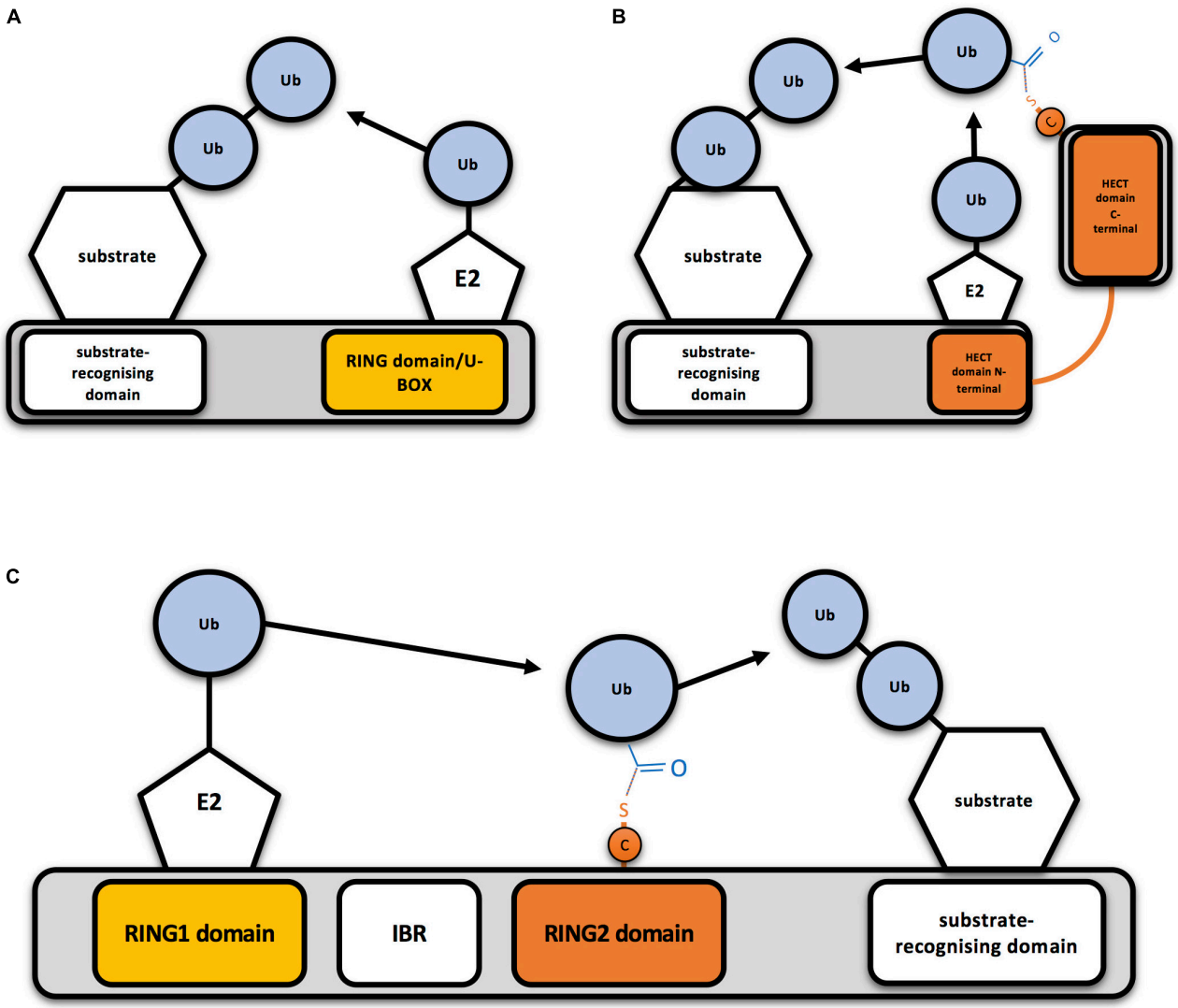

FIGURE 1 | Mechanism of action of RING-, HECT- and RBR-type E3 ubiquitin ligases **(A)** Schematic representation of a RING-type ubiquitin E3 ligase. RING E3s bind both the E2-ubiquitin and the substrate to be ubiquitinated, so bringing them together allows direct conjugation of ubiquitin (Ub) on the substrate by the E2. A monomeric RING E3 ligase is shown for illustrative purposes. **(B)** Schematic representation of a HECT-type ubiquitin E3 ligase. Ubiquitin is transferred first to a cysteine (C) of the HECT domain through a thioester bond and then to the substrate. **(C)** Schematic representation of an RBR-type ubiquitin E3 ligase. Two RING domains are separated by an in-between-RING (IBR) domain. Ubiquitin is first transferred to a cysteine (C) of the second RING domain through a thioester bond and then to the substrate.

of RING domains was elucidated by Bailly and co-workers (Bailly et al., 1997). Moreover, in 1999, Joazeiro and co-workers observed that the adapter protein c-Cbl bears two domains that act coordinately to mediate ubiquitination and subsequent degradation of substrates. Whereas the SH2 domain of c-Cbl served to recognize specific substrates, the RING domain was necessary to recruit and activate an ubiquitin-conjugating E2 (Joazeiro et al., 1999). After that, a similar role was conferred to a number of RING domain-containing proteins (Lorick et al., 1999). At present, it is accepted that the RING domain present in all RING E3s associates and activates E2-Ub conjugates promoting the direct transfer of ubiquitin from the E2 to the target protein (**Figure 1A**).

The interaction between the RING domain of E3 ligases and E2s was first elucidated with the crystal structure of Cbl's RING domain bound to UbcH7 E2 (Zheng et al., 2000). The combination of many structural studies allowed the characterization of the four residues of each protein that play a crucial role in the interaction, those are shown in green in **Figure 2**. Located between Cys residues C_1 and C_2 of the RING domain, a hydrophobic residue (Ile, Leu or Val) interacts with two Pro residues from the E2. Those two prolines are localised in one of the two loops that compose the accessible surface of the E2 enzyme. Additionally, another hydrophobic residue (typically Trp, His or Leu) from the E3 interacts with a Phe and a Pro present on the second loop of the E2. Simultaneously, this Pro

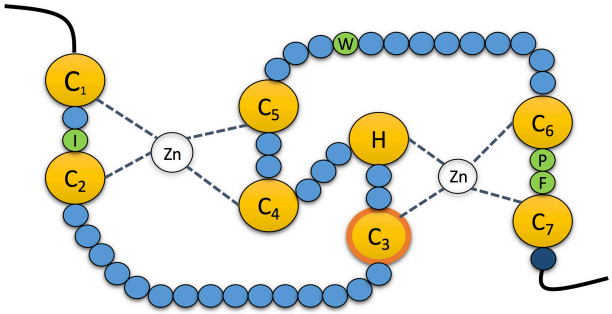

FIGURE 2 | The zinc coordinating residues in RING domains. Schematic representation of the cross-brace" topology of RING domains. The RING domain contains seven conserved cysteines and one histidine (yellow) which are involved in the coordination of two atoms of zinc. The third cysteine mediates the ubiquitin transfer in the second RING domain in RBR E3 ubiquitin ligases (contour labelled in orange). Four conserved residues (green) guide the interaction with the E2 conjugating enzyme. Mutation of the last residue of the domain (dark blue), which is normally a positively charged arginine or lysine, compromises the stability of the adjacent cysteine, affecting the coordination of the zinc atom.

interacts with a Pro of the E3 located between Cys residues C_6 and C_7. Which in turn, is also connected to an Ala localised in the same loop of the E2. Finally, this same Ala of the E2 also interacts with a hydrophobic amino acid (typically Val, Phe or Ile) located straight after the Pro between C_6 and C_7 of the E3 (Deshaies and Joazeiro, 2009).

More recently, structural studies focused on RING-type E3:E2-Ub complexes have revealed the mechanism by which this class of ubiquitin ligases facilitates Ub transfer to substrate proteins. The E2-Ub complex has a flexible topology with multiple inter-domain configurations that are altered upon E3 binding (Pruneda et al., 2011). More precisely, binding of RING E3 reduces the dynamics of E2-Ub and stabilizes in an ensemble of closed conformations. This modification facilitates the reactivity for substrate Lys that can perform the corresponding nucleophilic attack (Pruneda et al., 2012; Soss et al., 2013). Studies carried out on dimeric E3s such as RNF4 or BIRC7 also support the same mechanism by showing that a positively charged residue (Arg or Lys) conserved in many RING E3s just straight after the last zinc-coordinating Cys supports the non-covalent interaction with the E2-Ub complex (Dou et al., 2012; Plechanovov et al., 2012).

As mentioned above, although some RING-type E3s act independently, they have the tendency to form homo- and heterodimers. Most RING-type E3s dimerise through their RING domain, such as RNF4 homodimers or MDM2/MDMX and BRAC1/BARD1 heterodimers (Brzovic et al., 2001; Linke et al., 2008; Liew et al., 2010). Nevertheless, there are exceptions. For instance, MARCH9 E3 ligase can form active dimers with RING-less variants (Hoer et al., 2007), whereas viral RING-type E3s MIR1 and MIR2 are believed to homodimerise via their transmembrane domain (Lehner et al., 2005). The tripartite motif (TRIM) family members in metazoans contain an additional domain termed B-box. Like the above mentioned RING domain, the B-box domain is a zinc-binding domain. However, whereas the RING domain is essential for E2 binding and E3 ligase activity, it has recently been shown that the B-box domain is involved in chain assembly rate modulation (Lazzari et al., 2019). Similarly, the U-box domain is also related to the RING domain, but unlike the B-box, it can interact with E2s. Additionally, the U-box domain has no coordinating zinc, so in order to ensure the stability of the structure, zinc-binding residues present in RING are replaced by charged and polar residues (Aravind and Koonin, 2000; Vander Kooi et al., 2006).

Inactivating RING-Type E3s by Mutating the Zinc-Coordinating Residues

Since the coordination of the two atoms of zinc by the RING domain is crucial for E3 ligase activity, mutants that abolish such coordination have often been used to create ligase-dead versions of those E3 enzymes. Mutation of any of the conserved Cys and His involved in zinc binding should compromise the E3 activity, and so have all been, individually or jointly, mutated for that purpose (**Figure 3**). The mutated residue of choice to prevent E3 ligase activity appears the first conserved Cys (C_1) of the RING domain, followed by the His (H), C_2, C_3, and C_4. To our knowledge, C_7 is the only key residue on the domain that has not been individually mutated for this purpose. However, it has been shown that simultaneous mutations on either C_1+C_7 or C_6+C_7 abolish the ligase activity of AMFR and some TRIM family members, respectively (Wang et al., 2014; Liu et al., 2017a; Lee et al., 2018a). As shown in **Figure 3**, many E3 ligases have been inactivated by simultaneous mutations on C_1+C_2. Less frequently, additional double mutations and even the triple C_1+C_2+C_3 mutant have been efficiently applied to block the activity of distinct RING-type E3 ligases (**Figure 3**).

Zinc-coordinating Cys and His residues have been preferentially mutated into Ala in order to abolish the ubiquitin ligase activity of E3s (**Figure 3**). Nevertheless, in some cases, this type of substitution might be insufficient. In a recent research focused on studying TRIM27-dependent ubiquitination of UPS7, it was shown that a quadruple TRIM27 mutant, in which four zinc-coordinating residues of the RING domain (Cys16, Cys19, Cys31 and Cys33) were mutated into alanine, was still capable of ubiquitinating USP7. By contrast, the TRIM27 mutant, in which four zinc-binding residues of the B-box (Cys96, Cys99, His107, and Asp110) were simultaneously substituted by Ala, was incapable of ubiquitinating USP7 (not illustrated in **Figure 3**; Zaman et al., 2013). Moreover, it should be taken into account that in some cases a dominant negative effect may be acquired by the mutated E3 ligase. For example, CBL Cys381Ala mutant is not capable of ubiquitinating EGFR and thus, the subsequent desensitization of the receptor is abolished. However, CBL Cys381Ala mutant is still capable of interacting with EGFR, and consequently, competes with wild type CBL compromising CBL-mediated EGFR ubiquitination (Waterman et al., 1999). Similarly, the plant E3 ubiquitin ligase SINA1 mutant on the C_2 of the RING domain Cys47Ser mutant retains dimerisation

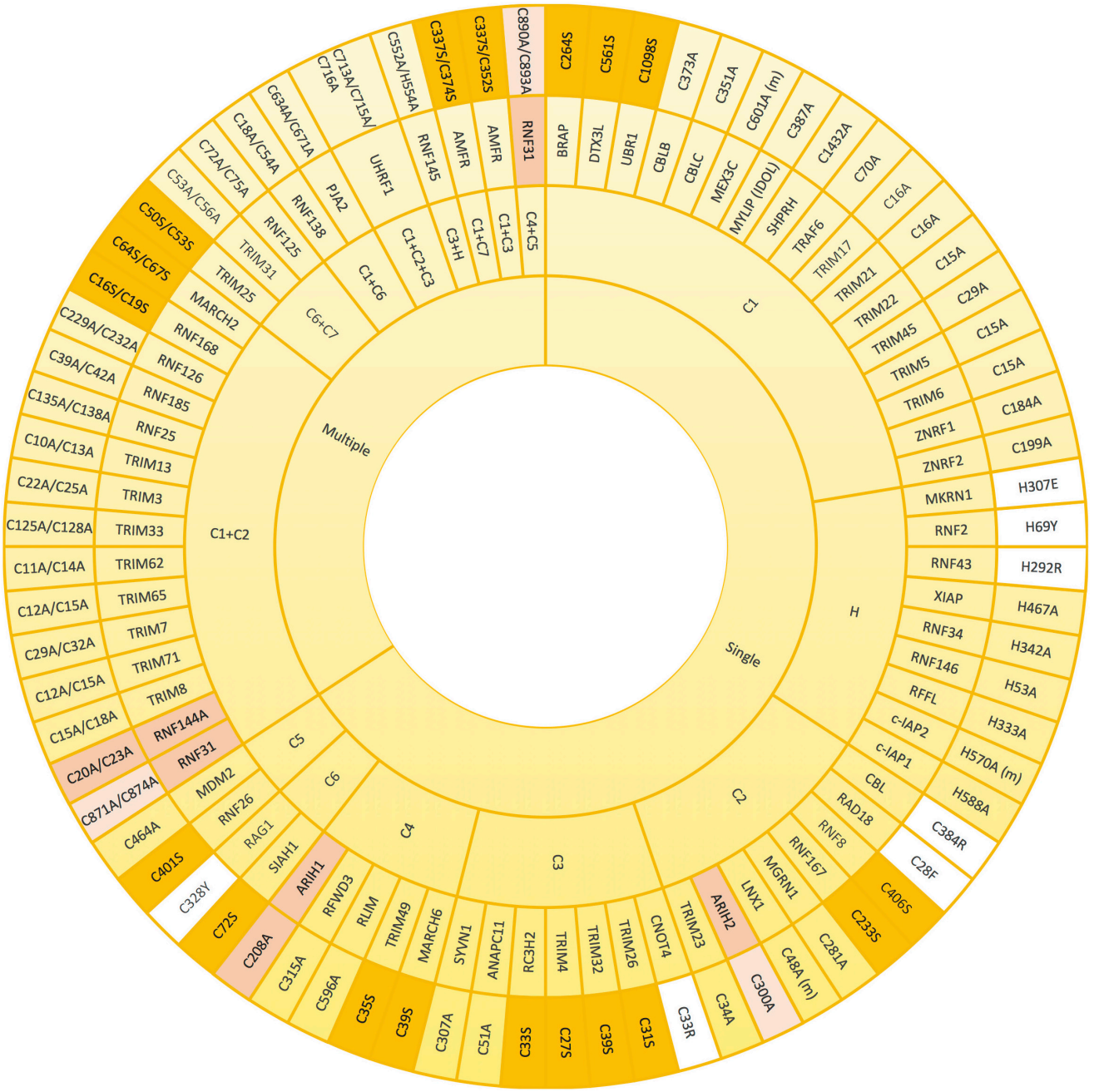

FIGURE 3 | Mutations that alter zinc coordinating residues in RING domains. Wheel diagram showing the reported mutations in RING domains, classified first whether a unique (single) or various (multiple) residues were mutated simultaneously. Most of the inactive E3 enzymes have been obtained by mutating key residues into alanine (yellow). Lack of activity can also be acquired by mutations into serine (orange). Mutations into other residues have been also employed (white). Zinc coordinating residues of the first (pink) and the second (light pink) RING domains in RBR-type E3 ubiquitin ligases (pink) have also be modified in order to achieve inactivation. References to all the mutations shown in this figure are provided in **Supplementary Table S1**.

and substrate binding ability but lacks ubiquitination activity (den Herder et al., 2012).

Despite less frequently, in a number of investigations, the Cys involved in zinc coordination have also been efficiently mutated into serine. Indeed, this type of point mutation that results on E3 ligase inactivation has served to uncover, among others, the role of MDM2, RNF8, and SIAH1 RING E3s in cell cycle regulation, DNA damage response and Wnt signalling, respectively (Ji et al., 2017; Tian et al., 2017; Tripathi and Smith, 2017). Additionally, although there are fewer examples, it has been demonstrated that mutating the His into Glu, Tyr or Arg is sufficient to inactivate the ligase activity of MKRN1, RNF2, and

RNF43 E3s, respectively (Xia et al., 2014; Loregger et al., 2015; Lee et al., 2018b; **Figure 3**). Similarly, it has been shown that mutating C_2 of RAD18 and CBL into Phe and Arg, respectively, as well as substituting C_3 of CNOT4 into Arg or C_6 of RAG1 into Tyr has an inhibitory effect (Albert et al., 2002; Jones and Gellert, 2003; Williams et al., 2011; Javadi et al., 2013). It should be noted, however, that in search of structure-function relationships, the safest approach is to mutate into the smaller Ala residue (Fersht et al., 1999). Introducing larger residues might -in addition to preventing the coordination of the zinc- result in further distortions on the overall fold of the protein.

Especially in the absence of the molecular structure, deciding the residues that should be mutated might not always be straightforward, but appropriate sequence alignments can provide sufficient insight. For instance, TRIM37 has two adjacent Cys residues (Cys36 and Cys37) that could correspond to the C_4 involved in zinc coordination (**Supplementary Figure S1**). Therefore, to ensure the inactivation of the enzyme, both Cys were simultaneously mutated (Kallijärvi et al., 2005; Wang et al., 2017). Similarly, ZNRF4 has two His nearby (His329 and His332) and in principle, either of them could be involved in coordinating zinc atoms. Once again, both His were mutated in order to obtain a catalytically inactive form of the E3 (Bist et al., 2017). Based on metal-binding studies, MDM2 His457 was initially confirmed to be the conserved His involved in zinc-coordination (Lai et al., 1998). Nevertheless, His452 is also essential, as demonstrated in auto-ubiquitination assays of this E3 ligase, with both His residues being necessary (Fang et al., 2000). It was later elucidated that His452 actually takes the place of the conserved Cys C_3 in the zinc coordination, as illustrated in the sequence alignment in **Figure 4B**.

Additionally, there are few E3s bearing RING domains in which a non-conserved amino acid plays an indirect but pivotal role in the coordination of the zinc atom, and therefore, can be mutated in order to disrupt the activity of the ligase. For example, Thr455, which was originally believed to be directly involved in the zinc-coordination based on an incorrect primary sequence alignment, has been reported to abolish -upon its mutation- MDM2-dependent p53 ubiquitination (Boddy et al., 1994; Fang et al., 2000).

Inactivating RING-Type E3s by Mutating the E2-Interacting Residues

It has previously been described that RING E3s interact with E2-Ub conjugates via their RING domain to directly transfer the ubiquitin to the substrate protein. Therefore, disrupting the interaction between E2s and RING-type E3s has also been extensively used to block, or at least reduce ubiquitination mediated by RING E3s. All three key hydrophobic residues on E3s that mediate the interaction with E2s (shown in green in **Figure 2**) have been recurrently mutated to compromise the activity of the E3s. As shown in **Figure 4A**, numerous RING-type E3 ligases have been successfully inactivated by mutating the first Ile/Leu, the second Trp/Leu or the last Ile/Val into Ala. The first Ile/Leu has been mutated in BRCA1, BMI-1, CHFR, CNOT4, RING1, RNF2, RNF8 and TRIM3 (Albert et al., 2002; Eakin et al., 2007; Alchanati et al., 2009; Kim et al., 2010; Mallette et al., 2012; Raheja et al., 2014; Liu et al., 2018; Shen et al., 2018). The second Trp/Leu was mutated abolishing ligase activity in BRAP, CBL, MARCH8, MARCH9, MDM2, and TRIM7 (Joazeiro et al., 1999; Chen et al., 2012; Hayes et al., 2012; Chakraborty et al., 2015; Fan and Wang, 2017; Tan et al., 2019). Finally, the last Ile/Val was successfully mutated in KIAP and TRIM3 (Dou et al., 2012; Raheja et al., 2014). All these hydrophobic residues are conserved as seen in **Figure 4B**. However, to our knowledge, no one has mutated the E2-interacting Pro (located between C6 and C7) with the aim to disrupt the association with the E2 enzyme. Given the special properties of this cyclic amino acid, one certainly would have to be weary of additional conformational effects that could be caused by its mutation to Ala. Additionally, MDM2 mutant variants Ile440Glu and Ile440Lys prevent MDM2-dependent ubiquitination of p53, by disrupting the E2–ubiquitin binding by the E3 ligase without altering its RING domain structure (Nomura et al., 2017). This residue, however, is barely conserved across the different RING domains.

However, other types of mutations have also been efficiently applied to disrupt the interaction between E2s and E3s. For instance, one of the few U-box-type E3s that has been mutated is CHIP, also known as STUB1, which was inactivated by substituting His260 into Glu (Seo et al., 2018). Likewise, the U-box domain-containing UBE4B E3 can be inactivated by mutating a Pro (Pro1140) that is conserved among U-box-type E3 ligases (Pro269 in CHIP) into Ala (not included in **Figure 4**; Okumura et al., 2004; Li et al., 2018).

Inactivating RING-Type E3s by Disrupting Substrate Recognition, E3 Dimerization and Stability

Many RING-type E3 ligases possess a conserved positively charged residue (Arg or Lys) in the last position of the RING domain, which appears to be essential for the ubiquitination activity of the E3. Nevertheless, it is still controversial whether the effect of mutating this residue results from the impaired interaction with E2s or from destabilization of the RING domain (**Figure 4A**, included in stabilization) (Albert et al., 2002; Linke et al., 2008; Lienlaf et al., 2011; Dou et al., 2012; Raheja et al., 2014; Nomura et al., 2017). But this uncertainty is not surprising given that mutations have been generated to substitute the positively charged residue by a very diverse choice of residues (mostly to Ala, but also to Glu, Pro and even Arg, as can be seen in **Figure 4A**. Future studies should preferably limit the mutations to substituting the positively charged residue by Ala.

As shown in **Figure 4A**, a number of other single point mutations, as well as multiple point mutations, have been generated along different positions of the RING domain to compromise protein stability and hence, E3 ligase activity, but no clear pattern can be predicted based on the studies reported so far. For example, the Tyr37Ala mutant in BRCA1 lack ligase activity, being therefore incapable of reversing γ-radiation hypersensitivity of BRCA1-null human breast cancer cells (Ruffner et al., 2001). In the case of the RAD18 ligase,

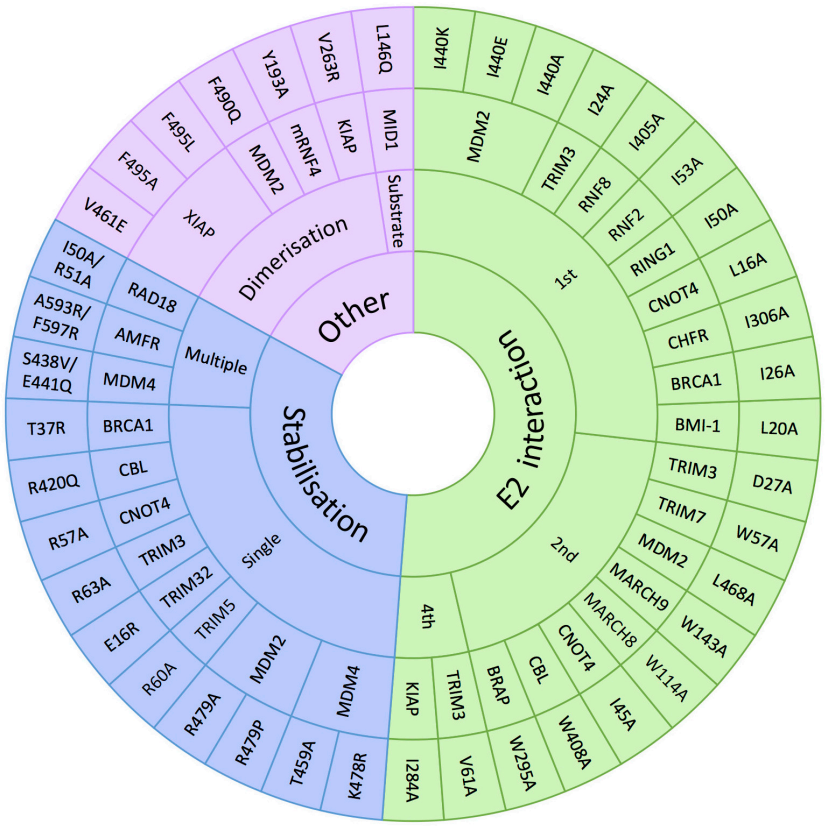

FIGURE 4 | Mutations on RING- and RBR-type E3s that affect E2-interaction, domain stabilisation, protein dimerization or substrate recognition. **(A)** In RING-type E3 ubiquitin ligases, inactivation can be obtained by abolishing the interaction with E2 ubiquitin-conjugating enzymes (green). This has mostly been achieved by mutating the conserved 1st (I/L) and 2nd (W/I/L) hydrophobic residues indicated in **Figure 2**. Other mutations affecting the stabilisation of key residues of the domain (blue), dimerization or the interaction with a specific substrate also abolish the ligase activity (purple). For the stabilisation affecting mutations, those have been classified whether a unique (single) or various (multiple) residues were mutated simultaneously. References to all the mutations shown in this figure are provided in **Supplementary Table S1**. **(B)** Alignment of the RING domains of the RING-type E3 ligases involved in E2-interacting and stabilisation mutations within the RING domain. Conserved amino acids are highlighted in yellow and orange, respectively, for the Zn-coordinating Cys and His residues, and in green for the E2-interacting residues. The conserved positively charged residues at the end of the RING domain are highlighted in blue. Mutated E2-interacting residues are shown in bold and underlined. Mutated residues involved in stabilisation are shown in bold. Mutated residues involved in dimerisation are underlined and shadowed.

the Ile50Ala/Arg51Ala inactive mutant allowed to study the formation of ternary complexes with RAD6A (Masuda et al., 2012); these two residues were selected due to being highly conserved among species.

RING-type E3s that act as dimers can also be inactivated by preventing their dimerization process. For instance, mutation of Val461Glu and Val263Arg within the RING domain diminishes oligomerisation and activity of XIAP and KIAP ligases, respectively (Poyurovsky et al., 2007; Dou et al., 2012; Nakatani et al., 2013). In other cases, however, the dimerization affecting residues are immediately after the RING domain (**Supplementary Figure S2**), as revealed for example by the mutation Phe490Gln in MDM2 (Poyurovsky et al., 2007). Another approach consists of inactivating oligomeric E3 ligases without affecting the oligomerisation process itself. For example, RNF4 Val134Ala and Ile153Ala mutants can form dimers but are catalytically incapacitated (Liew et al., 2010; Dou et al., 2012). Similarly, other E3 ligase mutants have been shown to act in a dominant negative due to their homo-dimeric nature. For example, mutant Fbw7 has a dominant-negative effect when dimerising with wild-type Fbw7, being able to effectively bind their substrate MYC but not to ubiquitinate and degrade it (Welcker et al., 2013).

Several experiments have also been carried out mutating specific residues on E3 ligases that are critical for the interaction with a given substrate, such as Leu146Gln mutation on the B-box containing E3 MID1 that cannot associate, nor ubiquitinate its substrate PP2A alpha-2 (Du et al., 2013; **Figure 4**).

MUTATIONS ON HECT TYPE E3 LIGASES

The human HECT-type E3 family consists of 28 members that are divided into three different groups depending on their N-terminal domain architecture: (i) the *NEDD4 subfamily*, characterized by containing a C2 domain, a HECT domain and two to four WW domains, which bind to the PY motifs of target proteins (Staub et al., 1996; Kanelis et al., 2001); (ii) the *HERC subfamily*, which integrates at least one regulator chromosome condensation 1 (RCC1)-like domain (RLDs) and a reduced HECT domain; and (iii) the *other HECT subfamily*, that embrace HECT-type E3s not fitting the above mentioned two subfamilies.

Despite those differences, all HECT-type E3s share a ∼350 amino acid long HECT domain, that was first described in human papilloma virus E6 associated protein (E6AP) (Huibregtse et al., 1995). In the HECT domain, a conserved Cys forms thioester-linked-intermediate complexes with ubiquitin (**Figure 1B**), before being transferred and attached to the substrate through a transthiolation reaction. This conserved Cys is located in the C-terminal region of the HECT domain, while the E2 interacting site is localised in the N-terminal site (**Figure 1B**; Rotin and Kumar, 2009).

Inactivating HECT-Type E3s

Given that an *active site Cys* is required for the formation of a thioester intermediate with ubiquitin, a typical approach is to mutate this specific Cys to generate ligase dead versions of HECT E3 ligases. As shown in **Figure 5A**, the majority of HECT-type E3 ligases have been inactivated by replacing this catalytic Cys by Ala. This approach has served to unveil, among others, the involvement of HERC3 in immune response (Hochrainer et al., 2015), the role of NEDD4L in EnaC receptor recycling (Zhou et al., 2007), and the contribution of SMURF1 to Axin degradation (Fei et al., 2013).

Less frequently, some ligase dead HECT-type E3s have been generated by substitution of the active Cys into Ser (**Figure 5A**). It has been reported that when the catalytic Cys of an E3 is mutated into Ser, the residue is still capable of binding through an oxyester bond with ubiquitin, but incapable to transfer it to substrates, which might result in a dominant-negative effect. In ubiquitination assays employing this type of ligase dead E3s, a stable monoubiquitinated version of the E3 has been detected (Lee et al., 2014). This approach has allowed, among other things to discover many substrates of distinct HECT-type E3 ligases. For instance, it was found that wild type version of HACE1 could ubiquitinate and target for degradation the small GTPase Rac1, but the Cys876Ser ligase dead version of the E3 ligase could not (Torrino et al., 2011). Similarly, HERC2 C4762S and HUWE C4341S mutants failed to ubiquitinate their substrates BRCA1 and N-Myc, respectively (Zhao et al., 2008; Wu et al., 2010). The sequence alignment for all the HECT domain E3 ligases illustrated in **Figure 5A** is shown around the catalytically active Cys in **Figure 5B**.

MUTATIONS ON RBR TYPE E3 LIGASES

RING between RING family members contain two RING domains (RING1 and RING2) that are separated by an in-between-RING (IBR) zinc-binding domain. Morett and Bork first characterised these domains in 1999 in a sequence profile-based characterisation (Morett and Bork, 1999). In the process of confirming reports that UbcH7 could also interact with RBR E3s, they discovered that these RBR E3s act as RING/HECT hybrids. The first RING domain serves as the E2 binding platform, while the C_3 of the second RING serves as the active site that mediates ubiquitination similarly to HECT E3 ligases (Wenzel et al., 2011; **Figures 1C**, **5C**).

Inactivating RBR-Type E3s

As it happens with HECT-type E3, the mutation of the catalytic Cys in the RING2 of RBR E3s results in the inactivation of these enzymes. However, unlike in HECT-type E3 ligases, in RBR E3s the active Cys has been mostly substituted by Ser, and less by Ala (**Figure 5A**). For example, C983S substitution in MIB2 resulted in ligase inactivation, and therefore, prevented ubiquitination of its substrate TANK-binding kinase 1 (Ye et al., 2014). Similarly, mutating the active Cys of ARIH2 (also called TRIAD1) into Ser or Ala completely abolished autoubiquitination of the RBR-type E3 ligase. Parkison disease has been shown to develop in patients carrying a Cys431Phe mutation at the catalytic Cys of the RBR-type E3 ligase PRKN; those mutants have also been characterized in the lab (Sarraf et al., 2013), in addition to the more common substitutions to Ser and Ala (Liu et al., 2017b; Xin et al., 2018).

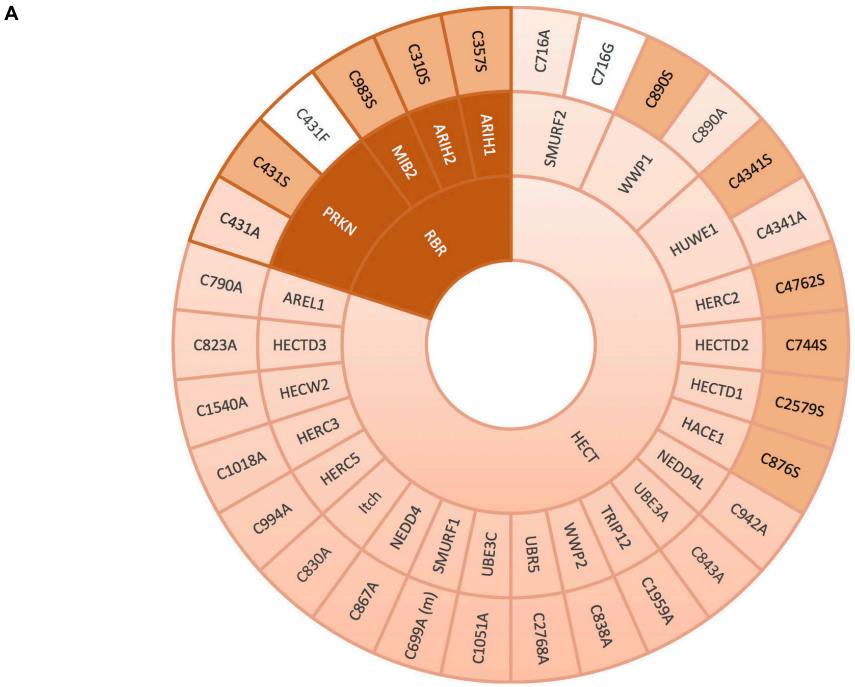

B

```
AREL1   (764-822)   GGFAALCPSFQIIAAP--THSTLP-TAHTCFNQLCLPTYDSYEEVHRMLQLAISEGCEGFGM
HACE1   (851-908)   GG-SGLQ-NFTIAAVPY-TPNLLP-TSSTCINMLKLPEYPSKEILKDRLLVALHCGSYGYTM
HECTD1  (2559-2617) GGLANLHPRLTVVRKVDATDASYP-SVNTCVHYLKLPEYSSEEIMRERLLAATMEK--GFHL
HECTD2  (719-775)   GGMADLN--FKIS-KNETSTNCLP-VAHTCFNQLCLPPYKSKKDLKQKLIIGISNS-EGFGL
HECTD3  (800-854)   ----ARIYIYPDKLGY-ETTDALP-ESSTCSSTLFLPHYASAKVCEEKLRYAAYNC-VAIDT
HECW2   (1516-1571) --GSNGPRRFCVEK-WGKI-TALP-RAHTCFNRLDLPPYPSFSMLYEKLLTAVEET-STFGL
HERC2   (4738-4793) --GRDFVIQVL-DKYNPPD-HFLP-ESYTCFFLLKLPRYSCKQVLEEKLKYAIHFC-KSIDT
HERC3   (992-1049)  -IYGMASLQIVIQSTASGE-EYLP-VAHTCYNLLDLPKYSSKEILSARLTQALDNY-EGFSL
HERC5   (967-1024)  -MKDLNNMKITFCCPESWN-ERDPIRALTCFSVLFLPKYSTMETVEEALQEAINNN-RGFG-
HUWE1   (4316-4373) --GMNGIQKFQIHRDDRS-TDRLP-SAHTCFNQLDLPAYESFEKLRHMLLLAIQECSEGFGL
ITCH    (846-902)   -MGSNGPQKFCIEKV-GKE-NWLP-RSHTCFNRLDLPPYKSYEQLKEKLLFAIEET-EGFGQ
NEDD4   (1261-1317) -YGSNGPQSFTVEQWGTP--EKLP-RAHTCFNRLDLPPYESFEELWDKLQMAIENT-QGFDG
NEDD4L  (917-973)   -YGSNGPQLFTIEQWGSP--EKLP-RAHTCFNRLDLPPYETFEDLREKLLMAVENA-QGFEG
mSMURF1 (673-730)   -TGAAGPRLFTIHLIDAN-TDNLP-KAHTCFNRIDIPPYESYEKLYEKLLTAVEET-CGFAV
SMURF2  (690-747)   -QGAAGPRLFTIHQIDAC-TNNLP-KAHTCFNRIDIPPYESYEKLYEKLLTAIEET-CGFAV
TRIP12  (1933-1991) -NPPLTIVRKTFESTENPD-DFLP-SVMTCVNYLKLPDYSSIEIMREKLLIAAREGQQSFHL
UBE3A   (818-874)   GGLG-KLKMIIA-KNG-PDTERLP-TSHTCFNVLLLPEYSSKEKLKERLLKAITYA-KGFGM
UBE3C   (1025-1082) -GFKELYPAFCI-HNGGSDLERLP-TASTCMNLLKLPEFYDETLLRSKLLYAIECA-AGFEL
UBR5    (2742-2798) -SEEGFQPMPSITIRPPDD-QHLP-TANTCISRLYVPLYSSKQILKQKLLLAIKTKNFGFV-
WWP1    (865-921)   -MGSNGPQKFCIEKVG-KD-TWLP-RSHTCFNRLDLPPYKSYEQLKEKLLFAIEET-EGFGQ
WWP2    (829-869)   -IGSNGPQKFCIDKVG-KE-TWLP-RSHTCFNRLDLPPYKSYEQLREKLLYAIEET-EGFGQ
```

C

```
ARIH1(344-375)  TKECPKCHVT-IEKDGGCNHMVCRNQNCKAEF---CWVCLGP-
ARIH2(297-326)  TKDCPKCNIC-IEKNGGCNHMQCS--KCKHDF---CWMCLGD-
MIB2 (969-1002) RITCPICIDSHIRLVFQCGHGACAP--CGSALSA-CPICRQPI
PRKN (418-449)  TKPCPRCHVP-VEKNGGCMHMKCPQPQCRLEWCWNCG-CE---
```

FIGURE 5 | Inactivation of HECT- and RBR-type E3 ligases by mutation of the catalytic cysteine. **(A)** Mutation of the catalytic cysteine into an alanine (light pink), a serine (pink) or another residue (white) abolishes transference of ubiquitin onto the substrate. Inactivation of the catalytic cysteine of RBR-type E3 ubiquitin ligases is obtained by mutation of the third conserved cysteine in the second RING domain. (m) indicates that this mutation has been done in the mice homolog of the protein. References to all the mutations shown in this figure are provided in **Supplementary Table S1**. **(B)** Alignment of the HECT domains of the HECT-type E3 ligases. The conserved catalytic cysteine is highlighted in pink. **(C)** Alignment of the RING2 domains of the RBR-type E3 ligases. Conserved zinc-coordinating cysteines and histidine on the second RING domain of mutated RBR E3 ligases are highlighted in yellow and the mutated catalytic cysteine is highlighted in pink.

In order to generate ligase dead versions of RBR-type E3s, it has been also shown to be plausible to preserve the active Cys, and instead mutate the zinc-coordinating residues in either of the two RING domains, substituting by Ala one or several of those key residues. For instance, ARIH1 and RNF144A have been successfully inactivated by modifying their RING1 domain (**Figure 3**, dark pink). Whereas mutating C4 of ARIH1 (Cys208) was sufficient to inhibit the ligase, Cys20 and Cys23 (C1+C2) were simultaneously modified to block the catalytic activity of the RBR-type E3 RNF144A (Ho et al., 2014; von Stechow et al., 2015). On the contrary, ARIH2 and RNF31 have been inactivated by mutating their RING2 domain zinc-coordinating Cys residues (**Figure 3**, light pink). Cells expressing an ARIH1 mutant in which the C2 of the RING2 domain was mutated into Ala (ARIH2 Cys300Ala mutant) was no longer able to ubiquitinate NLRPL3 (Kawashima et al., 2017). Similarly, Smit and co-workers generated various ligase dead versions of RNF31 by mutating simultaneously Cys871 and C874 (C1+C2) or Cys890 and Cys892 (C4+C5) of the RING2 domain (Smit et al., 2012).

CONCLUSION

Mutations on E3 ligases have been associated with a number of diseases, including neurological disorders (George et al., 2018; Osinalde et al., 2019). Thus, understanding their mechanism of action, as well as identifying which substrates are regulated by each E3 at different developmental stages and cell types, will provide invaluable knowledge that might contribute to develop therapeutic strategies to treat these diseases. Generation of E3 ligase dead mutants can certainly provide crucial information for this purpose. While the use of gene silencing techniques might be more appropriate to study the phenotypes derived from the loss of function of E3 ligases, the overexpression of ligase death versions can provide information about (i) the E2 enzymes they work with, (ii) substrate recognition domains and (iii) existing mechanism that regulate their activity. Additionally, a number of biochemical experiments do benefit from comparing the ectopic expression of wild type active E3 ligases with their mutated inactive variants.

As evident from all the examples shown in this review, there are multiple options to disrupt the activity of an E3 ligase. As illustrated by the sequence alignment in **Figure 4B**, the first necessary step is to identify which are the key residues in our ligase of interest. This is an essential step to ensure that any mutagenesis performed has a higher chance of success in disrupting the E3 ligase activity. For example, not all cysteine residues within a RING domain are involved in zinc coordination, as can be seen in the sequence alignment of Mdm2 in **Figure 4B**. When this cysteine of the Mdm2 RING domain was mutated (Kostic et al., 2006) the zinc coordination was maintained and no disruption to the ubiquitination activity of Mdm2 was detectable.

It is worth mentioning that mutating key residues involved either in the coordination of the zinc ions, dimerisation, proteins stabilization or E2 interaction might not always be sufficient to abolish the catalytic activity of the E3 ligase. The resulting mutation replacing the original residue that is substituted can actually be determinant in order to have a functional effect. For instance, mutating Phe495 of XIAP into either Ala, Tyr or Trp completely prevents E3 ligase autoubiquitination. However, XIAP Phe495Leu mutants appear to be functionally wild-type like (Nakatani et al., 2013); but might not be that surprising given the partial hydrophobic similarity between those two amino acids.

As illustrated within this review, so far one of the most frequent approaches for RING E3 ligases has been to mutate the residues involved in the zinc coordination (Cys and His residues, shaded in yellow and orange, respectively, in **Figure 4B**). Eliminating the zinc coordination on the RING domain is well known to severely disrupt the ubiquitination activity of those E3 ligases. However, this breakdown of the global structural integrity of the RING construct might lead to a severe effect in the folding and expression levels of the E3 ligase (Chasapis et al., 2010). Therefore, for certain experiments might be more effective to generate less disruptive point mutations. For example, the mutation of the hydrophobic residues (Ile, Leu, Trp, Val, shaded in green in **Figure 4B**) that mediate the interaction with the E2 conjugating enzyme, as demonstrated for a number of RING E3 ligases. To our knowledge this approach has not yet been employed for the E2-interacting RING domain of RBR E3 ligases, but it should indeed be an interesting experiment to perform.

Another approach that has been used as well is to eliminate by mutagenesis the positive charge of the Lys or Arg residue located straight after the last zinc-coordinating Cys of the RING domain. It is yet unclear, however, whether the effect caused by this mutation is on the interaction with E2s or from destabilization of the RING domain.

Mutations on the active Cys of HECT- and RBR-type E3 ligases are very straight forward, as they generate, without further effect to the structure and stability of the E3, ligase-dead versions of these enzymes. Those are of good value to be used as the best control in experiments overexpressing the wild type ligase, for example, to identify substrates in an unbiased manner. Additionally, if mutating the active site Cys to Ser, the formation of an oxyester to ubiquitin can be used with the aim to obtain a dominant-negative version of the ligase; the E3 will recruit the E2 and the substrate but the ubiquitination reaction cannot proceed since the ubiquitin cannot be released once it has conjugated to the E3.

To investigate the regulation of a specific protein by a particular HECT or RBR E3, however, it might be more suitable to mutate the ligase at the substrate recognition motif. Moreover, in some cases, as is the case of some RING E3s, the inactivation of E3 enzymes is not achieved by a single point mutation, even though such residue is defined as a key amino acid involved in substrate recognition. Hence, in such situations, several residues must be simultaneously mutated in order to disrupt the E3 ligase function. The generation and usage of E3 mutants have revealed unexpected and important lessons about the complexity of this family of enzymes. Nevertheless, a complete understanding of E3 ligases still requires more research, in which the generation of novel E3 ligase mutants will undoubtedly be decisive.

AUTHOR CONTRIBUTIONS

CG-B designed and wrote the first draft. All authors contributed to this manuscript.

FUNDING

This work was supported by Spanish MINECO (grant SAF2016-76898-P) cofinanced with FEDER funds. JR was funded with a postdoctoral fellowship from the University of the Basque Country (UPV/EHU).

ACKNOWLEDGMENTS

We would like to thank Jesus Mari Arizmendi for sharing the laboratory with our group. We would also like to thank all the people in the lab.

SUPPLEMENTARY MATERIAL

The Supplementary Material for this article can be found online at: https://www.frontiersin.org/articles/10.3389/fcell.2020.00039/full#supplementary-material

REFERENCES

Albert, T. K., Hanzawa, H., Legtenberg, Y. I. A., de Ruwe, M. J., van den Heuvel, F. A. J., Collart, M. A., et al. (2002). Identification of a ubiquitin-protein ligase subunit within the CCR4-NOT transcription repressor complex. *EMBO J.* 21, 355–364. doi: 10.1093/emboj/21.3.355

Alchanati, I., Teicher, C., Cohen, G., Shemesh, V., Barr, H. M., Nakache, P., et al. (2009). The E3 ubiquitin-ligase Bmi1/Ring1A controls the proteasomal degradation of Top2α cleavage complex - A potentially new drug target. *PLoS One* 4:e8104. doi: 10.1371/journal.pone.0008104

Aravind, L., and Koonin, E. V. (2000). The U box is a modified RING finger - a common domain in ubiquitination. *Curr. Biol.* 10, R132–R134. doi: 10.1016/S0960-9822(00)00398-395

Bailly, V., Lauder, S., Prakash, S., and Prakash, L. (1997). Yeast DNA repair proteins Rad6 and Rad18 form a heterodimer that has ubiquitin conjugating, DNA binding, and ATP hydrolytic activities. *J. Biol. Chem.* 272, 23360–23365. doi: 10.1074/jbc.272.37.23360

Bist, P., Cheong, W. S., Ng, A., Dikshit, N., Kim, B.-H., Pulloor, N. K., et al. (2017). E3 Ubiquitin ligase ZNRF4 negatively regulates NOD2 signalling and induces tolerance to MDP. *Nat. Commun.* 8:15865. doi: 10.1038/ncomms15865

Boddy, M. N., Freemont, P. S., and Borden, K. L. B. (1994). The p53-associated protein MDM2 contains a newly characterized zinc-binding domain called the RING finger. *Trends Biochem. Sci.* 19, 198–199. doi: 10.1016/0968-0004(94)90020-90025

Brzovic, P. S., Rajagopal, P., Hoyt, D. W., King, M. C., and Klevit, R. E. (2001). Structure of a BRCA1-BARD1 heterodimeric RING-RING complex. *Nat. Struct. Biol.* 8, 833–837. doi: 10.1038/nsb1001-833

Cao, R., Tsukada, Y. I., and Zhang, Y. (2005). Role of Bmi-1 and Ring1A in H2A ubiquitylation and hox gene silencing. *Mol. Cell* 20, 845–854. doi: 10.1016/j.molcel.2005.12.002

Chakraborty, A., Diefenbacher, M. E., Mylona, A., Kassel, O., and Behrens, A. (2015). The E3 ubiquitin ligase Trim7 mediates c-Jun/AP-1 activation by Ras signalling. *Nat. Commun.* 6:6782. doi: 10.1038/ncomms7782

Chasapis, C. T., Loutsidou, A. K., Orkoula, M. G., and Spyroulias, G. A. (2010). Zinc binding properties of engineered ring finger domain of arkadia e3 ubiquitin ligase. *Bioinorg. Chem. Appl.* 2010, 1–7. doi: 10.1155/2010/323152

Chen, R., Li, M., Zhang, Y., Zhou, Q., and Shu, H. (2012). The E3 ubiquitin ligase MARCH8 negatively regulates IL-1 β-induced NF-κB activation by targeting the IL1RAP coreceptor for ubiquitination and degradation. *Proc. Natl. Acad. Sci. U.S.A.* 109, 14128–14133. doi: 10.1073/pnas.1205246109

Ciechanover, A., and Ben-Saadon, R. (2004). N-terminal ubiquitination: more protein substrates join in. *Trends Cell Biol.* 14, 103–106. doi: 10.1016/j.tcb.2004.01.004

den Herder, G., Yoshida, S., Antolín-Llovera, M., Ried, M. K., and Parniskea, M. (2012). Lotus japonicus E3 ligase SEVEN IN ABSENTIA4 destabilizes the symbiosis receptor-like Kinase SYMRK and negatively regulates rhizobial infection. *Plant Cell* 24, 1691–1707. doi: 10.1105/tpc.110.082248

Deshaies, R. J., and Joazeiro, C. A. P. (2009). RING domain E3 ubiquitin ligases. *Annu. Rev. Biochem.* 78, 399–434. doi: 10.1146/annurev.biochem.78.101807.093809

Dou, H., Buetow, L., Sibbet, G. J., Cameron, K., and Huang, D. T. (2012). BIRC7-E2 ubiquitin conjugate structure reveals the mechanism of ubiquitin transfer by a RING dimer. *Nat. Struct. Mol. Biol.* 19, 876–883. doi: 10.1038/nsmb.2379

Du, H., Huang, Y., Zaghlula, M., Walters, E., Cox, T. C., and Massiah, M. A. (2013). The MID1 E3 ligase catalyzes the polyubiquitination of Alpha4 (α4), a regulatory subunit of protein phosphatase 2A (PP2A): novel insights into MID1-mediated regulation of PP2A. *J. Biol. Chem.* 288, 21341–21350. doi: 10.1074/jbc.M113.481093

Eakin, C. M., Maccoss, M. J., Finney, G. L., and Klevit, R. E. (2007). Estrogen receptor alpha is a putative substrate for the BRCA1 ubiquitin ligase. *Proc. Natl. Acad. Sci. U.S.A.* 104, 5794–5799. doi: 10.1073/pnas.0610887104

Fan, C., and Wang, X. (2017). Mdm2 Splice isoforms regulate the p53 / Mdm2 / Mdm4 regulatory circuit via RING domain-mediated ubiquitination of p53 and Mdm4. *Cell Cycle* 16, 660–664. doi: 10.1080/15384101.2017.1288327

Fang, S., Jensen, J. P., Ludwig, R. L., Vousden, K. H., and Weissman, A. M. (2000). Mdm2 is a RING finger-dependent ubiquitin protein ligase for itself and p53. *J. Biol. Chem.* 275, 8945–8951. doi: 10.1074/jbc.275.12.8945

Fei, C., Li, Z., Li, C., Chen, Y., Chen, Z., He, X., et al. (2013). Smurf1-mediated Lys29-linked nonproteolytic polyubiquitination of axin negatively regulates Wnt/β-catenin signaling. *Mol. Cell. Biol.* 33, 4095–4105. doi: 10.1128/MCB.00418-413

Fersht, A., Julet, M. R., and Britch, J. (1999). *Structure and Mechanicsm in Protein Science - A. Fersht (W H Freeman, 1999)*. Singapore: World Scientific.

Freemont, P. S., Hanson, I. M., and Trowsdale, J. (1991). A novel cysteine-rich sequence motif. *Cell* 64, 483–484. doi: 10.1016/0092-8674(91)90229-r

Fukutomi, T., Takagi, K., Mizushima, T., Ohuchi, N., and Yamamoto, M. (2014). Kinetic, thermodynamic, and structural characterizations of the association between Nrf2-DLGex degron and Keap1. *Mol. Cell. Biol.* 34, 832–846. doi: 10.1128/MCB.01191-1113

George, A. J., Hoffiz, Y. C., Charles, A. J., Zhu, Y., and Mabb, A. M. (2018). A comprehensive atlas of E3 ubiquitin ligase mutations in neurological disorders. *Front. Genet.* 9:29. doi: 10.3389/fgene.2018.00029

Gilberto, S., and Peter, M. (2017). Dynamic ubiquitin signaling in cell cycle regulation. *J. Cell Biol.* 216, 2259–2271. doi: 10.1083/jcb.201703170

Hayes, S. D., Liu, H., MacDonald, E., Sanderson, C. M., Coulson, J. M., Clague, M. J., et al. (2012). Direct and indirect control of mitogen-activated protein kinase pathway-associated components, BRAP/IMP E3 ubiquitin ligase and CRAF/RAF1 kinase, by the deubiquitylating enzyme USP15. *J. Biol. Chem.* 287, 43007–43018. doi: 10.1074/jbc.M112.386938

Hershko, A., and Ciechanover, A. (1998). the ubiquitin system. *Annu. Rev. Biochem.* 67, 425–479. doi: 10.1146/annurev.biochem.67.1.425

Ho, S.-R., Mahanic, C. S., Lee, Y.-J., and Lin, W.-C. (2014). RNF144A, an E3 ubiquitin ligase for DNA-PKcs, promotes apoptosis during DNA damage. *Proc. Natl. Acad. Sci. U.S.A.* 111, E2646–E2655. doi: 10.1073/pnas.1323107111

Hochrainer, K., Pejanovic, N., Olaseun, V. A., Zhang, S., Iadecola, C., and Anrather, J. (2015). The ubiquitin ligase HERC3 attenuates NF-κB-dependent transcription independently of its enzymatic activity by delivering the RelA subunit for degradation. *Nucleic Acids Res.* 43, 9889–9904. doi: 10.1093/nar/gkv1064

Hoer, S., Smith, L., and Lehner, P. J. (2007). MARCH-IX mediates ubiquitination and downregulation of ICAM-1. *FEBS Lett.* 581, 45–51. doi: 10.1016/j.febslet.2006.11.075

Huibregtse, J. M., Scheffner, M., Beaudenon, S., and Howley, P. M. (1995). A family of proteins structurally and functionally related to the E6-AP ubiquitin-protein ligase. *Proc. Natl. Acad. Sci. U.S.A.* 92, 5249. doi: 10.1073/pnas.92.11.5249-a

Javadi, M., Richmond, T. D., Huang, K., and Barber, D. L. (2013). CBL linker region and RING finger mutations lead to enhanced granulocyte-macrophage colony-stimulating factor (GM-CSF) signaling via elevated levels of JAK2 and LYN. *J. Biol. Chem.* 288, 19459–19470. doi: 10.1074/jbc.M113.475087

Ji, L., Jiang, B., Jiang, X., Charlat, O., Chen, A., Mickanin, C., et al. (2017). The SIAH E3 ubiquitin ligases promote Wnt/β-catenin signaling through mediating Wnt-induced Axin degradation. *Genes Dev.* 31, 904–915. doi: 10.1101/gad.300053.117

Joazeiro, C. A., Wing, S. S., Huang, H., Leverson, J. D., Hunter, T., and Liu, Y. C. (1999). The tyrosine kinase negative regulator c-Cbl as a RING-type, E2-dependent ubiquitin-protein ligase. *Science* 286, 309–312. doi: 10.1126/science.286.5438.309

Jones, J. M., and Gellert, M. (2003). Autoubiquitylation of the V(D)J recombinase protein RAG1. *Proc. Natl. Acad. Sci. U.S.A.* 100, 15446–15451. doi: 10.1073/pnas.2637012100

Joukov, V., Chen, J., Fox, E. A., Green, J. B. A., and Livingston, D. M. (2001). Functional communication between endogenous BRCA1 and its partner, BARD1, during Xenopus laevis development. *Proc. Natl. Acad. Sci. U.S.A.* 98, 12078–12083. doi: 10.1073/pnas.211427098

Kallijärvi, J., Lahtinen, U., Hämäläinen, R., Lipsanen-Nyman, M., Palvimo, J. J., and Lehesjoki, A.-E. (2005). TRIM37 defective in mulibrey nanism is a novel RING finger ubiquitin E3 ligase. *Exp. Cell Res.* 308, 146–155. doi: 10.1016/j.yexcr.2005.04.001

Kamadurai, H. B., Souphron, J., Scott, D. C., Duda, D. M., Miller, D. J., Stringer, D., et al. (2009). Insights into ubiquitin transfer cascades from a structure of a UbcH5B approximately ubiquitin-HECT(NEDD4L) complex. *Mol. Cell* 36, 1095–1102. doi: 10.1016/j.molcel.2009.11.010

Kanelis, V., Rotin, D., and Forman-Kay, J. D. (2001). Solution structure of a Nedd4 WW domain-ENaC peptide complex. *Nat. Struct. Biol.* 8, 407–412. doi: 10.1038/87562

Kawashima, A., Karasawa, T., Tago, K., Kimura, H., Kamata, R., Usui-Kawanishi, F., et al. (2017). ARIH2 Ubiquitinates NLRP3 and negatively regulates nlrp3 inflammasome activation in macrophages. *J. Immunol.* 199, 3614–3622. doi: 10.4049/jimmunol.1700184

Kim, J. M., Cho, E. N., Kwon, Y. E., Bae, S. J., Kim, M., and Seol, J. H. (2010). CHFR functions as a ubiquitin ligase for HLTF to regulate its stability and functions. *Biochem. Biophys. Res. Commun.* 395, 515–520. doi: 10.1016/j.bbrc.2010.04.052

Komander, D., and Rape, M. (2012). The ubiquitin code. *Annu. Rev. Biochem.* 81, 203–229. doi: 10.1146/annurev-biochem-060310-170328

Kostic, M., Matt, T., Martinez-Yamout, M. A., Dyson, H. J., and Wright, P. E. (2006). Solution structure of the Hdm2 C2H2C4 RING, a domain critical for ubiquitination of p53. *J. Mol. Biol.* 363, 433–450. doi: 10.1016/j.jmb.2006.08.027

Lai, Z., Freedman, D. A., Levine, A. J., and McLendon, G. L. (1998). Metal and RNA binding properties of the hdm2 RING finger domain. *Biochemistry* 37, 17005–17015. doi: 10.1021/bi980596r

Laney, J. D., and Hochstrasser, M. (1999). Substrate targeting in the ubiquitin system. *Cell* 97, 427–430. doi: 10.1016/S0092-8674(00)80752-80757

Lazzari, E., El-Halawany, M., De March, M., Valentino, F., Cantatore, F., Migliore, C., et al. (2019). Analysis of the zn-binding domains of TRIM32, the E3 ubiquitin ligase mutated in limb girdle muscular dystrophy 2H. *Cells* 8:254. doi: 10.3390/cells8030254

Lee, J. M., Choi, S. S., Lee, Y. H., Khim, K. W., Yoon, S., Kim, B.-G., et al. (2018a). The E3 ubiquitin ligase TRIM25 regulates adipocyte differentiation via proteasome-mediated degradation of PPARγ. *Exp. Mol. Med.* 50:135. doi: 10.1038/s12276-018-0162-6

Lee, M. S., Han, H. J., Han, S. Y., Kim, I. Y., Chae, S., Lee, C. S., et al. (2018b). Loss of the E3 ubiquitin ligase MKRN1 represses diet-induced metabolic syndrome through AMPK activation. *Nat. Commun.* 9:3404. doi: 10.1038/s41467-018-05721-5724

Lee, S. Y., Ramirez, J., Franco, M., Lectez, B., Gonzalez, M., Barrio, R., et al. (2014). Ube3a, the E3 ubiquitin ligase causing Angelman syndrome and linked to autism, regulates protein homeostasis through the proteasomal shuttle Rpn10. *Cell. Mol. Life Sci.* 71, 2747–2758. doi: 10.1007/s00018-013-1526-1527

Lehner, P. J., Hoer, S., Dodd, R., and Duncan, L. M. (2005). Downregulation of cell surface receptors by the K3 family of viral and cellular ubiquitin E3 ligases. *Immunol. Rev.* 207, 112–125. doi: 10.1111/j.0105-2896.2005.00314.x

Li, X., Zhong, L., Wang, Z., Chen, H., Liao, D., Zhang, R., et al. (2018). Phosphorylation of IRS4 by CK1γ2 promotes its degradation by CHIP through the ubiquitin/lysosome pathway. *Theranostics* 8, 3643–3653. doi: 10.7150/thno.26021

Li, Y., Wu, H., Wu, W., Zhuo, W., Liu, W., Zhang, Y., et al. (2014). Structural insights into the TRIM family of ubiquitin E3 ligases. *Cell Res.* 24, 762–765. doi: 10.1038/cr.2014.46

Lienlaf, M., Hayashi, F., Di Nunzio, F., Tochio, N., Kigawa, T., Yokoyama, S., et al. (2011). Contribution of E3-ubiquitin ligase activity to HIV-1 restriction by TRIM5αrh: structure of the RING domain of TRIM5. *J. Virol.* 85, 8725–8737. doi: 10.1128/jvi.00497-411

Liew, C. W., Sun, H., Hunter, T., and Day, C. L. (2010). RING domain dimerization is essential for RNF4 function. *Biochem. J.* 431, 23–29. doi: 10.1042/BJ20100957

Linke, K., Mace, P. D., Smith, C. A., Vaux, D. L., Silke, J., and Day, C. L. (2008). Structure of the MDM2/MDMX RING domain heterodimer reveals dimerization is required for their ubiquitylation in trans. *Cell Death Differ.* 15, 841–848. doi: 10.1038/sj.cdd.4402309

Liu, B., Zhang, M., Chu, H., Zhang, H., Wu, H., Song, G., et al. (2017a). The ubiquitin E3 ligase TRIM31 promotes aggregation and activation of the signaling adaptor MAVS through Lys63-linked polyubiquitination. *Nat. Immunol.* 18, 214–224. doi: 10.1038/ni.3641

Liu, J., Zhang, C., Zhao, Y., Yue, X., Wu, H., Huang, S., et al. (2017b). Parkin targets HIF-1α for ubiquitination and degradation to inhibit breast tumor progression. *Nat. Commun.* 8:1823. doi: 10.1038/s41467-017-01947-w

Liu, S., Jiang, M., Wang, W., Liu, W., Song, X., Ma, Z., et al. (2018). Nuclear RNF2 inhibits interferon function by promoting K33-linked STAT1 disassociation from DNA. *Nat. Immunol.* 19, 41–52. doi: 10.1038/s41590-017-0003-0

Loregger, A., Grandl, M., Mejías-Luque, R., Allgäuer, M., Degenhart, K., Haselmann, V., et al. (2015). The E3 ligase RNF43 inhibits Wnt signaling downstream of mutated β-catenin by sequestering TCF4 to the nuclear membrane. *Sci. Signal.* 8, 1–13. doi: 10.1126/scisignal.aac6757

Lorick, K. L., Jensen, J. P., Fang, S., Ong, A. M., Hatakeyama, S., and Weissman, A. M. (1999). RING fingers mediate ubiquitin-conjugating enzyme (E2)-dependent ubiquitination. *Proc. Natl. Acad. Sci. U.S.A.* 96, 11364–11369. doi: 10.1073/pnas.96.20.11364

Mallette, F. A., Mattiroli, F., Cui, G., Young, L. C., Hendzel, M. J., Mer, G., et al. (2012). RNF8- and RNF168-dependent degradation of KDM4A/JMJD2A triggers 53BP1 recruitment to DNA damage sites. *EMBO J.* 31, 1865–1878. doi: 10.1038/emboj.2012.47

Masuda, Y., Suzuki, M., Kawai, H., Suzuki, F., and Kamiya, K. (2012). Asymmetric nature of two subunits of RAD18, a RING-type ubiquitin ligase E3, in the human RAD6A-RAD18 ternary complex. *Nucleic Acids Res.* 40, 1065–1076. doi: 10.1093/nar/gkr805

Metzger, M. B., Pruneda, J. N., Klevit, R. E., and Weissman, A. M. (2014). RING-type E3 ligases: master manipulators of E2 ubiquitin-conjugating enzymes and ubiquitination. *Biochim. Biophys. Acta* 1843, 47–60. doi: 10.1016/j.bbamcr.2013.05.026

Morett, E., and Bork, P. (1999). A novel transactivation domain in parkin. *Trends Biochem. Sci.* 24, 229–231. doi: 10.1016/S0968-0004(99)01381-X

Morreale, F. E., and Walden, H. (2016). Types of ubiquitin ligases. *Cell* 165, 248-248.e1. doi: 10.1016/j.cell.2016.03.003

Muńoz-Escobar, J., Matta-Camacho, E., Kozlov, G., and Gehring, K. (2015). The MLLE domain of the ubiquitin ligase UBR5 binds to its catalytic domain to regulate substrate binding. *J. Biol. Chem.* 290, 22841–22850. doi: 10.1074/jbc.M115.672246

Nakatani, Y., Kleffmann, T., Linke, K., Condon, S. M., Hinds, M. G., and Day, C. L. (2013). Regulation of ubiquitin transfer by XIAP, a dimeric RING E3 ligase. *Biochem. J.* 450, 629–638. doi: 10.1042/BJ20121702

Nomura, K., Klejnot, M., Kowalczyk, D., Hock, A. K., Sibbet, G. J., Vousden, K. H., et al. (2017). Structural analysis of MDM2 RING separates degradation from regulation of p53 transcription activity. *Nat. Struct. Mol. Biol.* 24, 578–587. doi: 10.1038/nsmb.3414

Okumura, F., Hatakeyama, S., Matsumoto, M., Kamura, T., and Nakayama, K. I. (2004). Functional regulation of FEZ1 by the U-box-type ubiquitin ligase E4B contributes to neuritogenesis. *J. Biol. Chem.* 279, 53533–53543. doi: 10.1074/jbc.M402916200

Osinalde, N., Duarri, A., Ramirez, J., Barrio, R., Perez de Nanclares, G., and Mayor, U. (2019). Impaired proteostasis in rare neurological diseases. *Semin. Cell Dev. Biol.* 93, 164–177. doi: 10.1016/j.semcdb.2018.10.007

Pickart, C. M. (2001). Mechanisms underlying ubiquitination. *Annu. Rev. Biochem.* 70, 503–533. doi: 10.1146/annurev.biochem.70.1.503

Plechanovov, A., Jaffray, E. G., Tatham, M. H., Naismith, J. H., and Hay, R. T. (2012). Structure of a RING E3 ligase and ubiquitin-loaded E2 primed for catalysis. *Nature* 489, 115–120. doi: 10.1038/nature11376

Poyurovsky, M. V., Priest, C., Kentsis, A., Borden, K. L. B., Pan, Z. Q., Pavletich, N., et al. (2007). The Mdm2 RING domain C-terminus is required for supramolecular assembly and ubiquitin ligase activity. *EMBO J.* 26, 90–101. doi: 10.1038/sj.emboj.7601465

Pruneda, J. N., Littlefield, P. J., Soss, S. E., Nordquist, K. A., Chazin, W. J., Brzovic, P. S., et al. (2012). Structure of an E3:E2 Ub Complex Reveals an Allosteric Mechanism Shared among RING/U-box Ligases. *Mol. Cell* 47, 933–942. doi: 10.1016/j.molcel.2012.07.001

Pruneda, J. N., Stoll, K. E., Bolton, L. J., Brzovic, P. S., and Klevit, R. E. (2011). Ubiquitin in motion: structural studies of the ubiquitin-conjugating enzyme ubiquitin conjugate. *Biochemistry* 50, 1624–1633. doi: 10.1021/bi101913m

Raheja, R., Liu, Y., Hukkelhoven, E., Yeh, N., and Koff, A. (2014). The ability of TRIM3 to induce growth arrest depends on RING-dependent E3 ligase activity. *Biochem. J.* 458, 537–545. doi: 10.1042/BJ20131288

Ronchi, V. P., Klein, J. M., Edwards, D. J., and Haas, A. L. (2014). The active form of E6-associated protein (E6AP)/UBE3A ubiquitin ligase is an oligomer. *J. Biol. Chem.* 289, 1033–1048. doi: 10.1074/jbc.M113.517805

Rotin, D., and Kumar, S. (2009). Physiological functions of the HECT family of ubiquitin ligases. *Nat. Rev. Mol. Cell Biol.* 10, 398–409. doi: 10.1038/nrm2690

Ruffner, H., Joazeiro, C. A., Hemmati, D., Hunter, T., and Verma, I. M. (2001). Cancer-predisposing mutations within the RING domain of BRCA1: loss of ubiquitin protein ligase activity and protection from radiation hypersensitivity. *Proc. Natl. Acad. Sci. U.S.A.* 98, 5134–5139. doi: 10.1073/pnas.081068398

Sander, B., Xu, W., Eilers, M., Popov, N., and Lorenz, S. (2017). A conformational switch regulates the ubiquitin ligase HUWE1. *eLife* 6:e21036. doi: 10.7554/eLife.21036

Sarraf, S. A., Raman, M., Guarani-Pereira, V., Sowa, M. E., Huttlin, E. L., Gygi, S. P., et al. (2013). Landscape of the PARKIN-dependent ubiquitylome in response to mitochondrial depolarization. *Nature* 496, 372–376. doi: 10.1038/nature12043

Scheffner, M., and Kumar, S. (2014). Mammalian HECT ubiquitin-protein ligases: biological and pathophysiological aspects. *Biochim. Biophys. Acta* 1843, 61–74. doi: 10.1016/j.bbamcr.2013.03.024

Seo, J. H., Agarwal, E., Bryant, K. G., Caino, M. C., Kim, E. T., Kossenkov, A. V., et al. (2018). Syntaphilin ubiquitination regulates mitochondrial dynamics and tumor cell movements. *Cancer Res.* 78, 4215–4228. doi: 10.1158/0008-5472.CAN-18-0595

Shen, J., Li, P., Shao, X., Yang, Y., Liu, X., Feng, M., et al. (2018). The E3 ligase ring1 targets p53 for degradation and promotes cancer cell proliferation and survival. *Cancer Res.* 78, 359–371. doi: 10.1158/0008-5472.CAN-17-1805

Smit, J. J., Monteferrario, D., Noordermeer, S. M., Van, W. J., Reijden, B. A., and Van Der Sixma, T. K. (2012). The E3 ligase HOIP specifies linear ubiquitin chain assembly through its RING-IBR-RING domain and the unique LDD extension. *EMBO J.* 31, 3833–3844. doi: 10.1038/emboj.2012.217

Soss, S. E., Klevit, R. E., and Chazin, W. J. (2013). Activation of UbcH5c Ub is the result of a shift in interdomain motions of the conjugate bound to U-box E3 ligase E4B. *Biochemistry* 52, 2991–2999. doi: 10.1021/bi3015949

Staub, O., Dho, S., Henry, P., Correa, J., Ishikawa, T., McGlade, J., et al. (1996). WW domains of Nedd4 bind to the proline-rich PY motifs in the epithelial Na+ channel deleted in Liddle's syndrome. *EMBO J.* 15, 2371–2380. doi: 10.1002/j.1460-2075.1996.tb00593.x

Tan, C., Byrne, E. F. X., Ah-Cann, C., Call, M. J., and Call, M. E. (2019). A serine in the first transmembrane domain of the human E3 ubiquitin ligase MARCH9 is critical for down-regulation of its protein substrates. *J. Biol. Chem.* 294, 2470–2485. doi: 10.1074/jbc.RA118.004836

Tian, H., Tackmann, N. R., Jin, A., Zheng, J., and Zhang, Y. (2017). Inactivation of the MDM2 RING domain enhances p53 transcriptional activity in mice. *J. Biol. Chem.* 292, 21614–21622. doi: 10.1074/jbc.RA117.000122

Torrino, S., Visvikis, O., Doye, A., Boyer, L., Stefani, C., Munro, P., et al. (2011). The E3 ubiquitin-ligase HACE1 catalyzes the ubiquitylation of active Rac1. *Dev. Cell* 21, 959–965. doi: 10.1016/j.devcel.2011.08.015

Tripathi, E., and Smith, S. (2017). Cell cycle-regulated ubiquitination of tankyrase 1 by RNF8 and ABRO1/BRCC36 controls the timing of sister telomere resolution. *EMBO J.* 36, 503–519. doi: 10.15252/embj.201695135

Vander Kooi, C. W., Ohi, M. D., Rosenberg, J. A., Oldham, M. L., Newcomer, M. E., Gould, K. L., et al. (2006). The Prp19 U-box crystal structure suggests a common dimeric architecture for a class of oligomeric E3 ubiquitin ligases. *Biochemistry* 45, 121–130. doi: 10.1021/bi051787e

von Stechow, L., Typas, D., Carreras Puigvert, J., Oort, L., Siddappa, R., Pines, A., et al. (2015). The E3 ubiquitin ligase ARIH1 protects against genotoxic stress by initiating a 4EHP-Mediated mRNA translation arrest. *Mol. Cell. Biol.* 35, doi: 10.1128/mcb.01152-1114

Wang, H., Wang, L., Erdjument-Bromage, H., Vidal, M., Tempst, P., Jones, R. S., et al. (2004). Role of histone H2A ubiquitination in Polycomb silencing. *Nature* 431, 873–878. doi: 10.1038/nature02985

Wang, Q., Liu, X., Cui, Y., Tang, Y., Chen, W., Li, S., et al. (2014). The E3 Ubiquitin ligase AMFR and INSIG1 bridge the activation of TBK1 kinase by modifying the adaptor STING. *Immunity* 41, 919–933. doi: 10.1016/j.immuni.2014.11.011

Wang, W., Xia, Z.-J., Farré, J.-C., and Subramani, S. (2017). TRIM37, a novel E3 ligase for PEX5-mediated peroxisomal matrix protein import. *J. Cell Biol.* 216, 2843–2858. doi: 10.1083/jcb.201611170

Wang, X., Herr, R. A., and Hansen, T. H. (2012). Ubiquitination of substrates by esterification. *Traffic* 13, 19–24. doi: 10.1111/j.1600-0854.2011.01269.x

Waterman, H., Levkowitz, G., Alroy, I., and Yarden, Y. (1999). The RING finger of c-Cbl mediates desensitization of the epidermal growth factor receptor. *J. Biol. Chem.* 274, 22151–22154. doi: 10.1074/jbc.274.32.22151

Welcker, M., Larimore, E. A., Swanger, J., Bengoechea-Alonso, M. T., Grim, J. E., Ericsson, J., et al. (2013). Fbw7 dimerization determines the specificity and robustness of substrate degradation. *Genes Dev.* 27, 2531–2536. doi: 10.1101/gad.229195.113

Wenzel, D. M., Lissounov, A., Brzovic, P. S., and Klevit, R. E. (2011). UBCH7 reactivity profile reveals parkin and HHARI to be RING/HECT hybrids. *Nature* 474, 105–108. doi: 10.1038/nature09966

Williams, S. A., Longerich, S., Sung, P., Vaziri, C., and Kupfer, G. M. (2011). The E3 ubiquitin ligase RAD18 regulates ubiquitylation and chromatin loading of FANCD2 and FANCI. *Blood* 117, 5078–5087. doi: 10.1182/blood-2010-10-311761

Wu, W., Sato, K., Koike, A., Nishikawa, H., Koizumi, H., Venkitaraman, A. R., et al. (2010). HERC2 is an E3 ligase that targets BRCA1 for degradation. *Cancer Res.* 70, 6384–6392. doi: 10.1158/0008-5472.CAN-10-1304

Xia, P., Wang, S., Huang, G., Du, Y., Zhu, P., Li, M., et al. (2014). RNF2 is recruited by WASH to ubiquitinate AMBRA1 leading to downregulation of autophagy. *Cell Res.* 24, 943–958. doi: 10.1038/cr.2014.85

Xin, D., Gu, H., Liu, E., and Sun, Q. (2018). Parkin negatively regulates the antiviral signaling pathway by targeting TRAF3 for degradation. *J. Biol. Chem.* 293, 11996–12010. doi: 10.1074/jbc.RA117.001201

Ye, J. S., Kim, N., Lee, K. J., Nam, Y. R., Lee, U., and Joo, C. H. (2014). Lysine 63-linked TANK-binding kinase 1 ubiquitination by mindbomb E3 ubiquitin protein ligase 2 is mediated by the mitochondrial antiviral signaling protein. *J. Virol.* 88, 12765–12776. doi: 10.1128/JVI.02037-14

Zaman, M. M.-U., Nomura, T., Takagi, T., Okamura, T., Jin, W., Shinagawa, T., et al. (2013). Ubiquitination-deubiquitination by the TRIM27-USP7 complex regulates TNF-α-induced apoptosis. *Mol. Cell. Biol.* 33, 4971–4984. doi: 10.1128/MCB.00465-413

Zhao, X., Heng, J. I.-T., Guardavaccaro, D., Jiang, R., Pagano, M., Guillemot, F., et al. (2008). The HECT-domain ubiquitin ligase Huwe1 controls neural differentiation and proliferation by destabilizing the N-Myc oncoprotein. *Nat. Cell Biol.* 10, 643–653. doi: 10.1038/ncb1727

Zheng, N., and Shabek, N. (2017). Ubiquitin ligases: structure, function, and regulation. *Annu. Rev. Biochem.* 86, 129–157. doi: 10.1146/annurev-biochem-060815-14922

Zheng, N., Wang, P., Jeffrey, P. D., and Pavletich, N. P. (2000). Structure of a c-Cbl-UbcH7 complex: RING domain function in ubiquitin-protein ligases. *Cell* 102, 533–539. doi: 10.1016/s0092-8674(00)00057-x

Zhou, R., Patel, S. V., and Snyder, P. M. (2007). Nedd4-2 catalyzes ubiquitination and degradation of cell surface ENaC. *J. Biol. Chem.* 282, 20207–20212. doi: 10.1074/jbc.M611329200

Zuin, A., Isasa, M., and Crosas, B. (2014). Ubiquitin signaling: extreme conservation as a source of diversity. *Cells* 3, 690–701. doi: 10.3390/cells3030690

Conflict of Interest: The authors declare that the research was conducted in the absence of any commercial or financial relationships that could be construed as a potential conflict of interest.

frontiers in Chemistry

MINI REVIEW
published: 11 February 2020
doi: 10.3389/fchem.2020.00064

Reporter-Based Screens for the Ubiquitin/Proteasome System

*Maria E. Gierisch†, Tatiana A. Giovannucci† and Nico P. Dantuma**

Department of Cell and Molecular Biology, Karolinska Institutet, Stockholm, Sweden

Instant and adequate handling of misfolded or otherwise aberrant proteins is of paramount importance for maintaining protein homeostasis in cells. The ubiquitin/proteasome system (UPS) is a central player in protein quality control as it operates in a seek-and-destroy mode, thereby facilitating elimination of faulty proteins. While proteasome inhibition is in clinical use for the treatment of hematopoietic malignancies, stimulation of the UPS has been proposed as a potential therapeutic strategy for various neurodegenerative disorders. High-throughput screens using genetic approaches or compound libraries are powerful tools to identify therapeutic intervention points and novel drugs. Unlike assays that measure specific activities of components of the UPS, reporter substrates provide us with a more holistic view of the general functional status of the UPS in cells. As such, reporter substrates can reveal new ways to obstruct or stimulate this critical proteolytic pathway. Here, we discuss various reporter substrates for the UPS and their application in the identification of key players and the pursuit for novel therapeutics.

Keywords: reporter assay, ubiquitin-proteasome system, high-content screen, high-throughput drug screening, proteolysis

OPEN ACCESS

Edited by:
Benedikt M. Kessler,
University of Oxford, United Kingdom

Reviewed by:
Boris Rodenko,
Acerta Pharma, LLC, Netherlands
Wenshe R. Liu,
Texas A&M University, United States

***Correspondence:**
Nico P. Dantuma
nico.dantuma@ki.se

†These authors have contributed equally to this work

Specialty section:
This article was submitted to Chemical Biology, a section of the journal Frontiers in Chemistry

Received: *13 October 2019*
Accepted: *20 January 2020*
Published: *11 February 2020*

Citation:
Gierisch ME, Giovannucci TA and Dantuma NP (2020) Reporter-Based Screens for the Ubiquitin/Proteasome System. Front. Chem. 8:64. doi: 10.3389/fchem.2020.00064

TARGETING THE UBIQUITIN/PROTEASOME SYSTEM (UPS)

Cells need to balance production, maintenance and degradation of their proteome throughout their entire lifespan, which may vary depending on the type of cell from hours to decades. Proteins that fail protein quality control are a potential risk for protein homeostasis and are targeted for destruction by the ubiquitin/proteasome system (UPS) (Ciechanover, 2005). Proteasome-mediated degradation is initiated by conjugation of the protein modifier ubiquitin to lysine residues of proteins designated for destruction. This initial ubiquitin moiety can be used for the assembly of ubiquitin chains, which are formed through ubiquitylation of one out of seven internal lysine residues in ubiquitin (Komander and Rape, 2012). Conjugation of ubiquitin to substrates is regulated by an enzymatic cascade consisting of E1 ubiquitin-activating enzymes, E2 ubiquitin-conjugating enzymes, and E3 ubiquitin ligases (**Figure 1**). In some cases, specific E4 ubiquitin chain elongators are involved in extending the ubiquitin chains on substrates (Koegl et al., 1999). Subsequently, proteins are degraded into small peptide fragments inside the proteolytic chamber of proteasomes (Bard et al., 2018). Ubiquitylated substrates often require the unfoldase activity of the ubiquitin-targeted segregase valosin-containing protein (VCP), also known as p97, before they can be processed by the proteasome (Twomey et al., 2019). Moreover, several ubiquitin shuttle factors are responsible for the delivery of the substrate to the proteasome (Elsasser and Finley, 2005). To allow efficient degradation, ubiquitin chains have to be removed prior to degradation, which is facilitated by the POH1 deubiquitylating enzyme (DUB) at the entrance of the proteasome

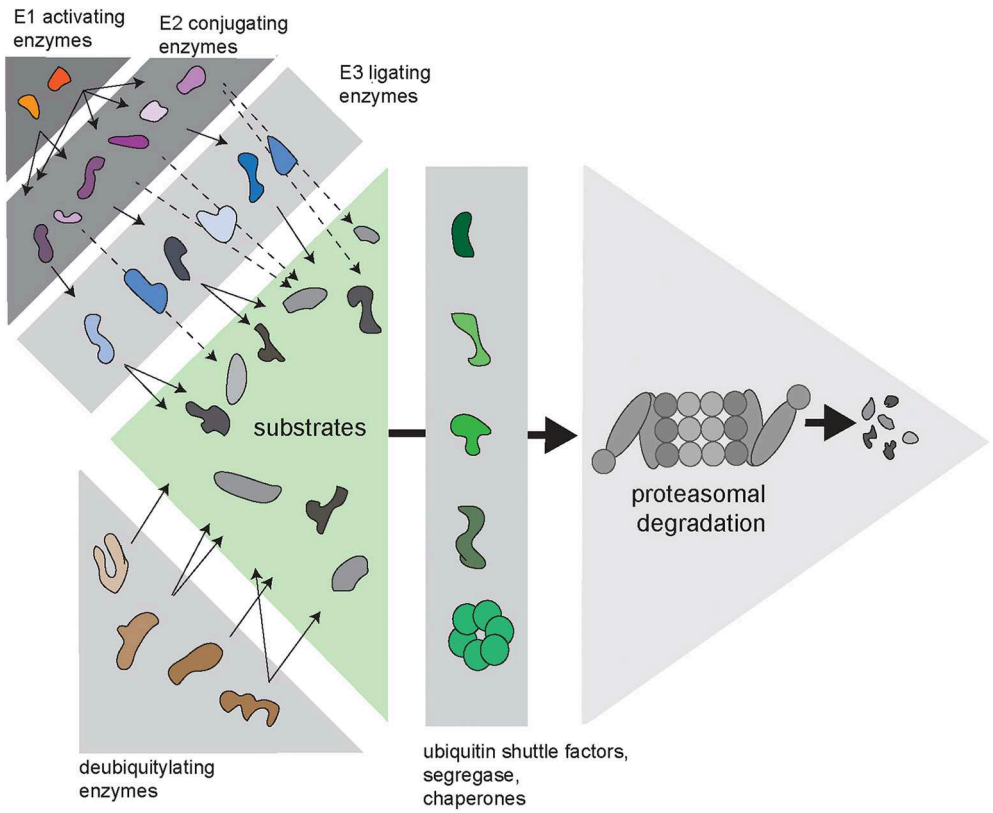

FIGURE 1 | Complexity of the ubiquitin/proteasome system (UPS). Via an enzymatic cascade consisting of E1 ubiquitin-activating enzymes, E2 ubiquitin-conjugating enzymes and E3 ubiquitin ligases, ubiquitin is transferred to substrate proteins. E2-bound ubiquitin can be passed on to an E3, which transfers it to the substrate (continuous arrows), or via E2–E3 complexes, where the E2 transfers the ubiquitin to the E3-bound substrate (dashed arrows). DUBs remove ubiquitin chains from proteins, which can either promote or inhibit degradation of substrates. Substrates are transferred to the proteasome by various ubiquitin shuttle factors and often require handling by the ubiquitin-selective seggregase VCP.

(Verma et al., 2002; Yao and Cohen, 2002). In contrast, the proteasome-associated DUB USP14 can rescue proteins from degradation by removing ubiquitin chains before the proteasome has initiated degradation (Kraut et al., 2007).

Due to their hyperactive state and compromised genome integrity, cancer cells produce elevated levels of aberrant proteins. This phenomenon is believed to make them more susceptible to drugs that restrict the activity of the UPS (Bruning and Juckstock, 2015). Pharmacological inhibition of the UPS is typically accomplished by targeting the proteasome (Kisselev and Goldberg, 2001). Bortezomib was the first FDA-approved proteasome inhibitor and currently serves as a drug for first-line treatment of multiple myeloma and mantle cell lymphoma (Adams, 2004). Despite the fact that the successful introduction of proteasome inhibition for treatment of hematopoietic malignancies has provided the field with an encouraging proof-of-principle, other therapeutic strategies for UPS inhibition remain in an early exploratory stage. The few clinically approved UPS-targeting drugs are rather crude in their action as they all target the main chymotrypsin-like activity of the proteasome (Fricker, 2019). Concerns regarding the observed adverse effects, the development of resistance against proteasome inhibitors and the poor activity of proteasome inhibitors toward solid tumors are strong arguments for the development of drugs directed against other targets within the UPS.

On the other hand, enhancing UPS activity may be desirable in diseases where accumulation of misfolded proteins is responsible for cellular dysfunction and decay, which is the case for a broad variety of neurodegenerative diseases characterized by accumulation of protein aggregates, such as Alzheimer's, Parkinson's and Huntington's disease as well as amyotrophic lateral sclerosis (Boland et al., 2018). As most compounds block catalytic activities of enzymes, pharmacological stimulation might potentially be more challenging. However, due to the complex nature of the UPS, overall stimulation may be feasible through inhibition of specific enzymes that slow down the process. In line with this notion, it has been shown that the USP14 inhibitor IU1 stimulates the degradation of aggregation-prone proteins, such as tau and TDP-43, both linked to neurodegenerative diseases (Lee et al., 2010).

One of the most daunting tasks in the development of new modulators of the UPS is the identification of proteins and processes that can be targeted. More than 40 E2 conjugation enzymes can pair with over 600 different E3 ligases, while around

100 DUBs are involved in the removal of ubiquitin chains. Moreover, a vast number of proteins is involved in coordinating this process, guiding substrates to the proteasome and prepare them for efficient degradation. It is hard to predict how inhibition of individual players will affect the overall efficacy of the UPS. Screening campaigns are often designed to interrogate the activity of a specific enzymatic target, which requires a preselection of a target-of-interest. An alternative approach are phenotypic assays that are based on the ectopic expression of engineered fluorescent UPS substrates, which lack a biological function but can be readily and quantitatively detected by their fluorescence (Neefjes and Dantuma, 2004). The latter assays are unbiased and allow the identification of novel ways to modulate UPS activity without requiring *a priori* knowledge on the mode of action of the targets.

UPS REPORTER SUBSTRATES

UPS reporter substrates are based on targeting an otherwise stable protein for proteasomal degradation through the introduction of a degradation signal (Neefjes and Dantuma, 2004) (**Figure 2A**). Degradation signals, so-called degrons, are conserved motifs that target proteins for proteasomal degradation. One of the first identified degrons is the N-terminal amino acid of proteins (Bachmair et al., 1986). This was discovered by expressing fusion proteins with an N-terminal ubiquitin moiety, which will be proteolytically cleaved in cells, leaving the C-terminal protein with an amino terminus that corresponds to the sequence following the DUB cleavage site. Depending on the nature of the new N-terminal amino acid, it may function as a degron that recruits ubiquitin ligases and determines the half-life of the protein.

When the DUB cleavage of the N-terminal ubiquitin was prevented by substituting the final glycine of ubiquitin to valine (G76V), proteins were still found to be destabilized, but this time another set of proteins was involved in their recognition and degradation (Johnson et al., 1992). In these fusions, the uncleavable N-terminal ubiquitin is marked with ubiquitin chains that target it for proteasomal degradation (Johnson et al., 1995). This type of engineered proteins are known as ubiquitin fusion degradation (UFD) substrates.

Both the N-end rule and UFD degradation signals are versatile motifs that can be used to target most proteins-of-interest for degradation. Both degrons were used for the development of the first green fluorescent protein (GFP)-based reporter substrates that were expressed in cells (Dantuma et al., 2000) and mice (Lindsten et al., 2003). Expression of a luciferase carrying multiple UFD signals enabled also *in vivo* analysis of the effect of drugs on UPS activity in xenograft transplants in mice (Luker et al., 2003), while a UFD-targeted version of a photoconvertable fluorescent protein allowed determination of the half-lives of UPS substrates in living nematodes (Hamer et al., 2010), illustrating the potential of this approach.

Another engineered degradation signal that has been used for the generation of reporter substrates is a short C-terminal linkage (CL) referred to as CL1. The CL1 peptide was identified in a yeast screen aimed at identifying peptide extensions that degrade proteins dependent on endoplasmic reticulum (ER)-anchored ubiquitin-conjugating enzymes involved in marking misfolded ER proteins for proteasomal degradation (Gilon et al., 1998, 2000). C-terminal tagging of GFP with CL1 resulted in a short-lived GFP, which has been used for generating cellular (Bence et al., 2001) and mouse UPS models (Bove et al., 2006; Liu et al., 2006). Fluorescent proteins destabilized by CL1 tend to aggregate most probably due to its hydrophobic nature (Menéndez-Benito et al., 2005; Link et al., 2006). As such, GFP-CL1 and related fluorescent reporters may be in particular suited to probe into the ability of cells to eliminate aggregation-prone proteins by proteasomal degradation.

In addition to these engineered motifs, naturally occurring degradation signals have also been exploited to destabilize reporter proteins. Fluorescent proteins have been provided with natural degradation signals or fused to full-length proteasome substrates. A natural motif used for this purpose is the PEST sequence of ornithine decarboxylase (ODC). The ODC degradation signal has the special feature that it can target proteins for ubiquitin-independent proteasomal degradation, thereby bypassing the complex machinery for ubiquitylation (Hoyt et al., 2005).

Other full-length proteins that have been used for the generation of reporter substrates are the heavy chain (HC) of major histocompatibility complex (MHC) class I molecules, which, in the presence of the viral proteins US2 or US11, is rapidly dislocated from the ER into the cytosol, ubiquitylated and disposed by the proteasome (Schust et al., 1998). MHC-HC shares this pathway with other proteins targeted for ER-associated degradation (ERAD) (Berner et al., 2018). Another commonly used ERAD reporter substrate is the T cell receptor subunit CD3δ. When expressed in other cells than T lymphocytes, CD3δ fusions are orphan subunits unable to find their binding partner, resulting in targeting of these fusions to the ERAD pathway (Yang et al., 1998).

While MHC class I and CD3δ require ERAD proteins that facilitate identification of the reporter as aberrant in the ER and its translocation into the cytosol, the CL1-destabilized reporter substrates, which are cytosolic reporters, will only engage the final steps of the ERAD pathway. Thus, different UPS reporters display differential sensitivities for different branches of the UPS: the N-end rule and UFD substrates behave as soluble, properly folded proteins, CL1 mimics aggregation-prone proteins, CD3δ and MHC class I HC are ERAD substrates and ODC-destabilized proteins report on the status of ubiquitin-independent degradation.

UPS REPORTER-BASED SCREENS

A number of genetic and compound screens have been published in which the usage of UPS reporters played a central role. In these screens, transiently transfected or stably integrated reporters in mammalian cells served as read-outs for global changes in the UPS in high-throughput screens for genetic or chemical modulators (**Figure 2B**).

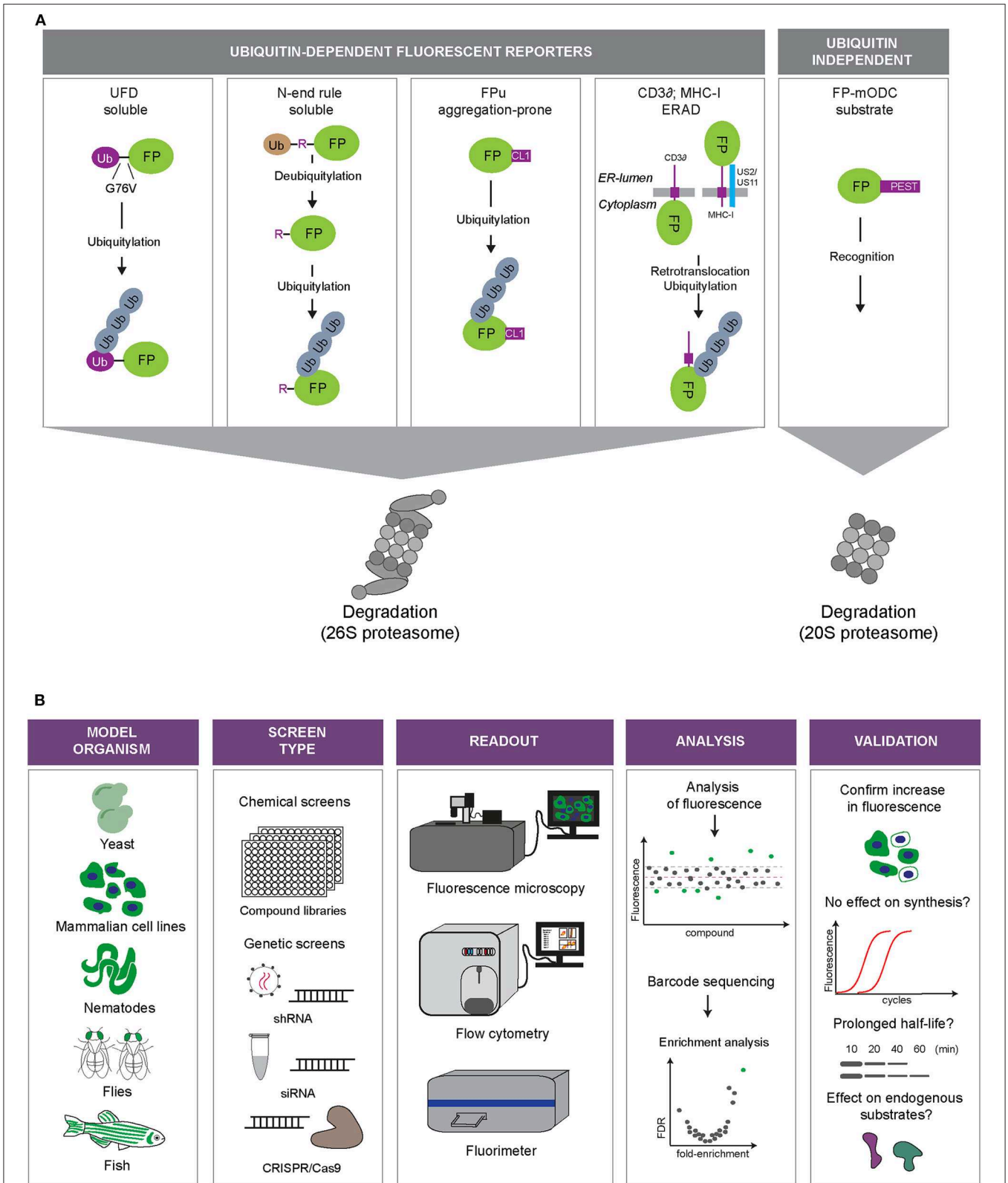

FIGURE 2 | Fluorescent UPS reporters and screening strategies. **(A)** UPS reporters. Fluorescent proteins (FP) are converted into UPS reporter substrates through introduction of degradation signals of different nature (depicted in purple). The different reporter proteins allow monitoring of different UPS activities: degradation of soluble proteins (Ub^{G76V}-FP and Ub-R-FP), degradation of aggregation-prone proteins (FP-CL1), ER-associated degradation (ERAD; MHC-I-FP and CD3δ-FP) or

(Continued)

FIGURE 2 | ubiquitin-independent degradation (FP-mODC). **(B)** Overview of the steps involved in high-throughput screens using fluorescent reporters of the UPS. Model: Fluorescent reporters are expressed in cell or animal models suited for high-throughput screening. Screening format: Compound libraries or genetic libraries can be used. Modulation of genetic expression can be achieved via siRNA, shRNA, or CRISPR/Cas9 approaches. Readout: Fluorescence microscopy, flow cytometry or fluorimetry can be used as a fluorescence readout or for sorting a specific cell population by fluorescence activated cell sorting (FACS). Analysis: Hits can be identified through readout of fluorescence intensity or sequencing of selected cells. Validation: Examples of various methods that can be used to validate hits.

Phenotypic assays based on reporter substrates have been used for the discovery of novel inhibitory compounds. A ChemBridge library consisting of around 16,000 compounds was screened using a cell line expressing the HC of enhanced green fluorescent protein (EGFP)-tagged MHC-I HC (EGFP-HC) and viral US2, resulting in targeting EGFP-HC for ERAD. This screen resulted in the identification of two structurally-related inhibitory compounds: Eeyarestatin 1 (Eer1) and 2 (Eer2) (Fiebiger et al., 2004). Follow-up studies revealed that Eer1 blocks EGFP-HC degradation by interfering with VCP-mediated segregation and suggested that this may be due to inhibition of the VCP-associated DUB ataxin-3 (Wang et al., 2008). In line with the model that Eer1 interferes with the function of VCP, Eer1 induced accumulation of a VCP-dependent reporter, while it did not interfere in the degradation of a VCP-independent substrate (Chou and Deshaies, 2011).

In another screening campaign for UPS inhibitors, the library of pharmacological active compounds (LOPAC) was tested in a high-throughput format using cells that expressed the ubiquitin-independent substrate ZsGreen-ODC. Surprisingly, disulfiram, an FDA-approved drug for treatment of alcohol addiction, was found to inhibit UPS activity and displayed cytotoxic effects on a myeloma cell line (Rickardson et al., 2007). Disulfiram had been previously found to interfere with NF-κB activity (Wang et al., 2003). This was later pinpointed to copper-dependent inhibition of the proteasome, whose activity is required for NF-κB translocation (Chen et al., 2006). In a more recent study, the ditiocarb-copper complex, a metabolite of disulfiram, was shown to also impair degradation of a UFD reporter substrate via inhibition of the VCP-adaptor protein NPL4 (Skrott et al., 2017), suggesting that disulfiram may modulate several targets within the UPS.

Genetic UPS screens are commonly based on manipulation of the gene expression in reporter cells using siRNA, shRNA or CRISPR/Cas9 technology. Cells expressing a UFD-destabilized reporter were used in a screen aimed at identifying proteins involved in the mammalian UFD pathway (Poulsen et al., 2012). An siRNA-based library targeting 558 genes was used in this screen. This led to the identification of several UFD components including HUWE1, a HECT domain ubiquitin ligase. A natural substrate of HUWE1 is UBB^{+1}, an aberrant ubiquitin found in neurological and non-neurological protein misfolding disorders (Van Leeuwen et al., 1998). UBB^{+1} has an uncleavable N-terminal ubiquitin moiety and resembles artificial UFD substrates (Lindsten et al., 2002). It is noteworthy that HUWE is overexpressed in lung, breast and colon carcinoma, suggesting also a possible role in tumorigenesis (Adhikary et al., 2005; Yoon et al., 2005; Kao et al., 2018).

A genome-wide CRISPR/Cas9 library was screened using a GFP-CL1-expressing cell line. Fluorescence-activated cell sorting (FACS) was employed to obtain a population enriched for cells with elevated GFP-CL1 levels, which were subsequently analyzed by barcode sequencing (Leto et al., 2019). This resulted in the identification of new genes of the ERAD ubiquitin conjugation machinery, including the ubiquitin ligase RNF139/TRC8 and ubiquitin-conjugating enzyme UBE3C. In a different screen, the near-haploid cell line KBM7 (Carette et al., 2009), stably expressing mCherry-CL1 was used to sort $mCherry^{High}$ cells by flow cytometry after insertional mutagenesis with a gene-trapping retrovirus (Stefanovic-Barrett et al., 2018). In addition to RNF139/TRC8, a second ER-resident E3 ligases, MARCH6, was found to function in ubiquitin-dependent degradation of soluble and tail anchored ER proteins.

In a UPS-specific and genome-wide siRNA-based screen, a fluorescently tagged, thermally unstable nuclear reporter was used to identify proteins involved in nuclear protein quality control (Pegoraro et al., 2012). The screen was performed by analyzing 384-well plates with automated fluorescence microscopy. Besides a number of hits that were anticipated, such as proteasome subunits, they found the proteasome assembly chaperone POMP (Burri et al., 2000; Fricke et al., 2007), and eIF3, a translation initiation complex (Abbott and Proud, 2004), to be important for efficient nuclear protein quality control.

Upon construction of two novel shRNA-based libraries, the fluorescent reporter ZsGreen-mODC was used to validate the functionality of these libraries (Paddison et al., 2004; Silva et al., 2005). Cells were transfected with an expression vector for the ZsGreen-mODC reporter together with either a plasmid library consisting of 7,000 unique shRNAs (Paddison et al., 2004) or a sub-library consisting of shRNAs specific for a large number of kinases and proteasome subunits shRNAs (Silva et al., 2005). The performance of the library and setup of the screen was confirmed as shRNAs directed against proteasome subunits were readily identified by accumulation of the reporter substrate. In this particular case, the UPS reporter were used as a fast and robust tool for validation of the screening libraries.

CONCLUDING REMARKS

With the appearance of advanced techniques and equipment, high-throughput and high-content screenings have become attractive approaches for addressing biological questions and drug development. Many different fluorescent substrate reporters have emerged over the years in parallel with a better

understanding of the UPS and an increased awareness of the UPS as therapeutic target. A number of opportunities for optimizing these reporter assays and tailoring them to specific purposes remain. Although some UPS reporter mouse strains have been generated, it is obvious that mouse models are not suited for large-scale screening efforts. However, other animal reporter models, such as nematodes (Hamer et al., 2010), fruit flies (Pandey et al., 2007), and zebrafish (Imamura et al., 2012), open possibilities to perform genetic and compound screens on a larger scale in *in vivo* models.

In addition to UPS inhibitors, there is an emerging interest for UPS stimulators, which may be harder to identify with the currently available assays. Hence, there is a need for the development of novel reporters that are more suited for detecting an increase in UPS activity. A point of improvement may be the use of internal stable reference proteins, which have been already applied in some screens (Yen and Elledge, 2008; Yen et al., 2008; Wu et al., 2016). These reference proteins can correct for differences in synthesis of the reporter and may give a more robust readout, thereby reducing the number of false hits. Due to the relatively low steady-state levels of the presently available reporter substrates, detection of enhanced degradation in high content screens may be problematic, even in the presence of a stable reference protein. Two recent studies elegantly overcame this limitation by creating a system in which the expression of the reporter protein is repressed by a transcriptional regulator (Zhao et al., 2014; Zeng et al., 2019). Fusion of the transcriptional repressor to a destabilizing signal results in an inverse correlation between the activity of the UPS and the levels of the reporter protein that are regulated by the repressor. However, the applicability of these reporter systems in high-throughput campaigns remains to be validated.

Genetic screens and compound screens each have their own strengths and weaknesses and can complement each other in screening campaigns. Genetic screens may result in the identification of interesting but poorly druggable candidates, while compound screens may identify powerful drug-like compounds but encounter difficulties in target identification. Upon combination of these complementary approaches and adapting the assays to more disease-relevant settings, fluorescent reporters can be used to their full potential in the pursuit for novel ways of modulating the UPS in human diseases.

AUTHOR CONTRIBUTIONS

MG, TG, and ND wrote the manuscript.

FUNDING

This work was supported by the Swedish Research Council, the Swedish Cancer Society; EU Joint Programme—Neurodegenerative Disease Research (JPND), the Karolinska Institute, and the German Research Foundation (DFG, GZ:GI-1329/1-1).

REFERENCES

Abbott, C. M., and Proud, C. G. (2004). Translation factors: in sickness and in health. *Trends Biochem. Sci.* 29, 25–31. doi: 10.1016/j.tibs.2003.11.006

Adams, J. (2004). The development of proteasome inhibitors as anticancer drugs. *Cancer Cell* 5, 417–421. doi: 10.1016/S1535-6108(04)00120-5

Adhikary, S., Marinoni, F., Hock, A., Hulleman, E., Popov, N., Beier, R., et al. (2005). The ubiquitin ligase HectH9 regulates transcriptional activation by Myc and is essential for tumor cell proliferation. *Cell* 123, 409–421. doi: 10.1016/j.cell.2005.08.016

Bachmair, A., Finley, D., and Varshavsky, A. (1986). *In vivo* half-life of a protein is a function of its amino-terminal residue. *Science* 234, 179–186. doi: 10.1126/science.3018930

Bard, J. A. M., Goodall, E. A., Greene, E. R., Jonsson, E., Dong, K. C., et al. (2018). Structure and Function of the 26S Proteasome. *Annu. Rev. Biochem.* 87, 697–724. doi: 10.1146/annurev-biochem-062917-011931

Bence, N. F., Sampat, R. M., and Kopito, R. R. (2001). Impairment of the ubiquitin-proteasome system by protein aggregation. *Science* 292, 1552–1555. doi: 10.1126/science.292.5521.1552

Berner, N., Reutter, K. R., and Wolf, D. H. (2018). Protein quality control of the endoplasmic reticulum and ubiquitin-proteasome-triggered degradation of aberrant proteins: yeast pioneers the path. *Annu. Rev. Biochem.* 87, 751–782. doi: 10.1146/annurev-biochem-062917-012749

Boland, B., Yu, W. H., Corti, O., Mollereau, B., Henriques, A., Bezard, E., et al. (2018). Promoting the clearance of neurotoxic proteins in neurodegenerative disorders of ageing. *Nat. Rev. Drug. Discov.* 17, 660–688. doi: 10.1038/nrd.2018.109

Bove, J., Zhou, C., Jackson-Lewis, V., Taylor, J., Chu, Y., Rideout, H. J., et al. (2006). Proteasome inhibition and Parkinson's disease modeling. *Ann. Neurol.* 60, 260–264. doi: 10.1002/ana.20937

Bruning, A., and Juckstock, J. (2015). Misfolded proteins: from little villains to little helpers in the fight against cancer. *Front. Oncol.* 5:47. doi: 10.3389/fonc.2015.00047

Burri, L., Hockendorff, J., Boehm, U., Klamp, T., Dohmen, R. J., and Levy, F. (2000). Identification and characterization of a mammalian protein interacting with 20S proteasome precursors. *Proc. Natl. Acad. Sci. U.S.A.* 97, 10348–10353. doi: 10.1073/pnas.190268597

Carette, J. E., Guimaraes, C. P., Varadarajan, M., Park, A. S., Wuethrich, I., Godarova, A., et al. (2009). Haploid genetic screens in human cells identify host factors used by pathogens. *Science* 326, 1231–1235. doi: 10.1126/science.1178955

Chen, D., Cui, Q. C., Yang, H., and Dou, Q. P. (2006). Disulfiram, a clinically used anti-alcoholism drug and copper-binding agent, induces apoptotic cell death in breast cancer cultures and xenografts via inhibition of the proteasome activity. *Cancer Res.* 66, 10425–10433. doi: 10.1158/0008-5472.CAN-06-2126

Chou, T.-F., and Deshaies, R. J. (2011). Quantitative cell-based protein degradation assays to identify and classify drugs that target the ubiquitin-proteasome system. *J. Biol. Chem.* 286, 16546–16554. doi: 10.1074/jbc.M110.215319

Ciechanover, A. (2005). Proteolysis: from the lysosome to ubiquitin and the proteasome. *Nat. Rev. Mol. Cell Biol.* 6:79. doi: 10.1038/nrm1552

Dantuma, N. P., Lindsten, K., Glas, R., Jellne, M., and Masucci, M. G. (2000). Short-lived green fluorescent proteins for quantifying ubiquitin/proteasome-dependent proteolysis in living cells. *Nat. Biotechnol.* 18, 538–543. doi: 10.1038/75406

Elsasser, S., and Finley, D. (2005). Delivery of ubiquitinated substrates to protein-unfolding machines. *Nat. Cell Biol.* 7, 742–749. doi: 10.1038/ncb0805-742

Fiebiger, E., Hirsch, C., Vyas, J. M., Gordon, E., Ploegh, H. L., and Tortorella, D. (2004). Dissection of the dislocation pathway for type I membrane proteins with a new small molecule inhibitor, eeyarestatin. *Mol. Biol. Cell* 15, 1635–1646. doi: 10.1091/mbc.e03-07-0506

Fricke, B., Heink, S., Steffen, J., Kloetzel, P. M., and Kruger, E. (2007). The proteasome maturation protein POMP facilitates major steps of 20S

proteasome formation at the endoplasmic reticulum. *EMBO Rep.* 8, 1170–1175. doi: 10.1038/sj.embor.7401091

Fricker, L. D. (2019). Proteasome inhibitor drugs. *Annu. Rev. Pharmacol. Toxicol.* doi: 10.1146/annurev-pharmtox-010919-023603

Gilon, T., Chomsky, O., and Kulka, R. G. (1998). Degradation signals for ubiquitin system proteolysis in Saccharomyces cerevisiae. *EMBO J.* 17, 2759–2766. doi: 10.1093/emboj/17.10.2759

Gilon, T., Chomsky, O., and Kulka, R. G. (2000). Degradation signals recognized by the Ubc6p-Ubc7p ubiquitin-conjugating enzyme pair. *Mol. Cell Biol.* 20, 7214–7219. doi: 10.1128/MCB.20.19.7214-7219.2000

Hamer, G., Matilainen, O., and Holmberg, C. I. (2010). A photoconvertible reporter of the ubiquitin-proteasome system *in vivo*. *Nat. Methods* 7:473. doi: 10.1038/nmeth.1460

Hoyt, M. A., Zhang, M., and Coffino, P. (2005). Probing the ubiquitin/proteasome system with ornithine decarboxylase, a ubiquitin-independent substrate. *Methods Enzymol.* 398, 399–413. doi: 10.1016/S0076-6879(05)98033-6

Imamura, S., Yabu, T., and Yamashita, M. (2012). Protective role of cell division cycle 48 (CDC48) protein against neurodegeneration via ubiquitin-proteasome system dysfunction during zebrafish development. *J. Biol. Chem.* 287, 23047–23056. doi: 10.1074/jbc.M111.332882

Johnson, E. S., Bartel, B., Seufert, W., and Varshavsky, A. (1992). Ubiquitin as a degradation signal. *EMBO J.* 11, 497–505. doi: 10.1002/j.1460-2075.1992.tb05080.x

Johnson, E. S., Ma, P. C., Ota, I. M., and Varshavsky, A. (1995). A proteolytic pathway that recognizes ubiquitin as a degradation signal. *J. Biol. Chem.* 270, 17442–17456. doi: 10.1074/jbc.270.29.17442

Kao, S. H., Wu, H. T., and Wu, K. J. (2018). Ubiquitination by HUWE1 in tumorigenesis and beyond. *J. Biomed. Sci.* 25:67. doi: 10.1186/s12929-018-0470-0

Kisselev, A. F., and Goldberg, A. L. (2001). Proteasome inhibitors: from research tools to drug candidates. *Chem. Biol.* 8, 739–758. doi: 10.1016/S1074-5521(01)00056-4

Koegl, M., Hoppe, T., Schlenker, S., Ulrich, H. D., Mayer, T. U., and Jentsch, S. (1999). A novel ubiquitination factor, E4, is involved in multiubiquitin chain assembly. *Cell* 96, 635–644. doi: 10.1016/S0092-8674(00)80574-7

Komander, D., and Rape, M. (2012). The ubiquitin code. *Annu. Rev. Biochem.* 81, 203–229. doi: 10.1146/annurev-biochem-060310-170328

Kraut, D. A., Prakash, S., and Matouschek, A. (2007). To degrade or release: ubiquitin-chain remodeling. *Trends Cell Biol.* 17, 419–421. doi: 10.1016/j.tcb.2007.06.008

Lee, B. H., Lee, M. J., Park, S., Oh, D. C., Elsasser, S., Chen, P. C., et al. (2010). Enhancement of proteasome activity by a small-molecule inhibitor of USP14. *Nature* 467, 179–184. doi: 10.1038/nature09299

Leto, D. E., Morgens, D. W., Zhang, L., Walczak, C. P., Elias, J. E., Bassik, M. C., et al. (2019). Genome-wide CRISPR analysis identifies substrate-specific conjugation modules in ER-associated degradation. *Mol. Cell* 73, 377–389 e311. doi: 10.1016/j.molcel.2018.11.015

Lindsten, K., De Vrij, F. M., Verhoef, L. G., Fischer, D. F., Van Leeuwen, F. W., Hol, E. M., et al. (2002). Mutant ubiquitin found in neurodegenerative disorders is a ubiquitin fusion degradation substrate that blocks proteasomal degradation. *J. Cell. Biol.* 157, 417–427. doi: 10.1083/jcb.200111034

Lindsten, K., Menéndez-Benito, V., Masucci, M. G., and Dantuma, N. P. (2003). A transgenic mouse model of the ubiquitin/proteasome system. *Nat. Biotechnol.* 21:897. doi: 10.1038/nbt851

Link, C. D., Fonte, V., Hiester, B., Yerg, J., Ferguson, J., Csontos, S., et al. (2006). Conversion of green fluorescent protein into a toxic, aggregation-prone protein by C-terminal addition of a short peptide. *J. Biol. Chem.* 281, 1808–1816. doi: 10.1074/jbc.M505581200

Liu, J., Chen, Q., Huang, W., Horak, K. M., Zheng, H., Mestril, R., et al. (2006). Impairment of the ubiquitin-proteasome system in desminopathy mouse hearts. *FASEB J.* 20, 362–364. doi: 10.1096/fj.05-4869fje

Luker, G. D., Pica, C. M., Song, J., Luker, K. E., and Piwnica-Worms, D. (2003). Imaging 26S proteasome activity and inhibition in living mice. *Nat. Med.* 9, 969–973. doi: 10.1038/nm894

Menéndez-Benito, V., Verhoef, L. G. G. C., Masucci, M. G., and Dantuma, N. P. (2005). Endoplasmic reticulum stress compromises the ubiquitin–proteasome system. *Hum. Mol. Genet.* 14, 2787–2799. doi: 10.1093/hmg/ddi312

Neefjes, J., and Dantuma, N. P. (2004). Fluorescent probes for proteolysis: tools for drug discovery. *Nat. Rev. Drug Discov.* 3, 58–69. doi: 10.1038/nrd1282

Paddison, P. J., Silva, J. M., Conklin, D. S., Schlabach, M., Li, M., Aruleba, S., et al. (2004). A resource for large-scale RNA-interference-based screens in mammals. *Nature* 428, 427–431. doi: 10.1038/nature02370

Pandey, U. B., Nie, Z., Batlevi, Y., Mccray, B. A., Ritson, G. P., Nedelsky, N. B., et al. (2007). HDAC6 rescues neurodegeneration and provides an essential link between autophagy and the UPS. *Nature* 447, 859–863. doi: 10.1038/nature05853

Pegoraro, G., Voss, T. C., Martin, S. E., Tuzmen, P., Guha, R., and Misteli, T. (2012). Identification of mammalian protein quality control factors by high-throughput cellular imaging. *PLoS ONE* 7:e31684. doi: 10.1371/journal.pone.0031684

Poulsen, E. G., Steinhauer, C., Lees, M., Lauridsen, A. M., Ellgaard, L., and Hartmann-Petersen, R. (2012). HUWE1 and TRIP12 collaborate in degradation of ubiquitin-fusion proteins and misframed ubiquitin. *PLoS ONE* 7:e50548. doi: 10.1371/journal.pone.0050548

Rickardson, L., Wickström, M., Larsson, R., and Lövborg, H. (2007). Image-based screening for the identification of novel proteasome inhibitors. *J. Biomol. Screen.* 12, 203–210. doi: 10.1177/1087057106297115

Schust, D. J., Tortorella, D., Seebach, J., Phan, C., and Ploegh, H. L. (1998). Trophoblast class I major histocompatibility complex (MHC) products are resistant to rapid degradation imposed by the human cytomegalovirus (HCMV) gene products US2 and US11. *J. Exp. Med.* 188, 497–503. doi: 10.1084/jem.188.3.497

Silva, J. M., Li, M. Z., Chang, K., Ge, W., Golding, M. C., Rickles, R. J., et al. (2005). Second-generation shRNA libraries covering the mouse and human genomes. *Nat. Genet.* 37, 1281–1288. doi: 10.1038/ng1650

Skrott, Z., Mistrik, M., Andersen, K. K., Friis, S., Majera, D., Gursky, J., et al. (2017). Alcohol-abuse drug disulfiram targets cancer via p97 segregase adaptor NPL4. *Nature* 552:194. doi: 10.1038/nature25016

Stefanovic-Barrett, S., Dickson, A. S., Burr, S. P., Williamson, J. C., Lobb, I. T., Van Den Boomen, D. J., et al. (2018). MARCH6 and TRC8 facilitate the quality control of cytosolic and tail-anchored proteins. *EMBO Rep.* 19:e45603. doi: 10.15252/embr.201745603

Twomey, E. C., Ji, Z., Wales, T. E., Bodnar, N. O., Ficarro, S. B., Marto, J. A., et al. (2019). Substrate processing by the Cdc48 ATPase complex is initiated by ubiquitin unfolding. *Science* 365:eaax1033. doi: 10.1126/science.aax1033

Van Leeuwen, F. W., De Kleijn, D. P., Van Den Hurk, H. H., Neubauer, A., Sonnemans, M. A., Sluijs, J. A., et al. (1998). Frameshift mutants of beta amyloid precursor protein and ubiquitin-B in Alzheimer's and Down patients. *Science* 279, 242–247. doi: 10.1126/science.279.5348.242

Verma, R., Aravind, L., Oania, R., Mcdonald, W. H., Yates, J. R. III, Koonin, E. V., et al. (2002). Role of Rpn11 metalloprotease in deubiquitination and degradation by the 26S proteasome. *Science* 298, 611–615. doi: 10.1126/science.1075898

Wang, Q., Li, L., and Ye, Y. (2008). Inhibition of p97-dependent protein degradation by Eeyarestatin I. *J. Biol. Chem.* 283, 7445–7454. doi: 10.1074/jbc.M708347200

Wang, W., Mcleod, H. L., and Cassidy, J. (2003). Disulfiram-mediated inhibition of NF-κB activity enhances cytotoxicity of 5-fluorouracil in human colorectal cancer cell lines. *Int. J. Cancer* 104, 504–511. doi: 10.1002/ijc.10972

Wu, Y., Zhou, L., Wang, X., Lu, J., Zhang, R., Liang, X., et al. (2016). A genome-scale CRISPR-Cas9 screening method for protein stability reveals novel regulators of Cdc25A. *Cell Discov.* 2:16014. doi: 10.1038/celldisc.2016.14

Yang, M., Omura, S., Bonifacino, J. S., and Weissman, A. M. (1998). Novel aspects of degradation of T cell receptor subunits from the endoplasmic reticulum (ER) in T cells: importance of oligosaccharide processing, ubiquitination, and proteasome-dependent removal from ER membranes. *J. Exp. Med.* 187, 835–846. doi: 10.1084/jem.187.6.835

Yao, T., and Cohen, R. E. (2002). A cryptic protease couples deubiquitination and degradation by the proteasome. *Nature* 419, 403–407. doi: 10.1038/nature01071

Yen, H. C., and Elledge, S. J. (2008). Identification of SCF ubiquitin ligase substrates by global protein stability profiling. *Science* 322, 923–929. doi: 10.1126/science.1160462

Yen, H. C., Xu, Q., Chou, D. M., Zhao, Z., and Elledge, S. J. (2008). Global protein stability profiling in mammalian cells. *Science* 322, 918–923. doi: 10.1126/science.1160489

Yoon, S. Y., Lee, Y., Kim, J. H., Chung, A. S., Joo, J. H., Kim, C. N., et al. (2005). Over-expression of human UREB1 in colorectal cancer: HECT domain of human UREB1 inhibits the activity of tumor suppressor p53 protein. *Biochem. Biophys. Res. Commun.* 326, 7–17. doi: 10.1016/j.bbrc.2004.11.004

Zeng, Y., Bachhav, B., Zhao, W., Nguyen, T., and Segatori, L. (2019). A hysteretic genetic circuit for detection of proteasomal degradation in mammalian cells. *ACS Synth. Biol.* 8:2025–35. doi: 10.1021/acssynbio.9b00074

Zhao, W., Bonem, M., Mcwhite, C., Silberg, J. J., and Segatori, L. (2014). Sensitive detection of proteasomal activation using the Deg-On mammalian synthetic gene circuit. *Nat. Commun.* 5:3612. doi: 10.1038/ncomms4612

Conflict of Interest: The authors declare that the research was conducted in the absence of any commercial or financial relationships that could be construed as a potential conflict of interest.

frontiers in Chemistry

METHODS
published: 21 February 2020
doi: 10.3389/fchem.2020.00111

Strategy for Development of Site-Specific Ubiquitin Antibodies

Ila van Kruijsbergen[1†], Monique P. C. Mulder[2†], Michael Uckelmann[3], Tibor van Welsem[1], John de Widt[3], Aldo Spanjaard[4], Heinz Jacobs[4], Farid El Oualid[5], Huib Ovaa[2] and Fred van Leeuwen[1,6*]*

[1] Division of Gene Regulation, Netherlands Cancer Institute, Amsterdam, Netherlands, [2] Leiden Institute for Chemical Immunology, Oncode Institute, Leiden University Medical Center, Leiden, Netherlands, [3] Division of Biochemistry, Netherlands Cancer Institute, Amsterdam, Netherlands, [4] Division of Tumor Biology & Immunology, Netherlands Cancer Institute, Amsterdam, Netherlands, [5] UbiQ Bio BV, Amsterdam, Netherlands, [6] Department of Medical Biology, Amsterdam UMC, University of Amsterdam, Amsterdam, Netherlands

OPEN ACCESS

Edited by:
Simone Brogi,
University of Pisa, Italy

Reviewed by:
Chunbin Zou,
University of Pittsburgh, United States
Qianzheng Zhu,
The Ohio State University, United States
Brian D. Strahl,
University of North Carolina at Chapel Hill, United States
Yue Chen,
University of Minnesota Twin Cities, United States

***Correspondence:**
Huib Ovaa
h.ovaa@lumc.nl
Fred van Leeuwen
fred.v.leeuwen@nki.nl

[†]These authors have contributed equally to this work

Specialty section:
This article was submitted to Chemical Biology, a section of the journal Frontiers in Chemistry

Received: 08 October 2019
Accepted: 05 February 2020
Published: 21 February 2020

Citation:
van Kruijsbergen I, Mulder MPC, Uckelmann M, van Welsem T, de Widt J, Spanjaard A, Jacobs H, El Oualid F, Ovaa H and van Leeuwen F (2020) Strategy for Development of Site-Specific Ubiquitin Antibodies. Front. Chem. 8:111. doi: 10.3389/fchem.2020.00111

Protein ubiquitination is a key post-translational modification regulating a wide range of biological processes. Ubiquitination involves the covalent attachment of the small protein ubiquitin to a lysine of a protein substrate. In addition to its well-established role in protein degradation, protein ubiquitination plays a role in protein-protein interactions, DNA repair, transcriptional regulation, and other cellular functions. Understanding the mechanisms and functional relevance of ubiquitin as a signaling system requires the generation of antibodies or alternative reagents that specifically detect ubiquitin in a site-specific manner. However, in contrast to other post-translational modifications such as acetylation, phosphorylation, and methylation, the instability and size of ubiquitin—76 amino acids–complicate the preparation of suitable antigens and the generation antibodies detecting such site-specific modifications. As a result, the field of ubiquitin research has limited access to specific antibodies. This severely hampers progress in understanding the regulation and function of site-specific ubiquitination in many areas of biology, specifically in epigenetics and cancer. Therefore, there is a high demand for antibodies recognizing site-specific ubiquitin modifications. Here we describe a strategy for the development of site-specific ubiquitin antibodies. Based on a recently developed antibody against site-specific ubiquitination of histone H2B, we provide detailed protocols for chemical synthesis methods for antigen preparation and discuss considerations for screening and quality control experiments.

Keywords: ubiquitin, histone H2B, H2B-K123ub, PCNA, monoclonal antibody

INTRODUCTION

The covalent attachment of ubiquitin (Ub) to proteins constitutes a key post-translational modification mechanism. Ubiquitin, a polypeptide of 76 amino acids, is perhaps best known for its role in protein degradation (Rosenbaum et al., 2011; Claessen et al., 2012; Geng et al., 2012; Komander and Rape, 2012; Varshavsky, 2012). However, more recently ubiquitin has also emerged as a powerful and versatile signaling system that regulates many different biological pathways (Chen and Sun, 2009; Husnjak and Dikic, 2012; Ramanathan and Ye, 2012; Oh et al., 2018; Rape, 2018; Clague et al., 2019; Mattern et al., 2019; Spit et al., 2019). Ubiquitin can influence protein-protein interactions, protein targeting and sorting, and regulates processes such as gene expression, and

DNA repair (Ranjitkar et al., 2010; Piro et al., 2012; Marteijn et al., 2014; van Cuijk et al., 2014; Zhao et al., 2014; Venkatesh and Workman, 2015). Ubiquitin impinges on many critical processes in the cell and thereby plays major roles in normal development and human aging and disease. The molecular mechanisms involved are topics of intensive research, both in basic science as well as in the clinic (Chen and Sun, 2009; Geng et al., 2012; Mattiroli and Sixma, 2014).

Ubiquitin-mediated protein degradation typically involves the attachment of poly-ubiquitin chains (poly-Ub) to target proteins (Varshavsky, 2012). Here, ubiquitin moieties are attached to each other via a lysine 48 (K48) residue of another ubiquitin molecule. This process has been studied extensively and is relatively well-understood because monitoring poly-ubiquitination requires simple non-specific detection methods and can be easily modulated by inhibition of the proteasome, the molecular machine that degrades K48-poly-ubiquitylated proteins. In contrast, the understanding of other signaling- and degradation-functions of ubiquitin is much less developed because of the lack of specific reagents required to study them. Different ubiquitination patterns involve the attachment of one ubiquitin molecule (Ub1) to a specific lysine residue of a target protein or the attachment of a poly-ubiquitin chain involving homogeneous or mixed chains by forming isopeptide bonds between the N-terminal methionine (Met1-linked ubiquitination) or any of the other internal lysines on ubiquitin (Lys6, Lys11, Lys27, Lys29, Lys33, Lys63) (Chen and Sun, 2009; Husnjak and Dikic, 2012; Ramanathan and Ye, 2012; Oh et al., 2018; Rape, 2018; Clague et al., 2019; Mattern et al., 2019; Spit et al., 2019). Efficient monitoring of these types of events requires reagents that specifically recognize the attachment of ubiquitin to one particular lysine residue of a protein or of ubiquitin itself (poly-Ub) (Fujimuro et al., 1994; Fujimuro and Yokosawa, 2005; Newton et al., 2008, 2012; Matsumoto et al., 2010, 2012; Fulzele and Bennett, 2018; Mattern et al., 2019; van Wijk et al., 2019). To date, very few reagents exist that fulfill these criteria. Whereas many antibodies have been developed to detect a range of known protein modifications (e.g., acetylation, methylation, phosphorylation), generation of antibodies against site-specific ubiquitination appears to be far from trivial. As a result, a limited number of suitable antibodies exists that allow for the monitoring and studying of specific ubiquitination events.

The development of site-specific ubiquitination antibodies faces several critical challenges due to the large size and reversibility of the ubiquitin modification. First, whereas a methylated lysine or phosphorylated serine can be easily incorporated into synthetic peptides by standard synthesis methods, incorporation of a ubiquitinated lysine requires advanced chemistry. As a way out, short fragments of ubiquitin have been used in immunization strategies. However, as evidenced by the small number of good antibodies this approach has not always been successful. Second, ubiquitin is covalently attached to lysine residues in proteins but can be readily removed by deubiquitinating enzymes that are also present in plasma, likely as a result of leakage from dead cells. Therefore, the native ubiquitin-lysine isopeptide linkage is likely to be cleaved upon immunization.

To solve these problems, we applied synthesis of full-length ubiquitin and derivatives thereof that can be attached to target peptides of choice and applied chemical ligation technologies that allow synthesis of well-defined Ub-modified polypeptides, either with a native isopeptide linkage using thiolysine mediated ligation or with a proteolytically stable bond using click chemistry. In the latter case the overall structure around the native Ub-Lysine environment is preserved to a maximum extent by only replacing the native isopeptide bond between Ub and the lysine residue with a proteolytically stable amide triazole isostere. This enables the use of immunization antigens that closely resemble the isopeptide linked Ub conjugate. The triazole isostere has been shown to be a good amide-bond mimic that is tolerated and has been utilized in biological settings involving triazole-based poly-Ub chains as well as in activity-based probes (Weikart et al., 2012; Dresselhaus et al., 2013; McGouran et al., 2013; Flierman et al., 2016). The introduction of the whole ubiquitin protein in a proteolytically stable form is expected to increase the chance of exposing a site-specific epitope for generating high quality antibodies. This idea is supported by the recent success of a monoclonal antibody specific for ubiquitin on lysine 123 of yeast histone H2B (yH2B-K123ub1), which was obtained using this approach (van Welsem et al., 2018; Vlaming et al., 2019). H2BK123ub in yeast or H2BK120 in metazoans is known to play key roles in regulating gene expression, chromatin dynamics, and DNA repair (Fuchs and Oren, 2014; Cole et al., 2015; Morgan and Wolberger, 2017; Marsh and Dickson, 2019; Worden and Wolberger, 2019). The antibody has successfully been used for immunoblots and chromatin immunoprecipitation assays (Vlaming et al., 2016, 2019; van Welsem et al., 2018) and thereby enabled the deconstruction of a bidirectional regulatory mechanism between histone methylation and histone ubiquitination (Vlaming et al., 2016, 2019; van Welsem et al., 2018).

The generation of monoclonal antibodies in mice involves multiple steps: (i) design and synthesis of non-hydrolyzable Ub-peptide conjugates for immunization; (ii) design and synthesis of extended native iso-peptide linked Ub-peptide conjugates for screening; (iii) immunization, and generation and screening of hybridomas; (iv) clone selection and antibody validation in native context (**Figure 1**). In this manuscript we focus on the steps that are specific for synthesis of ubiquitin-peptide conjugates for the generation of site-specific ubiquitin antibodies (steps i and ii), as detailed excellent general protocols for antibody development (step iii) and validation (step iv) have been described elsewhere (Egelhofer et al., 2010; Yokoyama et al., 2013; Greenfield, 2014; Ossipow and Fischer, 2014; Kungulovski et al., 2015; Marcon et al., 2015; Rothbart et al., 2015; Uhlen et al., 2016; Guillemette et al., 2017; Holzlöhner and Hanack, 2017; Edfors et al., 2018; Venkataraman et al., 2018; Weller, 2018; Marx, 2019). In addition, we discuss the rationale for the design of antigens used for immunization and screening. Finally, we provide examples of Ub-specific screening and validation assays and discuss possible pitfalls based on the immunization scheme to obtain site-specific antibodies against yeast H2B-K123ub (van Welsem et al., 2018; Vlaming et al., 2019) and attempts to develop antibodies specific for lysine 164 of human proliferating

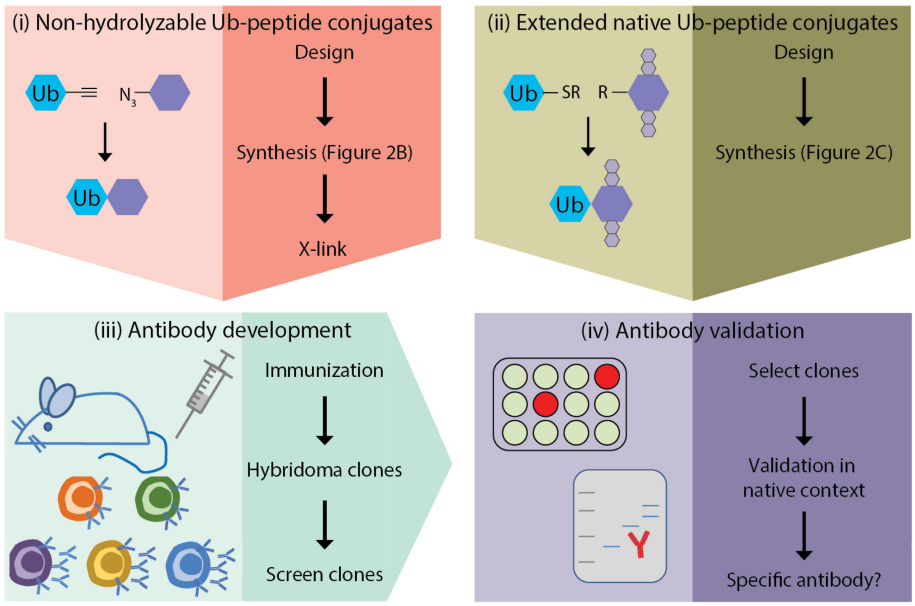

FIGURE 1 | Outline of site-specific Ub antibody development. **(i)** design and synthesis of non-hydrolyzable Ub-peptide conjugates for immunization; **(ii)** design and synthesis of extended native iso-peptide linked Ub-peptide conjugates for screening; **(iii)** immunization, and generation and selection of hybridomas; **(iv)** selection of clones and antibody validation.

cell nuclear antigen (huPCNA-K164ub). Modification of PCNA by ubiquitin critically regulates the function of PCNA in DNA damage tolerance (Hoege et al., 2002; Mailand et al., 2013; Kanao and Masutani, 2017; Uckelmann and Sixma, 2017).

Given the urgent need for site-specific ubiquitin antibodies in the field, our protocol and design strategies will be of great help to other researchers in the field of small-protein modifications and could facilitate the production of these reagents, thereby enabling insights into the dynamics of ubiquitination.

MATERIALS AND EQUIPMENT

In this section we describe the reagents and equipment required for the synthesis of Ub-conjugates. In section Methods we describe the synthesis methods and the rationale of the conjugate design. In section Anticipated Results we show how the conjugates are used for screening and clone selection in steps and we provide examples of validation experiments for step.

Reagents and Equipment Used for Ub-Conjugate Synthesis and Analysis

Reagents for Conjugate Synthesis

Fmoc-amino acids were purchased from Novabiochem, solvents, N,N-Diisopropylethylamine (DiPEA), and acetic anhydride from Biosolve, peptide coupling reagents Benzotriazol-1-yl-oxy-tripyrrolidinophosphonium hexafluorophosphate (PyBOP), 2-(1H-Benzotriazole-1-yl)-1,1,3,3-tetramethylaminium hexafluorophosphate (HBTU) and Hydroxybenzotriazole (HOBt) from Novabiochem (Merck).

Equipment and Software for Ub-Conjugate Synthesis and Analysis

Syro II MultiSyntech Automated Peptide synthesizer
Waters 2795 Separation Module (Alliance HT)
Waters 2996 Photodiode Array Detector (190–750 nm)
Phenomenex Kinetex C18 (2.1 × 100, 2.6 μm) column
LCTTM Orthogonal Acceleration Time of Flight Mass Spectrometer
Waters Atlantis T3 C18 (30 × 250 5 μm)
Waters Mass Lynx Mass Spectrometry Software 4.1.

Reagents Used for Ub-Conjugate Crosslinking

General Reagents

- KLH (Pierce 77600 Imject mcKLH)
- BCP (Pierce 77130 Imject Blue Carrier Protein)
- Glutaraldehyde solution 25%, EM grade (Sigma G5882).

Antibodies Used in This Study

- yH2BK123ub1 (mouse monoclonal #152107, Ximbio) RRID: AB_2737407
- yH2BK123ub1 (non-specific rabbit polyclonal serum; #NKI-162611, this study)
- yH2B (rabbit polyclonal; #39238, Active Motif) RRID: AB_2631110
- Ubiquitin (mouse monoclonal; #NKI-28B8A12/D7, this study)
- PCNA-K164ub (non-specific mouse monoclonal; #NKI-1G5B7/F10, this study)

- PCNA (mouse monoclonal; #PC10/Sc-56, lot I0710, Santa Cruz)
- PCNA-K164ub [rabbit monoclonal; #D5C7P, lot 11/2014, Cell Signaling Technology (CST)]
- H2A (rabbit polyclonal serum; #39235, Active Motif) RRID: AB_2687477
- H4 (rabbit monoclonal; #05-858, clone 62-141-13, lot: 2459608, Millipore).

METHODS

Rationale Antigen Design

Chemical ligation methods are used to synthesize well-defined Ub-modified polypeptides of ∼15–17 amino acids either with in the central residue a native isopeptide or proteolytically stable Ub bond (**Figure 2**). Proteolytically-stable Ub-polypeptide conjugates are used for the initial immunization. If the peptide corresponds to an internal sequence, immunization peptides are acetylated at the N-terminus to eliminate the positively charged N-terminal amino group, which is often erroneously recognized by antibodies raised against short peptides. Similarly, the C-terminus of the peptide is amidated. ELISA screens are performed with native iso-peptide linked Ub- polypeptides that are two amino acids longer at the N-terminus and/or C-terminus (depending on the position of the ubiquitination site in the protein) than the immunization antigen to more closely mimic the native protein (as discussed below and see **Figure 2**). When using mice, a complete 10-mouse immunization scheme, clone-selection, and screening protocol together typically requires 4 mg Ub conjugate. For the negative control ELISA screens, 4 mg non-modified peptide and 4 mg free Ub is required per protocol. Immunizations in larger animals typically require more material.

General Methods

LC-MS measurements are performed on a system equipped with a Waters 2795 Separation Module (Alliance HT), Waters 2996

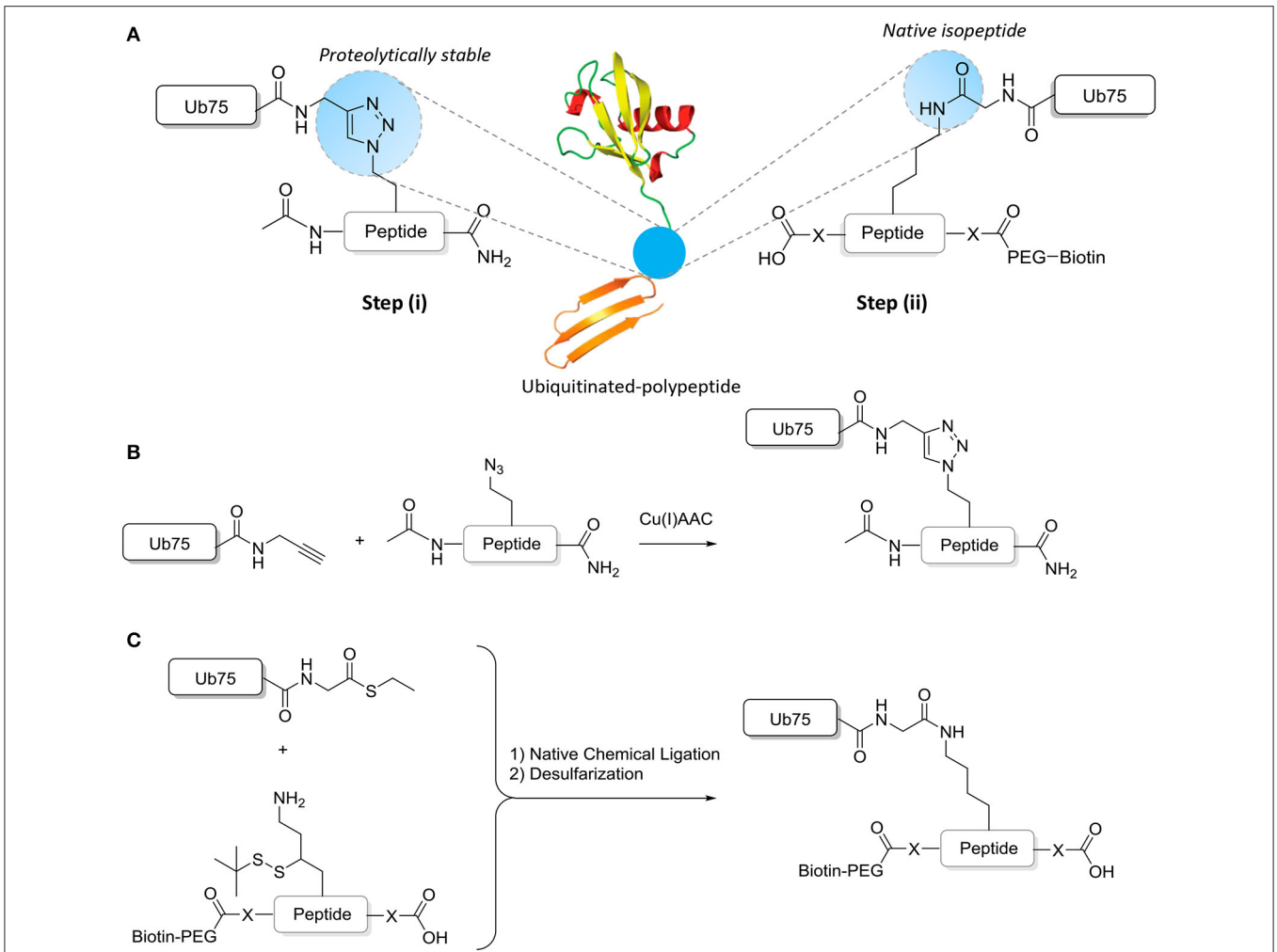

FIGURE 2 | Synthesis of ubiquitinated polypeptides. **(A)** Design of the proteolytically-stable and native isopeptide-linked ubiquitinated polypeptides; **(B)** Schematic representation of the key CuAAC reaction to generate non-hydrolyzable Ub-polypeptides; **(C)** Schematic representation of the key steps to generate isopeptide linked Ub-polypeptides in which the sequence used in panel B is extended (indicated by -X- and explained further in the text).

Photodiode Array Detector (190–750 nm), Phenomenex Kinetex C18 (2.1 × 100, 2.6 μm) column and LCTTM Orthogonal Acceleration Time of Flight Mass Spectrometer. Samples are run using 2 mobile phases: A (0.1% formic acid in H_2O/acetonitrile 99:1 v/v) and B (0.1 % formic acid in H_2O/acetonitrile 99:1 v/v) at a flow rate of 400 μL/min; gradient: 0–0.5 min, 5% B; 0.5–8 min, → 95% B; 8–10 min 95% B, 10–12 min, → 5% B. Data processing is performed using Waters Mass Lynx Mass Spectrometry Software 4.1 (deconvolution with Maxent1 function).

General Purification Procedures

The crude product is dissolved in a minimal amount of warm DMSO and then diluted by addition to MilliQ water and purified by RP-HPLC on a Waters Atlantis T3 C18 30 × 250 5 μm. Column Mobile phases: A = 0.05% aq. trifluoroacetic acid (TFA) and B = 0.05% TFA in CH_3CN. Ub peptides are purified with a gradient: 20→45% B over 25 min, while the short polypeptides (15–17 AA) are purified with a gradient: 5→95% B over 25 min, Flow rate = 37 mL/min. Pure fractions (>95%), as judged by LC-MS are pooled, lyophilized and used as such.

Synthesis of Mono-Ubiquitin Precursors

Ub

The Ub(1–75) and Ub(1–76) peptide sequences are synthesized on resin following the procedures described before (El Oualid et al., 2010; Mulder et al., 2014). In brief, (Ub) is synthesized on a Syro II MultiSyntech Automated Peptide synthesizer using standard 9-fluorenylmethoxycarbonyl (Fmoc) based solid phase peptide chemistry on a 25-μmol scale. Starting with the pre-loaded Fmoc-Gly trityl resin (0.18 mmol/g, Rapp Polymere GmbH), each successive amino acid (Novabiochem) is double coupled in 4 molar excess using PyBOP (4 equiv) and DiPEA (8 equiv) as coupling regents. The N-terminal methionine residue in the sequence is replaced by the known isostere Norleucine. Deprotection of the Fmoc group is achieved with 20% piperidine in N-Methyl-2-pyrrolidone (NMP) (2 × 2 and 1 × 5 min). After completion of all coupling cycles, the N-terminus is protected with a Boc group by overnight treatment with Boc-anhydride in Dichloromethane (DCM). The resin is rinsed with DCM (3×5 mL) and treated with 5 mL of DCM/Hexafluoroisopropanol (HFIP) (4:1 v/v) for 30 min and filtered. The resin is rinsed with DCM (3 × 5 mL) and the combined filtrates are concentrated to obtain the partially protected Ub peptide 1–75.

UbPA

The partially protected peptide residue Ub(1–75) (1 equiv) is redissolved in DCM and reacted with PyBOP (5 equiv), propargyl amine (10 equiv) and triethylamine (TEA) (20 equiv). The reaction mixture is stirred over night at room temperature. After removal of the solvent *in vacuo*, the residue is treated with TFA/H_2O/iPr_3SiH/phenol (90/5/2.5/2.5 v/v/v/v, 1 mL for 5 μmol Ub(1–75)-PA) for 3 h followed by precipitation with cold Et_2O/pentane (3/1 v/v). Purification by HPLC gives Ub-PA as a white powder.

UbSEt

The partially protected peptide residue Ub(1–76) (1 equiv) is redissolved in DCM and reacted with pyBOP (5 equiv), EtSH (10 equiv) and DiPEA (10 equiv). The reaction mixture is stirred overnight at room temperature. The solvent is removed in vacuo and the residue treated for 3 h with TFA/H_2O/iPr_3SiH/phenol (90/5/2.5/2.5 v/v/v/v, 1 mL for 5 μmol UbSEt) followed by precipitation with cold Et_2O/pentane (3/1 v/v). Purification by HPLC gives UbSEt as a white powder.

Synthesis of Peptide Precursors

Synthesis of Azidoornithine Peptide Precursor for Synthesis Non-hydrolyzable Conjugates

The peptides are synthesized on a Syro II MultiSyntech Automated Peptide synthesizer using standard Fmoc based solid phase peptide chemistry on a 100-μmol scale. Starting with pre-loaded resin for Fmoc Peptide synthesis (Rapp Polymere GmbH), each successive amino acid (Novabiochem) is double coupled (2 × 25 min, in the event of difficult coupling extended to 2 × 70 min) in 4 molar excess using PyBOP (4 equiv) and DiPEA (8 equiv) as coupling regents. Deprotection of the Fmoc group is achieved with 20% piperidine in NMP (2 × 5 min). After completion of all coupling cycles, the resin is treated with acetic anhydride to acetylate the N-terminus or modified with a biotin-PEG moiety to facilitate Surface Plasmon Resonance (SPR) measurements. In the latter case, a PEG spacer (8-Fmoc-amino)-3,6-dioxaoctanoic acid (AK Scientific, Inc., Union city, CA, 4 equiv), is coupled to the N-terminus using PyBOP (4 equiv) and DIPEA (4 equiv) in NMP for 25 min. at ambient temperature. The Fmoc protection group is removed as described and biotin is coupled subsequently using HBTU (2-(1H-benzotriazol-1-yl)-1,1,3,3-tetramethyluronium hexafluorophosphate, 4 equiv), HOBt (1-hydroxybenzotriazole, 4 equiv), DIPEA (8 equiv), and carboxy-functionalized biotin (Sigma-Aldrich, 4 equiv) in NMP and reacted for 2.5 h. After removal of the solvent *in vacuo*, the residue is treated for 3 h with TFA/H_2O/iPr_3SiH/phenol (90/5/2.5/2.5 v/v/v/v, 1 mL for 5 μmol peptide) followed by precipitation with cold Et_2O/pentane (3/1 v/v). Purification by HPLC gives the peptide as a white powder.

In the synthesis of immunization peptides, the lysine is replaced for an azidoornithine (azOrn) moiety and the choice for solid support is based upon the peptide sequence. Peptides corresponding to an internal protein sequence, as for the PCNA-K164 peptide (UniProtKB - P12004, AA 156-172: ac-DAVVISCAazOrnDGVKFSAS-$CONH_2$), are synthesized on a preloaded rink-amide resin. While peptide sequences corresponding to the C-termini of the protein, as for the H2B-K123 peptide (UniProtKB - P02294, AA 115–130: ac-SEGTRAVTazOrnYSSSTQA-COOH), are synthesized on a preloaded PEG-polystyrene support resin (PEG-PS).

Synthesis of γ-Thiolysine Peptide Precursor for Synthesis Native Conjugates

The peptides are synthesized on a Syro II MultiSyntech Automated Peptide synthesizer using standard Fmoc based solid phase peptide chemistry on a 100-μmol scale. Starting

with pre-loaded PEG-polystyrene support resin (PEG-PS) for Fmoc Peptide synthesis (Rapp Polymere GmbH), each successive amino acid (Novabiochem) is double coupled (2 × 25 min, in the event of difficult coupling extended to 2 × 70 min*) in 4 molar excess using PyBOP (4 equiv) and DiPEA (8 equiv) as coupling regents. Deprotection of the Fmoc group is achieved with 20% piperidine in NMP (2 × 5 min). After completion of all coupling cycles the resin is treated with acetic anhydride to acetylate the N-terminus. After removal of the solvent *in vacuo*, the residue is treated for 3 h with TFA/H_2O/iPr_3SiH/phenol (90/5/2.5/2.5 v/v/v/v, 1 mL for 5 μmol peptide) followed by precipitation with cold Et_2O/pentane (3/1 v/v). Purification by HPLC gives the peptide as a white powder.

*Note: We encountered difficulties in the synthesis of PCNA-K164 peptide (UniProtKB - P12004, AA 156-172: ac-DAVVISCAazOrnDGVKFSAS-$CONH_2$) following our regular procedure (double couplings 2 × 25 min) on the Syro II. The desired peptide could not be obtained and truncated versions of the peptide were found. To solve this, we synthesized this peptide on an Intavis MutiPep CF automated peptide synthesizer with a real-time UV monitoring enabling the optimization of reaction parameters like deprotection and coupling times during the synthesis. From cycle 13 onwards the coupling times were extended to 2 × 70 min (corresponding to peptide sequence DAVV).

Synthesis of Ub-Peptide Conjugate

Synthesis of Non-hydrolyzable End-Modified Ub-Peptide Conjugates

UbPA and the azidoornithine peptide are each dissolved in warm DMSO at a concentration of 50 mg/mL. 200 μL of the UbPA DMSO stock (10 mg) is added to 15 mL 8M urea, 100 mM phosphate buffer pH 7, followed by addition of 1.2 equiv of the azidoornithine peptide. To the resulting solution is added 600 μL of a freshly prepared CuAAC catalyst solution. This is made by first mixing 200 μL of a 25 mg/mL $CuSO_4 \cdot 5H_2O$ solution in MQ with 200 μL of a 120 mg/mL sodium ascorbate solution in MQ, affording a dark brown solution. Upon addition of 200 μL of a 50 mg/mL Tris((1-benzyl-4-triazolyl)methyl)amine (TBTA) solution in CH_3CN (Zhou and Fahrni, 2004), a colorless CuAAC catalyst solution is obtained. After the reactions are finished, as judged by LC-MS (∼1 h), the reaction is quenched by the addition of 1.5 mL of 0.5 M EDTA, pH 7.0 and the crude product purified by HPLC.

Synthesis of Native Iso-Peptide Linked Ub-Peptide Conjugates

A solution of UbSEt (50 mg/mL) in 6M guanidine hydrochloride (GdnHCl), 0.15 M sodium phosphate buffer, pH 7 and 250 mM MPAA is mixed with a solution of the γ-thiolysine peptide mutant (1.5 equiv, 50 mg/mL) in 6M GdnHCl, 0.2 M sodium phosphate buffer, pH 7 and 250 mM 4-mercaptophenylacetic acid (MPAA). After incubating the mixture overnight at 37°C, tris(2-carboxyethyl)phosphine (TCEP) is added to reduce the MPAA disulfide and the crude purified by HPLC.

Antigen Crosslinking

For coupling the synthesized antigen to carrier protein, several methods can be considered (Yokoyama et al., 2013; Greenfield, 2014; Ossipow and Fischer, 2014; Holzlöhner and Hanack, 2017), depending on the sequence of the peptide and the compatibility with the chemical synthesis of the Ub-peptide conjugates. Here we describe a general crosslinking protocol that uses glutaraldehyde for amine-to-amine coupling; the internal lysines on Ub provide several amines for efficient coupling to the carrier protein. To avoid selecting clones specific for the crosslinked conjugate, it is important to perform the screening of hybridomas with non-crosslinked peptide-Ub conjugates, as explained in more detail below in section 4. To use the synthesized Ub-peptide conjugate for immunization, prior to injection they are crosslinked to Keyhole limpet hemocyanin (KLH) or Blue Carrier Protein (BCP), or a mix of both carrier proteins. Generally, reacting equal mass amounts of Ub-peptide conjugate and carrier protein will achieve sufficient molar excess. Dissolving the Ub-peptide conjugate must be performed with great care to avoid precipitation of the conjugate. First, dissolve the peptide in warm DMSO at a concentration of 40 mg/mL. Then add the DMSO solution dropwise to PBS buffer (phosphate-buffered saline containing 100 mM phosphate buffer), while gently shaking the mixture. Next buffer exchange and concentrate the solution to a final concentration of 10 mg/mL Ub-peptide in PBS. Combine one volume carrier protein (10 mg/mL in PBS) with one volume Ub-peptide conjugate (10 mg/mL in PBS) and mix. Add 1/200 volume of glutaraldehyde (5% in H_2O) and mix briefly on a vortex. Incubate for 5 min at room temperature and repeat the addition of glutaraldehyde three times. Incubate 30 min on ice. Add 1/10 volume 1M glycine pH 8.5 and incubate for 5 min at room temperature. Dialyze overnight against PBS. Adjust the concentration to the equivalent of 2 mg/mL Ub-peptide conjugate. Store at −20°C. For primary and secondary immunizations of 10 mice, 4 mg Ub-peptide conjugate (400 μl of a 10 mg/mL solution) was combined with 4 mg carrier protein (400 μl of a 10 mg/mL solution). After addition of glutaraldehyde and during dialysis, some aggregation may occur. The immunizations are performed with the mix of soluble and insoluble conjugates since both have been reported to be immunogenic.

Immunization

Immunization of animals, monitoring the immune response and antibody production of selected clones by ELISA, production of hybridomas, and subcloning and isolation of specific hybridomas is frequently outsourced to a third party specialized in antibody development using proprietary protocols. All hybridomas described in this study were delivered by ThermoFisher Scientific (Life Technologies). All animals used by Thermo Scientific are assured by the Office of Laboratory Animal Welfare. Upon request additional accreditations can be provided. Here we focus on Ub-peptide conjugate synthesis and considerations for validation of site-specific Ub antibodies. Preferably, multiple mice (10 or more) and different genetic mouse backgrounds are immunized to maximize the diversity of the antibody repertoire

and immune response. Following primary immunization, the animals are boosted several times until the response stabilizes.

Antibody Production and Purification

Following hybridoma clone selection and expansion, the yH2B-K123ub1 and candidate PCNA-K164ub1 antibodies were produced and purified in house using the following protocol. Hybridoma clones are initially expanded in flasks in Dulbecco's Modified Eagle Medium (DMEM) or Iscove's Modified Dulbecco's Medium (IMDM) with L-glutamine containing Penicillin and 15-20% fetal calf serum (FCS). The percentage of serum is dropped by 1–2% on every passage until a concentration of 3–6% FCS is reached to minimize the amount of bovine IgG in the media. The final expansion is performed in roller bottles in which the cells are grown for 10–12 days until ∼50% of the cells die. The supernatant is collected and debris and cells are removed by centrifugation. The cleared supernatants are stored at 4°C in the presence of 0.02% sodium azide. The pooled supernatants are concentrated and dialyzed using an artificial kidney (Fresenius Medical Care Hemoflow F40S, Polysulfone Capillary Dialyzers; following the manufacturer's instructions) in MES buffer (25 mM 2N-morpholino ethanesulfonic acid, pH 5,5, set with 5 M NaOH), reaching a 20-fold concentration of proteins. The IgGs are purified over ABx resin (Bakerbond ABx prep scale 40 μm JT Baker 7269-00) on a fast protein liquid chromatography (FPLC) system (NGC Bio-Rad) (Ross et al., 1987; Chen et al., 1988) and eluted with an ammonium sulfate gradient (0–100% 500 mM $(NH_4)_2SO_4$ + 20 mM KH_2PO_4 pH6.7) to avoid pH shock (compared with classical ProtA and ProtG methods). Since every antibody has a different elution pattern, the peak fractions are identified by SDS-PAGE analysis for the presence of the IgG light and heavy chains, and subsequently pooled and dialyzed against PBS to remove the ammonium sulfate and azide. Antibodies are stored at 4 degrees for short term use, or frozen in aliquots.

ANTICIPATED RESULTS

Ub-Peptide Conjugates and Antigen Crosslinking

During the synthesis of the Ub-peptide conjugates, traces of monoUb precursors can remain present. Therefore, the purification of the proteolytically-stable Ub-polypeptide conjugates should be performed with great care, in particular as these are used for the immunization. Typically, purification by HPLC is sufficient to remove these traces as can be judged via LC-MS analysis (**Figure 3**). If difficulties are encountered, an additional size exclusion, or cation purification can be performed (El Oualid et al., 2010). To use the synthesized Ub-peptide conjugates for immunization, prior to injection they are crosslinked to carrier proteins. A crucial step here involves dissolving the Ub-conjugates in warm DMSO. When this step is overlooked and buffer added immediately to Ub, the protein will crash out of solution.

Immunization of Mice, Generation of Hybridomas, and Isolation of Stable Clones

The polyclonal serum after immunization with a non-hydrolyzable end-modified Ub-peptide conjugate will typically contain a mix of antibodies, e.g., anti-peptide, anti-ubiquitin, and anti-peptide-Ub (**Figure 4**). Given the relatively large size of the Ub moiety, a substantial anti-Ub response is expected,

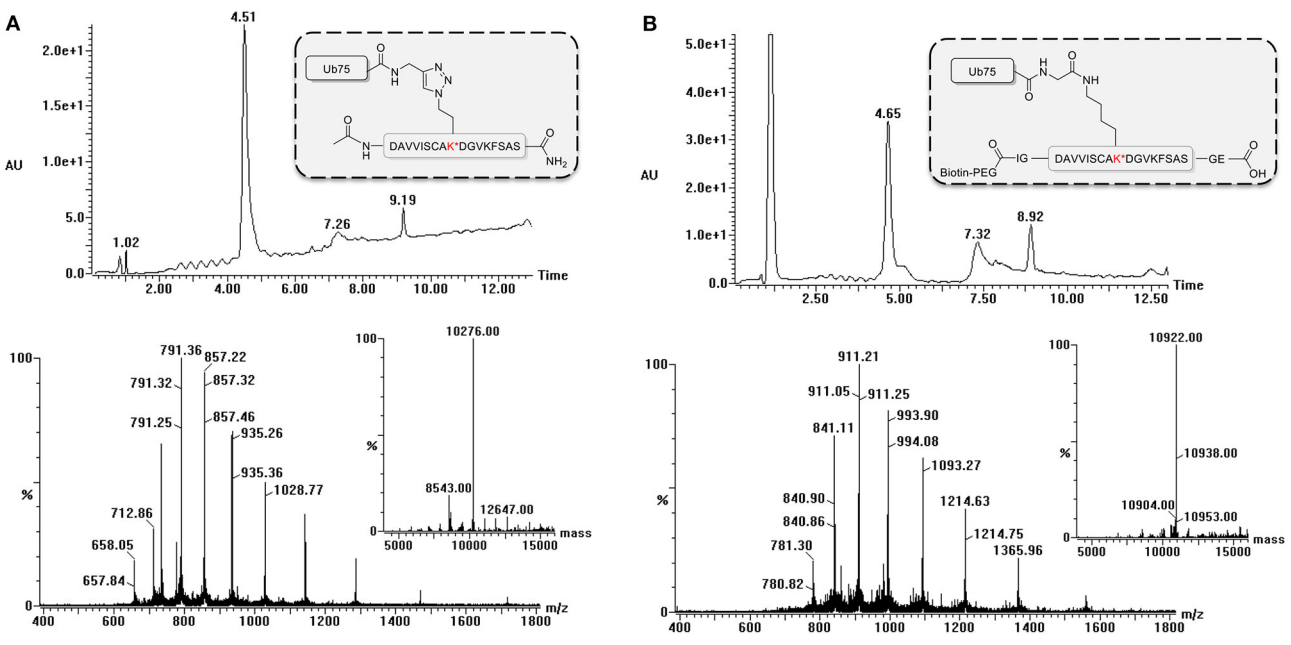

FIGURE 3 | LC-MS analysis of ubiquitinated polypeptides. Example of LC-MS analysis based on PCNA-K164 (UniProtKB P12004). Diode Array chromatogram (top), MS spectrum of peak (bottom) and Deconvoluted mass of product peak (insert) of **(A)** the non-hydrolyzable Ub-conjugate and **(B)** the isopeptide linked Ub-conjugate.

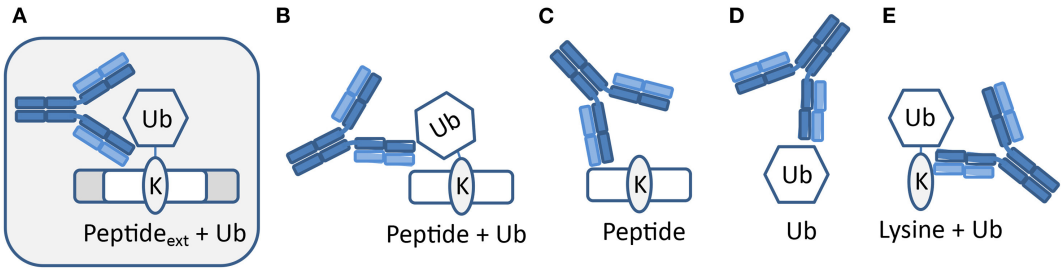

FIGURE 4 | Expected types of antibodies upon immunization with peptide-Ub conjugates. Polyclonal serum after immunization with a non-hydrolyzable end-modified Ub-peptide conjugate will typically contain a mix of antibodies. **(A)** Antibodies recognizing the site-specific ubiquitin on the native protein can be identified using an extended version of the antigen used for immunization. Other antibodies might recognize **(B)** an epitope that includes the terminus of the immunization antigen and hence these antibodies will not recognize ubiquitin in the native extended protein, **(C)** the peptide independent of Ub, **(D)** Ub independent of the peptide, and **(E)** a K-Ub conjugate independent of the peptide context.

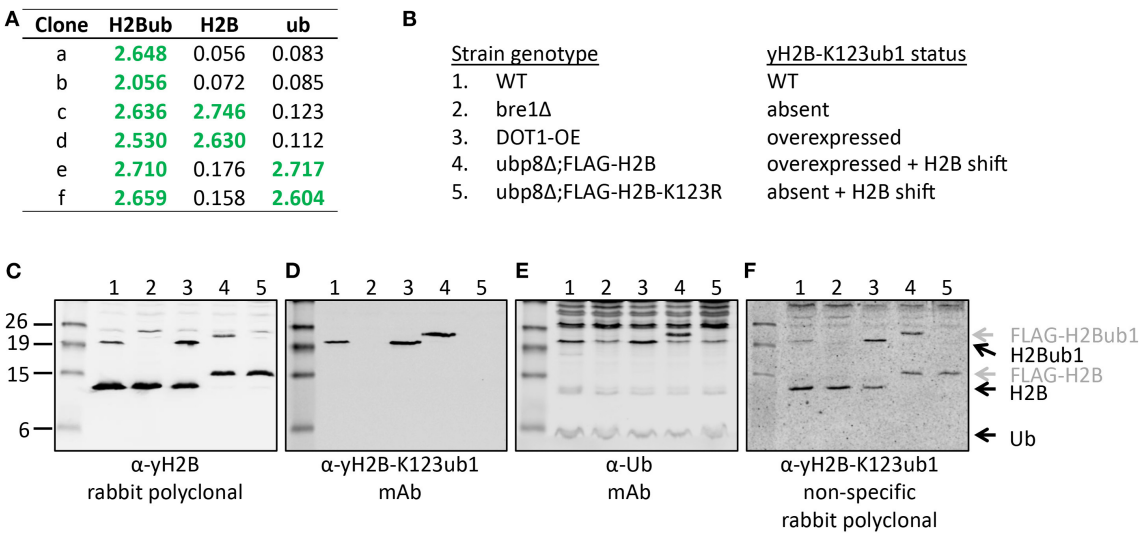

FIGURE 5 | Validation of the site-specific antibody against yeast histone H2B-K123ub1 using engineered cell lines. **(A)** Example of ELISA screening of supernatants of hybridoma cultures that identified clones specific for the H2B-K123ub1 conjugate (#a,b) and clones non-specifically recognizing the H2B peptide (#c,d) or ubiquitin (#e,f). **(B–F)** Following ELISA screens, antibodies produced from selected hybridomas against yH2B-K123ub were validated by immunoblot analysis using whole-cell extracts of a panel of engineered yeast strains. The panel includes (1) WT (normal H2B-K123ub1), (2) bre1Δ (no H2B-K123ub1), (3) DOT1-OE (more H2B-K123ub1), (4) ubp8Δ; FLAG-H2B (more H2B-K123ub1 and size shift due to FLAG-tag), (5) ubp8Δ; FLAG-H2B-K123R (no H2B-K123ub1 and H2B size shift due to FLAG-tag). The strains (BY4741, NKI4558, NKI4553, NKI2563, NKI2564) and protocols have been described previously (Vlaming et al., 2014; van Welsem et al., 2018). The antibodies and polyclonal serum indicated are described in the main text and section 2.2.2.

which we indeed observed in immunized mice (see below) and rabbits (**Figures 5A,E**). Nevertheless, it is useful to monitor the general immune response by ELISA to decide which of the mice will be used for hybridoma generation. After a final boost with antigen, spleens of three positive mice are harvested to isolate the antibody-producing cells for cell fusion to generate hybridomas. Hybridoma clones of ∼30 96-well plates are screened by ELISA using the native extended Ub-peptide conjugate and peptide and ubiquitin alone to identify clones that specifically recognize the site-specific ubiquitin attachment. Positive and specific clones identified by ELISA that show increased or stable production of specific antibodies (**Figure 5A**) are also screened by immunoblot analysis with recombinant proteins to confirm that antibodies in these clones recognize the native ubiquitin linkage on the complete protein (**Figures 5**, **6**).

Design Principles for Immunization- and Screening-Antigens

Since the validation assays are labor intensive, several design principles are recommended in the ELISA screening protocol to eliminate as many false positive clones as possible.

To identify clones that produce Ub site-specific antibodies, hybridoma culture supernatants are screened by ELISA. ELISA screens are performed with polypeptides that are two amino acids longer at the N-terminus and/or C-terminus (depending on the position of the ubiquitination site in the protein) than the antigen to more closely mimic the native protein and to eliminate clones

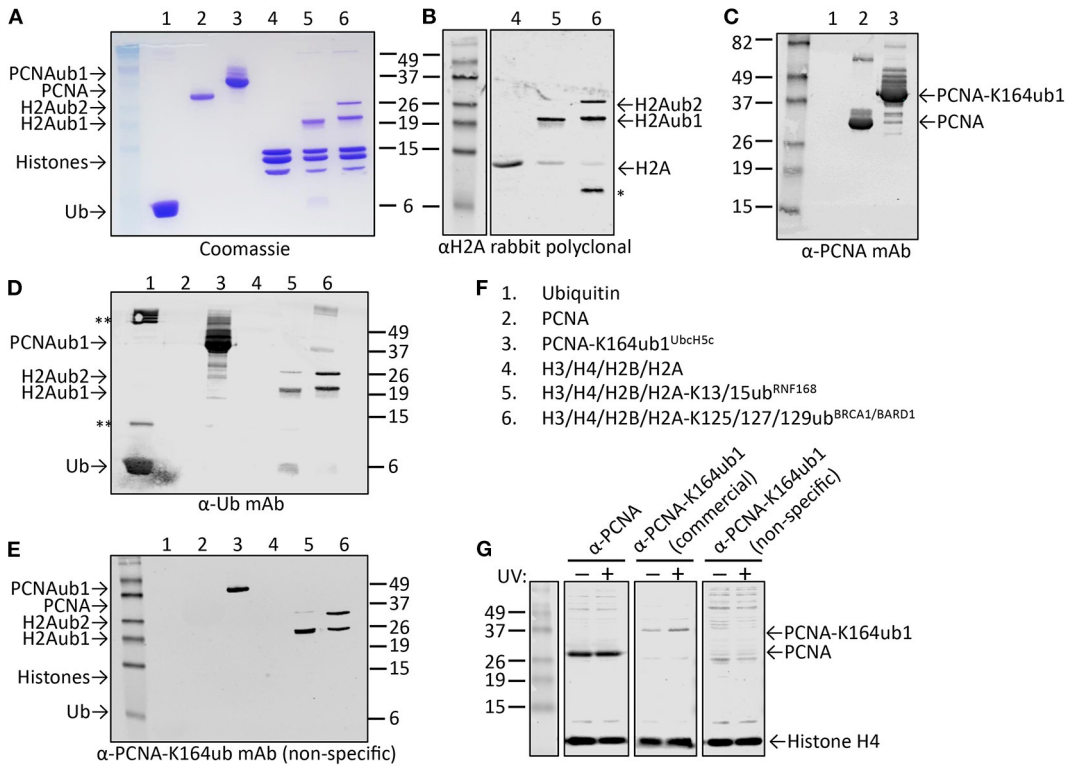

FIGURE 6 | Characterization of candidate site-specific antibody against human PCNA-K164ub1 using recombinant proteins and cell lysates. **(A)** Following ELISA screens, antibodies produced from selected hybridomas against PCNA-K164ub were examined by immunoblot analysis using recombinant proteins that were enzymatically ubiquitinated. The recombinant proteins used are shown on a Coomassie-stained gel. **(B–F)** Immunoblots of recombinant proteins with the indicated antibodies and recombinant proteins. Asterisk indicates degradation product; double asterisk indicates aggregation product. The selected PCNA-K164ub clone produced non-specific antibodies since ubiquitinated H2A was also detected. **(G)** Immunoblot analysis of whole-cell lysates of HEK-293T cells treated or not with 20 J/m^2 UV for 5 h, confirmed the lack of specificity of the selected clone (non-specific), while a UV-induced PCNA-K164ub1 increase was detected with a commercially available site-specific antibody (CST). Histone H4 was used as a loading control.

that recognize the N- and/or C terminal ends of the peptide normally not present in the full-length protein. The yH2B peptide was not extended at the C-terminus because it represents the C-terminal end of the native H2B protein.

While immunizations are performed with non-hydrolyzable Ub conjugates, ELISA tests are performed with a native peptide-ubiquitin linkage to avoid the selection of clones that recognize the non-native bond (**Figures 2**, **4**). A specific signal in the ELISA test is a requirement for a specific antibody but it does not guarantee that an antibody will be effective. An example of different ELISA results is shown in **Figure 5**. In our experience, not all ELISA-positive clones recognized the target in subsequent validation assays. This highlights the importance of validation assays using native substrates.

Validation of the Antibody

Validation of antibodies is critical but it has often been overlooked. Fortunately, there are many recent initiatives to improve the guidelines for quality control and thereby the value of the antibodies and the results that are generated with them (Egelhofer et al., 2010; Älgenäs et al., 2014; Bradbury and Plückthun, 2015; Kungulovski et al., 2015; Marcon et al., 2015; Rothbart et al., 2015; Uhlen et al., 2016; Guillemette et al., 2017; Edfors et al., 2018; Venkataraman et al., 2018; Weller, 2018; Marx, 2019). Validation of site-specific Ub-antibodies is very important given the abundance of ubiquitin modifications in the cell and the complexity of the epitope. Here we describe several examples of quality control experiments for site-specific Ub-antibodies. During the initial screening and validation tests, only a small amount of antibody is typically available, limiting the number of experiments that can be performed. On selected clones that give a positive and specific response by ELISA, immunoblots can be performed as a secondary screening to identify those antibodies that recognize the full-length ubiquitin conjugate but in a denatured form. Based on the combined screening results, clones are selected for expansion and purification of secreted immunoglobulins, as described above. It is also useful to consider the immunoglobulin class and subclass in the context of the downstream applications of the antibodies. If the peptides are synthesized with a biotin-moiety, this allows for using the conjugates in assays such as Surface Plasmon Resonance (SPR) to determine the binding properties of the antibodies in more detail.

A convenient method for validation of purified antibodies is the analysis of the full-length modified proteins by immunoblot.

Here we show two examples, taking advantage of different sets of reagents. **Figure 5** summarizes the screening and validation results of the yH2B-K123ub antibody. Yeast strains, antibodies and protocols to detect H2BK123ub1 by immunoblot assays have been described previously (Vlaming et al., 2016, 2019; van Welsem et al., 2018). In the ELISA screens, clones were identified that produced antibodies recognizing H2B-K123ub1 and not recognizing unmodified H2B or free Ub. We also observed clones that recognized Ub non-specifically (**Figures 5A,E** and see below), one of which we selected for expansion and antibody production. The clones with site-specific signals in ELISA (e.g., see **Figure 5A**) were examined on immunoblots with yeast strains in which yH2B-K123ub was wild-type, absent, increased, and shifted by the addition of a short epitope tag on H2B (**Figures 5B–F**). When using cell extracts, this has the added benefit that non-specific reactions to other cellular—ubiquitinated–proteins can be identified. Together, the signals observed in this panel of strains demonstrated the specificity of the antibody for yH2B-K123ub in yeast. Importantly, the specificity was subsequently confirmed by chromatin-immunoprecipitation assays, which demonstrated loss of signal in strains lacking yH2B-K123ub and gain of signal in strains with excess of it (van Welsem et al., 2018; Vlaming et al., 2019). Of note, injection of the yH2B-K123ub conjugate in rabbits resulted in a strong polyclonal response including non-specific antibodies against H2B and Ub (e.g., see **Figure 5F**), highlighting the need for selecting monoclonal antibodies. This is in contrast with antibodies against smaller modifications such as methylation, phosphorylation, or acetylation, for which specific polyclonal antisera have been successfully developed.

While cell extracts provide a powerful system to determine antibody specificity, it is not always straightforward or even possible to modulate the levels of the site-specific ubiquitination in cells, for example due to redundant enzyme activities, compensating ubiquitination and deubiquitination activities, fitness defects due to ubiquitination changes, or insufficient knowledge of the enzymes involved. However, in some cases the epitope in cells can be abolished by mutation of the target lysine to arginine, as we previously demonstrated for PCNA-K164 (Krijger et al., 2011). Another limitation is that for some sites, the endogenous, cellular levels may be too low to allow for detection during the screening and validation without an enrichment procedure. A powerful alternative to using cell extracts is the use of recombinant proteins and installing the ubiquitination with chemical and/or enzymatic methods. **Figures 6A–F** summarizes the results of the screening and validation phase of an antibody against ubiquitinated lysine 164 on human PCNA (PCNA-K164ub). Clones recognizing the PCNA-K164ub1 and not recognizing unmodified PCNA peptide or free Ub in ELISA were examined on immunoblots using recombinant proteins (**Figures 6A–F**). Recombinant human PCNA was purified and ubiquitinated enzymatically as described previously (Hibbert and Sixma, 2012). Recombinant nucleosomes enzymatically ubiquitinated at histone H2A-K13/15 by RNF168 and H2A-K125/127129 by BRCA1-BARD1 (Zhu et al., 2011; Mattiroli et al., 2012, 2014; Kalb et al., 2014; Uckelmann et al., 2018; Dharadhar et al., 2019; Horn et al., 2019) were included as controls (**Figures 6A–C**). Among the analyzed clones we observed antibodies recognizing PCNA and Ub alone. We also identified antibodies recognizing PCNA-K164ub1 but not unmodified full-length PCNA or Ub (**Figure 6D**). However, the selected clones appeared not to be site-specific because enzymatically ubiquitinated histone H2A on lysine 13/15 or 125/127/129 was also detected (**Figure 6D**). These results suggest that the selected clone produces antibodies recognizing the ubiquitinated lysine in PCNA but not specifically in the context of PCNA. Indeed, in cellular extracts, these antibodies detected a range of proteins, further indicating the lack of specificity for PCNA (**Figure 6G**). Therefore, when using recombinant proteins for validation, it is important to include independent ubiquitinated proteins in the analysis. It may also be beneficial to include independent peptide-Ub conjugates in the ELISA screens for selection and monitoring of hybridoma clones. Antibodies recognizing lysine-Ub conjugates provide powerful reagents for detecting poly- and mono-ubiquitinated proteins in cells and for affinity purification (Fujimuro and Yokosawa, 2005; Fulzele and Bennett, 2018; van Wijk et al., 2019). The clones we describe here potentially expand the toolbox for detecting protein ubiquitination but it will be important to determine their binding properties to the different types of linkages in more detail (Fujimuro et al., 1994; Newton et al., 2008, 2012; Matsumoto et al., 2010, 2012), and to do so in the assays of interest and not just on immunoblots.

DISCUSSION

Whereas polyclonal antibodies can specifically recognize sites carrying small post-translational modifications, a polyclonal response against ubiquitinated targets will lead to a mix of antibodies recognizing the ubiquitinated site, the unmodified peptide, any ubiquitinated lysine, and ubiquitin alone, as we experienced in yH2B-K123ub1 and PCNA-K164ub1 antibody screens. Therefore, the generation of site-specific ubiquitin antibodies will typically require the development of monoclonal antibodies. The antibodies we describe here were generated in mice. It has recently become possible and more popular to develop monoclonal antibodies in rabbits using different technologies (Weber et al., 2017). Since rabbits have highly distinctive antibody repertoires, this may offer powerful additional opportunities. Another powerful alternative is the generation of single-chain antibodies or nanobodies in llamas. Nanobodies recognizing linear and conformational epitopes can be obtained, which may be of special relevance for ubiquitinated conjugates (https://instruct-eric.eu/platform/nanobody-discovery). The synthesis of Ub-peptide conjugates and the suggestions for design and validation experiments are also applicable to rabbit monoclonals and nanobodies. However, with larger animals, more antigen is typically needed for immunization. Using automated linear solid phase peptide synthesis and the chemical synthesis ligation technologies described, we are able to fully synthesize site-selective ubiquitinated peptides in a native conformation as well as proteolytically stable non-hydrolyzable derivates. This synthetic approach enables the

specific incorporation of desired tags, labels, and mutations in high yields with high purities. Access to these well-defined ubiquitinated peptides, is of utmost importance in these types of studies.

The complexity and size of the site-specific ubiquitination epitope also means that stringent screening and validation strategies are required for the selection of appropriate antibodies. Initial screening of hybridoma clones is typically performed by ELISA. Recent advances in next generation sequencing offer powerful alternative strategies for antibody selection by identifying the genes encoding the antibody of interest. These methods are based on identifying clones dominating the total plasma cell repertoire following secondary immunization (Haessler and Reddy, 2014; Parola et al., 2018). However, when immunizations are performed with ubiquitinated peptides, the expanding clones will represent antibodies against peptide, ubiquitin, and non-specific lysine-ubiquitin conjugates and only a minority of the clones will produce site-specific antibodies (e.g., see **Figures 5**, **6**). Therefore, more targeted screening methods are still required when complex antigens are used and when site-specific ubiquitin antibodies are wanted. Validation of the antibodies by immunoblot analysis, as we describe in **Figures 5**, **6**, provides a convenient way of validating the specificity and sensitivity of the antibody. This is especially useful during the early stages of validation, when limiting amounts of antibody are available from the culture supernatants of the clones. However, this assay does not predict how well the antibody will work for other applications. Similarly, a specific signal on immunoblots does not guarantee that the antibody is specific in other assays. Therefore, once the antibody has been produced at larger scales, it should always be carefully tested in the application of interest. Validation assays, whether using cells or recombinant proteins, should include several critical negative controls, including the non-modified protein, free ubiquitin, and independent ubiquitinated proteins. Fortunately, the expanding tool sets for genome editing and *in vitro* ubiquitination allow for the generation of many powerful control settings for future antibody development. With regard to ubiquitination sites on chromatin, one protein of special interest is histone H2A or the histone variant H2AX (Mattiroli and Sixma, 2014; Du et al., 2019; Marsh and Dickson, 2019). H2A is ubiquitinated at several sites by specific enzyme complexes and each with a specific role in DNA damage response, DNA repair, and gene silencing (Mattiroli and Sixma, 2014; Marsh and Dickson, 2019). We hope that our protocols will be of use for others in the community to develop novel site-specific antibodies against these and other important epitopes.

DATA AVAILABILITY STATEMENT

All datasets generated for this study are included in the article/supplementary material.

ETHICS STATEMENT

Immunization of animals, monitoring the immune response and antibody production of selected clones by ELISA, production of hybridomas, and subcloning and isolation of specific hybridomas is frequently outsourced to a third party specialized in antibody development using proprietary protocols. All hybridomas described in this study were delivered by ThermoFisher Scientific (Life Technologies). All animals used by Thermo Scientific are assured by the Office of Laboratory Animal Welfare. Upon request additional accreditations can be provided.

AUTHOR CONTRIBUTIONS

IK, MM, FE, HO, and FL contributed conception and design of the study. IK and TW performed quality control experiments and coordinated the studies. MM was responsible for chemical synthesis. MU generated recombinant proteins. JW purified monoclonal antibodies. AS performed quality control experiments under supervision of HJ. IK, MM, FE, HO, and FL wrote sections of the manuscript. All authors contributed to manuscript revision, read and approved the submitted version.

FUNDING

This work was supported by grants from the Netherlands Organisation for Scientific Research (NWO); NWO-VICI-016.130.627, NWO-NCI-KIEM 731.013.102, NWO-NCI-LIFT-731.015.405 to FL. The funders had no role in study design, data collection and analysis, decision to publish, or preparation of the manuscript. The UvA-AMC provides support for open access publication.

ACKNOWLEDGMENTS

The authors thank Alfred Nijkerk (UbiQ) for advice, Dris el Atmioui and Cami Talavera for their assistance with solid-phase peptide synthesis, Patrick Celie (Netherlands Cancer Institute, Protein Production Facility) for support in generating recombinant protein reagents, and Matilda Ayidah for help with UV irradiation and western blotting. We thank Titia Sixma for advice and valuable suggestions.

REFERENCES

Älgenäs, C., Agaton, C., Fagerberg, L., Asplund, A., Björling, L., Björling, E., et al. (2014). Antibody performance in western blot applications is context-dependent. *Biotechnol J.* 9, 435–445. doi: 10.1002/biot.201300341

Bradbury, A., and Plückthun, A. (2015). Reproducibility: standardize antibodies used in research. *Nature* 518, 27–29. doi: 10.1038/518027a

Chen, F. M., Naeve, G. S., and Epstein, A. L. (1988). Comparison of mono Q, superose-6, and ABx fast protein liquid chromatography for the purification of IgM monoclonal antibodies. *J. Chromatogr.* 444, 153–164. doi: 10.1016/S0021-9673(01)94018-X

Chen, Z. J., and Sun, L. J. (2009). Nonproteolytic functions of ubiquitin in cell signaling. *Mol. Cell* 33, 275–286. doi: 10.1016/j.molcel.2009.01.014

Claessen, J. H., Kundrat, L., and Ploegh, H. L. (2012). Protein quality control in the ER: balancing the ubiquitin checkbook. *Trends Cell Biol.* 22, 22–32. doi: 10.1016/j.tcb.2011.09.010

Clague, M. J., Urbe, S., and Komander, D. (2019). Breaking the chains: deubiquitylating enzyme specificity begets function. *Nat. Rev. Mol. Cell. Biol.* 20, 338–352. doi: 10.1038/s41580-019-0099-1

Cole, A. J., Clifton-Bligh, R. J., and Marsh, D. J. (2015). Histone H2B monoubiquitination: roles to play in human malignancy. *Endocr. Relat. Cancer* 22, T19–T33. doi: 10.1530/ERC-14-0185

Dharadhar, S., Kim, R. Q., Uckelmann, M., and Sixma, T. K. (2019). Quantitative analysis of USP activity *in vitro*. *Methods Enzymol.* 618, 281–319. doi: 10.1016/bs.mie.2018.12.023

Dresselhaus, T., Weikart, N. D., Mootz, H. D., and Waller, M. P. (2013). Naturally and synthetically linked lys48 diubiquitin: a QM/MM study. *RSC Adv.* 3, 16122–16129. doi: 10.1039/c3ra42649a

Du, C., Hansen, L. J., Singh, S. X., Wang, F., Sun, R., Moure, C. J., et al. (2019). A PRMT5-RNF168-SMURF2 axis controls H2AX proteostasis. *Cell Rep.* 28, 3199–3211.e5. doi: 10.1016/j.celrep.2019.08.031

Edfors, F., Hober, A., Linderbäck, K., Maddalo, G., Azimi, A., Sivertsson, Å., et al. (2018). Enhanced validation of antibodies for research applications. *Nat. Comm.* 9:4130. doi: 10.1038/s41467-018-06642-y

Egelhofer, T. A., Minoda, A., Klugman, S., Lee, K., Kolasinska-Zwierz, P., Alekseyenko, A. A., et al. (2010). An assessment of histone-modification antibody quality. *Nat. Struct. Mol. Biol.* 18, 91–93. doi: 10.1038/nsmb.1972

El Oualid, F., Merkx, R., Ekkebus, R., Hameed, D. S., Smit, J. J., de Jong, A., et al. (2010). Chemical synthesis of ubiquitin, ubiquitin-based probes, and diubiquitin. *Angew. Chem. Int. Ed. Engl.* 49, 10149–10153. doi: 10.1002/anie.201005995

Flierman, D., van der Heden van Noort, G. J., Ekkebus, R., Geurink, P. P., Mevissen, T. E., Hospenthal, M. K., et al. (2016). Non-hydrolyzable diubiquitin probes reveal linkage-specific reactivity of deubiquitylating enzymes mediated by S2 pockets. *Cell Chem. Biol.* 23, 472–482. doi: 10.1016/j.chembiol.2016.03.009

Fuchs, G., and Oren, M. (2014). Writing and reading H2B monoubiquitylation. *Biochim. Biophys. Acta* 1839, 694–701. doi: 10.1016/j.bbagrm.2014.01.002

Fujimuro, M., Sawada, H., and Yokosawa, H. (1994). Production and characterization of monoclonal antibodies specific to multi-ubiquitin chains of polyubiquitinated proteins. *FEBS Lett.* 349, 173–180. doi: 10.1016/0014-5793(94)00647-4

Fujimuro, M., and Yokosawa, H. (2005). Production of antipolyubiquitin monoclonal antibodies and their use for characterization and isolation of polyubiquitinated proteins. *Methods Enzymol.* 399, 75–86. doi: 10.1016/S0076-6879(05)99006-X

Fulzele, A., and Bennett, E. J. (2018). Ubiquitin diGLY proteomics as an approach to identify and quantify the ubiquitin-modified proteome. *Methods Mol. Biol.* 1844, 363–384. doi: 10.1007/978-1-4939-8706-1_23

Geng, F., Wenzel, S., and Tansey, W. P. (2012). Ubiquitin and proteasomes in transcription. *Annu. Rev. Biochem.* 81, 177–201. doi: 10.1146/annurev-biochem-052110-120012

Greenfield, E. A. (2014). *Antibodies: A Laboratory Manual, 2nd Edn*. Cold Spring Harbor, NY: Cold Spring Harbor Laboratory Press.

Guillemette, B., Hammond-Martel, I., Wurtele, H., and Verreault, A. (2017). Production and purification of antibodies against histone modifications. *Methods Mol. Biol.* 1528, 149–164. doi: 10.1007/978-1-4939-6630-1_9

Haessler, U., and Reddy, S. T. (2014). Using next-generation sequencing for discovery of high-frequency monoclonal antibodies in the variable gene repertoires from immunized mice. *Methods Mol. Biol.* 1131, 191–203. doi: 10.1007/978-1-62703-992-5_12

Hibbert, R. G., and Sixma, T. K. (2012). Intrinsic flexibility of ubiquitin on proliferating cell nuclear antigen (PCNA) in translesion synthesis. *J. Biol. Chem.* 287, 39216–39223. doi: 10.1074/jbc.M112.389890

Hoege, C., Pfander, B., Moldovan, G. L., Pyrowolakis, G., and Jentsch, S. (2002). RAD6-dependent DNA repair is linked to modification of PCNA by ubiquitin and SUMO. *Nature* 419, 135–141. doi: 10.1038/nature00991

Holzlöhner, P., and Hanack, K. (2017). Generation of murine monoclonal antibodies by hybridoma technology. *J. Vis. Exp.* doi: 10.3791/54832

Horn, V., Uckelmann, M., Zhang, H., Eerland, J., Aarsman, I., le Paige, U. B., et al. (2019). Structural basis of specific H2A K13/K15 ubiquitination by RNF168. *Nat. Commun.* 10:1751. doi: 10.1038/s41467-019-09756-z

Husnjak, K., and Dikic, I. (2012). Ubiquitin-binding proteins: decoders of ubiquitin-mediated cellular functions. *Annu. Rev. Biochem.* 81, 291–322. doi: 10.1146/annurev-biochem-051810-094654

Kalb, R., Mallery, D. L., Larkin, C., Huang, J. T. J., and Hiom, K. (2014). BRCA1 is a histone-H2A-specific ubiquitin ligase. *Cell Rep.* 8, 999–1005. doi: 10.1016/j.celrep.2014.07.025

Kanao, R., and Masutani, C. (2017). Regulation of DNA damage tolerance in mammalian cells by post-translational modifications of PCNA. *Mutat. Res.* 803–805, 82–88. doi: 10.1016/j.mrfmmm.2017.06.004

Komander, D., and Rape, M. (2012). The ubiquitin code. *Annu. Rev. Biochem.* 81, 203–229. doi: 10.1146/annurev-biochem-060310-170328

Krijger, P. H., van den Berk, P. C., Wit, N., Langerak, P., Jansen, J. G., Reynaud, C. A., et al. (2011). PCNA ubiquitination-independent activation of polymerase eta during somatic hypermutation and DNA damage tolerance. *DNA Repair* 10, 1051–1059. doi: 10.1016/j.dnarep.2011.08.005

Kungulovski, G., Mauser, R., and Jeltsch, A. (2015). Affinity reagents for studying histone modifications & guidelines for their quality control. *Epigenomics* 7, 1185–1196. doi: 10.2217/epi.15.59

Mailand, N., Gibbs-Seymour, I., and Bekker-Jensen, S. (2013). Regulation of PCNA-protein interactions for genome stability. *Nat. Rev. Mol. Cell. Biol.* 14, 269–282. doi: 10.1038/nrm3562

Marcon, E., Jain, H., Bhattacharya, A., Guo, H., Phanse, S., Pu, S., et al. (2015). Assessment of a method to characterize antibody selectivity and specificity for use in immunoprecipitation. *Nat. Methods* 12, 725–731. doi: 10.1038/nmeth.3472

Marsh, D. J., and Dickson, K. A. (2019). Writing histone monoubiquitination in human malignancy-the role of RING finger E3 ubiquitin ligases. *Genes* 10, E67. doi: 10.3390/genes10010067

Marteijn, J. A., Lans, H., Vermeulen, W., and Hoeijmakers, J. H. (2014). Understanding nucleotide excision repair and its roles in cancer and ageing. *Nat. Rev. Mol. Cell. Biol.* 15, 465–481. doi: 10.1038/nrm3822

Marx, V. (2019). What to do about those immunoprecipitation blues. *Nat. Methods* 16, 289–292. doi: 10.1038/s41592-019-0365-3

Matsumoto, M. L., Dong, K. C., Yu, C., Phu, L., Gao, X., Hannoush, R. N., et al. (2012). Engineering and structural characterization of a linear polyubiquitin-specific antibody. *J. Mol. Biol.* 418, 134–144. doi: 10.1016/j.jmb.2011.12.053

Matsumoto, M. L., Wickliffe, K. E., Dong, K. C., Yu, C., Bosanac, I., Bustos, D., et al. (2010). K11-linked polyubiquitination in cell cycle control revealed by a K11 linkage-specific antibody. *Mol. Cell* 39, 477–484. doi: 10.1016/j.molcel.2010.07.001

Mattern, M., Sutherland, J., Kadimisetty, K., Barrio, R., and Rodriguez, M. S. (2019). Using ubiquitin binders to decipher the ubiquitin code. *Trends Biochem. Sci.* 44, 599–615. doi: 10.1016/j.tibs.2019.01.011

Mattiroli, F., and Sixma, T. K. (2014). Lysine-targeting specificity in ubiquitin and ubiquitin-like modification pathways. *Nat. Struct. Mol. Biol.* 21, 308–316. doi: 10.1038/nsmb.2792

Mattiroli, F., Uckelmann, M., Sahtoe, D. D., van Dijk, W. J., and Sixma, T. K. (2014). The nucleosome acidic patch plays a critical role in RNF168-dependent ubiquitination of histone H2A. *Nat. Commun.* 5:3291. doi: 10.1038/ncomms4692

Mattiroli, F., Vissers, J. H., van Dijk, W. J., Ikpa, P., Citterio, E., Vermeulen, W., et al. (2012). RNF168 ubiquitinates K13-15 on H2A/H2AX to drive DNA damage signaling. *Cell* 150, 1182–1195. doi: 10.1016/j.cell.2012.08.005

McGouran, J. F., Gaertner, S. R., Altun, M., Kramer, H. B., and Kessler, B. M. (2013). Deubiquitinating enzyme specificity for ubiquitin chain topology profiled by di-ubiquitin activity probes. *Chem. Biol.* 20, 1447–1455. doi: 10.1016/j.chembiol.2013.10.012

Morgan, M. T., and Wolberger, C. (2017). Recognition of ubiquitinated nucleosomes. *Curr. Opin. Struct. Biol.* 42, 75–82. doi: 10.1016/j.sbi.2016.11.016

Mulder, M. P., El Oualid, F., ter Beek, J., and Ovaa, H. (2014). A native chemical ligation handle that enables the synthesis of advanced activity-based probes: diubiquitin as a case study. *Chembiochem* 15, 946–949. doi: 10.1002/cbic.201402012

Newton, K., Matsumoto, M. L., Ferrando, R. E., Wickliffe, K. E., Rape, M., Kelley, R. F., et al. (2012). Using linkage-specific monoclonal antibodies

to analyze cellular ubiquitylation. *Methods Mol. Biol.* 832, 185–196. doi: 10.1007/978-1-61779-474-2_13

Newton, K., Matsumoto, M. L., Wertz, I. E., Kirkpatrick, D. S., Lill, J. R., Tan, J., et al. (2008). Ubiquitin chain editing revealed by polyubiquitin linkage-specific antibodies. *Cell* 134, 668–678. doi: 10.1016/j.cell.2008.07.039

Oh, E., Akopian, D., and Rape, M. (2018). Principles of ubiquitin-dependent signaling. *Annu. Rev. Cell. Dev. Biol.* 34, 137–162. doi: 10.1146/annurev-cellbio-100617-062802

Ossipow, V., and Fischer, N. (eds.). (2014). "Monoclonal antibodies: methods and protocols," in *Methods in Molecular Biology, 2nd Edn*, Vol. 1131 (Totowa, NJ: Humana Press), 1–575.

Parola, C., Neumeier, D., and Reddy, S. T. (2018). Integrating high-throughput screening and sequencing for monoclonal antibody discovery and engineering. *Immunology* 153, 31–41. doi: 10.1111/imm.12838

Piro, A. S., Mayekar, M. K., Warner, M. H., Davis, C. P., and Arndt, K. M. (2012). Small region of Rtf1 protein can substitute for complete Paf1 complex in facilitating global histone H2B ubiquitylation in yeast. *Proc. Natl. Acad. Sci. U.S.A.* 109, 10837–10842. doi: 10.1073/pnas.1116994109

Ramanathan, H. N., and Ye, Y. (2012). Cellular strategies for making monoubiquitin signals. *Crit. Rev. Biochem. Mol. Biol.* 47, 17–28. doi: 10.3109/10409238.2011.620943

Ranjitkar, P., Press, M. O., Yi, X., Baker, R., MacCoss, M. J., and Biggins, S. (2010). An E3 ubiquitin ligase prevents ectopic localization of the centromeric histone H3 variant via the centromere targeting domain. *Mol. Cell* 40, 455–464. doi: 10.1016/j.molcel.2010.09.025

Rape, M. (2018). Ubiquitylation at the crossroads of development and disease. *Nat. Rev. Mol. Cell. Biol.* 19, 59–70. doi: 10.1038/nrm.2017.83

Rosenbaum, J. C., Fredrickson, E. K., Oeser, M. L., Garrett-Engele, C. M., Locke, M. N., Richardson, L. A., et al. (2011). Disorder targets misorder in nuclear quality control degradation: a disordered ubiquitin ligase directly recognizes its misfolded substrates. *Mol. Cell* 41, 93–106. doi: 10.1016/j.molcel.2010.12.004

Ross, A. H., Herlyn, D., and Koprowski, H. (1987). Purification of monoclonal antibodies from ascites using ABx liquid chromatography column. *J. Immunol. Methods* 102, 227–231. doi: 10.1016/0022-1759(87)90081-0

Rothbart, S. B., Dickson, B. M., Raab, J. R., Grzybowski, A. T., Krajewski, K., Guo, A. H., et al. (2015). An interactive database for the assessment of histone antibody specificity. *Mol. Cell* 59, 502–511. doi: 10.1016/j.molcel.2015.06.022

Spit, M., Rieser, E., and Walczak, H. (2019). Linear ubiquitination at a glance. *J. Cell Sci.* 132:jcs208512. doi: 10.1242/jcs.208512

Uckelmann, M., Densham, R. M., Baas, R., Winterwerp, H. H. K., Fish, A., Sixma, T. K., et al. (2018). USP48 restrains resection by site-specific cleavage of the BRCA1 ubiquitin mark from H2A. *Nat. Commun.* 9:229. doi: 10.1038/s41467-017-02653-3

Uckelmann, M., and Sixma, T. K. (2017). Histone ubiquitination in the DNA damage response. *DNA Repair* 56, 92–101. doi: 10.1016/j.dnarep.2017.06.011

Uhlen, M., Bandrowski, A., Carr, S., Edwards, A., Ellenberg, J., Lundberg, E., et al. (2016). A proposal for validation of antibodies. *Nat. Methods* 13, 823–827. doi: 10.1038/nmeth.3995

van Cuijk, L., Vermeulen, W., and Marteijn, J. A. (2014). Ubiquitin at work: the ubiquitous regulation of the damage recognition step of NER. *Exp. Cell Res.* 329, 101–109. doi: 10.1016/j.yexcr.2014.07.018

van Welsem, T., Korthout, T., Ekkebus, R., Morais, D., Molenaar, T. M., van Harten, K., et al. (2018). Dot1 promotes H2B ubiquitination by a methyltransferase-independent mechanism. *Nucl. Acids Res.* 46, 11251–11261. doi: 10.1093/nar/gky801

van Wijk, S. J., Fulda, S., Dikic, I., and Heilemann, M. (2019). Visualizing ubiquitination in mammalian cells. *EMBO Rep.* 20:e46520. doi: 10.15252/embr.201846520

Varshavsky, A. (2012). The ubiquitin system, an immense realm. *Annu. Rev. Biochem.* 81, 167–176.doi: 10.1146/annurev-biochem-051910-094049

Venkataraman, A., Yang, K., Irizarry, J., Mackiewicz, M., Mita, P., Kuang, Z., et al. (2018). A toolbox of immunoprecipitation-grade monoclonal antibodies to human transcription factors. *Nat. Methods* 15, 330–338. doi: 10.1038/nmeth.4632

Venkatesh, S., and Workman, J. L. (2015). Histone exchange, chromatin structure and the regulation of transcription. *Nat. Rev. Mol. Cell. Biol.* 16, 178–189. doi: 10.1038/nrm3941

Vlaming, H., McLean, C., Korthout, T., Alemdehy, M. F., Hendriks, S., Lancini, C., et al. (2019). Conserved crosstalk between histone deacetylation and H3K79 methylation generates DOT1L-dose dependency in HDAC1-deficient thymic lymphoma. *EMBO J.* 38:e101564. doi: 10.15252/embj.2019101564

Vlaming, H., Molenaar, T. M., van Welsem, T., Poramba-Liyanage, D. W., Smith, D. E., Velds, A., et al. (2016). Direct screening for chromatin status on DNA barcodes in yeast delineates the regulome of H3K79 methylation by Dot1. *Elife* 5:e18919. doi: 10.7554/eLife.18919

Vlaming, H., van Welsem, T., de Graaf, E. L., Ontoso, D., Altelaar, A. M., San-Segundo, P. A., et al. (2014). Flexibility in crosstalk between H2B ubiquitination and H3 methylation *in vivo*. *EMBO Rep.* 15, 1077–1084. doi: 10.15252/embr.201438793

Weber, J., Peng, H., and Rader, C. (2017). From rabbit antibody repertoires to rabbit monoclonal antibodies. *Exp Mol Med.* 49:e305. doi: 10.1038/emm.2017.23

Weikart, N. D., Sommer, S., and Mootz, H. D. (2012). Click synthesis of ubiquitin dimer analogs to interrogate linkage-specific UBA domain binding. *Chem. Commun.* 48, 296–298. doi: 10.1039/C1CC15834A

Weller, M. G. (2018). Ten basic rules of antibody validation. *Anal. Chem. Insights* 13:1177390118757462. doi: 10.1177/1177390118757462

Worden, E. J., and Wolberger, C. (2019). Activation and regulation of H2B-Ubiquitin-dependent histone methyltransferases. *Curr. Opin. Struct. Biol.* 59, 98–106. doi: 10.1016/j.sbi.2019.05.009

Yokoyama, W. M., Christensen, M., Santos, G. D., Miller, D., Ho, J., Wu, T., et al. (2013). Production of monoclonal antibodies. *Curr. Protoc. Immunol.* 102:Unit 2.5. doi: 10.1002/0471142735.im0205s102

Zhao, Y., Brickner, J. R., Majid, M. C., and Mosammaparast, N. (2014). Crosstalk between ubiquitin and other post-translational modifications on chromatin during double-strand break repair. *Trends Cell Biol.* 24, 426–434. doi: 10.1016/j.tcb.2014.01.005

Zhou, Z., and Fahrni, C. J. (2004). A fluorogenic probe for the copper(I)-catalyzed azide-alkyne ligation reaction: modulation of the fluorescence emission via 3(n,pi)-1(pi,pi) inversion. *J. Am. Chem. Soc.* 126, 8862–8863. doi: 10.1021/ja049684r

Zhu, Q., Pao, G. M., Huynh, A. M., Suh, H., Tonnu, N., Nederlof, P. M., et al. (2011). BRCA1 tumour suppression occurs via heterochromatin-mediated silencing. *Nature* 477, 179–184. doi: 10.1038/nature10371

Conflict of Interest: FL, HO, and FE are entitled to royalties resulting from antibody licensing. FE and HO declare competing financial interests as co-founders and shareholders of UbiQ Bio BV.

The remaining authors declare that the research was conducted in the absence of any commercial or financial relationships that could be construed as a potential conflict of interest.

frontiers in Molecular Biosciences

REVIEW
published: 27 February 2020
doi: 10.3389/fmolb.2020.00021

Resolving the Complexity of Ubiquitin Networks

Katarzyna Kliza†* and *Koraljka Husnjak**

Institute of Biochemistry II, Medical Faculty, Goethe University, Frankfurt, Germany

Ubiquitination regulates nearly all cellular processes by coordinated activity of ubiquitin writers (E1, E2, and E3 enzymes), erasers (deubiquitinating enzymes) and readers (proteins that recognize ubiquitinated proteins by their ubiquitin-binding domains). By differentially modifying cellular proteome and by recognizing these ubiquitin modifications, ubiquitination machinery tightly regulates execution of specific cellular events in space and time. Dynamic and complex ubiquitin architecture, ranging from monoubiquitination, multiple monoubiquitination, eight different modes of homotypic and numerous types of heterogeneous polyubiquitin linkages, enables highly dynamic and complex regulation of cellular processes. We discuss available tools and approaches to study ubiquitin networks, including methods for the identification and quantification of ubiquitin-modified substrates, as well as approaches to quantify the length, abundance, linkage type and architecture of different ubiquitin chains. Furthermore, we also summarize the available approaches for the discovery of novel ubiquitin readers and ubiquitin-binding domains, as well as approaches to monitor and visualize activity of ubiquitin conjugation and deconjugation machineries. We also discuss benefits, drawbacks and limitations of available techniques, as well as what is still needed for detailed spatiotemporal dissection of cellular ubiquitination networks.

Keywords: ubiquitin, ubiquitin receptor, affinity purification, mass spectrometry, E3 ligase, deubiquitinating enzyme

OPEN ACCESS

Edited by:
Monique P. C. Mulder,
Leiden University Medical Center, Netherlands

Reviewed by:
Jun Yin,
Georgia State University, United States
Robert Layfield,
University of Nottingham, United Kingdom

***Correspondence:**
Katarzyna Kliza
K.Kliza@science.ru.nl
Koraljka Husnjak
K.Husnjak@biochem2.uni-frankfurt.de

†Present address:
Katarzyna Kliza,
Department of Molecular Biology, Faculty of Science, Radboud Institute for Molecular Life Sciences, Oncode Institute, Radboud University Nijmegen, Nijmegen, Netherlands

Specialty section:
This article was submitted to Cellular Biochemistry, a section of the journal Frontiers in Molecular Biosciences

Received: *22 October 2019*
Accepted: *04 February 2020*
Published: *27 February 2020*

Citation:
Kliza K and Husnjak K (2020) Resolving the Complexity of Ubiquitin Networks. Front. Mol. Biosci. 7:21. doi: 10.3389/fmolb.2020.00021

INTRODUCTION

Post-translational modifications (PTMs) greatly increase the complexity and functional diversity of the proteome, ensuring rapid and dynamic cellular responses to the environmental and intracellular factors (Walsh et al., 2005). Extensive research over the last few decades has revealed elaborate control of a variety of cellular processes by a small protein ubiquitin (Ub), including cellular proteostasis, DNA repair, trafficking and immunity (Varshavsky, 2006; Kulathu and Komander, 2012).

Ub is a small, highly compact globular protein, with the exception of its unrestrained and flexible C-terminal tail (**Figure 1A**). To achieve high cellular Ub concentrations, 4 different genes (UBB, UBC, RPS27, and UBA52) encode Ub in mammals. Genes UBB and UBC encode linear fusions of 3 and 9 Ub molecules, respectively, whereas RPS27A and UBA52 encode Ub as in-frame fusion to a small and large ribosomal protein, respectively (**Figure 1B**) (Ozkaynak et al., 1984; Finley et al., 1989).

Protein modification by Ub (ubiquitination) occurs through the formation of the covalent bond between α–carboxyl group of the terminal glycine (Gly) residue of Ub and, typically, ε-amino group

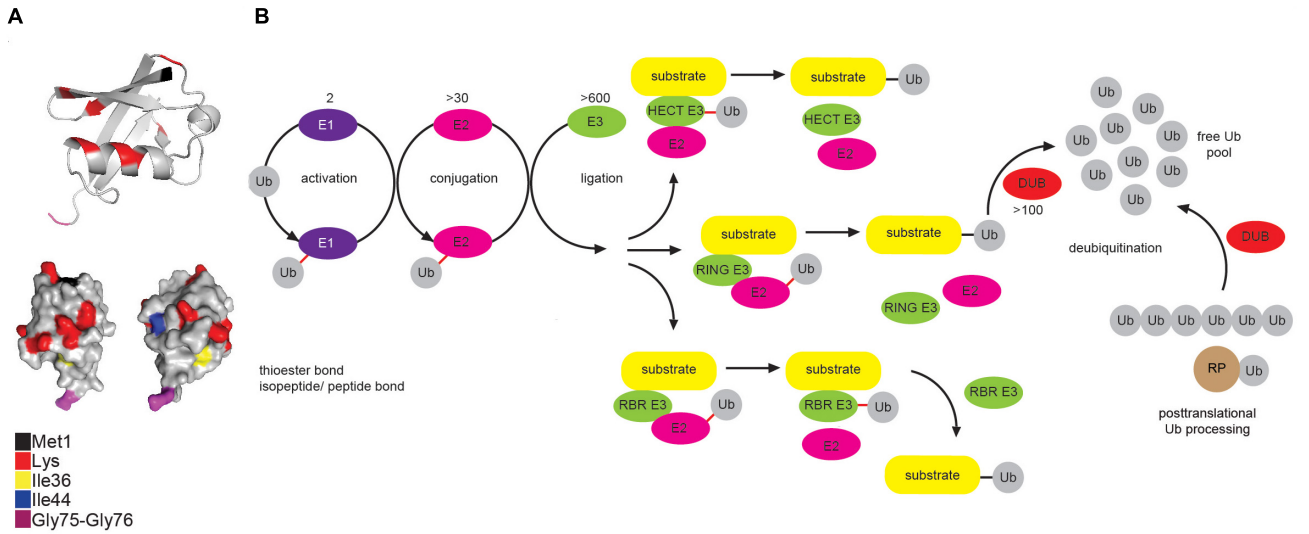

FIGURE 1 | Multicomponent enzymatic machineries assemble and disassemble ubiquitin modification. **(A)** Ub belongs to the β-grasp fold (β-GF) family (Vijay-Kumar et al., 1987), in which β-GF is formed by five-stranded β-sheet, a short 3_{10} helix and a 3.5-turn α-helix. The C-terminal Ub tail is essential for Ub conjugation and hence, for all the Ub functions. Functionally relevant Ub residues are depicted in different colors. The figure was generated from the PDB entry 1UBQ by PyMOL v1.7.6.0 software. **(B)** Coordinated activity of Ub-activating (E1), Ub-conjugating (E2), and Ub-ligating enzyme (E3) is required for Ub attachment to substrate protein. The action modes of the three main groups of E3 ligases (RING, HECT and RBR) are also depicted. In mammals, Ub is encoded by four different genes: UBA52 and RPS27A genes encode a single Ub molecule fused to the ribosomal subunits L40 and S27a, respectively (depicted as RP-Ub), UBB and UBC genes encode 2 different polyUb precursor proteins (exemplified here as Ub_6 fusion). More than 100 cellular DUBs process newly translated Ub-containing polypeptides, remove Ub from modified substrates and disassemble unanchored Ub chains.

of an internal lysine (Lys) residue of the substrate. Interestingly, some mammalian and viral E3 ligases target thiol group of cysteine (Cys) residue (Cadwell and Coscoy, 2005; Williams et al., 2007), whereas a subset of substrates, such as ataxin-3 and tau, is modified by the attachment of Ub to an α-amino group of their N-terminal residues, in a process known as N-terminal ubiquitination (Ciechanover and Ben-Saadon, 2004). Additionally, serine (Ser) and threonine (Thr) residues can also function as ubiquitination sites, forming hydroxyester bonds between Ub and target proteins (McDowell and Philpott, 2016) and thus expanding the biological importance of ubiquitination even further.

Ubiquitination is achieved by a coordinated and sequential enzymatic cascade (**Figure 1B**). Classically, Ub is activated in an ATP-dependent reaction by an Ub-activating (E1) enzyme and subsequently transferred to the active Cys residue of an Ub-conjugating (E2) enzyme, followed by Ub attachment to a substrate mediated by an Ub-ligating (E3) enzyme. Until now, two E1s, nearly 30 E2s and over 600 E3s have been identified in humans. Mechanistically, E3 ligases belong to either RING (really interesting new gene), HECT (homologous to E6-AP C terminus or RBR (RING-between-RING, hybrid RING-HECT) classes and can generate Ub linkages of different length and architecture (Metzger et al., 2012; Walden and Rittinger, 2018).

The activity of ubiquitination machinery can be reversed by more than 100 deubiquitinating enzymes (DUBs), which hydrolyze isopeptide or peptide bond resulting in Ub deconjugation from the ubiquitinated protein (**Figure 1B**) (Komander et al., 2009; Mevissen and Komander, 2017). DUBs affect cellular pool of free Ub by releasing newly synthesized Ub from Ub precursors, removing non-essential Ub molecules and recycling Ub from the former ubiquitination events (Reyes-Turcu et al., 2009; Grou et al., 2015).

Different Forms of Ubiquitin Modifications Exist in Nature

Cellular Ub modifications occur in various forms, which are usually referred to as "Ub code." Modification by a single Ub moiety (monoubiquitination) is the most abundant Ub modification that regulates DNA repair, transcription, signal transduction, viral budding, endocytosis and even proteasomal degradation (Chen and Mallampalli, 2009; Braten et al., 2016). After Ub is transferred to the ε-amino group of a target Lys, any of the eight amino groups of Ub (Met1, Lys6, Lys11, Lys27, Lys29, Lys33, Lys48, Lys63) can be attached to the C terminus of another Ub to form Ub chain of variable length, linkage type and configuration (homo- and heterotypic/branched Ub chains). Even though functional significance of several Ub modifications (such as Lys48- and Lys63-linked ubiquitination) is largely known, the biological significance of other Ub modifications is still far from being fully understood (**Figure 2**). Amongst the homotypic Ub chains, Lys48-linked Ub polymers were historically first identified and are predominant among homotypic polyUb chains (Peng et al., 2003; Swatek and Komander, 2016). These Ub linkages mark proteins for proteolytic degradation, which in turn regulates signal transduction, cell division, stress response, adaptive

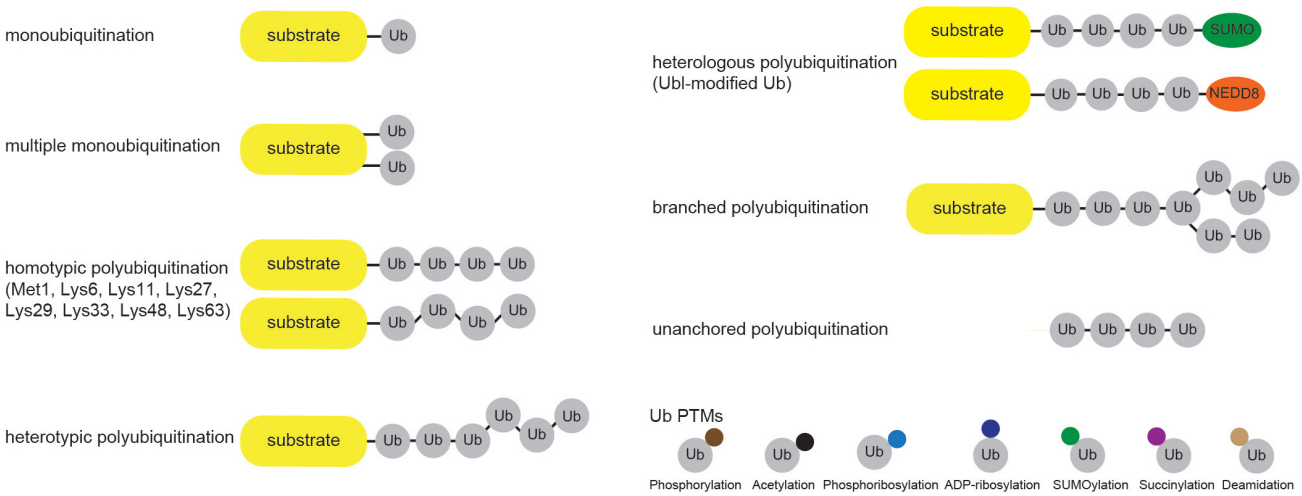

FIGURE 2 | Cellular ubiquitin modification comes in different formats. Single Ub moieties can modify proteins at one (monoubiquitination) or several (multiple monoubiquitination) Lys residues. Ub can form eight distinctive homotypic linkages, either through Met1 (linear Ub chain) or 7 internal Lys residues (Lys6-, Lys11-, Lys27-, Lys29-, Lys33-, Lys48-, and Lys63-linked Ub chains). Additional complexity is achieved through the formation of heterotypic Ub chains, which contain multiple Ub linkages and adopt mixed or branched topology. Furthermore, heterologous polymers contain additional UBLs, such as SUMO or NEDD8, within Ub chains. Ub molecules undergo various PTMs, including phosphorylation and acetylation, which regulate their binding properties and abilities to generate Ub chains.

immune system and development (Hershko and Ciechanover, 1998; Wang and Maldonado, 2006; Park et al., 2007). The remaining homotypic polyUb chains are collectively called atypical (Liu et al., 2015; Swatek and Komander, 2016), and their physiological roles are nicely summarized elsewhere (Kulathu and Komander, 2012; Akutsu et al., 2016). Branched Lys11/Lys48 and hybrid Met1/Lys63 linkages were recently implicated in proteasomal degradation and NFκB signaling, respectively (Emmerich et al., 2013; Meyer and Rape, 2014; Grice et al., 2015).

Besides by ubiquitination, Ub molecules can also be modified by acetylation, phosphorylation, ADP-ribosylation, phosphoribosylation, deamidation, SUMOylation and succinylation (**Figure 2**). Ub acetylation negatively regulates Ub chain elongation by competing with ubiquitination to regulate the stability of target proteins (Ohtake et al., 2015). By using mass spectrometry (MS) approach, Ohtake et al. (2015) identified acetylation of endogenous Ub at residues Lys6, Lys48, and Lys63. Since the same Ub residues are involved in Ub chain formation, it is not surprising that acetylation inhibits Lys11-, Lys48-, and Lys63-linked polyUb chain elongation by several E2 enzymes *in vitro*, without significantly affecting E1 and E2 charging or substrate monoubiquitination (Ohtake et al., 2015). Moreover, two of the major histones, H2A and H2B, were proposed as substrates for acetylated monoUb. Ser/Thr kinase PINK1 accumulates on depolarized mitochondria upon decrease in mitochondrial membrane potential and phosphorylates N-terminal Ub-like (UBL) domain of E3 ligase PARKIN (Kondapalli et al., 2012; Shiba-Fukushima et al., 2012; Kazlauskaite et al., 2014; Okatsu et al., 2018), as well as Ub itself (Kane et al., 2014; Koyano et al., 2014). Both modifications occur at the homologous position (Ser65) in PARKIN UBL domain and Ub. PARKIN UBL domain keeps PARKIN in autoinhibited state (Chaugule et al., 2011), and phosphorylated Ub is sufficient to allosterically activate it by unlocking its autoinhibition (Kane et al., 2014; Koyano et al., 2014; Wauer et al., 2015a). This topic was recently reviewed in great detail in Herhaus and Dikic (2015) and Swatek and Komander (2016). Interestingly, phosphorylation at Ser65 affects Ub structure, E2 discharging and formation of Ub chains by a subset of E2 and E3 enzymes, such as CDC34, UBC13/UEV1A, TRAF6 and HOIP (Wauer et al., 2015b). Some DUBs are also impaired in hydrolyzing Ser65-phosphoUb-containing chains (Wauer et al., 2015b). Even though other residues in Ub molecule have also been reported to be phosphorylated in various MS screens, the physiological significance of these modifications is not yet known.

Yang et al. (2017) have recently shown that Ub can undergo NAD^+-, E1- and E2-dependent monoADP-ribosylation. The process is catalyzed by a heterodimer of ADP-ribosyltransferase PARP9 and histone E3 ligase DTX3L. Since ADP-ribose is attached to the C-terminal Gly residue of Ub, monoADP-ribosylation of Ub prevents Ub conjugation and consequently impedes the Ub ligase activity and the function of DTX3L in non-homologous end joining (NHEJ) DNA repair pathway (Yang et al., 2017).

Many pathogens have evolved intricate mechanisms to hijack Ub system of the host, often mimicking components of the host Ub system, such as E3 ligases (Maculins et al., 2016) and DUBs (Pruneda et al., 2016). Recently discovered *Legionella pneumophila* effector SdeA utilizes unique, ATP-independent and NAD^+-dependent ubiquitination mechanism that does not involve host E1 and E2 enzymes (Qiu et al., 2016). SdeA possesses intrinsic monoADP-ribosyltransferase and phosphodiesterase activities, which enable intermediate ADP-ribosylation and subsequent phosphoribosylation of Ub Arg40 residue. SdeA subsequently mediates ubiquitination of the target protein by conjugating phosphoribosylated Ub to Ser residue of the

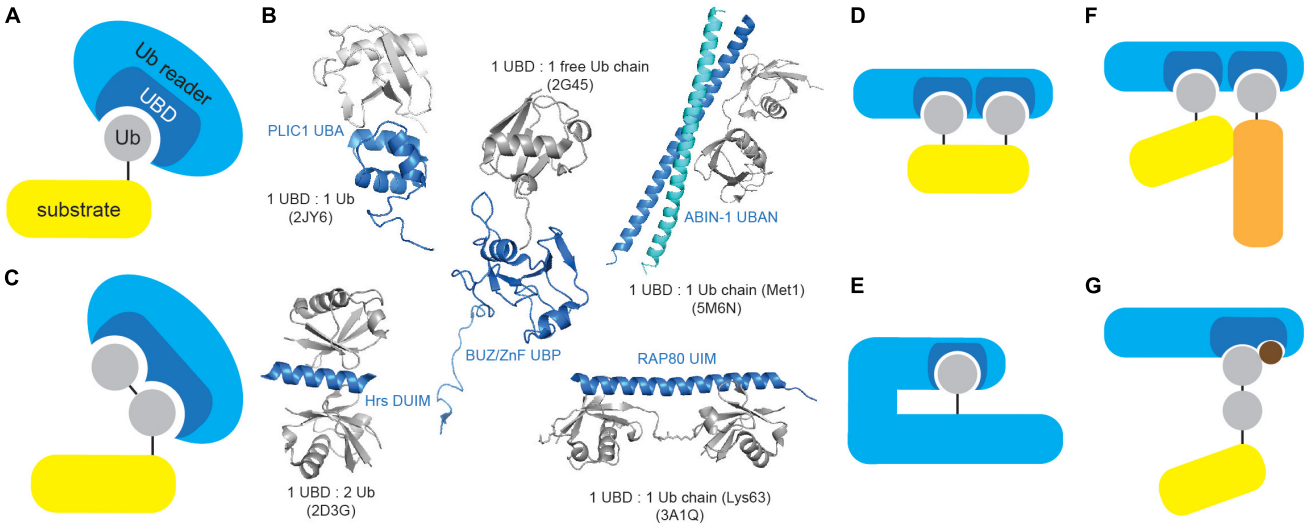

FIGURE 3 | Ubiquitin-binding domains come in different shapes and forms. **(A)** Ub receptors contain single or multiple (identical or different) motifs or domains that non-covalently bind Ub or Ub chains. **(B)** UBDs differ in shape and Ub/Ub chain specificity. Several UBDs in complex with Ub or Ub chains are depicted: PLIC1 UBA (Ub-associated, PDB code: 2JY6), Hrs DUIM (double-sided Ub-interacting motif, PDB code: 2D3G), ZnF UBP/BUZ (zinc-finger Ub-binding, PDB code: 2G45), ABIN-1 UBAN (Ub-binding domain in ABINs and NEMO, PDB code: 5M6N) and RAP80 tandem UIMs (Ub-interacting motif, PDB code: 3A1Q). Ub and UBD structures are depicted in gray and blue, respectively. The figure was generated from PDB entries by PyMOL v1.7.6.0 software. **(C)** A subset of UBDs recognizes specific types of Ub modifications, such as specific Ub linkages. **(D)** Cooperative recognition of Ub modifications by two or more UBDs is one of many approaches to increase avidity of Ub:UBD interaction. **(E)** Monoubiquitinated proteins can bind their intrinsic UBDs to regulate their function. The interaction between Ub modification and UBD (on the same protein) provides an efficient switch between active and inactive Ub receptor conformation. **(F)** Ub:UBD interactions often lead to formation of large protein complexes. Most of the Ub:UBD interactions are relatively weak. Multiple UBDs, due to avidity, contribute to the strengthened interaction between Ub and UBDs. Such multiple UBDs and Ub modifications enable formation of highly dynamic protein complexes. **(G)** A subset of UBDs could potentially recognize specific PTM-modified Ub modifications.

substrate through phosphodiester bond (Bhogaraju et al., 2016). Several proteins were shown to be ubiquitinated by SdeA, including small GTPase Rab33b and ER component RTN4 (Qiu et al., 2016; Kotewicz et al., 2017). Ser-linked ubiquitination of those proteins affects their cellular functions. Since SdeA-mediated ADP-ribosylation and phosphoribosylation of Ub inhibit activation of E1 and E2 enzymes, they also impair a plethora of essential Ub-dependent cellular processes, such as proteasomal degradation and mitophagy (Bhogaraju et al., 2016).

Cif proteins from enteropathogenic *Escherichia coli* (*E. coli*) (EPEC) and *Burkholderia pseudomallei* bacteria belong to the group of bacterial effectors targeting Ub signaling by catalyzing deamidatation of Ub at residue Gln40, which inhibits polyUb chain formation (Cui et al., 2010).

Recent proteomic studies have also revealed Ub modification by a small Ub-like modifier (SUMO) at multiple Lys residues (Galisson et al., 2011; Lamoliatte et al., 2013; Hendriks et al., 2014). Additionally, ubiquitinated SUMO has also been reported (Lamoliatte et al., 2013; Hendriks et al., 2014).

Ubiquitin Readers Decode Ubiquitin Code and Induce Specific Cellular Responses

Ub code is recognized by proteins containing single or multiple Ub-binding domains (UBDs), referred to as Ub readers or decoders that, more or less specifically, recognize Ub chain topology and length and enable execution of specific cellular processes (Husnjak and Dikic, 2012).

Ub readers interact with their targets in a transient, non-covalent way (**Figure 3A**) and are often found in a complex with E3 ligases and DUBs, where UBDs contribute to enzyme functionality and/or substrate selectivity, exemplified by the functional coupling between proteasomal Ub receptor RPN13 and DUB UCH37 (Reyes-Turcu and Wilkinson, 2009). Moreover, intrinsic UBDs often determine functionality of ubiquitinating and deubiquitinating enzymes.

UBDs utilize diverse surfaces to contact Ub or Ub polymers, which usually engage confined areas to interact with UBDs. Ub:UBD binding induces mild conformational changes in Ub surface, providing optimal Ub:UBD interface. Although majority of Ub surface is polar, it possesses few hydrophobic patches essential for Ub:UBD interaction, including the most frequently utilized Ile44/Val70 patch and the less common Ile36 and Phe4 patches (Sloper-Mould et al., 2001; Winget and Mayor, 2010). Another non-canonical hydrophobic area centered on Leu8 was identified in members of Y-family translesion synthesis (TLS) polymerases (Bienko et al., 2005). Interestingly, C-terminal part of Ub serves as a binding surface for DUB USP5/IsoT and assists in cleaving unanchored polyUb chains (Reyes-Turcu et al., 2006).

UBDs are typically independently folded, modular domains of up to 150 amino acids and with remarkable structural

heterogeneity that can accommodate a large number of known Ub modifications. UBDs have been classified into nearly 25 subfamilies based on adapted structural folds, which can be divided into helical (i.e., Ub-associated, UBA; Ub-interacting motif, UIM), zinc finger (ZnF), Ub-conjugating-like, pleckstrin homology (PH) and other domains (**Table 1** and **Figure 3B**). Interestingly, not all the members of a specific UBD family can bind Ub, as exemplified by SH3 (Stamenova et al., 2007) and CUE (Lim et al., 2019) domains.

Moreover, a subset of Ub readers with no obvious, structurally defined UBDs has been identified, including intrinsically disordered protein Dss1/SEM1 that binds Ub by binding sites characterized by acidic and hydrophobic residues (Paraskevopoulos et al., 2014). As such "Ub-binding activities" are hard to predict both structurally and bioinformatically, it is unclear how many of such proteins are yet to be identified.

The low-affinity interactions between UBDs and Ub are critical for rapid, timely and reversible cellular responses to a particular stimulus. However, specificity and amplification of Ub binding are required for effective and timely transmission of biological information. This is achieved by a number of different strategies. Approaches toward preferential recognition of various Ub linkages include: existence of Ub linkage-selective UBDs (**Figure 3C**), differential Ub recognition by UBDs with multiple Ub-binding surfaces, Ub chain specificity induced by UBD dimerization or through UBD conformational adaptation, as well as through contribution of sequences situated outside UBDs to Ub binding. On the other hand, increased avidity of Ub:UBD interaction is achieved by implementing various strategies, such as: ability of UBDs to sense Ub chain length, cooperative Ub binding by tandem of identical or combination of different UBDs (**Figure 3D**), regulation of accessibility of Ub-binding modules (through inter- and intramolecular interactions and steric hindrance) (**Figure 3E**), multimerization of Ub-modified proteins and/or Ub receptors (**Figure 3F**) and coupled ubiquitination of UBD-containing proteins (Husnjak and Dikic, 2012; Rahighi and Dikic, 2012).

Post-translational Modifications of Ubiquitin Receptors Affect Their Interactions With Ubiquitin

Ub receptors undergo PTMs that modify their affinity to Ub (**Figure 3G**). Phosphorylation of selective autophagy receptor p62/SQSTM1 UBA domain (at Ser403) by casein kinase 2 (CK2) and innate immunity regulator tank-binding kinase 1 (TBK1) increases its affinity toward Ub and regulates autophagic clearance of ubiquitinated proteins and pathogens (Matsumoto et al., 2011; Pilli et al., 2012). Furthermore, TBK1 also phosphorylates other autophagy receptors, including OPTINEURIN (OPTN), NDP52 (CALCOCO2) and TAX1BP1 (Richter et al., 2016). Phosphorylation of OPTN UBD (Ub-binding domain in ABIN proteins and NEMO; UBAN) at residue Ser473 increases its binding capacity to various Ub chains and enables binding to Ser65-pUb chains, implicating OPTN in PINK1-driven PARKIN-independent mitophagy (Richter et al., 2016).

SENSITIVE TOOLS HELP DISSECT CELLULAR PROCESSES REGULATED BY UBIQUITIN SYSTEM

In order to study spatiotemporal organization and dynamics of the Ub system, a set of powerful tools has been developed in the last decade, ranging from approaches that study Ub covalent targets, as well as non-covalent "executors" of Ub modifications. Moreover, recent advancement in techniques that enable measurement of the enzymatic activities within Ub system has significantly improved our understanding of the physiological significance of the Ub system (**Figure 4**).

Methods to Study Covalent Modifications by Ubiquitin

Identification of Substrates Modified by Ubiquitin and Ubiquitin Chains

Detection and characterization of Ub targets are often challenging due to typically small fraction of a specific protein being modified by Ub, as well as due to highly dynamic nature of Ub modifications. Several techniques enable enrichment and identification of ubiquitinated proteins. Among those, the most common method utilizes transient or ectopic expression of N-terminal epitope-tagged Ub variants, which can be directly conjugated to the substrates as monomers or incorporated into Lys-linked Ub polymers. The cellular epitope-tagged Ub conjugates are then enriched by affinity purification (AP) (**Figure 5A**). The original proteomic study identified 110 ubiquitination sites in 72 Ub targets isolated from Ub-deficient strain of *S. cerevisiae* expressing 6xHIS-Ub (Peng et al., 2003). Similar strategy enabled detection of 669 Ub-modified human proteins and 44 ubiquitinated peptides in HeLa cell line (Meierhofer et al., 2008). The use of 6xHIS tag enables protein purification under denaturing conditions, thus promoting disassembly of protein complexes and inhibition of DUB activity. Due to the existence of polyHIS stretches within eukaryotic proteins, alternative tags, such as STREP, have also been developed (Danielsen et al., 2011). Another technology takes advantage of the strong biotin:avidin and biotin:neutravidin interactions and is based on the existence of biotinylatable motifs (**Figure 5B**) (Franco et al., 2011; Lectez et al., 2014). Here, an N-terminal, 16-amino acids biotin-accepting tag is fused to Ub in tandem with *E. coli* biotin ligase BirA. Upon biotin treatment of cells, such Ub variant can be recognized and biotinylated by BirA, followed by AP. The strategy allows *in vitro* and *in vivo* identification of high and low abundant proteins and minimization of false positive hits due to very stringent denaturing conditions (Franco et al., 2011). Proteomic analysis of *in vivo* biotinylated Ub enabled detection of 48 neuronal Ub conjugates from *Drosophila melanogaster* (*D. melanogaster*) embryos, as well as 393 specific ubiquitinated substrates from mouse liver (Franco et al., 2011; Lectez et al., 2014).

TABLE 1 | List of currently known ubiquitin-binding domains.

Domains	Abbreviation	Name	Examples (proteins with specific UBD)
Helical	UIM	Ub-interacting motif	RPN10, VPS27, USP28, ATAXIN-3, EPS15, STAM1, STAM2, RAP80, DNAJB2, USP37, USP25, EPSINs
	MIU	Motif interacting with Ub	Rabex-5, RNF168
	UMI	UIM- and MIU-related UBD	RNF168
	DUIM	Double-sided UIM	HRS
	UBA	Ub-associated domain	PLIC1/2, HHR23A/B, p62, NBR1, Cbl-b, USP5, UBC1, HERC2, Vps13D, USP25
	CUE	Coupling of Ub to ER degradation domain	Cue2, Vps9
	GAT	GGA and TOM domain	GGA1, GGA2, GGA3, TOM1
	UBAN	Ub-binding domain in ABINs and NEMO	ABIN1, ABIN2, ABIN3, NEMO, OPTN
	VHS	VPS27, HRS and STA domain	VPS27, HRS, STAM1, STAM2, GGA1, GGA2, GGA3, TOM1
	UBM	Ub-binding motif	Polymerase iota, Rev1
	MyUb	Myosin VI UBD	Myosin VI
	AnkUBD	Ankyrin (Ank) repeat UBD	TRABID
Zinc finger (ZnF)	UBZ	Ub-binding ZnF domain	TAX1BP1, Polymerase eta, WRNIP1, FAAP20
	NZF	Npl4 ZnF domain	Npl4, Vps36, TAB2, TAB3, HOIP, HOIL-1L, SHARPIN
	ZnF A20	ZnF of A20 domain	A20, Rabex-5
	ZnF UBP (PAZ, BUZ)	ZnF of Ub-specific processing protease domain	USP5, USP20, HDAC6, BRAP2
Ub-conjugating-like	UBC	Ub-conjugating domain	UbcH5c
	UEV	Ub E2 variant domain	TSG101, Mms2
Pleckstrin-homology (PH)	GLUE	GRAM-like Ub-binding in EAP45 domain	Eap45
	PRU	Pleckstrin-like receptor for Ub	Rpn13
Others		Jab1/MPN domain	Prp8
	PFU	PLAA family UBD	Doa1, PLAA
		SH3, variant	Sla1, CIN85, amphiphysin
		WD40 repeat β-propeller	Doa1, PLAA, Fbxw8, Met30, WDR61, PAF, WDR5
		DC-UbP_N	UBTD2
		MDA-9 UBD	MDA-9

The observation that mutation of Ub residue Leu73 to Pro renders polyUb chains resistant to proteolytic cleavage by numerous DUB families led to generation of epitope-tagged Ub Leu73Pro variant that enables purification of stabilized Ub conjugates from cellular extracts and their subsequent proteomics-based identification (**Figure 5C**) (Bekes et al., 2013). Moreover, Ub and its single Lys variants, in which specific Lys residues are mutated to non-ubiquitinatable amino acids (either Arg or Ala), are frequently used to confirm ubiquitination of protein of interest and to determine the type of conjugated Ub linkage(s) (Kirisako et al., 2006; Kim and Huibregtse, 2009). Finally, since N-terminal tagging abolishes the ability of Ub to form Met1-linked (linear) Ub chains, recently developed Lys-less, internally STREP II-tagged Ub (INT-Ub.7KR) has been successfully used for the MS-based AP (AP-MS) of many novel linear Ub targets (**Figures 5D,E**) (Kliza et al., 2017).

The abovementioned methods can be combined with either MS or traditional Western blotting.

Identification of Substrates and Their Ubiquitin-Modified Sites

Since MS enables simultaneous identification of Ub-modified proteins and precise mapping of ubiquitination sites on these proteins, several approaches were specifically designed for MS-based identification of ubiquitinated proteins. Serine protease trypsin cleaves Ub after residue Arg74, leaving a diGly remnant from the C terminus of Ub covalently attached to the ubiquitinated Lys residue ("Ub remnant peptide"), thus allowing localization of Ub modification (Xu et al., 2010). Ub remnant profiling (**Figure 6A**) is a widely used immunopurification method for the identification of Lys ubiquitination sites by MS that exploits monoclonal antibody for selective enrichment of tryptic peptides containing Lys residue with diGly adduct (Xu et al., 2010; Kim et al., 2011; Wagner et al., 2011). Despite its substantial input in proteomic analysis of ubiquitinome, Ub remnant profiling has several limitations, such as additional enrichment of diGly-remnant peptides derived by tryptic digestion of UBL modifiers ISG15 and NEDD8, bias toward amino acid sequence of remnant peptides and inability to recognize linear Ub signature peptide.

Blagoy Blagoev's group has developed the StUbEx PLUS technique, which overcomes two drawbacks of Ub remnant profiling: recognition of UBL proteins and remnant peptide amino acid sequence preference (Akimov et al., 2018b). To detect ubiquitination sites, the method utilizes internally 6xHIS-tagged Ub in the endogenous Ub knockdown background (Akimov et al., 2018b). Insertion of 6xHIS tag near the C terminus of Ub

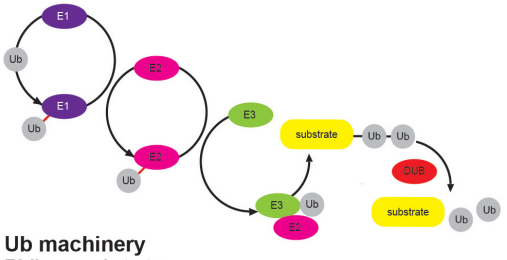

Ub machinery
E3 ligase substrates
>AP-MS, proximity labeling, Ub ligase trapping, NEDDylator, UBAIT, TUBEs, differential expression proteomics, protein microarray, Ub remnant profiling, yeast-two-hybrid, phage display, global protein stability profiling, high-throughput microscopy
DUB substrates
>AP-MS, proximity labeling techniques (i.e. BioID), *in vitro DUB* assay/Ub remnant profiling
Cellular activity
>ABPs, TUBE/TR-FRET, UPS-CONA
Cellular localization
>Antibodies, ABPs

Ub receptors
Identity
>UbIA-MS, yeast two-hybrid, Ub-PT
Ub chain specificity
>UbIA-MS, Octet/Biacore/ITC

Substrates
Identity
>Epitope-tagged Ub variants, TUBEs, Ligase trapping, NEDDylator, UBAIT
Ub-modified sites
>Ub remnant profiling, UbiSITE, StUbEx PLUS, Ub COFRADIC

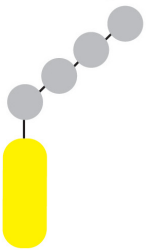

Ub & Ub chains
Linkage type
>Linkage-specific antibodies and affimers, TUBEs, UbiCRest
Architecture
>UbiCRest, UbiChEM-MS, Ub-clipping
Length
>Ub-ProT
Quantity
>Ub-AQUA, Ub-PSAQ, SILAC/TMT MS
Cellular localization
>Antibodies, TUBEs, UiFC
PTMs
> Antibodies, MS, Ub-clipping

FIGURE 4 | Tools to study ubiquitin system. Overview of different approaches to study features of Ub signaling: E3 ligase and DUB enzymes (enzyme abundance, activity, cellular localization), Ub chains (type, architecture, length, quantity, cellular localization, PTMs), ubiquitinated substrates (identity, modification site, type of modification) and Ub receptors (identity, Ub linkage preference).

enables enrichment of HIS-Ub-modified substrates (**Figure 5D**). Subsequent proteolytic cleavage after Lys residues generates ubiquitinated peptides, which can be detected by MS. In a proof of concept experiment, StUbEx PLUS identified over 41,000 unique diGly-Ub remnant peptides in nearly 7,800 Ub targets in U2OS cells upon proteasome inhibition (Akimov et al., 2018b). However, StUbEx PLUS is more laborious technique than Ub remnant profiling.

The same group has recently developed UbiSite antibody (**Figure 6B**), which shows significantly improved specificity toward ubiquitinated peptides, since it recognizes the C-terminal 13 amino acids of Ub that remain attached to modified peptides after proteolytic digestion with the endoproteinase LysC (Akimov et al., 2018a). Importantly, the antibody also allows detection of N-terminal ubiquitination and has enabled identification of over 63,000 unique ubiquitination sites on 9,200 proteins in two human cell lines (Akimov et al., 2018a). Nevertheless, just like Ub remnant profiling and StUbEx PLUS, it cannot recognize linear Ub signature peptide.

Noteworthy, in all of the MS-based approaches, sample preparation is critical for reliable identification of residues covalently modified by Ub. The iodoacetamide (IAA) is an alkylating chemical compound commonly used to block Cys residues in sample digestion procedures. However, IAA is not suitable for identification of ubiquitinated protein residues, as it can additionally react with unmodified Lys residues, leaving a modification of the same mass as a diGly remnant, thus mimicking ubiquitination site (Nielsen et al., 2008). Another alkylating agent, chloroacetamide, is therefore recommended for proteomic discovery of ubiquitination sites.

Combined fractional diagonal chromatography (Ub-COFRADIC) is a sensitive alternative approach for identification of ubiquitination sites, initially described in *Arabidopsis thaliana (A. thaliana)* cells (**Figure 6C**). This multi-step method exploits chemical modification of free primary amines by acetyl groups, which blocks unmodified Lys residues and leaves ubiquitinated Lys residues unmodified. The subsequent deubiquitination by catalytic core of USP2 (USP2cc) exposes the now free amine groups on previously ubiquitinated Lys residues and enables the attachment of Gly-BOC tags to non-acetylated Lys residues. Trypsin digestion of such modified proteins leads to proteolytic cleavage at the C-terminus of Arg, but not Lys residues. After reverse phase HPLC, fractions containing peptides are collected and treated with trifluoroacetic acid (TFA) to remove the BOC groups. Consequently, the residues previously targeted by Ub are now marked by the presence of Gly residues, which can be identified by MS. This proteomics-based approach enabled identification of 3,009 ubiquitination sites on 1,607 plant proteins (Walton et al., 2016). Alike Ub remnant profiling, UbiSite and StUbEx PLUS, Ub COFRADIC is limited to MS studies and is incompatible with standard validation techniques, such as Western blotting and immunofluorescence. Noteworthy, this method generates relatively large peptides, which make MS identification more challenging.

Assessment of Ubiquitin Linkage Type, Chain Size and Architecture

Antibodies specifically recognizing Ub modifications are yet another type of reagents for identification of ubiquitinated proteins. While some antibodies detect all Ub-modified proteins (FK2 antibody) (Fujimuro et al., 1994), the others were engineered to selectively recognize single or a subset of specific Ub modifications, such as polyUb chain-specific FK1 antibody (Fujimuro et al., 1994). Moreover, Ub chain topology can be determined by several Ub linkage-specific antibodies, which specifically recognize Met1, Lys11, Lys27, Lys48 and Lys63 Ub linkages (Matsumoto et al., 2010, 2012; Newton et al., 2012). Ub antibodies have been predominantly utilized to confirm

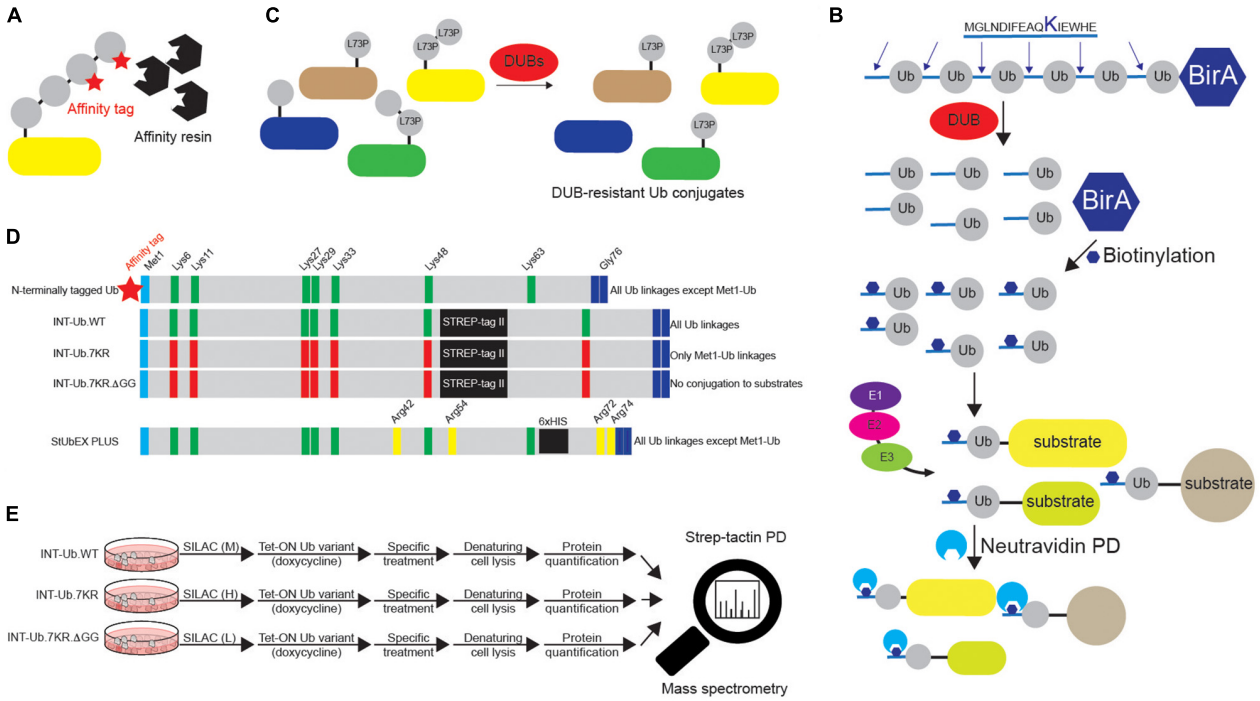

FIGURE 5 | Various approaches to study ubiquitination targets. **(A)** Various N-terminally tagged Ub variants can be exogenously added to cells to enable affinity purifications of ubiquitinated substrates upon denaturing lysis. Short and relatively linear tags (such as 6xHIS, STREP, HA and FLAG), combined with their respective affinity resins (Ni-NTA, strep-tactin, HA agarose and FLAG agarose) are often used in such experiments. Besides N-terminally tagged wild-type Ub, additional Ub variants are often used, such as specific Lys mutants (single or multiple Lys6, Lys11, Lys27, Lys29, Lys33, Lys48 and Lys63 residues mutated to either Arg or Ala). Additionally, residues relevant for Ub binding properties, such as Ile44 and Ile36, can also be mutated to either Arg or Ala. **(B)** Dual BirA system contains synthetic hexaUb sequence fused C-terminally to *E. coli* BirA gene (Ub_6-BirA). Each Ub in the construct contains 16 amino acids sequence at the N terminus that can be biotinylated by BirA. Once expressed in cells (or organisms), linear hexaUb is processed by cellular DUBs and undergoes biotinylation by BirA. When used by cellular ubiquitination machinery, biotin-containing Ub conjugates can be efficiently affinity purified with neutravidin resins and subsequently analyzed by Western blot and mass spectrometry. Due to the N-terminal tagging of Ub, such approach cannot be used to enrich linear ubiquitination targets. **(C)** DUB-resistant Ub variant Leu73Pro increases the half-life and stability of the formed Ub linkages and facilitates their subsequent identification. **(D)** Two MS-coupled approaches rely on the use of internally tagged Ub variants. Unlike N-terminally tagged Ub, INT-Ub and INT-Ub.7KR variants enable affinity purification of ubiquitinated proteins and Met1-Ub-modified substrates, respectively, due to the existence of internal affinity purification STREP-tag between Ub residues Lys48 and Lys63 that keeps Ub Met1 free to interact with Gly76 of another Ub molecule. **(E)** INT-Ub approach is based on inducible expression of INT-Ub variants in SILAC-treated cells, followed by denaturing lysis, strep-tactin pull-down and subsequent MS analysis. The presence of the internal tag does not affect the overall behavior of Ub. Similar to that, 6xHIS insertion near C-terminus of Ub in StUbEx PLUS approach enables enrichment of HIS-Ub-modified substrates under denaturing conditions. The latter approach can be combined with Ub remnant profiling to identify Ub-modified substrate sites.

substrate ubiquitination and only to a lesser extent in proteomic studies (Matsumoto et al., 2010, 2012; Newton et al., 2012). The FK2 antibody was the first antibody used for initial MS-based global ubiquitination analysis, which led to identification of 670 Ub substrates and 18 ubiquitination sites in HEK293T cells (Matsumoto et al., 2005). Similar approach resulted in detection of 70 Ub targets from MG132-treated MCF-7 cell line (Vasilescu et al., 2005). Moreover, proteomic analysis of immunoprecipitated Met1-linkages from *Salmonella*-infected HCT116 cells detected 32 putative linear Ub targets (Fiskin et al., 2016). Among advantages of Ub antibodies are detection of ubiquitinated proteins at the endogenous level and a wide applicability, including Western blotting, immunoprecipitation, immunofluorescence and flow cytometry. Since Ub linkage-specific antibodies often exhibit high cross-reactivity, their usage requires proper controls and highly defined experimental conditions (Beaudette et al., 2016).

Yet another technique for identification of Ub-modified proteins and evaluation of their Ub modifications is based on Ub-binding modules. Due to typically low binding affinity of UBDs toward Ub, synthetic multiple repeats of UBDs (tandem Ub-binding entities, TUBEs) were engineered (**Figure 7A**). Expressed as recombinant epitope-tagged fusions, those tools are characterized by high overall Ub-binding avidity and enable efficient capturing of both high and low abundant Ub targets from cellular lysates (Hjerpe et al., 2009; Mattern et al., 2019). A large number of available Ub traps differs in number and types of UBDs, length of linkers and type of epitope tags. While affinity UBD-based tools are widely used for the confirmation of specific protein ubiquitination, several reports demonstrated their applicability for proteomic analysis of ubiquitinated proteins. Identification of over 290 ubiquitination sites and 223 putative ubiquitinated proteins in HEK293T cells has been demonstrated in ubiquitinome

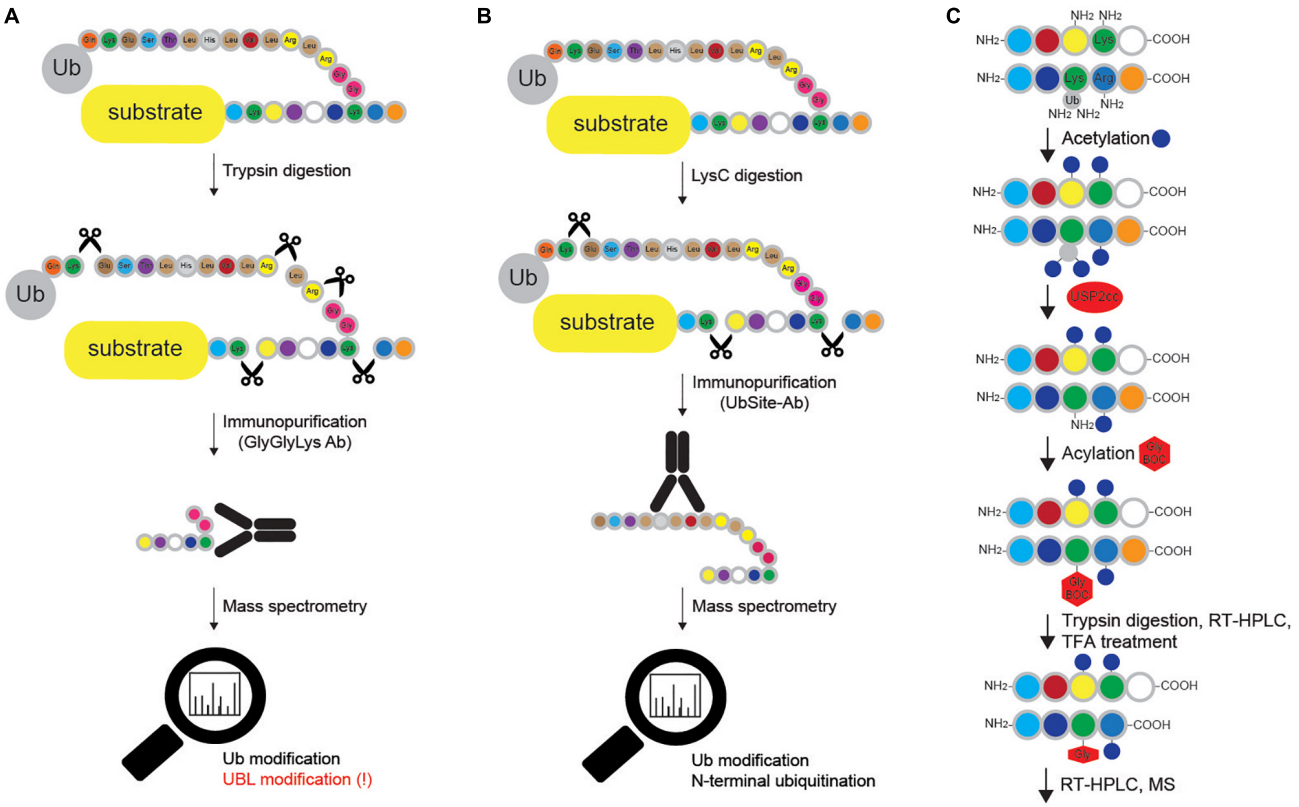

FIGURE 6 | Methods for mapping ubiquitination sites in proteins. **(A)** Ub remnant profiling is based on trypsin digestion of the proteome (cells are previously lysed in urea-containing buffer) combined with immunoprecipitation with monoclonal antibody raised against Lys-ε-Gly-Gly motif that remains on ubiquitinated substrate after trypsin cleavage. Samples are further processed and analyzed by LC-MS/MS. Such approach does not distinguish between modifications by Ub and other UBLs (such as NEDD8 and ISG15), and cannot be applied for Met1- and N-terminally Ub-modified proteins. **(B)** UbiSite antibody recognizes the last 13 amino acids of Ub that remain attached to ubiquitinated proteins upon LysC cleavage. Enriched ubiquitinated proteins are further analyzed by MS. Even though UbiSite approach distinguishes between modifications by Ub and other UBLs, it cannot be used for studying linear ubiquitination, as it does not recognize the signature peptide of linear ubiquitination after tryptic cleavage: Gly-Gly-Met-Gln-Ile-Phe-Val-Lys. **(C)** Ub-COFRADIC approach distinguishes between free (α or ε) and modified primary amines to enable identification of ubiquitinated Lys residues. Initial acetylation by NHS-acetate is only possible on free amines, leaving ubiquitinated Lys residues non-acetylated. Subsequent addition of USP2cc removes all the Ub moieties from Lys residues and enables the attachment of Gly linked to a hydrophobic tert-butyloxycarbonyl (Gly-BOC tag) to previously non-acetylated Lys residues. Trypsin then cleaves C-terminally of Arg residues (but not C-terminally of acetylated Lys). Peptides collected after the first reversed phase (RP)-HPLC run are treated with TFA to remove BOC groups, followed by additional RP-HPLC and MS. In enzyme setting during MS data analysis, ArgC (and not trypsin) should be selected, as cleavage after Lys residues is blocked.

analysis, which used PLIC-1 UBA-based TUBE (Shi et al., 2011). Another proteomic study utilized a tandem of hybrid UBDs (ThUBDs) to analyze total ubiquitinated proteins, which enabled detection of 1092 and 7487 Ub targets in yeast and liver MHCC97-H cell line, respectively (Gao et al., 2016). The recombinant HIS fusion of PLIC2 UBA domain enabled enrichment of polyUb chains from brains of Huntington's disease model mice, as well as patient samples (Bennett et al., 2007). Moreover, Ub linkage-selective affinity UBD-based probes have also been developed, including Lys29/Lys33 linkage-specific (TRABID NZF-based), Lys63 linkage-specific (TAB2 NZF- and VPS27 UIM-based) and Met1-linkage-specific (UBAN-based) TUBEs (Emmerich and Cohen, 2015). By using tandem VPS27 UIM-based probe, over 100 putative Lys63 Ub-modified proteins were identified in *A. thaliana* (Johnson and Vert, 2016). UBAN-based M1-SUB probe combined with proteomic analysis identified a single linear Ub-modified substrate in THP-1 cells upon NOD2 stimulation (Fiil et al., 2013). Furthermore, the tandem of ZnF UBP domain and hybrid Ub probe comprised of ZnF UBP and UBA domains were designed for isolation of unanchored Ub chains and unconjugated Lys48 linkages, respectively (Scott et al., 2016). To summarize, affinity UBD-based reagents efficiently enrich ubiquitinated endogenous substrates, protect Ub conjugates from DUB-mediated proteolysis and proteasomal degradation and have a wide range of applications, including MS, Western blotting and microscopy (Hjerpe et al., 2009; Shi et al., 2011; van Wijk et al., 2012). However, the use of UBD-based tools for discovery of ubiquitinated substrates requires non-stringent purification conditions that ultimately lead to purification of protein complexes rather than individual Ub-modified proteins. On top of that, some UBDs also bind proteins containing intrinsic UBL domains, which results in a relatively high number of contaminants.

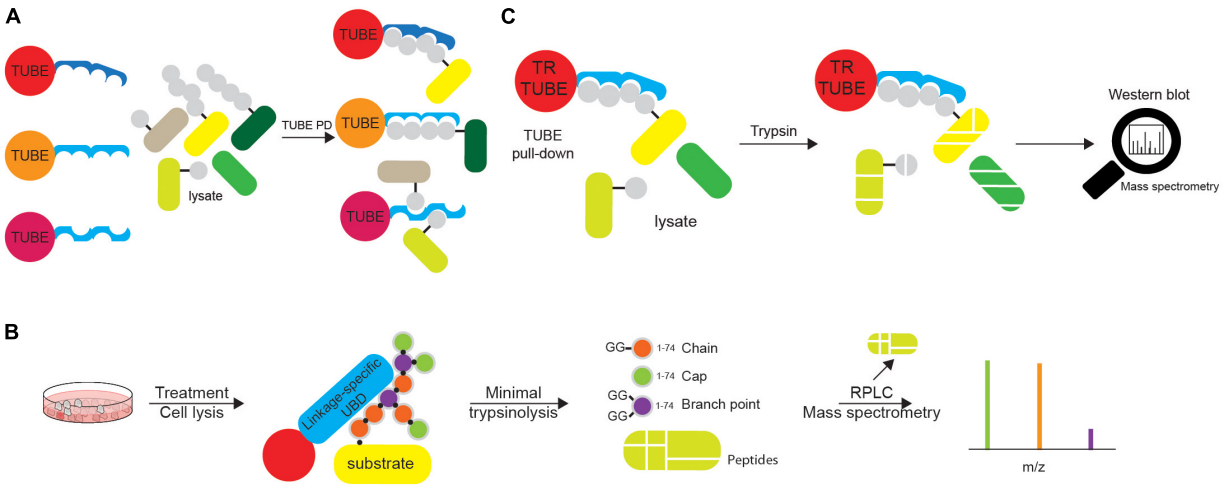

FIGURE 7 | Tandems of ubiquitin entities can be utilized in various ubiquitin tools. **(A)** Tandems of Ub chain-specific or promiscuous UBDs, additionally equipped with affinity tags (such as FLAG-, HA-, GST-, or 6xHIS) and bound to appropriate resins, can be used for affinity purification of ubiquitinated proteins. The use of tandem UBDs increases affinity toward Ub due to avidity, as well as protects ubiquitinated proteins from endogenous DUBs during purification steps. Purified ubiquitinated proteins can be further analyzed by either Western blotting or MS. **(B)** Ub chain enrichment middle-down MS (UbiChEM-MS) approach is based on the enrichment of the specific Ub linkages by linkage-specific UBDs or antibodies, combined with minimal trypsinolysis of Ub that induces a single Ub cleavage after Arg74 and leaves the rest of the Ub molecule intact. By using that approach, Ub molecules within chain, as well as capping and branched Ub conjugates can be detected and quantified by MS. **(C)** Ub-ProT (Ub chain protection from trypsinization) method determines the length of Ub chains bound to target proteins. Trypsin-resistant (TR)-TUBE (i.e., PLIC1 UBA domain lacking Arg residues) is used for the enrichment of ubiquitinated proteins that can be analyzed by Western blotting. Furthermore, since TR-TUBE-protected sample is resistant to trypsin digestion, it can be applied for the determination of the length of Ub chains by quantitative MS.

Since neither antibodies nor TUBEs selectively recognizing several atypical Ub linkages were available, David Komander's group used the affimer technology to screen libraries of small, non-antibody protein scaffolds with randomized surface to develop the linkage-specific Ub affinity reagents for detection of Lys6- and Lys33-linked polyUb chains (Michel et al., 2017). The Lys6 affimer exhibits high selectivity toward Lys6-linked polyUb chains, whereas the Lys33 Ub affinity reagent also recognizes Lys11 linkages. The proteomic analysis of proteins enriched by Lys6 Ub affimer enabled identification of mitofusin-2 and HUWE1 as the Lys6 polyUb-specific substrate and E3 ligase, respectively. Both linkage-specific Ub affinity reagents are suitable for *in vitro* and *in vivo* binding assays, MS, Western blotting and immunofluorescence.

Ub Chain Restriction (UbiCRest) approach is mainly utilized to confirm ubiquitination of putative substrates, which were identified by other methods (Hospenthal et al., 2015). UbiCRest kit provides a set of recombinant DUBs of defined linkage specificities that enable qualitative determination of the type(s) and architecture of Ub linkages modifying protein of interest (Hospenthal et al., 2015). Hitherto, several studies successfully applied UbiCRest, as shown by validation of linear polyUb targets BCL10, CASP8 and TNFR1 (Satpathy et al., 2015; Emmerich et al., 2016; Lafont et al., 2017). However, obtained results highly depend on numerous factors, including reaction conditions, concentration and enzymatic activity of DUBs, incubation period, as well as method used for the enrichment of Ub-modified substrate (Hospenthal et al., 2015).

Although linkage-specific antibodies can be used for studying endogenous polyUb-modified proteins, they cannot clearly distinguish between homotypic and heterotypic Ub chains. Bispecific antibodies detecting heterotypic Ub chains exist so far only for Lys11/LysK48-linked Ub chains (Yau et al., 2017). Complex topology of Ub chains, including branched Ub linkages, prompted the development of novel MS-based approaches for simultaneous detection of multiple modifications on a single Ub moiety. While bottom-up MS (such as Ub remnant profiling) enables characterization of linkages between two Ub molecules, it cannot assess chain length and topology due to trypsin digestion. Opposite to that, middle-down MS utilizes minimal protease digestion of protein samples to detect multiple PTMs on a single Ub molecule (**Figure 7B**). It is based on the notion that under optimized conditions, native folded polyUb is trypsinized only at the Arg74 residue (Xu and Peng, 2008). In that way, minimal trypsinolysis, by leaving Ub largely intact, enables detection of multiple modifications by MS (Xu and Peng, 2008; Valkevich et al., 2014). Ub chain enrichment middle-down MS (UbiChEM-MS) approach combines the enrichment of specific Ub chains using linkage-specific UBDs with minimal trypsinolysis and middle-down MS for the characterization of branched Ub conjugates (Crowe et al., 2017).

Furthermore, David Komander's group has recently published Ub-clipping approach that utilizes an engineered viral protease (Lb^{pro*}) to incompletely remove Ub from substrates, leaving the C-terminal diGly dipeptide conjugated to the modification site and enabling quantification of multiply diGly-modified branch-point Ub (Swatek et al., 2019). By using that approach they could estimate that around 10–20% of Ub in polymers can be found in branched Ub chains.

The length of substrate-attached Ub chains is usually estimated by monitoring their gel mobility in SDS-PAGE. However, due to the complex nature of ubiquitination (different Ub modifications can be simultaneously attached to a single protein), determining the length of Ub chains is not straightforward. Ub-ProT (Ub chain protection from trypsinization) method (**Figure 7C**) was recently developed for assessing the length of substrate-attached polyUb chains (Tsuchiya et al., 2018). The method is based on the use of Ub chain protector, i.e. trypsin-resistant (TR)-TUBE, which consists of biotin and 6xHIS tags and six tandem repeats of the PLIC1 UBA domain, in which all the Arg residues are replaced by Ala (to prevent trypsin digestion of the TUBE). When substrate-attached Ub chains are bound by TR-TUBE, they are resistant to trypsin digestion and can be analyzed using a gel-based assay. By combining this method with quantitative MS analysis, Tsuchiya et al. (2018) determined the length and composition of Ub chains in yeast, and of ligand-activated epidermal growth factor receptor (EGFR) in mammalian cells. The observed disadvantage of the Ub-ProT approach is differential protection of various Ub linkages, as some of them (such as Lys6, Lys27, Lys29, and Lys33) are less efficiently protected, similar to decreased protection of branched over homotypic Ub linkages, which will inevitably generate bias in data analysis. The development of novel TR-TUBEs, with a uniform affinity toward all Ub linkages and without preference for homotypic over heterotypic/branched Ub linkages should improve the quality of this approach.

Quantification of Ub Modification

In general, quantitative measurements of ubiquitination can be either relative or absolute and involve the use of various labeling approaches, such as metabolic labeling (stable isotope labeling with amino acids in cell culture; SILAC) or isobaric peptide tagging (isobaric tags for relative and absolute quantitation; iTRAQ and tandem mass tags; TMT).

Absolute quantification (AQUA) strategy is often used for absolute quantification of proteins or PTMs. Isotopically labeled synthetic peptide, corresponding to the tryptic peptide of the protein of interest, is used as an internal standard with a known concentration. In the Ub-AQUA approach, all eight ubiquitinated diGly peptides can be labeled with a stable isotope and used as internal standard that can be readily distinguished by MS and used for quantification of corresponding native peptides (**Figure 8A**) (Kirkpatrick et al., 2005). For examples, Ub-AQUA approach was used to quantify various types of Ub modifications of NEMO, an essential regulator of NFκB signaling (Ikeda et al., 2011).

Since Ub-AQUA approach cannot take into account any experimental loss of protein, Ub-PSAQ approach has additionally been developed. MS-based Ub protein standard absolute quantification (Ub-PSAQ) approach uses stable isotope–labeled free Ub and Ub conjugates as recovery standards, which are added into lysates and captured with affinity reagents either selective for free Ub (ZnF UBP domain that captures unconjugated Ub by interacting with C terminus of Ub) or Ub chains (PLIC2 UBA domain that binds Ub chains) (**Figure 8B**). Additionally, half of the sample is treated with USP2cc, which enables the conversion of all Ub species to free Ub in order to measure total Ub, and captured by UBD ZnF UBP/BUZ affinity reagent. Sample is subsequently washed, eluted, treated with trypsin and quantified by LC-ESI TOF MS relative to the peptide standard. The presence of DUB inhibitor in the assay prevents interconversion of Ub species during assay (Kaiser et al., 2011).

Determination of Cellular Localization of Ubiquitin Modifications

The techniques and approaches for visualizing Ub signals have recently been reviewed in details by van Wijk et al. (2019).

Engineered UBD-based biosensors containing fluorescent tags found important applications for Ub-binding modules in *in vivo* visualization of Ub modifications. The UBAN-based biosensor enabled monitoring of Met1 linkages in TNFα-mediated NFκB signaling and co-localization of linear Ub chains with cytosolic *Salmonella* during xenophagy, whereas Lys63-selective UIM- and NZF-based sensors traced localization and accumulation of Lys63 linkages during DNA damage response (DDR), mitophagy and upon IL-1β and TNF-related weak inducer of apoptosis (TWEAK) stimulation (Sims et al., 2012; van Wijk et al., 2012).

Ubiquitination-induced fluorescence complementation (UiFC) assay is a variation of TUBE-based biosensors. In this technique, visualization of polyUb chains is achieved by expression of two non-fluorescent, complementary fragments of a fluorescent protein fused to UBDs. Upon UBD-mediated binding to polyUb chains in close proximity, the fluorescence of two fragments is restored (Chen et al., 2013; Pinto et al., 2016). As a proof of concept, Lys48-linked Ub chains were visualized with Epsin1 UIM-based UiFC biosensors under various conditions (i.e., mitophagy, proteasome inhibition) (Chen et al., 2013). Importantly, levels of UBD-based biosensors have to be kept low during experiment, as their high expression could restrict activation of cellular signaling pathways (Sims et al., 2012; van Wijk et al., 2012).

Several aforementioned Ub and Ub linkage-specific antibodies (i.e., FK1 and FK2, Lys48- and Lys63-linked polyUb) are suitable for immunocyto- and immunohistochemistry and are widely used (Newton et al., 2008; Danielson and Hope, 2013; Nakazawa et al., 2016). Among others, Met1-linked polyUb-specific antibody was used to determine the effect of linear Ub binding-deficient OPTN mutations in the onset of amyotrophic lateral sclerosis (Nakazawa et al., 2016).

Identification of Post-translationally Modified Ubiquitin and Ubiquitin Chains

Discovery of PTMs that modify Ub monomers and polymers has predominantly been achieved by MS. As delineated previously, MS detection of tryptic Ub peptides containing specific modifications enabled identification of Ub PTMs such as deamidation and phosphoribosylation (Cui et al., 2010; Bhogaraju et al., 2019).

The abovementioned Ub-clipping method (Swatek et al., 2019) can also be used to determine the co-existing PTMs on Ub modifications. As a proof of principle, such approach was used to determine Ub architecture on depolarized mitochondria. The analysis revealed that, under mitophagy-inducing conditions,

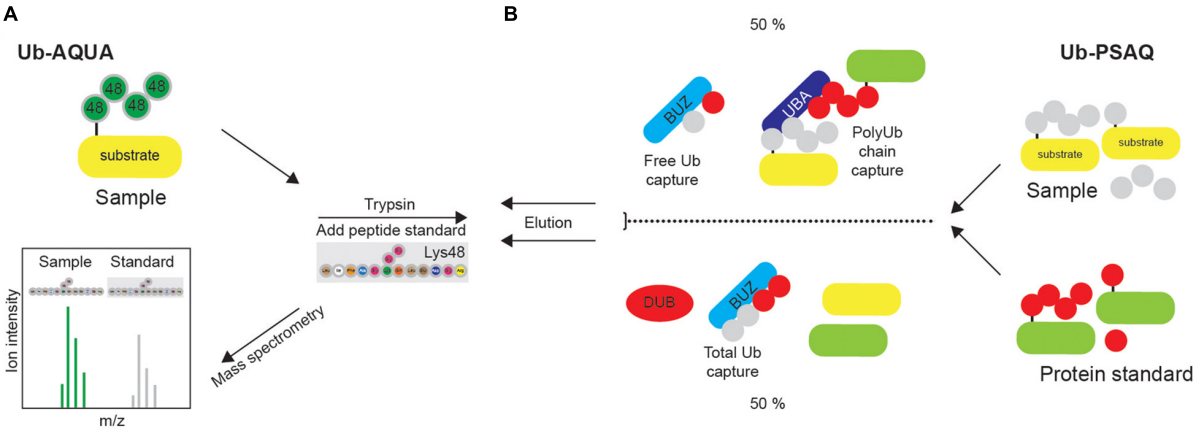

FIGURE 8 | Quantification of ubiquitination *in vivo*. **(A)** Synthetic peptide absolute quantification (Ub-AQUA) MS approach is based on synthetic peptides as quantification standards for both mono- and polyubiquitination. **(B)** Ub-PSAQ approach is based on the use of stable isotope-labeled free Ub and Ub conjugates as protein standards. They are added to lysates and captured with UBD BUZ that is selective for free Ub and UBD PLIC2 UBA (or similar) that recognizes Ub chains. Half of the sample is treated with USP2cc and total free Ub captured by BUZ affinity reagent. Sample is quantified by MS, relative to the peptide standard.

Ub coat on mitochondria is composed mainly of monoUb and oligoUb chains, with phosphoUb capping Ub chains and therefore, preventing further extension of Ub polymers (Swatek et al., 2019).

Currently, there are several available antibodies that detect specific PTMs on Ub. The antibody recognizing phosphorylation on Ub Ser65 is suitable for Western blotting and has been used to study the effect of Ub phosphorylation on the recruitment of Ub-binding mitophagy receptors to depolarized mitochondria (Ordureau et al., 2018). Moreover, the antibody detecting acetylation on Ub Lys48 residue, suitable for ELISA and Western blotting, is available on the market. However, it has not been reported in any publication thus far.

Methods to Study Ubiquitination Machinery

Identification of E3 Ligase Substrates

Identification of E3 ligase:substrate pairs is very challenging, since interactions between E3 ligases and their targets are very dynamic and of low affinity. Moreover, ubiquitination of the substrates often exhibits stimulus- and spatiotemporal dependency. Furthermore, individual substrates can be targeted by several E3 ligases at different residues and at different physiological conditions. Additionally, ubiquitinated substrates are often marked for proteasomal degradation, which leads to their fast removal from the cells.

A plethora of approaches has been established to enable identification of E3 ligase substrates and review by Iconomou and Saunders discusses them in details (Iconomou and Saunders, 2016). These include proximity-dependent biotin labeling (BioID) (Roux et al., 2012; Coyaud et al., 2015), Ub ligase substrate trapping (Mark et al., 2014, 2016; Loveless et al., 2015), Ub-activated interaction traps (UBAIT) (O'Connor et al., 2015, 2018) and NEDDylator approach (Zhuang et al., 2013).

BioID approach allows the identification of proteins in the close vicinity of a protein of interest in living cells. It is based on the fusion of the E3 ligase with mutated form of biotin ligase BirA, which biotinylates all the proteins in the close vicinity (around 10 nm), if biotin is available. Such "neighborhood tagging" allows AP and subsequent MS-based detection of all the labeled proteins, majority of which potentially being the E3 ligase substrates. This approach enabled identification of 50 putative substrates of $SCF^{\beta TrCP1/2}$ (Coyaud et al., 2015).

Ligase trapping is an AP approach in which E3 ligases fused to UBDs are used for isolation of ubiquitinated substrates (**Figure 9A**). The presence of UBD increases the binding affinity of the E3 ligase of interest toward its targets, thus increasing sensitivity of the method. This technique enabled successful identification of novel substrates of FBXL E3 ligases, including Prb1 (Mark et al., 2014). The selection of proper UBD (to ensure effective enrichment of substrates), as well as fusion point (that might potentially disrupt the substrate recruitment) is essential for the proper functionality of the ligase trap.

UBAIT is a method belonging to ligase trapping class and allows for identification of substrates for HECT and RING E3 ligases (**Figure 9B**). UBAIT tool consists of E3 ligase fused to Ub moiety and target-interacting domain. The presence of Ub enables E1- and E2-mediated activation of UBAIT and subsequent covalent capture of E3 ligase substrates. This technique was applied to identify proteins interacting with several Ub ligases, such as ITCH and RNF126 (O'Connor et al., 2015). The drawback of this approach is that it cannot distinguish between E3 ligase substrates and E3 ligase-interacting proteins.

NEDDylator approach relies on the fusion between NEDD8 E2 enzyme and substrate-binding region of desired E3 ligase (**Figure 9C**). Such configuration allows artificial NEDDylation of endogenous E3 ligase substrates, their enrichment (by denaturing immunoprecipitation of exogenous NEDD8 tag, such as 6xHIS) and subsequent MS identification. As NEDDylation does not

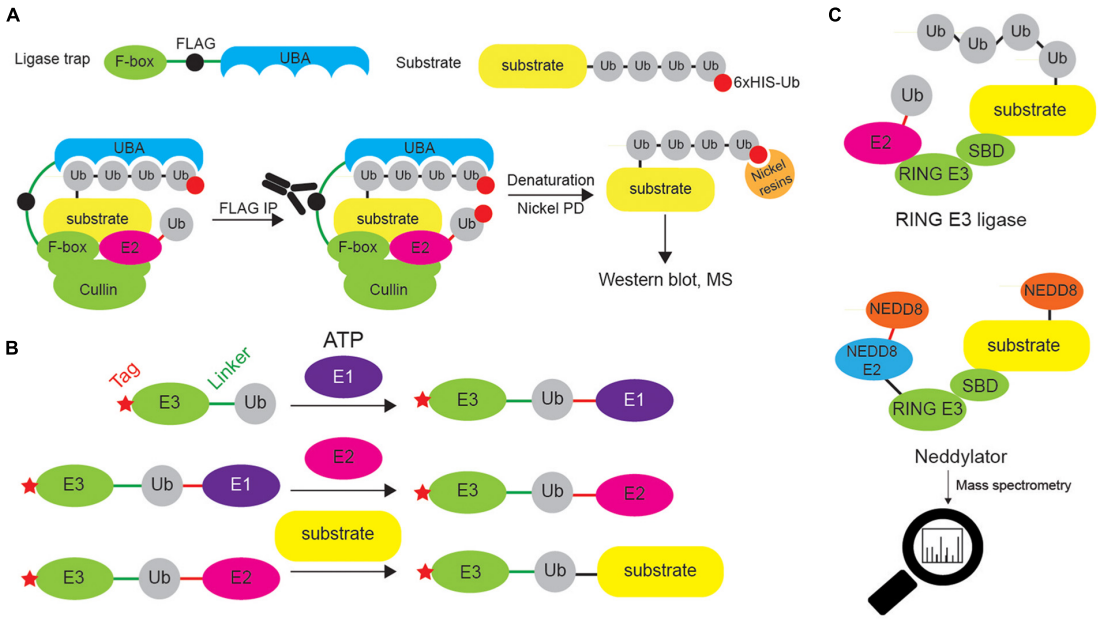

FIGURE 9 | Different approaches to identify E3 ligase substrates. **(A)** Ligase trapping approach "stabilizes" E3 ligase:substrate non-covalent interactions by UBDs (such as UBA domain) fused to E3 ligase substrate-interacting domains (such as F-box of the multi-protein E3 ligase complex SCF). When such ligase traps and 6xHIS-tagged Ub are overexpressed in cells, the UBA interacts with the nascent Ub chain on endogenous SCF substrates, thereby delaying their release. Cells are then lysed and subjected to an anti-FLAG coimmunoprecipitation under native conditions, to isolate ligase trap complexes (FLAG tag is inserted between F-box and UBA). FLAG eluates are then used in denaturing Ni-NTA agarose pull-down to exclusively enrich ubiquitinated substrates (and to remove any non-covalently interacting proteins). **(B)** UBAITs, similar to ligase traps, enable identification of E3 ligase substrates (for both HECT and RING E3 ligases), as well as their adaptors and regulators. Unlike ligase traps, UBAITs are fusions of N-terminal affinity-tagged E3 and C-terminal Ub molecule. With the help of cellular E1 and E2, UBAIT E3 component transfers UBAIT Ub component (by forming amide bond) to proteins that interact with the E3, such as E3 ligase substrates. Formed complex is easily affinity purified and analyzed by mass spectrometry. For HECT E3s, both E3 and E2 thioester-linked interacting proteins can be captured by UBAITs. **(C)** NEDDylator is a catalytic tagging tool, in which Ubc12, an E2 enzyme for NEDD8, is fused to an E3 ligase substrate-binding domain, allowing for the transfer of NEDD8 to the E3 substrate, and MS-based identification of E3 ligase-target pairs.

occur at a high level in a cell, it is not difficult to distinguish between endogenous and NEDDylator-induced modifications and as such, to identify E3 ligase substrates.

Identification of DUB Substrates

Identification of DUBs and their targets is difficult due to several reasons: the enzymatic activity of DUBs results in a rapid removal of Ub modifications from the DUB substrates, the interaction between DUBs and their substrates is often inducible and spatiotemporally restricted, DUBs typically bind their substrates with relatively low affinity and numerous DUBs require accessory proteins for specific interactions with their targets. Therefore, a limited number of studies have aimed to identify the substrates for specific DUBs thus far.

A common technique is substrate AP with either recombinant or ectopically expressed epitope-tagged DUB as bait (Bonacci et al., 2018). However, this approach preferentially identifies DUB interactors over DUB substrates. If known, point mutation of the active site of investigated DUB, which decreases/abolishes the proteolytic activity of the DUB, greatly facilitates identification of DUB targets as it enables entrapment of ubiquitinated substrates. This approach led to the identification of APC/C substrates (i.e., Cyclin B and Aurora A) as targets of Cezanne/OTUD7B, a Lys11 linkage-specific DUB (Bonacci et al., 2018). Another study utilized similar approach to identify NFX1-123 as a substrate of USP9X (Chen et al., 2019).

Yet another method for discovery of DUB targets is based on *in vitro* deubiquitination of cell lysate with recombinant DUB of interest. Together with reference lysate, samples are then digested with trypsin, peptides are isotopically labeled and subjected to Ub remnant profiling. This quantitative proteomic approach enabled identification of two substrates of *Salmonella Typhimurium* effector SseL (Nakayasu et al., 2015).

Measuring the Enzymatic Activity of Ubiquitination Machinery

E3 ligases and DUBs have evolved in the last several years as promising therapeutic targets in oncology and neurodegeneration, as they are often perturbed in various diseases and cancer types (Cromm and Crews, 2017; Harrigan et al., 2018; Yang et al., 2018). Many research groups and pharmaceutical industry are therefore developing specific inhibitors and activators of these enzymes, as well as improving and developing quantitative methods for measuring their enzymatic activity both *in vitro* and *in vivo*. A comprehensive review about activity-based probes (APBs) for ubiquitination machinery has recently been published by Huib Ovaa's group (Witting et al., 2017).

Initially developed ABPs contain Ub moiety with the C-terminal Gly76 residue chemically modified with an electrophilic warhead, such as aldehyde, vinyl sulfone (Ub-VS), vinyl methylester (Ub-VME) and propargylamide (Ub-Prg) to covalently bind proteins containing active Cys residue (Borodovsky et al., 2001, 2002; Ekkebus et al., 2013). They have been successfully used to identify novel DUBs and monitor DUB activity (Borodovsky et al., 2002; de Jong et al., 2012). The real advancement in the field came after the successful diUb chemical synthesis, which opened new possibilities in developing DUB probes (El Oualid et al., 2010; de Jong et al., 2012; Mulder et al., 2014; Flierman et al., 2016). Many approaches have also been developed for assessing DUB specificity, ranging from diUb probes mimicking all eight different Ub linkages combined with MS (McGouran et al., 2013), diUb probes resembling native diUb that contain a Michael addition acceptor for trapping the DUB active-site Cys (Li et al., 2014), seven synthetic isopeptide-linked diUb FRET probes with rhodamine-TAMRA for the absolute quantification of chain cleavage specificity (Geurink et al., 2016) or monitoring total cellular DUB activity by advanced chemoproteomics (Pinto-Fernandez et al., 2019).

Many assays for assessment of E3 ligase activity are based on monitoring E3 ligase autoubiquitination, either by Western blotting or by measuring fluorescence. By combining time-resolved fluorescence resonance energy transfer (TR-FRET) based on lanthanide chemistry and TUBEs, Marblestone et al. (2012) have developed an E3 ligase activity assay in which they monitored the proximity of the autoubiquitinated E3 ligase and biotinylated TUBEs in an E3-dependent polyUb chain formation assay based on endogenous Ub. The method is limited to studying E3 ligase activity of the specific, individual E3 ligase *in vitro* and might not work in cellular lysates. For E3 ligases that require PTMs or additional protein components for their enzymatic activity such approach can be technically very challenging.

The development of E1-E2-E3 activity probes was not as fast as the development of DUB probes. Some ABPs, such as Ub-Prg and Ub-VME, can also label active Cys in HECT E3 ligases (Ekkebus et al., 2013).

Recently published cascading E1-E2-E3 ABP (Mulder et al., 2016) is based on the use of the Ub variant in which Gly76 is replaced by dehydroalanine (Dha) that can be processed by the cellular ubiquitination machinery (Hodgins et al., 1992; Pickart et al., 1994; Mulder et al., 2016). Once added to lysate or electroporated into cells, UbDha is activated by E1 enzyme (through the formation of an adenylate intermediate) and the activated reactive methylene group of the Dha moiety can then either covalently trap the enzyme in an E1-UbDha thioether adduct or follow the native resulting in an E1∼UbDha thioester. Such thioester can then be transferred to an E2 enzyme and either form covalent thioether adduct with the probe or undergo native trans-thioesterification. Following the ubiquitination pathway UbDha can subsequently be transferred to an active site of either HECT or RBR E3 ligases.

In this manner, the probe can travel through the entire E1-E2-E3 cascade, where it "traps" catalytically active Ub-modifying enzymes along the way. Unlike endogenous Ub, the probe can irreversibly react with the active site Cys residue of target enzymes in living cells. It can be also combined with MS to identify or quantify E1-E2-E3 cellular activities. However, in its current form the probe is not selective for specific E2 or E3 enzymes and cannot capture RING E3 ligases in a mechanism-dependent manner (Mulder et al., 2016), which requires novel probe designs.

Pao et al. (2018) have recently developed a novel ABP consisting of Ub-charged E2 conjugate with C-terminal activated

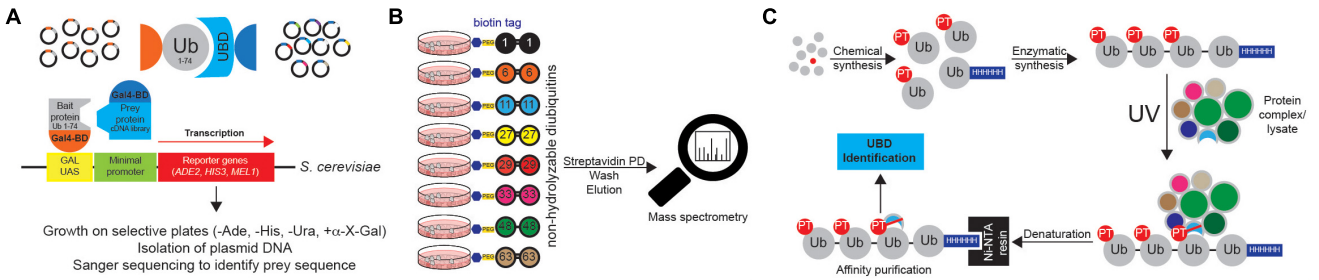

FIGURE 10 | Approaches to identify ubiquitin receptors. **(A)** A very common type of Y2H approach is based on the use of Ub sequence (lacking C-terminal Gly-Gly motif) as N-terminal fusion with the GAL4 binding domain (BD). The cDNA library containing putative UBDs consists of cDNAs cloned under the control of the lacZ promoter downstream of the DNA sequence encoding the activating domain (AD) of the yeast GAL4 transcription factor. Protein interaction induces the close proximity of GAL4AD and GAL4BD, forming the active transcription factor, which binds to the GAL1 upstream activating sequence (UAS) and activates the transcription of several GAL4-responsive genes, which are used as reporters. For example, yeast strain *S. cerevisiae* YTHGold (*Clontech*) enables very stringent quadruple selection, since it contains 4 reporters. In that way background growth and detection of false positive interacting proteins is significantly decreased, simplifying further evaluation steps. **(B)** UbIA-MS method relies on the use of 8 chemically synthesized non-hydrolyzable biotinylated diUbs that can be used for *in vitro* affinity purification of Ub interactors. These diUb linkages mimic native diUb, and have advantage of not being cleaved by cellular DUBs, which prevents the loss of captured material and decrease in Ub chain specificity. Upon purification, samples are digested on beads with trypsin, followed by liquid chromatography (LC)-MS/MS analysis. **(C)** Ub-PT is a synthetic Ub variant that contains a photo-activatable crosslinking Leu mimic photoleucine (pLeu) at positions 8 or 73 in Ub molecule. Importantly, these modifications do not affect Ub functionality, including its ability to bind UBDs. Enzymatic polymerization of Ub-PT into Ub chains of defined lengths and linkage types allows the use of Ub-PT as UV-activatable crosslinking reagent (phototrap) for irreversibly capturing Ub receptors. Furthermore, the existence of 6xHIS tag in Ub-PT-containing reagents allows stringent isolation of Ub interactors, without co-purification of their binding proteins.

vinylsulfide (E2-Ub-AVS) as the warhead for the detection and identification of novel E3 ligases. By using their probe, they identified MYCBP2/PHR1 as so far unique E3 ligase with esterification activity and intrinsic selectivity for Thr over Ser (Pao et al., 2018). Like E1-E2-E3 probe, this approach also lacks the ability to study specific E3 ligases and to monitor RING E3 ligase family.

Additionally, Dha-based E2-Ub ABP was also developed for monitoring HECT E3 activity *in vitro* and *in vivo* (Xu et al., 2019).

The UPS-confocal fluorescence nanoscanning (UPS-CONA) assay is based on the immobilization of the specific substrate of interest on micro-beads. Fluorescently labeled Ub is enzymatically conjugated to the substrate and can be quantitatively detected on the bead periphery by confocal microscopy. UPS-CONA approach can be used for studying specific enzymes of the ubiquitination machinery, as well as for measuring the selectivity of putative ubiquitination inhibitors (Koszela et al., 2018).

Methods to Study Non-covalent Ubiquitin Recognition

Identification of Novel Ubiquitin Readers and Determination of Their Specificity Toward Ubiquitin

The number of currently known Ub readers is relatively low in comparison to the number of proteins playing active roles in ubiquitination and deubiquitination or those modified by various Ub moieties. It is reasonable to speculate that there are still multiple UBDs that remain unknown at the moment, especially those specific for Ub linkages, those that are Ub chain length-dependent or can specifically recognize heterotypic/branched Ub linkages or even specific Ub PTMs.

The use of single Ub moiety lacking diGly motif at the C terminus (to prevent potential conjugation to yeast proteins) as bait in yeast two-hybrid (Y2H) screen led to the identification of several novel UBD-containing proteins, including Pru domain of RPN13 (**Figure 10A**) (Bienko et al., 2005; Husnjak et al., 2008; Wagner et al., 2008). This approach is limited to UBDs that bind single Ub moieties and cannot be used for Ub linkage-specific UBDs.

Ub chains cannot be efficiently used for the AP of Ub chain-specific UBDs, as cellular DUBs readily cleave them. However, by combining chemically synthesized non-hydrolyzable diUb molecules with AP/MS, Zhang et al. (2017) could successfully enrich and identify many known and novel Ub interactors with simultaneous evaluation of their Ub linkage specificity (**Figure 10B**). The novel method, termed Ub interactor affinity enrichment-MS (UbIA-MS) identified TAB2 and TAB3 as novel Lys6 interactors and characterized UCHL3 as Lys27-specific Ub receptor (Zhang et al., 2017).

Another promising approach for identifying novel UBDs is the use of synthetic Ub variant that contains a photoactivatable crosslinking side chain. Photoleucine (pLeu) incorporated into fully synthetic Ub monomer does not prevent UBD binding to its Ile44 patch and can be readily incorporated into polyUb chain, without affecting the specificity of the binding (**Figure 10C**). Once photoactivated by UV, it is able to crosslink nearby proteins, thus stabilizing often very weak UBD:Ub interactions. By using Ub-PT as a tool, Chojnacki et al. (2017) identified proteasomal subunit Rpn1 as a novel Ub receptor. Moreover, Ub-PT can have pLeu incorporated at multiple positions within Ub molecule, making it very useful for capturing UBDs that interact in different ways with Ub.

CONCLUDING REMARKS

Ub field has been extensively studied in the last several decades, and its recognition as the promising drug target has initiated a large number of studies aiming to improve our understanding of the complex nature of ubiquitination regulation. Novel DUB inhibitors have been developed, as well as multiple tools to identify novel components (enzymes, scaffolds, and receptors), to study enzymatic activity, cellular distribution, modes of regulation and potential chemical inhibition of Ub system.

The use of proteolysis targeting chimeras (PROTACs) for induction of specific protein degradation has emerged as promising approach for targeting proteins that are otherwise hard or impossible to target by small molecule approaches (Watt et al., 2019), making further research of the Ub system a priority. Still, there are many things that we do not know or that we have just started to elucidate. Newly developed tools and approaches will clearly shed a new light on our understanding of Ub systems and ways how we can explore it for treating diseases.

OUTSTANDING QUESTIONS

There are still no straightforward approaches for determining E3 ligases responsible for specific ubiquitination events. Furthermore, ABPs specific for single E3 ligases (and many DUBs) are still missing, as well as small molecules that can either specifically inhibit (or potentially activate) these enzymes.

Even though numerous high-throughput MS studies have identified tens of thousands of ubiquitination sites at the proteome level (Kim et al., 2011; Wagner et al., 2011), for only a small proportion of these modifications a specific E3 ligase is known. Methods such as Ub remnant profiling do not allow identification of E3 ligases that modify specific Lys residues on identified proteins.

Due to transient interaction between E3 ligases and their substrates, standard approaches (such as immunoprecipitation) are not appropriate for identification of specific E3 ligases:substrate pairs, even more so since many (but not all) E3 ligases target their substrates for proteasomal degradation, thus reducing their levels. In line with that, protein abundance upon E3 ligase removal/inhibition or activation/overexpression cannot be a good readout for identifying specific E3 ligase substrates.

As many E3 ligases are multicomponent complexes, whose activation often depends on various PTMs, many of these enzymes are difficult to be used in various high-throughput screening efforts for their regulators. As ubiquitination is a very complex PTM, with numerous heterotypic/branched and combinatorial ubiquitination events, it is clear that all the available methodology is still unable to fully comprehend the extent and importance of these modifications.

AUTHOR CONTRIBUTIONS

Both authors listed have made a substantial, direct and intellectual contribution to the work, and approved it for publication.

ACKNOWLEDGMENTS

We apologize to all the authors whose valuable work could not have been mentioned in this article due to size limitations.

REFERENCES

Akimov, V., Barrio-Hernandez, I., Hansen, S. V. F., Hallenborg, P., Pedersen, A. K., Bekker-Jensen, D. B., et al. (2018a). UbiSite approach for comprehensive mapping of lysine and N-terminal ubiquitination sites. *Nat. Struct. Mol. Biol.* 25, 631–640. doi: 10.1038/s41594-018-0084-y

Akimov, V., Olsen, L. C. B., Hansen, S. V. F., Barrio-Hernandez, I., Puglia, M., Jensen, S. S., et al. (2018b). StUbEx PLUS-A modified stable tagged ubiquitin exchange system for peptide level purification and in-depth mapping of ubiquitination sites. *J. Proteome Res.* 17, 296–304. doi: 10.1021/acs.jproteome.7b00566

Akutsu, M., Dikic, I., and Bremm, A. (2016). Ubiquitin chain diversity at a glance. *J. Cell Sci.* 129, 875–880. doi: 10.1242/jcs.183954

Beaudette, P., Popp, O., and Dittmar, G. (2016). Proteomic techniques to probe the ubiquitin landscape. *Proteomics* 16, 273–287. doi: 10.1002/pmic.201500290

Bekes, M., Okamoto, K., Crist, S. B., Jones, M. J., Chapman, J. R., Brasher, B. B., et al. (2013). DUB-resistant ubiquitin to survey ubiquitination switches in mammalian cells. *Cell Rep.* 5, 826–838. doi: 10.1016/j.celrep.2013.10.008

Bennett, E. J., Shaler, T. A., Woodman, B., Ryu, K. Y., Zaitseva, T. S., Becker, C. H., et al. (2007). Global changes to the ubiquitin system in Huntington's disease. *Nature* 448, 704–708.

Bhogaraju, S., Bonn, F., Mukherjee, R., Adams, M., Pfleiderer, M. M., Galej, W. P., et al. (2019). Inhibition of bacterial ubiquitin ligases by SidJ-calmodulin catalysed glutamylation. *Nature* 572, 382–386. doi: 10.1038/s41586-019-1440-8

Bhogaraju, S., Kalayil, S., Liu, Y., Bonn, F., Colby, T., Matic, I., et al. (2016). Phosphoribosylation of ubiquitin promotes serine ubiquitination and impairs conventional ubiquitination. *Cell* 167, 1636–1649.e13. doi: 10.1016/j.cell.2016.11.019

Bienko, M., Green, C. M., Crosetto, N., Rudolf, F., Zapart, G., Coull, B., et al. (2005). Ubiquitin-binding domains in Y-family polymerases regulate translesion synthesis. *Science* 310, 1821–1824.

Bonacci, T., Suzuki, A., Grant, G. D., Stanley, N., Cook, J. G., Brown, N. G., et al. (2018). Cezanne/OTUD7B is a cell cycle-regulated deubiquitinase that antagonizes the degradation of APC/C substrates. *EMBO J.* 37:e98701. doi: 10.15252/embj.201798701

Borodovsky, A., Kessler, B. M., Casagrande, R., Overkleeft, H. S., Wilkinson, K. D., and Ploegh, H. L. (2001). A novel active site-directed probe specific for deubiquitylating enzymes reveals proteasome association of USP14. *EMBO J.* 20, 5187–5196.

Borodovsky, A., Ovaa, H., Kolli, N., Gan-Erdene, T., Wilkinson, K. D., Ploegh, H. L., et al. (2002). Chemistry-based functional proteomics reveals novel members of the deubiquitinating enzyme. *Chem. Biol.* 9, 1149–1159.

Braten, O., Livneh, I., Ziv, T., Admon, A., Kehat, I., Caspi, L. H., et al. (2016). Numerous proteins with unique characteristics are degraded by the 26S proteasome following monoubiquitination. *Proc. Natl. Acad. Sci. U.S.A.* 113, E4639–E4647. doi: 10.1073/pnas.1608644113

Cadwell, K., and Coscoy, L. (2005). Ubiquitination on nonlysine residues by a viral E3 ubiquitin ligase. *Science* 309, 127–130.

Chaugule, V. K., Burchell, L., Barber, K. R., Sidhu, A., Leslie, S. J., Shaw, G. S., et al. (2011). Autoregulation of parkin activity through its ubiquitin-like domain. *EMBO J.* 30, 2853–2867. doi: 10.1038/emboj.2011.204

Chen, X., Lu, D., Gao, J., Zhu, H., Zhou, Y., Gao, D., et al. (2019). Identification of a USP9X substrate NFX1-123 by SILAC-Based quantitative proteomics. *J. Proteome. Res.* 18, 2654–2665. doi: 10.1021/acs.jproteome.9b00139

Chen, B. B., and Mallampalli, R. K. (2009). Masking of a nuclear signal motif by monoubiquitination leads to mislocalization and degradation of the regulatory enzyme cytidylyltransferase. *Mol. Cell. Biol.* 29, 3062–3075. doi: 10.1128/MCB.01824-08

Chen, Z., Zhong, Y., Wang, Y., Xu, S., Liu, Z., Baskakov, I. V., et al. (2013). Ubiquitination-induced fluorescence complementation (UiFC) for detection of K48 ubiquitin chains in vitro and in live cells. *PLoS One* 8:e73482. doi: 10.1371/journal.pone.0073482

Chojnacki, M., Mansour, W., Hameed, D. S., Singh, R. K., El Oualid, F., Rosenzweig, R., et al. (2017). Polyubiquitin-photoactivatable crosslinking reagents for mapping ubiquitin interactome identify Rpn1 as a proteasome ubiquitin-associating subunit. *Cell Chem. Biol.* 24, 443–457.e6. doi: 10.1016/j.chembiol.2017.02.013

Ciechanover, A., and Ben-Saadon, R. (2004). N-terminal ubiquitination: more protein substrates join in. *Trends Cell Biol.* 14, 103–106.

Coyaud, E., Mis, M., Laurent, E. M., Dunham, W. H., Couzens, A. L., Robitaille, M., et al. (2015). BioID-based identification of Skp cullin F-box (SCF)beta-TrCP1/2 E3 ligase substrates. *Mol. Cell. Proteomics* 14, 1781–1795. doi: 10.1074/mcp.M114.045658

Cromm, P. M., and Crews, C. M. (2017). Targeted protein degradation: from chemical biology to drug discovery. *Cell Chem. Biol.* 24, 1181–1190. doi: 10.1016/j.chembiol.2017.05.024

Crowe, S. O., Rana, A., Deol, K. K., Ge, Y., and Strieter, E. R. (2017). Ubiquitin chain enrichment middle-down mass spectrometry enables characterization of branched ubiquitin chains in cellulo. *Anal. Chem.* 89, 4428–4434. doi: 10.1021/acs.analchem.6b03675

Cui, J., Yao, Q., Li, S., Ding, X., Lu, Q., Mao, H., et al. (2010). Glutamine deamidation and dysfunction of ubiquitin/NEDD8 induced by a bacterial effector family. *Science* 329, 1215–1218. doi: 10.1126/science.1193844

Danielsen, J. M., Sylvestersen, K. B., Bekker-Jensen, S., Szklarczyk, D., Poulsen, J. W., Horn, H., et al. (2011). Mass spectrometric analysis of lysine ubiquitylation reveals promiscuity at site level. *Mol. Cell. Proteomics* 10:M110003590. doi: 10.1074/mcp.M110.003590

Danielson, C. M., and Hope, T. J. (2013). Using antiubiquitin antibodies to probe the ubiquitination state within rhTRIM5alpha cytoplasmic bodies. *AIDS Res. Hum. Retroviruses* 29, 1373–1385. doi: 10.1089/AID.2013.0029

de Jong, A., Merkx, R., Berlin, I., Rodenko, B., Wijdeven, R. H., El Atmioui, D., et al. (2012). Ubiquitin-based probes prepared by total synthesis to profile the activity of deubiquitinating enzymes. *Chembiochem* 13, 2251–2258. doi: 10.1002/cbic.201200497

Ekkebus, R., van Kasteren, S. I., Kulathu, Y., Scholten, A., Berlin, I., Geurink, P. P., et al. (2013). On terminal alkynes that can react with active-site cysteine nucleophiles in proteases. *J. Am. Chem. Soc.* 135, 2867–2870. doi: 10.1021/ja309802n

El Oualid, F., Merkx, R., Ekkebus, R., Hameed, D. S., Smit, J. J., de Jong, A., et al. (2010). Chemical synthesis of ubiquitin, ubiquitin-based probes, and diubiquitin. *Angew. Chem.* 49, 10149–10153.

Emmerich, C. H., Bakshi, S., Kelsall, I. R., Ortiz-Guerrero, J., Shpiro, N., and Cohen, P. (2016). Lys63/Met1-hybrid ubiquitin chains are commonly formed during the activation of innate immune signalling. *Biochem. Biophys. Res. Commun.* 474, 452–461. doi: 10.1016/j.bbrc.2016.04.141

Emmerich, C. H., and Cohen, P. (2015). Optimising methods for the preservation, capture and identification of ubiquitin chains and ubiquitylated proteins by immunoblotting. *Biochem. Biophys. Res. Commun.* 466, 1–14. doi: 10.1016/j.bbrc.2015.08.109

Emmerich, C. H., Ordureau, A., Strickson, S., Arthur, J. S., Pedrioli, P. G., Komander, D., et al. (2013). Activation of the canonical IKK complex by K63/M1-linked hybrid ubiquitin chains. *Proc. Natl. Acad. Sci. U.S.A.* 110, 15247–15252. doi: 10.1073/pnas.1314715110

Fiil, B. K., Damgaard, R. B., Wagner, S. A., Keusekotten, K., Fritsch, M., Bekker-Jensen, S., et al. (2013). OTULIN restricts Met1-linked ubiquitination to control innate immune signaling. *Mol. Cell* 50, 818–830. doi: 10.1016/j.molcel.2013.06.004

Finley, D., Bartel, B., and Varshavsky, A. (1989). The tails of ubiquitin precursors are ribosomal proteins whose fusion to ubiquitin facilitates ribosome biogenesis. *Nature* 338, 394–401.

Fiskin, E., Bionda, T., Dikic, I., and Behrends, C. (2016). Global analysis of host and bacterial ubiquitinome in response to *Salmonella* typhimurium infection. *Mol. Cell* 62, 967–981. doi: 10.1016/j.molcel.2016.04.015

Flierman, D., van der Heden van Noort, G. J., Ekkebus, R., Geurink, P. P., Mevissen, T. E., Hospenthal, M. K., et al. (2016). Non-hydrolyzable diubiquitin probes reveal linkage-specific reactivity of deubiquitylating enzymes mediated by S2 pockets. *Cell Chem. Biol.* 23, 472–482. doi: 10.1016/j.chembiol.2016.03.009

Franco, M., Seyfried, N. T., Brand, A. H., Peng, J., and Mayor, U. (2011). A novel strategy to isolate ubiquitin conjugates reveals wide role for ubiquitination during neural development. *Mol. Cell. Proteomics* 10:M110002188. doi: 10.1074/mcp.M110.002188

Fujimuro, M., Sawada, H., and Yokosawa, H. (1994). Production and characterization of monoclonal antibodies specific to multi-ubiquitin chains of polyubiquitinated proteins. *FEBS Lett.* 349, 173–180.

Galisson, F., Mahrouche, L., Courcelles, M., Bonneil, E., Meloche, S., Chelbi-Alix, M. K., et al. (2011). A novel proteomics approach to identify SUMOylated proteins and their modification sites in human cells. *Mol. Cell. Proteomics* 10:M110004796. doi: 10.1074/mcp.M110.004796

Gao, Y., Li, Y., Zhang, C., Zhao, M., Deng, C., Lan, Q., et al. (2016). Enhanced purification of ubiquitinated proteins by engineered tandem hybrid ubiquitin-binding domains (ThUBDs). *Mol. Cell. Proteomics* 15, 1381–1396. doi: 10.1074/mcp.O115.051839

Geurink, P. P., van Tol, B. D., van Dalen, D., Brundel, P. J., Mevissen, T. E., Pruneda, J. N., et al. (2016). Development of diubiquitin-based FRET probes to quantify ubiquitin linkage specificity of deubiquitinating enzymes. *Chembiochem* 17, 816–820. doi: 10.1002/cbic.201600017

Grice, G. L., Lobb, I. T., Weekes, M. P., Gygi, S. P., Antrobus, R., and Nathan, J. A. (2015). The proteasome distinguishes between heterotypic and homotypic lysine-11-linked polyubiquitin chains. *Cell Rep.* 12, 545–553. doi: 10.1016/j.celrep.2015.06.061

Grou, C. P., Pinto, M. P., Mendes, A. V., Domingues, P., and Azevedo, J. E. (2015). The de novo synthesis of ubiquitin: identification of deubiquitinases acting on ubiquitin precursors. *Sci. Rep.* 5:12836. doi: 10.1038/srep12836

Harrigan, J. A., Jacq, X., Martin, N. M., and Jackson, S. P. (2018). Deubiquitylating enzymes and drug discovery: emerging opportunities. *Nat. Rev. Drug Discov.* 17, 57–78. doi: 10.1038/nrd.2017.152

Hendriks, I. A., D'Souza, R. C., Yang, B., Verlaan-de Vries, M., Mann, M., and Vertegaal, A. C. (2014). Uncovering global SUMOylation signaling networks in a site-specific manner. *Nat. Struct. Mol. Biol.* 21, 927–936. doi: 10.1038/nsmb.2890

Herhaus, L., and Dikic, I. (2015). Expanding the ubiquitin code through post-translational modification. *EMBO Rep.* 16, 1071–1083. doi: 10.15252/embr.201540891

Hershko, A., and Ciechanover, A. (1998). The ubiquitin system. *Annu. Rev. Biochem.* 67, 425–479.

Hjerpe, R., Aillet, F., Lopitz-Otsoa, F., Lang, V., England, P., and Rodriguez, M. S. (2009). Efficient protection and isolation of ubiquitylated proteins using tandem ubiquitin-binding entities. *EMBO Rep.* 10, 1250–1258. doi: 10.1038/embor.2009.192

Hodgins, R. R., Ellison, K. S., and Ellison, M. J. (1992). Expression of a ubiquitin derivative that conjugates to protein irreversibly produces phenotypes consistent with a ubiquitin deficiency. *J. Biol. Chem.* 267, 8807–8812.

Hospenthal, M. K., Mevissen, T. E., and Komander, D. (2015). Deubiquitinase-based analysis of ubiquitin chain architecture using Ubiquitin Chain Restriction (UbiCRest). *Nat. Protoc.* 10, 349–361. doi: 10.1038/nprot.2015.018

Husnjak, K., and Dikic, I. (2012). Ubiquitin-binding proteins: decoders of ubiquitin-mediated cellular functions. *Annu. Rev. Biochem.* 81, 291–322. doi: 10.1146/annurev-biochem-051810-094654

Husnjak, K., Elsasser, S., Zhang, N., Chen, X., Randles, L., Shi, Y., et al. (2008). Proteasome subunit Rpn13 is a novel ubiquitin receptor. *Nature* 453, 481–488. doi: 10.1038/nature06926

Iconomou, M., and Saunders, D. N. (2016). Systematic approaches to identify E3 ligase substrates. *Biochem. J.* 473, 4083–4101.

Ikeda, F., Deribe, Y. L., Skanland, S. S., Stieglitz, B., Grabbe, C., Franz-Wachtel, M., et al. (2011). SHARPIN forms a linear ubiquitin ligase complex regulating NF-kappaB activity and apoptosis. *Nature* 471, 637–641. doi: 10.1038/nature09814

Johnson, A., and Vert, G. (2016). Unraveling K63 polyubiquitination networks by sensor-based proteomics. *Plant Physiol.* 171, 1808–1820. doi: 10.1104/pp.16.00619

Kaiser, S. E., Riley, B. E., Shaler, T. A., Trevino, R. S., Becker, C. H., Schulman, H., et al. (2011). Protein standard absolute quantification (PSAQ) method for the measurement of cellular ubiquitin pools. *Nat. Methods* 8, 691–696. doi: 10.1038/nmeth.1649

Kane, L. A., Lazarou, M., Fogel, A. I., Li, Y., Yamano, K., Sarraf, S. A., et al. (2014). PINK1 phosphorylates ubiquitin to activate Parkin E3 ubiquitin ligase activity. *J. Cell Biol.* 205, 143–153. doi: 10.1083/jcb.201402104

Kazlauskaite, A., Kondapalli, C., Gourlay, R., Campbell, D. G., Ritorto, M. S., Hofmann, K., et al. (2014). Parkin is activated by PINK1-dependent phosphorylation of ubiquitin at Ser^{65}. *Biochem. J.* 460, 127–139. doi: 10.1042/BJ20140334

Kim, H. C., and Huibregtse, J. M. (2009). Polyubiquitination by HECT E3s and the determinants of chain type specificity. *Mol. Cell. Biol.* 29, 3307–3318. doi: 10.1128/MCB.00240-09

Kim, W., Bennett, E. J., Huttlin, E. L., Guo, A., Li, J., Possemato, A., et al. (2011). Systematic and quantitative assessment of the ubiquitin-modified proteome. *Mol. Cell* 44, 325–340. doi: 10.1016/j.molcel.2011.08.025

Kirisako, T., Kamei, K., Murata, S., Kato, M., Fukumoto, H., Kanie, M., et al. (2006). A ubiquitin ligase complex assembles linear polyubiquitin chains. *EMBO J.* 25, 4877–4887.

Kirkpatrick, D. S., Gerber, S. A., and Gygi, S. P. (2005). The absolute quantification strategy: a general procedure for the quantification of proteins and post-translational modifications. *Methods* 35, 265–273.

Kliza, K., Taumer, C., Pinzuti, I., Franz-Wachtel, M., Kunzelmann, S., Stieglitz, B., et al. (2017). Internally tagged ubiquitin: a tool to identify linear polyubiquitin-modified proteins by mass spectrometry. *Nat. Methods* 14, 504–512. doi: 10.1038/nmeth.4228

Komander, D., Clague, M. J., and Urbe, S. (2009). Breaking the chains: structure and function of the deubiquitinases. *Nat. Rev. Mol. Cell Biol.* 10, 550–563. doi: 10.1038/nrm2731

Kondapalli, C., Kazlauskaite, A., Zhang, N., Woodroof, H. I., Campbell, D. G., Gourlay, R., et al. (2012). PINK1 is activated by mitochondrial membrane potential depolarization and stimulates Parkin E3 ligase activity by phosphorylating Serine 65. *Open Biol.* 2:120080. doi: 10.1098/rsob.120080

Koszela, J., Pham, N. T., Evans, D., Mann, S., Perez-Pi, I., Shave, S., et al. (2018). Real-time tracking of complex ubiquitination cascades using a fluorescent confocal on-bead assay. *BMC Biol.* 16:88. doi: 10.1186/s12915-018-0554-z

Kotewicz, K. M., Ramabhadran, V., Sjoblom, N., Vogel, J. P., Haenssler, E., Zhang, M., et al. (2017). A single legionella effector catalyzes a multistep ubiquitination pathway to rearrange tubular endoplasmic reticulum for replication. *Cell Host Microbe* 21, 169–181. doi: 10.1016/j.chom.2016.12.007

Koyano, F., Okatsu, K., Kosako, H., Tamura, Y., Go, E., Kimura, M., et al. (2014). Ubiquitin is phosphorylated by PINK1 to activate parkin. *Nature* 510, 162–166. doi: 10.1038/nature13392

Kulathu, Y., and Komander, D. (2012). Atypical ubiquitylation - the unexplored world of polyubiquitin beyond Lys48 and Lys63 linkages. *Nat. Rev. Mol. Cell Biol.* 13, 508–523. doi: 10.1038/nrm3394

Lafont, E., Kantari-Mimoun, C., Draber, P., De Miguel, D., Hartwig, T., Reichert, M., et al. (2017). The linear ubiquitin chain assembly complex regulates TRAIL-induced gene activation and cell death. *EMBO J.* 36, 1147–1166. doi: 10.15252/embj.201695699

Lamoliatte, F., Bonneil, E., Durette, C., Caron-Lizotte, O., Wildemann, D., Zerweck, J., et al. (2013). Targeted identification of SUMOylation sites in human proteins using affinity enrichment and paralog-specific reporter ions. *Mol. Cell. Proteomics* 12, 2536–2550. doi: 10.1074/mcp.M112.025569

Lectez, B., Migotti, R., Lee, S. Y., Ramirez, J., Beraza, N., Mansfield, B., et al. (2014). Ubiquitin profiling in liver using a transgenic mouse with biotinylated ubiquitin. *J. Proteome Res.* 13, 3016–3026. doi: 10.1021/pr5001913

Li, G., Liang, Q., Gong, P., Tencer, A. H., and Zhuang, Z. (2014). Activity-based diubiquitin probes for elucidating the linkage specificity of deubiquitinating enzymes. *Chem. Commun.* 50, 216–218. doi: 10.1039/c3cc47382a

Lim, M., Newman, J. A., Williams, H. L., Masino, L., Aitkenhead, H., Gravard, A. E., et al. (2019). A ubiquitin-binding domain that binds a structural fold distinct from that of ubiquitin. *Structure* 27, 1316–1325.e6. doi: 10.1016/j.str.2019.05.003

Liu, Z., Gong, Z., Jiang, W. X., Yang, J., Zhu, W. K., Guo, D. C., et al. (2015). Lys63-linked ubiquitin chain adopts multiple conformational states for specific target recognition. *eLife* 4:e05767.

Loveless, T. B., Topacio, B. R., Vashisht, A. A., Galaang, S., Ulrich, K. M., Young, B. D., et al. (2015). DNA damage regulates translation through beta-TRCP targeting of CReP. *PLoS Genet.* 11:e1005292. doi: 10.1371/journal.pgen.1005292

Maculins, T., Fiskin, E., Bhogaraju, S., and Dikic, I. (2016). Bacteria-host relationship: ubiquitin ligases as weapons of invasion. *Cell Res.* 26, 499–510. doi: 10.1038/cr.2016.30

Marblestone, J. G., Larocque, J. P., Mattern, M. R., and Leach, C. A. (2012). Analysis of ubiquitin E3 ligase activity using selective polyubiquitin binding proteins. *Biochim. Biophys. Acta* 1823, 2094–2097. doi: 10.1016/j.bbamcr.2012.06.013

Mark, K. G., Loveless, T. B., and Toczyski, D. P. (2016). Isolation of ubiquitinated substrates by tandem affinity purification of E3 ligase-polyubiquitin-binding domain fusions (ligase traps). *Nat. Protoc.* 11, 291–301. doi: 10.1038/nprot.2016.008

Mark, K. G., Simonetta, M., Maiolica, A., Seller, C. A., and Toczyski, D. P. (2014). Ubiquitin ligase trapping identifies an SCF(Saf1) pathway targeting unprocessed vacuolar/lysosomal proteins. *Mol. Cell* 53, 148–161. doi: 10.1016/j.molcel.2013.12.003

Matsumoto, G., Wada, K., Okuno, M., Kurosawa, M., and Nukina, N. (2011). Serine 403 phosphorylation of p62/SQSTM1 regulates selective autophagic clearance of ubiquitinated proteins. *Mol. Cell* 44, 279–289. doi: 10.1016/j.molcel.2011.07.039

Matsumoto, M., Hatakeyama, S., Oyamada, K., Oda, Y., Nishimura, T., and Nakayama, K. I. (2005). Large-scale analysis of the human ubiquitin-related proteome. *Proteomics* 5, 4145–4151.

Matsumoto, M. L., Dong, K. C., Yu, C., Phu, L., Gao, X., Hannoush, R. N., et al. (2012). Engineering and structural characterization of a linear polyubiquitin-specific antibody. *J. Mol. Biol.* 418, 134–144. doi: 10.1016/j.jmb.2011.12.053

Matsumoto, M. L., Wickliffe, K. E., Dong, K. C., Yu, C., Bosanac, I., Bustos, D., et al. (2010). K11-linked polyubiquitination in cell cycle control revealed by a K11 linkage-specific antibody. *Mol. Cell* 39, 477–484. doi: 10.1016/j.molcel.2010.07.001

Mattern, M., Sutherland, J., Kadimisetty, K., Barrio, R., and Rodriguez, M. S. (2019). Using ubiquitin binders to decipher the ubiquitin code. *Trends Biochem. Sci.* 44, 599–615. doi: 10.1016/j.tibs.2019.01.011

McDowell, G. S., and Philpott, A. (2016). New insights into the role of ubiquitylation of proteins. *Int. Rev. Cell Mol. Biol.* 325, 35–88. doi: 10.1016/bs.ircmb.2016.02.002

McGouran, J. F., Gaertner, S. R., Altun, M., Kramer, H. B., and Kessler, B. M. (2013). Deubiquitinating enzyme specificity for ubiquitin chain topology profiled by di-ubiquitin activity probes. *Chem. Biol.* 20, 1447–1455. doi: 10.1016/j.chembiol.2013.10.012

Meierhofer, D., Wang, X., Huang, L., and Kaiser, P. (2008). Quantitative analysis of global ubiquitination in HeLa cells by mass spectrometry. *J. Proteome Res.* 7, 4566–4576. doi: 10.1021/pr800468j

Metzger, M. B., Hristova, V. A., and Weissman, A. M. (2012). HECT and RING finger families of E3 ubiquitin ligases at a glance. *J. Cell Sci.* 125, 531–537.

Mevissen, T. E. T., and Komander, D. (2017). Mechanisms of deubiquitinase specificity and regulation. *Annu. Rev. Biochem.* 86, 159–192. doi: 10.1146/annurev-biochem-061516-044916

Meyer, H. J., and Rape, M. (2014). Enhanced protein degradation by branched ubiquitin chains. *Cell* 157, 910–921. doi: 10.1016/j.cell.2014.03.037

Michel, M. A., Swatek, K. N., Hospenthal, M. K., and Komander, D. (2017). Ubiquitin linkage-specific affimers reveal insights into K6-linked ubiquitin signaling. *Mol. Cell* 68, 233–246.e5. doi: 10.1016/j.molcel.2017.08.020

Mulder, M. P., El Oualid, F., ter Beek, J., and Ovaa, H. (2014). A native chemical ligation handle that enables the synthesis of advanced activity-based probes: diubiquitin as a case study. *Chembiochem* 15, 946–949. doi: 10.1002/cbic.201402012

Mulder, M. P., Witting, K., Berlin, I., Pruneda, J. N., Wu, K. P., Chang, J. G., et al. (2016). A cascading activity-based probe sequentially targets E1-E2-E3 ubiquitin enzymes. *Nat. Chem. Biol.* 12, 523–530. doi: 10.1038/nchembio.2084

Nakayasu, E. S., Sydor, M. A., Brown, R. N., Sontag, R. L., Sobreira, T. J., Slysz, G. W., et al. (2015). Identification of *Salmonella* typhimurium deubiquitinase SseL substrates by immunoaffinity enrichment and quantitative proteomic analysis. *J. Proteome Res.* 14, 4029–4038. doi: 10.1021/acs.jproteome.5b00574

Nakazawa, S., Oikawa, D., Ishii, R., Ayaki, T., Takahashi, H., Takeda, H., et al. (2016). Linear ubiquitination is involved in the pathogenesis of optineurin-associated amyotrophic lateral sclerosis. *Nat. Commu.* 7:12547. doi: 10.1038/ncomms12547

Newton, K., Matsumoto, M. L., Ferrando, R. E., Wickliffe, K. E., Rape, M., Kelley, R. F., et al. (2012). Using linkage-specific monoclonal antibodies to analyze cellular ubiquitylation. *Methods Mol. Biol.* 832, 185–196. doi: 10.1007/978-1-61779-474-2_13

Newton, K., Matsumoto, M. L., Wertz, I. E., Kirkpatrick, D. S., Lill, J. R., Tan, J., et al. (2008). Ubiquitin chain editing revealed by polyubiquitin linkage-specific antibodies. *Cell* 134, 668–678. doi: 10.1016/j.cell.2008.07.039

Nielsen, M. L., Vermeulen, M., Bonaldi, T., Cox, J., Moroder, L., and Mann, M. (2008). Iodoacetamide-induced artifact mimics ubiquitination in mass spectrometry. *Nat. Methods* 5, 459–460.

O'Connor, H. F., Lyon, N., Leung, J. W., Agarwal, P., Swaim, C. D., Miller, K. M., et al. (2015). Ubiquitin-activated interaction traps (UBAITs) identify E3 ligase binding partners. *EMBO Rep.* 16, 1699–1712. doi: 10.15252/embr.201540620

O'Connor, H. F., Swaim, C. D., Canadeo, L. A., and Huibregtse, J. M. (2018). Ubiquitin-activated interaction traps (UBAITs): tools for capturing protein-protein interactions. *Methods Mol. Biol.* 1844, 85–100. doi: 10.1007/978-1-4939-8706-1_7

Ohtake, F., Saeki, Y., Sakamoto, K., Ohtake, K., Nishikawa, H., Tsuchiya, H., et al. (2015). Ubiquitin acetylation inhibits polyubiquitin chain elongation. *EMBO Rep.* 16, 192–201. doi: 10.15252/embr.201439152

Okatsu, K., Sato, Y., Yamano, K., Matsuda, N., Negishi, L., Takahashi, A., et al. (2018). Structural insights into ubiquitin phosphorylation by PINK1. *Sci. Rep.* 8:10382. doi: 10.1038/s41598-018-28656-8

Ordureau, A., Paulo, J. A., Zhang, W., Ahfeldt, T., Zhang, J., Cohn, E. F., et al. (2018). Dynamics of PARKIN-dependent mitochondrial ubiquitylation in induced neurons and model systems revealed by digital snapshot proteomics. *Mol. Cell* 70, 211–227.e8. doi: 10.1016/j.molcel.2018.03.012

Ozkaynak, E., Finley, D., and Varshavsky, A. (1984). The yeast ubiquitin gene: head-to-tail repeats encoding a polyubiquitin precursor protein. *Nature* 312, 663–666.

Pao, K. C., Wood, N. T., Knebel, A., Rafie, K., Stanley, M., Mabbitt, P. D., et al. (2018). Activity-based E3 ligase profiling uncovers an E3 ligase with esterification activity. *Nature* 556, 381–385. doi: 10.1038/s41586-018-0026-1

Paraskevopoulos, K., Kriegenburg, F., Tatham, M. H., Rosner, H. I., Medina, B., Larsen, I. B., et al. (2014). Dss1 is a 26S proteasome ubiquitin receptor. *Mol. Cell* 56, 453–461. doi: 10.1016/j.molcel.2014.09.008

Park, S. H., Bolender, N., Eisele, F., Kostova, Z., Takeuchi, J., Coffino, P., et al. (2007). The cytoplasmic Hsp70 chaperone machinery subjects misfolded and endoplasmic reticulum import-incompetent proteins to degradation via the ubiquitin-proteasome system. *Mol. Biol. Cell* 18, 153–165.

Peng, J., Schwartz, D., Elias, J. E., Thoreen, C. C., Cheng, D., Marsischky, G., et al. (2003). A proteomics approach to understanding protein ubiquitination. *Nat. Biotechnol.* 21, 921–926.

Pickart, C. M., Kasperek, E. M., Beal, R., and Kim, A. (1994). Substrate properties of site-specific mutant ubiquitin protein (G76A) reveal unexpected mechanistic features of ubiquitin-activating enzyme (E1). *J. Biol. Chem.* 269, 7115–7123.

Pilli, M., Arko-Mensah, J., Ponpuak, M., Roberts, E., Master, S., Mandell, M. A., et al. (2012). TBK-1 promotes autophagy-mediated antimicrobial defense by controlling autophagosome maturation. *Immunity* 37, 223–234. doi: 10.1016/j.immuni.2012.04.015

Pinto, M. J., Pedro, J. R., Costa, R. O., and Almeida, R. D. (2016). Visualizing K48 ubiquitination during presynaptic formation by ubiquitination-induced fluorescence complementation (UiFC). *Front. Mol. Neurosci.* 9:43. doi: 10.3389/fnmol.2016.00043

Pinto-Fernandez, A., Davis, S., Schofield, A. B., Scott, H. C., Zhang, P., Salah, E., et al. (2019). Comprehensive landscape of active deubiquitinating enzymes profiled by advanced chemoproteomics. *Front. Chem.* 7:592. doi: 10.3389/fchem.2019.00592

Pruneda, J. N., Durkin, C. H., Geurink, P. P., Ovaa, H., Santhanam, B., Holden, D. W., et al. (2016). The molecular basis for ubiquitin and ubiquitin-like specificities in bacterial effector proteases. *Mol. Cell* 63, 261–276. doi: 10.1016/j.molcel.2016.06.015

Qiu, J., Sheedlo, M. J., Yu, K., Tan, Y., Nakayasu, E. S., Das, C., et al. (2016). Ubiquitination independent of E1 and E2 enzymes by bacterial effectors. *Nature* 533, 120–124. doi: 10.1038/nature17657

Rahighi, S., and Dikic, I. (2012). Selectivity of the ubiquitin-binding modules. *FEBS Lett.* 586, 2705–2710. doi: 10.1016/j.febslet.2012.04.053

Reyes-Turcu, F. E., Horton, J. R., Mullally, J. E., Heroux, A., Cheng, X., and Wilkinson, K. D. (2006). The ubiquitin binding domain ZnF UBP recognizes the C-terminal diglycine motif of unanchored ubiquitin. *Cell* 124, 1197–1208.

Reyes-Turcu, F. E., Ventii, K. H., and Wilkinson, K. D. (2009). Regulation and cellular roles of ubiquitin-specific deubiquitinating enzymes. *Annu. Rev. Biochem.* 78, 363–397. doi: 10.1146/annurev.biochem.78.082307.091526

Reyes-Turcu, F. E., and Wilkinson, K. D. (2009). Polyubiquitin binding and disassembly by deubiquitinating enzymes. *Chem. Rev.* 109, 1495–1508.

Richter, B., Sliter, D. A., Herhaus, L., Stolz, A., Wang, C., Beli, P., et al. (2016). Phosphorylation of OPTN by TBK1 enhances its binding to Ub chains and promotes selective autophagy of damaged mitochondria. *Proc. Natl. Acad. Sci. U.S.A.* 113, 4039–4044. doi: 10.1073/pnas.1523926113

Roux, K. J., Kim, D. I., Raida, M., and Burke, B. (2012). A promiscuous biotin ligase fusion protein identifies proximal and interacting proteins in mammalian cells. *J. Cell Biol.* 196, 801–810. doi: 10.1083/jcb.201112098

Satpathy, S., Wagner, S. A., Beli, P., Gupta, R., Kristiansen, T. A., Malinova, D., et al. (2015). Systems-wide analysis of BCR signalosomes and downstream phosphorylation and ubiquitylation. *Mol. Syst. Biol.* 11:810. doi: 10.15252/msb.20145880

Scott, D., Garner, T. P., Long, J., Strachan, J., Mistry, S. C., Bottrill, A. R., et al. (2016). Mass spectrometry insights into a tandem ubiquitin-binding domain hybrid engineered for the selective recognition of unanchored polyubiquitin. *Proteomics* 16, 1961–1969. doi: 10.1002/pmic.201600067

Shi, Y., Chan, D. W., Jung, S. Y., Malovannaya, A., Wang, Y., and Qin, J. (2011). A data set of human endogenous protein ubiquitination sites. *Mol. Cell. Proteomics* 10:M110002089. doi: 10.1074/mcp.M110.002089

Shiba-Fukushima, K., Imai, Y., Yoshida, S., Ishihama, Y., Kanao, T., Sato, S., et al. (2012). PINK1-mediated phosphorylation of the Parkin ubiquitin-like domain primes mitochondrial translocation of Parkin and regulates mitophagy. *Sci. Rep.* 2:1002. doi: 10.1038/srep01002

Sims, J. J., Scavone, F., Cooper, E. M., Kane, L. A., Youle, R. J., Boeke, J. D., et al. (2012). Polyubiquitin-sensor proteins reveal localization and linkage-type dependence of cellular ubiquitin signaling. *Nat. Methods* 9, 303–309. doi: 10.1038/nmeth.1888

Sloper-Mould, K. E., Jemc, J. C., Pickart, C. M., and Hicke, L. (2001). Distinct functional surface regions on ubiquitin. *J. Biol. Chem.* 276, 30483–30489.

Stamenova, S. D., French, M. E., He, Y., Francis, S. A., Kramer, Z. B., and Hicke, L. (2007). Ubiquitin binds to and regulates a subset of SH3 domains. *Mol. Cell* 25, 273–284.

Swatek, K. N., and Komander, D. (2016). Ubiquitin modifications. *Cell Res.* 26, 399–422. doi: 10.1038/cr.2016.39

Swatek, K. N., Usher, J. L., Kueck, A. F., Gladkova, C., Mevissen, T. E. T., Pruneda, J. N., et al. (2019). Insights into ubiquitin chain architecture using Ub-clipping. *Nature* 572, 533–537. doi: 10.1038/s41586-019-1482-y

Tsuchiya, H., Burana, D., Ohtake, F., Arai, N., Kaiho, A., Komada, M., et al. (2018). Ub-ProT reveals global length and composition of protein ubiquitylation in cells. *Nat. Commun.* 9:524. doi: 10.1038/s41467-018-02869-x

Valkevich, E. M., Sanchez, N. A., Ge, Y., and Strieter, E. R. (2014). Middle-down mass spectrometry enables characterization of branched ubiquitin chains. *Biochemistry* 53, 4979–4989. doi: 10.1021/bi5006305

van Wijk, S. J., Fiskin, E., Putyrski, M., Pampaloni, F., Hou, J., Wild, P., et al. (2012). Fluorescence-based sensors to monitor localization and functions of linear and K63-linked ubiquitin chains in cells. *Mol. Cell* 47, 797–809. doi: 10.1016/j.molcel.2012.06.017

van Wijk, S. J., Fulda, S., Dikic, I., and Heilemann, M. (2019). Visualizing ubiquitination in mammalian cells. *EMBO Rep.* 20:e46520. doi: 10.15252/embr.201846520

Varshavsky, A. (2006). The early history of the ubiquitin field. *Protein Sci.* 15, 647–654.

Vasilescu, J., Smith, J. C., Ethier, M., and Figeys, D. (2005). Proteomic analysis of ubiquitinated proteins from human MCF-7 breast cancer cells by immunoaffinity purification and mass spectrometry. *J. Proteome Res.* 4, 2192–2200.

Vijay-Kumar, S., Bugg, C. E., and Cook, W. J. (1987). Structure of ubiquitin refined at 1.8 A resolution. *J. Mol. Biol.* 194, 531–544.

Wagner, S., Carpentier, I., Rogov, V., Kreike, M., Ikeda, F., Lohr, F., et al. (2008). Ubiquitin binding mediates the NF-kappaB inhibitory potential of ABIN proteins. *Oncogene* 27, 3739–3745. doi: 10.1038/sj.onc.1211042

Wagner, S. A., Beli, P., Weinert, B. T., Nielsen, M. L., Cox, J., Mann, M., et al. (2011). A proteome-wide, quantitative survey of in vivo ubiquitylation sites reveals widespread regulatory roles. *Mol. Cell. Proteomics* 10:M111013284. doi: 10.1074/mcp.M111.013284

Walden, H., and Rittinger, K. (2018). RBR ligase-mediated ubiquitin transfer: a tale with many twists and turns. *Nat. Struct. Mol. Biol.* 25, 440–445. doi: 10.1038/s41594-018-0063-3

Walsh, C. T., Garneau-Tsodikova, S., and Gatto, G. J. Jr. (2005). Protein posttranslational modifications: the chemistry of proteome diversifications. *Angew. Chem.* 44, 7342–7372.

Walton, A., Stes, E., Cybulski, N., Van Bel, M., Inigo, S., Durand, A. N., et al. (2016). It's time for some "site"-seeing: novel tools to monitor the ubiquitin landscape in *Arabidopsis thaliana*. *Plant Cell* 28, 6–16. doi: 10.1105/tpc.15.00878

Wang, J., and Maldonado, M. A. (2006). The ubiquitin-proteasome system and its role in inflammatory and autoimmune diseases. *Cell. Mol. Immunol.* 3, 255–261.

Watt, G. F., Scott-Stevens, P., and Gaohua, L. (2019). Targeted protein degradation in vivo with proteolysis targeting chimeras: current status and future considerations. *Drug Discov. Today Technol.* 31, 69–80. doi: 10.1016/j.ddtec.2019.02.005

Wauer, T., Simicek, M., Schubert, A., and Komander, D. (2015a). Mechanism of phospho-ubiquitin-induced PARKIN activation. *Nature* 524, 370–374.

Wauer, T., Swatek, K. N., Wagstaff, J. L., Gladkova, C., Pruneda, J. N., Michel, M. A., et al. (2015b). Ubiquitin Ser65 phosphorylation affects ubiquitin structure, chain assembly and hydrolysis. *EMBO J.* 34, 307–325. doi: 10.15252/embj.201489847

Williams, C., van den Berg, M., Sprenger, R. R., and Distel, B. (2007). A conserved cysteine is essential for Pex4p-dependent ubiquitination of the peroxisomal import receptor Pex5p. *J. Biol. Chem.* 282, 22534–22543.

Winget, J. M., and Mayor, T. (2010). The diversity of ubiquitin recognition: hot spots and varied specificity. *Mol. Cell* 38, 627–635. doi: 10.1016/j.molcel.2010.05.003

Witting, K. F., Mulder, M. P. C., and Ovaa, H. (2017). Advancing our understanding of ubiquitination using the Ub-toolkit. *J. Mol. Biol.* 429, 3388–3394. doi: 10.1016/j.jmb.2017.04.002

Xu, G., Paige, J. S., and Jaffrey, S. R. (2010). Global analysis of lysine ubiquitination by ubiquitin remnant immunoaffinity profiling. *Nat. Biotechnol.* 28, 868–873. doi: 10.1038/nbt.1654

Xu, L., Fan, J., Wang, Y., Zhang, Z., Fu, Y., Li, Y. M., et al. (2019). An activity-based probe developed by a sequential dehydroalanine formation strategy targets HECT E3 ubiquitin ligases. *Chem. Commun.* 55, 7109–7112. doi: 10.1039/c9cc03739j

Xu, P., and Peng, J. (2008). Characterization of polyubiquitin chain structure by middle-down mass spectrometry. *Anal. Chem.* 80, 3438–3444. doi: 10.1021/ac800016w

Yang, C. S., Jividen, K., Spencer, A., Dworak, N., Ni, L., Oostdyk, L. T., et al. (2017). Ubiquitin modification by the E3 ligase/ADP-ribosyltransferase Dtx3L/Parp9. *Mol. Cell* 66, 503–516.e5. doi: 10.1016/j.molcel.2017.04.028

Yang, L., Chen, J., Huang, X., Zhang, E., He, J., and Cai, Z. (2018). Novel insights into E3 ubiquitin ligase in cancer chemoresistance. *Am. J. Med. Sci.* 355, 368–376. doi: 10.1016/j.amjms.2017.12.012

Yau, R. G., Doerner, K., Castellanos, E. R., Haakonsen, D. L., Werner, A., Wang, N., et al. (2017). Assembly and function of heterotypic ubiquitin chains in cell-cycle and protein quality control. *Cell* 171, 918–933.e20. doi: 10.1016/j.cell.2017.09.040

Zhang, X., Smits, A. H., van Tilburg, G. B., Jansen, P. W., Makowski, M. M., Ovaa, H., et al. (2017). An interaction landscape of ubiquitin signaling. *Mol. Cell* 65, 941–955.e8. doi: 10.1016/j.molcel.2017.01.004

Zhuang, M., Guan, S., Wang, H., Burlingame, A. L., and Wells, J. A. (2013). Substrates of IAP ubiquitin ligases identified with a designed orthogonal E3 ligase, the NEDDylator. *Mol. Cell* 49, 273–282. doi: 10.1016/j.molcel.2012.10.022

Conflict of Interest: The authors declare that the research was conducted in the absence of any commercial or financial relationships that could be construed as a potential conflict of interest.

frontiers in Chemistry

REVIEW
published: 11 June 2020
doi: 10.3389/fchem.2020.00485

Strategies to Investigate Ubiquitination in Huntington's Disease

*Karen A. Sap and Eric A. Reits**

Department of Medical Biology, Amsterdam UMC, Amsterdam, Netherlands

Many neurodegenerative disorders including Huntington's Disease are hallmarked by intracellular protein aggregates that are decorated by ubiquitin and different ubiquitin ligases and deubiquitinating enzymes. The protein aggregates observed in Huntington's Disease are caused by a polyglutamine expansion in the N-terminus of the huntingtin protein (Htt). Improving the degradation of mutant Htt via the Ubiquitin Proteasome System prior to aggregation would be a therapeutic strategy to delay or prevent the onset of Huntington's Disease for which there is currently no cure. Here we examine the current approaches used to study the ubiquitination of both soluble Htt as well as insolubilized Htt present in aggregates, and we describe what is known about involved (de)ubiquitinating enzymes. Furthermore, we discuss novel methodologies to study the dynamics of Htt ubiquitination in living cells using fluorescent ubiquitin probes, to identify and quantify Htt ubiquitination by mass spectrometry-based approaches, and various approaches to identify involved ubiquitinating enzymes.

Keywords: ubiquitin, Huntington's disease, huntingtin, neurodegenerative disease, proteasome, applications, toolbox

OPEN ACCESS

Edited by:
Zhihao Zhuang,
University of Delaware, United States

Reviewed by:
Zufeng Guo,
Johns Hopkins University, United States
T. Ashton Cropp,
Virginia Commonwealth University, United States

***Correspondence:**
Eric A. Reits
e.a.reits@amsterdamumc.nl

Specialty section:
This article was submitted to Chemical Biology, a section of the journal Frontiers in Chemistry

Received: *21 February 2020*
Accepted: *11 May 2020*
Published: *11 June 2020*

Citation:
Sap KA and Reits EA (2020) Strategies to Investigate Ubiquitination in Huntington's Disease. Front. Chem. 8:485. doi: 10.3389/fchem.2020.00485

INTRODUCTION

Protein Ubiquitination

Ubiquitin is a highly conserved small modular protein consisting of 76 amino acids that can be attached to other proteins as a post translational modification (PTM). Ubiquitination can modulate the properties of the target molecule, such as its cellular localization, interaction partners, protein activity, or it can send the target protein for degradation. As such ubiquitination controls major cellular processes including DNA repair, transcriptional regulation, cell cycle, protein turnover, and stress response. Protein ubiquitination is selectively mediated via the sequential action of three enzymes. First, ubiquitin is activated by a thioester bond formation with an internal active site cysteine residue of an E1 ubiquitin-activating enzyme in an ATP dependent manner. The activated ubiquitin is then transferred from the E1 enzyme to the cysteine residue of an E2 ubiquitin conjugating enzyme. Finally, an E3 ubiquitin ligase catalyzes the transfer of ubiquitin to specific target proteins (Hershko and Ciechanover, 1998). More than 600 different E3 ligases have been identified and they account for a high selectivity toward target protein ubiquitination. There are three main types of E3 ligases: RING/U-box ligases, RING-between-RING (RBR) ligases and HECT ligases, which have a different mode of action for the transfer of ubiquitin to target proteins. RING-type ligases transfer ubiquitin directly from the E2 enzyme to the target protein, while HECT-type ligases associate with ubiquitin via their active site cysteine before transferring it to the target protein. The RBR ligases use a combination of both strategies. These ligases harbor 2 RING

domains, of which the RING1 domain is used to associate with an E2 enzyme while the RING2 domain associates with ubiquitin via its active site cysteine, before ubiquitin is transferred to the target protein.

Ubiquitin associates with its C-terminal glycine residue to target proteins. The canonical site of isopeptide bond formation for ubiquitin is the epsilon-amino group of a lysine residue. Other residues that can become a target for ubiquitination are protein N-terminal methionine residues, cysteine, serine, and threonine residues (McDowell and Philpott, 2013). Proteins can become ubiquitinated with a single ubiquitin molecule, also called monoubiquitination, or with two or multiple ubiquitin molecules each bound to different target sites, which is called multi-monoubiquitination. Alternatively, proteins can become polyubiquitinated when ubiquitin associates with other ubiquitin molecules on the target protein thereby forming a polyubiquitin chain. Several residues of ubiquitin can be used for polyubiquitin chain formation, including its N-terminal methionine residue (M1) as well as several internal lysine residues: K6, K11, K27, K29, K33, K48, and K63. These different chains display different structures, thereby giving different signals which determines the target protein's fate (Akutsu et al., 2016). For instance, K48 and K11 polyubiquitination are associated with proteasome-mediated degradation, while K6 and K63 polyubiquitination play a role in DNA repair. Polyubiquitin chains could be formed through one single ubiquitin linkage type (homotypic) or via different ubiquitin linkage types (heterotypic). Heterotypic polyubiquitin chains could furthermore be mixed and/or branched, and contain ubiquitin-like proteins, like Small Ubiquitin-like Modifier (SUMO). SUMO is a ubiquitin-like protein that also associates with lysine residues on target proteins, and thereby it can affect multiple cellular processes such as protein translocation, DNA damage response and cell cycle progression. SUMO-targeted ubiquitin ligases (STUBLs) can attach ubiquitin to proteins that are already SUMOylated and target them for ubiquitin-dependent degradation (Uzunova et al., 2007). Finally, ubiquitin can be modified with other PTMs such as phosphorylation, SUMOylation, acetylation, and neddylation (Swatek and Komander, 2016). This all together makes ubiquitination a versatile modification, also called the ubiquitin code, and is reviewed in great detail elsewhere (Yau and Rape, 2016).

Protein ubiquitination can be reversed by deubiquitinating enzymes or DUBs which can cleave the peptide or isopeptide bond between a conjugated ubiquitin molecule and the modified protein. In humans over 100 different DUBs have been identified and they show selectivity toward specific protein substrates or toward specific polyubiquitin linkage types. The latter category can be divided in different subgroups, including DUBs that cleave within chains (endo-DUB-activity), DUBs that remove ubiquitin molecules from the end of polyubiquitin chains (exo-DUB activity), DUBs that prefer a specific chain length, and finally, DUBs that cleave off entire polyubiquitin chains. In general, members of the USP family of DUBs show little specificity for polyubiquitin linkage types, while members of the OTU family often display preferences for diverse polyubiquitin chain types. For instance, OTUB1 has a preference for K48-polyubiquitin linkages, while OTUD7B/Cezanne cleaves K11 ubiquitin linkages. Polyubiquitin linkage type specific DUBs have been elegantly reviewed elsewhere (Clague et al., 2019), but it is clear that the action of DUBs can suppress the abundance of polyubiquitinated proteins in the cell, thereby influencing the regulation of important cellular processes such as protein degradation and thus protein turnover rates. The important role of (de)ubiquitinating enzymes in selective protein turnover is also reflected in numerous protein misfolding disorders when efficient ubiquitination and turnover of particular proteins is impaired either due to mutations in involved (de)ubiquitinating enzymes or in disease-related target proteins. Mutations in E3 ligases and DUBs are linked to particular disorders, including the DUB ataxin-3 (Spinocerebellar ataxia 3) (Kawaguchi et al., 1994) and the E3 ligase Parkin (familiar form of Parkinson's Disease) (Kitada et al., 1998), which affects efficient target protein recognition and subsequent ubiquitination, thereby limiting protein degradation via the proteasome and autophagy. In addition, mutations in disease-related proteins including the Htt protein in Huntington's Disease (HD) results in the generation of aggregation-prone protein (fragments). Many neurodegenerative disorders are hallmarked by intracellular protein aggregates, and while these aggregates or inclusion bodies (IBs) are being decorated with ubiquitin, the turn-over of the disease-related proteins is apparently not efficient enough to prevent their accumulation. Due to the monogenetic cause, the availability of numerous *in vitro* and *in vivo* models, and the various techniques to monitor intracellular protein aggregates, HD became a commonly-used model to study ubiquitination dynamics and the role of the Ubiquitin Proteasome System (UPS) in protein misfolding diseases.

Huntington's Disease

HD is one of nine polyglutamine (polyQ) diseases, and is caused by an expansion of a CAG trinucleotide repeat in the exon-1 region of the *Huntingtin* (*Htt*) gene (MacDonald et al., 1993). The wild-type protein contains 6-35 polyQ repeats, while an expansion of more than 39 polyQ repeats in the mHtt protein causes HD (Finkbeiner, 2011). The polyQ expansion makes the protein aggregation prone and the aggregation of mHtt into IBs are a hallmark for the disease (Imarisio et al., 2008; Finkbeiner, 2011). The polyQ region is located close to the N-terminus of the Htt protein, which contains 17 N-terminal amino acids including 3 lysine residues, followed by the polyQ region and a polyproline region (Finkbeiner, 2011). Proteolysis of mHtt results in the formation of different mHtt protein fragments of which the N-terminal exon1 fragment containing the polyQ expansion was found to be the most pathogenic and is also observed in

Abbreviations: ABPs, activity-based probes; APEX, engineered ascorbate peroxidase; BioID, proximity-dependent biotin identification; DUBs, deubiquitinating enzymes; HD, Huntington's disease; Htt, huntingtin; IB, inclusion body; iPSCs, induced pluripotent stem cells; mHtt, mutant huntingtin; PolyQ, polyglutamine; PROTACs, proteolysis targeting chimeras; PTM, post-translational modification; UBA, ubiquitin-associated domain; UPS, ubiquitin-proteasome system.

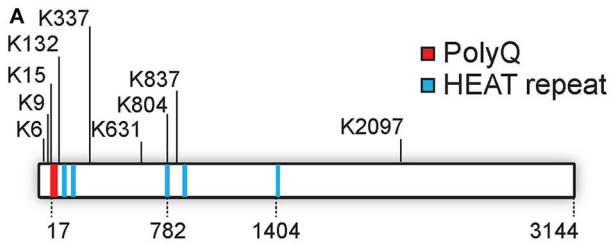

B

Ub site	Reference
K6, K9, K15	Steffan *et al.*, 2004
K6, K9, K132, K804, K837	Sap *et al.*, 2019
K337	Yau *et al.*, 2017
K631, K2097	Koyuncu *et al.*, 2018

FIGURE 1 | Overview of identified Htt ubiquitination sites**. (A)** Overview of identified Htt ubiquitination sites. **(B)** Overview of published studies on Htt ubiquitination site identification.

fibrillar aggregates in brains of HD patients (DiFiglia et al., 1997; Schilling et al., 2007; Landles et al., 2010) and overexpression of mutant Htt exon1 results in HD-like symptoms in mice (Mangiarini et al., 1996). The aggregation-prone fragments of mHtt can be present in cells as monomers, soluble oligomers or in insoluble aggregates including the insoluble IBs. The current model is that especially soluble oligomeric mHtt species are toxic to the cell, while large aggregates of mHtt sequester proteins from their normal cellular environment, thereby interfering with important processes such as transcriptional regulation (Schaffar et al., 2004), proteostasis (Park et al., 2013), and transport (Trushina et al., 2004). However, mHtt aggregates have also been described as protective as they reduce the level of toxic soluble mHtt species in the cell (Arrasate et al., 2004). Additionally, soluble mHtt induced apoptosis was found to be reduced by mHtt IB formation and led to a slower death by necrosis, which also suggests that IB formation functions as a rescue mechanism (Ramdzan et al., 2017).

Several PTMs of Htt, including phosphorylation, SUMOylation, ubiquitination, acetylation, and palmitoylation have been identified (as reviewed by Ehrnhoefer et al., 2011; Saudou and Humbert, 2016). Many PTMs are localized at the N-terminal region of Htt, and include acetylation, SUMOylation, and ubiquitination at lysines 6, 9, and 15 and phosphorylation at threonine 3 as well as at serines 13 and 16. These modifications can affect the subcellular localization, aggregation and clearance of Htt (Steffan et al., 2004; Thompson et al., 2009; Maiuri et al., 2013; DeGuire et al., 2018). Most PTMs were found to be localized in clusters within predicted unstructured domains and not in the structured HEAT repeats as determined by using label free quantitative mass spectrometry (Ratovitski et al., 2017). In addition, mutations in various phosphorylation sites located in protease-sensitive domains on the Htt protein affected cellular toxicity, and are thus important functional regions (Arbez et al., 2017). While various studies have mapped numerous phosphorylation and acetylation sites, the number of identified ubiquitination sites in Htt is so far limited to K6, K9, K15, K132, K337, K631, K804, K837, and K2097 (Steffan et al., 2004; Yau et al., 2017; Koyuncu et al., 2018; Sap et al., 2019; **Figures 1A,B**). Ubiquitination and SUMOylation of the N-terminus of mHtt was found to affect both aggregation and HD pathology in cells although the mechanism is still unclear (Steffan et al., 2004).

Htt Is a Target for Ubiquitin-Proteasome-System and Autophagy Dependent Degradation

Htt IBs are enriched with components of the protein quality control machinery including ubiquitin, proteasome complexes, and chaperones (DiFiglia et al., 1997; Wyttenbach et al., 2000). A decrease in proteostasis and quality control during aging are thought to play a role in the development and progression of HD, which may explain that the onset of HD starts typically at the 4th decade of life, although the mutant Htt protein is already expressed prior to birth (Arrasate and Finkbeiner, 2012). Several studies have shown that both wild-type Htt and mHtt can be degraded by both the UPS and via autophagosomal pathways. For example, mHtt protein fragments can be degraded by the proteasome, as shown by *in vitro* degradation assays using purified mHtt and proteasomes (Juenemann et al., 2013) or in cells (Bhat et al., 2014). Targeting mHtt to the proteasome by the N-end rule, or by using Atg5 knock-out MEF cells with impaired autophagy also shows efficient proteasomal degradation of mHtt (Juenemann et al., 2013). Inhibition of the proteasome increased the number of Htt aggregates in cells and in induced pluripotent stem cells (iPSCs) generated from HD-patients, which can be quantified by microscopy or filter retardation assays (Wyttenbach et al., 2000; Waelter et al., 2001; Koyuncu et al., 2018). Furthermore, protein levels of both normal and mutant full length Htt were increased by proteasome inhibition in heterozygous iPSCs (Koyuncu et al., 2018). Interestingly, longer mHtt fragments (508 a.a.) appear to be better targets for proteasomal degradation when compared to smaller fragments including Htt exon1 (Bhat et al., 2014) which might be due to the presence of unstructured HEAT-like repeat motifs in mHtt that facilitate initiation of proteasomal degradation. Htt levels are also regulated via autophagy, as shown by autophagy inhibition by 3-methyladenine (3-MA) and bafilomycin which increased the level of soluble mHtt protein fragments in striatal cells, as observed by SDS-PAGE Western blot (WB). Also, the number of cells with aggregates increased upon these treatments, as observed by microscopy (Qin et al., 2003), although autophagy inhibition also impairs protein degradation via the UPS (Korolchuk et al., 2009). The p62/SQSTM1 protein plays a role in targeting polyubiquitinated protein aggregates for degradation via the autophagy pathway (Bjørkøy et al., 2005), but the accumulation of the p62/SQSTM1 protein due to autophagy inhibition can also inhibit the clearance of ubiquitinated proteins destined for proteasomal degradation. Stimulation of autophagy with rapamycin or serum reduction lowered the levels of the

Htt protein, and fasting has been proposed in order to induce autophagy and thereby the clearance of mHtt (Ehrnhoefer et al., 2018). Concluding, Htt appears to be a target for both the UPS and autophagy, and enhanced selective degradation of mHtt via these pathways might be a therapeutic strategy to prevent or delay the onset of HD, with a key role for ubiquitin to target Htt for degradation. Here we give an overview of the current status of research focused on Htt ubiquitination, describe tools that are used to study ubiquitination of both soluble and insoluble mHtt, and discuss various developments including the development of novel tools such as proximity-dependent biotin identification (BioID), engineered ascorbate peroxidase (APEX), tandem ubiquitin binding entities (TUBEs), and proteolysis targeting chimeras (PROTACs).

TOOLS TO STUDY UBIQUITINATION OF SOLUBLE AND INSOLUBLE HTT

Methods to Study Aggregated Htt Ubiquitination

The mHtt protein can be present in either a soluble or insoluble fraction, and there are several methods available that one can use to study the insoluble fraction. Mutant Htt aggregates and IBs can be visualized using microscopy assays including immunostaining and fluorescently-tagged proteins, and various biochemical methodologies can be used to study differences in levels of mHtt aggregation. When studying the ubiquitination of Htt it is of importance to separate the soluble and insoluble fractions efficiently as aggregated proteins might be ubiquitinated differently when compared to their soluble counterparts. The use of a mild lysis buffer, for instance buffers based on 1% Triton X-100, was found to be suitable to separate the soluble fraction from the insoluble fraction (Ochaba et al., 2018). In contrast, stronger detergents such as SDS can solubilize the outer layer of aggregates, which would subsequently contaminate the soluble fraction, although it is a suitable protocol to access and study the ubiquitination of the inner core of the aggregates (Juenemann et al., 2015). Two frequently used biochemical techniques to study Htt aggregation are the filter retardation assay or filter trap assay, and the soluble/insoluble assay or solubilization assay. With a filter retardation assay, lysates are filtered through a cellulose acetate membrane, whereby the soluble fraction goes through the filter, while the insoluble fraction, including the IBs, remains on the filter allowing subsequent immunostaining similar to WB analysis (Wanker et al., 1999). Determining ubiquitination of mHtt aggregates by fluorescence or electron microscopy and the filter retardation assay can be performed using antibodies directed to ubiquitin or directed to specific polyubiquitin linkages. However, the obtained signal could be derived from ubiquitinated Htt but also from co-sequestered proteins that are modified by ubiquitin, and is thus not a proof for direct ubiquitination of Htt itself. Here, the soluble/insoluble assay has the advantage over the filter retardation assay to study PTMs in both the soluble and insoluble fractions (Juenemann et al., 2015). Briefly, in this assay the cell lysates containing 1.5% SDS are boiled after which the soluble and insoluble fractions are separated by centrifugation, and subsequently the SDS-insoluble fraction is dissolved and solubilized in 100% formic acid (Carra et al., 2008). Another advantage of the soluble/insoluble assay is that the samples are resolved by SDS-PAGE which gives information about the molecular weight of the studied proteins. Each ubiquitin molecule adds ∼8.5 kDa to the target protein, so an increased molecular weight of the protein of interest will be visible in the form of one or more higher molecular bands or a smear above the protein of interest when stained with an antibody against the protein of interest on a WB. Additional controls include the use of lysine-to-arginine (KR) mutants of the protein of interest, by which the potential ubiquitination sites of a protein of interest are mutated. The higher molecular bands should not appear if the protein of interest would have been ubiquitinated at the sites that were mutated. Lysine-to-arginine substitutions can also be used to identify ubiquitin sites for mHtt-exon1 (Steffan et al., 2004) which is described in more detail in paragraph Identification of Htt Ubiquitination Sites. Mutation of lysine residues to arginine residues can also be applied to the ubiquitin protein itself in order to study polyubiquitin linkage types of a protein of interest by expressing ubiquitin cDNA constructs with point mutations. For instance, a K48-only ubiquitin mutant, of which all lysines are mutated to arginines except for the lysine at position 48, can only make K48 homotypic polyubiquitin chains. In contrast, a K48R ubiquitin mutant, which contains all internal lysines except at the 48th amino acid where the lysine is replaced with an arginine, can make all polyubiquitin chains except for K48-linked chains. Such Ub mutants were used to study K48 and K63 polyubiquination in combination with stably expressed full length wtHtt (23Q) and mHtt (120Q) in HEK293 cells (Bhat et al., 2014). When full-length Htt was immunoprecipitated under native conditions and analyzed for polyubiquitination by SDS-PAGE WB, mHtt turned out to be mainly ubiquitinated via K63-polyubiquitin. However, it is important to note that immunoprecipitations under native conditions co-purify other ubiquitinated material, and a pull-down experiment under denaturation conditions (e.g., with the overexpression of His-tagged ubiquitin variants and a strong lysis buffer) is more suitable as to gain insights into ubiquitin linkage types onto soluble Htt. In addition, overexpression of ubiquitin with point mutations has its own shortcomings as overexpression of ubiquitin mutants will affect and hamper many processes in the cell. Concluding, typical approaches that could be used to study the ubiquitination of mHtt IBs include visualization by microscopy, and biochemical approaches such as the filter retardation assay and the soluble/insoluble assay, in combination with ubiquitin detection via specific antibodies and the use of arginine-to-lysine mutants.

Enrichment Protocols for Small Pools of Ubiquitinated Htt

A low stoichiometry of protein ubiquitination can make it necessary to enrich the pool of ubiquitin-modified proteins from the total pool of proteins, for example with the use of pull downs via immunoprecipitation. A pull down directed

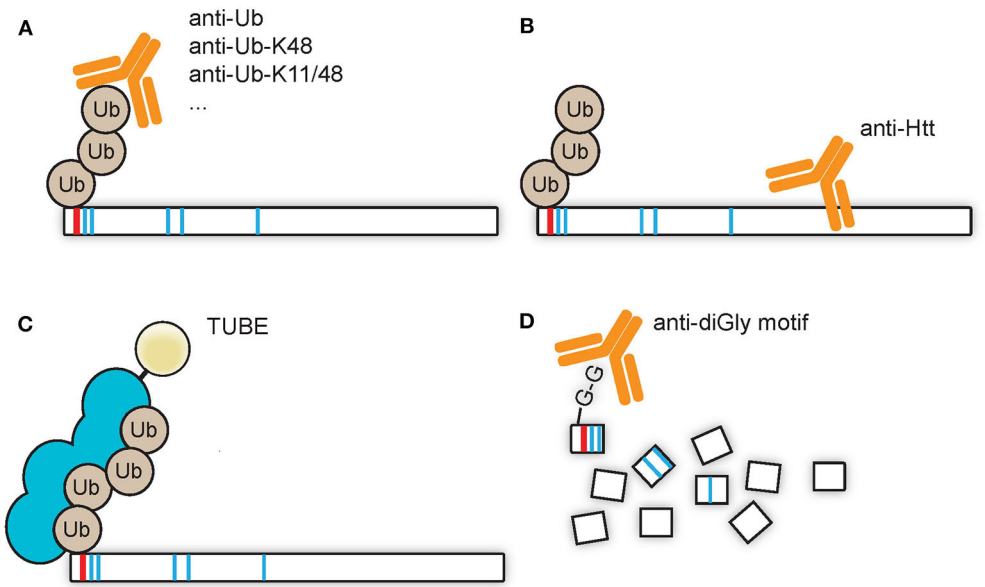

FIGURE 2 | Enrichment strategies for ubiquitinated Htt. **(A)** Antibodies directed against ubiquitin or a polyubiquitin linkage type can be used to enrich ubiquitin-modified Htt from samples, after which the enriched Htt species can be visualized by SDS-PAGE WB with Htt-specific staining. This is the method of choice in order to detect specific ubiquitination of a substrate. **(B)** Antibodies directed against Htt can be used to enrich Htt and ubiquitin modified Htt species from samples, after which the enriched proteins can be visualized by SDS-PAGE WB with ubiquitin-specific staining. This method could give false positive results as ubiquitin-modified co-sequestered proteins could contribute to the obtained ubiquitin detection signal. **(C)** TUBEs, which display a preferential affinity for M1, K48, or K63 tetra-ubiquitin, could be used to enrich polyubiquitinated Htt from samples. **(D)** diGly-modified peptides, derived from ubiquitinated proteins after trypsin digestion, could be enriched from samples with antibodies directed against this diGly remnant motif, and subsequently detected by LC-MS/MS.

against (poly)ubiquitin and subsequently visualized by SDS-PAGE WB with immunostaining for the protein of interest would be the best method to prove direct ubiquitination of the protein of interest (**Figure 2A**). Similarly, the overexpression of ubiquitin harboring an affinity tag could be used for pull downs under native conditions, such as with Myc, hemagglutinin (HA), FLAG, or glutathione S-transferase (GST) tags. Alternatively, pull downs under denaturing conditions, with for instance a poly-histidine (His) tag, could be done with the advantage of a reduction of the amount of co-purifying proteins. A pull down against Htt and a subsequent visualization of the (poly)ubiquitin signal might give a wrong impression due to putative co-purifying proteins which might be ubiquitinated (**Figure 2B**). Alternatively, TUBEs, which consists of a sequence of artificially generated and linked ubiquitin-associated (UBA) domains that recognize polyubiquitin linkages, can be used for pull downs (**Figure 2C**). The advantage of TUBEs over antibodies is that TUBEs protect the polyubiquitin chains from DUBs and proteasomal degradation in the cell lysate (Hjerpe et al., 2009). As described in the future perspectives paragraph Capturing Polyubiquitinated Proteins by Tandem Ubiquitin Binding Entities (TUBEs), TUBEs have to our knowledge not been applied to study Htt ubiquitination while it might yield valuable insight in the polyubiquitin landscape during HD, as the use of another isolated UBA domain, the UBA domain of ubiquilin-2, has been successfully applied to enrich K48-linked polyubiquitinated proteins from HD models and patient samples (Bennett et al., 2007). A different approach is the combination of immunoprecipitation and mass spectrometry in order to pull down so-called diGly peptides in order to define which lysines of proteins are ubiquitinated (**Figure 2D**). Ubiquitin associates with its C-terminal glycine residue to lysine residues of the target proteins, and upon digestion with trypsin a glycine-glycine (diGly) remnant motif derived from ubiquitin will remain on ubiquitin-modified lysine residues of proteins. The branched diGly motif is subsequently recognized by a specific antibody which could be used to enrich the diGly peptides from the samples and since the branched diGly motif on lysine residues results in mis cleavage of that specific lysine residue the site of ubiquitination can be identified using mass spectrometry (Kim et al., 2011; Wagner et al., 2011). The diGly peptides can be identified and quantified by LC-MS/MS, by which both ubiquitinated proteins and their ubiquitination sites can be characterized. The advantage of this technique is the unbiased nature and the direct proof of ubiquitination by mass spectrometry as well as a reduced complexity of the sample as compared to protein-targeted enrichments, as only the peptides that contain the diGly remnants are pulled down (**Figure 2D**). A disadvantage is the inability to discriminate between diGly remnants derived from ubiquitin and from ubiquitin-like proteins NEDD8 and ISG15. Recently an antibody named UbiSite has been generated which recognizes the 13 C-terminal amino acids

of ubiquitin (Akimov et al., 2018). This antibody is used in Lys-C digested samples and could recognize ubiquitination on lysine residues as well as ubiquitination of protein N-termini. This antibody is thus specific for remnants derived from ubiquitin.

Identification of Htt Ubiquitination Sites

Identification of Htt Ubiquitination Sites by Lysine-to-Arginine Mutants

Since lysine residues are the canonical sites for isopeptide bond formation with ubiquitin, mutation into residues that cannot become ubiquitinated, such as arginine residues, can reveal the lysine residues that function as sites for ubiquitin association. The lysine-to-arginine mutants are then compared to the original constructs to examine altered ubiquitination patterns. Htt exon1 contains 3 lysine residues, K6, K9, and K15, and several single and multiple lysine-to-arginine mutants have been generated in order to study SUMOylation and ubiquitination of Htt exon1 (Steffan et al., 2004). When these lysine-to-arginine mutants were used for pull downs in combination with overexpressed HIS-tagged SUMO and HIS-tagged ubiquitin, mutant Httex1 was shown to be modified both with SUMO-1 and ubiquitin, whereas mutation of all lysine residues did not show a signal for SUMOylation and ubiquitination. This indicates that Htt exon-1 was directly SUMOylated or ubiquitinated at either one or more of these lysine residues. Single and double mutations of the Httex1 lysine residues to arginines revealed that K6 and K9 were the main sites for ubiquitination and SUMOylation. Interestingly, mutation of the three lysines to arginines reduced HD pathogenicity, as expression of unmodified Httex1p 97QP resulted in a rough eye phenotype in *Drosophila*, while expression of the K6R, K9R, K15R mutant gave almost no detectable phenotype, and resulted in decreased abundance of the Htt exon1 protein which may indicate that ubiquitination is not a requirement for degradation.

Identification of Htt Ubiquitination Sites by Mass Spectrometry

Mass spectrometry has proven to be a powerful tool for the identification of PTMs, such as protein ubiquitination, and has been applied to characterize Htt ubiquitination sites. For instance, immunoprecipitation of the full-length Htt protein from HEK293 cells that overexpress Htt-Q100 followed by mass spectrometry revealed K631 and K2097 as Htt ubiquitination sites (Koyuncu et al., 2018). Another study identified K337 as ubiquitination site of endogenous Htt (Yau et al., 2017). As opposed to protein-level enrichment methods, the unbiased large-scale detection of ubiquitination sites in samples enriched for modified lysine-containing peptides has greatly enhanced the number of identified ubiquitination sites. These modified lysine-containing diGly peptides are pulled down with a K-ε-GG specific antibody, which is explained in more detail in paragraph Enrichment Protocols for Small Pools of Ubiquitinated Htt (**Figure 2D**) (Kim et al., 2011; Wagner et al., 2011). Pull down of diGly-modified peptides reduces the complexity of the sample as compared to a pull down with an antibody against the protein of interest or against ubiquitin. Furthermore, this technique can be combined with quantitative mass spectrometry approaches, and both qualitative and quantitative differences in ubiquitination can be found between different samples in an unbiased fashion. In this way K6, K9, K132, K804, and K837 were identified as ubiquitination sites of soluble full length Htt in brain lysates of 40 weeks old Q175 mice and wild-type controls (Sap et al., 2019). K6 and K9 were mainly ubiquitinated at the mutant soluble Htt protein, while K132, K804, and K837 were mainly ubiquitinated at the wild-type soluble Htt protein. This indicates that the polyQ expansion in the Htt protein affects ubiquitination.

STUDYING THE DYNAMICS OF HTT AGGREGATE UBIQUITINATION

Ubiquitin Is Dynamically Recruited to mHtt Aggregate IBs

Large intracellular Htt aggregates are often called IBs and are detected in the brain of HD-affected patients, especially in the cortex and striatum. These IBs were found to be decorated by ubiquitin as well as with other proteostasis-related proteins including proteasome complexes and chaperones, as shown in human postmortem cortical tissues, HD mouse model brain tissues and HD cell models (Davies et al., 1997; DiFiglia et al., 1997; Waelter et al., 2001). It is not clear yet which function ubiquitin fulfills at these IBs. Several microscopy-based studies revealed that the recruitment of ubiquitin is not essential for IB formation, since ubiquitination was not detected on nascent aggregates in mice brain tissue of juvenile R6/2 mice but only in later stages of disease, as demonstrated by using Ub antibody staining followed by microscopy (Davies et al., 1997; Gong et al., 2012). Furthermore, fluorescently-tagged ubiquitin (YFP-Ub) and Htt-exon1 (mCherry) were used to study the recruitment of ubiquitin to Htt exon1 IBs in living cells using fluorescent microscopy (Hipp et al., 2012). Upon transfection, Htt exon1 was initially diffusely distributed through the entire cytoplasm. However, when IBs became apparent, both IB size and fluorescence intensity increased rapidly, with the majority of fluorescently-labeled mHtt exon1 being recruited to IBs within 20–30 min. Interestingly, co-expressed YFP-tagged Ub was recruited toward mHtt exon1 IBs at a later stage when the IBs had already reached their mature size. This suggests that ubiquitination is not required for mHtt IB formation, and that Ub recruitment may depend on recruitment of ubiquitinating enzymes to IBs first. In addition, a 3xKR mutant Htt-exon1 with all lysines mutated to arginines and unable to form ubiquitin chains, can still form intracellular aggregates, indicating that mHtt IB formation is independent of ubiquitination of Htt itself (Juenemann et al., 2015).

Initial experiments to study dynamics of Ub recruitment to mHtt IBs were done using GFP or YFP-tagged ubiquitin combined with Fluorescent Recovery After Photobleaching (FRAP) protocols in living cells. Here, a small region of the fluorescent aggregate is photobleached and recovery of fluorescence is monitored in time. Since photobleaching is permanent, recovery can only occur when bleached proteins exchange with fluorescent proteins from the surroundings by

diffusion or active transport. Since no recovery was observed when fluorescently-tagged Ub present in IBs was photobleached, these studies indicate that Ub is irreversibly sequestered into IBs (Raspe et al., 2009; Bersuker et al., 2016). However, the commonly-used GFP (or variant) tags are relatively large as compared to the size of the labeled target protein, especially when considering that GFP is ∼27 kDa in size, while ubiquitin is ∼8.5 kDa. By using synthetic ubiquitin labeled at the N-terminus with Tetramethylrhodamine (TAMRA-Ub) and electroporated into living cells (**Figures 3A,B**) it was more recently shown that ubiquitin is reversibly recruited to mHtt IBs (Juenemann et al., 2018). The TAMRA label is with its mass of only ∼0.5 kDa much smaller than GFP (and variants) tags and it was found that TAMRA-labeled Ub behaves more similar to endogenous Ub when compared to GFP-tagged Ub. While GFP-tagged Ub can be expressed following transfection of cells with cDNAs, the TAMRA-Ub has to enter the cell via micro-injection or electroporation. Electroporation involves the application of a very short electrical pulse (few microseconds or milliseconds) which disturbs the phospholipid bilayer and forms temporary small pores through which the TAMRA-Ub can enter the cell. Electroporation can be performed using a cuvette with cells in suspension, or alternatively an adherent cell electrode can be used to electroporate adherent cells on coverslips, allowing for immediate visualization by microscopy. Note that in both cases electroporation has to be performed at low temperature to prevent uptake of TAMRA-Ub via endocytosis, as resulting fluorescent puncta represent internalized TAMRA-Ub in vesicles instead of cytoplasmatic TAMRA-Ub being involved in mono-ubiquitination and internalization of endosomes. Upon electroporation, TAMRA-Ub is mainly present in the nucleus and on cytoplasmic vesicles, but when mHtt induced IBs are present most TAMRA-Ub is recruited to IBs (**Figure 3C**). Both TAMRA-Ub and endogenous Ub are present in the entire mHtt aggregates, including the inner core, and TAMRA-Ub was incorporated into Ub linkages including poly-ubiquitinated mHtt itself (Juenemann et al., 2018). This can be visualized by SDS-PAGE WB after lysing cells and solubilizing the insoluble fraction including aggregated mHtt (**Figure 3D**). FRAP experiments showed that TAMRA-Ub was reversibly recruited to mHtt IBs, which was prevented when either E1 ligase or DUB inhibitors were used (Juenemann et al., 2018). This indicates that (de)ubiquitinating enzymes recruited to IBs are involved in mHtt ubiquitination as well as of other proteins sequestered into IBs, resulting in ongoing ubiquitination and deubiquitination of proteins present in IBs with reversible recruitment of ubiquitin.

Recruitment of Ubiquitin Related Enzymes to Htt IBs

The reversible recruitment of Ub into mHtt IBs and the dependency on active E3 ligase and DUB activities as described above indicate that different E3 ligases and DUBs are recruited to aggregates. Indeed, several ubiquitin ligases and DUBs have been observed to co-localize with mHtt IBs, but only a few E3 ligases have so far been identified to affect mHtt aggregation, including Ube3a, CHIP, WWP1, and UBR5. Ube3A is an E3 ligase known to promote proteasomal degradation of misfolded proteins by enhancing K48-linkage type poly-ubiquitination, and Ube3A protein levels were found to be reduced during aging. When Ube3A levels were selectively decreased in HD mouse brains an increase in aggregate formation was observed combined with reduced ubiquitination of the IBs (Maheshwari et al., 2014). In contrast, overexpression of Ube3A reduced mHtt accumulation and aggregation (Bhat et al., 2014), suggesting that Ube3A is at least involved in ubiquitination of mHtt or sequestered proteins. Another E3 ligase that is recruited to mHtt IBs is the C-terminus of Hsc70-interacting protein (CHIP). Both the ubiquitination and the rate of degradation of mHtt was increased when CHIP was transiently overexpressed in cells, while aggregation and cell death were reduced (Jana et al., 2005). *In vivo* studies using mice that were haploinsufficient for CHIP showed an accelerated HD disease phenotype, while overexpression of CHIP showed a reduction in mHtt aggregates in zebra fish models of HD (Miller et al., 2005). Similar to Ube3A and CHIP, also the E3 ligase WPP1 is recruited to mHtt aggregates, but its activity appears to enhance mHtt levels and aggregation in both *in vivo* and *in vitro* models. This may be the result of ineffective ubiquitination as WWP1 ubiquitinates mHtt at an atypical position of Lys-63, which may impair efficient targeting to the UPS (Lin et al., 2016). More recently the role of UBR5 in mHtt IB formation was demonstrated, which appears to be required for proteasomal degradation of both normal and mutant Htt. Knockdown of UBR5 increased mHtt aggregation and neurotoxicity in invertebrate models, while loss of UBR5 increased Htt levels and IB formation in iPSCs expressing mHtt (Koyuncu et al., 2018). Intriguingly, this effect may be mediated by UBR5-mediated heterotypic ubiquitin K11/K48-linked chains that are also present in mHtt IBs, and which promote rapid proteasomal clearance of aggregation-prone proteins (Yau et al., 2017). Besides these E3 ligases also the E2 enzyme Ube2W has been reported to affect mHtt aggregation (Wang et al., 2018), which could be the result of the preference of Ube2W to ubiquitinate proteins with a disordered N-terminus.

The recruitment of E3 ligases and DUBs to mHtt IBs is likely to be due to the presence of numerous target proteins present in IBs either due to active recruitment or sequestration. By using fluorescent reporter proteins that can become reversibly and conditionally misfolded it was shown that the misfolded conformation of the reporter was targeted for ubiquitin-dependent degradation unless mHtt aggregates were present, resulting in the sequestration of these reporter proteins (Bersuker et al., 2016). Interestingly, only reporter constructs in a misfolded conformation accumulated at mHtt IBs, whereas constitutively ubiquitinated reporters which were not misfolded were not recruited to mHtt IBs. These data suggest that the folding state of a protein is the primary determinant for sequestration of proteins in an IB, instead of active recruitment of ubiquitinated proteins toward mHtt IBs. This reporter system nicely shows that the sequestration of misfolded proteins, possibly in a promiscuous fashion, contributes to mHtt aggregation. However, several recruited (de)ubiquitinating enzymes appear to be functional and enzymatically active as shown by using activity-based probes (ABPs) to label recruited

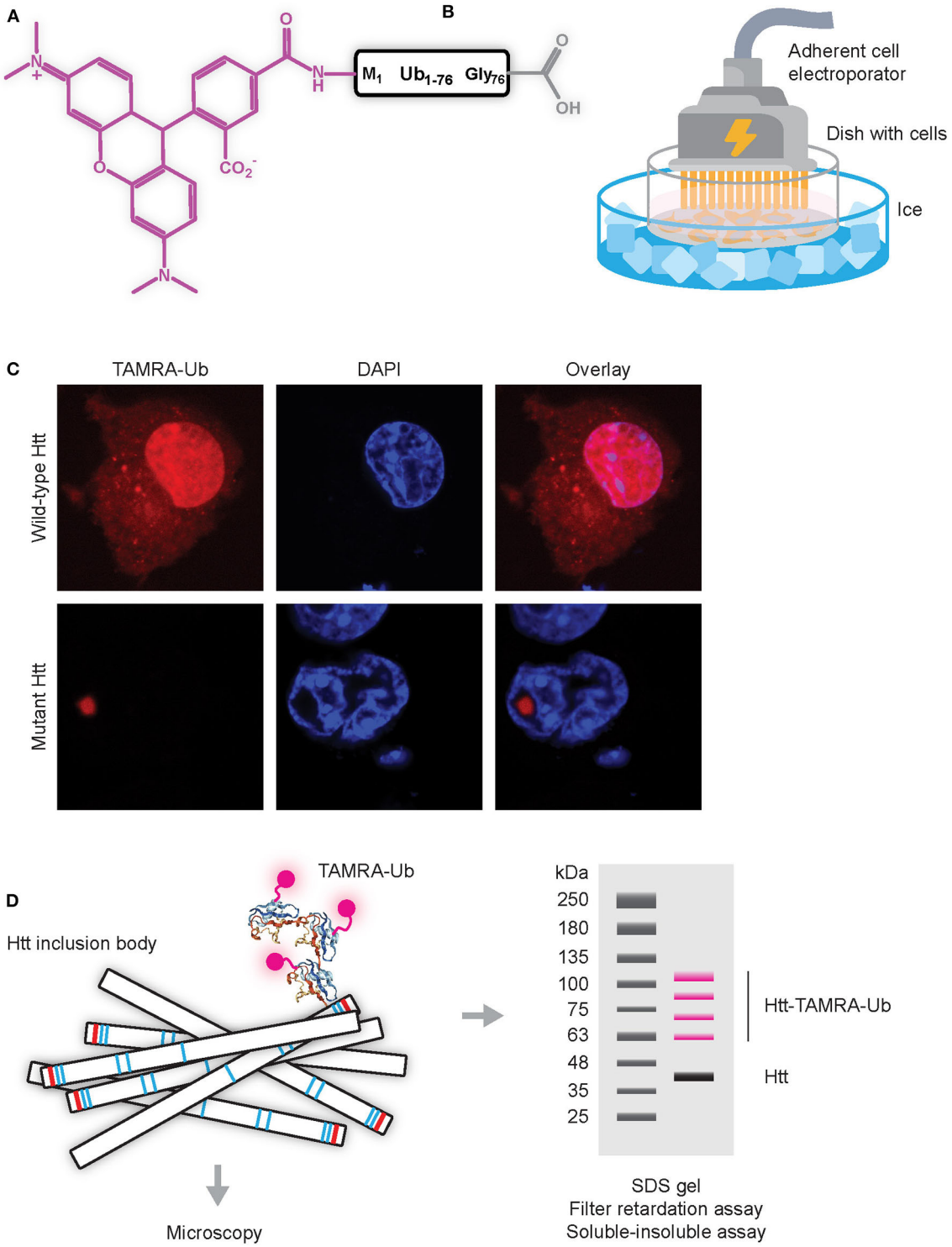

FIGURE 3 | Application of TAMRA-Ub to study ubiquitination of mHtt aggregates **(A)** Scheme of TAMRA-Ub with Ub being fluorescently labeled on the N-terminus with TAMRA (5-tetramethylrhodamine, excitation 550 nm, emission 590 nm). **(B)** Electroporation of adherent cells with TAMRA-Ub dissolved in mannitol buffer, placed on ice to prevent intravesicular staining due to uptake by endocytosis. **(C)** TAMRA-Ub electroporated into cells is mainly localized in the nucleus and present on vesicles, while upon mHtt expression most TAMRA-Ub is recruited into the mHtt aggregate. **(D)** Upon electroporation of TAMRA-Ub, cells can be lysed and aggregates can be solubilized and separated by SDS-PAGE, with fluorescent bands representing TAMRA-Ub conjugated proteins.

enzymes. ABPs target only the active form of an enzyme, which allows for the identification and quantification of the pool of active enzymes in a biological sample. The development and application of ABPs for protein (de)ubiquitination was recently reviewed by Mulder and colleagues (Mulder et al., 2019). Recent examples for the usage of two chemically synthesized ABPs in HD are Cy5-Ub-Dha and Cy5-Ub-PA. Cy5-Ub-Dha is an ABP which reacts with active cysteine residues of E1, E2, and E3 enzymes and can irreversibly label active enzymes involved in protein ubiquitination (Mulder et al., 2016). Cy5-Ub-PA is a specific inhibitor of DUBs of the UCH, USP, and OTU DUB families, and fluorescently labels them (Ekkebus et al., 2013). Similar to TAMRA-Ub, most ABPs are not cell permeable and electroporation was used to introduce the ABPs into cells. These probes were electroporated into cells expressing GFP-tagged mHtt-exon1 to visualize aggregates. While the Cy5-Ub-Dha staining for active E1, E2, and E3 enzymes showed staining of entire aggregates, the Cy5-Ub-PA staining was present as a ring around the aggregates (Juenemann et al., 2018), suggesting that DUBs were mainly active in the periphery of mHtt IBs, while ubiquitinating enzymes were also active in the core of Htt IBs. Similarly, when using GFP-tagged enzymes, GFP-tagged ubiquitin ligase NEDD4.1 showed a complete co-localization with Htt aggregate staining, while co-transfection of GFP-tagged DUB USP5 resulted in a ring-formed staining around the aggregates (Juenemann et al., 2018). Together these data suggest that enzymes are active at mHtt aggregates, and that active ubiquitin ligases are found in both the core and periphery of IBs, while DUBs were found to be active at the periphery.

Detecting Polyubiquitination of the Htt Protein

Degradation-Associated Polyubiquitination in HD Pathology

Mass spectrometry is an important tool to characterize ubiquitin association sites, and to distinguish different forms of ubiquitination, such as mono- and polyubiquitination. Whereas, tryptic peptides derived from mono-ubiquitin contain only unbranched peptides, tryptic peptides derived from polyubiquitin chains contain branched peptides as a result of isopeptide-bond formation between the C-terminal glycine residue of one ubiquitin molecule and the internal lysine residue of the other ubiquitin molecule. The ubiquitin-AQUA method was developed for the absolute quantification of ubiquitin, using isotope-labeled internal standard peptides for all seven possible polyubiquitin chain linkages, as well as internal standard peptides specific for mono-ubiquitination (Kirkpatrick et al., 2006). When known amounts of (heavy) isotope-labeled internal standard peptides were added to (light) samples, heavy and light peptides were subsequently separated by reversed phase high-performance liquid chromatography (HPLC) and analyzed by a targeted quantitative mass spectrometry approach named multiplexed Selected Reaction Monitoring (SRM). With this method one can measure the amount of total ubiquitin, the amount of monoubiquitin and polyubiquitin, as well as the amount of targeted substrate. This technique has been applied to study the function of the UPS in HD, using the UBA domain from human ubiquilin 2 (UBQLN2) to capture polyubiquitin chains from HD samples (Bennett et al., 2007). Here, polypeptides were eluted, digested with trypsin and measured by mass spectrometry and the abundance of the ubiquitin K48 diGly peptide was compared with a heavy labeled spiked-in peptide. K48 diGly peptide abundance was used as a measure of the UPS functioning as an increase in abundance of the ubiquitin K48 diGly peptide correlated with an increase in MG132 proteasome inhibitor concentration in cell culture. The authors observed an increase in the pool of K48 polyubiquitin linkages during HD pathology while the increase in the unconjugated ubiquitin pool was minimal or absent. In R6/2 HD mice expressing expanded mHtt exon1, elevated levels of K48 polyubiquitin linkages were first detected in cortex and striatum of 6 weeks old mice. Furthermore, a small increase in K48 polyubiquitin linkages was observed in 22 months old $Hdh^{Q150/Q150}$ "knock-in" HD mice expressing full-length mHtt. Finally, half of the tested human HD cortex and striatum samples showed increased levels of the UbK48 isopeptide as compared to control (Bennett et al., 2007). Together these results suggest that the proteasome function is impaired during HD and that levels of polyubiquitin K48 linkages could be used as a biomarker for UPS impairment.

A recent global proteome and global ubiquitinome analysis of brain tissues of 40 weeks old homozygous Q175FDN mice that express full-length Htt with 175 polyQ repeats, and Q20 wild-type mice as control, used the diGly remnant of ubiquitin left on protein substrates after trypsin digestion to enrich peptides derived from ubiquitinated proteins using a specific antibody. When label-free quantification was used to compare relative protein and diGly peptide levels between HD and wild-type samples, increased levels of the ubiquitin protein and of ubiquitin K48-diGly peptides were observed in the insoluble fraction of HD mice brains (Sap et al., 2019). A similar result was obtained when HA-tagged ubiquitin mutants were transfected into cells expressing mHtt. These ubiquitin mutants contained lysine-to-arginine substitutions at all lysine residues except for either K48 or K63 and can therefore only make K48- or K63-linked polyubiquitin chains. Upon co-transfection of these mutants with mHtt into cells only co-localization of Htt-positive inclusions and K48 polyubiquitin was observed by fluorescence microscopy following immunostaining for K48 and K63 polyubiquitin, indicating that mutant Htt inclusions are K48-polyubiquitinated (Kah et al., 2005). Interestingly, mHtt IBs were also shown to be ubiquitinated via K11/K48 branched chains, which are mainly associated with enhanced degradation of regulators of mitosis by the proteasome. Heterotypic ubiquitination has been difficult to study, and to identify these branched chains bispecific antibodies were developed that detect K11 and K48 polyubiquitin linkages which are in close proximity, which allows for the identification of K11/K48 heterotypic polyubiquitin chains (Yau et al., 2017). Heterotypic chains adopt a branched or mixed topology due to ubiquitin-modification of more than one site on a single ubiquitin molecule. K11/K48-branched chains were identified on mitotic regulators, misfolded nascent proteins but also on mutant Htt, as fluorescent staining with

the bispecific K11/K48 antibody co-localized with Htt-Q73-GFP aggregate staining in HeLa cells, embryonic stem cells and in differentiated neurons as observed by microscopy. Also aggregates of Q175 mHtt in mice brain were recognized by the K11/K48 bispecific antibody. Furthermore, purification of His-tagged wtHtt and mHtt from HeLa cell lysates under denaturing conditions followed by SDS-PAGE WB revealed that primarily mHtt samples were polyubiquitinated with K11- and K48-polyubiquitin linkages. The branched chains on mHtt were confirmed by using an ubiquitin$^{TEV/FLAG}$ system, which results in ∼2 kDa stamps on wild-type ubiquitin molecules whereby the presence of two or more stamps on one ubiquitin molecule indicates branched chains (Meyer and Rape, 2014; Yau et al., 2017). Also, proteins with a role in the K11/K48 quality control pathway co-localized with Q73 mHtt aggregates in HeLa cells, such as BAG6, p97/VCP, UBQLN2, and P62/SQSTM1, as was shown by microscopy. Inhibition of protein degradation and inhibition of the stabilization of newly synthesized misfolded proteins led to a loss of co-localization of K11/K48 Ub with Htt aggregates. In contrast, co-localization was maintained when new protein synthesis was blocked during these treatments. These results suggest that mHtt aggregates compete with newly synthesized misfolded proteins for a limited pool of enzymes involved in the Ub K11/K48-specific quality control system, including ubiquitin E3 ligases UBR4 and UBR5, ubiquitin-selective segregase P97/VCP and proteasome shuttles of the UBQLN family.

Atypical Forms of Polyubiquitination in HD

Also other polyubiquitin linkages have been associated with mHtt IBs. E3 ubiquitin ligase TRAF6 was found to be localized with mHtt IBs, especially at the outside. Overexpression of ubiquitin mutants which could only make homotypic chains revealed that TRAF6 facilitates atypical polyubiquitination of wildtype and mutant Htt with K6, K27, or K29 polyubiquitin chains. TRAF6 expression also enhanced aggregate formation and atypical ubiquitination of mHtt aggregates (Zucchelli et al., 2011). Htt aggregates were shown to be modified with linear M1-linked polyubiquitin chains (van Well et al., 2019). Usually ubiquitin associates with its C-terminal glycine residue to a lysine residue on a target protein, but in M1-linked ubiquitination the protein's N-terminal methionine is the target for ubiquitination. A M1-linked polyubiquitin chain is then formed by incoming ubiquitin molecules that associate with their C-termini to the N-terminal methionine of the preceding ubiquitin molecule. N-terminal polyubiquitination is catalyzed by the linear ubiquitin chain assembly complex (LUBAC), which comprises HOIL-1, HOIL-1 interacting protein (HOIP) and SHARPIN (Kirisako et al., 2006). M1 polyubiquitination can be reversed by the DUBs CYLD and OTULIN (Komander et al., 2009; Keusekotten et al., 2013). Van Well and colleagues also observed recruitment of components of the LUBAC complex (responsible for linear ubiquitination) including HOIP, HOIL-1L, and Sharpin to mHtt aggregates, as well as the recruitment of proteins that are known to associate specifically to M1-linked ubiquitination such as NEMO (NF-κB essential modifier) and Optineurin. Several sample types were studied including human neuronal SH-SY5Y cells expressing wild-type or mHtt, human frontal cortex HD samples and cortex and striatum of R6/2 HD mice. Both soluble and insoluble mHtt appeared to be directly ubiquitinated with linear ubiquitin as shown by immunoprecipitation of HA-tagged Htt exon1 and 3xKR variants of Htt-exon1. In addition, sequestration of transcription factor Sp1 to mHtt aggregates was affected by the levels of linear ubiquitin. Results of this study suggest that linear ubiquitination prevents unfavorable protein sequestration in aggregates, and promotes the degradation of misfolded proteins in a P97/VCP- and proteasome-dependent manner.

FUTURE PERSPECTIVES

While many aspects of the role of ubiquitination in HD, including identification of Htt ubiquitination sites, dynamics of ubiquitin recruitment to IBs, and alterations in the ubiquitinome during HD progression can be studied with current methodologies, various remaining challenges remain to be addressed. These include the quantification of low levels of polyubiquitination and the identification of polyubiquitin linkages as well as the identification of involved (de)ubiquitinating enzymes.

Identification of Ubiquitin Ligases Involved in Htt Ubiquitination

Standard techniques for the identification of ubiquitin ligases specific for Htt would include microscopy-based co-localization assays, siRNA knockdown screens to determine the effect of knockdown of individual E3 ligases on soluble and insoluble mHtt levels, or the identification of a physical interaction using a yeast two hybrid assay or affinity-purification followed by mass spectrometry. Immunoprecipitation assays rely on the specificity of the antibody and the stable interaction between proteins throughout the procedure. There are a number of challenges when aiming to identify a specific E3 ligase. First of all is the typically very transient nature of their interaction (Pierce et al., 2009), which makes it difficult to identify these interactions with the standard techniques. Secondly, the rapid targeting of ubiquitinated substrates for protein degradation decreases the abundance of ligase substrates in the sample. Thirdly, ubiquitination is a reversible modification and rapid deubiquitination can make it challenging to identify ubiquitinated substrates. Finally, substrates could be ubiquitinated by different ubiquitin ligases, which hampers identification of involved E3 ligases by selective knockdown. Several novel approaches may enhance the possibility to identify new ubiquitin ligase-substrate pairs, including BioID and APEX.

Proximity-Dependent Biotin Identification (BioID)

BioID can be used to identify proteins in close proximity of a protein of interest in living cells (Roux et al., 2012, 2018). This approach makes use of the fusion of a protein of interest with a mutant form of the biotin ligase enzyme BirA (BirA*), which has been engineered in such a way that it can biotinylate neighboring proteins in a promiscuous fashion. Upon addition of biotin, proteins which are in close proximity (∼10 nm) of the fusion protein are biotinylated and these could be efficiently

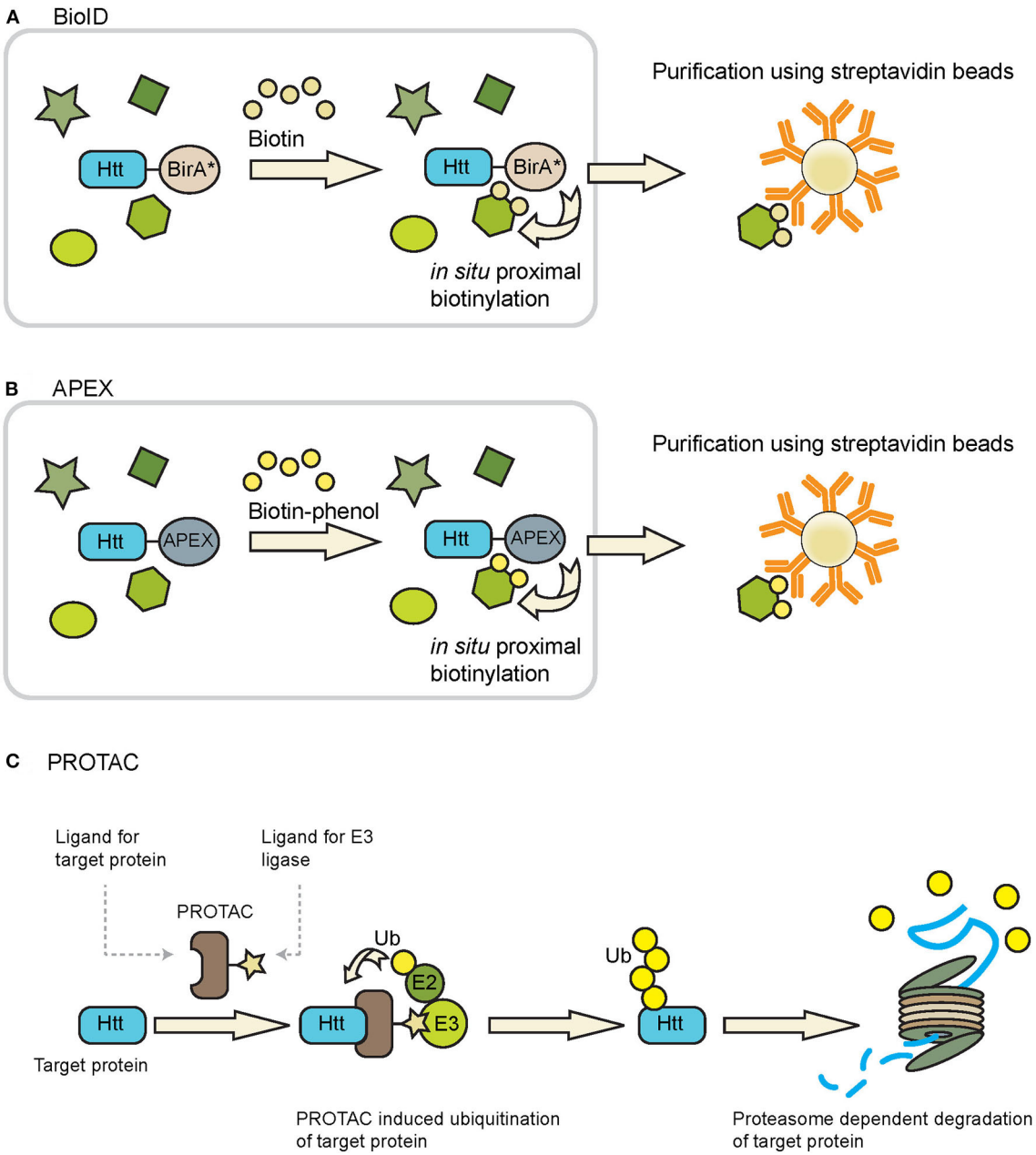

FIGURE 4 | Tools that can be used to study Htt ubiquitination and degradation. **(A)** BioID and **(B)** APEX can be used to identify ubiquitin ligases and DUBs that putatively interact with Htt, as both techniques identify transient interacting proteins via promiscuous biotinylation of proteins in close proximity of the BirA* or APEX fusion protein. Biotinylated proteins can be purified using avidin/streptavidin beads and are subsequently identified by mass spectrometry. Figures adapted from Ueda et al. (2015) and Chu et al. (2017). **(C)** PROTACs can be used to induce ubiquitination of a protein of interest followed by proteasome-dependent degradation. PROTACs bring together the protein of interest (Htt in this case) and a ubiquitin ligase, leading to ubiquitination of the protein of interest and subsequent proteasome-dependent degradation.

enriched from samples due to the strong interaction of biotin with avidin/streptavidin conjugated beads (**Figure 4A**), which also makes it possible to study insoluble proteins, while a spatial resolution can be obtained by targeting BirA* to a location-specific protein. Additionally, with the use of split-BioID constructs, consisting of a split BirA* molecule, it is possible to confirm the interaction of two proteins of interest while also biotinylating other members of the protein complex (Schopp et al., 2017). After enrichment of the biotinylated proteins mass spectrometry is used to identify the interactomes of the fusion proteins. The advantages of BioID are the identification of weak and/or transient protein-protein interactions of both soluble and

insoluble proteins, and the possibility to study protein-protein interactions at specific subcellular localizations. Disadvantages of the BioID approach include fusion of BirA* to the protein of interest which accounts for an additional mass of ∼ 35 kDa, which could affect the structure, function and localization of the protein of interest. However, a smaller and improved version of BioID, named BioID2, is also available (Kim et al., 2016). Whether the optimal location of the BirA* is at the N-terminal or C-terminal side of the protein of interest will depend on the target protein. The expression of the fusion protein should ideally be done at endogenous levels, as high expression levels, as for instance obtained via transient expression systems, might result in increased levels of false positives. Hence expression under the control of an endogenous promotor is advised. Another limitation of this method is the relatively slow labeling kinetics of the BioID, which results in labeling timeframes of typically 12–24 h (Varnaite and MacNeill, 2016). However, also improved versions, called TurboID and miniTurbo, were recently developed and can label neighboring proteins within 10 min (Branon et al., 2018). BioID experiments could result in a large number of unspecific hits, which makes selection of the right control experiments important in order to discriminate between specific and unspecific interactors. Negative controls that could be used are either the parental cell line, or the expression of an epitope-tagged BirA* protein at similar levels as the BirA* fusion protein (Lambert et al., 2015). Quantitative proteomics could be used in combination with BioID in order to eliminate background proteins. BioID has been successfully applied to identify substrates of E2 ubiquitin conjugating and E3 ubiquitin ligase enzymes (Coyaud et al., 2015; Bakos et al., 2018; Dho et al., 2019). The fusion of a BioID molecule with wtHtt or mHtt might lead to the identification of novel enzymes with a role in the ubiquitin pathway.

Engineered Ascorbate Peroxidase (APEX)

A functionally related method to BioID is the 28 kDa APEX (Rhee et al., 2013). Upon treatment with hydrogen peroxide and biotin-phenol, APEX catalyzes the oxidation of biotin-phenol to generate the short-lived biotin-phenoxyl radical, which results in the biotinylation of proteins in close proximity to APEX. An improved version of APEX, APEX2, exhibits a higher sensitivity as compared to the original (Lam et al., 2015). Similar as with the BioID approach the biotinylated proteins can be enriched with streptavidin beads and subsequently identified by mass spectrometry (**Figure 4B**). APEX labeling times as short as 1 min could be used to biotinylate neighboring proteins, making it a much faster method as compared to BioID. This higher temporal resolution makes it possible to study interactome dynamics over time. Disadvantages of APEX are the fusion of a tag with the protein of interest, as well as the toxic effect that the biotin-phenol reagent can have in living cells, making it unsuitable for *in vivo* studies (Che and Khavari, 2017).

Capturing Polyubiquitinated Proteins by Tandem Ubiquitin Binding Entities (TUBEs)

TUBEs can be used to enrich polyubiquitinated substrates from the cell (Hjerpe et al., 2009). TUBEs consist of four UBA domains separated by flexible linkers and fused to a tag or agarose bead to facilitate purification and detection. They have a higher affinity for polyubiquitin as compared to single UBA domains, and can be expressed in cell lines where they associate with polyubiquitinated proteins and protect them from proteasomal degradation as well as from the action of DUBs, thus stabilizing polyubiquitinated proteins. These polyubiquitinated proteins can subsequently be enriched by standard immunoprecipitations. Currently, TUBEs with specificity for M1, K48, and K63 homotypic polyubiquitin chains are available. A disadvantage of TUBEs is that they recognize homotypic polyubiquitin chains and it is not clear which part of the ubiquitin landscape consists of homotypic chains vs. mixed and branched polyubiquitin chains. Trypsin-resistant TUBEs (TR-TUBEs) could be used for protein identification by mass spectrometry, as otherwise high abundant peptides derived from the TUBE proteins will not be generated and measured by mass spectrometry. The application of TUBEs might increase the pool ubiquitinated Htt species by protecting them from the action of DUBs and proteasomal degradation, which might facilitate the identification of novel Htt ubiquitination sites or might shed more light on the regulation of K48-linked polyubiquitin targeting for degradation by the UPS.

Targeted Protein Degradation by Proteolysis Targeting Chimeras (PROTACs)

Therapeutic strategies for HD focus on mHtt lowering in order to slow down or delay the onset of disease, either by reducing synthesis of mHtt or by accelerating the turnover of mHtt prior to aggregation. Various antisense oligonucleotide approaches are entering the clinic with the aim to reduce Htt mRNA levels, often requiring invasive approaches including repeated CSF injections or direct delivery of AAV viruses in the brain. Alternatively, one could aim to reduce mHtt protein levels by improving the turnover of mHtt via the UPS. This would require the identification of involved ubiquitinating enzymes and manipulating their activities.

Novel strategies also include the development of PROTACs to induce proteasome-dependent protein degradation via a targeting molecule (reviewed by Gu et al., 2018; Schapira et al., 2019; Zou et al., 2019). The designed hybrid molecule contains a moiety to recognize the substrate protein, and another moiety to recruit an E3 ligase to induce ubiquitination and subsequent proteasome-dependent degradation (**Figure 4C**). In the case of HD, one could use moieties recognizing the expanded polyQ tract of mHtt, or other Htt-specific domains that are accessible for PROTAC molecules. The challenge will be to generate a ligand with sufficient specificity for mHtt over wtHtt or other proteins with a polyQ repeat. Both peptide-based and small molecule-based PROTACs have been developed to recruit E3 ligases, with the latter being preferred as they can easier enter the human body (An and Fu, 2018). An important benefit of the PROTAC approach is that it is not required to identify the natural E3 ligase that targets Htt, as recruiting an E3 ligase to a substrate is often sufficient to trigger activity. In the case of HD, an E3 ligase able to generate K48-linkages might be sufficient, or E3 ligases like UBR5 to generate bi-specific K11/K48 linkages for accelerated

degradation. In this way, the PROTAC takes advantage of the intracellular proteostasis pathways to selectively target and degrade disease-related proteins. Yet while representing a short-cut to accelerate Htt turnover via ubiquitination, PROTAC strategies may also encounter problems with permeability (especially by crossing the blood-brain barrier), off-target effects and stability.

Final Remarks

The toolbox to study ubiquitination in HD is quickly expanding with new technologies including the possibility to use fluorescent activity probes to detect alterations in (de)ubiquitinating enzyme activities, new developments in proteomics to study alterations in the ubiquitinome, and chemical synthesis of ubiquitin with a variety of modifications including fluorophores and linkages. The possibility to synthesize Htt peptides with PTMs and the advances made in the field of chemical derived ubiquitin tools opens the door to generate specialized Ub-Htt peptides able to trap and identify enzymes involved in Htt ubiquitination. Together this will allow examination of the complexity of PTM crosstalk in HD and the intriguing role of the UPS in HD in more depth, which may lead to novel therapeutic strategies to lower mHtt levels and delay onset and progression of disease.

AUTHOR CONTRIBUTIONS

KS and ER wrote the manuscript and generated the figures.

FUNDING

This work was funded by CHDI and Campagneteam Huntington.

REFERENCES

Akimov, V., Barrio-Hernandez, I., Hansen, S. V. F., Hallenborg, P., Pedersen, A. K., Bekker-Jensen, D. B., et al. (2018). UbiSite approach for comprehensive mapping of lysine and N-terminal ubiquitination sites. *Nat. Struct. Mol. Biol.* 25, 631–640. doi: 10.1038/s41594-018-0084-y

Akutsu, M., Dikic, I., and Bremm, A. (2016). Ubiquitin chain diversity at a glance. *J. Cell Sci.* 129, 875–880. doi: 10.1242/jcs.183954

An, S., and Fu, L. (2018). Small-molecule PROTACs: an emerging and promising approach for the development of targeted therapy drugs. *EBiomedicine* 36, 553–562. doi: 10.1016/j.ebiom.2018.09.005

Arbez, N., Ratovitski, T., Roby, E., Chighladze, E., Stewart, J. C., Ren, M., et al. (2017). Post-translational modifications clustering within proteolytic domains decrease mutant huntingtin toxicity. *J. Biol. Chem.* 292, 19238–19254. doi: 10.1074/jbc.M117.782300

Arrasate, M., and Finkbeiner, S. (2012). Protein aggregates in Huntington's disease. *Exp. Neurol.* 238, 1–11. doi: 10.1016/j.expneurol.2011.12.013

Arrasate, M., Mitra, S., Schweitzer, E. S., Segal, M. R., and Finkbeiner, S. (2004). Inclusion body formation reduces levels of mutant huntingtin and the risk of neuronal death. *Nature* 431, 805–810. doi: 10.1038/nature02998

Bakos, G., Yu, L., Gak, I. A., Roumeliotis, T. I., Liakopoulos, D., Choudhary, J. S., et al. (2018). An E2-ubiquitin thioester-driven approach to identify substrates modified with ubiquitin and ubiquitin-like molecules. *Nat. Commun.* 9:4775. doi: 10.1038/s41467-018-07251-5

Bennett, E. J., Shaler, T. A., Woodman, B., Ryu, K. Y., Zaitseva, T. S., Becker, C. H., et al. (2007). Global changes to the ubiquitin system in Huntington's disease. *Nature* 448, 704–708. doi: 10.1038/nature06022

Bersuker, K., Brandeis, M., and Kopito, R. R. (2016). Protein misfolding specifies recruitment to cytoplasmic inclusion bodies. *J. Cell Biol.* 213, 229–241. doi: 10.1083/jcb.201511024

Bhat, K. P., Yan, S., Wang, C., Li, S., and Li, X. (2014). Differential ubiquitination and degradation of huntingtin fragments modulated by ubiquitin-protein ligase E3A. *Proc. Natl. Acad. Sci. U.S.A.* 111, 5706–5711. doi: 10.1073/pnas.1402215111

Bjørkøy, G., Lamark, T., Brech, A., Outzen, H., Perander, M., Øvervatn, A., et al. (2005). p62/SQSTM1 forms protein aggregates degraded by autophagy and has a protective effect on huntingtin-induced cell death. *J. Cell Biol.* 171, 603–614. doi: 10.1083/jcb.200507002

Branon, T. C., Bosch, J. A., Sanchez, A. D., Udeshi, N. D., Svinkina, T., Carr, S. A., et al. (2018). Efficient proximity labeling in living cells and organisms with TurboID HHS public access author manuscript. *Nat. Biotechnol.* 36, 880–887. doi: 10.1038/nbt.4201

Carra, S., Seguin, S. J., Lambert, H., and Landry, J. (2008). HspB8 chaperone activity toward poly(Q)-containing proteins depends on its association with Bag3, a stimulator of macroautophagy. *J. Biol. Chem.* 283, 1437–1444. doi: 10.1074/jbc.M706304200

Che, Y., and Khavari, P. A. (2017). Research techniques made simple: emerging methods to elucidate protein interactions through spatial proximity. *J. Invest. Dermatol.* 137, e197–e203. doi: 10.1016/j.jid.2017.09.028

Chu, Q., Rathore, A., Diedrich, J. K., Donaldson, C. J., Yates, J. R., and Saghatelian, A. (2017). Identification of microprotein-protein interactions via APEX tagging. *Biochemistry* 56, 3299–3306. doi: 10.1021/acs.biochem.7b00265

Clague, M. J., Urbé, S., and Komander, D. (2019). Breaking the chains: deubiquitylating enzyme specificity begets function. *Nat. Rev. Mol. Cell Biol.* 20, 338–352. doi: 10.1038/s41580-019-0099-1

Coyaud, E., Mis, M., Laurent, E. M. N., Dunham, W. H., Couzens, A. L., Robitaille, M., et al. (2015). BioID-based identification of skp cullin F-box (SCF)β-TrCP1/2 E3 ligase substrates. *Mol. Cell. Proteomics* 14, 1781–1795. doi: 10.1074/mcp.M114.045658

Davies, S. W., Turmaine, M., Cozens, B. A., DiFiglia, M., Sharp, A. H., Ross, C. A., et al. (1997). Formation of neuronal intranuclear inclusions underlies the neurological dysfunction in mice transgenic for the HD mutation. *Cell* 90, 537–548. doi: 10.1016/s0092-8674(00)80513-9

DeGuire, S. M., Ruggeri, F. S., Fares, M. B., Chiki, A., Cendrowska, U., Dietler, G., et al. (2018). N-terminal Huntingtin (Htt) phosphorylation is a molecular switch regulating Htt aggregation, helical conformation, internalization, and nuclear targeting. *J. Biol. Chem.* 293, 18540–18558. doi: 10.1074/jbc.RA118.004621

Dho, S. E., Silva-Gagliardi, N., Morgese, F., Coyaud, E., Lamoureux, E., Berry, D. M., et al. (2019). Proximity interactions of the ubiquitin ligase Mind bomb 1 reveal a role in regulation of epithelial polarity complex proteins. *Sci. Rep.* 9:12471. doi: 10.1038/s41598-019-48902-x

DiFiglia, M., Sapp, E., Chase, K. O., Davies, S. W., Bates, G. P., Vonsattel, J. P., et al. (1997). Aggregation of huntingtin in neuronal intranuclear inclusions and dystrophic neurites in brain. *Science* 277, 1990–1993. doi: 10.1126/science.277.5334.1990

Ehrnhoefer, D. E., Martin, D. D. O., Schmidt, M. E., Qiu, X., Ladha, S., Caron, N. S., et al. (2018). Preventing mutant huntingtin proteolysis and intermittent fasting promote autophagy in models of Huntington disease. *Acta Neuropathol. Commun.* 6:16. doi: 10.1186/s40478-018-0518-0

Ehrnhoefer, D. E., Sutton, L., and Hayden, M. R. (2011). Small changes, big impact: Posttranslational modifications and function of huntingtin in Huntington disease. *Neuroscientist.* 17, 475–492. doi: 10.1177/1073858410390378.Small

Ekkebus, R., Van Kasteren, S. I., Kulathu, Y., Scholten, A., Berlin, I., Geurink, P. P., et al. (2013). On terminal alkynes that can react with active-site cysteine nucleophiles in proteases. *J. Am. Chem. Soc.* 135, 2867–2870. doi: 10.1021/ja309802n

Finkbeiner, S. (2011). Huntington's disease. *Cold Spring Harb. Perspect. Biol.* 3, 1–24. doi: 10.1101/cshperspect.a007476

Gong, B., Kielar, C., and Morton, A. J. (2012). Temporal separation of aggregation and ubiquitination during early inclusion formation in transgenic

mice carrying the Huntington's disease mutation. *PLoS ONE* 7:e41450. doi: 10.1371/journal.pone.0041450

Gu, S., Cui, D., Chen, X., Xiong, X., and Zhao, Y. (2018). PROTACs: an emerging targeting technique for protein degradation in drug discovery. *Bioessays* 40:e1700247. doi: 10.1002/bies.201700247

Hershko, A., and Ciechanover, A. (1998). The ubiquitin system. *Annu. Rev. Biochem.* 67, 425–479. doi: 10.1146/annurev.biochem.67.1.425

Hipp, M. S., Patel, C. N., Bersuker, K., Riley, B. E., Kaiser, S. E., Shaler, T. A., et al. (2012). Indirect inhibition of 26S proteasome activity in a cellular model of Huntington's disease. *J. Cell Biol.* 196, 573–587. doi: 10.1083/jcb.201110093

Hjerpe, R., Aillet, F., Lopitz-Otsoa, F., Lang, V., England, P., and Rodriguez, M. S. (2009). Efficient protection and isolation of ubiquitylated proteins using tandem ubiquitin-binding entities. *EMBO Rep.* 10, 1250–1258. doi: 10.1038/embor.2009.192

Imarisio, S., Carmichael, J., Korolchuk, V., Chen, C.-W., Saiki, S., Rose, C., et al. (2008). Huntington's disease: from pathology and genetics to potential therapies. *Biochem. J.* 412, 191–209. doi: 10.1042/BJ20071619

Jana, N. R., Dikshit, P., Goswami, A., Kotliarova, S., Murata, S., Tanaka, K., et al. (2005). Co-chaperone CHIP associates with expanded polyglutamine protein and promotes their degradation by proteasomes. *J. Biol. Chem.* 280, 11635–11640. doi: 10.1074/jbc.M412042200

Juenemann, K., Jansen, A. H. P., Van Riel, L., Merkx, R., Mulder, M. P. C., An, H., et al. (2018). Dynamic recruitment of ubiquitin to mutant huntingtin inclusion bodies. *Sci. Rep.* 8:1405. doi: 10.1038/s41598-018-19538-0

Juenemann, K., Schipper-Krom, S., Wiemhoefer, A., Kloss, A., Sanz, A. S., and Reits, E. A. J. (2013). Expanded polyglutamine-containing N-terminal huntingtin fragments are entirely degraded by mammalian proteasomes. *J. Biol. Chem.* 288, 27068–27084. doi: 10.1074/jbc.M113.486076

Juenemann, K., Wiemhoefer, A., and Reits, E., a. (2015). Detection of ubiquitinated huntingtin species in intracellular aggregates. *Front. Mol. Neurosci.* 8:1. doi: 10.3389/fnmol.2015.00001

Kah, L. L., Chew, K. C. M., Tan, J. M. M., Wang, C., Chung, K. K. K., Zhang, Y., et al. (2005). Parkin mediates nonclassical, proteasomal-independent ubiquitination of synphilin-1: Implications for lewy body formation. *J. Neurosci.* 25, 2002–2009. doi: 10.1523/JNEUROSCI.4474-04.2005

Kawaguchi, Y., Okamoto, T., Taniwaki, M., Aizawa, M., Inoue, M., Katayama, S., et al. (1994). CAG expansions in a novel gene for Machado-Joseph disease at chromosome 14q32.1. *Nat. Genet.* 8, 221–228. doi: 10.1038/ng1194-221

Keusekotten, K., Elliott, P. R., Glockner, L., Fiil, B. K., Damgaard, R. B., Kulathu, Y., et al. (2013). OTULIN antagonizes LUBAC signaling by specifically hydrolyzing Met1-linked polyubiquitin. *Cell* 153, 1312–1326. doi: 10.1016/j.cell.2013.05.014

Kim, D. I., Jensen, S. C., Noble, K. A., Kc, B., Roux, K. H., Motamedchaboki, K., et al. (2016). An improved smaller biotin ligase for BioID proximity labeling. *Mol. Biol. Cell* 27, 1188–1196. doi: 10.1091/mbc.E15-12-0844

Kim, W., Bennett, E. J., Huttlin, E. L., Guo, A., Li, J., Sowa, M. E., et al. (2011). Systematic and quantitative assessment of the ubiquitin modified proteome. *Mol. Cell* 44, 325–340. doi: 10.1016/j.molcel.2011.08.025

Kirisako, T., Kamei, K., Murata, S., Kato, M., Fukumoto, H., Kanie, M., et al. (2006). A ubiquitin ligase complex assembles linear polyubiquitin chains. *EMBO J.* 25, 4877–4887. doi: 10.1038/sj.emboj.7601360

Kirkpatrick, D. S., Hathaway, N. A., Hanna, J., Elsasser, S., Rush, J., Finley, D., et al. (2006). Quantitative analysis of *in vitro* ubiquitinated cyclin B1 reveals complex chain topology. *Nat. Cell Biol.* 8, 700–710. doi: 10.1038/ncb1436

Kitada, T., Asakawa, S., Hattori, N., Matsumine, H., Yamamura, Y., Minoshima, S., et al. (1998). Mutations in the parkin gene cause autosomal recessive juvenile parkinsonism. *Nature* 392, 605–608. doi: 10.1038/33416

Komander, D., Reyes-Turcu, F., Licchesi, J. D. F., Odenwaelder, P., Wilkinson, K. D., and Barford, D. (2009). Molecular discrimination of structurally equivalent Lys 63-linked and linear polyubiquitin chains. *EMBO Rep.* 10, 466–473. doi: 10.1038/embor.2009.55

Korolchuk, V. I., Mansilla, A., Menzies, F. M., and Rubinsztein, D. C. (2009). Autophagy inhibition compromises degradation of ubiquitin-proteasome pathway substrates. *Mol. Cell* 33, 517–527. doi: 10.1016/j.molcel.2009.01.021

Koyuncu, S., Saez, I., Lee, H. J., Gutierrez-Garcia, R., Pokrzywa, W., Fatima, A., et al. (2018). The ubiquitin ligase UBR5 suppresses proteostasis collapse in pluripotent stem cells from Huntington's disease patients. *Nat. Commun.* 9, 1–9. doi: 10.1038/s41467-018-05320-3

Lam, S. S., Martell, J. D., Kamer, K. J., Deerinck, T. J., Ellisman, M. H., Mootha, V. K., et al. (2015). Directed evolution of APEX2 for electron microscopy and proximity labeling. *Nat. Methods* 12, 51–54. doi: 10.1038/nmeth.3179

Lambert, J.-P., Tucholska, M., Go, C., Knight, J. D. R., and Gingras, A.-C. (2015). Proximity biotinylation and affinity purification are complementary approaches for the interactome mapping of chromatin-associated protein complexes. *J. Proteomics* 118, 81–94. doi: 10.1016/j.jprot.2014.09.011

Landles, C., Sathasivam, K., Weiss, A., Woodman, B., Moffitt, H., Finkbeiner, S., et al. (2010). Proteolysis of mutant huntingtin produces an exon 1 fragment that accumulates as an aggregated protein in neuronal nuclei in huntington disease. *J. Biol. Chem.* 285, 8808–8823. doi: 10.1074/jbc.M109.075028

Lin, L., Jin, Z., Tan, H., Xu, Q., Peng, T., and Li, H. (2016). Atypical ubiquitination by E3 ligase WWP1 inhibits the proteasome-mediated degradation of mutant huntingtin. *Brain Res.* 1643, 103–112. doi: 10.1016/j.brainres.2016.03.027

MacDonald, M. E., Ambrose, C. M., Duyao, M. P., Myers, R. H., Lin, C., Srinidhi, L., et al. (1993). A novel gene containing a trinucleotide repeat that is expanded and unstable on Huntington's disease chromosomes. *Cell* 72, 971–983. doi: 10.1016/0092-8674(93)90585-E

Maheshwari, M., Shekhar, S., Singh, B. K., umar, Jamal, I., Vatsa, N., Kumar, V., et al. (2014). Deficiency of Ube3a in Huntington's disease mice brain increases aggregate load and accelerates disease pathology. *Hum. Mol. Genet.* 23, 6235–6245. doi: 10.1093/hmg/ddu343

Maiuri, T., Woloshansky, T., Xia, J., and Truant, R. (2013). The huntingtin N17 domain is a multifunctional CRM1 and ran-dependent nuclear and cilial export signal. *Hum. Mol. Genet.* 22, 1383–1394. doi: 10.1093/hmg/dds554

Mangiarini, L., Sathasivam, K., Seller, M., Cozens, B., Harper, A., Hetherington, C., et al. (1996). Exon I of the HD gene with an expanded CAG repeat is sufficient to cause a progressive neurological phenotype in transgenic mice. *Cell* 87, 493–506. doi: 10.1016/S0092-8674(00)81369-0

McDowell, G. S., and Philpott, A. (2013). Non-canonical ubiquitylation: mechanisms and consequences. *Int. J. Biochem. Cell Biol.* 45, 1833–1842. doi: 10.1016/j.biocel.2013.05.026

Meyer, H. J., and Rape, M. (2014). Enhanced protein degradation by branched ubiquitin chains. *Cell* 157, 910–921. doi: 10.1016/j.cell.2014.03.037

Miller, V. M., Nelson, R. F., Gouvion, C. M., Williams, A., Rodriguez-Lebron, E., Harper, S. Q., et al. (2005). CHIP suppresses polyglutamine aggregation and toxicity *in vitro* and *in vivo*. *J. Neurosci.* 25, 9152–9161. doi: 10.1523/JNEUROSCI.3001-05.2005

Mulder, M. P. C., Witting, K., Berlin, I., Pruneda, J. N., Wu, K.-P., Chang, J.-G., et al. (2016). A cascading activity-based probe sequentially targets E1–E2–E3 ubiquitin enzymes. *Nat. Chem. Biol.* 12, 523–530. doi: 10.1038/nchembio.2084

Mulder, M. P. C., Witting, K. F., and Ovaa, H. (2019). Cracking the ubiquitin code: the ubiquitin toolbox. Sumoylation ubiquitination. *Curr. Emerg. Concepts* 37, 1–20. doi: 10.21775/9781912530120.02

Ochaba, J., Morozko, E. L., O'Rourke, J. G., and Thompson, L. M. (2018). Fractionation for resolution of soluble and insoluble huntingtin species. *J. Vis. Exp.* 132:e57082. doi: 10.3791/57082

Park, S. H., Kukushkin, Y., Gupta, R., Chen, T., Konagai, A., Hipp, M. S., et al. (2013). PolyQ proteins interfere with nuclear degradation of cytosolic proteins by sequestering the Sis1p chaperone. *Cell* 154, 134–145. doi: 10.1016/j.cell.2013.06.003

Pierce, N. W., Kleiger, G., Shan, S., and Deshaies, R. J. (2009). Detection of sequential polyubiquitylation on a millisecond time-scale. *Nature* 462, 615–619. doi: 10.1038/nature08595

Qin, Z. H., Wang, Y., Kegel, K. B., Kazantsev, A., Apostol, B. L., Thompson, L. M., et al. (2003). Autophagy regulates the processing of amino terminal huntingtin fragments. *Hum. Mol. Genet.* 12, 3231–3244. doi: 10.1093/hmg/ddg346

Ramdzan, Y. M., Trubetskov, M. M., Ormsby, A. R., Newcombe, E. A., Sui, X., Tobin, M. J., et al. (2017). Huntingtin inclusions trigger cellular quiescence, deactivate apoptosis, and lead to delayed necrosis. *Cell Rep.* 19, 919–927. doi: 10.1016/j.celrep.2017.04.029

Raspe, M., Gillis, J., Krol, H., Krom, S., Bosch, K., van Veen, H., et al. (2009). Mimicking proteasomal release of polyglutamine peptides initiates aggregation and toxicity. *J. Cell Sci.* 122, 3262–3271. doi: 10.1242/jcs.045567

Ratovitski, T., O'Meally, R. N., Jiang, M., Chaerkady, R., Chighladze, E., Stewart, J. C., et al. (2017). Post-Translational Modifications (PTMs), identified on endogenous huntingtin, cluster within proteolytic domains between HEAT repeats. *J. Proteome Res.* 16, 2692–2708. doi: 10.1021/acs.jproteome.6b00991

Rhee, H.-W., Zou, P., Udeshi, N. D., Martell, J. D., Mootha, V. K., Carr, S. A., et al. (2013). Proteomic mapping of mitochondria in living cells via spatially restricted enzymatic tagging. *Science* 339, 1328–1331. doi: 10.1126/science.1230593

Roux, K. J., Kim, D. I., Burke, B., and May, D. G. (2018). BioID: a screen for protein-protein interactions. *Curr. Protoc. Protein Sci.* 91, 19.23.1–19.23.15. doi: 10.1002/cpps.51

Roux, K. J., Kim, D. I., Raida, M., and Burke, B. (2012). A promiscuous biotin ligase fusion protein identifies proximal and interacting proteins in mammalian cells. *J. Cell Biol.* 196, 801–810. doi: 10.1083/jcb.201112098

Sap, K. A., Guler, A. T., Bezstarosti, K., Bury, A. E., Juenemann, K., Demmers, J. A. A., et al. (2019). Global proteome and ubiquitinome changes in the soluble and insoluble fractions of Q175 Huntington mice brains. *Mol. Cell. Proteomics* 18, 1705–1720. doi: 10.1074/mcp.RA119.001486

Saudou, F., and Humbert, S. (2016). The biology of huntingtin. *Neuron* 89, 910–926. doi: 10.1016/j.neuron.2016.02.003

Schaffar, G., Breuer, P., Boteva, R., Behrends, C., Tzvetkov, N., Strippel, N., et al. (2004). Cellular toxicity of polyglutamine expansion proteins: mechanism of transcription factor deactivation. *Mol. Cell* 15, 95–105. doi: 10.1016/j.molcel.2004.06.029

Schapira, M., Calabrese, M. F., Bullock, A. N., and Crews, C. M. (2019). Targeted protein degradation: expanding the toolbox. *Nat. Rev. Drug Discov.* 18, 949–963. doi: 10.1038/s41573-019-0047-y

Schilling, G., Klevytska, A., Tebbenkamp, A. T. N., Juenemann, K., Cooper, J., Gonzales, V., et al. (2007). Characterization of huntingtin pathologic fragments in human Huntington disease, transgenic mice, and cell models. *J. Neuropathol. Exp. Neurol.* 66, 313–320. doi: 10.1097/nen.0b013e318040b2c8

Schopp, I. M., Amaya Ramirez, C. C., Debeljak, J., Kreibich, E., Skribbe, M., Wild, K., et al. (2017). Split-BioID a conditional proteomics approach to monitor the composition of spatiotemporally defined protein complexes. *Nat. Commun.* 8:15690. doi: 10.1038/ncomms15690

Steffan, J. S., Agrawal, N., Pallos, J., Rockabrand, E., Trotman, L. C., Slepko, N., et al. (2004). SUMO modification of Huntingtin and Huntington's disease pathology. *Science* 304, 100–104. doi: 10.1126/science.1092194

Swatek, K. N., and Komander, D. (2016). Ubiquitin modifications. *Cell Res.* 26, 399–422. doi: 10.1038/cr.2016.39

Thompson, L. M., Aiken, C. T., Kaltenbach, L. S., Agrawal, N., Illes, K., Khoshnan, A., et al. (2009). IKK phosphorylates Huntingtin and targets it for degradation by the proteasome and lysosome. *J. Cell Biol.* 187, 1083–1099. doi: 10.1083/jcb.200909067

Trushina, E., Dyer, R. B., Badger, J. D., Ure, D., Eide, L., Tran, D. D., et al. (2004). Mutant huntingtin impairs axonal trafficking in mammalian neurons *in vivo* and *in vitro*. *Mol. Cell. Biol.* 24, 8195–8209. doi: 10.1128/MCB.24.18.8195-8209.2004

Ueda, S., Blee, A. M., Macway, K. G., Renner, D. J., and Yamada, S. (2015). Force dependent biotinylation of myosin IIA by α-catenin tagged with a promiscuous biotin ligase. *PLoS ONE* 10:e0122886. doi: 10.1371/journal.pone.0122886

Uzunova, K., Göttsche, K., Miteva, M., Weisshaar, S. R., Glanemann, C., Schnellhardt, M., et al. (2007). Ubiquitin-dependent proteolytic control of SUMO conjugates. *J. Biol. Chem.* 282, 34167–34175. doi: 10.1074/jbc.M706505200

van Well, E. M., Bader, V., Patra, M., Sánchez-Vicente, A., Meschede, J., Furthmann, N., et al. (2019). A protein quality control pathway regulated by linear ubiquitination. *EMBO J.* 38:e100730. doi: 10.15252/embj.2018100730

Varnaite, R., and MacNeill, S. A. (2016). Meet the neighbors: mapping local protein interactomes by proximity-dependent labeling with BioID. *Proteomics* 16, 2503–2518. doi: 10.1002/pmic.201600123

Waelter, S., Boeddrich, A., Lurz, R., Scherzinger, E., Lueder, G., Lehrach, H., et al. (2001). Accumulation of mutant huntingtin fragments in aggresome-like inclusion bodies as a result of insufficient protein degradation. *Mol. Biol. Cell* 12, 1393–1407. doi: 10.1091/mbc.12.5.1393

Wagner, S. A., Beli, P., Weinert, B. T., Nielsen, M. L., Cox, J., Mann, M., et al. (2011). A proteome-wide, quantitative survey of *in vivo* ubiquitylation sites reveals widespread regulatory roles. *Mol. Cell. Proteomics* 10:M111.013284. doi: 10.1074/mcp.M111.013284-1

Wang, B., Zeng, L., Merillat, S. A., Fischer, S., Ochaba, J., Thompson, L. M., et al. (2018). The ubiquitin conjugating enzyme Ube2W regulates solubility of the Huntington's disease protein, huntingtin. *Neurobiol. Dis.* 109, 127–136. doi: 10.1016/j.nbd.2017.10.002

Wanker, E. E., Scherzinger, E., Heiser, V., Sittler, A., Eickhoff, H., and Lehrach, H. (1999). Membrane filter assay for detection of amyloid-like polyglutamine- containing protein aggregates. *Methods Enzymol.* 309, 375–386. doi: 10.1016/S0076-6879(99)09026-6

Wyttenbach, A., Carmichael, J., Swartz, J., Furlong, R. A., Narain, Y., Rankin, J., et al. (2000). Effects of heat shock, heat shock protein 40 (HDJ-2), and proteasome inhibition on protein aggregation in cellular models of Huntington's disease. *Proc. Natl. Acad. Sci. U.S.A.* 97, 2898–2903. doi: 10.1073/pnas.97.6.2898

Yau, R., and Rape, M. (2016). The increasing complexity of the ubiquitin code. *Nat. Publ. Gr.* 18, 579–586. doi: 10.1038/ncb3358

Yau, R. G., Doerner, K., Castellanos, E. R., Matsumoto, M. L., Dixit, V. M., Rape, M., et al. (2017). Assembly and function of heterotypic ubiquitin chains in cell-cycle and protein quality control. *Cell* 171, 918–933. doi: 10.1016/j.cell.2017.09.040

Zou, Y., Ma, D., and Wang, Y. (2019). The PROTAC technology in drug development. *Cell Biochem. Funct.* 37, 21–30. doi: 10.1002/cbf.3369

Zucchelli, S., Marcuzzi, F., Codrich, M., Agostoni, E., Vilotti, S., Biagioli, M., et al. (2011). Tumor necrosis factor receptor-associated factor 6 (TRAF6) associates with Huntingtin protein and promotes its atypical ubiquitination to enhance aggregate formation. *J. Biol. Chem.* 286, 25108–25117. doi: 10.1074/jbc.M110.187591

Conflict of Interest: The authors declare that the research was conducted in the absence of any commercial or financial relationships that could be construed as a potential conflict of interest.

Advantages of publishing in Frontiers

OPEN ACCESS
Articles are free to read for greatest visibility and readership

FAST PUBLICATION
Around 90 days from submission to decision

HIGH QUALITY PEER-REVIEW
Rigorous, collaborative, and constructive peer-review

TRANSPARENT PEER-REVIEW
Editors and reviewers acknowledged by name on published articles

Frontiers
Avenue du Tribunal-Fédéral 34
1005 Lausanne | Switzerland

Visit us: www.frontiersin.org
Contact us: info@frontiersin.org | +41 21 510 17 00

REPRODUCIBILITY OF RESEARCH
Support open data and methods to enhance research reproducibility

DIGITAL PUBLISHING
Articles designed for optimal readership across devices

FOLLOW US
@frontiersin

IMPACT METRICS
Advanced article metrics track visibility across digital media

EXTENSIVE PROMOTION
Marketing and promotion of impactful research

LOOP RESEARCH NETWORK
Our network increases your article's readership